National Research Council Canada

Conseil national de recherches Canada

NRC·CNRC

Canadian Journal of Fisheries and Aquatic Sciences

Journal canadien des sciences halieutiques et aquatiques

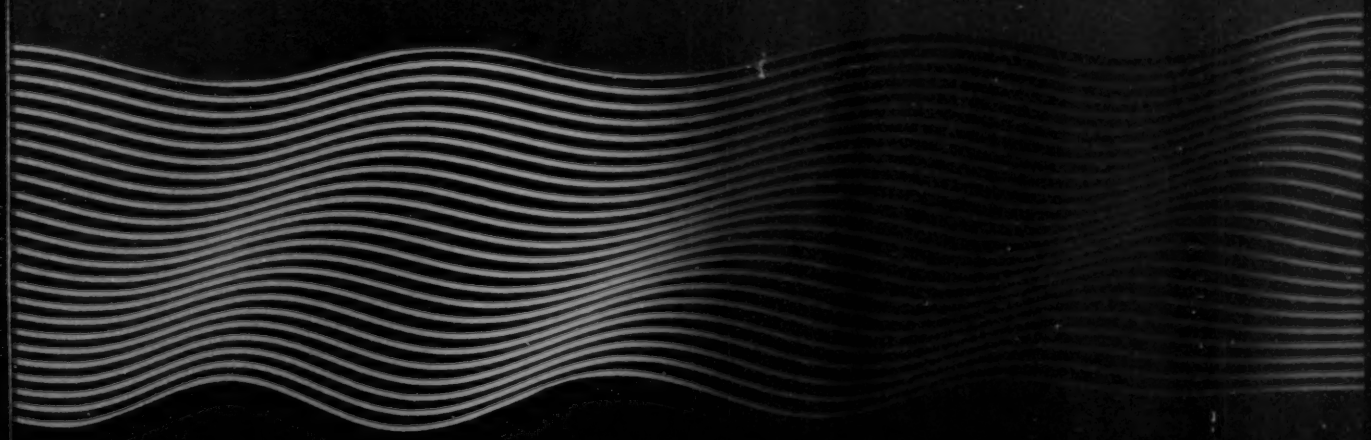

http://cjfas.nrc.ca

http://jcsha.cnrc.ca

ISSN 0706-652X / CJFSDX 59(4) 587–753 (2002)

The *Canadian Journal of Fisheries and Aquatic Sciences*, previously published as *Contributions to Canadian Biology* 1901–1925, *Contributions to Canadian Biology and Fisheries* 1926–1934, *Journal of the Biological Board of Canada* 1934–1937, and *Journal of the Fisheries Research Board of Canada* 1938–1979, is issued monthly to form annual volumes of 12 numbers plus supplements.

Editorial policy: The Journal publishes original research articles, perspectives (syntheses, critiques, re-evaluations), discussions (comment and reply), and rapid communications. Manuscripts may concern cells, organisms, populations, communities, ecosystems, or processes that affect aquatic systems. They may cover a range of disciplines including biology and ecology of marine and freshwater organisms, limnology, oceanography, physiology, toxicology, genetics, economics, disease, and management. Preference will be given to manuscripts that emphasize understanding of observed phenomena and interpretation of experimental results. The Journal encourages papers that lead from clearly stated purpose or rationale and from testable hypotheses, concepts, or questions to identifiable conclusions or syntheses. Such papers may amplify, modify, question, or redirect accumulated knowledge embodied in contemporary perceptions of a particular state of aquatic sciences. The Journal discourages papers that are essentially descriptive, except in emerging disciplines; have only site-specific or local applications (a certain year, place, taxon, chemical compound, etc.); only confirm previously established principles; or apply standard techniques without breaking new methodological ground.

Manuscripts for publication should be submitted to the Editors, *Canadian Journal of Fisheries and Aquatic Sciences*, Department of Zoology, University of Guelph, Guelph, ON N1G 2W1, Canada (519-824-4120 ext. 2646; fax: 519-767-9798; e-mail: cjfas@uoguelph.ca).

Submissions in either English or French are acceptable. The information must be original, that is, not copyrighted, published, or submitted elsewhere except in abstract form or unless by written consent of the Editor. NRC accepts no responsibility for statements or opinions expressed by a contributor. Acceptance of an advertisement, announcement, or other material does not imply endorsement by either the Journal's Editors or NRC. The use of proprietary names does not imply endorsement of the product or company.

Correspondence concerning accepted manuscripts and corrected proofs should be sent to NRC Research Press, National Research Council of Canada, Ottawa, ON K1A 0R6, Canada (fax: 613-952-7656; e-mail: research.press@nrc.ca).

Instructions to Authors are published once a year in the first issue of each volume. Copies are available from NRC Research Press or at http://cjfas.nrc.ca. The **Publication Policy** of NRC Research Press is available at http://cjfas.nrc.ca.

The National Research Council of Canada accepts no responsibility for statements or opinions expressed by a contributor. Acceptance of an advertisement, announcement, or other material does not imply endorsement by either the Journal's Editors or NRC.

Microfilm: Issues from 1934 through the current volume can be purchased on 16- or 35-mm microfilm. Photocopies of individual articles or issues can be purchased from University Microfilms International, 330 North Zeeb Road, Ann Arbor, MI 48106, U.S.A.

U.S. periodical postage paid at Champlain, N.Y., and at additional mailing offices. Attention U.S. POSTMASTER: Send address changes to **Canadian Journal of Fisheries and Aquatic Sciences**, c/o USACAN Media Distribution Center, P.O. Box 2888, Plattsburg, NY 12901, U.S.A.

Publié sans interruption depuis 1901, le *Journal canadien des sciences halieutiques et aquatiques* a paru sous plusieurs titres : *Contributions to Canadian Biology* 1901–1925, *Contributions to Canadian Biology and Fisheries* 1926–1934, *Journal of the Biological Board of Canada* 1934–1937, et *Journal of the Fisheries Research Board of Canada* 1938–1979. Le Journal paraît tous les mois, formant ainsi un volume de 12 numéros, et offre en plus jusqu'à deux suppléments par année.

Politique éditoriale : On publie, dans le Journal, des articles rendant compte de recherche originale, des perspectives (synthèses, critiques et réévaluations), des discussions (commentaires et réponses) et des communications rapides. Les documents peuvent porter sur les cellules, organismes, populations, communautés, écosystèmes ou processus qui affectent les systèmes aquatiques. Ils peuvent relever de divers domaines y compris la biologie et l'écologie des organismes marins et d'eau douce, la limnologie, l'océanographie, la physiologie, la toxicologie, la génétique, l'économie, la pathologie et la gestion. On accorde la préséance aux articles qui contribuent à la compréhension de phénomènes observés et à l'interprétation de résultats expérimentaux. On invite les auteurs à soumettre des articles ayant des objectifs précis ou relevant d'hypothèses, de concepts ou de questions vérifiables et se terminant par de solides conclusions ou d'utiles synthèses. Ces articles enrichissent, changent, mettent en question ou réorientent les connaissances acquises sur divers aspects des sciences aquatiques. On décourage toutefois la soumission d'articles simplement descriptifs (à moins qu'il ne s'agisse de nouvelles disciplines), d'application très limitée (applicables à une seule année, une seule région ou un seul taxon, portant sur un unique composé chimique, etc.); d'articles qui ne font que reprendre les principes énoncés dans des articles précédents; et d'articles rendant compte de l'application de normes sans gain de méthodologie.

Les auteurs voudront adresser leurs **manuscrits** aux directeurs scientifiques, *Journal canadien des sciences halieutiques et aquatiques*, Department of Zoology, University of Guelph, Guelph, ON N1G 2W1, Canada (519-824-4120 poste 2646; télécopieur : 519-767-9798; courriel : cjfas@uoguelph.ca).

Les contributions peuvent être en anglais ou en français. Elles doivent être originales, c.-à.-d. qu'elles ne doivent pas avoir fait l'objet d'un copyright, avoir été publiées ou soumises ailleurs, sauf sous forme abrégée ou avec le consentement du rédacteur. Le CNRC ne se tient en aucune façon responsable des opinions exprimées par un collaborateur ou des déclarations qui pourrait faire ce dernier. La publication d'annonces publicitaires, d'avis et autres n'implique pas l'endossement de leur contenu par les directeurs du Journal ou du CNRC. L'utilisation des noms de marques de commerce ne signifie aucunement une sanction du produit en question ou de la compagnie qui le fabrique.

La correspondance ayant trait aux manuscrits acceptés et les **épreuves corrigés** doivent être envoyées aux Presses scientifiques du CNRC, Conseil national de recherches du Canada, Ottawa, ON K1A 0R6, Canada (télécopieur : 613-952-7656; courriel : presses.scientifiques@cnrc.ca).

Les Recommandations aux auteurs sont publiées une fois par année dans le premier numéro de chaque volume. Des copies sont disponibles auprès du Bureau de la rédaction aux Presses scientifiques du CNRC ou au http://jcsha.cnrc.ca. **La Politique de publication** est disponible auprès des Presses scientifiques du CNRC ou au http://jcsha.cnrc.ca.

Le Conseil national de recherches du Canada ne se tient en aucune façon responsable des opinions exprimées par un collaborateur ou des déclarations que pourrait faire ce dernier. La publication d'annonces publicitaires, d'avis et autres n'implique pas l'endossement de leur contenu par les directeurs de la Revue ou du CNRC.

Microfilms : On peut acheter sur microfilms de 16 ou 35 mm tous les numéros depuis 1934. Des photocopies d'articles ou de numéros individuels sont aussi en vente auprès de University Microfilms International, 330 North Zeeb Road, Ann Arbor, MI 48106, É.-U.

This Journal is indexed or abstracted in / Cette revue est signalée ou résumée dans

ABSEARCH, Aquatic Sciences and Fisheries Abstracts, Biological Abstracts, Biological & Agricultural Index, CAB Abstracts, Chemical Abstracts, Current Contents, Elsevier BIOBASE, Environmental Abstracts, Environmental Periodicals Bibliography, GEOBASE, GeoRef, Internationale Bibliographie der Zeitschriftenliteratur, Life Sciences Collection, Meteorological and Geoastrophysical Abstracts, Oceanic Abstracts, PASCAL Database, and Science Citation Index.

Volume 59, Number 4, April 2002

Canadian Journal of Fisheries and Aquatic Sciences

Published by the National Research Council of Canada

Volume 59, numéro 4, avril 2002

Journal canadien des sciences halieutiques et aquatiques

Publié par le Conseil national de recherches du Canada

Editors / directeurs scientifiques John C. Roff and Moira M. Ferguson

Assistant to the Editors / adjointe aux directeurs scientifiques **Holly Foster**

Associate Editors / directeurs scientifiques associés

M.T. Arts, *Environment Canada, Burlington*
D. Boisclair, *Université de Montréal*
U. Borgmann, *Environment Canada, Burlington*
S.E. Campana, *DFO/MPO, Dartmouth*
R. Carignan, *Université de Montréal*
D.G. Dixon, *University of Waterloo*
A.E. Dizon, *National Marine Fisheries Service, La Jolla, Calif.*
J.J. Dodson, *Université Laval*
J.A. Downing, *Iowa State University*
K.T. Frank, *DFO/MPO, Dartmouth*
D.F. Houlihan, *University of Aberdeen, Aberdeen, Scotland*
F.A. Huntingford, *University of Glasgow*
J.A. Hutchings, *Dalhousie University*
G.S. Jamieson, *DFO/MPO, Nanaimo*
B. Jonsson, *Norwegian Institute for Nature Research, Oslo, Norway*
D.M. Mason, *NOAA-Great Lakes Environmental Research Laboratory, Ann Arbor, Mich.*
A. Mazumder, *University of Victoria*
D.L. Parrish, *Vermont Cooperative Fish and Wildlife Research Unit (USGS/BRD), University of Vermont*
P. Pepin, *DFO/MPO, St. John's*
T.M. Powell, *University of California, Berkeley, Calif.*
E.E. Prepas, *University of Alberta*
T.J. Quinn II, *University of Alaska–Fairbanks, Juneau, Alaska*
T.P. Quinn, *University of Washington*
R.D. Robarts, *Environment Canada, Saskatoon*
B. Sainte-Marie, *DFO/MPO, Mont-Joli*
D.W. Schindler, *University of Alberta*
S.J. Smith, *DFO/MPO, Dartmouth*
W.G. Sprules, *University of Toronto*
R.J. Thompson, *Memorial University of Newfoundland*
C.J. Walters, *University of British Columbia*
R.D. Ward, *CSIRO Marine Research, Australia*
C.M. Wood, *McMaster University*
B. de Young, *Memorial University of Newfoundland*

NRC Research Press / Presses scientifiques du CNRC

Editor-in-chief / directeur général **Bruce P. Dancik**

Assistant Editor-in-chief / directeur général adjoint **Iain E.P. Taylor**

Journals Program / Programme des revues

(Fax / télécopieur : 613-952-7656; e-mail / courriel : research.press@nrc.ca;
URL: http://researchpress.nrc.ca)

Director / directrice **Aldyth Holmes**

Business Manager / gestionnaire des affaires **Paul McClymont**

Managing Editor / rédactrice administrative **Cecily M. Pearson (613-993-9099)**

Publication Officers / agentes de publication **Jennifer McColl and Lee Murphy**

Advertising / annonces publicitaires **Judy Gorman (613-993-0151)**

Reprints / tirés à part **Roxanne Landriault (613-990-2254)**

Subscriptions / abonnements **Helen Goulet (613-993-9084)**

© National Research Council of Canada 2002. World rights reserved.
No part of this publication may be reproduced, stored, or transmitted in any form or by any means, without the written permission of the publisher, except as stated below.

The National Research Council of Canada grants **permission*** to individuals to make single copies of articles for personal use. Any person may reproduce short excerpts from articles in the journal for any purpose that respects the moral rights of authors, provided that the source is fully acknowledged. As a courtesy, the consent of authors of such material should be obtained directly from the author.

Authorization to reproduce items for other than personal use, as stated above, is granted by the National Research Council of Canada provided that the copyright fee of $7.00 per copy is paid directly to CANCOPY, One Yonge Street, Suite 1900, Toronto, ON M5E 1E5, Canada.

*The above permission does not extend to other kinds of copying, such as copying for general distribution, for advertising, or promotional purposes, for creating new collective works, or for resale. For such copying, arrangements must be made with the publisher, National Research Council of Canada, Ottawa, ON K1A 0R6, Canada.

© Conseil national de recherches du Canada 2002. Tous droits réservés.
Il est interdit de reproduire, de sauvegarder ou de transmettre quelque partie de la présente publication dans quelque format ou de quelque façon sans le consentement écrit de l'éditeur, à l'exception des conditions suivantes.

Le Conseil national de recherches du Canada accorde aux particuliers le droit de faire des copies individuelles pour leur usage personnel. Toute personne peut reproduire de courts extraits des articles de la Revue pour autant que les droits moraux de l'auteur soient respectés et que la mention de provenance soit clairement indiquée. Il est de convenance de demander le consentement de l'auteur avant de faire mention de son travail.

On obtiendra l'autorisation de reproduire des articles à d'autres fins que l'usage personnel (tel qu'on l'a décrit ci-dessus) auprès du Conseil national de recherches du Canada pour autant que des redevances de droits d'auteurs de 7,00 $/copie soient versées au CANCOPY, 1, rue Yonge, bureau 1900, Toronto, ON M5E 1E5, Canada.

*La permission ci-dessus ne s'applique pas à la reproduction à grande échelle, telle que la reproduction aux fins de distribution générale, publicitaire ou promotionnelle, de compilation de nouveaux ouvrages collectifs ou de revente. Dans de tels cas, il faudra ratifier une entente particulière avec l'éditeur, le Conseil national de recherches du Canada, Ottawa, ON K1A 0R6, Canada.

Subscription information

The *Canadian Journal of Fisheries and Aquatic Sciences* (ISSN 0706-652X) is published monthly by the National Research Council of Canada. 2002 annual subscription rates (second class postage) for Canada are $732CAN institutional and $227CAN personal, for US & foreign $732US institutional and $227US personal. For air mail add $175US to foreign rate. Canadian customers please include 7% GST (business no. 12149 1807 RT 0275). Subscriptions are entered for the calendar year. Remittances should be made payable to the Receiver General for Canada credit NRC. Price for regular single issues: institutional, $95.00; personal, $30.00. Supplements will be priced separately. Special rates apply to members of Canadian scientific and engineering societies if they subscribe through their respective societies.

There are no refunds on cancelled subscriptions once delivery has begun. Claims for missing issues should be made within four months (N. America) or six months (outside N. America) following the date of publication. The publisher expects to supply missing issues only when losses have occurred in transit and when the reserve stock will permit. For change of address and subscription enquiries: Subscription Office, NRC Research Press, National Research Council of Canada, Ottawa, ON K1A 0R6, Canada; tel.: 613-993-9084; fax: 613-952-7656; e-mail: research.press@nrc.ca.

Microform backfiles are available from UMI, P.O. Box 1346, Ann Arbor, MI 48106-1346, U.S.A., and Micromedia Ltd., 20 Victoria St., Toronto, ON M5C 2N8, Canada.

All issues of the *Canadian Journal of Fisheries and Aquatic Sciences* since 1996 are available on the Web. Pricing information can be found at http://cjfas.nrc.ca.

Renseignements sur l'abonnement

Journal canadien des sciences halieutiques et aquatiques (ISSN 0706-652X) est une publication mensuelle du Conseil national de recherches du Canada. Le prix de l'abonnement annuel au Canada (courrier de deuxième classe) est de 732 $CAN pour les organismes et de 227 $CAN pour les particuliers. À l'étranger (y compris les É.-U.), le prix de l'abonnement est de 732 $US pour les organismes et de 227 $US pour les particuliers. L'expédition par avion exige des frais de 175 $US en sus du prix d'abonnement à l'étranger. Les clients du Canada doivent ajouter la TPS de 7% (numéro d'entreprise 12149 1807 RT 0275). Les abonnements sont pour l'année civile. Tout paiement doit être adressé au Receveur général du Canada, crédit du CNRC. Le prix par numéro est de 95 $ pour les organismes et de 30 $ pour les particuliers. Le prix des hors-série varie. Les membres des sociétés canadiennes de sciences et de génie bénéficient de taux préférentiels en s'abonnant via leurs sociétés respectives.

Aucun remboursement ne sera accordé ni aucune annulation acceptée une fois que les livraisons auront commencé. Les réclamations de numéros manquants devront être soumises dans les quatre mois (Amérique du Nord) ou dans les six mois (à l'extérieur de l'Amérique du Nord) suivant la date de publication. L'éditeur ne fournira de numéros manquants que si le document a été perdu pendant l'expédition et que si le stock le permet. Adressez tout changement d'adresse ou toute question quant à l'abonnement au : Bureau des abonnements, Presses scientifiques du CNRC, Conseil national de recherches Canada, Ottawa, ON K1A 0R6, Canada; téléphone : 613-993-9084; télécopieur : 613-952-7656; courriel : presses.scientifiques@nrc.ca.

On peut obtenir les fichiers rétrospectifs sur **microforme** auprès de UMI, P.O. Box 1346, Ann Arbor, MI 48106-1346, É.-U., et auprès de Micromedia Ltée, 20 rue Victoria, Toronto, ON M5C 2N8, Canada.

À partir de 1996, tous les numéros de *Journal canadien des sciences halieutiques et aquatiques* sont accessibles sur le Web. On trouvera des renseignements sur les tarifs à http://jcsha.cnrc.ca.

RAPID COMMUNICATION / COMMUNICATION RAPIDE

Otolith sulfur isotope method to reconstruct salmon (*Oncorhynchus tshawytscha*) life history

Peter K. Weber, Ian D. Hutcheon, Kevin D. McKeegan, and B. Lynn Ingram

Abstract: We report a new ion microprobe method to reconstruct aspects of fish life history based on sulfur isotopes ($^{34}S/^{32}S$, expressed as $\delta^{34}S$). Selected hatchery raised and naturally spawned juvenile chinook salmon (*Oncorhynchus tshawytscha*) are shown to have a 12.96 ± 0.27‰ (mean ± 2 standard errors) difference in muscle $\delta^{34}S$ values, corresponding to $\delta^{34}S$ differences between the hatchery and freshwater diets. Isotopic microanalyses of otoliths demonstrate that this 13‰ difference is preserved in the otoliths. We interpret the otolith $\delta^{34}S$ record to be a chronology of dietary $\delta^{34}S$, with approximately one-week temporal resolution, preserved in these banded calcium carbonate structures. Potential applications of this method include identifying hatchery raised fish and reconstructing nutrition sources, migration, and other aspects of fish life history.

Résumé : Une nouvelle méthode qui utilise une microsonde ionique permet de reconstituer certains aspects du cycle biologique d'un poisson à l'étude des isotopes de soufre ($^{34}S/^{32}S$, soit $\delta^{34}S$). De jeunes saumons quinnat (*Oncorhynchus tshawytscha*) sélectionnés, certains élevés en pisciculture et d'autres nés en nature, présentent des différences de 12,96 ± 0,27‰ (moyenne ± 2 fois l'erreur type) dans les $\delta^{34}S$ de leurs muscles, ce qui correspond aux différences de $\delta^{34}S$ entre les régimes alimentaires en pisciculture et en milieu d'eau douce. Des microanalyses des isotopes des otolithes révèlent que cette différence de 13‰ se maintient dans les otolithes. Nous interprétons cet enregistrement du $\delta^{34}S$ dans les couches de carbonate de calcium des otolithes comme le reflet de l'évolution dans le temps du $\delta^{34}S$ alimentaire avec une précision de l'ordre de 1 semaine. L'identification des poissons élevés en pisciculture, ainsi que la reconstitution des sources alimentaires, de la migration et d'autres aspects du cycle biologique des poissons sont parmi les applications potentielles de cette nouvelle méthodologie.

[Traduit par la Rédaction]

Introduction

Sulfur isotopes are useful for the study of nutrient flows and migratory patterns in large part because marine and continental food webs typically have substantially different sulfur isotopic compositions (Peterson et al. 1986; Nriagu et al. 1991). Bacterial sulfate (SO_4^{2-}) reduction in the oceans enriches marine SO_4^{2-} in ^{34}S relative to sulfur in the earth's crust ($\delta^{34}S$ of +21‰ versus a mean of ~0‰) (Thode 1991). The $\delta^{34}S$ of river water SO_4^{2-} varies regionally between –5‰ and +15‰ according to bedrock lithology, anthropogenic inputs, and atmospheric deposition from natural sources, with a global average value of approximately +7‰ (Nriagu et al. 1991). Photosynthetic plants use inorganic sulfur, like SO_4^{2-}, to synthesize S-bearing compounds with a small amount of isotopic fractionation (0 to –3‰ for marine, and –5‰, on average, for freshwater plants) (Nriagu et al. 1991). The $\delta^{34}S$ signal established by primary producers is maintained in the food web because the essential sulfur-bearing compounds are incorporated into the tissue of consumers without significant fractionation (Peterson et al. 1986; Nriagu et al. 1991), generating a substantial difference in $\delta^{34}S$ between marine and most continental food webs. Smaller but still useful differences can be found within freshwater systems (Nriagu et al. 1991). In fish, $\delta^{34}S$ can readily be determined in muscle and organ samples by standard isotope ratio mass spectrometry techniques, providing time-averaged dietary $\delta^{34}S$ information (Hesslein et al. 1993).

We hypothesize that the otolith organic matrix contains a permanent record of a fish's dietary sulfur history. Otoliths are calcium carbonate concretions in the inner ear of bony fish (salmon, in this study) that accrete with daily and sea-

Received 4 January 2002. Accepted 10 April 2002. Published on the NRC Research Press Web site at http://cjfas.nrc.ca on 23 April 2002. J16683

P.K. Weber.[1] Department of Geography, University of California, Berkeley, CA 94720, U.S.A.
I.D. Hutcheon. Analytical & Nuclear Chemistry Division, Lawrence Livermore National Laboratory, Livermore, CA 94551, U.S.A.
K.D. McKeegan. Department of Earth and Space Sciences, University of California, Los Angeles, CA 90095, U.S.A.
B.L. Ingram. Department of Earth and Planetary Science, University of California, Berkeley, CA 94720, U.S.A.

[1]Corresponding author (email: pweber@socrates.berkeley.edu)

 DOI: 10.1139/F02-038 © 2002 NRC Canada

sonal growth increments, preserved by successive growth layers. Sulfur (100–600 $\mu g \cdot g^{-1}$) is associated with the otolith organic matrix (Kalish 1989). Otolith chemistry has been extensively analyzed (Campana 1999), but no measurements of otolith $\delta^{34}S$ have ever been reported. We expect the organic matrix in the centre of each salmon otolith to reflect the marine sulfur isotopic composition of the mother, transmitted via the egg to the fish. Once the juvenile salmon hatches out and begins to feed, the $\delta^{34}S$ of each otolith growth increment should reflect the diet of the fish at that particular time (i.e., the otolith layers preserve a temporal record of fish diet).

We test this hypothesis by making in situ measurements of otolith $\delta^{34}S$ for hatchery raised and naturally spawned juvenile chinook salmon (*Oncorhynchus tshawytscha*). Hatchery raised and naturally spawned salmon should have distinct juvenile dietary $\delta^{34}S$ histories in most river systems. In the hatchery, juvenile salmon are raised on commercial feeds typically consisting of 80–90% protein from marine sources, whereas in the wild, juvenile salmon have a freshwater diet. We analyze tissue and food samples to show that hatchery raised and naturally spawned juvenile chinook salmon have distinct dietary sulfur histories. We compare hatchery and source river water dissolved sulfur content to exclude significant additions of exogenous sulfur from hatchery operations (e.g., feeding). Finally, we analyze otolith $\delta^{34}S$ by ion microprobe, generating a spatially resolved $\delta^{34}S$ record.

Methods

Five sets of juvenile chinook salmon from the Sacramento – San Joaquin river system (~38°N, 122°W) were used in this study. One set of fish came from a river with no hatchery stocking (Butte Creek), another set was captured in August in a river that last received hatchery fish four months before (Sacramento River at Red Bluff), the third set was taken directly from a hatchery (Feather River), the fourth set were naturally spawned chinook salmon fry recently emerged from the gravel (34- to 38-mm fork length, FL), and the fifth set were tagged hatchery raised salmon (Merced River) released in the Tuolumne River and recaptured in the Sacramento – San Joaquin Delta 25 days later. With the exception of the fry, the fish caught in the wild were all larger than 60-mm FL, and the fish taken directly from the hatchery were larger than 45-mm FL.

The Butte Creek, Sacramento River, and Feather River Hatchery fish were used to characterize dietary and resultant bulk muscle tissue $\delta^{34}S$ for the naturally spawned and hatchery raised juvenile salmon because these fish were expected to be in equilibrium with their diets. Whole prey items were extracted from the stomachs of salmon caught in the wild, three commercial chinook salmon feeds were obtained from the Feather River and Merced River hatcheries, and stomach contents were extracted from three of the hatchery salmon. To characterize prefeeding salmon $\delta^{34}S$, two sets of chinook salmon eggs and the four naturally spawned chinook salmon fry were analyzed. All muscle, stomach content, feed, and egg samples were dried at 60°C and ground to a fine powder. Lipids were extracted using methylene chloride and methanol (2:1, v/v). The lipid-extracted samples were analyzed for ^{34}S:^{32}S by an Isochrom Continuous Flow Stable Isotope Mass Spectrometer (Micromass, Manchester, U.K.) coupled to a Carlo Erba Elemental Analyzer (ThermoFinnigan Italia, Milan, Italy) at the Environmental Isotope Laboratory, University of Waterloo, Ont., Canada.

Fig. 1. Transmitted light micrograph of a polished otolith from a juvenile chinook salmon (*Oncorhynchus tshawytscha*) showing concentric growth increments and ion microprobe traverse used to determine $\delta^{34}S$. In situ ion microprobe analyses reveal variations in $\delta^{34}S$, correlated with radial position (salmon age), that track changes in nutrient-source and (or) diet $\delta^{34}S$, which can in turn be related to aspects of salmon life history (Fig. 3).

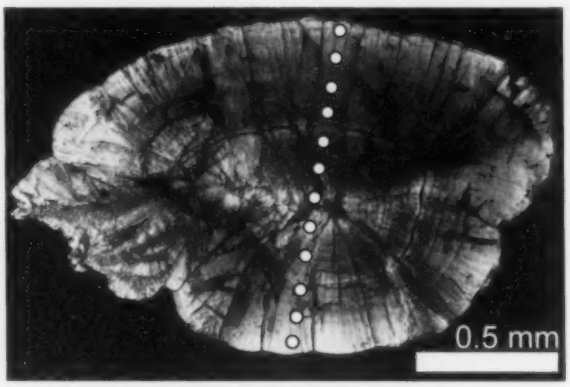

To test for sulfur additions in the hatchery (Merced River), matched pairs of filtered water samples (0.4 µm) were collected from the hatchery raceways and the adjacent river when salmon were present (February 1998, March 1998, and January 1999). Total sulfur was determined by inductively coupled plasma atomic emission spectrometer (Thermo Jarrell Ash Iris HR, Thermo Elemental, Franklin, Mass., U.S.A.) at the University of California, Berkeley. Replicate analyses of matched pairs were made using concentrated and spiked aliquots.

We selected otoliths from the Butte Creek juvenile salmon for analysis to characterize otolith $\delta^{34}S$ in the wild because these fish were the most likely to be naturally spawned. Otoliths from the recaptured Merced River Hatchery salmon were selected to characterize otolith $\delta^{34}S$ in the hatchery and after release. Otoliths were removed, cleaned in deionized water, dried at 60°C, mounted in Araldite epoxy, and polished to expose banding (Fig. 1).

The spatial distribution of sulfur isotopes in otoliths was determined using ion microprobes (Cameca, Courbevoie, France) at the University of California at Los Angeles (Cameca IMS 1270, National Ion Microprobe Facility) and the Lawrence Livermore National Laboratory (Cameca IMS 3f, Livermore, Calif.). Techniques for the IMS 1270 were similar to those described previously for oxygen-isotope analyses (McKeegan et al. 1998). A 20-keV, ~4-nA Cs^+ primary ion beam, defocused to produce a uniformly illuminated spot, was used to sputter gold-coated sections of otoliths. Low-energy (<30 eV) negative secondary ions were accelerated to 10 keV and mass analyzed at high resolving power ($m/\Delta m = 4000$). A normal incidence electron flood gun was used to provide charge compensation. Secondary ions were detected by static multicollection: ^{32}S (~4×10^6 ions$\cdot s^{-1}$) on a Faraday cup and ^{34}S by ion counting on an

© 2002 NRC Canada

Fig. 2. Sulfur isotope composition of muscle tissue (□) from hatchery raised (>45 mm fork length, FL) and naturally spawned juvenile (>60-mm FL) chinook salmon (*Oncorhynchus tshawytscha*), with comparison to $\delta^{34}S$ of diet (○; ● for Merced River Hatchery feed), eggs (×), and recently hatched, naturally spawned fry (△). The egg (n = 2) and fry (n = 4) data demonstrate that the maternal marine $\delta^{34}S$ signal is transmitted to the prefeeding juvenile fish. The data for the larger juvenile fish (n = 7, 12, and 10 from left to right) show an unambiguous difference in $\delta^{34}S$ (12.96 ± 0.27‰ (2 SE)) between hatchery raised and naturally spawned fish. The larger fish are in approximate equilibrium with their diets (n = 6, 6, and 6), as expected based on known history and size. Butte Creek salmon are expected to be naturally spawned in the wild because the river is not stocked with hatchery salmon. The Sacramento River samples were collected at the Red Bluff diversion dam four months after the last releases from the upstream hatchery; therefore, any hatchery fish still in the river would reflect a freshwater diet in the wild. Data point size represents two standard errors.

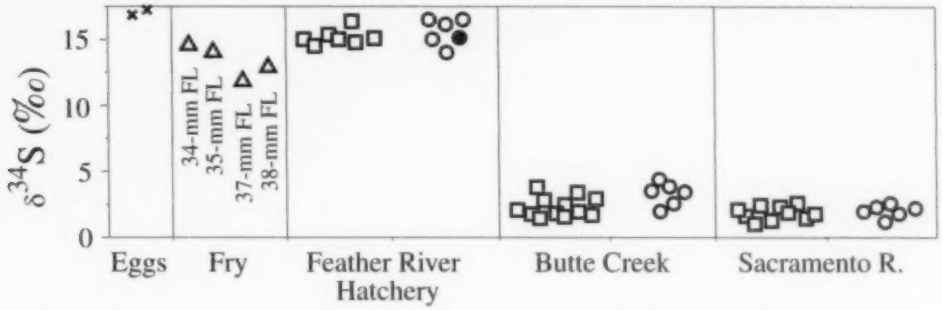

electron multiplier. Techniques for the IMS 3f were generally similar, with the major differences being a reduction in the Cs^+ beam energy to 14.5 keV, reduction in secondary ion energy to 4.5 keV, and the measurement of both S isotopes by pulse counting and magnetic peak switching. The ^{34}S–^{32}S ratios were corrected for instrumental mass-dependent fractionation by comparison to analyses of pressed standards composed of 95% calcium carbonate and 5% dried, lipid-extracted fish muscle with known sulfur isotopic compositions. All ^{34}S–^{32}S ratios are expressed as $\delta^{34}S$ values, the deviation in per mil relative to the Canyon Diablo Troilite (CDT) standard

$$\delta^{34}S = \left[\frac{(^{34}S/^{32}S)_{sample}}{(^{34}S/^{32}S)_{CDT}} - 1\right] \times 1000$$

Measurement uncertainty is presented as two standard errors (2 SE). The sulfur concentration in these otoliths (100–500 ppm) is sufficient to measure $\delta^{34}S$ at a single spot to 1–2‰ (external precision) with the Cameca IMS 1270, and to 3–5‰ with the Cameca IMS 3f. The temporal resolution of the analyses is limited by the ~20-μm diameter of the primary beam. Juvenile salmon otoliths have 2- to 10-μm daily growth increments and each single spot analysis averages four to eight daily bands in these otoliths. The $\delta^{34}S$ data thus provide a chronology with roughly one-week resolution.

Results and discussion

Our $\delta^{34}S$ data for eggs and fry (Fig. 2) demonstrate that the adult salmon $\delta^{34}S$ signal (+17‰ to +18‰; Krouse et al. 1991) is transmitted to the juvenile fish via the egg. With time and growth (>45-mm FL), this signal in the tissue is replaced by the dietary $\delta^{34}S$ value (Fig. 2), as expected (Hesslein et al. 1993). Our results show a substantial difference in muscle tissue $\delta^{34}S$ (12.96 ± 0.27‰) between juvenile salmon feeding in the hatchery and those feeding in the rivers. This difference is large relative to both sample variability (2 standard deviations, SD, of 1.0–1.8‰) and measurement precision (2 SE of 0.6‰). Wild salmon $\delta^{34}S$ values for muscle (+1.0‰ to +3.8‰) and stomach content (+1.3‰ to +4.5‰) are in the range expected for freshwater sulfur sources. In contrast, the $\delta^{34}S$ values in the muscle tissue of the hatchery raised fish (+14.6‰ to +16.4‰) are indicative of sulfur derived from the hatchery feeds (+14.1‰ to +16.6‰), reflecting a marine signature modified by the admixture of sulfur from continental sources.

Filtered water samples from the Merced River Hatchery and adjacent river contain S at 0.7–1.5 $\mu g \cdot g^{-1}$. Matched pairs have the same sulfur content within error ($mean_{river-hatchery}$ = 0.03 ± 0.25 $\mu g \cdot g^{-1}$), suggesting that hatchery operation does not add significant amounts of exogenous dissolved sulfur to river water diverted to the hatchery raceways. This observation is consistent with strontium isotope and major and minor elemental data for this hatchery and others in the Sacramento – San Joaquin river system, which also suggest that hatchery operation does not alter source water chemistry (Weber 2002). If little exogenous sulfur is added to hatchery water, then the hatchery water sulfate $\delta^{34}S$ cannot be significantly elevated relative to river water sulfate $\delta^{34}S$.

We present the in situ analyses of $\delta^{34}S$ in two otoliths, from a naturally spawned juvenile salmon and a recaptured juvenile hatchery raised salmon (Fig. 3). The data show large differences in sulfur isotope composition correlated with nutritional history. For the naturally spawned fish, the $\delta^{34}S$ of the otolith core (14.4 ± 2.2‰, 2 SE, external precision) reflects the marine signal from the egg. The $\delta^{34}S$ values abruptly decrease to near zero (–0.4 ± 1.3‰) ~150 μm from the centre, reflecting growth of the salmon in fresh water. In contrast, the bulk of the otolith from the hatchery raised salmon (Merced River Hatchery) reflects the marine and hatchery-feed $\delta^{34}S$ signal (+12.9 ± 1.5‰). Only the outermost 25 growth bands (~100 μm wide) of the otolith, formed during the 25 days between release of the salmon and its subsequent capture downstream, have the freshwater $\delta^{34}S$ value (–0.6 ± 2.0‰). Pooling the data for the two oto-

© 2002 NRC Canada

Fig. 3. Spatially resolved otolith $\delta^{34}S$ values for (*a*) a juvenile naturally spawned chinook salmon (*Oncorhynchus tshawytscha*) and (*b*) a recaptured juvenile hatchery raised chinook salmon. The data reveal an unambiguous difference in the distribution of $\delta^{34}S$ values across individual otoliths, correlated with salmon diet and life history. Elevated $\delta^{34}S$ values in the core of the wild salmon otolith, reflecting the marine S signal transmitted to the fish from the mother via the egg, decrease to values near zero once the hatchling begins to feed in the river. The hatchery raised salmon otolith exhibits uniformly high $\delta^{34}S$ values until release to freshwater (indicated by ▼; shaded area represents the period when the nutrition source is marine), 25 days before capture. The difference in $\delta^{34}S$ (13.33 ± 0.97‰ (2 SE)) between hatchery-feeding and river-feeding zones reflects dietary and muscle tissue $\delta^{34}S$. Distance from the centre of the otolith is related to days since first feeding based on visible daily banding. These data were collected on the Cameca IMS 1270 ion microprobe and replicated on the Cameca IMS 3f ion microprobe (see Methods). Error bars represent two standard errors.

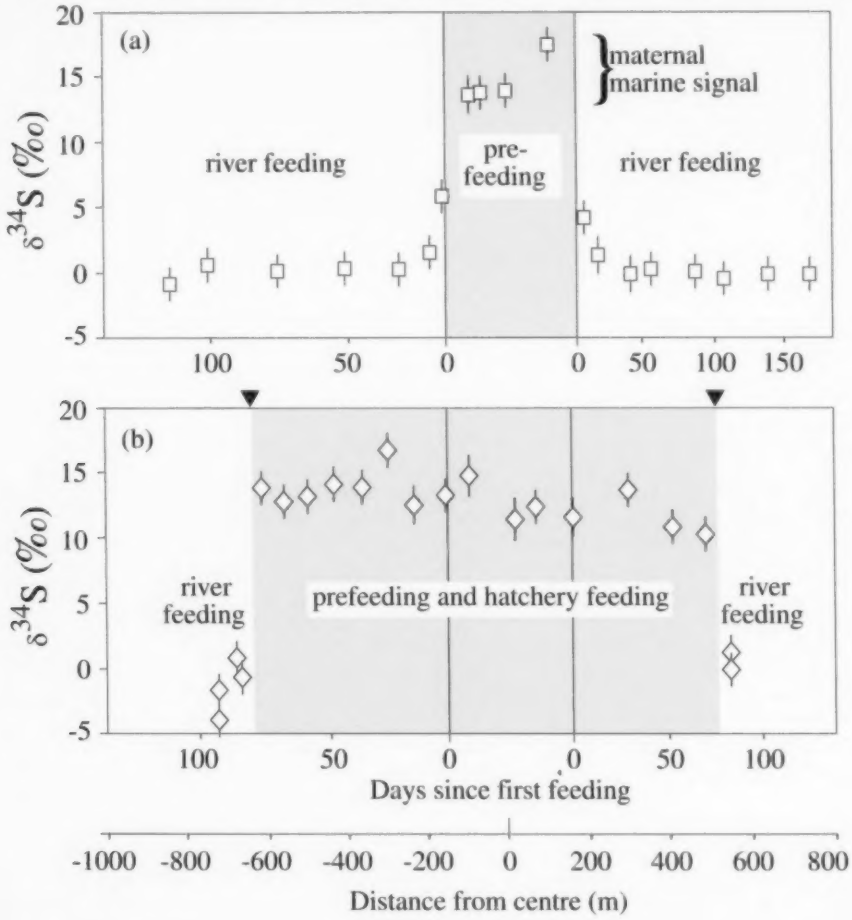

liths, the sulfur isotope composition of the hatchery-feeding and river-feeding zones differs by 13.33 ± 0.97‰ (2 SE, internal precision).

At our current levels of accuracy and precision, we are unable to distinguish between the marine $\delta^{34}S$ signal in the otolith core and the (largely) marine signal derived from the hatchery feed. We are also unable to determine whether the offset in otolith $\delta^{34}S$ relative to muscle $\delta^{34}S$ is an artifact of the mass-fractionation correction or whether it is an actual difference between otolith and muscle $\delta^{34}S$.

Based on the observations that (*i*) the spatial variation of otolith sulfur content is consistent with the spatial variation in otolith protein content and (*ii*) the sulfur content of an otolith is consistent with the total amount of sulfur in the proteins of the organic matrix, Kalish (1989) inferred that S-bearing amino acids in the organic matrix are the primary source of sulfur in otoliths. Otoliths are 0.2–10% protein, containing 1–3% cysteine and methionine (Degans et al. 1969), which are 26.5% and 21.5% S by weight, respectively (Kalish 1989). However, sulphated acid mucopolysaccharides have also been detected in otoliths (Asano and Mugiya 1993), and their abundance and provenance have not been studied. Mugiya and Iketsu (1987) demonstrated that inorganic sulfate in ambient water is incorporated into an otolith under experimental conditions, most likely in the organic matrix as sulphated acid mucopolysaccharides. Our sulfur concentration results for matched pairs of water samples exclude hatchery water sulfate as a significant source of

© 2002 NRC Canada

elevated $\delta^{34}S$ for the otolith hatchery-feeding zone, supporting the thesis that diet is the primary source of otolith sulfur under river and hatchery conditions.

Applications

Hatchery managers can use a number of physical, chemical, and thermal methods to tag hatchery fish, but not all hatchery fish are marked. In California's Sacramento – San Joaquin river system, only 10 to 20 percent of hatchery chinook salmon are tagged, primarily because of concerns about physiological stress to the fish and cost (compiled from personal communications with: Rich Bryant, Mokelumne River Hatchery, Clemments, Calif.; Mike Cozart, Merced River Hatchery, Snelling, Calif.; Anna Kastern, Feather River Hatchery, Oroville, Calif.; John Scott, Coleman Hatchery, Anderson, Calif.; Terry West, Nimbus Hatchery, Rancho Cordova, Calif.). In this river system, otolith $\delta^{34}S$ will be useful for identifying hatchery salmon. This method will also work in other systems where (*i*) fish are released from the hatchery after significant feeding and growth occur, (*ii*) the hatchery feed is marine-based, and (*iii*) exceptionally high $\delta^{34}S$ lithologies do not dominate the freshwater $\delta^{34}S$ signal (Nriagu et al. 1991; Thode 1991). Where hatchery raised fish can be identified, the timing of the release of fish to the river can also be determined.

More generally, in situ analyses of $\delta^{34}S$ can be used to reconstruct aspects of fish life history, given sufficient differences in $\delta^{34}S$ between geographic regions and food sources of interest. The presence of the marine $\delta^{34}S$ value in the centre of the otolith can be used to distinguish anadromous from resident populations. Regional differences in river $\delta^{34}S$ (Nriagu et al. 1991) should be useful for determining fish origin and reconstructing migration. For estuary or migratory fish, bulk tissue $\delta^{34}S$ provides time-averaged information on nutrition sources (Hesslein et al. 1993). By contrast, spatially resolved otolith $\delta^{34}S$ analyses provide a time-resolved record of dietary $\delta^{34}S$.

Acknowledgements

We thank the California Department of Fish and Game, the California Department of Water Resources, and the U.S. Fish and Wildlife Service for samples; C. Coath, M. Grove, and D. Phinney for ion probe technical assistance; R. Stewart for early discussions; C. Beeman, A. Kapuscinski, J. Kirchner, J. Stella, E. Volk, and an anonymous reviewer for comments on the manuscript; and T. Nguyen and E. Pickett for sample preparation. This work was supported financially by the California Department of Water Resources and the Institute for Geophysics and Planetary Physics, and performed under the auspices of the U.S. Department of Energy by Lawrence Livermore National Laboratory under contract No. W-7405-Eng-48. The UCLA ion probe facility is partially supported by a grant from the National Science Foundation Instrument Fund.

References

Asano, M., and Mugiya, Y. 1993. Biochemical and calcium-binding properties of water-soluble proteins isolated from otoliths of the tilapia, *Orechromis niloticus*. Comp. Biochem. Physiol. B, **104**: 201–205.

Campana, S.E. 1999. Chemistry and composition of fish otoliths: pathways, mechanisms and applications. Mar. Ecol. Prog. Ser. **188**: 263–297.

Degans, E.T., Deuser, W.G., and Haedrich, R.L. 1969. Molecular structure and composition of fish otoliths. Mar. Biol. **2**: 105–113.

Hesslein, R.H., Hallard, K.A., and Ramlal, P. 1993. Replacement of sulfur, carbon and nitrogen in tissue of growing broad whitefish (*Coregonus nasus*) in response to a change in diet traced by $\delta^{34}S$, $\delta^{13}C$, and $\delta^{15}N$. Can. J. Fish. Aquat. Sci. **50**: 2071–2076.

Kalish, J.M. 1989. Otolith microchemistry: validation of the effects of physiology, age and environment on otolith composition. J. Exp. Mar. Biol. Ecol. **132**: 151–178.

Krouse, H.R., Stewart, J.W.B., and Grinenko, V.A. 1991. Pedosphere and biosphere. *In* Stable isotopes: natural and anthropogenic sulphur in the environment. *Edited by* H.R. Krouse and V.A. Grinenko. John Wiley & Sons, New York. SCOPE, **43**: 267–306.

McKeegan, K.D., Leshin, L.A., Russell, S.S., and MacPherson, G.J. 1998. Oxygen isotopic abundances in calcium-aluminum-rich inclusions from ordinary chondrites: implications for nebular heterogeneity. Science (Washington, D.C.), **280**: 414–418.

Mugiya, Y., and Iketsu, H. 1987. Uptake of aspartic acid and sulfate by calcified tissues in goldfish and tilapia. Bull. Fac. Fish. Hokkaido Univ. **38**: 185–190.

Nriagu, J.O., Rees, C.E., Mekhtiyeva, V.L., Lein, A.Y., Fritz, P., Drimmie, R.J., Pankina, R.G., Robinson, B.W., and Krouse, H.R. 1991. Hydrosphere. *In* Stable isotopes: natural and anthropogenic sulphur in the environment. *Edited by* H.R. Krouse and V.A. Grinenko. John Wiley & Sons, New York. SCOPE, **43**: 177–265.

Peterson, B.J., Howarth, R.W., and Garritt, R.H. 1986. Sulfur and carbon isotopes as tracers of salt-marsh organic matter flow. Ecology, **67**: 865–874.

Thode, H.G. 1991. Sulfur isotopes in nature and the environment: an overview. *In* Stable isotopes: natural and anthropogenic sulphur in the environment. *Edited by* H.R. Krouse and V.A. Grinenko. John Wiley & Sons, New York. SCOPE, **43**: 1–26.

Weber, P.K. 2002. Geochemical markers in the otoliths of chinook salmon in the Sacramento-San Joaquin river system, California. Ph.D. thesis, University of California, Berkeley.

© 2002 NRC Canada

RAPID COMMUNICATION / COMMUNICATION RAPIDE

Throwing light on straddling stocks of *Illex argentinus*: assessing fishing intensity with satellite imagery

C.M. Waluda, P.N. Trathan, C.D. Elvidge, V.R. Hobson, and P.G. Rodhouse

Abstract: Marine fisheries provide around 20% of animal protein consumed by man worldwide, but ineffective management can lead to commercial extinction of exploited stocks. Fisheries that overlap nationally controlled and high seas waters cause particular problems, as few management data are available for the high seas. The Argentinean short-finned squid, *Illex argentinus*, exemplifies such a "straddling stock". Here we demonstrate that light emitted by fishing vessels to attract squid can be detected via remote-sensing. Unlike conventional fisheries data, which are restricted by political boundaries, satellite imagery can provide a synoptic view of fishing activity in both regulated and unregulated areas. By using known levels of fishing effort in Falkland Islands waters to calibrate the images, we are able to estimate effort levels on the high seas, providing a more comprehensive analysis of the overall impact of fishing on the stock. This innovative tool for quantifying fishing activity across management boundaries has wide-ranging applications to squid fisheries worldwide.

Résumé : La pêche en mer fournit environ 20 % des protéines animales consommées par les humains à l'échelle mondiale, mais la gestion inefficace de la pêche commerciale peut causer l'extinction des stocks exploités. Les pêches commerciales qui s'étendent à la fois sur des eaux territoriales et en haute mer posent des problèmes particuliers, puisqu'il existe peu de données sur la gestion en haute mer. L'encornet rouge argentin, *Illex argentinus*, est un exemple d'un tel stock en chevauchement. Nous démontrons que la lumière émise par les navires de pêche pour attirer les encornets peut être décelée par télédétection. Alors que les données de pêches conventionnelles sont restreintes par les frontières politiques, l'imagerie satellitaire peut produire une vue synoptique des activités de pêche tant dans les zones réglementées que dans celles qui ne le sont pas. En utilisant des taux connus d'effort de pêche dans les eaux autour des îles Falkland pour calibrer les images, il est possible d'estimer l'intensité de l'effort de pêche en haute mer et d'obtenir ainsi une analyse plus complète de l'impact global de la pêche sur le stock. Ce nouvel outil de quantification de l'activité de pêche au-delà des frontières des zones de gestion a des applications potentielles très variées pour la pêche aux calmars partout dans le monde.

[Traduit par la Rédaction]

Introduction

A "straddling stock" of a species of squid, or other living marine resource, is one that is harvested in both nationally controlled (exclusive economic zone; EEZ) and high-seas (international) waters. EEZs typically extend up to 200 miles from the coastline of a country, whereas the "high seas" incorporate the open ocean outside EEZ regions (Doulman 1995). Within an EEZ, fishing is usually regulated and managed by the relevant authorities, whereas on the high seas, fishing is generally unregulated. Fisheries data, on the number and size of vessels, catch rate, and effort spent fishing, are usually available for EEZ waters, but rarely for the high seas. Straddling stocks inhabit both areas, so the overall fishing impact on a stock is uncertain, potentially undermining long-term sustainable management methods for a fishery.

The winter spawning stock of *Illex argentinus* in the Southwest Atlantic is an important example of a highly mi-

Received 1 February 2002. Accepted 17 April 2002. Published on the NRC Research Press Web site at http://cjfas.nrc.ca on 26 April 2002.
J16741

C.M. Waluda,[1] **P.N. Trathan, and P.G. Rodhouse.** British Antarctic Survey, National Environmental Research Council, High Cross, Madingley Road, Cambridge CB3 0ET, U.K.
C.D. Elvidge. Office of the Director, NOAA National Geophysical Data Center, 325 Broadway, Boulder, CO 80303, U.S.A.
V.R. Hobson. University of Colorado, Cooperative Institute on Research in the Environmental Sciences, Boulder, CO 80303, U.S.A.

[1]Corresponding author (e-mail: clwa@bas.ac.uk).

 DOI: 10.1139/F02-049 © 2002 NRC Canada

gratory straddling stock. This stock is fished on the southern Patagonian shelf, south of 42°S (Haimovici et al. 1998). This is one of the widest shelf areas in the world, extending up to 500 miles from the coast of South America (Longhurst 1998). Here the stock straddles both the high seas and two nationally controlled areas: the Falkland Islands Conservation Zone (comprising the interim conservation and management zone (FICZ) and outer conservation zone (FOCZ); extending 150 and 200 miles from the coast, respectively), and the Argentinean EEZ (extending 200 miles from the coast).

In common with the majority of commercially exploited squid species, *I. argentinus* has a life span of one year, so the fishery exploits a new year-class at the start of each fishing season. Management of the stock in the Falkland Islands fishery is based on allowing sufficient numbers of squid to escape at the end of the fishing season to propagate the next generation, which then becomes the sole target of the fishery in the following year (Rosenberg et al. 1990). Fishing in Falkland Islands and Argentinean waters has been licensed since 1987 and 1993, respectively (Rosenberg et al. 1990; FIGFD 1997). Despite the strict regulations in place in these areas, squid must pass through unregulated high seas waters on their return migration to the spawning grounds. This may have significant consequences for stock conservation, as it exploits some of the squid that fishery management has allowed to escape for spawning.

As with most major squid fisheries targeting the family ommastrephidae (i.e., "short-finned" squid), *I. argentinus* is predominantly caught by jigging vessels, which fish at night. These operate using jigs—coloured lures armed with a crown of barbless hooks. A typical vessel deploys at least 2500 jigs simultaneously and may catch more than 30 tonnes of squid in one night (Rodhouse et al. 2001). To attract squid to the jigs, powerful incandescent lamps are used. These are usually 2 kW each and a typical vessel uses up to 300 kW for light production (Rodhouse et al. 2001). The emission of light from squid fishing vessels is detectable throughout the worlds oceans using imagery from the United States Air Force Defence Meteorological Satellite Program (DMSP) Operational Linescan System (OLS) (Rodhouse et al. 2001). This paper presents the first application of DMSP-OLS imagery, coupled with geographical information system (GIS) techniques to observe and quantify fishing activity throughout the whole of the Southwest Atlantic squid fishery, including the high seas area. We test the hypothesis that light emitted by vessels in Falkland Islands waters can be used to estimate the number of vessels fishing, and thus used to calculate the number of vessels fishing in high seas waters. This potentially provides a tool to better account for fishing across the range of the species distribution, which could improve estimates of the total catch of *I. argentinus*, and aid in stock management.

Materials and methods

Fishery description

A series of 15 single-pass visible-band images were obtained from the DMSP-OLS for the region shown in Fig. 1. Images (with a maximum pixel resolution of 2.7 km, or 0.008°) were selected for the period January–June 1999, corresponding to the period during which the Falkland Islands *I. argentinus* fishery was operational. All satellite passes were made between the hours of 2300 and 0100 local time. Each image was georeferenced and cloud-cleared using algorithms developed by the National Geophysical Data Center (NGDC), Boulder, Colo. (Elvidge et al. 1999). Using a GIS, images were overlaid with spatial data comprising the 200-m bathymetric contour and the boundaries of the Falkland Islands, high seas, and Argentinean fishery zones (see Fig. 1). The selected images were examined visually to describe the distribution of the fleet throughout the season, to relate fleet distribution to the known distribution and life-cycle of *I. argentinus*.

Calibration and estimation of vessel numbers

Data on fishing effort in Falkland Islands waters was obtained from the Falkland Islands Government Fisheries Department (FIGFD). Effort was measured as the number of vessels fishing in Falkland Islands waters for the night corresponding to each image. The number of illuminated pixels in the Falkland Islands and high seas regions were obtained from each image, using algorithms developed by the NGDC (Elvidge et al. 1999). Using fishery data from Falkland Islands waters and data on the number of illuminated pixels in this region, a regression equation relating the number of pixels and the number of vessels was derived (Fig. 2*a*). Using this calibration, the number of vessels fishing in high seas waters were estimated based on the number of illuminated pixels recorded in the high seas area. Additionally, the number of vessels fishing in Falkland Islands waters was calculated using the regression equation (Fig. 2*a*) to test the reliability of using the method.

Results

Fishery description

We provide a chronological series of satellite images from the 1999 fishing season in the Southwest Atlantic (Fig. 1). In January, fishing lights are observed towards the north of the region, specifically on the high seas at around 46°S (Fig. 1). In February, the fleet spreads southward along the shelf-break, moving into the Argentinean EEZ and the western part of the Falkland Islands Conservation Zone. In early April, fishing concentrations form to the north of the Falkland Islands and close to the shelf-break in all three regions. The fleet reaches the southwesterly point of its distribution (around 52°S, 61°W) by 24 April. Fishing continues to occur in Falkland Islands waters and along the shelf-break until early June, when the fleet disperses and moves northwest into the Argentinean EEZ and the high seas. By 17 June the Falklands fishery is closed, whereas vessels continue to operate in Argentinean and high seas waters north of 48°S. Of particular note is that portion of the shelf-edge that lies in the high seas area (between 45°S and 47°S), which supports substantial fishing activity throughout the season, as evidenced by the presence of fishing lights in each of the images shown (Fig. 1).

Calibration and estimation of vessel numbers

In Falkland Islands waters, the number of vessels operating in 1999 (over the period of the images presented in Fig. 1) ranged between 48 and 86 vessels (mean = 75 ± 13,

© 2002 NRC Canada

Fig. 1. Defence Meteorological Satellite Program (DMSP) images for the period 31 January to 17 June 1999. Yellow areas represent light emitted by fishing vessels and land is shaded in green. Images are overlaid with bathymetry (200-m isobath, shown in blue) and political regions (Argentinean exclusive economic zone (EEZ), top left; high seas, top right; Falkland Islands Conservation Zone, bottom of images, delimited in red).

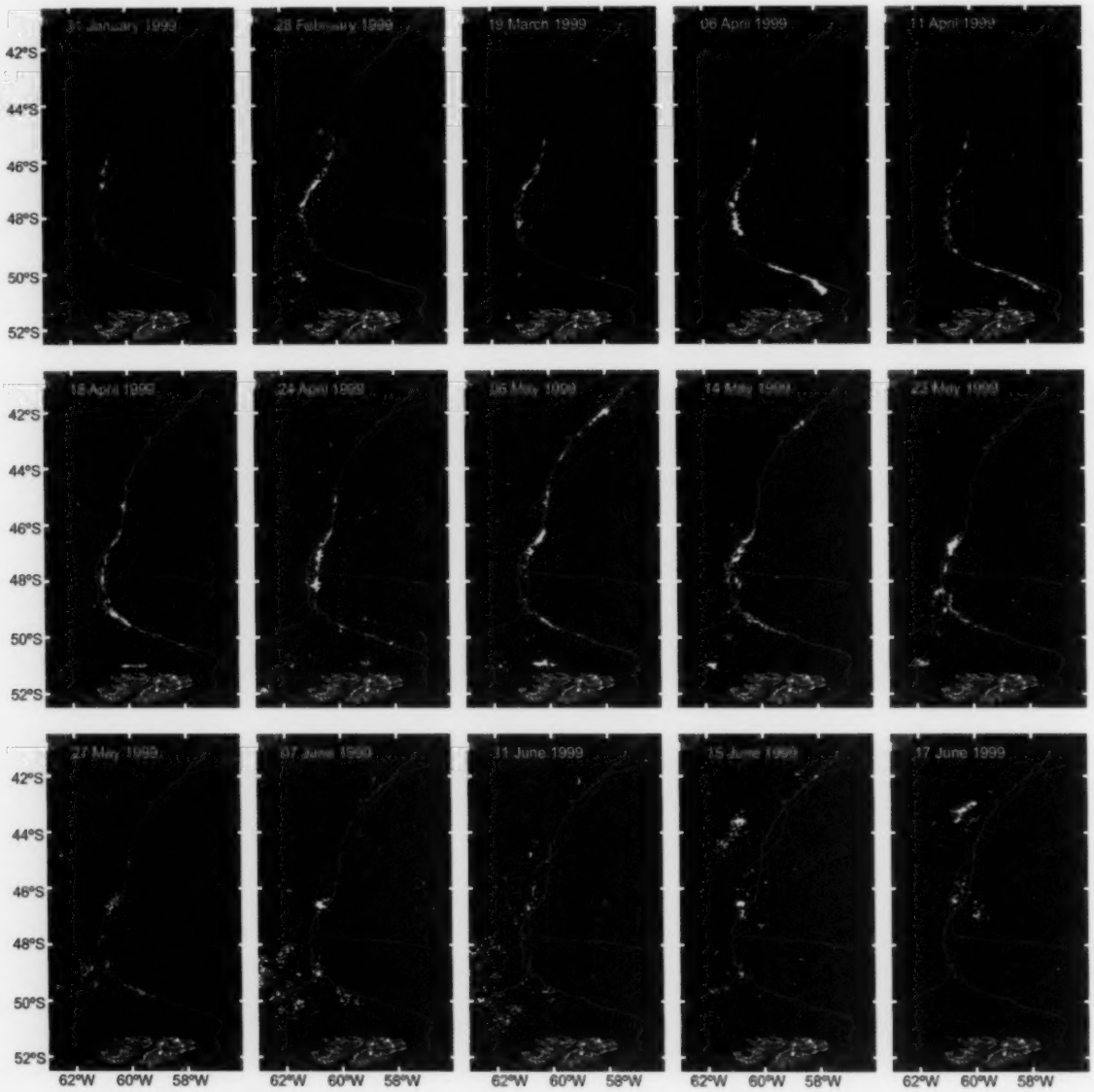

SD (standard deviation)) (Fig. 2*b*). Using the calibration given in Fig. 2*a* to indicate fishing intensity in terms of number of vessels fishing, we estimate that from January to June 1999 between 61 and 82 vessels (mean = 58 ± 6, SD) were operating in the high seas fishery (Fig. 2*b*). The estimated number of vessels present on the high seas varied throughout the season, and was less consistent than in Falkland Islands waters. During the 1999 season, the estimated number of vessels fishing on the high seas was usually lower than or equivalent to that in Falklands waters (Fig. 2*b*). However, after the close of the Falkland Islands fishery (15 June 1999), when a proportion of the surviving squid were migrating north along the shelf-edge to the spawning grounds, significant fishing continued on the high seas (an estimated 69 vessels on 17 June 1999; Figs. 1 and 2). Estimation of fishing in Falkland Islands waters suggested that between 61 and 95 vessels were fishing (mean = 75 ± 9, SD) during the period of the study (Fig. 2*b*). This suggests a discrepancy of between 2 and 15 vessels with a mean of 8 (i.e., within ±11%) between the observed and actual number of vessels fishing.

Discussion

Satellite images obtained from DMSP-OLS can be success-

© 2002 NRC Canada

Fig. 2. (*a*) The number of vessels fishing in Falkland Islands waters versus the number of illuminated pixels in corresponding Defence Meteorological Satellite Program (DMSP) images. Dates as in Fig. 1. (—) Regression line (R^2 = 0.51); (- – -) 95% confidence intervals. (Regression equation: $N_{vessels}$ = 55.3 + 0.0101 × $N_{lit\ pixels}$; n = 13; $F_{[1,12]}$ = 11.4; P = 0.006). (*b*) Number of fishing vessels in Falkland Islands waters (observed and estimated) and high-seas waters (estimated), Southwest Atlantic. Dates are given as days from 1 January 1999, corresponding to images in Fig. 1. Observed Falkland Islands data (closed circles, solid lines) obtained from Falkland Islands Government Fisheries Department. Estimated data from: the high seas (open circles, dashed line) and the Falkland Islands (triangles, dashed-dotted line) calculated using the regression equation given above.

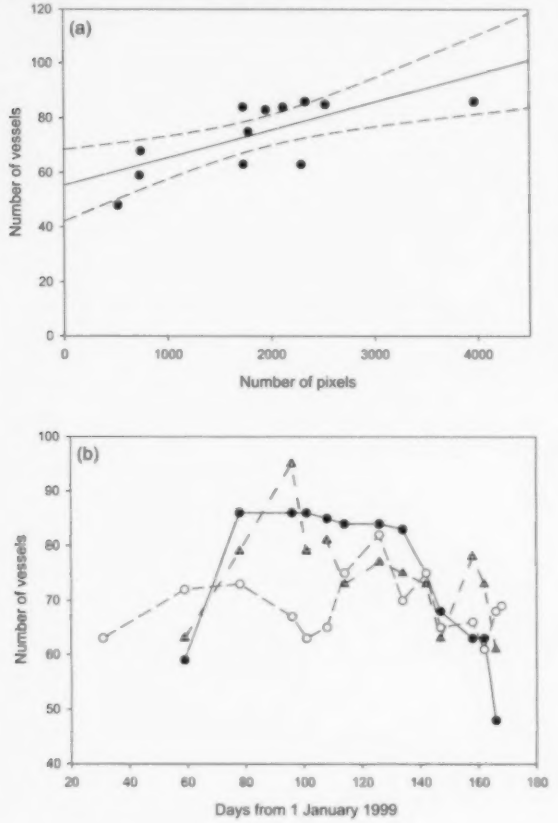

fully used to observe the distribution of the fleet throughout the fishing season, and it is possible to interpret the fleet distribution in light of the known life cycle of *I. argentinus*. In the austral winter, before the fishing season begins, squid eggs hatch over the northern Patagonian shelf (Haimovici et al. 1998). During late winter, newly hatched "paralarval" squid are most commonly found off the Rio de la Plata in latitudes of 32°S to 39°S (Brunetti and Ivanovic 1992; Haimovici et al. 1998). Early in the season (January–March), the fishery follows feeding migrations of squid travelling south from the nursery areas of the northern Patagonian shelf (Haimovici et al. 1998). This can be clearly seen in the southerly progress of fishing lights along the shelf-edge, with the location of fishing vessels closely tracking the shelf-break (200-m bathymetric contour).

The largest catches are made mid-season (April–May) when the fishery targets feeding aggregations of squid over the southern Patagonian shelf, particularly near the Falkland Islands (Rodhouse et al. 1995). Late in the season (June), the fleet moves northwards, following squid as they leave Falkland Islands waters on their return migration to the northern Patagonian shelf. Here, squid spawn and die, completing their one-year life cycle (Rodhouse et al. 1995; Haimovici et al. 1998). It is clear that the distribution of the fleet closely tracks the adult phase of the annual migratory cycle. We have shown that the high seas region supports substantial fishing throughout the season, which has significant consequences for the management of the stock as a whole.

The management of the Falkland Islands fishery has been arguably among the most successful in the world (Pierce and Guerra 1994). However, despite the strict regulations in Falkland Island (and Argentinean) waters, *I. argentinus* must pass through unregulated high seas fishing areas during their northerly migration. Total escapement levels set by management authorities does include an element associated with unregulated fishing during migration (D.J. Agnew, Renewable Resources Assessment Group, Imperial College, London, U.K. personal communication), and the use of DMSP-OLS imagery potentially provides a tool for enhancing management procedures to better account for the exploitation of the stock in the high seas region. The use of a linear regression model provides a simple method that has been shown to estimate the number of vessels fishing in the Falkland Islands region to within around 11% of the actual number of vessels. Extrapolating this to the high seas suggests that the estimates of fishing are likely to be reasonable, and useful during those periods where data on high seas fishing are not available.

The regression equation indicates that there was a "background level" of around 55 vessels. This may relate to the range of data used and the fact that the regression may not be linear. In addition, it is not always possible to view individual vessels, as the light signatures of vessels fishing closely together tend to merge into one continuous lit area. This may result in an underestimate of the numbers of vessels fishing. To address this problem, further work will focus on improving the calibration between lit pixel and vessel numbers by using high-resolution data on specific vessel locations. In addition, the inclusion of additional satellite images, and more rigorous statistical analyses are required to provide a more precise estimate of high seas fishing and to further account for noise caused by factors such as high cloud, glare, and atmospheric scintillation.

The work presented here demonstrates an innovative method for estimating the number of vessels fishing on a highly migratory squid stock that straddles several political regions. This technique is transferable to other squid fisheries that operate using lights, for example, in the Sea of Japan, the South China Sea, the Gulf of Thailand, and the eastern Pacific (Rodhouse et al. 2001). In terms of global productivity, squid fisheries are becoming increasingly important, particularly with the decline in catches from many traditional finfisheries (Caddy and Rodhouse 1998).

© 2002 NRC Canada

Using satellite imagery to monitor the exploitation of straddling stocks across their entire distributional range has the potential to contribute to the sustainable management of stocks, and hence maintain the wider ecosystem structure. *Illex argentinus* is an important link in the food web of the southern Patagonian shelf as both a predator and a prey species (Haimovici et al. 1998). The Patagonian shelf-edge is an important feeding area for many higher predators, such as elephant seals, albatrosses, and petrels (see, e.g., Grémillet et al. 2000). These species forage in the shelf-break region and are dependent on the sustainable management of the ecosystem. Proper management of *I. argentinus* is therefore critical not only for sustainable exploitation, but also for maintaining ecological balance.

Acknowledgements

Support from the British Antarctic Survey (Natural Environmental Research Council) is gratefully acknowledged. We would like to thank J. Barton, Falkland Islands Fisheries Department, for supplying the fishery data, and for helpful comments on the manuscript. We thank D.J. Agnew, Renewable Resources Assessment Group (RRAG), Imperial College, for valuable discussions and input to this research, and L.S. Peck and A.L. George for useful comments on an earlier draft. This research forms part of an Independent Project awarded to P.G.R. and funded under the British Antarctic Survey's Antarctic Science in the Global Context Programme.

References

Brunetti, N.E., and Ivanovic, M.L. 1992. Distribution and abundance of early life stages of squid (*Illex argentinus*) in the south-west Atlantic. ICES J. Mar. Sci. **49**: 175–183.

Caddy, J.F., and Rodhouse, P.G. 1998. Cephalopod and groundfish landings: evidence for ecological change in global fisheries. Rev. Fish Biol. Fish. **8**: 1–14.

Doulman, D.J. 1995. Structure and process of the 1993–1995 United Nations conference on straddling fish stocks and highly migratory fish stocks. FAO Fish. Circ. No. 898.

Elvidge, C.D., Baugh, K.E., Dietz, J.B., Bland, T., Sutton, P.C., and Kroehl, H.W. 1999. Radiance calibration of DMSP-OLS low-light imaging data of human settlements. Remote Sens. Environ. **68**: 77–88.

FIGFD (Falkland Islands Government Fisheries Department). 1997. Fisheries Statistics, Vol. 1. Falkland Islands Government Printing Office, Stanley, Falkland Islands.

Grémillet, D., Wilson, R.P., Wanless, S., and Chater, T. 2000. Black-browed albatrosses, international fisheries and the Patagonian Shelf. Mar. Ecol. Prog. Ser. **195**: 269–280.

Haimovici, M., Brunetti, N.E., Rodhouse, P.G., Csirke, J., and Leta, R.H. 1998. *Illex argentinus*. *In* Squid recruitment dynamics. *Edited by* P.G. Rodhouse, E.G. Dawe, and R.K. O'Dor. FAO, Rome. pp. 27–58.

Longhurst, A.R. 1998. Ecological Geography of the Sea. Academic Press, San Diego.

Pierce, G.J., and Guerra, A. 1994. Stock assessment methods used for cephalopod fisheries. Fish. Res. **21**: 255–285.

Rodhouse, P.G., Barton, J., Hatfield, E.M.C., and Symon, C. 1995. *Illex argentinus*: life cycle, population structure and fishery. ICES Mar. Sci. Symp. **199**: 425–432.

Rodhouse, P.G., Elvidge, C.D., and Trathan, P.N. 2001. Remote sensing of the global light-fishing fleet: an analysis of interactions with oceanography, other fisheries and predators. Adv. Mar. Biol. **39**: 261–303.

Rosenberg, A.A., Kirkwood, G.P., Crombie, J.A., and Beddington, J.R. 1990. The assessment of stocks of annual squid species. Fish. Res. **8**: 335–350.

© 2002 NRC Canada

RAPID COMMUNICATION / COMMUNICATION RAPIDE

Estimating and testing non-additivity in fishing mortality: implications for detecting a fisheries collapse

Ransom A. Myers and Terrance J. Quinn II

Abstract: Common in many fisheries collapses is a disproportionate increase in fishing mortality at younger ages. One mechanism by which this increase could occur is sufficient depletion of the population at older ages due to strong overfishing, which leads to targeting of younger fish. Thus, it is essential for assessments to estimate and test for a change in selectivity in the fishery. We introduce a simple and powerful approach based upon Tukey's one degree of freedom test for non-additivity. This approach can be applied within any statistical age-structured population model that estimates selectivity. We illustrate the approach with data from Atlantic cod (*Gadus morhua*) from St. Pierre Bank, Canada. The results show significant non-additivity in fishing mortality that translates into an increase in selectivity on younger ages when fishing mortality is high. This approach also can be applied to the output of an age-structured model that assumes catch-at-age is known without error or to any survey or catch-per-unit-effort data for which estimates of abundance are made by year and age. We believe that this approach should be routinely applied in assessments, particularly when overfishing has led to depletion of the overall population or to truncation of the age structure.

Résumé : On observe souvent dans les cas d'effondrement de stocks de poissons une augmentation disproportionnée de la mortalité des jeunes due à la pêche. Un mécanisme qui peut expliquer ce phénomène est une réduction telle de la densité des poissons plus âgés dans la population à cause de la forte surpêche que les poissons plus jeunes deviennent ciblés. Il est donc essentiel dans les évaluations de stocks d'estimer et de tester les changements dans la sélectivité de la pêche. Nous présentons ici une méthode simple et puissante, basée sur le test de non-additivité de Tukey avec un degré de liberté, qui peut s'appliquer à tout modèle statistique de population qui est structuré d'après l'âge et qui estime la sélectivité. En exemple, nous l'appliquons à des données sur la morue franche (*Gadus morhua*) du banc de St-Pierre, Canada. Les résultats révèlent une non-additivité significative de la mortalité due à la pêche qui se reflète dans la sélectivité accrue des poissons de bas âge lorsque la mortalité due à la pêche est élevée. La méthode peut aussi s'appliquer aux données de sortie de modèles structurés d'après l'âge qui assument que les captures spécifiques aux différents âges sont connues sans erreur ou à tout inventaire ou série de données de captures par unité d'effort dans lesquels l'estimation d'abondance se fait pour chaque année et chaque âge. Cette approche devrait être appliquée de façon systématique aux évaluations de stocks lorsque la surpêche réduit la population générale ou produit une structure d'âges tronquée.

[Traduit par la Rédaction]

Introduction

Most of the spectacular, rapid collapses of fish populations due to overfishing have shared a characteristic change in fishery selectivity: a reduction of the mean age of selectivity by the fishery as the population collapsed. This is evident in the collapse of herring (*Clupea* spp.) stocks in the North Pacific and the North Atlantic, and the cod (*Gadus morhua*) stocks in the Northwest Atlantic (Myers et al. 1997). This process of targeting younger fish occurs across a wide range of gear types.

A good illustration of this phenomenon is the collapse of the walleye (*Stizostedion vitreum*) in Lake Erie (Shuter et al. 1979) (Fig. 1*a*). The population plummeted in the 1950s as overall fishing mortality increased. More interestingly, the selectivity pattern changed, because fishers harvested younger fish as older fish were depleted (Fig. 1*b*). First the relative fishing mortality on three year olds increased, and later the relative fishing mortality on two year olds increased.

This change in targeting is a key factor in a rapid collapse of a population, because harvesting at a sustainable rate can, with a small change in age of selectivity, become unsustainable, leading to commercial extinction of the stock (Myers

Received 14 March 2002. Accepted 23 April 2002. Published on the NRC Research Press Web site at http://cjfas.nrc.ca on 1 May 2002.
J16803

R.A Myers.[1] Department of Biology, Dalhousie University, Halifax, NS B3H 4J1, Canada.
T.J. Quinn II. Juneau Center, School of Fisheries and Ocean Sciences, 11120 Glacier Highway, Juneau, AK 99801-8677, U.S.A.

[1]Corresponding author (e-mail: ransom.myers@dal.ca).

 DOI: 10.1139/F02-048 © 2002 NRC Canada

Fig. 1. (*a*) The spawner biomass (average catch per trap set of mature fish), instantaneous adult fishing mortality (year^{-1}), and (*b*) the ratio of juvenile to adult fishing mortality for walleye (*Stizostedion vitreum*) in the east and central Lake Erie. The ratio of juvenile to adult fishing mortality is given as the ratio of 3 year olds to the average fishing mortality on adults (ages 4+), and the ratio of fishing mortality on 2 year olds to the adult fishing mortality.

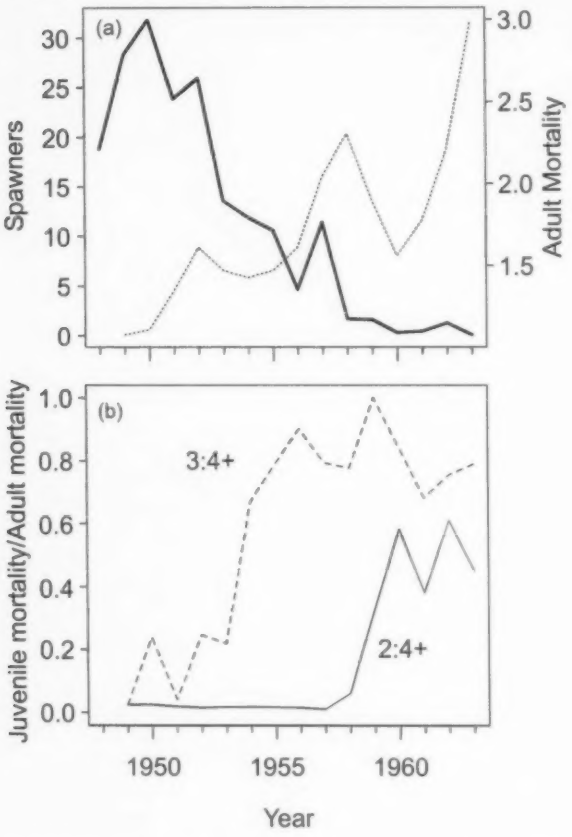

and Mertz 1998). This rapid collapse can occur in any fishery if the mean age of selectivity to the fishery decreases below the mean age of maturity, because fish have a relatively small maximum reproductive rate in spite of their high fecundity (Myers et al. 1999). Attempts to harvest a constant quota from a declining stock are especially apt to cause increases in selectivity of younger fish (through alteration of gear or changes in fishing grounds when there is spatial segregation of fish by age). Risk evaluations based on simulations of population trajectories apparently never include this phenomenon, despite the likelihood of its occurrence during stock declines. Realistic evaluations of the risk incurred by employment of a given strategy should not ignore this effect.

Furthermore, statistical age-structured assessment models (Quinn and Deriso 1999) often make the assumption that fishing mortality is separable into age and year effects. That is, after log transformation, fishing mortality can be considered the sum of a year effect and an age effect.

One solution is to make selectivity (or fishing mortality) a random walk process, in which selectivity in one year is equal to that of the previous year plus a random error (Gudmundsson 1994; Ianelli 1996). A large number of additional parameters for these errors must be included, thereby increasing the complexity of the model greatly. A simpler solution would be advantageous in terms of model parsimony.

The purpose of this paper is to provide a simple and powerful approach to estimate and test for an increase in gear selectivity at younger ages associated with increased fishing mortality that can be easily incorporated into almost any age-structured assessment model. The statistician John Tukey developed such a solution for two-way tables in the analysis of variance (ANOVA) more than 50 years ago!

Approach

Fishing mortality is often assumed to be separable into an effect of age (the selectivity of the fishery) and an effect of year (the intensity of the fishing mortality) (Fournier and Archibald 1982; Quinn and Deriso 1999). If the fishing mortality in year y on age a is denoted $F_{y,a}$, then the separability assumption is that $F_{y,a} = E_y S_a$, where E_y is the year effect and S_a is the age effect (Quinn and Deriso 1999, section 8.2.5). Usually S_a is set to 1 for those ages of maximal selectivity, so that E_y is the full-recruitment fishing mortality.

If we log transform fishing mortality, and let lower case letters correspond to logarithms (e.g., $\log S_a = s_a$), we can write this multiplicative relationship as an additive relationship, i.e., $f_{y,a} = e_y + s_a$. We are interested in testing a particular systematic departure from this pattern because we expect that as total fishing mortality goes up that s_a should increase for younger ages.

Tukey (1949) considered a slightly nonlinear function as an alternative to the additive form and showed that a suitable approximation for one degree of freedom for non-additivity (abbreviated ODOFFNA) involves the crossproduct of the deviations of the additive terms from their mean values. In our situation, the log-transformed fishing mortality should display a simple form of non-additivity that can be described by an addtional parameter, or

$$(1) \qquad f_{y,a} = e_y + s_a + \gamma \tilde{e}_y \tilde{s}_a$$

where γ is Tukey's (1949) ODOFFNA parameter and the tildes (~) over the letters denote deviations from the means of the effects. γ can be thought of as a simple control on the age-specific selectivity as the average fishing mortality increases. For ease in implementation, we reparameterize eq. 1 as

$$(2) \qquad f_{y,a} = \mu + \tilde{e}_y + \tilde{s}_a + \gamma \tilde{e}_y \tilde{s}_a$$

where μ is the average log fishing mortality across ages and years. The year and age deviations are implicitly assumed to sum to 0 over their respective subscripts. Conversion of eq. 2 back to original units results in

$$(3) \qquad F_{y,a} = \overline{F}\, \tilde{E}_y\, \tilde{S}_a^{1+\gamma \tilde{e}_y}$$

in which $\overline{F} = \exp(\mu)$. The latter term in eq. 3 is age and year dependent, in contrast to the additive model in which it is simply $\tilde{S}_a$. By varying γ, one can produce non-additive patterns that range from nearly additive (when $\gamma = 0$) to those in which the trends in selectivity are completely opposite over

© 2002 NRC Canada

time for some ages. Which patterns occur depends on the magnitudes and signs of the deviations and γ.

The implementation of the ODOFFNA parameter is straightforward. Separate log fishing mortality parameters are used for each fleet for a block of years (Quinn and Deriso 1999). Then, the ODOFFNA term is added using eq. 3. Parameters μ, $\tilde{e}_y$, $\tilde{s}_a$, and γ are estimated jointly with other model parameters for abundance, constraining the age and year deviations to sum to 0. A likelihood ratio test with the two alternative models then indicates whether non-additivity is present: $F = (RSS_a - RSS_{na})/RMS_{na}$, where RSS is residual sum of squares, RMS is residual mean square, and subscripts a and na are used for the additive and non-additive models, respectively. This ODOFFNA test is an F test with one degree of freedom in the numerator and the residual degrees of freedom for the non-additive model in the denominator (Quinn and Deriso 1999, p. 152).

Also, it is often useful to examine indices of mortality from research survey estimates of relative abundance at age. Mortality can be estimated as $\hat{z}_{y,a} = -\log(r_{y+1,a+1}/r_{y,a})$, where $r_{y,a}$ is the estimate of abundance in year y at age a. The variable $\hat{z}_{y,a}$ can again be easily analyzed in a two-way ANOVA with ODOFFNA. A similar analysis can be carried out with the catch-at-age data. Two-way plots can be used to visually assess the non-additivity (Morgenthaler and Tukey 2001).

Illustration

So that others can easily try out and evaluate this approach, we provide a simple example that is programmed in a Microsoft Excel spreadsheet (go to website fish.dal.ca/~myers/papers.html) on Atlantic cod (*Gadus morhua*) from St. Pierre Bank, south of Newfoundland (the stock designated as 3Ps in the notation of the Northwest Atlantic Fisheries Organization (NAFO)). This is one of the cod stocks in eastern Canada that collapsed in the early 1990s; the data set is discussed in some detail in (Myers et al. 1997). The data consist of catch-at-age data from 1978 to 1993 for ages 3 to 10+, the latter being a plus group. The Canadian research trawl survey was used for the same years, but also included age 2. Natural mortality is assumed to be 0.2 for all ages except 0.4 for age 2. A typical lognormal analysis is made with the objective function

$$(4)\qquad RSS = \sum_y \sum_a (c'_{y,a} - c_{y,a})^2 + \sum_y \sum_a (\log I'_{y,a} - \log Q_a N_{y,a})^2$$

where c is log catch, N is abundance, I is the research survey index, Q is the catchability of the survey as a function only of age, and a prime denotes a data value. Full-recruitment selectivity of the catch was assumed constant for ages 6 to 10+. All parameters were estimated on a log scale and we gave equal weight to the two sums of squares for this example. This example was kept as simple as possible to focus on non-additivity; a full assessment would include other evaluations, such as correlated errors among ages in a year (Myers and Cadigan 1995) or alternative error structure (Cadigan and Myers 2001).

The results show that estimated abundance peaked for the presented time series in 1987 and decreased rapidly shortly thereafter (Fig. 2*a*). There was an overall increase in estimated fishing mortality onward from 1984 until the fishery was partially closed in 1993 (Fig. 2*a*). These trends were the same for the additive and non-additive models. The estimates of selectivity on the younger ages from the non-additive model increase rapidly as shown by the increasing ratios in Fig. 2*b*. The estimates of fishing mortality from the additive model are proportional across year by design. The two values on the right-hand side of Fig. 2*b* with the largest positive deviation are for the two years with highest fishing mortality, 1991 and 1992. The RSS drops from 63 to 61, a highly significant difference (F test, $P = 0.008$). Thus, the estimate $\hat{\gamma} = -0.35$ is significantly different from 0; therefore, we conclude that fishing mortality is non-additive. This example demonstrates the shift in fishing mortality to younger fish as the stock declines; however, the extent is underestimated because of discarding (Myers et al. 1997).

We also applied the ODOFFNA analysis for just the catch-at-age data. We found a very large difference in the fit of the additive model for the log catch ratios ($c_{y,a} - c_{y+1,a+1}$) compared with the ODOFFNA model (F test, $P < 0.001$). This analysis shows that a change of selectivity can be detected for this stock even without the research surveys. A similar analysis of the survey data failed to show significant non-additivity, presumably because the survey variability at age was too high.

We conducted a sensitivity study of the ODOFFNA parameter γ on the estimates of population parameters from the age-structured model. We selected various values of γ between –1 and 1 for illustration (γ is not confined to this range), and refitted the model each time. Detailed results are given in the spreadsheet. Negative values of γ generally produced better fits to the catch data and worse fits to the survey data than positive values, with the best overall fit obviously occurring at the estimated value of –0.35.

Estimates of abundance and year deviations in the early years, age deviations in all years, and survey catchabilities were not sensitive to the value of γ. Negative values of γ generally produced markedly lower estimates of the year deviations as well as resultant higher estimates of age-specific selectivity and fishing mortality at younger ages in the most recent years than did the additive model ($\gamma = 0$). However, the opposite occurred in some years, like 1993. Positive values of γ produced both lower and higher estimates of the year deviations than did the additive model. Therefore, the effect of γ is complex and not monotonic, depending on the interactions among the data components and population parameters.

The resulting effect of γ on abundance in the most recent year differs among ages (Fig. 2*c*). Negative values of γ are associated with lower values of abundance than in the additive model, whereas no clear pattern emerges with positive values of γ. Nevertheless, the implication is that if significant non-additivity in fishing mortality occurs as in this example, then there may be a large overestimation of abundance and a corresponding inability to detect the imminent collapse of a fish population.

Discussion

Fishery selectivity can change for a variety of reasons.

© 2002 NRC Canada

Fig. 2. (*a*) Estimated abundance (solid line) and fishing mortality (dashed line) of older (age-6+) cod (*Gadus morhua*) on St. Pierre Bank. (*b*) Results from the additive (lines) and non-additive models (symbols) showing the ratio of fishing mortality for 1978 to 1993 for ages 3 (△), 4 (◇), and 5 (□) to the fully recruited fishing mortality, i.e., for ages 6 and above, as a function of the fully recruited fishing mortality. The additive results for the three younger ages are the three flat horizontal lines nearest the corresponding symbols. (*c*) Ratio of abundance for the non-additive model to that for the additive model ($\gamma = 0$) as a function of ODOFFNA parameter γ for ages 2 to 5 in 1993.

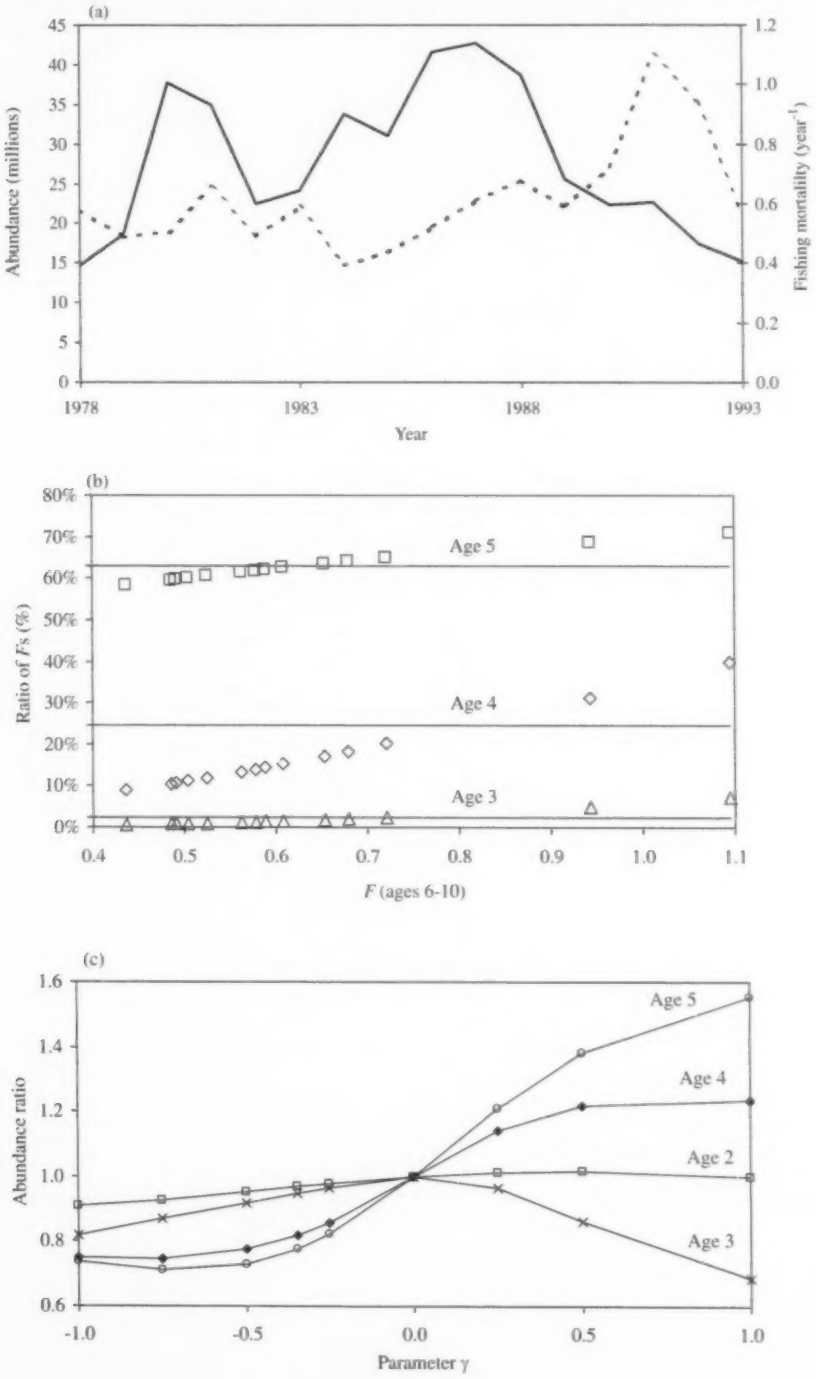

© 2002 NRC Canada

First, regulatory changes such as gear restrictions or time-area closures can influence the catching properties of the gear or the availability of fish to be caught. Second, environmental changes can alter the spatial distribution of fish or susceptibility of fish to the gear. More pernicious is the mechanism discussed in this paper: Overfishing leads to depletion of the population that is not recognized in the assessment, catch remains constant because of increased effort and changes in selectivity, and there is no evidence to indicate that reduction in fishing is needed. This leads to increased overfishing; harvesters increasingly target younger fish to accommodate their catch needs. Density-dependent growth would exacerbate this problem.

Assessing changes in selectivity is often not easy owing to measurement error in data sources and because alternative hypotheses may appear equally likely. The random walk model has been a useful approach for modeling changes in selectivity over a long time period, but it is not clear whether it would be able to detect recent changes in selectivity accompanying overfishing. The ODOFFNA approach may provide a parsimonious approach suitable for some assessments, but cannot deal with autocorrelation in selectivity like the random walk model can—likely an important phenomenon. However, the ODOFFNA approach can be implemented with a modicum of extra work, so we recommend its routine application. In the ODOFFNA approach, only a single degree of freedom is used to represent non-additivity, which limits the range of behaviour allowed. We encourage researchers to explore the sensitivity of their models to different values of γ to ensure that the results are plausible.

The ODOFFNA approach can easily be incorporated into other types of age-structured assessments. In many formulations of age-structured models, the catch-at-age is assumed to be known without error and the fishing mortality at year and age matrix is estimated separately with no or limited constraints. For these models, it is a simple matter to output the estimated fishing mortality at age, take logarithms, analyze it with a two-way ANOVA, and apply the ODOFFNA test.

Unobserved discarding may increase for younger fish as the stock collapses (Myers et al. 1997), as well as selectivity. For this reason we recommend that the ODOFFNA test be applied to any survey data as well as in the catch-at-age model, where discarding may not be well estimated. Such discarding could be confounded with an increase in natural mortality of juveniles. The ODOFFNA test on survey data detects changes in total mortality, whether due to changes in selectivity or in natural mortality. Therefore, auxiliary information would be necessary to attribute a significant test result to selectivity, natural mortality, or both.

Acknowledgments

We thank S. Morgenthaler for an inspiring seminar and J. Baum, C. Field, and S. Morgenthaler for helpful discussions. We appreciate the advice from two very helpful referees.

References

Cadigan, N.G., and Myers, R.A. 2001. A comparison of gamma and lognormal maximum likelihood estimators in a sequential population analysis. Can. J. Fish. Aquat. Sci. **58**: 560–567.

Fournier, D.A., and Archibald, C. 1982. A general theory for analyzing catch at age data. Can. J. Fish. Aquat. Sci. **39**: 1195–1207.

Gudmundsson, G. 1994. Time series analysis of catch-at-age observations. Appl. Stat. **43**: 117–126.

Ianelli, J. 1996. An alternative stock assessment model of the eastern Bering Sea pollock fishery. *In* Stock assessment and fishery evaluation report for the groundfish resources of the Bering Sea / Aleutian Islands regions, November 1996. North Pacific Fisheries Management Council, Anchorage, Alaska. pp. 81–104.

Morgenthaler, S., and Tukey, J.W. 2001. Multipolishing and two-way plots. Metrika, **53**: 245–2.

Myers, R.A., and Cadigan, N.G. 1995. Statistical analysis of catch-at-age data with correlated errors. Can. J. Fish. Aquat. Sci. **52**: 1265–1273.

Myers, R.A., and Mertz, G. 1998. The limits of exploitation: a precautionary approach. Ecol. Appl. **8**(Suppl. 1): S165–S169.

Myers, R.A., Hutchings, J.A., and Barrowman, N.J. 1997. Why do fish stocks collapse? The example of cod in Canada. Ecol. Appl. **7**: 91–106.

Myers, R.A., Bowen, K.G., and Barrowman, N.J. 1999. The maximum reproductive rate of fish at low population sizes. Can. J. Fish. Aquat. Sci. **56**: 2404–2419.

Quinn, T.J., II, and Deriso, R.B. 1999. Quantitative fish dynamics. Oxford University Press, New York.

Shuter, B.J., Koonce, J.F., and Regier, H.A. 1979. Modeling the Western Lake Erie walleye population: a feasibility study. Gt. Lakes Fish. Comm. Tech. Rep. No. 32.

Tukey, J.W. 1949. One degree of freedom for non-additivity. Biometrics, **5**: 232–242.

© 2002 NRC Canada

Predation on marine-phase Atlantic salmon (*Salmo salar*) by gannets (*Morus bassanus*) in the Northwest Atlantic

W.A. Montevecchi, D.K. Cairns, and R.A. Myers

Abstract: Predation on Atlantic salmon (*Salmo salar*) has been recorded in rivers and estuaries, but there is little documentation of predation at sea. Prey landed by gannets (*Morus bassanus*) over 24 years in a large colony off northeast Newfoundland included small proportions of post-smolt Atlantic salmon. Before 1990, when shifts in oceanographic conditions and pelagic food webs occurred in the Labrador Sea, post-smolts, on average, made up 0.29% of estimated intake by gannets during August 1977–1989. In contrast, during the 1990s, this estimate increased to 2.53%, peaking at 6.37% in 1993. Model estimates with wide error margins projected that gannets consumed a mean of 1.6 t and 19.2 t of post-smolts during August 1977–1989 and 1990–2000, respectively, making up 0.22% and 2.70% of estimated North American post-smolt biomass during these periods. The migratory routes of post-smolt Atlantic salmon pass through the foraging ranges of gannet colonies, but limited sampling at colonies other than Funk has not revealed salmon in gannet diets. Sampling seabird diets is an economic, biological means of investigating the ecology and natural mortality of Atlantic salmon. Spatial and temporal expansion of this sampling would enhance its oceanographic context and reduce uncertainty associated with estimates of predation by seabirds.

Résumé : La prédation exercée sur le saumon de l'Atlantique (*Samo salar*) a été étudiée dans les rivières et les estuaires, mais elle reste mal connue en mer. Les proies capturées par les fous de Bassan (*Morus bassanus*) d'une grande colonie au large de la côte nord-est de Terre-Neuve au cours d'une période de 24 ans incluent une faible proportion de saumons de l'Atlantique de stade post-saumoneau. Avant 1990, lorsque les changements des conditions océaniques et des réseaux alimentaires pélagiques se sont produits, les post-saumoneaux représentaient en moyenne 0,29% de la valeur estimée du régime alimentaire des fous durant la période d'août 1977–1989. En revanche, durant les années 1990, l'estimation a augmenté à 2,53 % pour atteindre un sommet de 6,37 % en 1993. Les estimations d'un modèle avec de grandes marges d'erreur indiquent que les fous ont consommé en moyenne 1,6 t de saumons au stade post-saumoneau durant la période d'août 1977–1989 et 19,2 t en 1990–2000, quantités qui représentent respectivement 0,22 % et 2,70 % de la biomasse estimée des saumons de ce stade en Amérique du Nord à ces périodes. Les routes migratoires des saumons de l'Atlantique au stade post-saumoneau traversent les territoires d'alimentation des colonies de fous, mais un échantillonnage restreint des colonies autres que celle de Funk n'indique pas la présence de saumons dans le régime alimentaire des fous. L'échantillonnage des régimes alimentaires des oiseaux marins est une méthode biologique économique d'étudier l'écologie et la mortalité naturelle des saumons de l'Atlantique. En étendant cet échantillonnage dans l'espace et le temps, on élargirait le contexte océanique de l'étude et on réduirait l'incertitude associée aux estimations de prédation par les oiseaux marins.

[Traduit par la Rédaction]

Introduction

Numbers of adult Atlantic salmon (*Salmo salar*) of North American origin have been declining since the early 1980s, a trend that intensified in the 1990s (ICES 1999). In November 2000, the U.S. Fish and Wildlife Service listed Atlantic salmon in the Gulf of Maine as endangered, and in May 2001 the Committee on the Status of Endangered Wildlife in Canada (COSEWIC) listed Atlantic salmon associated with rivers in the inner Bay of Fundy as endangered (WWF 2001). Fisheries, predation, disease, parasites, degradation of riverine habitat, forest pesticide spraying, and marine environmental conditions have all been suggested as causative agents of the decline, but there is no clear evidence to link the decrease to any or any combination of these factors (Dempson et al. 1998). During the Atlantic salmon's de-

Received 20 August 2001. Accepted 8 February 2002. Published on the NRC Research Press Web site at http://cjfas.nrc.ca on 1 May 2002.
J16491

W.A. Montevecchi.[1] Biopsychology Programme, Memorial University of Newfoundland, St. John's, NF A1B 3X9, Canada.
D.K. Cairns. Science Branch, Department of Fisheries and Oceans, Box 1236, Charlottetown, PEI C1A 7M8, Canada.
R.A. Myers. Biology Department, Dalhousie University, Halifax, NS B3J 4J1, Canada.

[1]Corresponding author (e-mail: mont@mun.ca).

 DOI: 10.1139/F02-033 © 2002 NRC Canada

cline, the densities of fry and parr in many major salmon rivers have remained high (ICES 1999). These circumstances and an evaluation of hypotheses that might explain the decline of Atlantic salmon (Cairns 2001) suggest that much or most of the decrease is due to increased mortality during the fish's marine phase. Similar arguments have been advanced regarding the recent decline of steelhead (*Oncorhynchus mykiss*) in British Columbia (Welch et al. 2000).

Almost all studies of predation on Atlantic salmon have been conducted in rivers and in estuaries (Scheel and Hough 1997; Beland et al. 2001). Avian, fish, and mammalian predators often aggregate near estuaries, and predation rates can be high in such restricted environments (e.g., Scheel and Hough 1997). Yet, elucidation of mortality factors affecting marine-phase salmon, especially during the first year, is hampered by limited understanding of salmon movements, behavior, and ecology at sea (Reddin and Friedland 1993). Information on migratory patterns in the Northwest Atlantic has been derived primarily from previous captures of tagged fish in commercial nets, yet because there were no directed fisheries for post-smolts, very little is known about their movement patterns following departure from natal rivers (Ritter 1989; Reddin and Short 1991). Aspects of post-smolt biology have also been inferred from characteristics of scales and otoliths obtained from returning adults (Friedland et al. 1999).

Seabirds have provided additional information on post-smolts that is not readily obtained by conventional survey techniques (Cairns 1992). Northern gannets (*Morus bassanus*), the largest seabird species breeding in Canada, plunge-dive into surface waters to capture pelagic prey (Garthe et al. 2000), including post-smolt Atlantic salmon that frequently swim in surface waters. Levels of prey consumption by gannets nesting on Funk Island off the northeast Newfoundland coast is positively correlated with fishery catches and research indices of abundance over multiple spatial and temporal scales (Montevecchi and Myers 1995). During the late 1970s and 1980s, the gannets' prey landings were dominated by warm-water pelagic migrants (mackerel, *Scomber scombrus*; short-finned squid, *Illex illecebrosus*; Atlantic saury, *Scomberesox saurus*). These prey were essentially replaced in the gannets' diets during the 1990s by cold-water pelagic species (capelin, *Mallotus villosus*; herring, *Clupea harengus*). Interdecadal dietary changes and concomitant fisheries and physical data suggested that cold surface water events (Drinkwater 1996) inhibited movements of warmwater pelagic prey into the region and amplified effects of apparent overfishing of squid in the late 1970s (Montevecchi and Myers 1995, 1996). Incidence of salmon in the gannets' food loads on Funk Island has been rare and sporadic but increased notably from the 1980s to the 1990s (Montevecchi and Myers 1997).

Atlantic salmon smolts leave natal rivers in the spring. Some post-smolts from rivers in Maine, the Maritime Provinces, Quebec, and Newfoundland move to the Newfoundland Shelf within several weeks of river exit, and others remain in local waters at least until autumn (Dutil and Coutu 1988; Ritter 1989). Some post-smolts migrate east of Newfoundland, while others, primarily those from the Gulf of St. Lawrence, move through the Strait of Belle Isle (Montevecchi et al. 1988*b*). Much of the habitat moved through or occupied by the post-smolts is within the foraging radius (approximately 180 km, Kirkham et al. 1985) of the three gannet colonies in the Gulf of St. Lawrence and of the three in eastern Newfoundland.

This paper examines avian predation on post-smolt Atlantic salmon at sea, using dietary data collected from northern gannets in the colony on Funk Island from 1977 through 2000. Gannet diet is used to (*i*) infer salmon movements and distributions in the context of recent oceanographic changes, (*ii*) assess potential predation by gannets on Atlantic salmon populations, and (*iii*) recommend research activities to improve understanding of the behavior, abundance, and mortality of Atlantic salmon at sea.

Methods

Prey items were sampled from gannets at their breeding colony on Funk Island off Newfoundland's northeast coast in North Atlantic Fisheries Organization (NAFO) Area 3K (Fig. 1) from 1977 through 2000, excluding 1981 when sea conditions prevented access to the island. A total of 7521 regurgitations were sampled with an annual range from 50 to 914. These regurgitations contained 40 120 prey items. Food samples were obtained by approaching gannets at roosts and in the colony, which induces birds to regurgitate (Montevecchi and Myers 1997). Regurgitations usually include multiple items, and regurgitations of the smallest prey (capelin) contained the highest number of individual prey. About 5% of the regurgitations contain more than one species. Samples were collected almost entirely during August with a small portion taken in July and September. Prey were identifiable to species, and lengths of relatively intact specimens were measured and relatively fresh ones were weighed with Pesola spring scales.

The gannets' consumption of salmon was estimated using a bioenergetics model (e.g., Cairns et al. 1991). Adult energy requirements were estimated as 4865 kJ·day^{-1}, based on doubly labeled water measurements of energy use by gannets on Funk Island (Birt-Friesen et al. 1989). Our energetic model sums energy needs of adult and chick metabolism and egg formation and divides them by assimilation efficiency to obtain food requirements (see Table 1 for input parameters). Food requirements are in turn converted to consumption estimates using dietary data and the energy densities of prey. All calculations were based on estimated prey mass, rather than numbers. Colony populations for 1977–2000 were taken from aerial photographic censuses (Nettleship and Chapdelaine 1988; Chardine 2000; G. Chapdelaine, Canadian Wildlife Service, Ste. Foy, QC G1V 4H5, unpublished data) and from linear interpolation and extrapolation for uncensused years (Fig. 2). Pre-breeder numbers were estimated with the aid of a life table submodel based on literature values of age of first breeding, hatching and fledging success, and adult survivorship (Cairns et al. 1991). Numbers of pre-breeders as a proportion of breeders were calculated from the life table after post-fledging survival was varied until the population exhibited the increase estimated for that year.

Our energetics model operates in deterministic mode, with fixed input values, and in stochastic mode, in which inputs are randomly varied according to a normal distribution whose mean is the original input value. Input distributions

© 2002 NRC Canada

Fig. 1. Locations of the six northern gannet (*Morus bassanus*) colonies in North America: Funk Island, Baccalieu Island (BAC), Cape St. Marys (CSM), Magdalen Bird Rocks (MAG), Anticosti Island (ANT), and Bonaventure Island (BON). Circles are 60 and 180 km in radius and represent the median and maximum foraging ranges of northern gannets. Populations (pairs) are from a 1999 census (Chardine 2000; G. Chapdelaine, Canadian Wildlife Service, Ste. Foy, QC G1V 4H5, unpublished data). Arrows indicate post-smolt migration routes as proposed by Reddin (1988) and Montevecchi et al. (1988*b*).

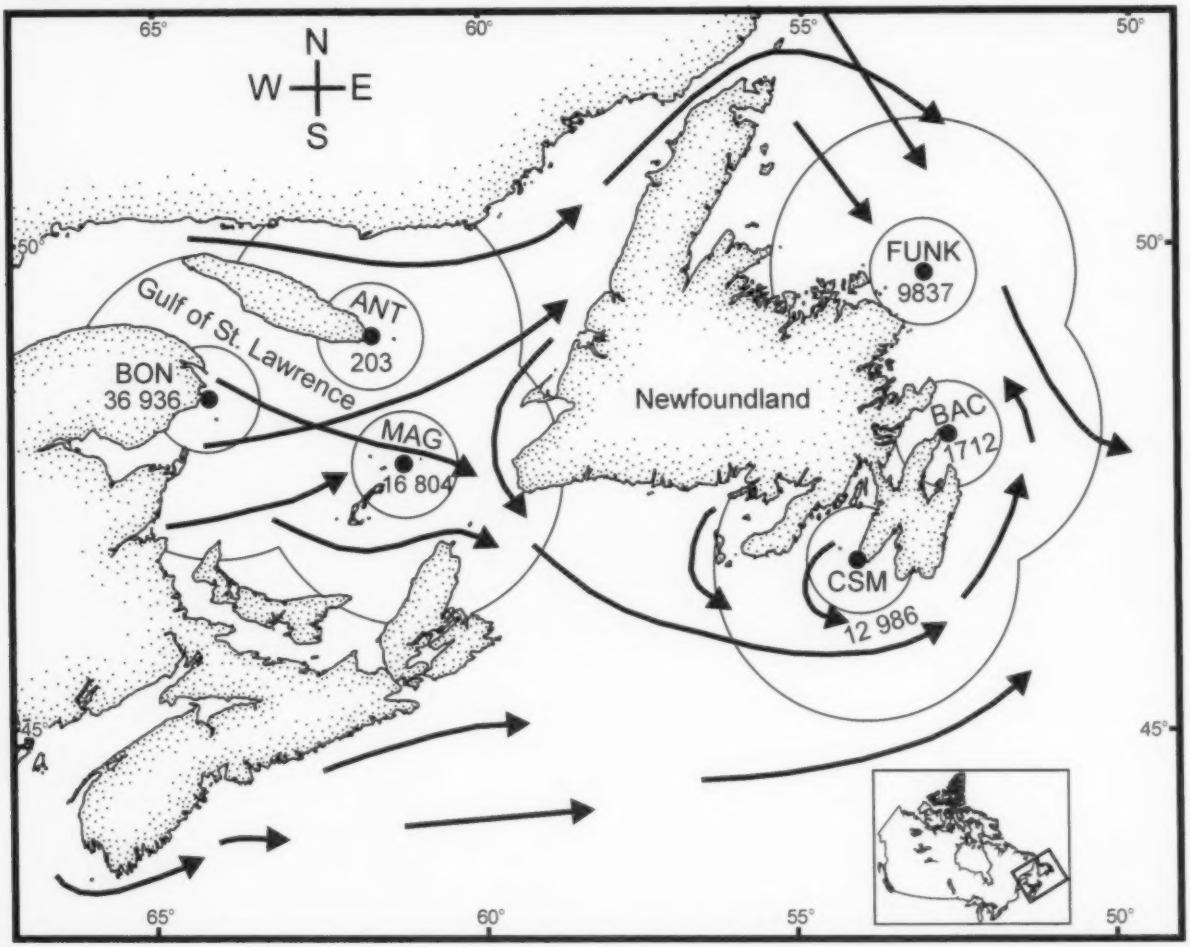

are truncated at 0 (and 1 in the case of proportions). In stochastic runs the standard deviation (SD) of the randomized input value was set at one half of the mean for percentage of salmon in the gannets' diet and for pre-breeders as a proportion of breeders, and one fourth of the mean for all other inputs. Stochastic results are presented as means, medians, SD, and as 5th, 50th (median), and 95th percentiles of 10 000 Monte Carlo outcomes.

The consumption of Atlantic salmon by gannets in the Funk Island colony was estimated for August of each year. Consumption estimates were compared with biomass of post-smolt salmon, as estimated by Cairns and Reddin (2000) for the same period. Briefly, these authors fitted logistic curves to observed weights of marine-phase salmon to derive weight curves, and estimated numbers alive from Lorenzen's (1996) equation for ocean fish, which estimates mortality as an allometric function of body weight. Estimates of post-smolt biomass involve substantial uncertainty because total North American smolt production is poorly known and because there are no empirical measures of mortality during the post-smolt year (Cairns and Reddin 2000).

We compared the gannets' estimated consumption of salmon from 1990 to 2000 with the period 1977–1989. We did this to reflect differences consistent with a shift in the gannets' diet from warm- to cold-water pelagic prey (Montevecchi and Myers 1995) that indicated a larger regime shift in pelagic food webs on the Newfoundland Shelf (Montevecchi and Myers 1996), coincident with decadally anomalous cold-water events (Drinkwater 1996).

The percentage of salmon in the gannets' diet was compared with mean August sea surface temperature (SST) east of St. John's, Newfoundland, at Station 27, whose signals indicate condition fluctuations over the Labrador Shelf (Myers et al. 1990). August temperatures for 1978, 1981, and 1982,

© 2002 NRC Canada

Table 1. Input values for energy model of gannet (*Morus bassanus*) requirements breeding on Funk Island in the Northwest Atlantic.

	Value	CV[a]	Source
Breeding population (pairs, 1999)	9837	0.25	Chardine 2000
Age at first breeding (years)	5		Nelson 1978
Adult annual survivorship	0.94		Nelson 1978
Clutch size	1	0.25	Nelson 1978
Hatching success (eggs hatched·eggs laid^{-1})	0.88	0.25	Montevecchi et al. 1988*a*
Incubation period (days)	44	0	Poulin 1968
Fledging success (chicks fledged·eggs hatched^{-1})	0.8	0.25	Montevecchi et al. 1988*a*
Chick period (days)	91	0	Poulin 1968
Pre-breeding population as proportion of the breeding population	0.321	0.50	Life table model (see text)
Adult metabolism (kJ·day^{-1})	4865	0.25	Birt-Friesen et al. 1989
Energy content of an egg (kJ)	442	0.25	Ricklefs and Montevecchi 1979
Chick metabolism (kJ·day^{-1})	136–2228	0.25	Montevecchi et al. 1984
Assimilation efficiency	0.836	0.25	Bennett and Hart 1993

Note: See text for explanations of model design and functions.
[a]Coefficient of variation (standard deviation·mean^{-1}) of the randomized parameter values used in SHAGIT (program available from CairnsD@dfo-mpo.gc.ca).

Fig. 2. Breeding populations of northern gannets (*Morus bassanus*) in North America. Data are from Nettleship and Chapdelaine (1988), Chardine (2000), and G. Chapdelaine, Canadian Wildlife Service, Ste. Foy, QC G1V 4H5, unpublished data. Colonies (from top to bottom) are open, Funk Island; dots, Baccalieu Island; diagonal lines, Cape St. Mary's; vertical lines, Magdalen Islands; solid, Bonaventure Island. The population of the Anticosti colony is too small to be visible at this scale.

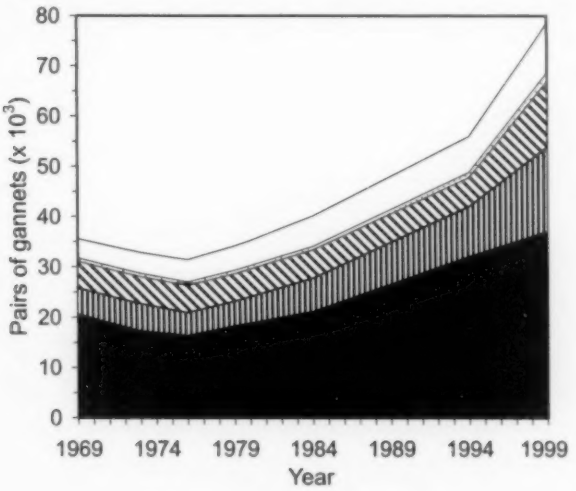

for which data were missing, were estimated from July and September data by a regression equation.

Results

Salmon constituted from 0 to 6.37% of the food that gannets were recorded to have landed on Funk Island during 1977–2000 (Table 2). Before 1990, salmon was a rare item that contributed less than 1% to diet in all but one year. The percentage of salmon in food loads rose sharply during the 1990s, peaking at 6.37% in 1993, and thereafter declined to 0% in 1999 and 2000 (Fig. 3). During 1977–1989 and 1990–2000, the mean relative contributions of salmon to the gannets' diet were 0.29% and 2.78%, respectively (Table 2).

The mean (±SD) fork length of 21 fresh Atlantic salmon regurgitated by gannets on Funk Island on a mean date of 9 August was 23.4 ± 1.9 cm (range 18.5–26.1 cm, Fig. 4). Based on the length–mass relationship calculated for post-smolt Atlantic salmon taken in September–October in the Labrador Sea (mass = 0.181 × length$^{2.213}$, masses in g and lengths in cm; Cairns and Reddin 2000), these fish had a mean mass of 196 g. Figure 4 also shows the length distributions of other fish species preyed on by gannets at Funk Island. Owing to decadal dietary shifts from predominantly large pelagic fishes during the 1970s and 1980s to predominantly small ones during the 1990s, the length of prey decreased while the number of prey per food load increased (Fig. 5).

In 1991, SST in the region around Funk Island dropped precipitously, but temperatures returned to previous levels by mid-decade (Fig. 3). The temperature decrease during 1991 occurred one year after the initial increase in salmon in the gannets' diets, and the percent salmon consumed was not significantly correlated with SST ($r = 0.343$, $n = 23$, $P = 0.110$).

Estimates from model simulations of the tonnes of salmon consumed during years of high (1993), medium (1996), and low (1998) predation by gannets were skewed to the right (Fig. 6). As a consequence, means of these distributions were greater than medians (Table 2). Consumption estimates from deterministic model runs were intermediate between stochastic mean and median values. The estimated consumption of Atlantic salmon by gannets on Funk Island during August varied from 0 to 43.4 t (median values; Table 2). Means of median consumption levels were 1.6 t for 1977–1989 and 18.1 t for 1990–2000. The gannet population of Funk Island more than doubled between 1977 and 1999 (Fig. 2) and contributed to the higher estimated consumption of salmon during later years.

Estimated salmon consumption by gannets on Funk Island during August was less than 1% of total estimated biomass of post-smolt Atlantic salmon of North American origin in all but one year between 1977 and 1989 (Table 2). During the 1990s, when salmon predation by gannets increased, the

© 2002 NRC Canada

Table 2. Estimated consumption by gannets (*Morus bassanus*) at Funk Island, Newfoundland, of post-smolt Atlantic salmon (*Salmo salar*) and of total prey, and estimated consumption (t) of post-smolt salmon as a percentage of post-smolt biomass, during August, based on deterministic and stochastic model runs.

						Salmon consumption in August[a]						
							Stochastic					
Year	No. gannet samples	No. prey	% salmon in gannet diet	Post-smolt biomass August (t)	Annual consumption, all prey[b](t)	Deterministic	Mean[b]	Median[b]	SD[b]	5th percentile[b]	95th percentile[b]	% post-smolt biomass[b,c]
1977	146	332	0.00	810	2922	0.0	0.0	0.0	0.0	0.0	0.0	0.00
1978	914	1 080	0.00	496	3082	0.0	0.0	0.0	0.0	0.0	0.0	0.00
1979	393	586	0.36	1020	3242	1.8	2.0	1.7	1.4	0.3	4.5	0.16
1980	219	608	0.00	1783	3401	0.0	0.0	0.0	0.0	0.0	0.0	0.00
1982	193	360	1.06	450	3742	6.1	6.6	5.6	5.8	0.9	14.9	1.25
1983	494	1 242	0.32	1264	3982	1.9	2.1	1.8	1.6	0.3	4.8	0.15
1984	227	882	0.00	1240	4078	0.0	0.0	0.0	0.0	0.0	0.0	0.00
1985	184	770	0.00	1123	4177	0.0	0.0	0.0	0.0	0.0	0.0	0.00
1986	493	1 294	0.91	1103	4246	5.9	6.5	5.5	4.7	0.9	14.7	0.50
1987	354	2 506	0.45	986	4367	3.0	3.3	2.8	2.4	0.5	7.5	0.28
1988	572	1 836	0.33	706	4405	2.2	2.5	2.1	3.2	0.3	5.6	0.29
1989	410	1 388	0.00	763	4480	0.0	0.0	0.0	0.0	0.0	0.0	0.00
1990	342	4 550	2.94	630	4555	20.3	21.9	18.9	15.8	2.9	50.1	3.00
1991	405	3 468	2.23	954	4617	15.6	17.1	14.8	12.2	2.2	39.3	1.55
1992	288	1 710	3.87	914	4723	27.5	30.1	26.0	22.2	4.3	68.6	2.84
1993	255	1 508	6.37	555	4780	45.9	50.1	43.5	36.0	6.9	114.9	7.84
1994	50	779	1.62	523	4800	11.9	13.0	11.1	9.6	1.8	29.7	2.12
1995	278	3 951	5.72	715	5132	45.1	49.3	42.8	35.0	7.1	112.1	5.99
1996	334	3 834	3.68	647	5553	31.4	34.6	29.9	24.4	4.9	78.1	4.62
1997	244	1 376	1.07	706	5980	9.7	10.8	9.4	7.6	1.5	24.3	1.33
1998	445	4 398	0.33	706	6277	3.2	3.5	3.0	2.5	0.5	7.9	0.43
1999	97	551	0.00	706	6652	0.0	0.0	0.0	0.0	0.0	0.0	0.00
2000	184	1 111	0.00	706	7100	0.0	0.0	0.0	0.0	0.0	0.0	0.00
$\bar{x}$1977–1989			0.29	979	3844	1.7	1.9	1.6	1.6	0.3	4.3	0.22
$\bar{x}$1990–2000			2.53	706	5470	19.2	20.9	18.1	15.0	2.9	47.7	2.70
$\bar{x}$1977–2000			1.42	855	4479	10.5	11.4	9.9	8.3	1.6	26.1	1.41
Totals	7521	40 120										

Note: SD, standard deviation.

[a]Based on a mortality of 20% at river exit. Post-smolt biomasses for 1997–2000 are the mean of values for 1990–1996.

[b]Based on 10 000 Monte Carlo simulations of gannet consumption.

[c]Based on median estimated consumption of salmon.

© 2002 NRC Canada

Fig. 3. Mean sea surface temperature (diamonds) at Station 27 (east of St. John's, Newfoundland) and the percent contribution of Atlantic salmon (*Salmo salar*) (open bars) to diets of gannet (*Morus bassanus*) chicks at Funk Island during August 1977–2000. Dietary data are unavailable for 1981.

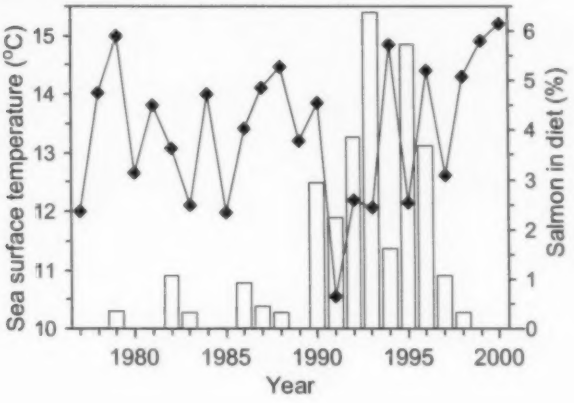

Fig. 4. Length–frequency distributions of (*a*) capelin (*Mallotus villosus*), (*b*) Atlantic salmon (*Salmo salar*), (*c*) Atlantic herring (*Clupea harengus*), (*d*) Atlantic saury (*Scomberesox saurus*), and (*e*) mackerel (*Scomber scombrus*) preyed on by gannets (*Morus bassanus*) from the breeding colony on Funk Island during August.

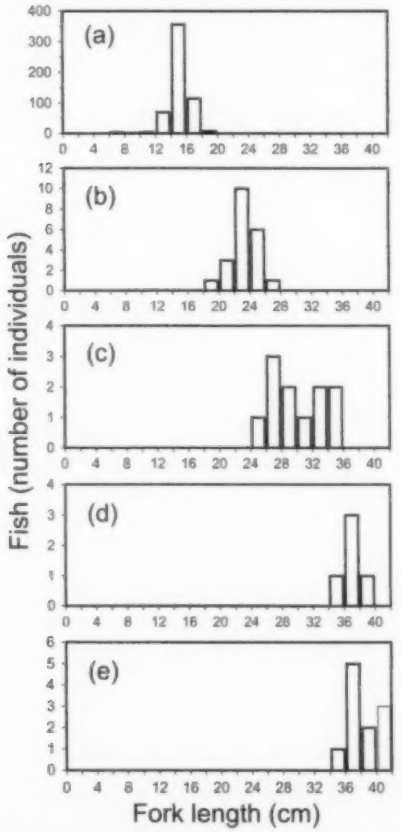

Fig. 5. (*a*) Average number of prey per food load and (*b*) average length of prey landed by gannets (*Morus bassanus*) on Funk Island, 1977–2000.

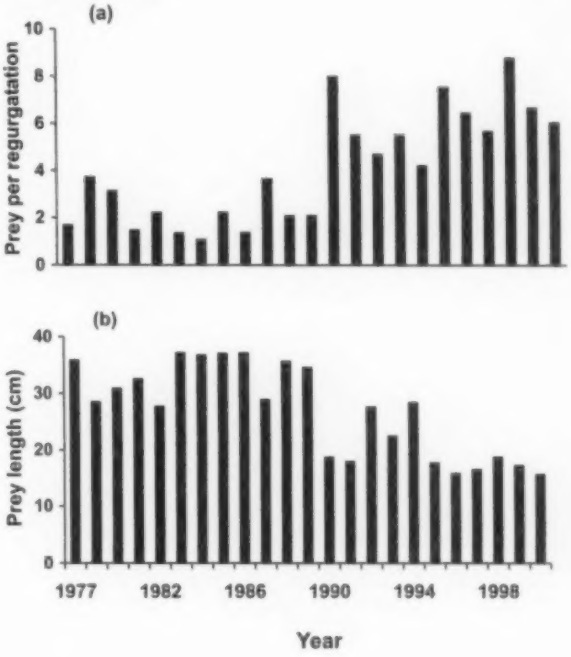

birds' estimated consumption relative to post-smolt biomass increased, peaking at 7.84% in August 1993. Overall, gannets consumed an estimated 0.22% of post-smolt biomass in August 1977–1989 and 2.70% in August 1990–2000.

Foraging gannets range up to 180 km or more from their colonies to obtain food, although feeding effort is most intense within 60 km of the colony (Kirkham et al. 1985). The probable migratory routes of post-smolt Atlantic salmon overlap with the foraging ranges of all North American gannet colonies (Fig. 1). Dietary samples from two colonies in the Gulf of St. Lawrence (Bonaventure Island and Great Bird Rock, Magdalen Islands) include a variety of pelagic fishes and squid, but no Atlantic salmon (Table 3), although sampling efforts at these sites has not been nearly as intensive and extensive as those at Funk Island. Dietary data are unavailable for other North American colonies.

Lengths of nonsalmon prey were compiled from samples from Funk Island to assess the range of prey lengths that are vulnerable to predation by gannets. Capelin, the smallest prey, had mean and minimum lengths of 15.2 cm and 7.6 cm, respectively (Fig. 3). Mackerel, the largest prey, had mean and maximum lengths of 38.6 cm and 41.7 cm, respectively. Post-smolt Atlantic salmon enter the sea at lengths that range from 13 to 18 cm and attain an estimated length of ~42 cm by early November (Hutchings and Jones 1998; Cairns and Reddin 2000). Thus, post-smolt salmon are of a size that could be preyed on by gannets throughout the entire period between river departure until gannets depart from eastern Canadian waters (mid- to late October).

When the mean salmon contribution to diet at Funk Island

© 2002 NRC Canada

Fig. 6. Frequency distributions of estimated consumption of Atlantic salmon (*Salmo salar*) by gannets (*Morus bassanus*) on Funk Island during August during years of (*a*) high (1993), (*b*) medium (1996), and (*c*) low (1998) predation from 10 000 stochastic runs for each year.

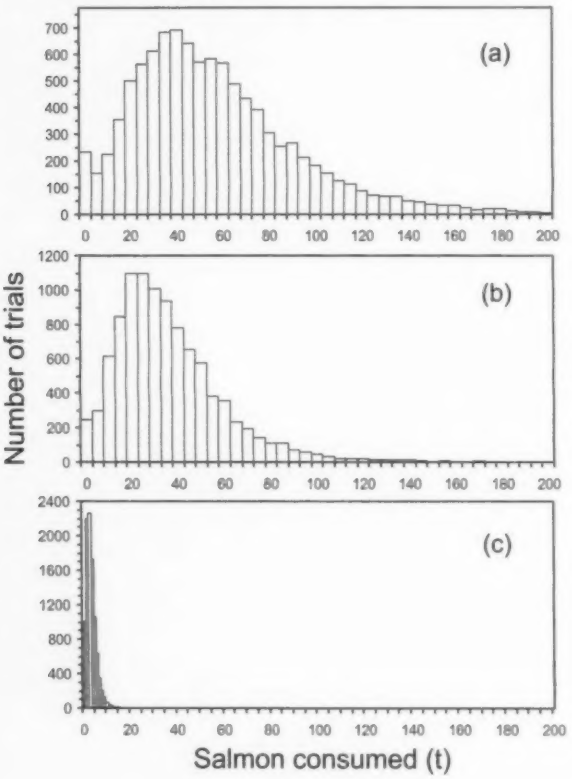

for August 1990–2000 (2.53%) was assumed to apply to all Newfoundland colonies, estimated consumption during August totaled 5.0% of post-smolt biomass. Enumerated diet samples from the Gulf of St. Lawrence total 321 (Table 3), indicating that salmon would not likely be detected if they were less than 1/321 (0.31%) of diet. When salmon were assumed to contribute 2.53% of Newfoundland diet and 0.31% of Gulf diet throughout the breeding season, estimated consumption of post-smolt biomass by gannets increased markedly.

Discussion

Gannets as indicators of the marine ecology of Atlantic salmon

Dietary records of gannets on Funk Island in NAFO Area 3K provide the only long-term time series of post-smolt salmon in the Northwest Atlantic. Post-smolts have been taken in small numbers on research cruises in the Labrador Sea during September–October in 1987, 1988, 1991, and 1998, and the area is viewed as a major staging area for post-smolt salmon (Reddin and Short 1991). The occurrence of salmon in gannet regurgitations at Funk Island demon-

Table 3. Diet of northern gannets (*Morus bassanus*) in the Gulf of St. Lawrence taken from the literature.

Prey	*N*	Date	Location	Prey size range	Source
Herring *Clupea harengus*, mackerel *Scomber scombrus*, *Loligo* squid	NR	June–Sept. 1966–1967	Bonaventure I		Poulin 1968
Herring, mackerel, *Loligo* squid, redfish *Sebastes* spp.	NR	1968	Bonaventure I	18–30 cm	Lafleur 1969
Mackerel, herring, smelt *Osmerus mordax*, sand lance *Ammodytes* spp., cunner *Tautogolabrus adspersus*	80	15–17 Aug. 1995	Bonaventure I		Rail et al. 1996
Capelin *Mallotus villosus*, sand lance, mackerel, smelt, *Crangon* shrimp, American eel *Anguilla rostrata*, lumpfish *Cyclopterus lumpus*, *Illex* squid, cod *Gadus morhua*, yellowtail *Limanda ferruginea*, other flatfish	189	3 June – 10 Aug. 1977–1978	Bird Rock, Magdalens	7–41 cm	Burton 1980
Mackerel, Atlantic saury *Scomberesox saurus*, herring, sand lance, *Loligo* squid	52	17–29 Sept. 1987–1988	Bird Rock, Magdalens	20–520 g	Cairns et al. 1991; D.K. Cairns, unpublished data

Note: NR, sample sizes not reported.

© 2002 NRC Canada

strates that post-smolts also occupy the southern Labrador Sea in August.

Post-smolts were found in gannet regurgitations at Funk Island in six of 12 years from 1977 to 1989 and in nine of 11 years from 1990 to 2000. The increase of salmon in the birds' diets was associated with a radical shift from warm-water (mackerel, saury, squid) to cold-water (capelin, herring) pelagic prey (Montevecchi and Myers 1996, 1997). This dietary shift occurred during a period of megascale physical and biological change on the Newfoundland and Labrador Shelf. Changes included the extreme cold surface water event of 1991 (Drinkwater 1996), breeding failures of surface-feeding seabirds (Regehr and Montevechi 1997), the southward influx of polar cod (*Boreogadus saida*) as a dominant pelagic species (Frank et al. 1996), and the collapse of groundfish stocks (Hutchings 1996). The shift in the gannets' diet during the 1990s, including the increased consumption of Atlantic salmon, does not appear to be a simple consequence of cold surface water. A major dietary change occurred in 1990, one year before the extreme cold SST event of 1991, and continued after surface water temperatures warmed during the mid-1990s (Drinkwater 1996). In a somewhat parallel finding in the Pacific Ocean, Welch et al. (1998) related a long-term response of sockeye salmon (*Oncorhynchus nerka*) to a short-term oceanographic perturbation. Such a long-term biological change in response to rapid onset, relatively discrete perturbations reflects a large-scale regime shift (sensu Steele 1998).

The increase in salmon in the gannets' diet could be due to any of a number or combination of factors: (*i*) an increase in the abundance of post-smolts, (*ii*) an increase in their relative abundance related to the changing abundances or alternative prey, and (or) (*iii*) an increase in availability due to a change in the salmon's migratory patterns, with higher numbers of post-smolts occupying the southern Labrador Sea during the 1990s. Decreased mackerel abundance in the region could favor greater predation on salmon by gannets that are opportunistic generalist predators on pelagic prey. The mean energy density for major warmwater prey is 7.1 $kJ \cdot g^{-1}$ (mackerel 10.3, squid 4.3, saury 6.8) and 5.7 $kJ \cdot g^{-1}$ for cold-water prey (herring 7.2, capelin 4.2; Montevecchi et al. 1984). Thus, alternative prey were energetically more valuable relative to Atlantic salmon (4.4 $kJ \cdot g^{-1}$, Cairns 1998) during 1977–1989, the period of warmwater prey, than during 1990–2000, the period of cold-water prey. Moreover, the number of prey per food load increased while the average length of prey decreased over the 24-year sampling period, as gannets shifted from dominant consumption of large pelagic species like mackerel before 1990 to small ones like capelin during the 1990s. As post-smolt salmon in August are substantially larger than capelin, this might also have favored an increase in the gannets' consumption of salmon during the 1990s. It would, however, be unlikely to account for all the change given that mean percentage of salmon in the birds' diets rose by an order of magnitude between 1977–1989 (0.29%) and 1990–2000 (2.53%). Had comparable numbers of post-smolt salmon been present within the gannets' foraging range around Funk Island during the 1970s and 1980s, we expect that more of them would have been found in the birds' regurgitations.

Summer occurrences of post-smolt Atlantic salmon in the Labrador Sea does not preclude their presence elsewhere. Of 420 tags returned from post-smolts that had been marked in rivers in Quebec, the Maritimes, and New England, only 30 (7.6%) were recovered from the Atlantic coasts of Newfoundland and Labrador (Ritter 1989; Cairns and Reddin 2000). Return dates from the Labrador Sea and from southern areas ranged from June to September–October, suggesting either a diffuse and asynchronous migration, or one with routes and timing that vary from year to year (Friedland et al. 1999). Research and commercial fishing in the Bay of Fundy and in the northwestern Gulf of St. Lawrence demonstrates also that post-smolt Atlantic salmon can remain in coastal waters during summer and fall (Dutil and Coutu 1988).

Tag recoveries from salmon originating from rivers in New England, the Bay of Fundy, and southwestern Nova Scotia on Funk Island have been interpreted as evidence of a salmon migration route east of Newfoundland (Montevecchi et al. 1988*b*). Tags from these areas have, however, also been recovered in the northern and eastern Gulf of St. Lawrence (Ritter 1989), suggesting that post-smolts from the southern part of the range can also reach the Labrador Sea via the Gulf of St. Lawrence, passing through the foraging ranges of gannet colonies there.

Consumption of Atlantic salmon by gannets

Estimates of seabird consumption are usually derived from deterministic bioenergetic models that yield single-value outputs (e.g., Cairns et al. 1991). We used stochastic model runs to evaluate error in our estimates. Model outputs varied over wide ranges, indicating substantial uncertainty in consumption estimates. Comparisons of estimated consumption by gannets with indirect estimates of post-smolt Atlantic salmon biomass and numbers introduce additional uncertainty (Cairns and Reddin 2000).

These limitations notwithstanding, our data and simulations suggest that gannet predation on post-smolts could influence the population dynamics of Atlantic salmon in the Northwest Atlantic. Some post-smolts are likely to be within the foraging range of gannet colonies for a substantial period between river exit and mid-autumn, when the gannets depart from eastern Canadian waters. Much more extensive dietary sampling at gannet colonies other than Funk Island and at other times is needed to critically assess the potential influences of gannet predation on the population dynamics of post-smolt Atlantic salmon in the Northwest Atlantic.

North American gannet numbers increased 2.4 fold between 1977 and 1999. Growing gannet populations could have consumed increasing numbers of post-smolts since the 1970s. Most of the tags from post-smolt Atlantic salmon recovered in the gannet colony on Funk Island have come from hatchery-reared fish released in the Penobscot River, Maine. Tags could make post-smolts more vulnerable to gannets and other avian predators that prey proportionally more heavily on hatchery-reared fishes than on wild ones. If so, predation on hatchery-reared fish could inflate estimates of predation on wild post-smolts. Salmon vertebrae and ring patterns on scales (Friedland et al. 1999) regurgitated by gannets could help determine relative predation rates of wild and hatchery-released fish. Nevertheless, hatchery fish are a small fraction of the Atlantic salmon post-smolts in the re-

© 2002 NRC Canada

gion, so their increased susceptibility would have negligible effects on predation opportunities by gannets.

In some restricted environments, marine birds consume small proportions of salmonid numbers and biomass. For example, below a dam on the Columbia River 2% of juvenile Pacific salmon (*Oncoryhynchus* spp.) and steelhead were estimated to be preyed upon by seabirds (Ruggerone 1986). Notably, whereas prey swamping of predators may have occurred, this mortality estimate is lower than some of those generated for predation on post-smolt Atlantic salmon by gannets in the open ocean, where overall predation by birds might be expected to be less intense. Presumably the predation imposed by gannets on Atlantic salmon smolts represents an additive source of mortality.

Atlantic salmon are extremely rare in the diets of Atlantic cod (*Gadus morhua*), common murres (*Uria aalge*), and harp (*Phoca groenlandica*), harbor (*Phoca vitulina*), and grey (*Halichoerus grypus*) seals in the Northwest Atlantic (Cairns and Reddin 2000). Post-smolt salmon may be more vulnerable to gannets than other large marine predators, owing to the gannets' large size and specialized feeding habit of plunge-diving into surface waters (Garthe et al. 2000), the habitat favored by salmon (Dutil and Coutu 1988). The decreasing incidence of post-smolts in gannet diets since 1995 and their absence in 1999 and 2000 could also reflect decreased availability of Atlantic salmon in the region (see Montevecchi and Myers 1995).

Many complexities and controversies surround considerations of the consumption of commercial prey by large predators (Lavigne 1996). Arguments for culls of large marine predators whose diets contain small proportions of commercial prey for portions of the year ignore uncertainties inherent in multispecies and ecosystem interactions (Swain and Sinclair 2000). Wild Atlantic salmon will likely best benefit from the mitigation of human impacts, including aquacultural practices, releases of hatchery fishes, pesticide use, and the damming, pollution, and degradation of rivers (e.g., Gross 1998; Fairchild et al. 1999; Levin et al. 2001) and their cumulative effects. Influences of these cumulative effects are likely reflected in the general inverse relationship between human and Atlantic salmon populations along a North American latitudinal gradient from New England through the Maritime Provinces, Gulf of St. Lawrence, and Newfoundland and Labrador.

Given the precarious state of wild Atlantic salmon and risk to the species' population integrity, understanding of the marine ecology of Atlantic salmon is urgently needed. The use of gannet diets to sample post-smolts, despite its many associated uncertainties, has provided some insight into their marine distribution, movements, abundance, and mortality.

There are many practical implications for integrating seabird studies in multidisciplinary ecosystem and fisheries research. The systematic sampling of gannets' diets at multiple colonies and from June through September can provide an efficient and cost-effective means of obtaining biological and ecological data on post-smolt Atlantic salmon. Research cruises are constrained by high costs, whereas colony-based sampling of gannets' diets can be repeated annually at modest expense, without harm to the birds. The foraging ranges of gannets around breeding colonies in North America cover a substantial portion of the presumed marine distribution of post-smolt Atlantic salmon. Sampling seabird diets could provide samples of salmon tissue for genetic assessments of origins, as well as samples of scales and otoliths that can be used to elucidate individual histories (Friedland et al. 1999). Findings from the gannets' dietary data could be used to help clarify post-smolt migratory movements, growth rates, natural mortality, and food habits.

Acknowledgements

We thank Keith Bowen for assistance with data management, John Gibson, Jeff Hutchings, Fred Whorisky, Rod Bradford, and anonymous reviewer for comments on the manuscript, Ken Drinkwater for stimulating discussions, and the many people who helped in field collections, especially Iain Stenhouse, Stefan Garthe, Gail Davoren, Nicholas Montevecchi, Janet Russell, and Laura Dominguez who crewed our expeditions in the 1990s. Gilles Chapdelaine and David Nettleship generously provided unpublished gannet census data. Research was supported by grants from the Natural Sciences and Engineering Research Council of Canada (NSERC) and the Department of Fisheries and Oceans to WAM.

References

Beland, K.F., Kocik, J.F., vandeSande, J., and Sheehan, T.F. 2001. Striped bass predation upon Atlantic salmon smolts in Maine. Northeast. Nat. **8**: 267–274.

Bennett, D.C., and Hart, L.E. 1993. Metabolizable energy of fish when fed to captive great blue herons (*Ardea herodias*). Can. J. Zool. **71**: 1767–1771.

Birt-Friesen, V.L., Montevecchi, W.A., Cairns, D.K., and Macko, S.A. 1989. Activity-specific metabolic rates of free-living northern gannets and other seabirds. Ecology, **70**: 357–367.

Burton, J. 1980. L'alimentation estivale du fou de bassan (*Sula bassana* L.) au Rocher aux Oiseaux, Iles-de-la-Madeleine, Quebec. Nat. Can. (Ottawa), **107**: 289–291.

Cairns, D.K. 1992. Bridging the gap between ornithology and fisheries science: use of seabird data in stock assessment models. Condor, **94**: 811–824.

Cairns, D.K. 1998. Diet of cormorants, mergansers, and kingfishers in northeastern North America. Can. Tech. Rep. Fish. Aquat. Sci. No. 2225.

Cairns, D.K. 2001. An evaluation of possible causes of the decline in pre-fishery abundance of North American Atlantic salmon. Can. Tech. Rep. Fish. Aquat. Sci. No. 2358.

Cairns, D.K., and Reddin, D.G. 2000. The potential impact of seal and seabird predation on North American Atlantic salmon. Can. Stock Assess. Secretariat Res. Doc. 2000/12. (http://www.dfo-mpo.gc.ca/CSAS/CSAS/DocREC/2000/PDF/2000_012e.pdf)

Cairns, D.K., Chapdelaine, G., and Montevecchi, W.A. 1991. Prey exploitation by seabirds in the Gulf of St. Lawrence. *In* The Gulf of St. Lawrence: small ocean or big estuary? *Edited by* J.-C. Therriault. Can. Spec. Publ. Fish. Aquat. Sci. No. 113. pp. 277–291.

Chardine, J.W. 2000. Census of northern gannet colonies in the Atlantic region. Can. Wildl. Serv. Atl. Reg. Tech. Rep. Ser. 361. *Available from* Canadian Wildlife Service, Sackville, NB E4L 1G6.

Dempson, J.B., Reddin, D.G., O'Connell, M.F., Helbig, J., Bourgeois, C.E., Mullins, C., Porter, T.R., Lilly, G., Carscadden, J., Stenson, G.B., and Kulka, D. 1998. Spatial and temporal varia-

© 2002 NRC Canada

tion in Atlantic salmon abundance in the Newfoundland–Labrador region with emphasis on factors that may have contributed to low returns in 1997. Can. Stock Assess. Secretariat Res. Doc. 98/114. *Available from* Department of Fisheries and Oceans, Northwest Atlantic Fisheries Centre, P.O. Box 5667, St. John's, NF A1C 5X1.

Drinkwater, K.F. 1996. Atmospheric and oceanic variability in the northwest Atlantic during the 1980s and early 1990s. J. Northw. Atl. Fish. Sci. **18**: 77–97.

Dutil, J.-D., and Coutu, J.M. 1988. Early marine life of Atlantic salmon, *Salmo salar*, postsmolts in the northern Gulf of St. Lawrence. Fish. Bull. **86**: 197–212.

Fairchild, W.L., Swanberg, E.O., Arsenault, J.T., and Brown, S.B. 1999. Does an association between pesticide use and subsequent declines in catch of Atlantic salmon (*Salmo salar*) represent a case of endocrine disruption? Environ. Health Perspect. **107**: 349–357.

Frank, K.T., Carscadden, J.E., and Simon, J.E. 1996. Recent excursions of capelin (*Mallotus villosus*) to the Scotian Shelf and Flemish Cap during anomalous hydrographic conditions. Can. J. Fish. Aquat. Sci. **53**: 1473–1486.

Friedland, K.D., Dutil, J.-D., and Sadusky, T. 1999. Growth patterns in postsmolts and the nature of the marine juvenile nursery for Atlantic salmon, *Salmo salar*. Fish. Bull. **97**: 472–481.

Garthe, S., Benvenuti, S., and Montevecchi, W.A. 2000. Pursuit-plunging by northern gannets (*Sula bassana*) feeding on capelin. Proc. R. Soc. Lond. Ser. B Biol. Sci. **267**: 1717–1722.

Gross, M.R. 1998. One species with two biologies: Atlantic salmon (*Salmo salar*) in the wild and in aquaculture. Can. J. Fish. Aquat. Sci. **55**(Suppl. 1): 131–144.

Hutchings, J.A. 1996. Spatial and temporal variation in the density of northern cod and a review of hypotheses for the stock's collapse. Can. J. Fish. Aquat. Sci. **53**: 943–962.

Hutchings, J.A., and Jones, M.E.B. 1998. Life history variation and growth rate thresholds for maturity in Atlantic salmon, *Salmo salar*. Can. J. Fish. Aquat. Sci. **55**(Suppl. 1): 22–47.

International Council on the Exploration of the Sea (ICES). 1999. Report of the working group on North Atlantic salmon. ICES CM 1999/ACFM:14.

Kirkham, I.R., McLaren, P., and Montevecchi, W.A. 1985. The food habits and distribution of northern gannets off eastern Newfoundland and Labrador. Can. J. Zool. **63**: 181–188.

Lafleur, Y. 1969. Île Bonaventure 1968. Unpublished report. Université Laval, Quebec City.

Lavigne, D.M. 1996. Ecological interactions between marine mammals, commercial fisheries, and their prey: unravelling the tangled web. *In* Studies of high-latitude seabirds 4: Trophic relationships and energetics of endotherms in cold ocean systems. *Edited by* W.A. Montevecchi. Can. Wildl. Serv. Occas. Pap. No. 91. pp. 59–71.

Levin, P.S., Zabel, R.W., and Williams, J.G. 2001. The road to extinction is paved with good intentions: negative association of fish hatcheries with threatened salmon. Proc. R. Soc. Lond. Ser. B Biol. Sci. **268**: 1153–1158.

Lorenzen, K. 1996. The relation between body weight and natural mortality in juvenile and adult fish: a comparison of natural ecosystems and aquaculture. J. Fish Biol. **49**: 627–647.

Montevecchi, W.A., and Myers, R.A. 1995. Prey harvests of seabirds reflect pelagic fish and squid abundance on multiple spatial and temporal scales. Mar. Ecol. Prog. Ser. **117**: 1–9.

Montevecchi, W.A., and Myers, R.A. 1996. Dietary changes of seabirds indicate shifts in pelagic food webs. Sarsia, **80**: 313–322.

Montevecchi, W.A., and Myers, R.A. 1997. Centurial and decadal oceanographic influences on changes in northern gannet populations and diets in the north-west Atlantic: implications for climate change. ICES J. Mar. Sci. **54**: 608–614.

Montevecchi, W.A., Ricklefs, R.E., Kirkham, I.R., and Gabaldon, D. 1984. Growth energetics of nestling northern gannets (*Sula bassanus*). Auk, **101**: 334–341.

Montevecchi, W.A., Birt, V.L., and Cairns, D.K. 1988*a*. Dietary changes of seabirds associated with local fisheries failures. Biol. Oceanogr. **5**: 153–161.

Montevecchi, W.A., Cairns, D.K., and Birt, V.L. 1988*b*. Migration of post-smolt Atlantic salmon, *Salmo salar*, off northeastern Newfoundland, as inferred by tag recoveries in a seabird colony. Can. J. Fish. Aquat. Sci. **45**: 568–571.

Myers, R.A., Akenhead, S.A., and Drinkwater, K.F. 1990. The influence of Hudson Bay runoff and ice melt on the salinity of the inner Newfoundland Shelf. Atmos. Ocean. **28**: 241–256.

Nelson, J.B. 1978. The gannet. T & AD Poyser, Berkhamsted.

Nettleship, D.N., and Chapdelaine, G. 1988. Population size and status of the northern gannet *Sula bassanus* in North America, 1984. J. Field Ornithol. **59**: 120–127.

Poulin, J.-M. 1968. Reproduction du fou de Bassan (*Sula bassana*), Île Bonaventure (Québec). M.Sc. thesis, Université Laval, Quebec City.

Rail, J.-F., Chapdelaine, G., Brousseau, P., and Savard, J.-P.L. 1996. Utilisation des oiseaux marins comme bioindicateurs de l'écosystème marin de l'estuaire et du Golfe Saint-Laurent. Can. Wildl. Serv. Tech. Rep. No. 254. *Available from* Canadian Wildlife Service, Ste. Foy, QC G1V 4H5.

Reddin, D.G. 1988. Ocean life of Atlantic salmon (*Salmo salar* L.) in the Northwest Atlantic. *In* Atlantic salmon: preparing for the future. *Edited by* D.H. Mills and D.J. Piggins. Croon Helm, London. pp. 483–511.

Reddin, D.G., and Friedland, K.D. 1993. Marine environmental factors influencing the movement and survival of Atlantic salmon. *In* Salmon in the sea and new enhancement strategies. *Edited by* D.H. Mills. Blackwell Scientific, London. pp. 79–103.

Reddin, D.G., and Short, P.B. 1991. Postsmolt Atlantic salmon (*Salmo salar*) in the Labrador Sea. Can. J. Fish. Aquat. Sci. **48**: 2–6.

Regehr, H.M., and Montevecchi, W.A. 1997. Interactive effects of food shortage and predation on breeding failure of black-legged kittiwakes: indirect effects of fishery activities and and implications for indicator species. Mar. Ecol. Prog. Ser. **155**: 249–260.

Ricklefs, R.E., and Montevecchi, W.A. 1979. Size, organic composition and energy content of North Atlantic gannet *Morus bassanus* eggs. Comp. Biochem. Physiol. A Comp. Physiol. **64**: 161–165.

Ritter, J.A. 1989. Marine migration and natural mortality of North American Atlantic salmon (*Salmo salar* L.). Can. Manuscr. Rep. Fish. Aquat. Sci. No. 2041.

Ruggerone, G.T. 1986. Consumption of migrating juvenile salmonids by gulls foraging below a Columbia River dam. Trans. Am. Fish. Soc. **115**: 736–742.

Scheel, D., and Hough, K.R. 1997. Salmon fry predation by seabirds near an Alaskan hatchery. Mar. Ecol. Prog. Ser. **150**: 35–48.

Steele, J.H. 1998. Regime shifts in marine ecosystems. Ecol. Appl. **8**: 533–536.

Swain, D.P., and Sinclair, A.F. 2000. Pelagic fishes and the cod recruitment dilemma in the Northwest Atlantic. Can. J. Fish. Aquat. Sci. **57**: 1321–1325.

Welch, D.W., Ishida, Y., and Nagasawa, K. 1998. Thermal limits and ocean migrations of sockeye salmon (*Oncorhychus nerka*): long-term consequences of global warming. Can. J. Fish. Aquat. Sci. **55**: 937–948.

© 2002 NRC Canada

Welch, D.W., Ward, B.R., Smith, B.D., and Eveson, J.P. 2000. Temporal and spatial responses of British Columbia steelhead (*Oncorhynchus mykiss*) populations to ocean climate shifts. Fish. Oceanogr. **9**: 17–32.

World Wildlife Fund (WWF). 2001. The status of wild salmon: a river by river assessment. World Wildlife Fund, Washington, D.C.

© 2002 NRC Canada

Landscape characteristics, land use, and coho salmon (*Oncorhynchus kisutch*) abundance, Snohomish River, Wash., U.S.A.

George R. Pess, David R. Montgomery, E. Ashley Steel, Robert E. Bilby, Blake E. Feist, and Harvey M. Greenberg

Abstract: We used temporally consistent patterns in the spatial distribution of returning adult coho salmon (*Oncorhynchus kisutch*) to explore relationships between salmon abundance, landscape characteristics, and land use patterns in the Snohomish River watershed, Wash. The proportion of total adult coho salmon abundance supported by a specific stream reach was consistent among years, even though interannual adult coho salmon abundance varied substantially. Wetland occurrence, local geology, stream gradient, and land use were significantly correlated with adult coho salmon abundance. Median adult coho salmon densities in forest-dominated areas were 1.5–3.5 times the densities in rural, urban, and agricultural areas. Relationships between these habitat characteristics and adult coho salmon abundance were consistent over time. Spatially explicit statistical models that included these habitat variables explained almost half of the variation in the annual distribution of adult coho salmon. Our analysis indicates that such models can be used to identify and prioritize freshwater areas for protection and restoration.

Résumé : L'étude des patterns temporels stables dans la répartition spatiale des saumons coho (*Oncorhynchus kisutch*) qui retournent en rivière nous a permis d'examiner les relations entre l'abondance des saumons, les caractéristiques du paysage et l'utilisation des terres dans le bassin versant de la Snohomish. La proportion du nombre total de saumons adultes maintenue par chaque section de cours d'eau est constante d'une année à l'autre, bien que l'abondance des saumons adultes varie considérablement au cours des années. Il y a des corrélations significatives entre la présence de terres humides, la géologie locale, le gradient du cours d'eau et l'utilisation des terres, d'une part, et l'abondance des saumons coho adultes, d'autre part. Les densités médianes de saumons coho adultes dans les zones à prédominance de forêts sont de 1,5 à 3,5 fois plus élevées que dans les zones rurales, urbaines et agricoles. Les relations entre ces caractéristiques de l'habitat et l'abondance des saumons coho adultes sont constantes dans le temps. Des modèles statistiques spatiaux explicites qui incluent ces variables de l'habitat expliquent presque la moitié de la variation dans la répartition annuelle des saumons coho adultes. Notre analyse laisse croire que de tels modèles peuvent servir à identifier les sites d'eau douce nécessaires à la protection et à la restauration des saumons et à les placer par ordre d'importance.

[Traduit par la Rédaction]

Introduction

Relationships between land use, freshwater habitat condition, and the productivity of salmonid populations traditionally have been examined at fine spatial scales (individual habitat-units or stream reaches) and over short periods of time (1–5 years). Much of this research has attempted to associate an environmental condition with a life stage specific response by the fish, such as the effect of fine sediment on egg survival or average densities of juveniles during summer or winter rearing periods (Everest et al. 1987). Such research is critical for evaluating population control mechanisms and provides a sound basis for evaluating the potential impacts of land use. However, extrapolating site- and life history specific relationships throughout a watershed or to regional scales has been difficult for a number of reasons, including the high degree of temporal and spatial variation in salmon production and the lack of detailed data across large regions.

Central to the development of recovery strategies for depressed salmonid populations across the Pacific Northwest is a quantitative understanding of the relationship between salmon population levels and freshwater habitat condition

Received 18 February 2002. Accepted 15 March 2002. Published on the NRC Research Press Web site at http://cjfas.nrc.ca on 4 May 2002.
J16768

G.R. Pess,[1] E.A. Steel, R.E. Bilby,[2] and B.E. Feist. Northwest Fisheries Science Center, National Marine Fisheries Service, 2725 Montlake Boulevard E., Seattle, WA 98112-2097, U.S.A.
D.R. Montgomery and H.M. Greenberg. Department of Earth & Space Sciences, University of Washington, Seattle, WA 98195, U.S.A.

[1]Corresponding author (e-mail: george.pess@noaa.gov).
[2]Present address: Weyerhaeuser Company, Tacoma, WA 98477, U.S.A.

 DOI: 10.1139/F02-035 © 2002 NRC Canada

Fig. 1. Map of the Snohomish River basin on the west slope of the North Cascades in northwestern Washington. Solid black denotes each adult coho salmon index reach. Grey watersheds within the basin denote areas inaccessible to anadromous fishes.

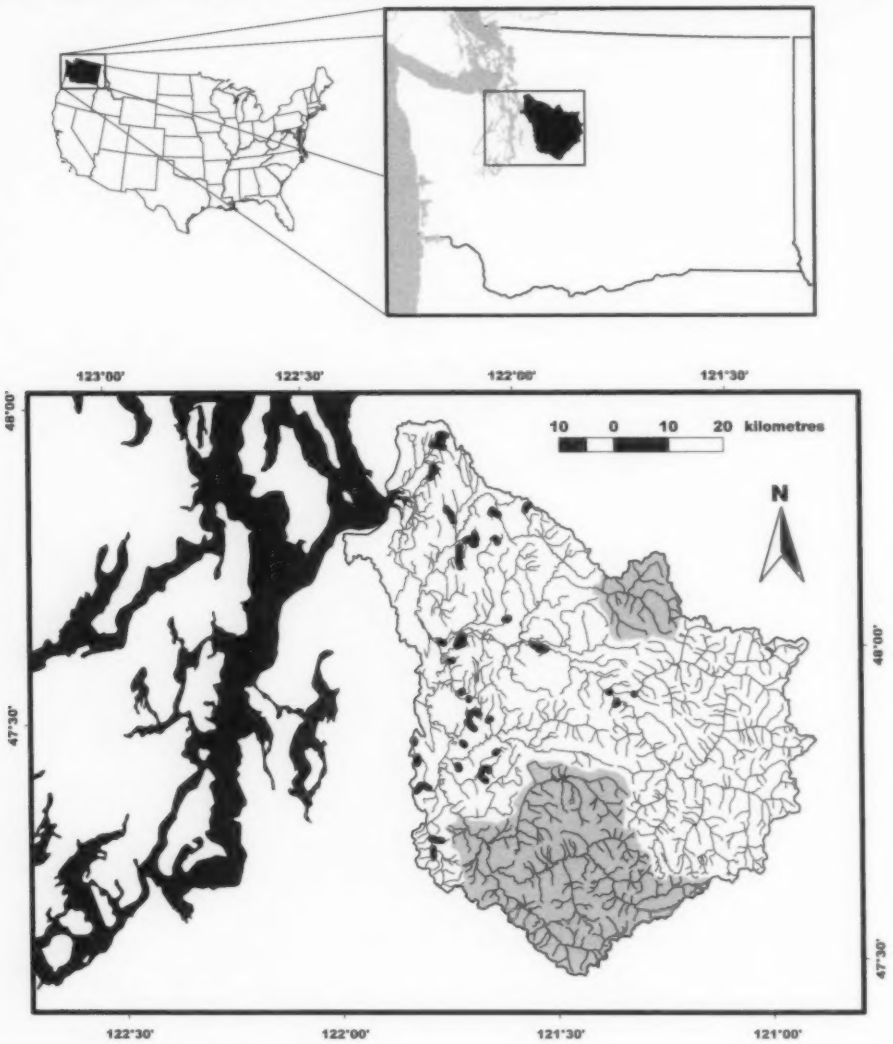

(Holtby and Scrivener 1989). Several methods for relating salmonid population response to changes in freshwater habitat condition have been developed in the Pacific Northwest over the past several decades. One approach is based on reach-scale relationships between potential fish capacity and habitat condition (Reeves et al. 1989). Potential fish capacity by life stage is calculated by applying life stage specific salmonid densities and survival estimates to reach-level habitat data for the entire watershed (Beechie et al. 1994). Although this approach can be used to estimate potential salmon population size and spatial distribution, it has not been used for regional analysis because detailed field data are not available across all watersheds. Various methods of stream habitat classification also have been used to predict salmon response to habitat condition. For example, a priori classification of channel types can explain substantial variance in salmonid spawner densities (Montgomery et al. 1999), but other important habitat variables also influence salmonid population dynamics such as stream temperature and flow conditions.

In this paper, we develop a broad-scale analysis that correlates coho salmon abundance with habitat characteristics and land use in the Snohomish River Basin of western Washington. Specifically, we combine stream-reach and watershed area characteristics, such as the amount and quality of wetland and floodplain habitat, riparian vegetation, geology, or land use to determine correlations between adult coho salmon (*Oncorhynchus kisutch*) abundance levels, land use, and the underlying physical features. We address the interannual variation in fish abundance using a hierarchical anal-

© 2002 NRC Canada

ysis strategy in which each year of data is examined independently and the results summarized across years.

Materials and methods

Study site

The 4610-km^2 Snohomish River watershed, located in the Puget Sound basin of western Washington, includes the Skykomish and Snoqualmie rivers that flow west from the Cascade range through the glaciated Puget lowlands, forming the mainstem Snohomish at their confluence (Fig. 1). The Snohomish River flows through a broad alluvial floodplain and delta for 33 river kilometers before entering Puget Sound northeast of Seattle, Wash. The basin ranges in elevation from sea level to 2438 meters above sea level (ASL) and has an average annual precipitation range between 762 mm·year^{-1} at Puget Sound and 4064 mm·year^{-1} at the crest of the Cascade range.

Lower-elevation forests of the drainage (<700 m ASL) are within the western hemlock zone (Franklin and Dyrness 1973). Dominant conifer species are western hemlock (*Tsuga heterophylla*), Douglas fir (*Pseudotsuga menziesii*), western red cedar (*Thuja plicata*), and Sitka spruce (*Picea sitchensis*). Deciduous broadleaf species include red alder (*Alnus rubra*), black cottonwood (*Populus trichocarpa*), and bigleaf maple (*Acer macrophyllum*). More than 75% of the Snohomish River basin is forested, with the vast majority in upland areas. The floodplains and neighboring foothills along the major river channels are located predominantly in rural-residential, agricultural, and urbanized areas. Nearly all salmon spawning and rearing occurs within the low-elevation western hemlock zone.

Returning adult coho salmon enter the Snohomish River from October through January to spawn in their natal streams, which are primarily small, gravel-bedded, low-gradient tributaries. Run timing and population status vary by stock, four of which (Snohomish, Skykomish, South Fork Skykomish, and Snoqualmie) are recognized as distinct stocks by the Washington Department of Fisheries and Wildlife (WDFW) and Western Washington Treaty Indian Tribes (WDFW and Western Washington Treaty Indian Tribes 1993). Coho salmon eggs incubate in spawning gravel through the winter and emerge as fry in March through May. After rearing in freshwater for one to two years, coho salmon smolts migrate to salt water usually during March and April. Most coho in the Snohomish spend 14–18 months in freshwater and 16–20 months in the Pacific Ocean before returning to spawn at 3 years of age.

Approach

Our approach included several steps. First, we characterized coho salmon distribution and abundance in the Snohomish River Basin of western Washington. We expressed local adult coho salmon population levels relative to the total population for the entire drainage basin and found strong interannual consistency in the spatial distribution of spawners. Next, we characterized multiple habitat characteristics at both the stream-reach and watershed area scales. Finally, we combined the spawner abundance data with the habitat data at each scale to identify relationships between adult coho salmon abundance levels and broad-scale habitat characteristics.

Data

Fish abundance data used in our analysis were based on annual surveys of spawning coho salmon collected by the WDFW at 54 index stream reaches from 1984 to 1998. The analysis approach we used requires data collected at numerous sites over a long period of time within a basin. The best salmon abundance data available over broad spatial and long temporal scales are adult salmon counts. Thus, our analysis compares adult salmon abundance with physical habitat characteristics.

Index reaches averaged 0.90 km in length, and ranged from 0.20 to 3.80 km. Each index reach was surveyed every 7–10 days from the beginning of November through January over the entire period of record. Abundance of spawners at the index reaches was reported as fish-days. Fish-days were calculated by multiplying the live fish observed on each survey date by the number of days between surveys. These values were then summed for the entire observation period to generate a relative index of spawner abundance at a reach for any given year.

Habitat geospatial data layers used in the analysis were characterized at two spatial scales: the reach and watershed. Habitat attributes were explored at two scales because the effects of certain factors on salmon are likely to be limited to the area immediately adjacent to the channel (reach scale), whereas the effect of other factors depends on upstream conditions (watershed scale). For example, a loss of forested riparian area may have a greater effect on reach-scale wood recruitment and subsequently reach-scale habitat characteristics (such as the loss of pools), whereas the influence of local geology on overall sediment input into the reach can only be captured on a watershed scale. Reach-level habitat data were delineated for the area within 100 m of the channel edge for each index reach and watershed-level data included the entire drainage area contributing to the downstream end of the index reach (Table 1; Fig. 2). Habitat data were determined for the index reaches by locating each reach on a 1 : 24 000 scale digital hydrographic data layer developed by the Washington Department of Natural Resources.

At each spatial scale, a wide array of habitat geospatial-related datalayers that represented natural (or landform variables) and anthropogenic (or land cover variables) characteristics were analyzed. All habitat data, with the exception of the potential for slope instability, were derived from existing data sources (Table 1). Potential for slope instability, a variable relating to sediment delivery to the index reach, was generated by a model that uses hill-slope gradient, drainage area, and slope form derived from a 10-m digital elevation model to estimate the relative potential for shallow landsliding (Montgomery and Dietrich 1994). Habitat data for the stream reach and watershed included geology (Booth 1990*a*), wetland abundance and type (Cowardian et al. 1979), wetland modification (defined as hydrologically altered wetlands that had been ditched or separated from the stream channel by bank armoring or diking) (Cowardian et al. 1979), land cover classification (forest, agriculture, rural, and urban), and the relative potential for slope instability.

© 2002 NRC Canada

Table 1. Summary table of stream reach and watershed-scale landform and land use data layers used in habitat analysis for the Snohomish River Basin, Washington.

Data layer	Source (year)	Category	Scale	Grid cell size/resolution	Description
Surficial geology	Booth (1990[a])	vashon till advance outwash recessional outwash undifferentiated drift alluvium bedrock peat	1 : 100 000	Vector data/polygons	Classification of geologic map units according to major surficial geology. All bedrock types were grouped together.
Wetlands	United States Fish and Wildlife Service National Wetlands Inventory (Cowardian et al. 1979)	% wetlands wetland class	1 : 58 000	Vector data/polygons	Classification of wetland types from aerial photo analysis.
Potential for slope instability	Montgomery and Dietrich (1994)	steady state rainfall values necessary to trigger slope failure		10 m	Relative index of topographic control on shallow landslide potential.
Land use and (or) land cover	Puget Sound Regional Council LANDSAT™ thematic mapper (1992)	forest rural residential agriculture urban roads	1 : 100 000	30 m	Classification of LANDSAT™ imagery into land cover categories developed from 1992 LANDSAT™ imagery.

Fig. 2. An example of the stream-reach and watershed area spatial analysis in the Snohomish River basin. Thick, solid, grey lines indicate 100-m buffer around index reaches. Broken black line denotes drainage area to an index reach.

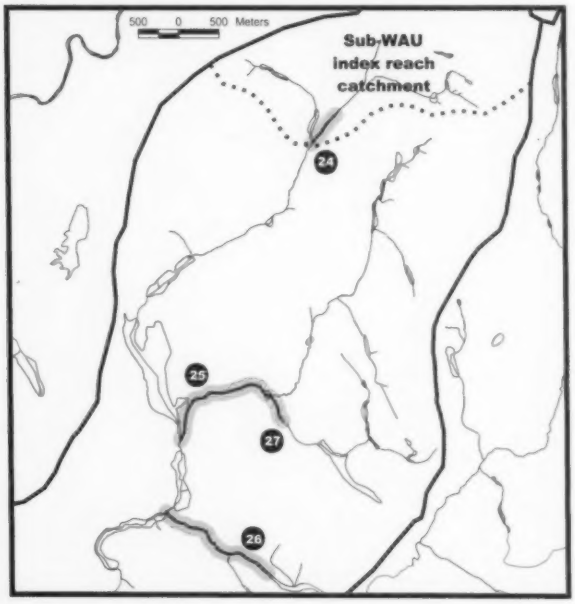

Data analysis

We examined the relationships between habitat characteristics and fish abundance using a simplified hierarchical linear model (HLM) (Bryk and Raudenbush 1992). Hierarchical models are common in the social sciences for modeling nested social units; for example, students within classrooms (Bryk and Raudenbush 1992). We used it here to describe nested observations: spawner counts within years. In biometric applications, these models are often called mixed- or random-effects models (Laird and Ware 1982). We used a simplified version of the hierarchical linear model because we were limited to only one estimate of fish abundance per site per year.

We examined the data using exploratory single-variable and multiple-regression models. In both cases, our analysis consisted of two steps. In the first step, we fit a weighted, log-linear model to each year of data independently; the model explained variation in fish density as a function of single habitat characteristics (for the exploratory analyses) or suites of habitat characteristics (for the explanatory models). Models were weighted by the inverse of the coefficient of variation in fish-days to reduce the impact of highly variable sites on the model parameters. In the second step, the distribution of regression coefficients over all years was examined for consistent patterns. Because of small sample sizes and concerns about distributional assumptions, the statistical significance of the pattern of regression coefficients was assessed using a randomization test (Good 1994). The observed t statistic, which tested whether or not the mean regression coefficient (over all years) was significantly different from zero, was compared with 1000 t statistics calculated from random permutations of the dependent variable (within year). An exact P value was calculated and expressed as the percent of t statistics from the permuted data sets that were more extreme than the observed t statistic. We used an alpha level of 0.002 to indicate a significant relationship. A conservative cutoff was chosen because of the multitude of statistical tests required to explore all potential predictors. We tested for sites with particularly high leverage, the ability to affect the regression coefficients dramatically, using a leave-one-out approach. No single site was responsible for the consistent patterns in regression coefficients over time.

To identify the suite of habitat characteristics most closely

© 2002 NRC Canada

associated with the sites that had the highest salmon abundance, we constructed a multiple regression model of salmon spawner abundance. Independent multiple regression models were developed using the stream-reach and watershed data. We examined only the main effects of habitat predictors because of our limited sample size and large number of potential predictors. Because of moderate correlation between potential predictors at both the reach and the watershed scale (Table 2), individual regression coefficients in the multiple regression context should be interpreted with caution; inference should be made about the suite(s) of habitat characteristics significantly associated with spawner abundance. Models were fit independently to each year of data and the behavior of the set of regression coefficients was analyzed over time. Coefficients in the final model were calculated as the mean of the coefficients from the independent annual models. The set of predictors used in the model was chosen using a backward and forward selection process. Final model selection was based on total adjusted r^2 (over all years), minimum adjusted r^2 (in any particular year), and statistical significance of all regression coefficients. For the reach-scale model, differences between model performance did not provide a clear break between one or two best models and the other possible models. As a result, we chose to present a set of best models.

Results

Adult coho salmon distribution and abundance

The proportion of total coho salmon abundance supported by particular index reaches in the Snohomish River basin was consistent over time, even though adult coho salmon return levels varied by a factor of three (Fig. 3). Relatively few reaches supported a large proportion of the fish. The 25% of the index reaches with the highest average abundance of spawning salmon accounted for nearly 50% of the fish counted in the index reaches. In contrast, the 25% of the index reaches with the fewest salmon on average supported less than 5% of the spawning coho salmon.

HLM analysis

Hierarchical linear modeling of the habitat variables against fish abundance revealed temporally consistent, statistically significant relationships for a number of stream-reach and watershed-scale variables (Figs. 4*a* and 4*b*; Table 3). At both the reach and watershed scales, there were negative correlations over time between coho abundance and the percentage of the area that is in urban and agricultural use, and positive correlations over time with the percentage of the area forested. Surficial geology also was related to salmon abundance. The percent of the drainage basin or riparian area underlain by shallow bedrock had a negative correlation at both spatial scales. In contrast, the proportion of peat and glacial till was positively related to salmon abundance at the watershed scale and peat was also positively correlated at the reach scale. Although there appear to be trends through time for some of the regression coefficients, few are significant, and in all but two cases, those trends that are significant are weak. In only two cases (percent recession outwash and percent potentially unstable slopes) was the ratio of the slope of the time trend over the mean regression coefficient

Table 2. Correlations between each of the potential predictor variables at the stream reach and watershed scales.

	Urban	Rural	Agriculture	Forest	Roads	Wetland	Water	Unstable slopes	Advanced outwash	Recessional outwash	Till	Peat	Alluvium	Bedrock	Stream gradient
Urban		**0.34**	**0.12**	**–0.41**	**0.18**	**0.06**	**–0.14**	**–0.09**	**0.28**	**0.35**	**–0.23**	**–0.19**	**–0.13**	**0.01**	**–0.08**
Rural	0.58		**–0.09**	**–0.53**	**0.21**	**0.08**	**–0.18**	**–0.16**	**0.43**	**–0.03**	**–0.10**	**–0.19**	**0.08**	**0.00**	**–0.09**
Agriculture	0.32	0.13		**–0.66**	**–0.18**	**–0.10**	**0.00**	**–0.20**	**0.06**	**0.06**	**–0.44**	**–0.15**	**0.29**	**–0.05**	**–0.14**
Forest	–0.70	–0.88	–0.46		**–0.12**	–0.09	0.08	0.36	–0.23	–0.11	0.42	0.25	–0.21	0.06	0.21
Roads	0.41	0.70	0.16	–0.66		**0.06**	**–0.02**	**–0.03**	**0.26**	**–0.07**	**0.01**	**–0.13**	**–0.03**	**–0.11**	**0.18**
Wetland	0.06	0.33	0.04	–0.34	0.11		**0.27**	**–0.19**	**0.24**	**0.04**	**–0.17**	**0.15**	**0.02**	**–0.18**	**–0.33**
Water	0.17	0.06	0.17	–0.22	–0.07	0.47		**–0.22**	**–0.12**	**–0.28**	**–0.13**	**–0.09**	**0.37**	**–0.10**	**0.03**
Unstable slopes	–0.24	–0.68	0.01	0.55	–0.42	–0.21	0.07		**0.07**	**–0.13**	**0.17**	**0.32**	**0.05**	**0.10**	**0.31**
Advanced outwash	0.27	0.59	0.28	–0.57	0.50	0.20	0.22	–0.39		**–0.26**	**–0.05**	**–0.11**	**–0.02**	**–0.11**	**–0.13**
Recessional outwash	0.33	0.10	0.09	–0.14	–0.06	–0.15	–0.07	–0.11	–0.18		**–0.30**	**0.11**	**–0.55**	**0.17**	**–0.14**
Till	–0.09	0.42	–0.30	–0.21	0.23	0.28	–0.27	–0.59	0.34	–0.31		**0.03**	**–0.45**	**–0.17**	**0.05**
Peat	–0.09	–0.03	–0.18	0.09	0.00	0.41	–0.07	–0.12	–0.08	–0.12	0.23		**–0.19**	**0.19**	**0.08**
Alluvium	0.14	–0.18	0.41	–0.03	–0.04	–0.09	0.20	0.36	–0.24	–0.12	–0.61	–0.03		**–0.10**	**0.12**
Bedrock	–0.01	–0.50	0.20	0.36	–0.37	–0.24	0.29	0.62	–0.36	–0.01	–0.84	–0.21	0.52		**0.07**
Drainage area	0.15	–0.13	0.17	–0.11	–0.10	0.27	0.31	0.06	0.05	–0.13	–0.06	0.27	0.23	0.03	

Note: Bolded numbers in upper right (above the diagonal) are reach-scale variables. Numbers in lower left (below the diagonal) are watershed-scale variables. For those variables that were transformed in the analysis (Table 3), correlations are presented for the transformed data.

© 2002 NRC Canada

Fig. 3. Percentage of adult coho salmon returns (in fish-days) per kilometre of stream length to each index site (1984 to 1998). Open squares are median values; top and bottom of open rectangles are the 25th and 75th percentiles, respectively; horizontal lines at the top and bottom are 5th and 95th percentiles, respectively; and open circles are outliers.

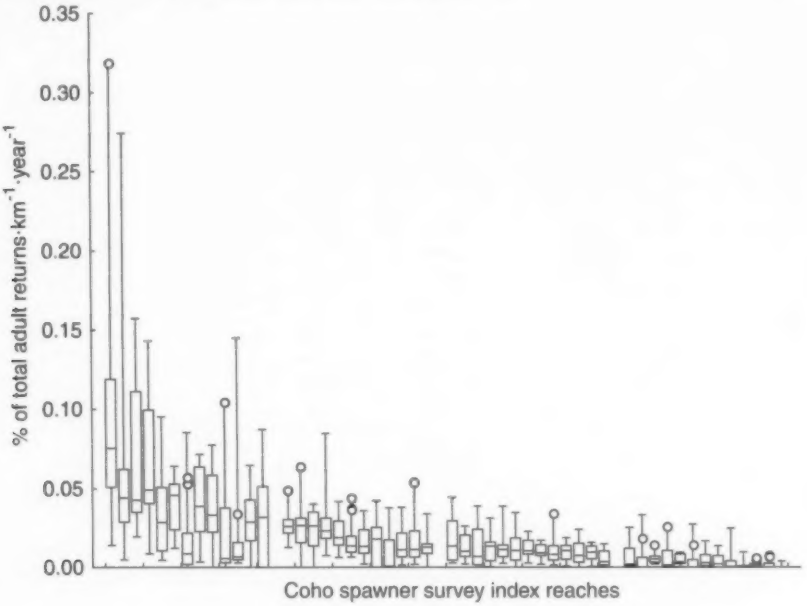

greater than 1; in nearly all other cases this ratio was less than 0.2. Although there may be some subtle shifts in the effects of certain habitat variables over time, these shifts are minor when compared with the magnitude of the correlation of the habitat variable.

Three predictive models were developed at the reach scale, using different combinations of habitat variables (Table 4). The three models explained similar amounts of the variability in salmon spawner abundance. One model was developed at the watershed scale. Model fit ranged between an adjusted multiple r^2 of 0.20 to 0.42 (Fig. 5). Land-use variables were major factors in all of the final models at both spatial scales.

Land cover and landscape variables

The magnitude of the correlation of some of the land use variables on salmon abundance becomes clear when relative abundance is plotted against these attributes. Index reaches bordered by lands designated as forest supported far more fish than areas under other types of land use. Average adult coho salmon abundance increased with an increase in proportion of the streamside area in forest at the reach scale (Fig. 6*a*). Average adult coho salmon abundance in index reaches where more than 50% of the riparian area was designated as forest land was 1.5–3.5× greater than in index reaches with less than 50% forest. In addition, the 10 index reaches supporting the highest salmon abundance were forested over 60% of the riparian area (Fig. 6*a*). Average coho salmon abundance was positively correlated with amount of forest at the watershed scale (Fig. 6*b*). An increase in percent total area of other land use categories (e.g., rural, agriculture, urban) at the reach and watershed scales was negatively correlated with adult coho salmon abundance. Salmon abundance was two to three times greater in index reaches that had less than 10% of the contributing watershed in agriculture (Fig. 6*c*).

Discussion

Implications of correlating habitat characteristics and adult coho salmon distribution and abundance

Our analysis provides a method to identify which habitat attributes correlate with the greatest adult coho salmon abundance and identifies their location based on 14 years of record. Even though substantial variability in salmon abundance remained unexplained by our multivariate models, our model fit was similar to what others have found linking more site-specific habitat variables to coho response (Rosenfield et al. 2000). Our results show that adult coho abundance is correlated to a suite of habitat characteristics shared by sites across space and time, despite interannual variation in population size. Given the high degree of spatial variability in salmon abundance, our results indicate that population monitoring should occur at multiple sites representative of the range of conditions occurring in the watershed. The consistency between these correlative results and our mechanistic understanding of the relationship between salmonids and their habitats suggest that these patterns will remain consistent over time. Our study also demonstrates the utility of this approach for evaluating the role of habitat conditions on salmon abundance.

Understanding the habitat characteristics of a watershed associated with the spatial distribution of salmon abundance

© 2002 NRC Canada

Fig. 4. Relationships of individual predictors at (*a*) the stream-reach scale and (*b*) the watershed scale to the natural log of fish-days over time. The *y* axis describes the mean regression coefficient ± 2 SE for natural log of fish-days as a function of one independent variable. All variables are calculated as a percent of the watershed area of influence except drainage area (km^2), roads (road density in $km \cdot km^{-2}$), and stream channel gradient. Stream channel gradient was calculated as the elevation change (m) divided by index reach length (m) multiplied by 100, and was determined for each index reach using 1 : 24 000 scale United States Geological Survey (USGS) quadrangle maps. Wetland modification was determined by the United States Fish and Wildlife Service (USFWS) National Wetlands Inventory (NWI).

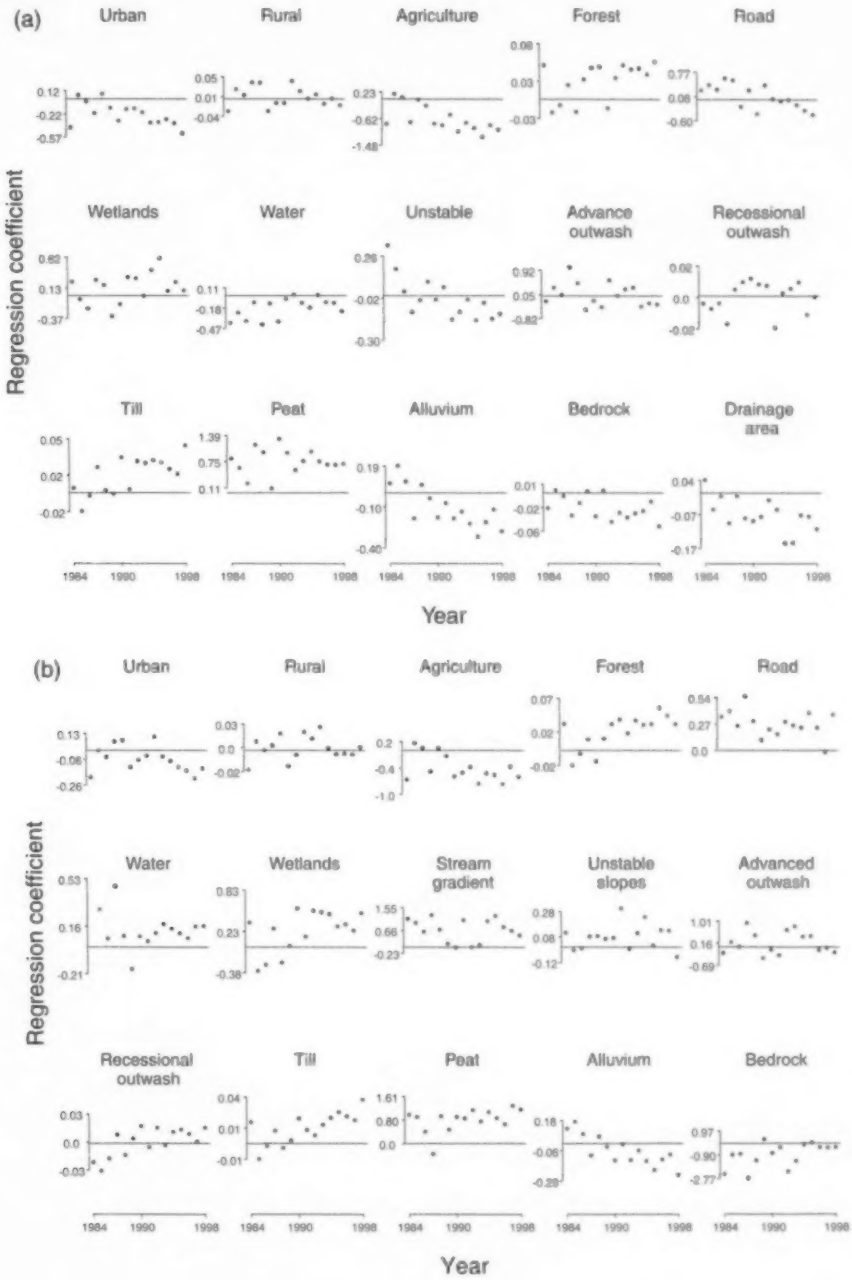

© 2002 NRC Canada

Table 3. Summary of exploratory analysis results.

		Watershed scale		Reach scale	
Variable	Transformation	Mean	*P* value	Mean	*P* value
Urban	log(x + 0.001)	–0.222	0	–0.065	0.022
Rural		0.005	0.390	0.003	0.394
Agriculture	log(x + 0.1)	–0.622	0	–0.282	0
Forest		0.026	0	0.025	0
Roads		0.083	0.412	0.274	0
Percent wetlands	Square root	0.128	0.088	0.229	0.018
Nonmodified wetland	Indicator (1 = non-modified)			0.638	0
Wetland	Indicator (1 = wetland)			0.543	0
Channel gradient				0.661	0
Lowest channel gradient	Square root			0.102	0.320
Water	log(x + 0.01)	–0.180	0	0.162	0.010
Partially unstable ground	log(x + 0.001)	–0.016	0.670	0.080	0.008
Advance outwash	Indicator AdvOut <0.1	0.049	0.634	0.157	0.178
Recessional outwash		–0.001	0.680	0.001	0.742
Till		0.016	0	0.013	0.004
Peat	Indicator peat <0.1	0.749	0	0.803	0.002
Alluvium	log(x + 0.0001)	–0.103	0.030	–0.055	0.110
Bedrock		–0.023	0	–0.186	0
Drainage area		–0.066	0		

Note: Independent variables were transformed to stabilize the variance by the function identified in the transformation column. The mean columns describe the mean coefficient over all years for linear regression models using only one independent variable to predict the natural log of adult coho returns·km^{-1}. *P* values are from randomization tests (1000 iterations).

Table 4. Reach- and watershed-scale predictive models.

Area of influence	Equation
Reach	= 3.89 – 0.18 · %bedrock + 0.27 · roads (km·km^{-2}) + 0.028 · %forest
	= 378 – 0.25 · ln(%agriculture + 0.01) + 0.22 · %bedrock + 0.56 · sqrt(gradient(m·m^{-1})) + 1.29 · *I*(%peat > 0.1)
	= 3.14 + 0.027 · %forest + 0.32 · roads (km·km^{-2}) + 0.26 · sqrt(%wetlands)
Watershed	= 6.49 – 0.32 · ln(%agriculture + 0.01) – 0.011·%till 0.029 · %bedrock0.13 · ln(%urban + 0.001)

Note: Response variable is the natural log of adult coho returns (fish days)·km^{-1}. *I* stands for indicator of peat.

Fig. 5. Adjusted *r*-squared values for the four predictive models. Filled circles denote watershed model. Open squares denote average for three reach models.

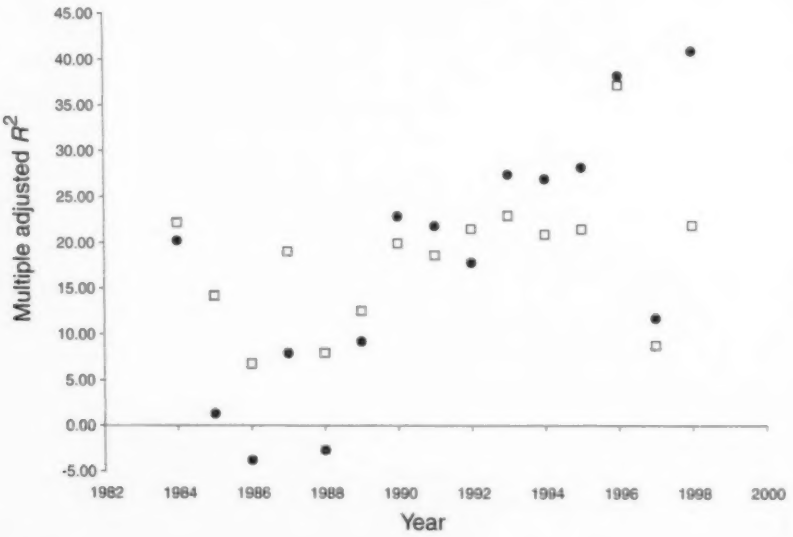

© 2002 NRC Canada

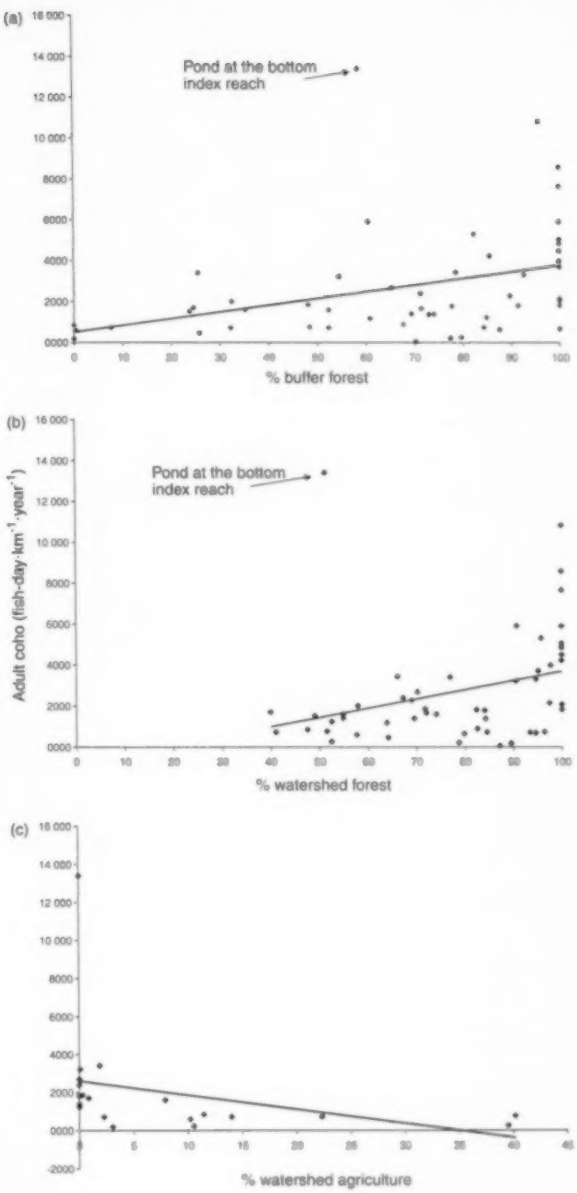

Fig. 6. (*a*) Average adult coho salmon return per kilometre of stream length per year in fish-days versus percent of 100-m buffer that was forested. Regression equation is average adult coho salmon per kilometre of stream length per year = 513 + 32.7(% of 100-m forested buffer) (r^2 = 0.22, P = 0.007). (*b*) Average adult coho salmon return per kilometre of stream length per year in fish-days versus percent of total upstream drainage area that was forested. Regression equation is average adult coho salmon per kilometre of stream length per year = –824 + 45.3(% total upstream drainage area that is forested) (r^2 = 0.28, P = 0.02). (*c*) Percent of total drainage area upstream of index reach that was agricultural and average adult coho salmon per kilometre of stream length per year in fish-days. Regression equation is average adult coho salmon per kilometre of stream length per year = 3007 – 89.6 (% of total drainage area that was agricultural) (r^2 = 0.28, P = 0.04).

provides a means of prioritizing areas for protection or restoration based on their contribution to overall abundance levels. For example, this approach could either be used to identify sites with potentially greater abundance levels that are currently impaired by land use or be used to identify existing high-abundance areas with a high risk of habitat degradation in the future. Restoration activities could also be prioritized to first address those impaired locations with the appropriate habitat attributes to support high salmon abundance. For example, in the Snohomish River basin, these priority restoration sites would include forested locations with wetlands that have been modified. Maintaining and restoring these sites is considered critical to the long-term recovery of salmonids in the watershed, especially during periods when ocean conditions are unfavorable (Bradford and Irvine 2000).

Temporal changes in adult coho salmon distribution and abundance

The variability explained by the models differed dramatically among years, suggesting that fish are distributing themselves differently in different years. It is also possible that changes over time in those habitat variables included in the model might contribute to variability in model fit. Such changes would be found in the land-use variables, percent-agricultural area, percent-urbanized area, percent-forested area, and road density. A time-series of remotely sensed data describing changes in land use over the entire basin might be used to test this possibility. The low correlation coefficients of the models also suggest that variables for which no data were available may play a role in determining abundance patterns for different reaches. These patterns might be influenced by habitat factors that vary annually (e.g., flow, water temperature) or by the influence of variables other than large-scale habitat characteristics such as ocean conditions.

Landscape characteristics, land use, and adult coho salmon distribution and abundance

The correlations between landform and coho salmon abundance that we detected are consistent with our understanding of how underlying physical attributes can influence fish habitat potential. Geology and geomorphic processes dictate the range of morphological characteristics a stream reach can exhibit, thus partially determining the physical and biological characteristics of fish habitat (Montgomery and Buffington 1998). We suspect that in the Snohomish Basin areas dominated by bedrock terrain generally produce channels that are too steep to support spawning habitat for coho salmon. Steep channels also lack the pool habitat favored by coho salmon for rearing (Bisson et al. 1982) and often possess very limited amounts of gravel used by the fish for spawning (Beechie and Sibley 1997).

The relationship between spawner abundance and land-use activities also indicates that adult coho densities reflect large-scale land-use patterns. We found that forested areas

© 2002 NRC Canada

maintained positive correlations to spawner abundance, whereas those converted for agricultural or urban uses had negative correlations to spawner abundance. Wetlands and other indicators of wetland environments, like peat, also had consistent positive correlations to spawner abundance.

Human disturbances, such as agriculture and urbanization, can lead to a decrease in coho salmon habitat availability and quality (Beechie et al. 1994; Bradford and Irvine 2000). A study in the nearby Skagit River watershed revealed a decrease in tributary and off-channel habitats (e.g., wetlands, sloughs, and ponds) of up to 75%, almost all of which was due to deliberate modifications of the channel and floodplain (Beechie et al. 1994). The vast majority of these impacts are related to the conversion of forested areas to agricultural and subsequently to residential use. Maintained channelization can increase channel incision to the point where the streambed is disconnected from its floodplain (Booth 1990*b*). Floodplain isolation reduces the amount of off-channel habitat available for adult salmonid spawning and juvenile rearing, which can lead to the downstream displacement of newly emerged salmonids to less-desirable habitats (Seegrist and Gard 1972; Erman et al. 1988). Stream cleaning and riparian vegetation removal reduces the amount of in-channel wood, leading to a loss of pool habitat quantity (Montgomery et al. 1995; Collins et al. 2002), which can substantially reduce coho redd density (Montgomery et al. 1999).

Urbanization can lead to an increase in impervious surface area and increase stream-flooding frequency and magnitude (Hollis 1975). The pre-urbanized 10-year recurrence interval flow event can occur every 2–5 years in urbanized areas of the Puget Sound region (Booth 1990*b*), which can lead to declines in adult coho (Moscrip and Montgomery 1997). Urban watersheds also generate high concentrations of compounds that are toxic to salmon or alter their behavior in ways that could reduce survival (Scholz et al. 2000).

Acknowledgements

We thank Don Hendrick, Larry Lowe, and Curt Kraemer of the Washington Department of Fish and Wildlife for giving us the spawner survey data and showing us many of the spawner survey index reaches. We thank Dick Gersib and Susan Grigsby of the Washington State Department of Ecology for providing many of the GIS data layers. We thank Peter Kiffney, Phil Roni, Bill Reichert, John Stein, Jason Dunham, and one anonymous reviewer for providing constructive comments on earlier versions of the manuscript.

References

Beechie, T.J., Beamer, E., and Wasserman, L. 1994. Estimating coho salmon rearing habitat and smolt production losses in a large river basin, and implications for restoration. N. Am. J. Fish. Manag. **14**: 797–811.

Beechie, T.J., and Sibley, T.H. 1997. Relationships between channel characteristics, woody debris, and fish habitat in northwestern Washington streams. Trans. Am. Fish. Soc. **126**: 217–229.

Bisson, P.A., Nielson, R.A., Palmason, R.A., and Gore, L.E. 1982. A system of naming habitat types in small streams with examples of habitat utilization by salmonids during low stream flow. *In* Acquisition and utilization of aquatic habitat information. *Edited by* N.A. Armatrout. American Fisheries Society, Bethesda, Md. pp. 62–73.

Booth, D.B. 1990*a*. Surficial geologic map of the Skykomish and Snoqualmie rivers area, Snohomish and King counties, Washington. U.S. Department of the Interior, U.S. Geological Survey, miscellaneous investigations series, Map I-1745. Denver, Colo.

Booth, D.B. 1990*b*. Stream channel incision following drainage basin urbanization. Water Resour. Bull. **26**: 407–417.

Bradford, M.J., and Irvine, J.R. 2000. Land use, fishing, climate change, and the decline of Thompson River, British Columbia, coho salmon. Can. J. Fish. Aquat. Sci. **57**: 13–16.

Bryk, A.S., and Raudenbush, S.W. 1992. Hierarchical linear models. Sage publications, Newbury Park, Calif.

Collins, B.D., Montgomery, D.R., and Haas, A. 2002. Historical changes in the distribution and functions of large wood in Puget Lowland rivers. Can. J. Fish. Aquat. Sci. **59**: 66–76.

Cowardian, L.M., Carter, V., Golet, F.C., and LaRoe, E.T. 1979. Classification of wetland and deepwater habitats of the United States. FWS/OBS-79/31. U.S. Fish and Wildlife Service, U.S. Department of the Interior. Washington, D.C.

Erman, D.C., Andrews, E.D., and Yoder-Williams, M. 1988. Effects of winter floods on fishes in the Sierra Nevada. Can. J. Fish. Aquat. Sci. **45**: 2195–2200.

Everest, F.H., Beschta, R.L., Scrivener, J.C., Koski, K.V., Sedell, J.R., and Cederholm, C.J. 1987. Fine sediment and salmonid production – a paradox. *In* Streamside management and forestry and fishery interactions. *Edited by* E. Salo and T. Cundy. University of Washington, College of Forest Resources, Contribution 57, Seattle, Wash. pp. 98–142.

Franklin, J.F., and Dyrness, C.T. 1973. Natural vegetation of Oregon and Washington. U.S. For. Serv. Gen. Tech. Rep. PNW-8.

Good, P. 1994. Permutation tests: a practical guide to resampling methods for testing hypotheses. Springer-Verlag, New York.

Hollis, G.E. 1975. The effects of urbanization on floods of different recurrence intervals. Water Resour. Res. **11**: 431–435.

Holtby, L.B., and Scrivener, J.C. 1989. Observed and simulated effects of climate variability, clear-cut logging, and fishing on the numbers of chum salmon (*Oncorhynchus keta*) and coho salmon (*O. kisutch*) returning to Carnation Creek, British Columbia. Can. J. Fish. Aquat. Sci. Contrib. No. 124 of the Carnation Creek Experimental Watershed Project. pp. 62–81.

Laird, N.M., and Ware, H. 1982. Random effects models for longitudinal data. Biometrics, **38**: 963–974.

Montgomery, D.R., and Buffington, J.M. 1998. Channel processes, classification, and response potential. *In* River ecology and management. *Edited by* R.J. Naiman and R.E. Bilby. Springer-Verlag Inc., New York. pp. 13–42.

Montgomery, D.R., and Dietrich, W.E. 1994. A physically based model for the topographic control on shallow landsliding. Water Resour. Res. **30**: 1153–1171.

Montgomery, D.R., Buffington, J.M., Smith, R.D., Schmidt, K.M., and Pess, G.R. 1995. Pool spacing in forest channels. Water Resour. Res. **31**:1097–1105.

Montgomery, D.R., Beamer, E.M., Pess, G.R., and Quinn, T.P. 1999. Channel type and salmonid spawning distribution and abundance. Can. J. Fish. Aquat. Sci. **56**: 377–387.

Moscrip, A.L., and Montgomery, D.R. 1997. Urbanization, flood frequency, and salmon abundance in Puget lowland streams. J. Am. Water Resour. Assoc. **33**: 1289–1297.

Reeves, G.H., Everest, F.H., and Nickelson, T.E. 1989. Identification of physical habitats limiting the production of coho salmon in western Oregon and Washington. U.S. For. Serv. Gen. Tech. Rep. PNW-GTR-245.

Rosenfield, J., Porter, M., and Parkinson, E. 2000. Habitat factors affecting the abundance and distribution of juvenile cutthroat

© 2002 NRC Canada

trout (*Oncorhynchus clarki*) and coho salmon (*Oncorhynchus kisutch*). Can. J. Fish. Aquat. Sci. **57**: 766–774.

Scholz, N.L., Truelove, N.K., French, B.L., Berejikian, B.A., Quinn, T.P., Casillas, E., and Collier, T.K. 2000. Diazinon disrupts anitpredator and homing behaviors in Chinook salmon (*Oncorhynchus tshawytscha*). Can. J. Fish. Aquat. Sci. **57**: 1911–1918.

Seegrist, D.W., and Gard, R. 1972. Effects of floods on trout in Sagehen Creek, California. Trans. Am. Fish. Soc. **101**: 478–482.

Washington Department of Fisheries and Wildlife (WDFW) and Western Washington Treaty Indian Tribes. 1993. Washington State salmon and steelhead stock inventory (SASSI): appendix 1. Puget Sound stocks, north Puget Sound volume. Washington Department of Fisheries and Wildlife. Olympia, Wash.

© 2002 NRC Canada

Estimation of mortality of juvenile blacktip sharks, *Carcharhinus limbatus*, within a nursery area using telemetry data

M.R. Heupel and C.A. Simpfendorfer

Abstract: A population of young blacktip sharks (*Carcharhinus limbatus*) was monitored over three years to determine their mortality rates using a series of acoustic listening stations. Based on these data it was possible to use several mortality estimators, including indirect life history based methods and direct methods such as the Kaplan-Meier and SURVIV methods, to estimate natural, fishing, and total mortality. Kaplan-Meier (61–91%) and SURVIV (62–92%) methods provided nearly identical total mortality rates during the first six months of life. This agreement suggests that these estimates are accurate for this population. All natural and fishing mortality occurred within the first 15 weeks of the study. This suggests that young sharks are most vulnerable to all types of mortality during this period. Sharks that survived beyond the first 15 weeks successfully left the nursery and were presumed to have migrated southward during fall months. These results provide critical information concerning the early life history of sharks and the importance of nursery areas to the survival of young animals.

Résumé : Un réseau de stations d'écoute nous a permis de suivre une population de jeunes requins bordés (*Carcharhinus limbatus*) pendant 3 ans pour en déterminer les taux de mortalité. Il a été possible avec ces données acoustiques d'utiliser divers estimateurs de la mortalité, en particulier des méthodes démographiques indirectes et des méthodes directes, telles que celle de Kaplan-Meier et SURVIV, pour estimer la mortalité naturelle, la mortalité due à la pêche et la mortalité totale. Les méthodes de Kaplan-Meier (61–91 %) et SURVIV (62–92 %) donnent des estimations presque identiques de la mortalité totale durant les premiers 6 mois de vie. Cet accord laisse croire que ces estimations sont exactes pour cette population. Toute la mortalité naturelle et la mortalité due à la pêche se sont produites pendant les 15 premières semaines de l'étude, ce qui fait penser que les jeunes requins sont vulnérables aux diverses causes de mortalité durant cette période. Les requins qui survivent au-delà de cette période initiale de 15 semaines quittent la zone d'alevinage et migrent sans doute vers le sud durant les mois d'automne. Ce sont là des renseignements essentiels sur les premières étapes du cycle biologique des jeunes requins et sur l'importance des zones d'alevinage pour la survie des jeunes.

[Traduit par la Rédaction]

Introduction

Estimation of mortality is a critical factor in determining the status of fished species and is typically one of the most difficult parameters to define. Many scientists have estimated the mortality of fishes, including sharks, based on life history characteristics (e.g., Pauly 1980; Vetter 1988; Simpfendorfer 1999*a*). However, as Branstetter (1990) pointed out, many of these analyses are based on the adult portion of the population. In fact, to account for the higher vulnerability of young sharks to natural mortality, researchers routinely double estimates calculated from life history methods to represent increased mortality of the first year class (e.g., Smith and Abramson 1990; Sminkey and Musick 1996; Simpfendorfer 1999*b*). Unfortunately, this calculation is often made with no direct evidence concerning the survivorship of this portion of the population. The early life history of elasmobranchs may be a critical period for recruitment, and survival of young sharks and needs to be examined more closely.

Survival estimates in terrestrial studies are commonly calculated from telemetry data and these methods have recently been applied to aquatic populations (e.g., Bendock and Alexandersdottir 1993; Hightower et al. 2001). The use of telemetry data allows the researcher to define the fate of animals within the study site by continuously monitoring or relocating an animal. This removes the need to recapture marked individuals or to rely on tag reports from other individuals. Advancements in telemetry technology are providing opportunities to use these methodologies in aquatic systems where mortality estimates have mostly been based on life history characteristics or mark-recapture data. Mortality data have been particularly sparse in relation to juvenile stages of aquatic populations, and elasmobranchs are no exception.

Many coastal elasmobranch species are known to use nursery areas (e.g., Branstetter 1990; Castro 1993; Simpfendorfer and Milward 1993). These areas are mostly shallow-water, nearshore areas of high productivity that are thought to provide

Received 29 November 2001. Accepted 28 March 2002. Published on the NRC Research Press Web site at http://cjfas.nrc.ca on 2 May 2002.
J16640

M.R. Heupel[1] and C.A. Simpfendorfer. Center for Shark Research, Mote Marine Laboratory, Sarasota, FL 34236, U.S.A.

[1]Corresponding author (e-mail: mheupel@mote.org).

 DOI: 10.1139/F02-036 © 2002 NRC Canada

young sharks with ample food and protection from predators. These characteristics theoretically make the use of nursery areas critical to the survival of young sharks. However, the precise benefits and costs to young sharks living in nursery areas, and in particular their rates of mortality within these areas, are largely unknown. In this paper we will describe mortality for a population of juvenile blacktip sharks (*Carcharhinus limbatus*) within a coastal nursery area based on long-term acoustic telemetry data.

Materials and methods

Study site

Terra Ceia Bay, a small bay adjacent to the southeastern region of Tampa Bay along the Gulf of Mexico coast of Florida, is a nursery area for neonate and juvenile *C. limbatus*. The open water area of Terra Ceia Bay is approximately 10 km^2 with a maximum water depth of approximately 4 m. The bay is fringed by mangroves, has one major opening where it joins Tampa Bay (Fig. 1), and has a limited freshwater input in the extreme northern portion of the bay. Water quality parameters (e.g., salinity, temperature, dissolved oxygen) are similar throughout the study site (M.R. Heupel, unpublished data), which has a daily tidal range of less than 1 m.

Terra Ceia Bay is commonly used as a nursery area by neonate and juvenile *C. limbatus* from May to November (Heupel and Hueter 2001). Pups are born in May–June and migrate from the nursery area when water temperatures decline in the fall. Although general information about pupping time and location of nursery areas is well known (e.g., Castro 1993), the use of the nursery during the early life history of *C. limbatus* is still unclear.

Field methods

Blacktip sharks were collected by rod and reel fishing, were landed in less than one minute and fitted with 16 × 65 mm acoustic transmitters (Vemco Ltd., Nova Scotia). Transmitters were surgically implanted into the abdominal cavity of sharks using the same procedure in all years. Sharks were anesthetized prior to insertion of the transmitter, were stitched under anesthetic and were revived post-surgery in an oxygenated bath of fresh seawater (see Heupel and Hueter 2001 for detailed methods). All sharks were marked with an external dart tag (Hallprint, South Australia) for identification purposes, measured, weighed, sexed, length of handling time recorded, and condition of release assessed. Upon release, the long-term movement patterns of sharks were recorded by a series of acoustic listening stations (Heupel and Hueter 2001; Simpfendorfer et al. 2002). The acoustic array allowed sharks to be continuously monitored for the entire period they were present within the nursery area.

Animal release condition was assessed as follows (based upon a rating system developed by Hueter and Manire 1994): condition 1 (good), no revival time required when shark is returned to the water, rapid swimming upon release, usually with a vigorous splash; condition 2 (fair), no revival time required when shark is returned to the water, slow but strong swimming upon release; condition 3 (poor), short revival time (up to 30 s) required, slow but sometimes atypical swimming upon release; condition 4 (very poor), long revival time (more than 30 s), limited or no swimming observed upon release but respiration functional.

Defining fates of tagged sharks

The fate of individuals in the nursery area was determined through analysis of the long-term monitoring data. Sharks were classified into three categories. (*i*) Survivals; individuals that maintained continuous movement within the study site and (or) were observed to swim out of the study site. (*ii*) Natural mortalities; individuals that ceased movement within the study site or showed movement patterns more rapid than, and inconsistent with previous or typical movements (consistent with the faster rate of movement of a large predator that had consumed the small shark). This category includes all types of natural mortality (e.g., predation, starvation, disease). (*iii*) Removals (censored); individuals removed from the study site because of factors other than natural mortality or swimming out, such as harvest by fishermen. These individuals were typified by loss of signal detection from the animal while it was within the acoustic array. Many of these instances were validated by tag and (or) transmitter returns from recreational fishermen. Although removals could include transmitter failure, it was assumed that transmitter failure would be negligible. This assumption is based on the large numbers of transmitters that functioned throughout the duration of the season and that all transmitters returned by fishermen were still functioning. The study site is a very popular location for recreational fishermen and it is more likely that these animals were harvested. The fate of each individual was assigned to one of these categories at the end of each week to construct monitoring histories.

A generalized linear model with a logistic link function was used to test if a range of release factors (shark size, shark sex, water temperature, handling time, release condition) influenced the chances of postrelease mortality. For this analysis, animals that were swimming in the study site at least 90 days after release and those that had swum out of the study site were considered to have survived. Individuals that were captured by fishermen also were considered to have survived since fishing mortality is not considered to be a source of postrelease mortality.

Mortality estimation from life history data

Natural mortality of *C. limbatus* was estimated using a range of indirect techniques based on life history data to provide a comparison to those estimated from telemetry data. Six estimators of constant lifetime mortality (Pauly 1980; Hoenig 1983; Jensen 1996) and one method of age-specific mortality (Peterson and Wroblewski 1984) were used. The Peterson and Wroblewski (1984) method uses age-specific weight to estimate natural mortality

$$M = 1.92W_a^{-0.25}$$

where W_a is the weight at age a in grams. All life history data for *C. limbatus* were taken from Killam and Parsons (1989) and Castro (1996).

Kaplan-Meier estimation

Survival of juvenile *C. limbatus* was estimated with the nonparametric Kaplan-Meier procedure (Cox and Oakes 1984; Pollock et al. 1989*a*, 1995). This approach computes

© 2002 NRC Canada

Fig. 1. Map of the study site, Terra Ceia Bay, and its location on the Gulf of Mexico coast of Florida. Circles represent the locations of acoustic hydrophones inside the study area, cross-hatching indicates seagrass beds.

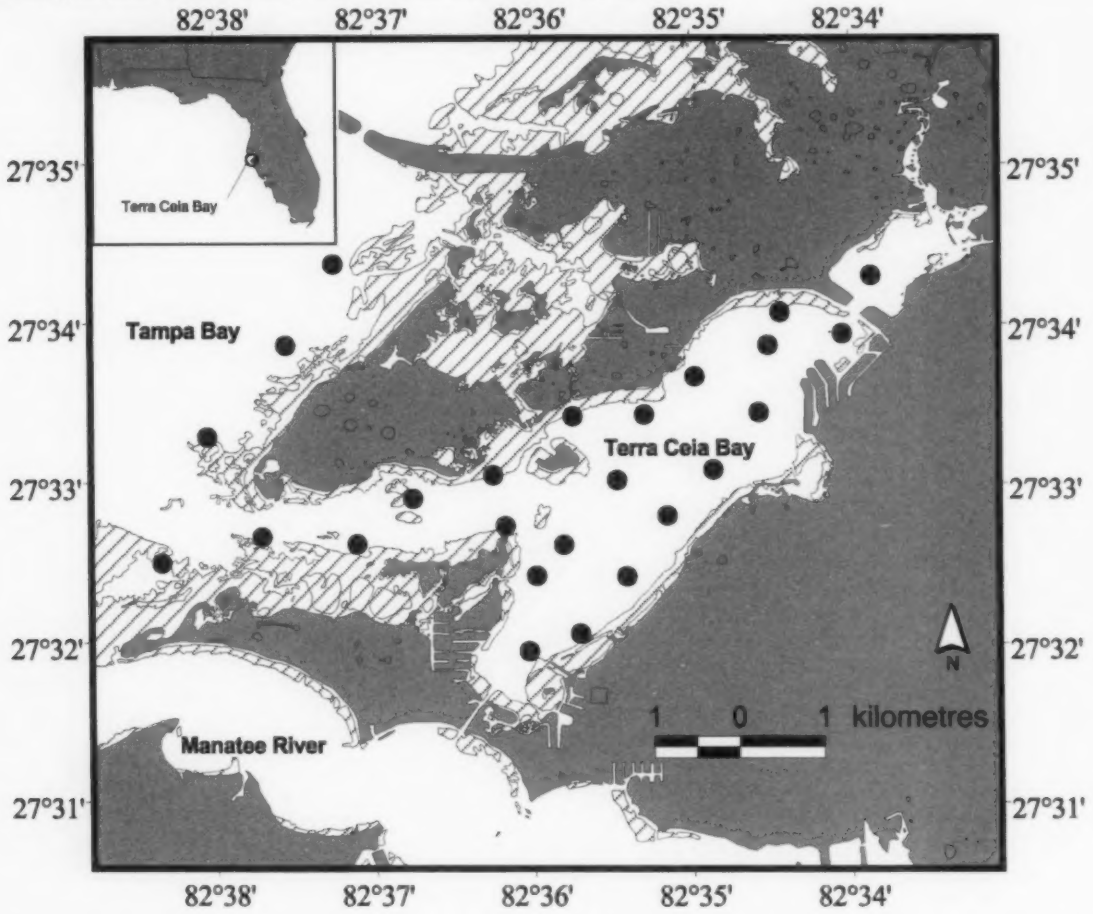

the proportion of fish that die within the study period and allows for animals that are censored from the population (Pollock et al. 1989*b*).

Survival estimates are based on the Kaplan-Meier staggered entry method as defined by Pollock et al. (1989*b*)

$$\hat{S}(t) = \prod (1 - d_j / r_j)$$

where $\hat{S}(t)$ is the survival function (the probability of an arbitrary animal in a population surviving t units of time from the beginning of the study), d_j is the number of deaths at time j, and r_j is the number of animals at risk at time j. The number of animals at risk in one time period included the number of animals present at the end of the previous period, plus the number added in the previous period, minus the number of deaths and censored animals. In this calculation the number of animals censored included those that were recorded to have swum out of the study site. Variance was calculated by

$$\text{var}(\hat{S}[t]) = \frac{[\hat{S}(t)^2][1 - \hat{S}(t)]}{r(t)}$$

as discussed by Cox and Oakes (1984). Two forms of survival were calculated. The first was with the number of deaths equal to the number of animals that had died from all sources of mortality except fishing (referred to as survival from natural mortality). The second was with the number of deaths equal to those censored (removed via fishing), and was referred to as survival from fishing mortality.

Program SURVIV estimates

Natural and fishing mortality were estimated from the telemetry data using a method described by Hightower et al. (2001) for striped bass. This method considers that for R_i animals released in the study site at time t, the expected number of animals surviving at time $t + 1$ (S_{t+1}) (here t is one week) is

$$S_{t+1} = R_t e^{-F_t - M_t} p_{t+1}$$

where F_t is the instantaneous fishing mortality during period t, M_t is the instantaneous natural mortality during period t, and p_{t+1} is the probability of relocating animals at time $t + 1$. The expected number of deaths of fish relocated at time $t + 1$ (D_{t+1}) is

© 2002 NRC Canada

Fig. 2. Monitoring histories of sharks (*Carcharhinus limbatus*) for (*a*) 1999, (*b*) 2000, and (*c*) 2001. Week one is the second week of May in each year. The fate of individuals is listed at the end of the animal history where S is survival (swam out of the study site), M is natural mortality, and R is removal (fished).

© 2002 NRC Canada

Table 1. Effect of release factors on time of mortality of neonate *Carcharhinus limbatus*.

Effect	Degrees of freedom	Wald statistic	*p*
Intercept	1	1.6277	0.2020
Size (fork length)	1	1.0502	0.3055
Handling time	1	0.4047	0.5247
Water temperature	1	0.7026	0.4019
Sex	1	1.0949	0.2954
Release condition	1	3.1892	0.0741
Sex * release condition	1	1.4137	0.2344

Note: Results of a generalized linear model with a binomial error distribution and a logit link function.

$$D_{t+1} = R_t M_t \frac{1 - e^{-F_t - M_t}}{F_t + M_t} p_{t+1}$$

Animals that survive to time $t + 1$ are then considered releases for the next time period and were added to new releases in that period.

Since the acoustic system used in the current study provided practically total coverage in the study site on a continuous basis we assumed that $p = 1$. Thus, unlike Hightower et al. (2001), it was not necessary to consider the possibility that an animal had died during one period, but was not detected until a few periods later. This made specification of the model simpler. The computer program SURVIV (White 1983) was used to estimate the model parameters (F_t and M_t). To arrange the monitoring history data into the appropriate form for input to SURVIV, it was first converted to a full-m array (a summary table of relocations for each release period) using the computer program RELEASE (Burnham et al. 1987). Each year of data was considered separately, with two different models run for each. The first model assumed that mortality rates were constant across all periods within a year, and the second allowed mortality rates to vary between time periods.

Results

A total of 92 *C. limbatus* were collected and fitted with transmitters over the course of three years. The sample size in 1999 was 18 (11 male, 7 female), in 2000 was 33 (20 male, 13 female), and in 2001 was 41 (14 male, 27 female). All individuals collected were neonates with open umbilical scars (mean total length 62 cm) and were monitored within the study site from 1 to 167 days. All sharks were assessed as being in condition 2 or 3 upon release. Owing to the need to resuscitate animals on board after surgery none could be classified as condition 1, but all sharks were swimming well at the time of release. Handling time for surgical procedures and revival ranged from 8 to 43 min with a mean of 14 min and a median of 13 min. One individual was revived, but would not swim, so this individual was revived longer than most (43 min) to ensure it swam away in good condition.

Monitoring histories were defined for all sharks in each year (Fig. 2). During the three years, 23 sharks (25.3%) were censored, or removed from the study site (5 in 1999, 7 in 2000, 11 in 2001). Eight tagged shark recaptures were reported (34.8% of censored animals) from local anglers during this period with five transmitters returned. Twenty-eight (30.8%) cases of natural mortality occurred during the course of the study (7 in 1999, 9 in 2000, and 12 in 2001). Five sharks died within 24 h of release, with at least two of these animals appearing to have been consumed by a predator (see below). These five individuals were excluded from mortality estimates since it is likely that their deaths were a direct result of the surgical procedure and (or) handling. Most natural mortalities occurred within the first month of the study (mean = 12 days) but there were two animals that died after 55 and 66 days at liberty. Forty-one (42.9%) sharks were observed to have swum out of the study site and were considered survivals (6 in 1999, 17 in 2000, and 18 in 2001). Logistic regression analysis showed no significant relationship between survival and shark size, sex, environmental variables, handling time, or release condition (Table 1).

Two individuals appeared to have been consumed by the same large predator a few hours after release. Both animals simultaneously exited the study site at a faster rate than normally exhibited by juvenile *C. limbatus*. The next day both sharks were recorded to return, swim to identical locations simultaneously, and rapidly leave together. Neither individual was recorded by the monitoring system after this time. This behavior is very uncharacteristic of the other juvenile *C. limbatus* monitored and suggests that both transmitters were recorded returning to the study site within the stomach of a predator. Great hammerhead (*Sphyrna mokarran*) and bull (*Carcharhinus leucas*) sharks have both been observed in Terra Ceia Bay and are potential predators on young *C. limbatus*.

Results of mortality estimates based on life history characteristics were calculated for *C. limbatus* (Table 2). Constant mortality estimates varied slightly between males and females, but were generally within the range of 0.35–0.45·year^{-1}. The age-specific mortality estimates from the Peterson and Wroblewski (1984) method declined from 0.30·year^{-1} for newborn individuals to 0.14·year^{-1} at maximum age (10 years).

Calculation of Kaplan-Meier survival estimates varied among years (Fig. 3). Survival estimates were lower for year 1 than those for years 2 and 3, probably owing to small sample sizes in year 1 (Table 3). Similarly, animals tagged early in year 2 had to be excluded because small sample sizes caused exaggerated mortality for that year. Natural mortality was greatest within the first 15 weeks of the study period in each year before leveling off at zero. Rates of fishing mortality also varied among years (Fig. 4), but appeared to be greatest early in the season (May–July). After this point, fishing mortality leveled off at zero for the remainder of the summer months. Pooling data from all years to estimate survival from natural mortality revealed that survival initially decreases, followed by a leveling off at approximately 0.5 (Fig. 5). Survival from fishing mortality also showed a decline early in the season, followed by a level period at a rate of approximately 0.5 (Fig. 5). The combined effects of fishing and natural mortality resulted in total mortality estimates ranging from 0.61 to 0.91 (Table 3).

Natural and fishing mortality rates were calculated by week based on the output of the program SURVIV (Fig. 6). Natural mortality estimates ranged from 0 to 0.69·week^{-1} and fishing mortality estimates ranged from 0 to 0.79·week^{-1}, but both

© 2002 NRC Canada

Table 2. Methods used to calculate mortality rates (M, natural mortality; Z, total mortality) for *Carcharhinus limbatus* based on life history parameters.

Method	Relationship	Male	Female
Hoenig (1983) (fish)	$\ln(Z) = 1.46 - 1.01 \ln(t_{max})$	0.47	0.42
Hoenig (1983) (cetacean)	$\ln(Z) = 0.941 - 0.873 \ln(t_{max})$	0.38	0.34
Pauly (1980)	$\ln(M) = -0.0066 - 0.279 \log(L_\infty) + 0.6543 \log(K) + 0.4634 \log(T)$	0.46	0.35
Jensen (1996) (age)	$M = 1.65/x_m$	0.37	0.25
Jensen (1996) (growth)	$M = 1.5K$ (theoretical)	0.42	0.30
Jensen (1996) (Pauly)	$M = 1.6K$	0.44	0.32

Note: K, Brody growth coefficient (males = 0.276·year^{-1}, females = 0.197·year^{-1}); L_∞, maximum length (males = 166.5 cm, females = 195 cm); T, mean temperature (25°C); t_{max}, maximum age (males = 9 years, females = 10 years); x_m, age at maturity (males = 4.5 years, females = 6.5 years).

Fig. 3. Kaplan-Meier estimation of survival from natural mortality for juvenile *Carcharhinus limbatus* in Terra Ceia Bay during (*a*) 1999, (*b*) 2000, and (*c*) 2001. Dashed lines indicate 95% confidence intervals. All graphs use the second week of May as week 1.

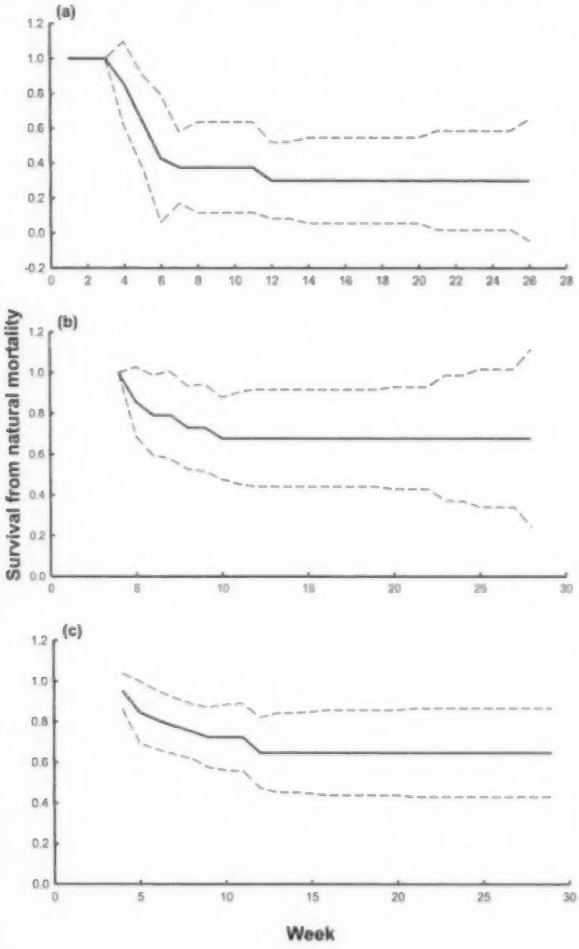

were generally below 0.2·week^{-1}. While mortality rates varied among years, all years showed a consistent pattern where both natural and fishing mortality occurred within the first 15 weeks of the season (Fig. 6).

Discussion

Natural and fishing mortality rates of elasmobranch populations have traditionally been difficult to estimate and analyses have generally relied on life history parameters. However, results of the current study have gone beyond previously available methods to provide a temporally explicit definition of mortality in a population of juvenile sharks. There are few available data with which to compare mortality estimates for neonate *C. limbatus*. Manire and Gruber (1993) provided the most comparable data by conducting a census of a closed population of neonate lemon sharks (*Negaprion brevirostris*) in Bimini, Bahamas, for which they estimated that 44 to 61% of sharks die in the first year of life. The total mortality estimate for lemon sharks was lower than for neonate blacktip sharks, in part because there was little or no fishing mortality for the lemon shark population (Manire and Gruber 1993). The natural mortality estimate for neonate blacktip sharks for the period from May to November was similar to that for neonate lemon sharks for their entire first year. This suggests that the natural mortality of blacktip sharks in their first full year of life in Terra Ceia Bay is higher than for lemon sharks in Bimini, Bahamas.

Natural mortality estimates for other elasmobranch species have come mostly from indirect life history methods (e.g., Waring 1984; Smith and Abramson 1990; Cortes and Parsons 1996). These indirect methods have resulted in a range of estimates, from 0.14·year^{-1} for leopard sharks, *Triakis semifasciata* (Smith and Abramson 1990), to 0.35–0.70·year^{-1} for bonnethead sharks, *Sphyrna tiburo* (Cortes and Parsons 1996), and 0.56·year^{-1} for Australian sharpnose sharks, *Rhizoprionodon taylori* (Simpfendorfer 1999*a*). Applying similar life history methods to *C. limbatus* resulted in estimates of natural mortality lower than those from direct estimation methods. The technique of doubling natural mortality rates for the first year of life increased these mortality estimates but they are still lower than those estimated by direct methods (40–60% dying in the first year). The limitation of most life history methods is that it is necessary to assume that the mortality rate is constant across all year classes. Results of the current study clearly show that this assumption cannot be met within the first year of life and therefore is unlikely to hold for the duration of a lifetime. While the Peterson and Wroblewski (1984) method provided age-specific mortality estimates, this method also produced mortality estimates lower than direct methods.

The direct methods applied to *C. limbatus* in this study as-

© 2002 NRC Canada

Table 3. Kaplan-Meier estimates of mortality for young of the year *Carcharhinus limbatus* based on natural, fishing, and total mortality rates.

	1999	2000	2001	Pooled data
Natural mortality	0.70 (0.032)	0.32 (0.049)	0.44 (0.011)	0.52 (0.010)
Fishing mortality	0.60 (0.048)	0.41 (0.047)	0.42 (0.012)	0.51 (0.010)
Total mortality	0.91 (0.004)	0.61 (0.031)	0.66 (0.006)	0.75 (0.003)

Note: Values in parentheses are variance estimates.

Fig. 4. Kaplan-Meier estimation of survival from fishing mortality for juvenile *Carcharhinus limbatus* in Terra Ceia Bay during (*a*) 1999, (*b*) 2000, and (*c*) 2001. Dashed lines indicate 95% confidence intervals. All graphs use the second week of May as week 1.

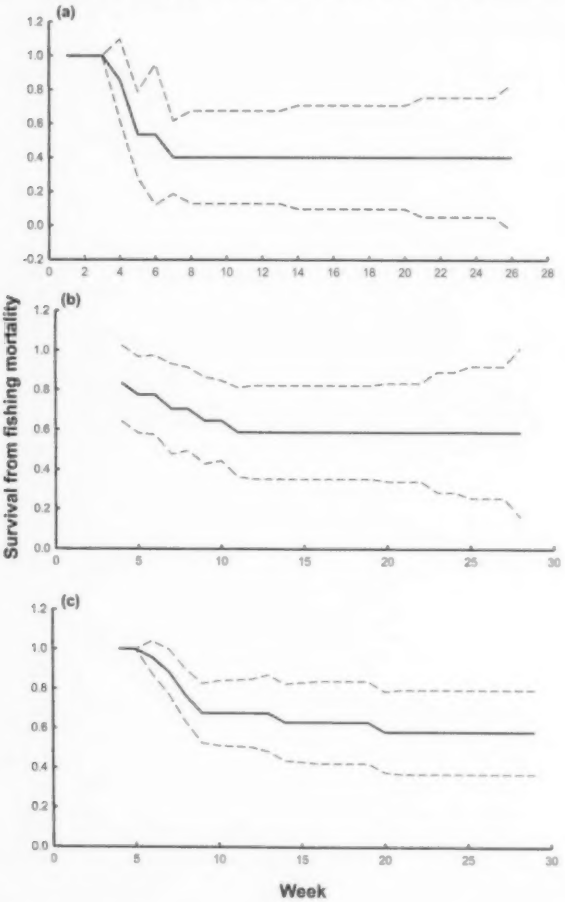

Fig. 5. Kaplan-Meier estimates of survival from (*a*) natural mortality and (*b*) fishing mortality for juvenile *Carcharhinus limbatus* combined from all three years. Dashed lines indicate 95% confidence intervals. Graphs use the second week of May as week 1.

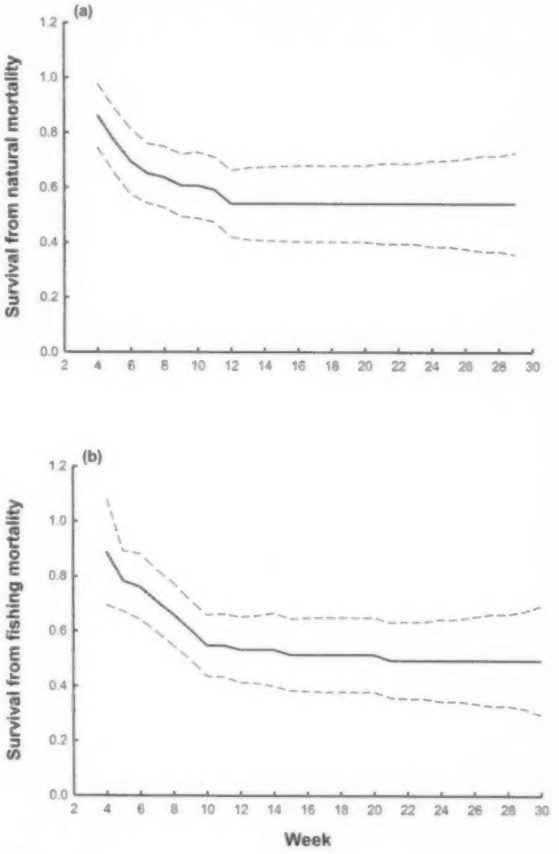

sume that all animals in the study have an equal chance of survival. The results of the generalized linear model for release factors showed no differences in survival between sex, size, and environmental conditions, suggesting that this assumption was met. However, it was not possible to determine if survival is different between tagged and untagged individuals.

Analysis of telemetry data in the present study provided the ability to directly estimate mortality for neonate *C. limbatus*. The Kaplan-Meier method estimated that over the course of a summer between 61 and 91% of neonates died, with all mortality occurring prior to week 15. The upper end of this range was based on the fewest data and is likely to overestimate mortality, as deaths among a small number of animals released early in the season heavily weighted the estimates. SURVIV results provided estimates of weekly natural and fishing mortality rates that were generally less than 0.2·week^{-1} for the first 12 to 15 weeks in each year. However, these results are independent weekly estimates that are not directly comparable to Kaplan-Meier results. If the total mortality rates estimated by the SURVIV method are applied to a population equivalent to the total number of tags released in each year of the current study, a comparable estimate is obtained.

© 2002 NRC Canada

Fig. 6. Weekly estimates of instantaneous (*a*) natural mortality and (*b*) fishing mortality based on program SURVIV calculations for juvenile *Carcharhinus limbatus* during 1999 (solid line), 2000 (dotted line), and 2001 (dashed line). Graphs use the second week of May as week 1.

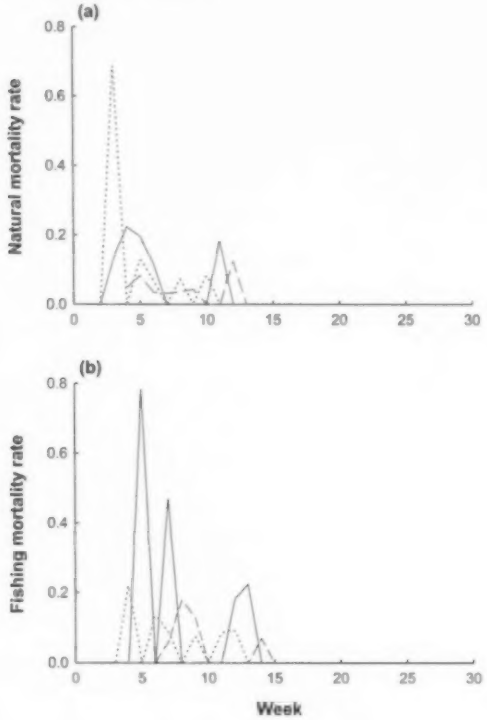

This technique resulted in an estimate where 62–92% of neonate *C. limbatus* died. This result is almost identical to that estimated by the Kaplan-Meier method. The agreement between these two models suggests that the calculated natural and fishing mortality estimates are accurate for the population within Terra Ceia Bay.

The magnitude of the mortality rates for *C. limbatus* in Terra Ceia Bay (61–91%) probably represents a conservative estimate. Terra Ceia Bay is part of an aquatic buffer preserve and does not suffer from high pollution loads. Although this area is not the most pristine estuary in Florida waters, it is a relatively healthy habitat with thick mangrove stands fringing most of the shoreline. As such, the bay represents a good model of continental nursery areas for blacktip sharks. In addition, predation levels appear to be relatively low, probably due to the semi-enclosed nature of the bay (M.R. Heupel, unpublished data). Comparison of the mortality estimates from Terra Ceia Bay to other nursery areas with lower environmental quality and (or) higher predation will provide an understanding of the range of mortality rates possible for young-of-the-year *C. limbatus*.

The results of the Kaplan-Meier and SURVIV methods at times estimated high levels of mortality in individual weeks. In all cases these were the result of animals dying or being removed while there were small numbers of tagged animals in the population. This occurred in both 1999 and 2000 when small numbers of animals were released over time, but did not occur in 2001 when relatively large numbers of animals were released over a short period. It is thus possible that mortality was overestimated in 1999 and 2000. Future studies employing this technique may wish to avoid the situation where estimates are based on small numbers of animals initially released.

The results of this study demonstrate that natural and fishing mortality of neonate *C. limbatus* in Terra Ceia Bay occurs in the first 12–15 weeks of life. If an animal survives this period, it has a high likelihood of surviving until leaving the nursery area in the fall. All of the animals released in the study were less than a month old, and many were only a few days old. Anecdotal evidence suggests that one cause of early mortality may be inexperience. When fishing within the study site early in the summer it was not uncommon to have several sharks around the boat within 5–15 min of putting bait in the water. Sharks were caught in quick succession with a new shark caught almost immediately upon release of the previous animal. This suggests that these young animals are hungry and will bite at any potential prey. This tendency has obvious consequences when considering fishing mortality and the number of sharks removed from the nursery early in the year. This is supported by the fact that during this study sharks became increasingly difficult to capture and by August were rarely captured, although monitoring data indicate that sharks were still present in the area. Another learning experience these young sharks had to contend with is predator avoidance. While fishing in the northern portion of Terra Ceia Bay in June 2001 a hammerhead (approximately 2 m in length) was observed chasing a juvenile *C. limbatus*. Although some of these observations are anecdotal, they are consistent with the results of the mortality estimation that suggests that if sharks can survive beyond 15 weeks they will have a good chance of surviving the rest of the summer. This 15-week period is obviously critical to the learning, development, and survival of these animals, even within what is defined as a protected nursery area.

Estimation of natural mortality within elasmobranch populations is a common problem that has limited efforts to define the dynamics of species and design appropriate fishery management plans (Cortes 1998). Previous authors have suggested that mortality rates for juvenile sharks are highest in the first year of life (e.g., Hoenig and Gruber 1990; Manire and Gruber 1993; Simpfendorfer 1999*b*). The results presented here support those conclusions. In fact, the first few months of life appear to be the most critical time for survival of neonate *C. limbatus* in Terra Ceia Bay. Therefore, the protection of nursery areas would be of significant value to animals in the first few months of life when mortality rates appear to be highest. The added impact of fishing pressure on this young portion of the population increases total mortality and future management plans may consider closing fishing for these young animals during the first few months of life.

Acknowledgements

Funding from the National Science Foundation to M.R. Heupel (Award No. OCE-991295) and National Oceanic and Atmospheric Administration/National Marine Fisheries Ser-

© 2002 NRC Canada

vice (grant Nos. NA97FM0223 and NA07FM0459) to R.E. Hueter supported this work. We thank J. Hightower and K. Pollock for their advice on data manipulation and analyses. We also thank T. Wilkie, J. Tyminski, M. Conn, J. Morris, S. Robbins, R. Phillips, C. Chutsz, and D. Rowles for assistance with field efforts.

References

Bendock, T., and Alexandersdottir, M. 1993. Hooking mortality of Chinook salmon released in the Kenai River, Alaska. N. Am. J. Fish. Manag. **13**: 540–549.

Branstetter, S. 1990. Early life-history implications of selected carcharhinoid and lamnoid sharks of the northwest Atlantic. NOAA Tech. Rep. NMFS, **90**: 17–28.

Burnham, K.P., Anderson, D.R., White, G.C., Brownie, C., and Pollock, K.H. 1987. Design and analysis methods for fish survival experiments based on release-recapture data. Am. Fish. Soc. Monogr. No. 5, Bethesda, Md.

Castro, J.I. 1993. The shark nursery of Bulls Bay, South Carolina, with a review of the shark nurseries of the southeastern coast of the United States. Environ. Biol. Fishes, **38**: 37–48.

Castro, J.I. 1996. Biology of the blacktip shark, *Carcharhinus limbatus*, off the southeastern United States. Bull. Mar. Sci. **59**: 508–522.

Cortes, E. 1998. Demographic analysis as an aid in shark stock assessment and management. Fish. Res. **39**: 199–208.

Cortes, E., and Parsons, G.R. 1996. Comparative demography of two populations of the bonnethead shark (*Sphyrna tiburo*). Can. J. Fish. Aquat. Sci. **53**: 709–718.

Cox, D.R., and Oakes, D. 1984. Analysis of survival data. Chapman and Hall, New York.

Heupel, M.R., and Hueter, R.E. 2001. Use of an automated acoustic telemetry system to passively track juvenile blacktip shark movements. *In* Electronic tagging and tracking in marine fisheries. *Edited by* J.R. Sibert and J.L. Nielsen. Kluwer Academic Publishers, Netherlands. pp. 217–236.

Hightower, J.E., Jackson, J.R., and Pollock, K.H. 2001. Use of telemetry methods to estimate natural and fishing mortality of striped bass in Lake Gaston, North Carolina. Trans. Am. Fish. Soc. **130**: 557–567.

Hoenig, J.M. 1983. Empirical use of longevity data to estimate mortality rates. Fish. Bull. **82**: 898–903.

Hoenig, J.M., and Gruber, S.H. 1990. Life-history patterns in the elasmobranchs: implications for fisheries management. NOAA Tech. Rep. NMFS, **90**: 1–16.

Hueter, R.E., and Manire, C.A. 1994. Bycatch and catch-release mortality of small sharks in the Gulf coast nursery grounds of Tampa Bay and Charlotte Harbor. Mote Mar. Lab. Tech. Rep. No. 368. Final report to NOAA/NMFS, MARFIN (Marine Fisheries Initiative) Project NA17FF0378-01.

Jensen, A.L. 1996. Beverton and Holt life history invariants result from optimal trade-off of reproduction and survival. Can. J. Fish. Aquat. Sci. **53**: 820–822.

Killam, K.A., and Parsons, G. R. 1989. Age and growth of the blacktip shark, *Carcharhinus limbatus*, near Tampa Bay, Florida. Fish. Bull. **87**: 845–857.

Manire, C.A., and Gruber, S.H. 1993. A preliminary estimate of natural mortality of age-0 lemon sharks, *Negaprion brevirostris*. NOAA Tech Rep. NMFS, **115**: 65–71.

Pauly, D. 1980. On the interrelationship between natural mortality, growth parameters, and mean environmental temperature in 175 fish stocks. J. Cons. Int. Explor. Mer, **39**: 175–192.

Peterson, I., and Wroblewski, J.S. 1984. Mortality rates of fishes in the pelagic ecosystem. Can. J. Fish. Aquat. Sci. **41**: 1117–1120.

Pollock, K.H., Winterstein, S.R., and Conroy, M.J. 1989*a*. Estimation and analysis of survival distributions for radio-tagged animals. Biometrics, **45**: 99–109.

Pollock, K.H., Winterstein, S.R. Bunck, C.M., and Curtis, P.D. 1989*b*. Survival analysis in telemetry studies: the staggered entry design. J. Wildl. Manag. **53**: 7–15.

Pollock, K.H. Bunck, C.M., Winterstein, S.R., and Chen, C. 1995. A capture-recapture survival analysis model for radio-tagged animals. J. Appl. Stat. **22**: 661–672.

Simpfendorfer, C.A. 1999*a*. Mortality estimates and demographic analysis for the Australian sharpnose shark, *Rhizoprionodon taylori*, from northern Australia. Fish. Bull. **97**: 978–986.

Simpfendorfer, C.A. 1999*b*. Demographic analysis of the dusky shark fishery in southwestern Australia. *In* Life in the slow lane: ecology and conservation of long-lived marine animals. *Edited by* J.A. Musick. Am. Fish. Soc. Symp. (Bethesda), **23**: 149–160.

Simpfendorfer, C.A., and Milward, N.E. 1993. Utilisation of a tropical nursery area by sharks of the families Carcharhinidae and Sphyrnidae. Environ. Biol. Fishes, **37**: 337–345.

Simpfendorfer, C.A., Heupel, M.R., and Hueter, R.E. 2002. Estimation of short-term centers of activity from an array of omnidirectional hydrophones, and its use in studying animal movements. Can. J. Fish. Aquat. Sci. **59**: 23–32.

Sminkey, T.R., and Musick, J.A. 1996. Demographic analysis of the sandbar shark, *Carcharhinus plumbeus*, in the western north Atlantic. Fish. Bull. **94**: 341–347.

Smith, S.E., and Abramson, N.J. 1990. Leopard shark, *Triakis semifasciata* distribution, mortality rate, yield, and stock replenishment estimates based on a tagging study in San Francisco Bay. Fish. Bull. **88**: 371–381.

Vetter, E.F. 1988. Estimation of natural mortality in fish stocks: a review. Fish. Bull. **86**: 25–43.

Waring, G.T. 1984. Age, growth and mortality of the little skate off the northwest coast of the United States. Trans. Am. Fish. Soc. **113**: 314–321.

White, G.C. 1983. Numerical estimation of survival rates from band recovery and biotelemetry data. J. Wildl. Manag. **47**: 716–728.

© 2002 NRC Canada

Vorticity and circulation: spatial metrics for evaluating flow complexity in stream habitats

David W. Crowder and Panayiotis Diplas

Abstract: Channel topography, formed by boulders, submerged bars, and meanders, creates complex flow patterns. These flow patterns exist over a variety of spatial scales and provide habitat for many aquatic organisms. Spatial flow features cannot be adequately characterized with qualitative descriptions or hydraulic metrics such as depth and velocity. Two-dimensional hydraulic model simulations, based on detailed channel geometry, are used to develop and test vorticity (a point metric) and a circulation-based metric (an area metric) as means of quantifying spatial flows occurring within micro-, meso-, and macro-habitat features. The proposed spatial metrics are computed throughout distinctly different regions of a study site. The vorticity metric produces small absolute values in uniform flows and large absolute values in complex flows. Circulation metric values varied by a factor of 11.7 within distinctly different regions of the modeled study site and suggest that the metric provides a means of quantifying flow complexity within a study reach or within individual mesoscale habitats such as pools, eddies, riffles, and transverse flows. The circulation metric is used to quantify flow complexity around three brown trout (*Salmo trutta*) redds to provide an example of how the proposed metric might be employed in habitat studies.

Résumé : La topographie d'un chenal formé de blocs de pierre, de barres submergées et de méandres crée des patterns d'écoulement complexes qui existent à différentes échelles spatiales et qui fournissent des habitats à de nombreux organismes aquatiques. Les caractéristiques spatiales de l'écoulement ne peuvent être adéquatement représentées par des descriptions qualitatives ou des métriques hydrauliques, telles que la profondeur et la vitesse du courant. Des modèles de simulation bidimensionnels, basés sur la géométrie détaillée des chenaux, permettent de développer et de tester la vorticité (une métrique ponctuelle), ainsi qu'une métrique basée sur la circulation (une métrique de surface) dans le but de quantifier les écoulements spatiaux qui existent dans les structures des micro-, méso- et macro-habitats. Les métriques spatiales proposées ont pu être calculées à divers sites très distincts du milieu d'étude. La métrique de vorticité prend des valeurs absolues basses dans les écoulements uniformes et de fortes valeurs absolues dans les écoulements complexes. Les valeurs de la métrique de circulation peuvent varier par un facteur de 11,7 d'une région à l'autre du site d'étude, ce qui démontre que cette métrique permet de quantifier la complexité de l'écoulement dans une section de cours d'eau ou alors entre des méso-habitats individuels, tels que des profonds, des tourbillons, des rapides et des écoulements transversaux. La métrique de circulation a servi à quantifier la complexité de l'écoulement autour de trois frayères de truites brunes (*Salmo trutta*), illustrant ainsi comment elle peut être utilisée dans les études d'habitats.

[Traduit par la Rédaction]

Introduction

Flow within natural rivers is typically highly complex. The presence of boulders, submerged bars, meanders, and other topographic features create eddies, transverse flows, velocity gradients, and other spatial flow patterns. Observers of stream flow phenomena know that even rivers that appear to be tranquil have complex flow patterns created by topographic features within the streambed (e.g., Whiting and Dietrich 1991). Such flow complexity provides micro-, meso-, and macro-scale habitat features from which aquatic organisms can choose to inhabit.

Growing evidence suggests that different aquatic organisms use and surround themselves with flow patterns that are not readily quantifiable or differentiable using standard habitat metrics (e.g., point depth, velocity, and substrate data). Fausch and White (1981) and Hayes and Jowett (1994) suggest that velocity gradients are important features of brown trout (*Salmo trutta*) and brook trout (*Salvelinus fontinalis*) feeding stations. Shields et al. (1995) reported the placement of spur dykes, which create vortices, in degraded warmwater streams could substantially increase fish biomass. Freeman and Grossman (1993) suggest that, during the summer, rosyside dace (*Clinostomus funduloides*) dispersion may be dependent on the availability of depositional zones found near swift adjacent water.

How channel topography and discharge interact to create and provide the different types and amounts of habitat used by various aquatic organisms is poorly understood. A major obstacle to understanding this interaction is the inability to

Received 5 July 2001. Accepted 27 March 2002. Published on the NRC Research Press Web site at http://cjfas.nrc.ca on 2 May 2002.
J16434

D.W. Crowder.[1,2] Civil and Environmental Engineering Department, Virginia Polytechnic Institute and State University, Blacksburg, VA 24061, U.S.A.
P. Diplas. 200 Patton Hall, Department of Civil and Environmental Engineering, Virginia Polytechnic Institute and State University, Blacksburg, VA 24061, U.S.A.

[1]Corresponding author (e-mail: crowderd@sws.uiuc.edu).
[2]Present address: Illinois State Water Survey, 2204 Griffith Drive, Champaign, IL 61820, U.S.A.

 DOI: 10.1139/F02-037 © 2002 NRC Canada

quantify and differentiate between flow features within a river. Routinely, point depth, velocity, and substrate values are employed to quantify the hydraulic habitat within streams. However, these measurements are point metrics and quantify only what is occurring at a single point within the river. Hence, one cannot use point measurements to accurately quantify the hydraulic habitats of aquatic organisms that prefer, or use, spatial flow features surrounding a particular point or within an extended area.

The inability to quantify such spatially varying features forces one to adopt qualitative descriptions of flow features, (e.g., pools, riffles, runs, and eddies). A significant drawback to this qualitative approach is that the characteristics and functions of pools, eddies, and runs differ from stream to stream, depending on discharge, channel roughness, slope, and channel morphology. Moreover, many of these features occur over a variety of spatial scales, making comparisons between similar features even more difficult. The development of spatial metrics that quantify flow complexity and differentiate between specific flow features might lead to better means of assessing stream habitat, restoring degraded streams, and predicting how specific land activities might impact a stream's ecology.

Recently, researchers have begun looking at the usefulness of employing two-dimensional (2-D) hydraulic models to evaluate the hydraulic conditions in stream habitat studies (e.g., Leclerc et al. 1995; Ghanem et al. 1996). Two-dimensional hydraulic models, unlike commonly used 1-D hydraulic models, are capable of reproducing transverse flows, eddies, velocity gradients, and other complex flow patterns found within streams. Hence, 2-D hydraulic models provide a spatially explicit representation of a river reach that stream biologists can analyze with traditional habitat metrics and (or) spatial hydraulic metrics to identify important features such as velocity gradients, eddies, and vortices. Unfortunately, there is a paucity of research focusing on modeling and quantifying the spatial flow patterns of biological importance that are created by topographic features (exposed boulders, submerged bars, etc.). Crowder and Diplas (2000*a*, 2000*b*) used a 2-D hydraulic model to reproduce flow patterns induced by exposed boulders and proposed a spatial hydraulic metric to quantify biologically important velocity–kinetic energy gradientslike those used by brown and brook trout. The metric proposed by Crowder and Diplas (2000*b*) computes the spatial rate at which a flow's kinetic energy is changing relative to the kinetic energy at that point. The metric can be used to distinguish between two points having similar depth and velocity values, but surrounded by different velocity–kinetic energy gradients. Mathematically, the metric is expressed as follows:

$$(1) \qquad \frac{\dfrac{\partial}{\partial x}\dfrac{V^2}{2}}{\dfrac{V^2}{2}}$$

where V is the magnitude of the depth-averaged velocity at a point and x represents the direction in which the spatial change in kinetic energy ($V^2 \div 2$) is being evaluated. This metric provides an indication of how flow is changing spatially around a point and provides a useful means of quantifying microhabitat features within a stream. The development of additional spatial hydraulic metrics designed to characterize different types of flow features, occurring within arbitrary areas, can complement the usefulness of this metric and allow stream biologists to more fully describe biologically important micro-, meso-, and macro-habitat features found within streams.

Here, the 2-D hydraulic model simulations and spatial energy metric proposed by Crowder and Diplas (2000*a*, 2000*b*) are used to develop and evaluate two new spatial metrics capable of quantifying flow complexity within rivers. The first spatial metric, vorticity, measures the rate at which a tiny fluid element rotates around its axes. As vorticity describes flow conditions only at a point, comparisons between vorticity and the previously proposed spatial energy gradient metric are made to determine how these metrics complement each other in their ability to quantify and locate points of biological importance. A second metric, one that integrates the absolute vorticity values over a specified region, is then proposed and evaluated as a means of quantifying flow complexity within any arbitrary area, whether it is a mesoscale habitat or the entire stream reach. The resulting combination of spatial metrics, measuring different flow properties, can be used to better quantify spatial flow patterns existing at the micro-, meso-, or macro-scale levels.

Methods

The development of vorticity and circulation as spatial hydraulic metrics

In fluid mechanics, it is well established that the motion of a small fluid element within a flow field can be described in terms of its translation, linear deformation, rotation, and angular deformation. For a full discussion on this topic and how vorticity and circulation relate to fluid motion the reader should refer to a basic fluid mechanics book, for example, Batchelor (1967), Munson et al. (1990), and others. Of particular importance here is the vorticity vector, $\overline{\xi}$, which describes the rotation rate of a small fluid element about its axes. For a 3-D flow field, vorticity can be expressed mathematically as follows:

$$(2) \qquad \overline{\xi} = 2\overline{\omega} = \nabla \times \overline{V}$$

where $\overline{\omega}$ is the rotation vector and $\overline{V}$ is the fluid's velocity vector. The right-hand side of the expression is known as the curl of the velocity vector and is expressed below

$$(3) \qquad \nabla \times \overline{V} = \left(\frac{\partial w}{\partial y} - \frac{\partial v}{\partial z}\right)\hat{i} + \left(\frac{\partial u}{\partial z} - \frac{\partial w}{\partial x}\right)\hat{j} + \left(\frac{\partial v}{\partial x} - \frac{\partial u}{\partial y}\right)\hat{k}$$

where u, v, and w are a flow's x-, y-, and z-velocity components and $\hat{i}$, $\hat{j}$, and $\hat{k}$ are unit vectors in the x-, y-, and z-directions (for this paper, x and y are the downstream and cross-stream directions, respectively, and z is the vertical direction).

For 2-D flow fields, which this paper models and analyzes, the z-velocity component in the above equation is ignored and the vorticity vector simplifies to the following expression:

© 2002 NRC Canada

$$(4) \qquad \bar{\xi} = 2\bar{\omega} = \left(\frac{\partial v}{\partial x} - \frac{\partial u}{\partial y}\right)\hat{k}$$

and represents twice the rate at which a very small fluid element is rotating about its vertical axis. The vorticity vector is considered as positive when the fluid is rotating in the counterclockwise direction. Vorticity at a point within a flow is zero under two conditions. (*i*) When both $\partial v \div \partial x$ and $\partial u \div \partial y$ are zero; and (*ii*) when $\partial v \div \partial x = \partial u \div \partial y$. In the first case, a fluid element, as it moves with the flow, may undergo pure translation and (or) linear deformation (stretching), but does not rotate or undergo angular deformation (change in shape). In the second case, a fluid element may undergo translation, linear and (or) angular deformation, but will not rotate or "spin" about its vertical axis as it moves. Flows falling within either of these two categories are referred to as potential flows. Perhaps one of the most important potential flows is uniform flow. In natural streams, however, channel topography creates velocity gradients, transverse flows, eddies, and other complex, nonuniform flow patterns that are characterized by nonzero vorticity. Consequently, vorticity provides a physically meaningful basis for identifying these complex or spatially varying flows, and distinguishing them from uniform flow conditions within a stream.

Vorticity does not necessarily reflect whether the fluid surrounding that location has circular motion similar to that associated with tornadoes, whirlpools, or hurricanes. For example, in a free vortex (a form of potential flow), flow occurs in concentric circles around a central point and has velocity values that increase toward the center of the circle, but has zero vorticity at every point within the flow ($\partial v \div \partial x = \partial u \div \partial y$ everywhere). In a forced vortex, the fluid rotates like a solid body and therefore the velocity decreases linearly towards the centre of the circle. In this case, vorticity is nonzero, and in fact, has the same value throughout the flow. It can also be shown that velocity gradients, created by channel banks, produce nonzero vorticity values even when the flow is largely in the downstream direction and lacks the circular motions associated with vortices.

Since vorticity is computed at a single point in the flow field, it cannot directly quantify the flow complexity within an arbitrary area or throughout a river reach. However, a commonly used mathematical term, circulation, is closely related to vorticity and sums the vorticity values of all the fluid elements within an arbitrary area *S*. The mathematical expression for circulation, Γ, follows:

$$(5) \qquad \Gamma = \oint_L \bar{V} \cdot d\bar{L} = \iint_S \bar{\xi} \cdot d\bar{A}$$

where $d\bar{L}$ is the unit vector along the length of a closed path, *L*. The closed line, *L*, surrounds a surface area *S*, and $d\bar{A}$ represents the area of an infinitesimal element of the surface *S*. Circulation can be used to measure the strength of vortices, like those responsible for making scour holes behind spur-dykes. Depending on the vorticity values that are within the area of interest, circulation can be positive, negative, or zero. A positive circulation value suggests a vortex spinning in a counterclockwise direction.

If circulation is computed within a region containing areas of positive and negative vorticity, the areas of opposing sign will work to cancel each other out and may result in a positive, negative, or zero circulation value. Moreover, the resulting circulation value will not be reflective of the total flow complexity within the region. For example, computing circulation within a region that contains two distinct eddies circulating in opposite directions can result in a zero or near-zero circulation value. Such a value is what one expects to find in uniform flow conditions and clearly does not reflect the flow complexity of the two eddies. However, a simple and effective means of quantifying the overall flow complexity within the region would be to compute the sum of the absolute values of vorticity throughout the area. Hence, the flow complexity found in each eddy would contribute to the resulting "absolute circulation" value and be clearly distinguishable from uniform flow conditions. Moreover, by dividing the resulting circulation value by the total area being analyzed, a measure of the average stream complexity over the area of interest can be obtained. For the 2-D flows discussed here, the mathematical expression for this variation on circulation follows:

$$(6) \qquad \frac{\Gamma_{ABS}}{A_{tot}} = \frac{\iint_S |\xi| dA}{A_{tot}} = \frac{\sum |\xi| \Delta A}{A_{tot}}$$

where Γ_{ABS} is the modified or "absolute" circulation parameter, A_{tot} is the total wetted area over which Γ_{ABS} is being computed, and ΔA represents the area of an element of surface *S*.

While vorticity and circulation are numerical means of quantifying the physical nature of vortices and other flow complexity, vorticity and circulation also appear to have biological significance. Bandyopoadhyay et al. (2000) found that vortices generated by the movement of a fish's fins play a part in determining a fish's maneuverability. Hanke et al. (2000) and Kiorboe and Visser (1999) suggest that piscivorous predators and copepods can detect the presence of prey through the vortex structures left behind by fish and other organisms as they swim. Way et al. (1995) found that grooved blocks used to line parts of the Mississippi River create small eddies that allow macroinvertebrates to build feeding structures that are sheltered from high velocity flows, but remain in contact with faster feeding flows. Such observations suggest that aquatic organisms use vortices and other complex flows in different manners and at different scales. The proposed vorticity and circulation metrics may be appropriate means of quantifying these habitats.

Testing vorticity as a spatial metric applied at a point

The ability of the vorticity and circulation metrics to quantify flow patterns of biological importance is evaluated through numerical simulations performed with the 2-D hydraulic model RMA2 (King 1990). RMA2 is a well-known 2-D finite element program that solves the shallow water equations for depth and depth-averaged velocities (in the *x* and y directions) at every node within a finite element mesh. The two specific simulations employed here to evaluate the proposed metrics were previously used and described in detail by Crowder and Diplas (2000*a*, 2000*b*). These simulations modeled a 61-m reach of a regulated mountain stream (The North Fork of the Feather River in California) that has

© 2002 NRC Canada

a summer discharge of 4.24 $m^3 \cdot s^{-1}$, an average width of 15 m, and a maximum depth of about 1.5 m. The first simulation modeled the study site without incorporating topographic data on exposed boulders found within the study site. The resulting flow field for this simulation is largely uniform and similar to what one would expect to see in urban channels having rather simple geometry. The second simulation incorporated topographic data on exposed boulders found within the study site and generated highly complex flow patterns within the upper 21 m of the study site. Together the simulations provide a means to evaluate the role that channel topography has on creating potentially important flow patterns and how such flows can be quantified.

To test the ability of vorticity to identify locations within a stream containing nonuniform flows, vorticity was plotted throughout the study site for both simulations (with and without boulders). By dividing a location's absolute vorticity value by the mean absolute vorticity value found within the entire study reach, regions having relative high and low vorticity values were then identified for each simulation. Comparisons of regions with relatively high and low vorticity values are found within the two simulations are then made to quantify the influence that channel complexity has on creating vorticity within a stream. Likewise, the spatial energy metric proposed by Crowder and Diplas (2000*b*) was computed throughout the study reach for both simulations. The absolute energy metric values found at each point within the study site are then divided by the mean absolute energy metric value obtained within the study reach. Plotting this ratio throughout the study site for both simulations allows one to identify areas within the stream having relatively high and low energy metric values and to discern how channel topography influences stream energy gradients. Comparisons between the vorticity and energy metric ratios were then made to help determine the similarities and differences between the vorticity and energy metrics (Figs. 1–3).

Testing circulation as a spatial metric applied over an area

To compute the proposed circulation metric value within an arbitrary area of the study site, a FORTRAN 90 program was developed. The program allows a user to define a rectangular area surrounding a specific location within the study reach where one wants to compute the circulation metric. The author's FORTRAN program, using data files generated from SMS (EMRL 1999) (a commercially available pre- and post-processor for RMA-2V), computes the average nodal energy metric value, average nodal vorticity value, and average nodal velocity value for each wet element in the finite element mesh that lies completely within the rectangle area of interest. For each wet element, the program multiplies the absolute value of its average nodal vorticity value by its area. The resulting values for each wet element within the predefined area are then summed to provide the circulation value, as defined by the right-hand term in eq. 6. The program also computes the proportion of area within the defined rectangular region that has vorticity and energy metric values falling within user-specified "bins" or ranges of metric values. This information is used to plot and compare the vorticity and energy metric distributions found within the two different simulations and within distinct areas of the study site. For each simulation, circulation metric values are computed for the entire site, its upper 20 m, and within three distinct regions of the site. The three distinct regions have areas of approximately 36 m^2 (Figs. 1–2). The first region (A) surrounds an area in the middle portion of the site having uniform flow. The second region (B) is found within the upper portion of the site where a significant transverse flow exists and the third region (C) encompasses an area containing four exposed boulders that create highly complex flow patterns. The resulting circulation metric values are compared to determine if circulation metric values differed significantly between the two simulations and the three distinct areas of varying spatial complexity.

Computing the circulation metric with velocity data obtained in field studies

To ascertain the ability and usefulness of applying the circulation metric in field studies, the proposed circulation metric was computed for a 10.75-m^2 area and a 21.4-m^2 area within a reach of the Smith River in Virginia (Fig. 4). The first area (Area D), identified with the aid of fishery biologists, was within a portion of the river reach devoid of redds, but appeared to have substrate, depth, and velocity values similar to those of areas where numerous brown trout redds have been found. The second area (Area E) surrounded an area where fishery biologists studying the site previously found and recorded the locations of three brown trout redds. With no overhead vegetation observed at Area D or Area E, the two locations appeared to have quite similar habitat characteristics, except in terms of flow complexity. The flow in Area D was uniform and no visually identifiable vortices existed within it. In Area E, a large exposed boulder and a smaller submerged boulder created local flow constriction and two distinct regions in which one could see vortices rotating in opposite directions.

Using a compass and a Flo-Rate model 2000 velocity meter (Marsh-McBirney), velocity magnitude and direction were measured at 0.3-m intervals along each side of the perimeter encompassing Area D. These measurements, combined with the bearing of each side of Area D's perimeter, provided the information needed to use the line integral expression in eq. 5 to compute Γ within Area D. As no distinct positive and negative vorticity zones existed within Area D, the proposed circulation metric (Γ_{ABS}) value for Area D is equal to the absolute value of the circulation value.

The same approach was employed to calculate the circulation metric value for Area E. However, as Area E has both positive and negative vorticity regions, circulation (Γ) was computed for each of these regions separately. Areas LMNO and PLOQ represent the negative and positive vorticity regions, respectively (Fig. 4). The absolute circulation values for both regions were then summed to obtain the circulation metric (Γ_{ABS}) for the entire Area E. To capture the spatial variations in velocity occurring along the perimeters of areas LMNO and PLOQ, velocity magnitude and direction were measured at 0.15-m intervals, except on line LO where measurements were taken every 0.3 m. Because the velocity varied slowly along line LO and the line integral contributions along this line ultimately cancel out, larger spacing along LO was justified. Comparisons of the circulation and circu-

© 2002 NRC Canada

Fig. 1. Plot of the absolute energy metric value at a point divided by the reach's mean absolute energy metric value (|energy metric|/|energy metric|$_{average}$) (*a*) without boulders and (*b*) with boulders. Contours represent the magnitude of the energy metric ratio. The arrows indicate the direction of flow at a point within the river and are scaled to the velocity magnitude found at that point. The white spots in Fig. 1*b* represent the location of exposed boulders within the stream. Areas A, B, and C represent locations where the circulation metric values were computed. Area A is in the middle portion of the 61-m study reach where the flow is uniform. Area B has a transverse flow within it and Area C surrounds the location of the largest exposed boulder.

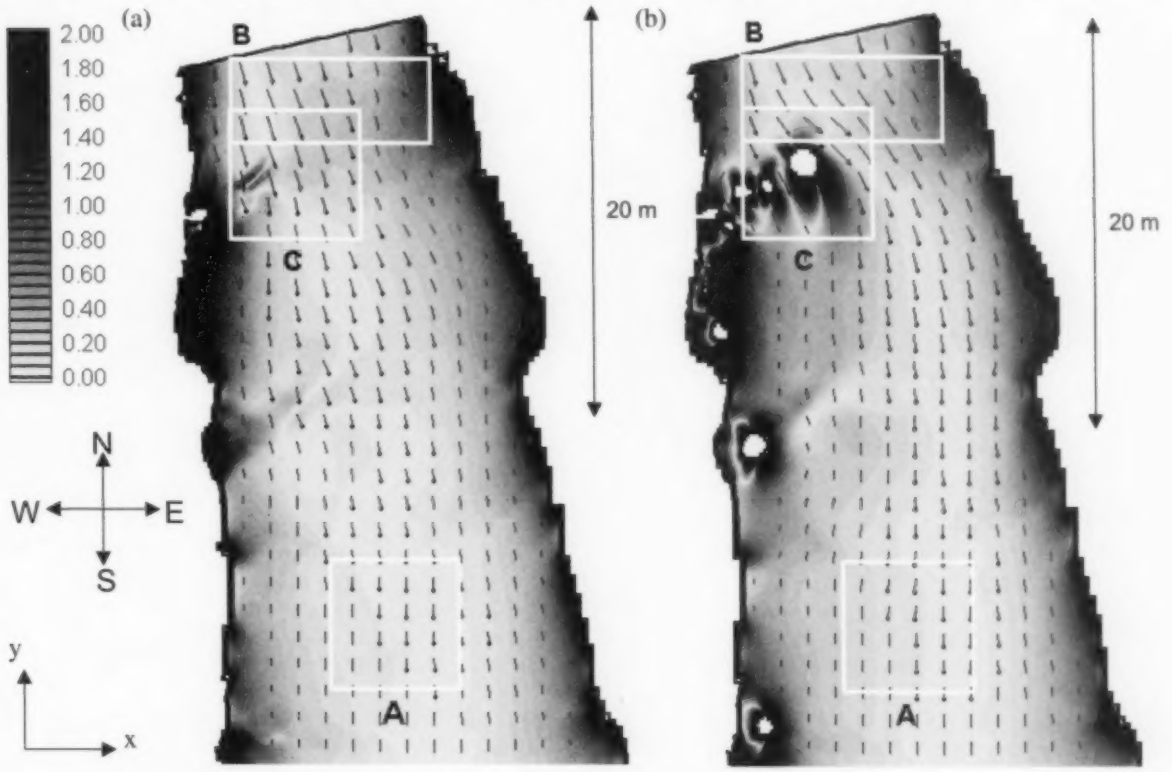

lation metric values obtained in areas D and E and areas LMNO and PLOQ are made.

Results

Sensitivity of the energy and vorticity metrics to locating spatial flow patterns

The absolute energy metric value divided by the mean absolute energy metric value found within the reach (|energy metric|/|energy metric|$_{average}$) is plotted for each of the two model simulations (Fig. 1). When boulders are present, the absolute mean energy metric value for the entire reach is 1.333 m^{-1}. Without boulders present this value becomes 0.947 m^{-1}. However, for consistency purposes, energy metric ratios were computed based on the 1.333 value in both modeling scenarios. The resulting energy metric ratios ranged between 0 and 677 in the no boulder simulation and from 0 to 1168 in the simulation containing boulders. Energy metric ratios having very large magnitudes (>15) are artifacts of having very low velocity values found in modest or large velocity–energy gradients. Hence, such values can be expected immediately next to channel banks and boulders. However, in both simulations, the total proportion of area having energy metric ratios greater than 1.5 (or with underlying absolute energy metric values greater than 2.00 m^{-1}) is only 6–7% of the reach's area.

Without incorporating exposed boulders into the model, the larger energy metric ratios are found only near the banks of the river. When boulders are incorporated into the model, the steep velocity–energy gradients produced in the vicinity of the boulders are reflected by the higher energy metric ratios found in the vicinity of the exposed boulders. The boulders also create a transverse flow in the upper portion of the study site. The main flow can be seen shifting from the west bank toward the east bank, as indicated by a comparison of the velocity vectors in the upper portion of the plots. However, the transverse flow, a form of flow complexity, does not contain significant velocity–energy gradients, as reflected by the low energy metric values found in this region (Area B).

The results of dividing absolute vorticity values by the mean absolute vorticity found within the study reach (|vorticity|/|vorticity|$_{average}$) for each model simulation are illustrated (Fig. 2). As with the computation of the energy metric ratios, the mean absolute vorticity value obtained in the simulation containing boulders was used to compute all

© 2002 NRC Canada

Fig. 2. Plot of the absolute vorticity value found at a point divided by the reach's mean absolute vorticity value ($|\text{vorticity}|/|\text{vorticity}|_{\text{average}}$) (*a*) without boulders and (*b*) with boulders.

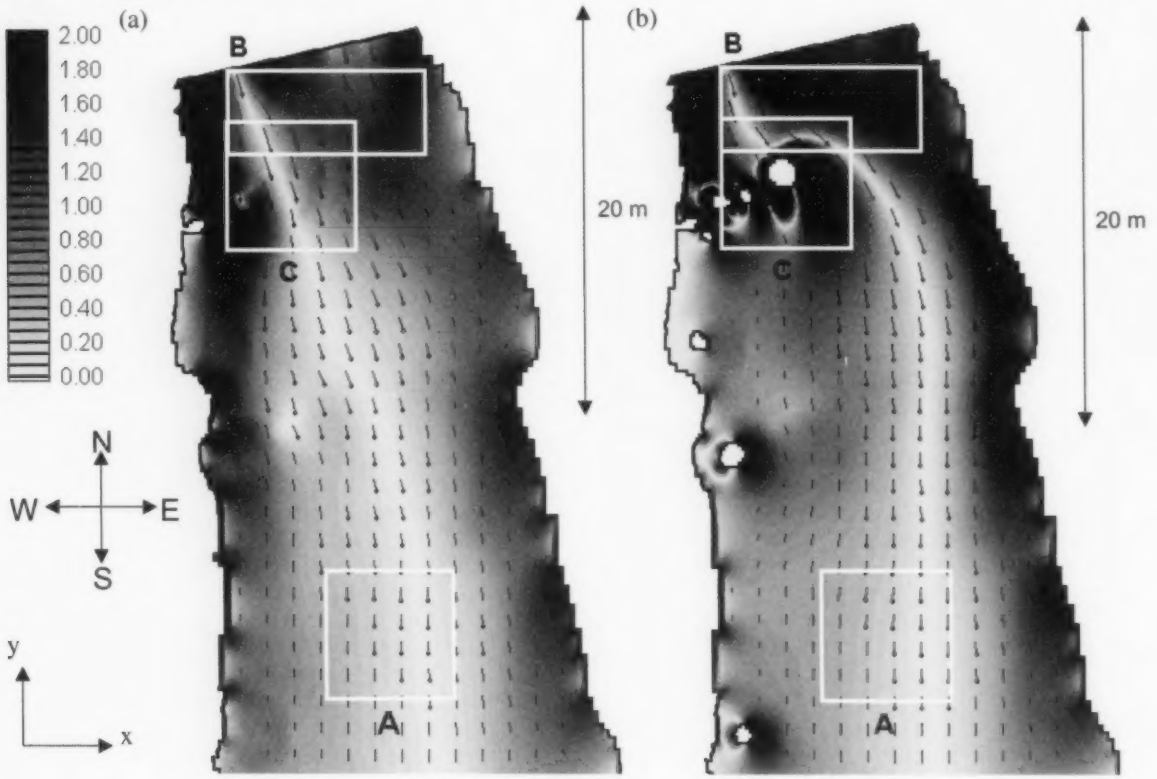

vorticity ratios. The mean absolute vorticity value for the simulation containing boulders is 0.0676 s^{-1} compared with the 0.0507 s^{-1} value obtained for the no boulder simulation. The resulting vorticity metric ratios ranged between 0 and 13.593 in the no boulder simulation and from 0 to 47.673 in the simulation containing boulders. Without boulders, 93% of the study reach has vorticity ratios less than 1.48 (or with underlying vorticity values between –0.1 and 0.1 s^{-1}). With boulders present, 88% of the study reach has vorticity ratios less than 1.48 s^{-1}. Thus, only a small range of vorticity values occupies most of the area within the study site, despite the wide range of vorticity values actually present (–3.223 to 3.008 s^{-1}).

Without boulders, the vorticity metric ratios, like the energy metric ratios, tend to have values greater than 1.5 only near the banks. When boulders are incorporated into the model, relatively large vorticity ratios (>1.5) are found near the banks and around the localized flow patterns created by the boulders. Hence, the vorticity metric, like the energy metric, reflects the presence of the velocity–energy gradients induced by channel banks and exposed boulders. Additionally, with the boulders present, a large portion of Area B has vorticity metric ratios greater than 1.5, whereas without boulders a much smaller portion of Area B's area contains vorticity ratios greater than 1.5. These higher metric ratio values are a reflection of the vorticity generated by the transverse flow, which was induced by the presence of the boulders. This shift in the main flow from the west bank toward the east bank is also responsible for increasing velocity gradients and vorticity ratios along the upper 20 m of the channel's east bank.

A direct comparison of the energy and vorticity ratios obtained throughout the study site when boulders are incorporated into the model simulations (Figs. 1*b* and 2*b*) demonstrates that the proportion of the river reach having vorticity ratios exceeding 1.0 is substantially larger than the proportion of river having energy metric ratios exceeding 1.0. One reason for these larger ratios is that the transverse flow occurring within Area B appears to create relatively large vorticity values, but relatively low energy gradients. Hence, vorticity ratios highlight this region as having complex flow, whereas the energy metric does not. The vorticity effects created by the presence of the boulders (Area C) also appear to permeate through a larger area surrounding the boulders than the energy gradient effects created by the boulder. Hence, the vorticity ratio highlights a larger portion of area surrounding the boulders as having complex flow than the energy ratio does. These results suggest that, in this case, vorticity is more sensitive to detecting flow complexity induced by channel topography than the energy metric. However, unlike vorticity, the energy metric provides information that can be linked to bioenergetic concepts and remains a useful spatial metric (Crowder and Diplas 2000*b*). For example, in the case of a free vortex, the flow is highly

© 2002 NRC Canada

Fig. 3. Comparison of the energy metric ratios (|energy metric|/|energy metric|$_{average}$) and vorticity ratios (|vorticity|/|vorticity|$_{average}$) surrounding four exposed boulders found within the study site. (*a*) Energy metric ratios; (*b*) vorticity ratios.

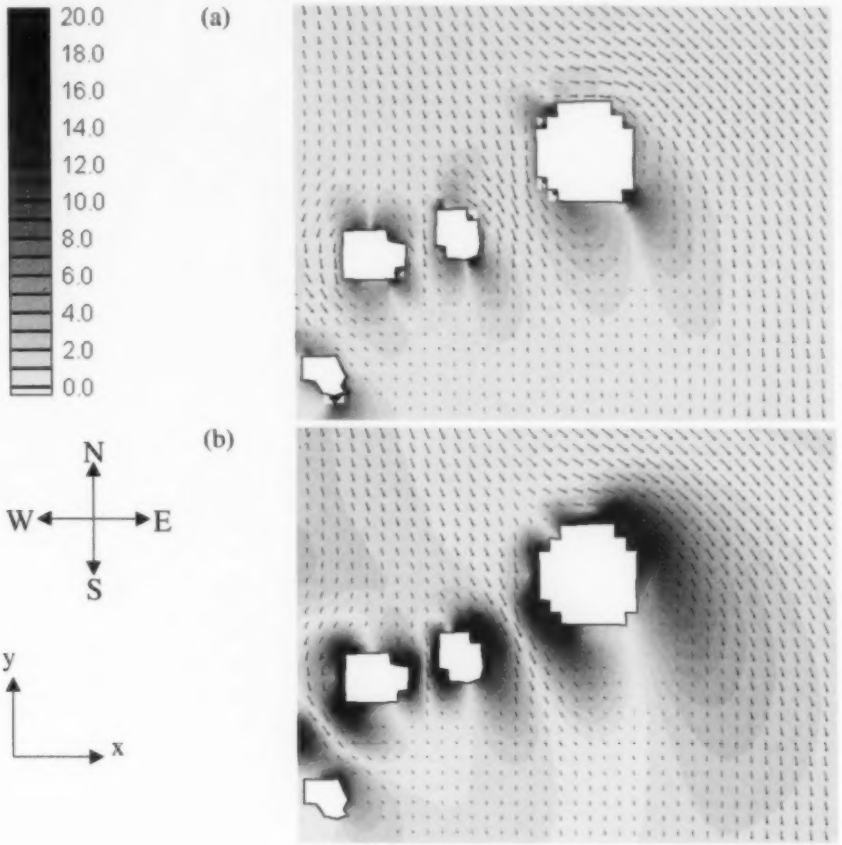

complex but has zero vorticity. Hence, vorticity cannot be used to describe its complexity. However, the high energy gradients within this flow can be quantified with the energy metric.

The differences between the energy and vorticity metrics are demonstrated further (Fig. 3) by comparing the vorticity and energy metric ratios in the immediate vicinity of the boulders found in Area C. For both of these metrics, ratio values are very large (>20) immediately next to the boulders. However, two important differences exist between them. First, the proportion of area having ratio values greater than 20 is much smaller for the energy metric, even though the maximum energy ratios near the boulders are higher than those of the highest vorticity ratio. Second, as one moves away from the boulders, the energy ratio values drop much quicker than the vorticity ratios. Hence, the area containing vorticity ratios between 1 and 20 is much larger than the area containing energy ratios between 1 and 20.

Circulation computations for the numerical simulations

For both simulations, the circulation metric, $\Gamma_{ABS} \div A_{tot}$, was computed for the entire study reach, the upper 20 m of the study reach, and within areas A, B, and C (Figs. 1 and 2). The circulation metric values calculated within each of these five areas for both simulations are summarized (Table 1). Circulation metric values measured in a field study (discussed later) are also summarized (Table 1). To provide a measure of how the circulation metric values in Table 1 differ among each of the various areas and simulations, the value of each area is divided by the circulation metric of every other area for which a circulation metric value was computed. The resulting circulation metric ratios are used to make three comparisons (Table 2). First, a paired comparison is made to determine how the absence or presence of boulders influences circulation values in each of the five identified areas in the model simulations. Second, for each model simulation, the circulation value obtained for the entire reach is compared with the circulation values obtained in the upper 20 m of the reach and in areas A, B, and C. This comparison reveals how the flow complexities within different portions of the modeled study site compare with the site's overall flow complexity. Third, the flow complexity within areas A, B, and C are compared for each model simulation. This comparison reveals how flow complexity within three different locations of similar size differs and is analogous to comparing three different mesoscale habitat features in terms of their flow complexity.

A side-by-side comparison of the five areas analyzed in

© 2002 NRC Canada

Fig. 4. Schematic (not to scale) of the two areas for which the circulation metric was computed within the Smith River, Va. (*a*) Area D without brown trout redds; (*b*) Area E with the three brown trout redds. Area LMNO contains negative vorticity values, whereas Area PLOQ contains positive vorticity values. The arrows indicate flow direction and magnitude along the lines for which velocity was measured.

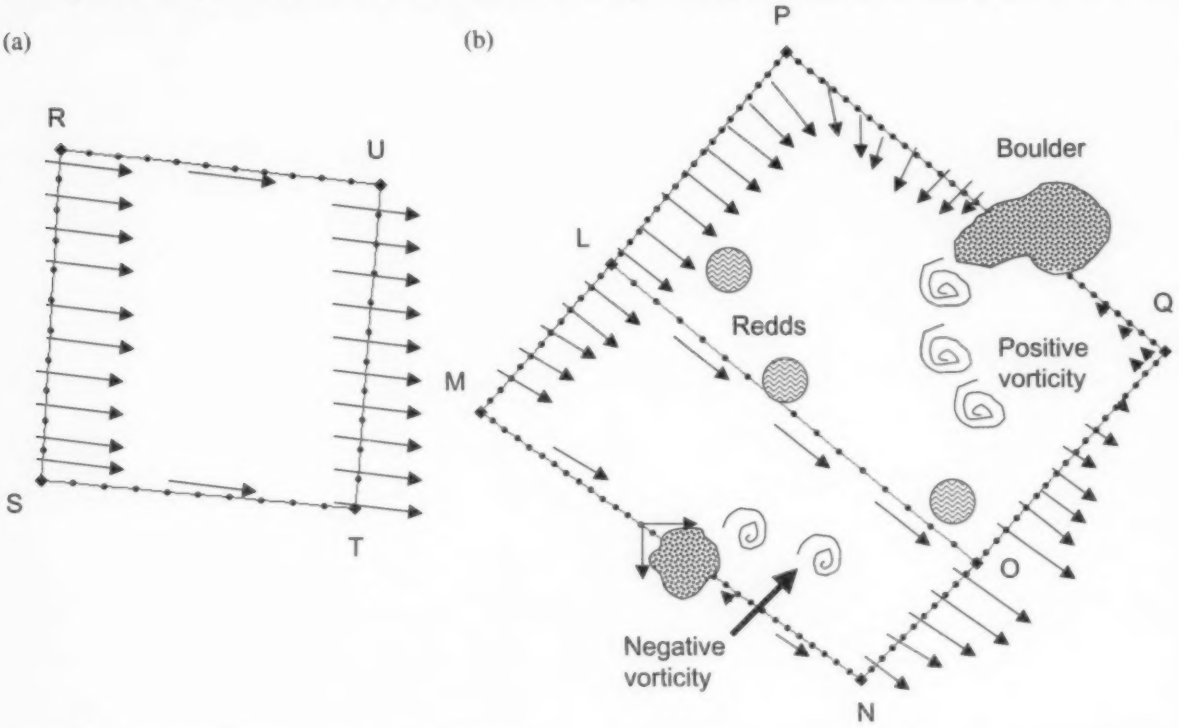

the model simulations (Tables 1 and 2) shows that two scenarios (with and without boulders) generate different circulation metric values within each of the areas. The magnitude of the differences in circulation values, for a particular area, depends greatly on the total area and location over which the metric was computed. With boulders, the 61-m-long reach (1029.190 m^2) has a circulation metric value of 0.054 s^{-1} and is 1.200 times greater than the circulation metric calculated for the same area without boulders. Assuming that $\Gamma_{ABS} \div A_{tot}$ is a measure of flow complexity, then one can state that the entire reach is 1.200 (column 2, row 1 of Table 2) times more complex when boulders are incorporated into the model. A 20% increase in complexity may not seem significant given the differences highlighted between the two model scenarios. However, a large portion of the study site has very similar flow patterns for both model scenarios. It is only within the upper 20 m of the study site that the presence of the boulders clearly creates different flow patterns. Consequently, by computing the circulation metric at the reach-scale, the differences in vorticity values produced by the boulders in the upper 20 m of the site are masked by the large portion of the study site having similar vorticity values.

When the circulation metric is computed for the upper 20 m of the site (272.910 m^2), one sees a more pronounced difference between model simulations. According to the circulation metric values, the flow within this region becomes 1.443 times more complex when boulders are present. Similarly, in the 31.997-m^2 area immediately surrounding the boulders (Area C) where the boulders have their strongest influence and the two simulations are the most different, the flow becomes 3.443 times more complex when boulders are incorporated into the model. These results show the relative influence that the boulders have on flow complexity at different scales and different locations within the study site. In this case, at the reach-scale, the boulders play a minor role in the channel's overall complexity. Had more exposed boulders been present throughout the site, the reach-scale results could have been significantly different. However, within areas B and C, where the flows are most influenced by the presence of the boulders, one obtains significantly different circulation metric values that reflect the diversity of flow features created under the two different simulations.

The variation of circulation values within different parts of the study site compared with a simulation's reach-scale circulation value is also observed (Table 2). For both simulations, the circulation metric for Area A is about a third of the circulation value one obtains for the entire reach. The flow pattern found within Area A is quite uniform and has very little flow complexity compared with the average flow complexity found throughout the site. For the simulation without boulders, areas B and C have circulation metric values 1.667 and 1.356 times that of the entire reach, respectively. For the simulation with boulders, areas B and C have circulation metric values 1.963 and 3.889 times that of the entire reach, respectively. If the circulation metric value is

© 2002 NRC Canada

Table 1. Summary of circulation metric values.

Area analyzed	Reach[a]	Reach[b]	20 m[a]	20 m[b]	Area A[a]	Area A[b]	Area B[a]	Area B[b]	Area C[a]	Area C[b]	Area D[c]	Area LMNO[c]	Area PLOQ[c]	Area E[c]
A_{tot} (m^2)[d]	1034.237	1029.190	275.967	272.910	32.783	32.783	32.037	32.037	34.057	31.997	10.750	8.188	13.250	21.438
Γ ($m^2 \cdot s^{-1}$)	—	—	—	—	—	—	—	—	—	—	–0.016	–0.377	1.666	—
Γ_{ABS} ($m^2 \cdot s^{-1}$)	46.034	55.197	19.324	27.532	0.463	0.585	2.419	3.401	2.068	6.727	0.016	0.377	1.666	2.043
$\Gamma_{ABS} \div A_{tot}$ (s^{-1})	0.045	0.054	0.070	0.101	0.014	0.018	0.075	0.106	0.061	0.210	0.001	0.046	0.123	0.095

[a]Results obtained from model simulations of the North Fork of the Feather River (California) without boulders.
[b]Results obtained from model simulations of the North Fork of the Feather River with boulders.
[c]Results obtained from field measurements taken at locations in the Smith River (Virginia).
[d]Total wetted area within a given analyzed area varies slightly between the model simulations because of wetting and drying and because elements do not always fall completely within the regions.

Table 2. Matrix comparing the flow complexity of all the regions for which circulation metric values were computed.

Area analyzed	Reach[a]	Reach[b]	20 m[a]	20 m[b]	Area A[a]	Area A[b]	Area B[a]	Area B[b]	Area C[a]	Area C[b]	Area D[c]	Area LMNO[c]	Area PLOQ[c]	Area E[c]
Reach[a]	1.000	1.200	1.556	2.244	0.311	0.400	1.667	2.356	1.356	4.667	0.022	1.022	2.733	2.111
Reach[b]	0.833	1.000	1.296	1.870	0.259	0.333	1.389	1.963	1.130	3.889	0.019	0.852	2.278	1.759
20 m[a]	0.643	0.771	1.000	1.443	0.200	0.257	1.071	1.514	0.871	3.000	0.014	0.657	1.757	1.357
20 m[b]	0.446	0.535	0.693	1.000	0.139	0.178	0.743	1.050	0.604	2.079	0.010	0.455	1.218	0.941
Area A[a]	3.214	3.857	5.000	7.214	1.000	1.286	5.357	7.571	4.357	15.00	0.071	3.286	8.786	6.786
Area A[b]	2.500	3.000	3.889	5.611	0.778	1.000	4.167	5.889	3.389	11.67	0.056	2.556	6.833	5.278
Area B[a]	0.600	0.720	0.933	1.347	0.187	0.240	1.000	1.413	0.813	2.800	0.013	0.613	1.640	1.267
Area B[b]	0.425	0.509	0.660	0.953	0.132	0.170	0.708	1.000	0.575	1.981	0.009	0.434	1.160	0.896
Area C[a]	0.738	0.885	1.148	1.656	0.230	0.295	1.230	1.738	1.000	3.443	0.016	0.754	2.016	1.557
Area C[b]	0.214	0.257	0.333	0.481	0.067	0.086	0.357	0.505	0.290	1.000	0.005	0.219	0.586	0.452
Area D[c]	45.00	54.00	70.00	101.00	14.00	18.00	75.00	106.0	61.00	210.0	1.000	46.00	123.0	95.00
Area LMNO[c]	0.978	1.174	1.522	2.196	0.304	0.391	1.630	2.304	1.326	4.565	0.022	1.000	2.674	2.065
Area PLOQ[c]	0.366	0.439	0.569	0.821	0.114	0.146	0.610	0.862	0.496	1.707	0.008	0.374	1.000	0.772
Area E[c]	0.474	0.568	0.737	1.063	0.147	0.189	0.789	1.116	0.642	2.211	0.011	0.484	1.295	1.000

[a]Results obtained from model simulations of the North Fork of the Feather River (California) without boulders.
[b]Results obtained from model simulations of the North Fork of the Feather River with boulders.
[c]Results obtained from field measurements taken at locations in the Smith River (Virginia).

© 2002 NRC Canada

considered an indicator of flow complexity, then the most complex flow pattern occurs within Area B when the boulders are absent and in Area C when the boulders are present.

For a given simulation, the circulation metrics computed in areas A, B, and C vary significantly (Table 2). Without boulders, the flow in areas B and C are 5.357 and 4.357 times as complex as the flow in Area A. With boulders, the flow in areas B and C are 5.889 and 11.67 times more complex than the flow in Area A. In both scenarios, the uniform flow patterns found in Area A have small circulation values and are clearly distinguishable from the circulation values computed within areas B and C. Hence, the circulation metric adequately differentiates between the uniform and non-uniform flows predicted in the two model scenarios. Without boulders, the circulation values for areas B and C (0.075 and 0.061 s^{-1}, respectively) do not suggest that these are substantially different in terms of their flow complexity. A visual analysis of the vorticity metric ratio plot (Fig. 2*a*) confirms that finding. When the boulders are included in the model, the circulation metric values clearly distinguish between the highly complex flows surrounding the boulders and the moderately complex flows found in Area B. The sensitivity of the circulation metric in distinguishing between the visually observed flow patterns makes it a potentially useful tool for identifying meso- or macro-scale habitat features of biological importance.

Circulation metrics computed from velocity data measured in the field

The circulation metric values computed within the two areas of the Smith River are significantly different. Consistent with the results of the previous numerical simulations, a large circulation metric value (0.095 s^{-1}) was computed in Area E (where significant flow complexity exists) and a small circulation metric (0.001 s^{-1}) was computed in Area D (where uniform flow exists). Moreover, the circulation values computed in areas LMNO and PLOQ are consistent in sign with the clockwise and counterclockwise motion of the vortices observed within these regions. A summary of the circulation (Γ), absolute circulation (Γ_{ABS}), circulation metric ($\Gamma_{ABS} \div A_{tot}$), and area ($A_{tot}$) corresponding to areas D and E, as well as the positive and negative vorticity regions (areas LMNO and PLOQ), is provided (Table 1). A comparison of the results for Area D and areas LMNO and PLOQ shows that the flow in Area D, which had no visually identifiable vortices, has the smallest absolute circulation (0.016 $m^2 \cdot s^{-1}$) and circulation per unit area (0.001 s^{-1}) values. Area LMNO, which had subtle but visually identifiable vortices, has absolute circulation and circulation per unit area values 23.5 and 46 times larger than those found in Area D. However, the absolute circulation and circulation per unit area values found in Area PLOQ, which had stronger and distinctly visible vortices, were 4.4 and 2.67 times larger than those found in Area LMNO. When the circulation metrics of the positive and negative vorticity regions are combined to represent the area surrounding the location of the three redds (Area E), the resulting circulation per unit area metric value is 95 times that found in Area D, where no redds were found. Hence, the proposed circulation metric clearly distinguished between the flow complexity surrounding the three redd locations and an area in which no redds were found.

The locations of the three redds within Area E (Fig. 4) are close to line LO, which separates the positive and negative vorticity zones visually observed in the field. Along line LO, little, if any vorticity could be seen and flow direction was largely parallel to the line LO. However, significant energy gradients and vorticity exist immediately adjacent to line LO. These flow conditions are analogous to the flow patterns found between the two easternmost boulders (Fig. 3). Specifically, a line having near-zero vorticity, and energy metric values passes between positive and negative vorticity zones. Hence, the hydraulic conditions surrounding the three brown trout redds can be described at two different scales using the proposed metrics. At the "microhabitat scale", or at the exact locations of the redds, relatively small vorticity and energy gradient metric values are present. At the "mesohabitat scale" (the 21.44-m^2 area surrounding the redds) the flow is highly complex and yields a high circulation per unit area value. In contrast, any location within Area D (containing no redds) will have low vorticity and energy metric values at the microhabitat scale and low circulation per unit area values at the mesohabitat scale because of the uniform flow conditions found throughout this location. Consequently, if the flow complexity at the mesohabitat scale (surrounding the redds) is biologically important, then Area E's circulation metric per unit area value used in conjunction with vorticity, energy gradient, and other habitat variables evaluated at the microhabitat scale is likely to best describe the overall flow patterns and differentiate between the flow conditions in areas D and E.

While the proposed circulation metric provides a means of quantifying flow complexity at the mesoscale or macroscale level, it is not known how large an area (or at what scale) the circulation metric should be computed over to best quantify biologically important flow patterns. In this example, a 21.44-m^2 area surrounding the locations of three redds was selected as an appropriate scale to test the metric and explore whether flow complexity might be an important component of brown trout spawning habitat. It is possible that only the flow patterns within about a metre of the redd's locations are biologically important and that the circulation metric should be computed at this scale and not the larger one used. However, an advantage of the circulation metric is that it can be computed at the scale stream biologists determine to be appropriate for quantifying specific flow patterns.

Discussion

A better understanding of how channel topography and discharge interact to create spatially varying flows and suitable habitat features may lead to improved techniques of quantifying the types and amounts of habitat available within a stream. A stream's flow interacts with a river's topographic features to create complex flow patterns that can occur over a range of spatial scales. Often, these features are described qualitatively and not quantitatively (eddies, pools, riffles, and runs). Moreover, commonly used point metrics such as depth, velocity, and substrate values cannot be used to quantify the spatial characteristics within these features. Two-dimensional hydraulic models and spatial hydraulic metrics provide stream biologists with the ability to analyze and quantify how channel topography interacts within the

© 2002 NRC Canada

flow to create vorticity, velocity–energy gradients, and other spatial flow features of potential biological importance.

The energy, vorticity, and circulation metrics discussed here are all spatial hydraulic metrics that quantify physical attributes of flows and can be used to help locate and distinguish between flow features of biological importance. The energy and vorticity metrics describe how flow is changing around a point. Hence, two locations having the same depth and velocity values surrounded by different flow features can be distinguished from each other by comparing their local vorticity and (or) energy metric values. A high vorticity or energy metric value would suggest that a point is located within an area having significant spatial variation, or flow complexity, occurring around that point. Consequently, one can employ these metrics to help identify important microhabitat features like the velocity–energy gradients used by brown and brook trout to feed.

The circulation metric extends the concept behind the energy and vorticity metrics to an arbitrary area. Specifically, the circulation metric provides stream biologists a means of quantifying flow complexity within a given area. The higher the circulation metric value is, the higher is the flow complexity within the area being analyzed. Note that a distribution of velocity values within a stream reach does not necessarily reflect the reach's flow complexity. Instead, flow complexity depends greatly on the spatial arrangement of the velocity values within a reach. For example, a river reach that gradually transitions from uniform high-velocity values at its upstream section to uniform low-velocity values at a downstream cross-section may, statistically, have the same depth and velocity distributions as a reach having complex topography that creates heterogeneous pockets of high- and low-velocity areas throughout the reach. Although they are statistically similar, the latter stream would have far more flow complexity in terms of velocity gradients, eddies, etc. In the circulation metric, vorticity values dependent on the spatial arrangement of the velocity values are summed. Hence, the circulation metric reflects and accounts for the spatial arrangement of the velocity field within a river and provides stream biologists with a means to quantify flow conditions within mesoscale habitat features (e.g., pools, riffles, and runs). Moreover, one can conjecture on what types of physical processes (aeration, erosion, and deposition) might be associated with a circulation metric value. High circulation values are indicative of high vorticity, local aeration, and scour patterns. In fact, local aeration processes and erosional features were visually observed immediately adjacent to and downstream of the large exposed boulder near the three redd locations (Area E) in the Smith River. Specifically, one could see vortices entraining air and purging finer particles from the bed material immediately adjacent to the boulders, whereas finer materials were found deposited immediately downstream of the boulders. The circulation metric may also be useful in quantifying important differences between urban and nonurban streams and developing stream restoration techniques that create and maintain the flow characteristics found in natural streams.

The spatial hydraulic metrics proposed here can be incorporated into stream habitat studies in a number of ways. One means of using and calculating these metrics within an area is through the use of 2-D hydraulic model output. Two-dimensional models provide the depth, velocity, substrate, and cover data traditionally used in stream habitat assessments. Moreover, the spatially explicit output provided by 2-D models provides a means of directly computing the proposed spatial hydraulic metrics throughout a study site to help identify and distinguish between features within the river having biological importance. Plots like those generated in this study can be used to determine if specific ranges of energy gradients, vorticity values, or circulation values are characterizing biologically significant areas.

The energy, vorticity, and circulation metrics proposed here can also be computed in the field with standard velocity meters and a compass. One can collect the data needed to compute the energy and vorticity metrics at a particular point within the river by measuring the depth-averaged velocity at the midpoints of the four sides of a small imaginary square centered over the point where the vorticity or energy gradient is being calculated. Using the compass to measure the direction of the flow at each of the four points, one can decompose the velocity magnitudes at each point into the depth-averaged x- and y-velocity components needed to compute vorticity (eq. 4). Circulation (not the circulation metric) can be computed by measuring velocity magnitude and direction around the perimeter of an area. By observing the locations of positive and negative vorticity zones within an area of interest, one can compute and then sum the absolute circulation values for each region to obtain the proposed circulation metric value for the entire area of interest. This procedure was adopted to compute the flow complexity around two locations within the Smith River.

One cannot compute the proposed spatial hydraulic metrics with model output from one-dimensional hydraulic models like the one used in PHABSIM (physical habitat simulation system, Milhous et al. 1989). One-dimensional models represent a river reach as a series of rectangular areas each having uniform depth, and velocity (Bovee 1978). By assuming uniform flow within each cell, the energy metric, vorticity metric, and circulation values within a cell must be zero, as there is no spatial variation occurring within a cell. However, the inability to compute spatial hydraulic metrics from 1-D model output does not exempt the use of spatial hydraulic metrics in a habitat study employing a 1-D model. Spatial hydraulic metric values measured at key locations within the study site may provide valuable insights on a stream's characteristics and complement the depth, velocity, and substrate, values computed in 1-D models.

Input from stream biologists is needed to further develop and validate meaningful spatial metrics. Aquatic organisms of different species and life stages are likely to require or respond to different types of vorticity, energy gradients, and flow complexities. Field studies need to be performed to determine what types and scales of spatial flow attributes different aquatic organisms are using. If a specific spatial metric is determined to be biologically significant, one can then begin to incorporate it into habitat suitability criteria for that particular organism.

The 2-D hydraulic model results suggest that vorticity is a potentially useful metric for detecting spatial flow patterns of biological importance. The highest vorticity values computed in the study site were found in the immediate vicinity of exposed boulders located in the river's main channel.

© 2002 NRC Canada

Vorticity values were also relatively high along the channel banks and within an area containing a transverse flow. A comparison of the vorticity and energy metric values within the study site revealed that both vorticity and energy gradients are present in the spatial flow patterns generated by channel banks and exposed boulders. However, vorticity values appeared to be more sensitive to detecting spatial flow patterns. Specifically, the vorticity effects created by the presence of boulders were detected further downstream than the energy gradients created by the boulders. Vorticity also reflected the location of a transverse flow whereas the energy metric did not. However, as each metric quantifies a different physical attribute of flow, both metrics provide useful means of differentiating between locations having similar depth and velocity values surrounded by different flow patterns. The best metric to use in a specific instance will depend on the type of flow pattern being analyzed and the physical attributes within that flow that aquatic organisms are utilizing. In some situations, both metrics might be necessary to describe the important attributes of a particular location within a river.

Circulation metric values computed over the entire reach, over the upper 20 m of the study site, and within three distinct areas of the site were consistently higher when boulder geometry was incorporated into the model. The magnitude of the differences in circulation metric values for the two simulations depended on the location and total area over which the metric was computed. At the reach scale, a difference of 20% was found. In the vicinity of the boulders, a difference of 350% was found. Circulation metric values computed within separate segments of the study site show that the metric can distinguish between the visually different flow patterns observed within the study reach. The circulation metric obtained around the locations of four exposed boulders is twice as large as the same metric computed within a region containing a transverse flow and twelve times larger than the metric value obtained within a region of the river having uniform flow.

By collecting velocity magnitude and direction data, circulation metric values were also computed (without the use of 2-D model output) for an area containing three brown trout redds and a location devoid of brown trout redds within the Smith River. The resulting circulation metric values varied by a factor of 95 and differentiated between the uniform flow conditions surrounding the area containing no redds and the complex flow patterns surrounding the three redds. However, given that the circulation metric was computed for the flow surrounding the locations of only three redds, no definitive statements can be made regarding whether or not flow complexity is actually an important factor in quantifying brown trout spawning habitat, especially as important nonhydraulic factors such as cover and predation were not addressed. Consequently, the circulation metric results for the redd comparison should be viewed solely as an example of how the proposed metric might be employed in future studies and a method of further exploring the metric's suitability to describe flow complexity.

The proposed spatial metrics provide stream biologists, engineers, and managers the ability to describe micro-, meso-, and macro-habitat-scale features in a quantitative and physically meaningful way. This quantitative description allows one to compare how specific pools, or other habitat features, between or within streams, are hydraulically similar or different and how these differences might reflect a stream's aquatic health. The spatial hydraulic metrics proposed here are only a few of the many potential metrics that could be employed in evaluating stream conditions. Input from stream biologists is needed to help determine the best and most appropriate use of such metrics. The metrics provided here quantify well-established attributes of fluid motion and can be readily calculated in the field with standard velocity meters or from 2-D hydraulic model output.

Acknowledgements

The support provided by the United States Environmental Protection Agency, the National Science Foundation, and Pacific Gas and Electric is gratefully acknowledged. The field and technical support provided by Matt Chan, Doug Novinger, and Yi Shen is also appreciated.

References

Bandyopadhyay, P.R., Castano, J.M., Nedderman, W.H., and Donnelly, M.J. 2000. Experimental simulation of fish-inspired unsteady vortex dynamics on a rigid cylinder. Journal of Fluids Engineering—Transactions of the ASME, **122**: 219–238.

Batchelor, G.K. 1967. An introduction to fluid dynamics. Cambridge University Press, London.

Bovee, K.D. 1978. The incremental method of habitat potential for coolwater species with management implications. Am. Fish. Soc. Spec. Publ. **11**: 340–346.

Crowder, D.W., and Diplas, P. 2000*a*. Using two-dimensional hydrodynamic models at scales of ecological importance. J. Hydrol. **230**: 172–190.

Crowder, D.W., and Diplas, P. 2000*b*. Evaluating spatially explicit metrics of stream energy gradients using hydrodynamic model simulations. Can. J. Fish. Aquat. Sci. **57**: 1497–1507.

Environmental Modeling Research Laboratory (EMRL). 1999. SMS surface water modeling system reference manual, version 6.0. Brigham Young University, Provo, Utah.

Fausch, K.D., and White, R.J. 1981. Competition between brook trout (*Salvelinus fontinalis*) and brown trout (*Salmo trutta*) for position in a Michigan stream. Can. J. Fish. Aquat. Sci. **38**: 1220–1227.

Freeman, M.C., and Grosssman, G.D. 1993. Effects of habitat availability on dispersion of a stream cyprinid. Environ. Biol. Fish. **37**: 121–130.

Ghanem, A., Steffler, P., Hicks, F., and Katopodis, C. 1996. Two-dimensional hydraulic simulation of physical habitat conditions in flowing streams. Regul. Rivers, **12**: 185–200.

Hanke, W., Brucker, C., and Bleckmann, H. 2000. The ageing of the low-frequency water disturbances caused by swimming foldfish and its possible relevance to prey detection. J. Exp. Biol. **203**: 1193–1200.

Hayes, J.W., and Jowett, I.G. 1994. Microhabitat models of large drift-feeding brown trout in three New Zealand rivers. N. Am. J. Fish. Manag. **14**: 710–725.

King, I.P. 1990. Program documentation RMA-2V, two-dimensional finite element model for flow in estuaries and streams, version 4.3. Resource Management Associates, Lafayette, Calif.

Kiorboe, T., and Visser, A.W. 1999. Predator and prey perception in copepods due to hydromechanical signals. Mar. Ecol. Prog. Ser. **179**: 81–95.

© 2002 NRC Canada

Leclerc, M., Boudreault, A., Bechara, J.A., and Corfa, G. 1995. Two-dimensional hydrodynamic modeling: a neglected tool in the instream flow incremental methodology. Trans. Am. Fish. Soc. **124**: 645–662.

Milhous, R.T., Updike, M.A., and Schneider, D.M. 1989. Physical habitat simulation system (PHABSIM) reference manual, version II. Instream Flow Information Paper No. 26, U.S. Fish Wild. Serv. Biol. Rep. 89(16), Fort Collins, Colo.

Munson, B.R., Young, D.F., and Okiishi, T.H. 1990. Fundamentals of fluid mechanics. 2nd ed. John Wiley and Sons, Inc., New York.

Shields, F.D., Jr., Cooper, C.M., and Knight, S.S. 1995. Experiment in stream restoration. Journal of Hydraulic Engineering (ASCE), **121**: 494–502.

Way, C.M., Burky, A.J., Bingham, C.R., and Miller, A.C. 1995. Substrate roughness, velocity refuges, and macroinvertebrate abundance on artificial substrates in the lower Mississippi River. J. North Am. Benthol. Soc. **14**: 510–518.

Whiting, P.J., and Dietrich, W.E. 1991. Convective acccelerations and boundary shear stress over a channel bar. Water Resour. Res. **27**: 783–796.

© 2002 NRC Canada

Atlantic mackerel (*Scomber scombrus*) recruitment fluctuations in relation to copepod production and juvenile growth

Marc Ringuette, Martin Castonguay, Jeffrey A. Runge, and François Grégoire

Abstract: A previous study identified relationships linking variations in the physical environment to fluctuations in zooplankton biomass and Atlantic mackerel (*Scomber scombrus*) recruitment. Diets of mackerel larvae were compared among four years, one of these years producing an exceptional year-class (1982). Comparisons were standardized for larval length and time of day. Stomach fullness differed significantly among years, with highest values observed in 1982. Stomach content wet weights were significantly larger in 1982 than in 1987 and 1996. The mean weight of *Calanus finmarchicus* nauplii prey in the diet was also significantly greater in 1982 than in 1985, 1987, or 1996. Female *C. finmarchicus* were more abundant and more widely distributed in the southern Gulf of St. Lawrence in 1982 compared with 1985, 1987, and 1990. These findings are consistent with the hypothesis of a link between production of copepod nauplii, feeding of mackerel larvae, and recruitment success. However, mackerel size at the end of the first year, as measured on otoliths, varied significantly between years and was smallest in 1982. We propose hypotheses to account for the coupling between high larval food abundance, small juvenile growth, and strong cohorts.

Résumé : Une étude précédente a identifié une relation liant les variations de l'environnement physique aux fluctuations de la biomasse zooplanctonique et à la force du recrutement du maquereau bleu (*Scomber scombrus*) du sud du golfe du Saint-Laurent. L'alimentation des larves de maquereau a été comparée entre quatre années, l'une d'entre elle produisant une classe d'âge exceptionnelle (1982). L'indice de plénitude des estomacs a varié significativement entre les années avec les valeurs les plus fortes en 1982. Le poids du contenu stomacal était significativement plus grand en 1982 qu'en 1987 et 1996 et le poids des proies nauplii *Calanus finmarchicus* dans les estomacs était significativement plus grand en 1982 qu'en 1985, 1987 ou 1996. Les *C. finmarchicus* femelles étaient plus abondantes et avaient une distribution plus vaste dans le sud du Golfe du St-Laurent en 1982 qu'en 1985, 1987 et 1990. Ces observations supportent l'hypothèse d'un lien entre la production de nauplii de copépodes, l'alimentation des larves de maquereau et la force du recrutement. Toutefois, la taille des maquereaux juvéniles mesurée à partir des otolithes, a varié significativement entre les années et était la plus faible en 1982. Nous proposons des hypothèses qui pourraient expliquer le couplage entre la forte abondance de nourriture pour les larves, la faible croissance juvénile et les fortes cohortes.

Introduction

Very strong year-classes occasionally occur in populations of pelagic fishes (Anderson 1988; Cushing 1995), including Atlantic mackerel (*Scomber scombrus*) (Anderson and Paciorkowski 1980). These cohorts are of crucial importance for the commercial fishery because they dominate the catch even several years after their first appearance. Survival and recruitment are believed to be determined primarily during the larval stage. Biotic factors such as prey availability (Cushing 1990), growth, and predation (Hunter 1981; Anderson 1988; Pepin 1991) along with abiotic factors such as temperature (Houde 1987) and currents all have impacts on larval survival and thus influence recruitment success. However, the interactions and mechanisms that give rise to very strong year-classes and the connections to environmental variations are not well understood. This paper focuses on the early larval stage as a critical period for recruitment. Processes occurring during the late larval or juvenile stages could also play a significant role but are not examined here.

The mackerel of the Northwest Atlantic overwinter off the east coast of the United States, on the outer part of the conti-

Received 21 January 2002. Accepted 18 March 2002. Published on the NRC Research Press Web site at http://cjfas.nrc.ca on 2 May 2002.
J16726

M. Ringuette.[1] Institut des Sciences de la Mer, Université du Québec à Rimouski, 310 Allée des Ursulines, Rimouski, QC G5L 3A1, Canada.
M. Castonguay,[2] **J.A. Runge,**[3] **and F. Grégoire.** Pêches et Océans Canada, Institut Maurice-Lamontagne, C.P. 1000, Mont-Joli, QC G5H 3Z4, Canada.

[1]Present address: GIROQ, Département de Biologie, Université Laval, QC G1K 7P4, Canada.
[2]Corresponding author (e-mail: CastonguayM@dfo-mpo.gc.ca).
[3]Present address: Ocean Process Analysis Laboratory, 142 Morse Hall, University of New Hampshire, Durham, NH 03824, U.S.A.

 DOI: 10.1139/F02-039 © 2002 NRC Canada

nental shelf. In spring, schools of the Canadian stock swim toward the coast and begin a migration that takes them northward into the Gulf of St. Lawrence (Anderson and Paciorkowski 1980). They typically enter the Gulf in late May – early June. Spawning takes place over a short period, at most a few weeks, throughout the southern Gulf of St. Lawrence, at temperatures close to 10°C (Ouellet 1987).

Runge et al. (1999) found a significant inverse relationship between RIVSUM, an index of freshwater discharge from the St. Lawrence River watershed for January through May, and variations in both zooplankton biomass in the southern Gulf of St. Lawrence in June and year-class strength of the Canadian mackerel stock. The mesozooplankton community of the southern Gulf is typically dominated by the planktonic copepods *Temora longicornis* and *Pseudocalanus* spp. One hypothesis that is consistent with the observations is that in some years there is a much greater proportion of adult and copepodite stages of *Calanus finmarchicus* and *Calanus hyperboreus*, two other copepod species found in the southern Gulf, perhaps because of interannual variability in transport from the *Calanus*-rich Laurentian Channel (de Lafontaine et al. 1991). This phenomenon correlates with years of low freshwater discharge (RIVSUM) and strong mackerel recruitment (Runge et al. 1999). *Calanus finmarchicus* is reproductively active in early summer and has the potential to produce large numbers of eggs, and consequently, early naupliar stages relative to the smaller dominant southern Gulf copepod species (Runge 1988). The exceptionally high abundance of *C. finmarchicus* females that was observed to coincide with the very high mackerel recruitment is hypothesized to have produced eggs that hatched and overwhelmed the local prey field for mackerel larvae with high-quality nauplii prey, resulting in unusually high survival.

The diet of mackerel larvae varies with age. Young larvae feed mainly on the eggs and nauplii of copepods (Fortier and Villeneuve 1996; Hillgruber et al. 1997), cladocerans (Grave 1981), and appendicularians (Grave 1981). As the larvae grow, the size of their prey increases, consisting of copepodite stages of various species and often other fish larvae (Last 1980; Grave 1981; Fortier and Villeneuve 1996). However, most studies have not examined the composition of prey species ingested, especially when these prey are nauplii. This knowledge is needed to understand the linkage between zooplankton production and larval survival.

Here we probe further the hypothesis of a link in the southern Gulf of St. Lawrence between copepod production, feeding of mackerel larvae on copepod nauplii, and the subsequent growth and recruitment of juvenile mackerel into the adult population. First, we analyzed the potential prey field for mackerel larvae in the southern Gulf based on samples collected with finer mesh nets during one survey year, for the purpose of testing the assumption that samples from the 333-μm-mesh survey nets provide proxies for the production of prey. Second, we analyzed the stomach contents of mackerel larvae captured during the June surveys in the southern Gulf to test the hypothesis that larvae fed more on *C. finmarchicus* during the year of high recruitment (1982). Third, annual indices of growth of juvenile mackerel (at age 1) and of recruitment at age 3 were obtained from the commercial fishery in eastern Canada and are used to examine relationships between diet, growth, and year-class strength.

Materials and methods

Sampling of zooplankton and mackerel larvae

The reproductive biomass of adult mackerel in the southern Gulf of St. Lawrence is assessed by estimating egg abundance in the water column during the spawning period (e.g., Grégoire 1997; see also Priede and Watson 1993). This work has been conducted each year since 1982 with the exception of 1995 and 1997. A ship twice visits a grid of 65 stations covering the entire southern Gulf of St. Lawrence in late June (Fig. 1), which typically covers the period of peak mackerel spawning (Ouellet 1987). One pass of the grid usually requires 7–8 days.

Fish eggs, fish larvae, and zooplankton were collected using 61-cm-diameter bongo nets with mesh size of 333 μm. The nets were towed diagonally at a speed of 1 $m \cdot s^{-1}$ for 10 min between the surface and 50 or 5 m above bottom in shallower water. A General Oceanics (model 2031, Miami, Fla.) flow meter was attached in the middle of each net. Until 1986, water column temperature was measured with an expendable bathythermograph (XBT). After 1986, salinity and temperature profiles were taken with an Applied Microsystems STD-12 or a Guildline CTD (model 8715). The zooplankton was preserved directly after capture in 4% formaldehyde.

The mackerel eggs and larvae were sorted, counted, and stored separately. The species composition of the zooplankton sampled in 1982, 1985, 1987, and 1990 was determined by the Huntsman Marine Science Centre at St. Andrews, N.B., Canada (Castonguay et al. 1998). The beaker method was used to divide the samples to obtain a minimum of 500 individuals (van Guelpen et al. 1982) and the organisms were identified to the lowest possible taxonomic level. Here, we will use data on variations in the distribution of females; raw data on species composition are published in Castonguay et al. (1998).

The composition of multicellular microzooplankton in the southern Gulf was examined during an additional survey in 1996. Because of the mesh size of the Bongo nets (333 μm), the mackerel egg survey samples underestimated the abundance of very small zooplankton such as cyclopoids and the copepodite stages of small calanoids. An analysis of the abundance of small zooplankton species provides a more complete description of the abundance of the potential prey available to fish larvae immediately following yolk-sac resorption. Samples for microzooplankton composition were collected at 13 stations with nets 1 m in diameter and 200- and 500-μm mesh between 10:00 and 12:00. (Sampling time was standardized to avoid biases in estimation of zooplankton production.) The nets were towed vertically, between the bottom and the surface at stations <70 m and between 70 m and the surface at stations >70 m. The volume of water filtered was computed based on the depth of the water column sampled and the net diameter. We observed no clogging of the nets. Abundance of the different zooplankton species for these net samples was determined from a subsample of at least 300 individuals obtained with a Stemple pipette. The

© 2002 NRC Canada

Fig. 1. Sampling grid for the mackerel egg survey in the southern Gulf of St. Lawrence. The open circles are regular stations of the egg survey, but also show where vertical net tows with 50- and 200-μm-mesh nets were carried out in 1996.

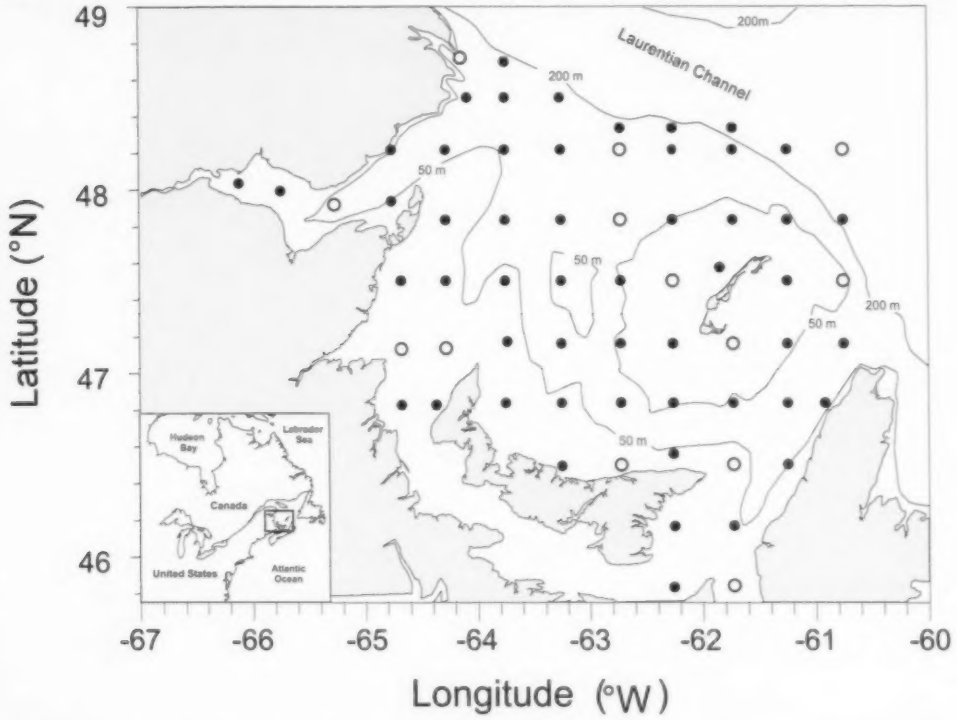

organisms were identified to the lowest possible taxonomic level using a stereomicroscope (Leica M-10). Egg production of the various copepod species was estimated based on the literature.

Stomach content analysis

To eliminate biases due to a diel feeding pattern, only mackerel larvae collected between 18:00 and 24:00 were analyzed. As larval mackerel diet varies with size (Grave 1981; Fortier and Villeneuve 1996), the standard length of each larva was measured with a Bioquant image analysis system. Based on previous studies (Hunter and Kimbrell 1980; Ware and Lambert 1985), larvae were expected to start feeding at a size of 3.5 mm, which takes into account effects of shrinkage due to preservation (Theilacker 1980).

Dissection of larval stomachs was performed under a stereomicroscope (Leica M-10) using entomology needles. The isolated gut was evaluated for fullness using a qualitative index consisting of five classes (empty, 1/4, 1/2, 3/4, and full) based on the degree of stomach distension. After the stomach was cut open, the prey (usually nauplii) were counted and identified to the most precise taxonomic level possible. Each prey item was measured with an optical micrometer for maximum length not including body curvature. The wet weight biomass of the prey in the stomachs was estimated according to the method of Bainbridge and McKay (1968). In the present study, the biomass of nauplii for any species represents a mean value and does not take into account their developmental stage.

A comprehensive analysis, including determination of zooplankton species composition and spatial distribution and stomach content analysis of mackerel larvae, was done for the survey years 1982, 1985, and 1987. For 1990, only the zooplankton analyses were carried out. According to the mackerel recruitment index calculated by Runge et al. (1999), 1990 was a year of low recruitment. Because we already had data for a low recruitment year, we decided to invest the time and effort involved in detailed stomach content analysis in another way. The collection of larvae in 1996 allowed us to work on fresh material, an advantage from the standpoint of sample quality. Accordingly, an analysis of stomach contents of mackerel larvae and an analysis of species composition of the microzooplankton fraction was carried out in that year.

Mackerel growth and recruitment

Because of the formaline solution, the otoliths had dissolved in the larval collection used for stomach content analysis. To compare growth among year-classes, we used the only material available, otoliths sampled from the commercial fishery. The mean size of otoliths at age 1 (L_1) was used as a proxy of the first year of growth for mackerel born between 1982 and 1990. L_1 is measured as the distance between the centre of the otolith and the demarcation representing the end of the first growth season in the fall (e.g., Dawson 1991). A total of 7391 otoliths were examined (see Grégoire and Gagnon 1993 for details).

Growth at age 1 reflects both larval and juvenile growth. In the southern Gulf of St. Lawrence, mackerel larvae meta-

© 2002 NRC Canada

Fig. 2. Spatial distribution and abundance of females of *Calanus finmarchicus*, *Pseudocalanus* spp., and *Temora longicornis* (no·m^{-2}) in the southern Gulf of St. Lawrence in June 1982, 1985, 1987, and 1990.

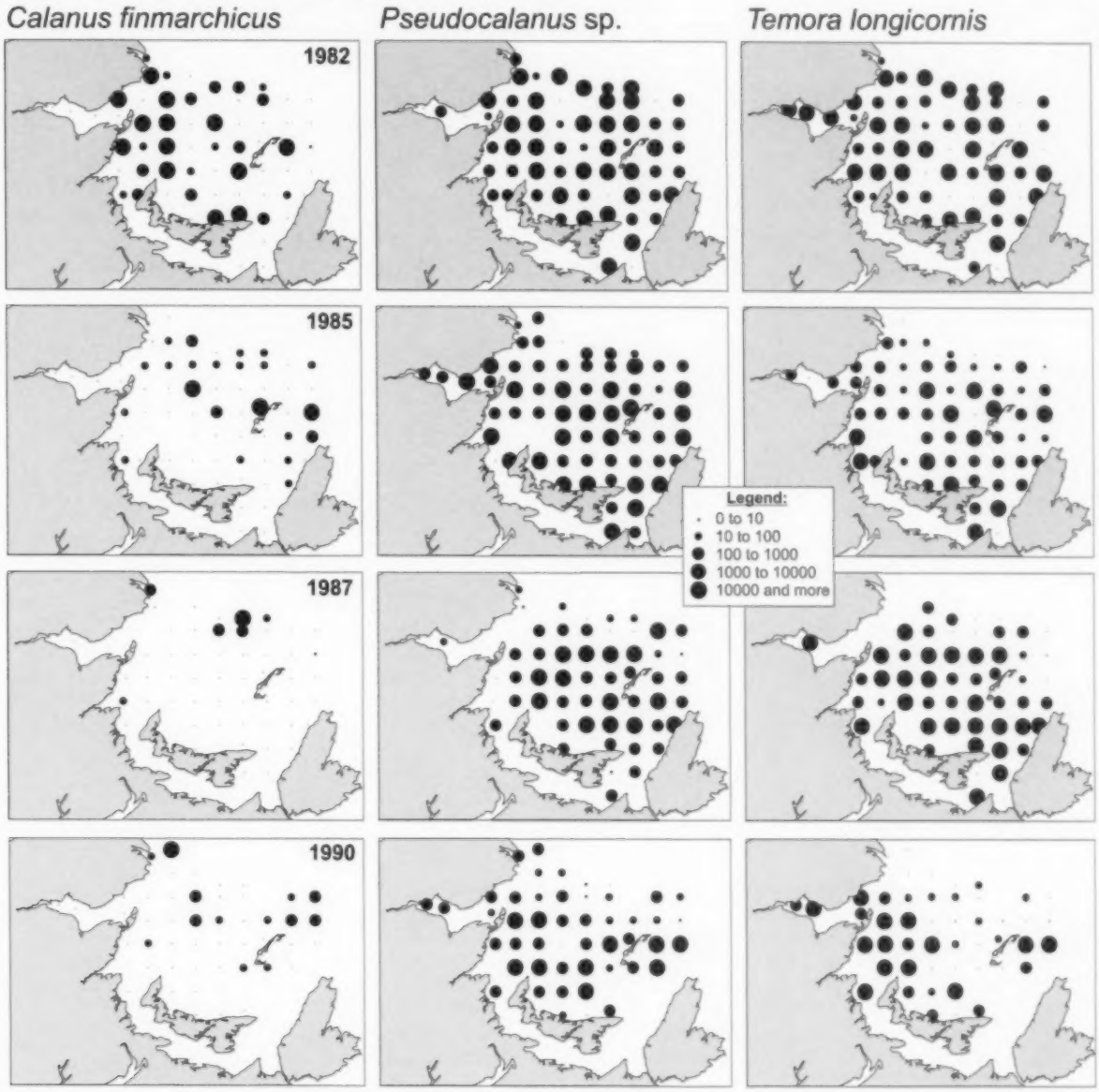

morphose into juveniles approximately 20 days after hatching. Juveniles then grow for about 80 days before growth ceases in the fall (see Simard et al. 1992). Therefore, body size at age 1 primarily reflects growth achieved during the juvenile stage rather than the larval stage.

An index of mackerel recruitment was back-calculated from the proportion of 3-year-olds in the age distribution of the Canadian commercial fishery of each year, as described in Runge et al. (1999). For example, in 1985, 3-year-old mackerel made up 62% of the total number of fish harvested by the fishery (hence a recruitment index of 0.62), indicating a strong year-class in 1982. No other recruitment index is available for this stock. See Runge et al. (1999) for a more complete discussion of the recruitment index.

Statistics

The distribution of gut fullness indices was compared among years with a contingency table testing the null hypothesis that fullness did not differ among years. Statistical comparisons of ($\log_{10}$ + 1) prey number and ($\log_{10}$ + 1) wet weight in mackerel larvae stomachs were carried out using planned analysis of variance (ANOVA) comparisons (Sokal and

© 2002 NRC Canada

Table 1. Mean abundance (thousands) and percent of the main zooplankton taxa from two mesh sizes in 1996.

(A) 200 μm (N = 11).

	Total			Female		
Taxon	No·m^{-2}	SD	%	No·m^{-2}	SD	%
Oithona sp.	24.7	27.0	37.2	12.83	16.66	66.1
Pseudocalanus sp.	11.2	10.9	16.9	4.34	4.01	22.4
Temora longicornis	10.1	13.4	15.2	1.77	1.40	9.1
Echinoderm larvae	3.9	6.6	5.9			
Calanus finmarchicus	3.8	2.3	5.7	0.054	0.07	0.3
Copepod nauplii	2.8	1.6	4.3			
Crustacean eggs	1.3	1.4	2.0			
Larvacea	1.0	1.1	1.5			
Calanus hyperboreus	1.0	0.8	1.5	0.01	0.04	0.1
Tortanus discaudatus	0.6	0.9	1.0	0.29	0.41	1.5
Others (<1%)	5.9	66.0	8.9	0.11	0.10	0.6
Total	66.4	11.5	100.0	19.40	5.26	100.0

(B) 50 μm (N = 13).

	Total			Female		
Taxon	No·m^{-2}	SD	%	No·m^{-2}	SD	%
Crustacean eggs						
Oithona sp.	80.6	241.6	27.1			
T. longicornis	16.0	48.3	5.4			
Pseudocalanus sp.	11.5	25.3	3.9			
C. finmarchicus	5.2	17.6	1.7			
Others, eggs	5.7	27.3	1.9			
Subtotal	118.9	81.4	40.0			
Oithona sp.	63.9	55.2	21.5	12.76	17.62	82.6
Pseudocalanus sp.	36.7	40.6	12.4	1.46	1.46	9.5
Temora longicornis	19.7	14.7	6.6	0.83	0.81	5.3
Microsetella gracilis	13.1	18.5	4.4	0.09	0.13	0.6
Bivalve larvae	11.0	11.1	3.7			0.0
Calanus finmarchicus	6.8	8.8	2.3	0.02	0.04	0.1
Metridia longa	3.4	4.9	1.1			0.0
Others (<1%)	23.8	21.8	8.0	0.29	0.50	1.9
Total	297.4	38.9	100.0	15.44	4.46	100.0

Note: N indicates the number of net casts analyzed. "Others" is mainly represented by unidentified invertebrate larvae, and less abundant copepods like *Centropages* spp, *Eurythometra* spp., and *Oncaea borealis*. SD, standard deviation.

Rohlf 1995), testing the a priori hypothesis (H_1) that mean number and weight of prey were larger in 1982 than in the other years. Because the 1982 distribution was used in all tests (1982 vs. 1985, 1982 vs. 1987, 1982 vs. 1996), the tests were nonorthogonal. Hence the Dunn–Šidák method was used to determine α (0.017) to avoid making a type-I error (Sokal and Rohlf 1995). Log-transformed prey number and weight followed a normal distribution and the variance was homogeneous, as determined by the F_{max} test.

Larval lengths were compared using ANOVA followed by an a posteriori Scheffé test. The assumption of normality of distribution was not met in the analysis of the mean length of mackerel larvae. However, as discussed by Sokal and Rohlf (1995), non-normality generally does not pose a problem when equality of variances is respected, which was the case here. L_1 values were compared among years (1982 to 1990) with a Kruskal–Wallis test because variances were not homogeneous.

Results

Examination of interannual variation in the spatial distribution of females of the dominant copepod species collected in survey Bongo nets shows that *C. finmarchicus* is the most variable in time and space. In 1982, this species extended far south into the southern Gulf, whereas in other years *C. finmarchicus* females remained in the Laurentian Channel and barely appeared in the southern Gulf (Fig. 2). The spatial distribution of the other species, *Pseudocalanus* sp., and *Temora longicornis*, was less variable between years (Fig. 2).

In samples collected with the finer mesh (200-μm) net in 1996, four copepod species constituted 75% by number of the zooplankton community in the southern Gulf: *Oithona similis* (37.2%), virtually absent in surveys with a 333-μm-mesh net (Castonguay et al. 1998), *Pseudocalanus* spp. (16.9%), *T. longicornis* (15.2%), and *C. finmarchicus* (5.7%) (Table 1). Crustacean eggs constituted 40% of the total number of zooplankton collected in the 50-μm-mesh nets (Table 1). *Oithona* eggs accounted for 27% of the total number of organisms present in the 50-μm-mesh net. Paralleling the results of the larger mesh net, the other dominant groups were the eggs of *T. longicornis* (5.4%), *Pseudocalanus* (3.9%), and *C. finmarchicus* (1.7%). Other taxa in the fine-mesh samples that would not be well sampled during mack-

© 2002 NRC Canada

Fig. 3. Estimated mean (±standard deviation) daily egg production rates (μg C·L^{-1}·day^{-1}) of the major copepod species of the southern Gulf of St. Lawrence calculated as the product of female abundance and the specific egg production rates. Symbols represent *Calanus finmarchicus* (●), *Temora longicornis* (◇), *Pseudocalanus* spp. (△), and *Oithona similis* (□). Specific egg production rates, assumed to be constant across all stations and years, were estimated to be 50 eggs·female^{-1}·day^{-1} for *C. finmarchicus* (Runge and de Lafontaine 1996), 30 eggs·female^{-1}·day^{-1} for *T. longicornis* (Peterson and Kimmerer 1994), and 5 eggs·female^{-1}·day^{-1} for *Pseudocalanus* spp. (Corkett and McLaren 1978). Egg production from *O. similis* is measured from the egg–female ratio (Nielsen and Sabatini 1996). Conversion from egg number to carbon was *C. finmarchicus*, 0.23 μg C·egg^{-1} (Runge and Plourde 1996); *Pseudocalanus*, 0.14 μg C·egg^{-1}; *T. longicornis*, 0.04 μg C·egg^{-1} (Frost 1980); *O. similis*, 0.75 × 10^{-6} μg C·egg^{-1} (Kiørboe et al. 1985). Note that *O. similis* was sampled only in 1996.

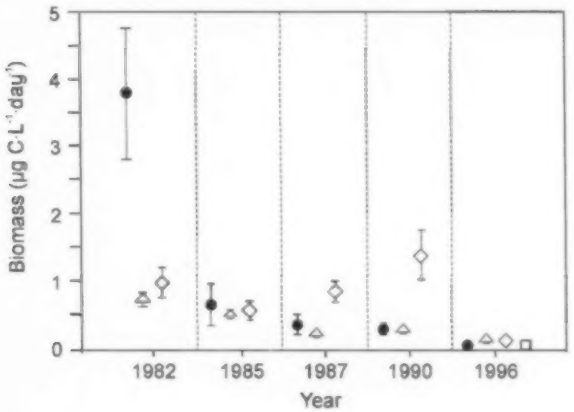

Fig. 4. Standard lengths (mm) by year of mackerel larvae selected for stomach content analysis. Means followed by different letters indicate significant statistical difference (ANOVA, $p < 0.0001$ and Scheffé post hoc test, $p < 0.001$). (*a*) 1982, (*b*) 1987, (*c*) 1985, and (*d*) 1996. SD, standard deviation.

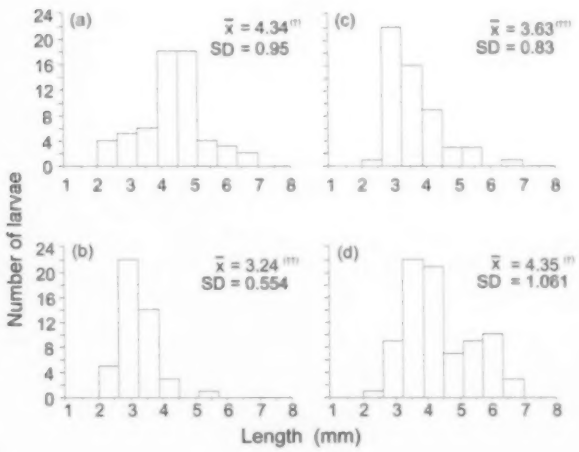

Fig. 5. Gut fullness stages (%) per length class of mackerel larvae for each year. The maximal larval size analyzed were 6.6 mm (1982), 5.1 mm (1985), 6.5 mm (1987), and 7.0 mm (1996). (*a*) <3.5 mm, (*b*) 3.5–5.4 mm, (*c*) >5.4 mm.

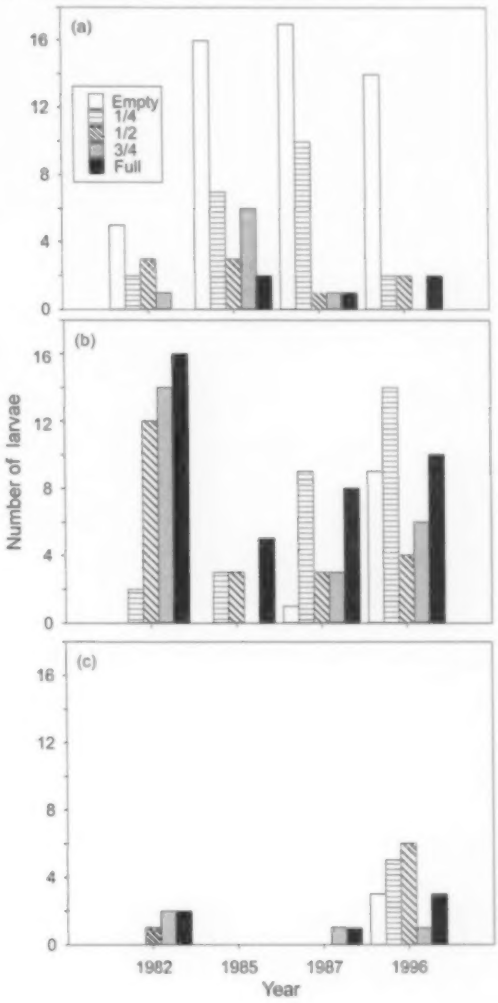

erel assessment cruises include the harpacticoid copepod, *Microsetella* sp., along with *Oncaea borealis*, another cyclopoid copepod.

The variations in estimated total egg biomass production, based on the abundance of females and values found in the literature, are even more pronounced (Fig. 3). The estimated egg biomass produced daily by *C. finmarchicus* was very large in 1982 (3.8 μg C·L^{-1}·day^{-1}) compared with the other years (between 0.6 μg C·L^{-1}·day^{-1} and 0.02 μg C·L^{-1}·day^{-1}). In 1996, the year in which *Calanus* constituted <2% of the microzooplankton captured with the very fine mesh net (Table 1), its daily production is estimated as 0.02 μg C·L^{-1}·day^{-1}. Estimated egg production of the other dominant copepod species was less variable and always less (from 1.5–0.02 μg C·L^{-1}·day^{-1}) than *Calanus* in 1982. Although *Oithona* was numerically dominant in 1996 (Table 1) and presumably in

© 2002 NRC Canada

Fig. 6. Mean prey abundance (numbers) and biomass (±standard error) per mackerel larva 3.5–5.4 mm long. The number above each bar is the number of stomachs analyzed. Statistical analysis was conducted on log-transformed data.

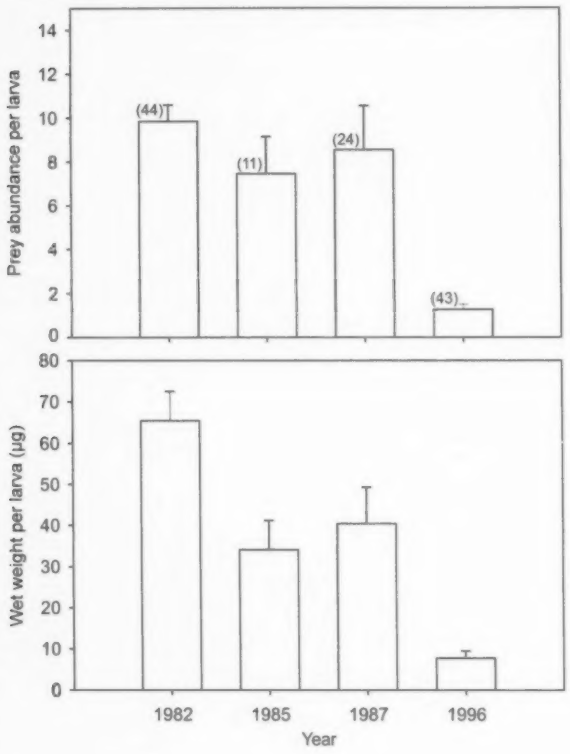

other years, its egg production converted to biomass amounted to only 0.1 µg C·L^{-1}·day^{-1} (Fig. 3).

Feeding success

The mean size of mackerel larvae was similar between 1982 and 1996 and between 1985 and 1987 (Fig. 4); however, the former group was significantly larger than the latter one (ANOVA, $p < 0.0001$, Scheffé test, $p < 0.001$). Interannual comparisons of feeding success should be based on comparable size classes within each of these years.

Larvae in the smallest size class (<3.5 mm) had a low gut fullness index regardless of the year considered. Distributions of gut fullness indices in this size were not significantly different among years ($\chi^2_{[12]} = 17.2$; $p > 0.05$) (Fig. 5). Larvae in the 3.5- to 5.4-mm size class appeared to eat more in 1982 than during the other years, as 95% of stomachs were half full or more in 1982 compared with 73%, 58%, and 47% of stomachs in 1985, 1987, and 1996, respectively (Fig. 5). Accordingly, the distribution of gut fullness indices of these larvae was significantly different among years ($\chi^2_{[12]} = 37.8$; $p < 0.001$) (Fig. 5). There were too few larvae >5.4 mm to conduct a valid interannual comparison (Fig. 5). For the rest of the analyses, statistical comparisons were carried out only on the 3.5- to 5.4-mm size class, which comprises most individuals sampled in each year.

The log-transformed mean total number of prey in stomachs of 3.5- to 5.4-mm larvae in 1982 was significantly higher than in 1996 (ANOVA, $F_{[1,85]} = 11.48$, $p < 0.005$) but not significantly different from 1985 (ANOVA, $F_{[1,53]} = 0.60$, $p = 0.44$) or 1987 (ANOVA, $F_{[1,66]} = 0.87$, $p = 0.35$) (Fig. 6). The log-transformed mean total prey weight was significantly larger in 1982 than in 1987 (ANOVA, $F_{[1,66]} = 11.59$, $p < 0.005$) or in 1996 (ANOVA, $F_{[1,85]} = 101.09$, $p < 0.001$) (Fig. 6). The mean prey weight in stomachs of larvae from 1985 was approximately half the level observed in larvae from 1982 (Fig. 6); however, this difference was not statistically significant (ANOVA, $F_{[1,53]} = 1.57$, $p = 0.22$). We note that the number of larvae available for analysis in 1985 was small (11).

Comparing numbers and wet weights of the dominant prey taxa (*Pseudocalanus* spp. and *C. finmarchicus* nauplii) between 1982 and the other years, significant differences were found (Fig. 7). In 1982, the log-transformed mean weight of *C. finmarchicus* nauplii in mackerel larvae stomachs was significantly greater than in 1985, 1987, or 1996, whereas their log-transformed mean number was significantly larger than in 1985 and 1996 (Table 2). Moreover, the log-transformed mean number and weight of *Pseudocalanus* nauplii in 1982 were significantly larger than in 1987 or 1996 (Table 2). For other taxa, significant differences occurred primarily when comparing 1982 with 1996 (Table 2).

In this mackerel stock, the two strongest recruitment years between 1982 and 1991 were first 1982 and second 1988 (Fig. 8). The mean size of otoliths at age one (L_1) exhibited significant interannual variability between 1982 and 1990 (Kruskal–Wallis test, $p < 0.001$) and L_1 was lowest in 1982 and third-lowest in 1988, suggesting that large year-classes may be associated with low juvenile growth (Fig. 8). However, the 1983 year-class appears to be an outlier. There were no L_1 measurements in 1991.

Discussion

The hypothesis of a trophic link between zooplankton and mackerel recruitment in the southern Gulf of St. Lawrence implies a variation in the quantity and (or) quality of the prey available during the larval or juvenile stages (Runge et al. 1999). If the abundance of females is used as an indicator of prey production, the high densities of female *C. finmarchicus* and its extensive distribution in the southern Gulf in 1982 represents a major fluctuation that could explain the tremendous success of this mackerel year-class.

The comparison of gut fullness indices takes into account the entire alimentary bolus. Given the spherical shape of the stomach, a reliable assessment can be made of the quantity of food in larval guts, including prey species that could not be identified. Stomachs tended to be fuller in 1982 than in the other years, suggesting that the larvae had consumed more food in 1982 than during the other years under study. The mean weight of stomach contents in the dominant larval length class was significantly higher in 1982 than in 1987 and 1996. The significantly larger abundance and mean weight of *C. finmarchicus* nauplii prey in mackerel larvae guts in 1982, a highly successful mackerel year-class, is further evidence of a strong link between the abundance of fe-

© 2002 NRC Canada

Fig. 7. Mean numbers and wet weights (±standard error) of nauplii prey per species in 3.5- to 5.4-mm mackerel larvae. Statistical analysis was conducted on log-transformed data. Wet weights were calculated following Bainbridge and McKay (1968). Copepodites were mostly *Temora longicornis* in 1982 and only *Oithona similis* in 1987.

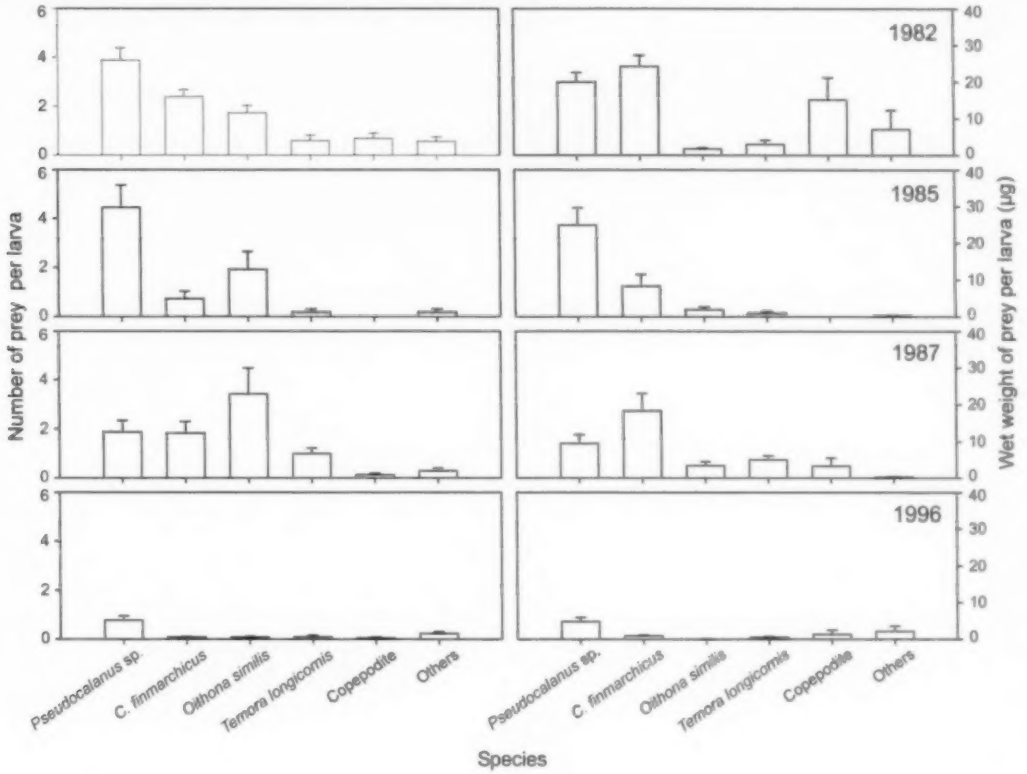

Fig. 8. Mackerel recruitment index (MACREC) as a function of L_1 (the otolith radius at the end of the first year). L_1 is calculated from otolith measurements on fish between 1 and 16 years old.

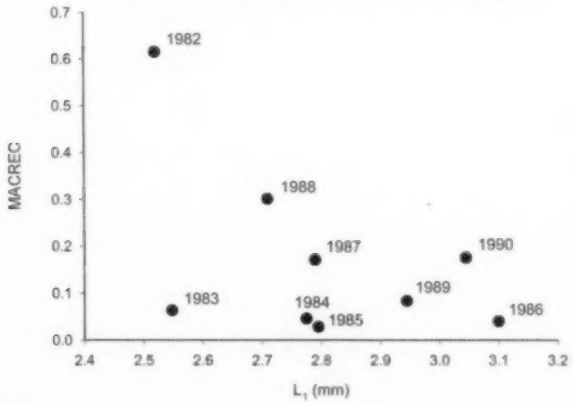

male *C. finmarchicus* and mackerel larval survival in the southern Gulf of St. Lawrence.

Feeding success, reflected here by the quality and quantity of prey ingested, if combined with to rapid growth, would allow larvae to reach the juvenile stage quickly and then survive to the adult stage (Litvak and Leggett 1992; Meekan and Fortier 1996). However, in light of the size achieved at age 1 estimated from otoliths, the juveniles arising from the very strong year-class of 1982 were smaller on average than those of other years. Lett (1980) noted that the 1967 cohort, which was the other exceptional year-class of the past 40 years in this stock, represented the smallest individuals ever observed after the first few years of growth. Based on a comparison of L_1 with stock size, Agnalt (1989) and Dawson (1991) suggested that a density-dependent mechanism was operating within the mackerel stock of the North Sea. The size of juveniles at the end of their first year was found to be inversely correlated with stock size ($R^2 = -0.72$), and was 3 cm smaller during years of very strong recruitment (Dawson 1991).

The fact that the 1983 year-class is an outlier (small recruitment associated with small juvenile growth) could be due to aging errors. Aging errors on the order of 20% are not uncommon (Hilborn and Walters 1992), which implies a 10% probability of misclassifying the large 1982 year-class as 1983. When weak cohorts follow strong cohorts such as in this case, the weak cohort may mistakenly be assigned attributes (like growth) of the strong year-class (see Hilborn and Walters 1992 for a more complete discussion of this phenomenon).

© 2002 NRC Canada

Table 2. Results of a priori ANOVA comparisons between 1982 and other years for number and wet weight of individual prey taxa in stomachs of 3.5- to 5.4-mm larvae.

		Number of prey		Wet weight of prey	
Taxon	Comparison	*F*	*P*	*F*	*P*
Calanus finmarchicus	1982–1985	11.90	<0.005*	6.01	0.0175*
	1982–1987	5.43	0.023	8.76	<0.005*
	1982–1996	81.96	<0.001*	105.48	<0.001*
Pseudocalanus sp.	1982–1985	0.74	0.39	1.35	0.25
	1982–1987	9.32	<0.005*	8.61	<0.005*
	1982–1996	40.60	<0.001*	40.23	<0.001*
Oithona similis	1982–1985	0.01	0.93	0.01	0.93
	1982–1987	0.63	0.43	0.63	0.43
	1982–1996	25.94	<0.001*	25.94	<0.001*
Temora longicornis	1982–1985	0.11	0.74	0.88	0.35
	1982–1987	0.63	0.43	7.09	<0.01*
	1982–1996	0.59	0.45	5.93	0.017*
Copepodites[a]	1982–1987	6.31	0.014*	4.40	0.04
	1982–1996	15.12	<0.001*	11.47	<0.005*

Note: All prey taxa are at the nauplius stage (except for copepodites). Data were ($\log_{10}$ + 1) transformed prior to analysis. Degrees of freedom are 1, 53 (1982–1985); 1, 66 (1982–1987); and 1, 85 (1982–1996).
*Indicates significance at the adjusted α level of 0.017, calculated using the Dunn–Šidák method.
[a]Copepodites were not compared between 1982 and 1985 because none were found in 1985.

The low growth rates noted at the end of the first year for the 1982 year-class may relate to a density-dependent phenomenon operating during the juvenile stage. During years of higher food availability, higher larval growth rates are hypothesized to allow more larvae to survive to the juvenile stage. The absence of predators, such as medusae, which are generally associated with warmer water masses, could act in synergy with feeding and growth to result in very large larval survival. The subsequent arrival of juveniles in large numbers in nearshore habitats could have a negative impact on the abundance of food available for juvenile growth as shown by Romare et al. (1999) through mesocosm experiments. This would not much impact on survival rates, but fish would grow more slowly as a consequence. Cowan et al. (2000) provided a combination of empirical evidence and conceptual arguments suggesting that consumption by fish populations and effects on prey resources are likely to be highest during the juvenile stage. Their individual-based modeling results further indicated that juvenile fishes can exert density-dependent pressures on prey resources that are sufficient to reduce fish growth.

Another hypothesis, proposed by Meekan and Fortier (1996), is that when larval food supply is abundant, the selective pressure for fast growth is relaxed such that slow-growing larvae survive in larger proportion than when the larval food is scarce, with the resulting effect that the mean size of a cohort will be smaller. In this scenario, the mean growth rate of a large cohort would be small at both larval and juvenile stages, as opposed to the density-dependent hypothesis where a fast growth rate at the larval stage would be followed by a slow growth rate at the juvenile stage.

Unfortunately, we cannot determine larval growth rates on the basis of this historical plankton collection because otoliths have been dissolved in formaldehyde. However, there are early indications that the 1999 year-class could be of comparable magnitude to the 1982 and 1967 ones (DFO 2001). We may be able to further our understanding of mackerel recruitment dynamics with this recent year-class for which samples in ethanol from another collection are available. Interestingly, 1999 was also the year with the lowest RIVSUM (as measured between January and May) since 1982 (D. Lefaivre, Institut Maurice-Lamontagne, Mont-Joli, Que., Canada, unpublished data). Furthermore, analysis currently underway also suggests that the June 1999 zooplankton biomass in the southern Gulf could be as large or larger than in 1982.

Mackerel recruitment could also be compensatory. Small stock size may promote strong recruitment through a decrease in cannibalism on eggs and larvae. Stock size was relatively small in 1982 and 1999, when very strong year-classes were produced. This could act in synergy with an abundant larval food supply to produce exceptional cohorts.

High water temperatures allow eggs to develop more quickly and hatch faster, and hence survive better. However, the mixed-layer temperature during the survey was colder in 1982 than during 1985, 1987, 1990 (Runge et al. 1999), or 1996 (F. Grégoire, unpublished data). Moreover, water temperature in 1985, a year of weak recruitment, was relatively warm (Runge et al. 1999).

The significant interannual difference in larval sizes can be attributed primarily to three factors: sampling date, spawning date, and water temperature. In 1982 and 1985, the collection dates of larvae used in the diet analysis were similar, whereas larvae were sampled approximately one week earlier in 1987 and 1996. Grégoire (1997) estimated that the date of peak mackerel spawning occurred earlier than usual in 1982.

In conclusion, the large zooplankton biomass and the great abundance of female *C. finmarchicus* in 1982 contributed to producing a high nauplius prey density that seems to have favored the feeding success of mackerel larvae and the success of this year-class. Although the evidence presented here supports a trophic link hypothesis, it is difficult to draw a clear and unequivocal conclusion based on the field data

© 2002 NRC Canada

available at present. Our study nevertheless suggests that *C. finmarchicus* can play a key role in determining mackerel year-class strength in the southern Gulf of St. Lawrence.

Acknowledgments

We thank Jean-Louis Beaulieu for help with data analysis and Pierre Joly for assistance with data management and experiments at sea. Dr. P. Archambault's advice on a priori ANOVAS is also appreciated. Constructive suggestions by Drs. J.A. Gagné, P. Ouellet, and three anonymous referees improved the manuscript substantially. Laure Devine proofed the paper.

References

Agnalt, A.-L. 1989. Long-term changes in growth and age at maturity of mackerel, *Scomber scombrus* L., from the North Sea. J. Fish Biol. **35**(Suppl. A): 305–311.

Anderson, E.D., and Paciorkowski, A.J. 1980. A review of the Northwest Atlantic mackerel fishery. Rapp. P.-V. Reun. Cons. Int. Explor. Mer, **177**: 175–211.

Anderson, J.T. 1988. A review of size-dependent survival during pre-recruit stages of fishes in relation to recruitment. J. Northw. Atl. Fish. Sci. **8**: 55–66.

Bainbridge, V., and McKay, B.J. 1968. The feeding of cod and redfish larvae. Int. Comm. Northwest Atl. Fish. (ICNAF) Spec. Publ. No. 7. pp. 187–217.

Castonguay, M., de Lafontaine, Y., and Runge, J.A. 1998. Annual and spatial variability in zooplankton biomass and species composition, and in eggs and larvae of mackerel and cod in the southern Gulf of St. Lawrence between 1982 and 1991. Can. Data Rep. Fish. Aquat. Sci. No. 1035.

Corkett, C.J., and McLaren, I.A. 1978. The biology of *Pseudocalanus*. Adv. Mar. Biol. **15**: 1–231.

Cowan, J.H., Rose, K.A., and DeVries, D.R. 2000. Is density-dependent growth in young-of-the-year fishes a question of critical weight? Rev. Fish Biol. Fish. **10**: 61–89.

Cushing, D.H. 1990. Plankton production and year-class strength in fish populations: an update of the match/mismatch hypothesis. Adv. Mar. Biol. **26**: 249–293.

Cushing, D.H. 1995. The long-term relationship between zooplankton and fish. ICES J. Mar. Sci. **52**: 611–626.

Dawson, W.A. 1991. Otolith measurement as a method of identifying factors affecting first-year growth and stock separation of mackerel (*Scomber scombrus* L.). ICES J. Mar. Sci. **47**: 303–317.

de Lafontaine, Y., Demers, S., and Runge, J.A. 1991. Pelagic food web interactions and productivity in the Gulf of St. Lawrence: a perspective. *In* The Gulf of St. Lawrence: small ocean or big estuary? *Edited by* J.-C. Therriault. Can. Spec. Publ. Fish. Aquat. Sci. No. 113. pp. 99–123.

Department of Fisheries and Oceans (DFO). 2001. Atlantic mackerel of the northwest Atlantic. Fisheries and Oceans Canada Science, Laurentian Region. Stock Status Report B4-04 (2001). (http://www.dfo-mpo.gc.ca/CSAS/CSAS/status/2001/B4-04e.pdf)

Fortier, L., and Villeneuve, A. 1996. Cannibalism and predation on fish larvae by larvae of Atlantic mackerel, *Scomber scombrus*: trophodynamics and potential impact on recruitment. Fish. Bull. U.S. **94**: 268–281.

Frost, B.W. 1980. The inadequacy of body size as an indicator of niches in the zooplankton. *In* Evolution and ecology of zooplankton communities. *Edited by* W.C. Kerfoot. University Press of New England. Hanover, N.H. pp. 742–753.

Grave, H. 1981. Food and feeding of mackerel larvae and juveniles in the North Sea. Rapp. P.-V. Reun. Cons. Int. Explor. Mer, **178**: 454–459.

Grégoire, F. 1997. Évaluation de la méthode de la réduction journalière de la fécondité pour estimer la biomasse du maquereau bleu (*Scomber scombrus* L.). Can. Stock Assess. Sec. Res. Doc. 97/84. (http://www.dfo-mpo.gc.ca/csas/Csas/English/Publications/Research_Doc_e.htm)

Grégoire, F., and Gagnon, P. 1993. Analyse préliminaire des mesures de L_1 sur des otolithes de maquereau bleu (*Scomber scombrus* L.) du golfe du Saint-Laurent. DFO Atl. Fish. Res. Doc. 93/62.

Hilborn, R., and Walters, C.J. 1992. Quantitative fisheries stock assessment: choice, dynamics and uncertainty. Chapman & Hall, New York.

Hillgruber, N., Kloppmann, M., Wahl, E., and Westernhagen, H.-V. 1997. Feeding of larval blue whiting and Atlantic mackerel: a comparison of foraging strategies. J. Fish Biol. **51**: 230–249.

Houde, E.D. 1987. Fish early life dynamics and recruitment variability. Am. Fish. Soc. Symp. **2**: 17–29.

Hunter, J.R. 1981. Predation of marine fish larvae. *In* Marine fish larvae: Morphology, ecology and relation to fisheries. *Edited by* R. Lasker. Washington Sea Grant Program, University of Washington Press, Seattle. pp. 60–79.

Hunter, J.R., and Kimbrell, C.A. 1980. Early life history of Pacific mackerel, *Scomber japonicus*. Fish. Bull. U.S. **78**: 89–101.

Kiørboe, T., Møhlenberg, F., and Riisgård, H.U. 1985. In situ feeding rates of planktonic copepods: A comparison of four methods. J. Exp. Mar. Biol. Ecol. **88**: 67–81.

Last, J.M. 1980. The food of twenty species of fish larvae in the west-central North Sea. Ministry of Agriculture, Fisheries and Food. Fish. Res. Tech. Rep. Dir. Fish. Res. (Great Britain) No. 60.

Lett, P.F. 1980. A comparative study of the recruitment mechanisms of cod and mackerel, their interaction, and its implication for dual assessment. Can. Tech. Rep. Fish. Aquat. Sci. No. 988.

Litvak, M.K., and Leggett, W.C. 1992. Age and size-selective predation on larval fishes: the bigger-is-better hypothesis revisited. Mar. Ecol. Prog. Ser. **81**: 13–24.

Meekan, M.G., and Fortier, L. 1996. Selection for fast growth during the larval life of Atlantic cod *Gadus morhua* on the Scotian Shelf. Mar. Ecol. Prog. Ser. **137**: 25–37.

Nielsen, T.G., and Sabatini, M. 1996. Role of cyclopoid copepods *Oithona* spp. in the North Sea plankton communities. Mar. Ecol. Prog. Ser. **139**: 79–93.

Ouellet, P. 1987. Mackerel (*Scomber scombrus*) egg abundance in the southern gulf of St. Lawrence from 1979 to 1986, and the use of the estimate for stock assessment. Can Atl. Fish. Sci. Adv. Comm. Res. Doc. 87/67.

Pepin, P. 1991. Effect of temperature and size on development, mortality, and survival rates of the pelagic early life history stages of marine fish. Can. J. Fish. Aquat. Sci. **48**: 503–518.

Peterson, W.T., and Kimmerer, W.J. 1994. Processes controlling recruitment of the marine calanoid copepod *Temora longicornis* in Long Island Sound: egg production, egg mortality and cohort rates. Limnol. Oceanogr. **39**: 1594–1605.

Priede, I.G., and Watson, J.J. 1993. An evaluation of the daily egg production method for estimation biomass of mackerel (*Scomber scombrus*). Bull. Mar. Sci. **53**: 891–911.

Romare, P., Bergman, E., and Hansson, L.-A. 1999. The impact of larval and juvenile fish on zooplankton and algal dynamics. Limnol. Oceanogr. **44**: 1655–1666.

Runge, J.A. 1988. Should we expect a relationship between primary production and fisheries? The role of copepod dynamics as a filter of trophic variability. Hydrobiologia, **167/168**: 61–71.

© 2002 NRC Canada

Runge, J.A., and de Lafontaine, Y. 1996. Characterization of the pelagic ecosystem in surface waters of the northern Gulf of St. Lawrence in early summer: the larval redfish-Calanus-microplankton interaction. Fish. Oceanogr. **5**: 21–37.

Runge, J.A., and Plourde, S. 1996. Fecundity characteristics of *Calanus finmarchicus* in coastal waters of eastern Canada. Ophelia, **44**: 171–187.

Runge, J.A., Castonguay, M., de Lafontaine, Y., Ringuette, M., and Beaulieu, J.-L. 1999. Covariation in climate, zooplankton biomass and mackerel recruitment in the southern Gulf of St. Lawrence. Fish. Oceanogr. **8**: 139–149.

Simard, P., Castonguay, M., D'Amours, D., and Magnan, P. 1992. Growth comparison between juvenile Atlantic mackerel (*Scomber scombrus*) from the two spawning groups of the northwest Atlantic. Can. J. Fish. Aquat. Sci. **49**: 2242–2248.

Sokal, R.R., and Rohlf, F.J. 1995. Biometry. 3rd ed. W.H. Freeman and Co., San Francisco.

Theilacker, G.H. 1980. Changes in body measurements of larval northern anchovy, *Engraulis mordax*, and other fishes due to handling and preservation. Fish. Bull. U.S. **78**: 685–692.

van Guelpen, L., Markle, D.F., and Duggan, D.J. 1982. An evaluation of accuracy, precision, and speed of several zooplankton subsampling techniques. J. Cons. Int. Explor. Mer, **40**: 226–236.

Ware, D.M., and Lambert, T.C. 1985. Early life history of Atlantic mackerel (*Scomber scombrus*) in the southern of St. Lawrence. Can. J. Fish. Aquat. Sci. **42**: 577–592.

© 2002 NRC Canada

Estimating abundance from gillnet samples with application to red drum (*Sciaenops ocellatus*) in Texas bays

Clay E. Porch, Mark R. Fisher, and Lawrence W. McEachron

Abstract: A model of gillnet selection is developed to accommodate the possibility that some catch observations will be known more precisely than others and allow for nonlinear relationships between the selection parameters and mesh size. The model is used to show that gillnet selection for red drum (*Sciaenops ocellatus*) in Texas bays may be explained as a unimodal process approximating a skewed Laplace distribution, where the optimal length varies in proportion to mesh size and the variance in proportion to the optimal length. It is also suggested that the number of encounters with the net ought to depend on swimming speed of the quarry, which in turn varies predictably with length. This information, along with the estimates of selection, is used to develop indices of abundance for each length-class. The results indicate that the recruitment of year-old red drum to Texas bays has fluctuated markedly since 1975, but without any persistent trends. However, the survival of these and older fish has increased dramatically owing to various regulations promulgated since 1981.

Résumé : Un nouveau modèle de sélection des filets maillants permet de tenir compte de la possibilité que certaines observations de captures soient plus précises que d'autres et qu'il y ait des relations non-linéaires entre les paramètres de sélection et la dimension de la maille du filet. Le modèle est utilisé pour démontrer que la sélection exercée par les filets maillants sur le tambour rouge (*Sciaenops ocellatus*) des baies du Texas s'explique comme un processus unimodal s'approchant d'une distribution de Laplace asymétrique dans laquelle la logueur optimale varie en proportion de la dimension de la maille et la variance, en fonction de la longueur optimale. Nous avançons aussi l'hypothèse que le nombre de rencontres avec le filet dépend de la vitesse de nage de la proie, qui est, elle-même, fonction de sa longueur. Ces renseignements, ajoutés aux estimations de sélection, nous ont permis de calculer des indices d'abondance pour chaque classe de longueur. Il en ressort que le recrutement des tambours rouges de 1 an dans les baies du Texas a fluctué de façon importante depuis 1975, mais sans tendance bien marquée. Néanmoins, la survie de ces poissons et celle des poissons plus âgés a augmenté de façon spectaculaire à cause de diverses réglementations en vigueur depuis 1981.

[Traduit par la Rédaction]

Introduction

Gillnets are widely used to monitor the abundance of fish populations, but are highly selective. As a result, the length structure of the catch may differ substantially from that of the sampled population. This difference is usually corrected for by dividing the catch of each length-class with an estimate of the net's selectivity towards that length-class. If the length structure of the population is known for some portion of the time series, then the estimation of selection is straightforward (catch divided by abundance). Otherwise, selection can be estimated indirectly from the length–frequency distributions of several different mesh sizes fished simultaneously.

Most "indirect" methods operate by fitting selection curves to the length–frequency distributions of each mesh size or the mesh frequency distributions of each length-class. The earliest applications assumed that the shape of the selection curve was the same for all mesh sizes. Helser et al. (1991) and Hovgard (1996) have since developed numerical methods that relax this assumption somewhat, but the former still requires the height of the selection curve to be the same for all mesh sizes and the latter requires the variance of the selection curve to be proportional to the square of the mesh size (essentially implying a constant coefficient of variation). Both methods also assume that the most vulnerable length-class (optimal length) is a linear function of mesh size.

Another important limitation of existing indirect methods is that they are conditioned on the number of fish that actually encounter the net, which means that the selection estimates reflect the proportion of fish captured from the encountered population rather than from the population as a whole. Thus, if the desire is to construct indices of abundance, account must be taken of factors that may cause the number of encounters to differ from the number of animals in the population.

The purpose of this paper is to present a generalized

Received 1 February 2001. Accepted 27 March 2002. Published on the NRC Research Press Web site at http://cjfas.nrc.ca on 11 May 2002.
J16202

C.E. Porch.[1] Southeast Fisheries Science Center, Sustainable Fisheries Division, NOAA Fisheries, 75 Virginia Beach Drive, Miami, FL 33149, U.S.A.
M.R. Fisher and L.W. McEachron.[2] Texas Parks and Wildlife, Coastal Fisheries Division, 4200 Smith School Road, Austin, TX 78744, U.S.A.

[1]Corresponding author (e-mail: clay.porch@noaa.gov).
[2]Deceased.

 DOI: 10.1139/F02-034 © 2002 NRC Canada

method for estimating selection and population abundance from gillnet catches. The proposed methodology builds on the least-squares approach of Hovgard (1996) by accommodating nonlinear relationships between the selection parameters and mesh size as well as variations in selection over time and space. The least-squares estimation procedure is also extended to allow for the fact that some catch observations are known more precisely than others. Finally, the encounter rate is modeled as a function of the swimming speed of the quarry, which provides a means for converting estimates of the number of encounters to estimates of abundance. The proposed models are applied to catch-at-length observations from red drum (*Sciaenops ocellatus*) collected during gillnet surveys conducted in Texas bays.

Materials and methods

Selection model

The expected number of fish caught (C) by a gillnet may be expressed as a function of effort (f), fishing power (p), selection (S), and encounters per unit effort (E)

$$(1) \qquad C_{mkl} = f_{mk}p_{mk}S_{mkl}E_{kl}$$

where the subscripts m, l, and k refer to mesh size, length, and stratum (e.g., time or area). In this notation, p is the probability of capture for the length-class that is most vulnerable upon encountering the net and S gives the probability of capture for each length-class relative to p. Together they dictate the height and shape of the S curve.

The system described in eq. 1 has more unknowns than equations, making it necessary to impose some additional structure. Most methods accomplish this by assuming that p is the same for all m and requiring S to be of a particular functional form. However, the assumption that p is the same for all m is generally untrue and can lead to substantial bias (Hamley 1975). Moreover, p may be expected to vary in space and time. Fortunately, the need to assume a constant p arose principally as a matter of algebraic convenience and is unnecessary in numerical schemes. Unique solutions to the system in eq. 1 can be shown to exist whenever two fairly liberal conditions are met: (*i*) the p value for each mesh is constant over several, but not necessarily all, k and (*ii*) the shape of S can be described by a mathematical function with reasonably few parameters compared with the number of l categories. In practice, the estimates for the absolute magnitude of the ps will be poorly determined unless there is considerable contrast in the data. Therefore it will usually be prudent to fix the value of p for one of the m to an arbitrary standard (say 1.0) over several k. The estimates of E and p for the remaining k must be regarded as relative values, but this should be of little consequence inasmuch as the "absolute" values themselves typically represent an unknown fraction of the population that is available to the gear.

Several mathematical functions have been used to model the curve S to the satisfaction of condition (*ii*) above, including the normal, lognormal, gamma, and Pearson type 1 curves. Another potential candidate is the Laplace curve, which can accommodate narrower peaks and thicker tails than the others. The equations for these curves may all be expressed in terms of the size of most vulnerable length-class (optimal l) λ and variance in length, σ^2 (see Table 1). However, the model's ability to produce precise estimates may be enhanced if λ and σ^2 can be expressed as a function of m.

Most researchers have adopted Baranov's similarity principle and assumed that λ is proportional to m and that σ^2 is constant. Regier and Robson (1966) and Hovgard (1996), however, allowed σ^2 to be proportional to m^2. In point of fact, it is quite possible that λ and σ^2 are both nonlinearly related to m owing to asymmetries in growth, net elasticity, and other factors. Therefore, it is useful to express them as more general functions of, such as the power functions $\lambda = \alpha m^{\beta}$ and $\sigma^2 = \gamma\lambda^{\delta}$. Similarly, additional skew may be admitted by use of the Gram-Charlier series (Table 1), where the skew parameter θ can be expressed as the quadratic $\theta = \theta_1 + \theta_2 m + \theta_3 m^2$ rather than a power function to allow for changes in sign (Helser et al. 1991).

Parameter estimation

The selection model in system (1) has now been reduced to a function of p, optimal length (α and β), variance (γ and δ), and skewness (θ_1, θ_2, θ_3). In principle, all of these parameters may be estimated by minimizing an objective function involving one of the S curves in Table 1, provided of course they are each invariant over some subset of k. Hovgard (1996) advocated the use of least squares, which implies an additive error with constant variance. It is likely, however, that the variance in catch-at-length will increase with larger catches or fewer samples. Accordingly, we adopted a weighted least-squares ($\mathfrak{L}$) procedure that minimizes

$$(2) \qquad \mathfrak{L} = \sum_{l}\sum_{k}\sum_{m}\frac{(C_{mkl} - f_{mk}p_{mk}S_{mkl}E_{kl})^2}{2V[C_{mkl}]}$$

where V denotes the variance of the catch-at-length observation (see Appendix A).

A practical difficulty with applying eq. 2 is that the number of E parameters will often be very large (there are 8421 in the red drum example below) and the search time for optimization algorithms increases geometrically with the number of parameters. However, as Hovgard (1996) pointed out for ordinary least squares, analytical expressions for E may be obtained by setting the derivatives of eq. 2 equal to zero and solving with respect to E, p and S being regarded as constant

$$(3) \qquad E_{kl} = \frac{\sum_{m} C_{mkl}f_{mk}p_{mk}S_{mkl} / V[C_{mkl}]}{\sum_{m} f_{mk}^2 p_{mk}^2 S_{mkl}^2 / V[C_{mkl}]}$$

Substituting eq. 3 into eq. 2 produces an objective function with the same minimum as the original problem (Seber and Wild 1989). Covariances and percentile confidence limits for the p, S, and E parameters were derived by use of a parametric bootstrap (see Appendix B).

Model building

Akaike's information criteria for small samples (AIC_c) was used to determine the combination of selection parameters and type of S curve that provided the most parsimonious explanation of the data (Hurvich and Tsai 1995; Buckland et

© 2002 NRC Canada

Table 1. Mathematical functions used to model selection (S).

Function name	Mathematical representation	Comments
Normal	$\frac{1}{\sqrt{2\pi\sigma^2}} e^{-0.5(l-\lambda)^2/\sigma^2}$	Most common choice in the literature (e.g., Baranov 1948; Holt 1963)
Laplace (double exponential)	$\frac{1}{\sqrt{2}\sigma} e^{-\sqrt{2}\lvert l-\lambda\rvert/\sigma}$	Similar to normal curve, but with thicker tails
Lognormal	$\frac{1}{\sqrt{2\pi\sigma^2 l}} e^{-0.5(\log_e[l]-\log_e[\lambda])^2/\sigma^2}$	Asymmetric curve used by McCombie and Fry (1960)
Gamma	$\frac{1}{\Gamma(A)} B^{-A} l^{A-l} e^{-l/B}$	Asymmetric curve used by Regier and Robson (1966) (Note: $A = (\lambda/\sigma)^2$ and $B = \sigma^2/\lambda$)
Pearson type 1	$\left(1.0 + \frac{l-\lambda}{b}\right)^{bd}\left(1.0 + \frac{l-\lambda}{c}\right)^{cd}$	Asymmetric curve (Hamley and Regier 1973) (Note: b and c are distance to the right and left of λ where $S = 0$; d determines kurtosis)
Gram-Charlier series	$1.0 - 0.5\theta\sigma^{3/2}\left(\frac{(l-\lambda)}{\sigma} - \frac{(l-\lambda)^3}{3\sigma^3}\right)$	A multiplicative factor used to skew other functions (see Croxton et al. 1967; McCombie and Berst 1969)

Note: The variables λ and σ refer to the optimal length and standard deviation in length, respectively. In practice, the equations are discretized by allowing l to represent the midpoint of each length-class and dividing by the sum over all length-classes.

Table 2. Number of gillnet sets by fishing year and bay system.

Fishing year	Sabine Lake	Galveston	Matagorda	San Antonio	Aransas	Corpus Christi	Upper Laguna Madre	Lower Laguna Madre	East Matagorda	Total
1975	2	12	7	7	7	7	8	7	0	57
1976	0	20	14	14	14	14	14	14	8	112
1977	0	16	16	16	16	16	16	16	16	128
1978	0	20	20	20	20	20	20	20	20	160
1979	0	32	32	32	32	32	32	32	24	248
1980	0	20	20	20	20	20	20	20	20	160
1981	0	90	90	90	90	90	90	90	16	646
1982	0	90	90	90	90	90	90	90	20	650
1983	0	90	90	90	90	90	90	90	20	650
1984	0	90	90	90	90	90	90	90	40	670
1985	45	90	90	90	90	90	90	90	40	715
1986	90	90	90	90	90	90	90	90	40	760
1987	90	90	90	90	90	90	90	90	40	760
1988	90	90	90	90	90	90	90	90	40	760
1989	90	90	90	90	90	90	90	90	40	760
1990	90	90	90	90	90	90	90	90	40	760
1991	90	90	90	90	90	90	90	90	40	760
1992	90	90	90	90	90	90	90	90	40	760
1993	90	90	90	90	90	90	90	90	40	760
1994	90	90	90	90	90	90	90	90	40	760
1995	90	90	90	90	90	90	90	90	40	760
1996	90	90	90	90	90	90	90	90	40	760
1997	90	90	90	90	90	90	90	90	40	760
1998	45	45	45	45	45	45	45	45	20	380
Total	1172	1695	1684	1684	1684	1684	1685	1684	724	13 696

al. 1997). Essentially, this amounted to minimizing the statistic

$$\text{(4)} \qquad AIC_c = -2\log_e(\mathcal{L}) + 2\phi\left(1 + \frac{\phi+1}{n-\phi-1}\right)$$

where n is the number of data points and ϕ is the number of estimated parameters (including the Es).

The very large number of possible combinations made examining each potential model formulation impractical; therefore, the model building procedure was conducted in a stepwise fashion. The first step was to establish the simplest form of the model that could reasonably be expected to explain the data: a null hypothesis. The second step identified the S curve that gave the lowest AIC_c value under the null hypothesis. This curve was then used in all subsequent eval-

© 2002 NRC Canada

Table 3. Parameter estimates for the model resulting from the stepwise selection procedure with bootstrap estimates of the coefficient of variation (CV, %), bias (%), and correlation coefficients.

				Correlation coefficients										
	Estimate	CV	Bias	$p_{f,102}$	$p_{s,102}$	$p_{f,126}$	$p_{s,126}$	$p_{f,152}$	$p_{s,152}$	β	α	γ_f	γ_s	θ_1	θ_2
$p_{f,102}$	0.7098	6	0												
$p_{s,102}$	0.9056	15	–1	0.3											
$p_{f,126}$	0.5207	18	–9	0.1	0.0										
$p_{s,126}$	0.6168	26	–9	0.0	0.4	0.6									
$p_{f,152}$	0.3351	25	3	–0.1	–0.1	0.8	0.6								
$p_{s,152}$	0.3658	34	–2	–0.1	0.3	0.5	0.8	0.6							
β	0.9859	1	0	–0.4	–0.2	0.1	0.2	0.3	0.3						
α	1.9000	2	0	0.4	0.2	0.1	0.0	–0.2	–0.1	–1.0					
γ_f	0.0861	5	–3	–0.1	–0.1	0.0	–0.1	0.0	–0.1	0.0	0.0				
γ_s	0.0976	13	–11	0.1	0.0	–0.3	–0.2	–0.3	–0.3	–0.2	0.2	0.1			
θ_1	0.2256	10	0	0.2	0.4	0.0	0.1	0.0	0.0	–0.1	0.1	0.0	–0.1		
θ_2	–0.0398	–10	3	0.0	0.1	0.0	0.0	0.0	0.1	0.0	0.0	0.0	–0.1	–0.3	
θ_3	–0.0024	–37	14	–0.2	–0.3	0.1	0.0	0.1	0.0	0.1	–0.1	0.0	0.1	–0.6	–0.5

Note: The subscripts s and f indicate spring and fall. The bootstrap procedure and bias estimator are discussed in Appendix B.

uations until a final model was selected (at which point the choice of curves was re-evaluated).

The third step proceeded with the goal of identifying the most parsimonious choice of selectivity parameters given the S curve chosen in the previous step and assuming selectivity was invariant among the various k. This was accomplished by adding the parameters to the initial model one at a time and keeping the parameter that gave the lowest AIC_c value. The remaining parameters were then added one at a time to the updated version of the model and the one with the lowest AIC_c score used to update the model further and so on. This procedure was continued until no further improvement in the AIC_c could be obtained. The fourth and final step proceeded similarly, adding seasonal terms to the model that emerged from the third step.

Relationship between encounter rates and abundance

The discussion so far has been framed in terms of S and E rates, but it is changes in abundance that are of most interest to fisheries managers. The local abundance (N) of the population may be derived by dividing the estimates of E by the number of encounters per fish (ε)

$$(5) \qquad N_{kl} = E_{kl}/\varepsilon_{kl}$$

The encounter rate will index N if ε is constant, but this seems unlikely because larger fish tend to move about more and are therefore more likely to swim into the net (Lagler 1968).

Random walk and advection–diffusion models indicate that the number of times a fish would be expected to encounter a particular region in space (such as a unit of net) is proportional to its average swimming speed (see, e.g., Okubo 1980), which in turn increases in proportion to l raised to a power (τ) between 0.5 and 1.0 (Beamish 1978; Blake 1983). This suggests

$$(6) \qquad \tilde{N}_{kl} = E_{kl}(l / l_\omega)^{-\tau}$$

where $\tilde{N}$ is a measure of relative abundance obtained by dividing N in eq. 5 by the swimming speed at some reference length l_ω (perhaps the largest length-class defined in the model).

Unfortunately, the exponent τ cannot be estimated from catch and effort data alone, which are conditioned on the number of encounters, and must be determined independently. No such values have been published for red drum; however, Blake (1983) estimated an overall value of 0.8 for the combined observations from a large variety of nonscombrioid fish and we suspect red drum will be better represented by this value than by either extreme (0.5 or 1.0). Note that the choice of τ in eq. 6 does not affect the estimates of the selectivity parameters.

Application to red drum in Texas bays

The Texas Parks and Wildlife Department (TPWD) has used overnight sets of monofilament gillnets to monitor the abundance of red drum and other fish in Texas bays since November of 1975. The nets, composed of four 1.2 × 45.7 m panels with ms of 76, 102, 127, and 152 mm (stretched), have been deployed in the same way since the program's inception (McEachron and Green 1985; Hensley and Fuls 1998). Over 13 000 sets were made at randomly chosen positions along the shorelines of the nine major bays (Table 2) during two 10-week time periods beginning in the second full week of April (spring) and the second full week of September (fall).

The data were aggregated into strata defined by mesh, bay, season, and fishing year. Fishing years began during the fall, when red drum recruit to the bays, and included the following spring (e.g., the 1976 fishing year includes the fall of 1976 and spring of 1977). Not all of the fish were measured in some sets. Therefore, catch-at-length vectors were obtained by multiplying the relative length–frequency distribution of the measured fish by the total catch of all sets (for a total of 32 676 catch-at-length observations). Effort was measured in terms of the hours each net spent immersed.

Baranov's (1948) similarity principle, which states that S is the same for any given l:m if the quarry grows symmetrically and the primary mode of capture is gilling or wedging, was adopted as the null hypothesis because red drum grow

© 2002 NRC Canada

Fig. 1. Final estimates of (*a*) selection curves for each mesh size in the spring (thin lines) and fall (thick lines) and (*b–e*) selectivity parameters from the final model. Circles and triangles represent the estimates corresponding to the fall and spring (where they are different). The squares represent the null hypothesis for the fishing power coefficients.

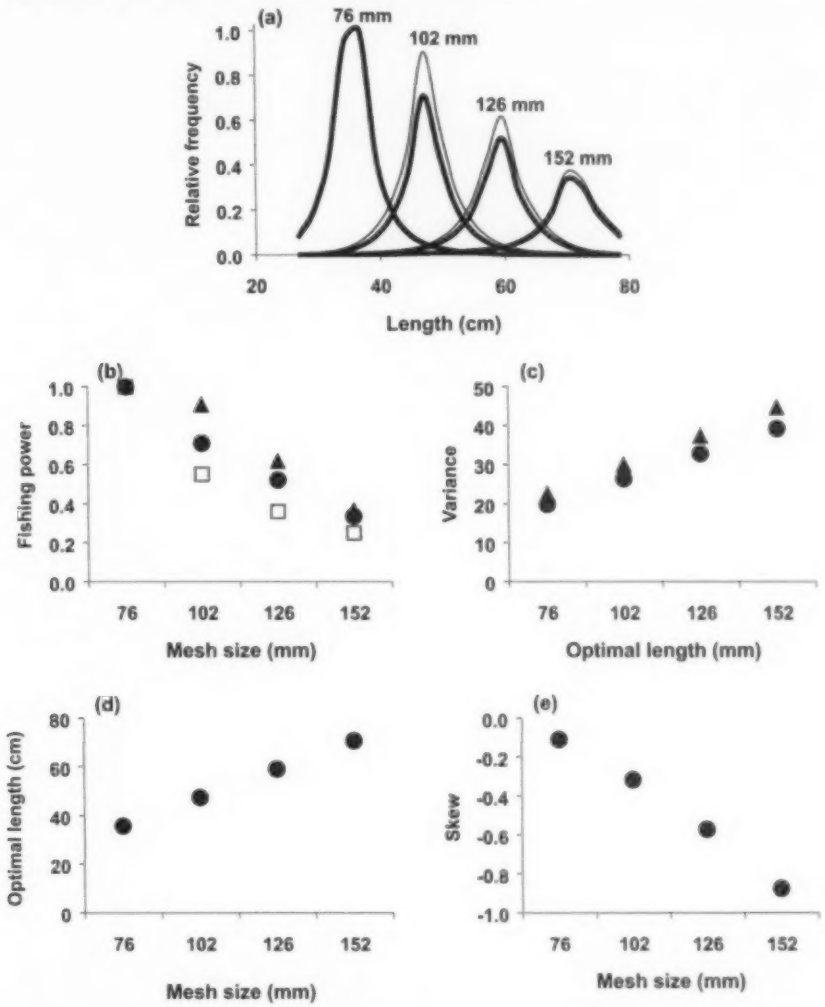

symmetrically and have few protuberances to encourage tangling. The similarity principle implies a linear relationship between λ and m ($\beta = 1$), constant σ^2 ($\delta = 0$), and no added skew ($\theta = 0$). Initially it was also assumed that p is proportional to the number of potential gilling sites per unit area inasmuch as fish have a tendency to move along the net until they find a place they can pass through or are captured (resulting in fixed relative p values of 1.0, 0.54, 0.33, and 0.23 for the 76-, 102-, 127-, and 152-mm-mesh panels). Subsequently, the statistical contribution of estimating the β, δ, θ, and p terms was evaluated via the model-building procedure discussed earlier. Owing to the consistent manner in which the survey was conducted, the same selection parameters were applied to all years. However, allowance was made for possible differences between the spring and fall, which have very different environmental characteristics.

Coast-wide estimates of $\tilde{N}$ were constructed from the results of the final model by weighting the bay-specific estimates according to the length of their coastlines (see Hensley and Fuls 1998). Approximate 90% confidence intervals were constructed from the ordered bootstrap results (Appendix B). Sabine lake was not sampled before 1985 (except sparsely in 1975) and East Matagorda bay was not sampled in 1975; however, this should have little impact on the results because both bays together account for only about 7% of the total coastline.

Results

The initial model representing the null hypothesis had only two selection terms (α and γ)

$$(7) \qquad C_{mbtyl} = f_{mbty} p_m S\{\lambda = \alpha m,\ \sigma^2 = \gamma,\ \theta = 0\} E_{btyl}$$

where the subscripts b, t, and y denote bay, season, and year,

© 2002 NRC Canada

Fig. 2. Model fits (lines) to observed catch-at-length (points) for all bays and years combined.

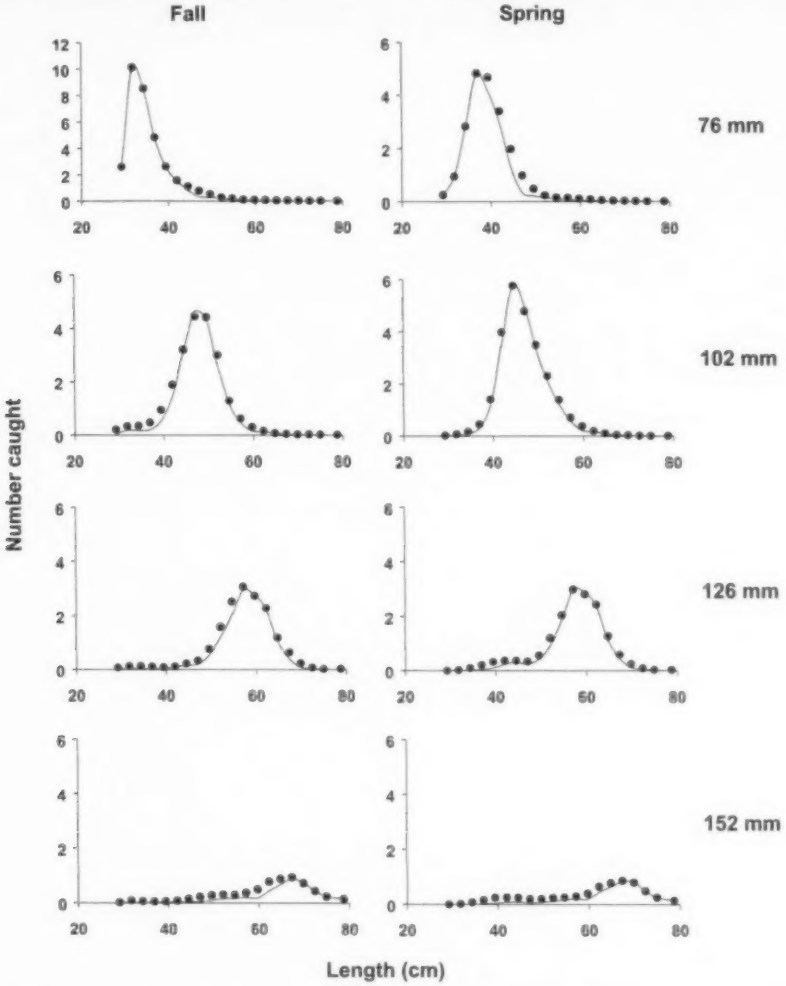

p_m = [1.0, 0.54, 0.33, and 0.23], and S is the unknown selection curve. The final model that emerged from the stepwise procedure added five more selection terms (β, θ_1, θ_2, θ_3, seasonal γs) and 6 seasonal ps ($p_{76} = 1.0$),

$$(8) \qquad C_{mbtyl} = f_{mbty} p_m S\{\lambda = \alpha m\beta,\ \sigma^2 = \gamma_t \lambda,\ \theta = \theta_1 + \theta_2 m + \theta_3 m^2\} E_{btyl}$$

The Laplace distribution was selected to model the shape of S because it gave the lowest AIC_c value for both eqs. 7 and 8.

A total of 8434 parameters, including the 8421 E terms, were estimated from 32 676 data points. Nevertheless, the results of the bootstrap procedure indicated that the S and p parameters were well estimated, having low coefficients of variation, negligible bias, and moderate correlations (Table 3). The estimated S curves had the narrow peaks and thick-tailed characteristic of the Laplace distribution and were slightly skewed (Fig. 1*a*). p was estimated to decrease with m, but less rapidly than postulated by the null hypothesis (Fig. 1*b*). λ increased almost linearly with m as hypothesized (Fig. 1*c*), the estimated exponents (β) being close to, but statistically different from, 1.0. The σ^2 was not constant, as originally hypothesized, but increased linearly with λ (Fig. 1*d*). The estimates for the skew parameters (θ_1, θ_2, θ_3) were significantly different from 0 and suggest increasingly negative skew with m (Fig. 1*e*). The variance and fishing power coefficients were significantly higher in the spring than in the fall, but no significant seasonal effects were found for the optimal length and skew parameters.

The model provided a good overall fit to the catch data (Fig. 2), but the predictions along the tails of the distributions tended to be somewhat lower than the observed values. This pattern is largely due to the proportionally higher variances associated with the low catch rates in the tails and was much less conspicuous when each catch observation was weighted equally. In any case, the estimates of abundance were similar for the variance-weighted and equally weighted fitting procedures, suggesting that they are robust with respect to the model's ability to fit the tails.

The coast-wide estimates of abundance fluctuate markedly

© 2002 NRC Canada

Fig. 3. Estimated relative abundance of red drum (*Sciaenops ocellatus*) in Texas bays during the fall (heavy centerline) with 90% confidence intervals (thin lines).

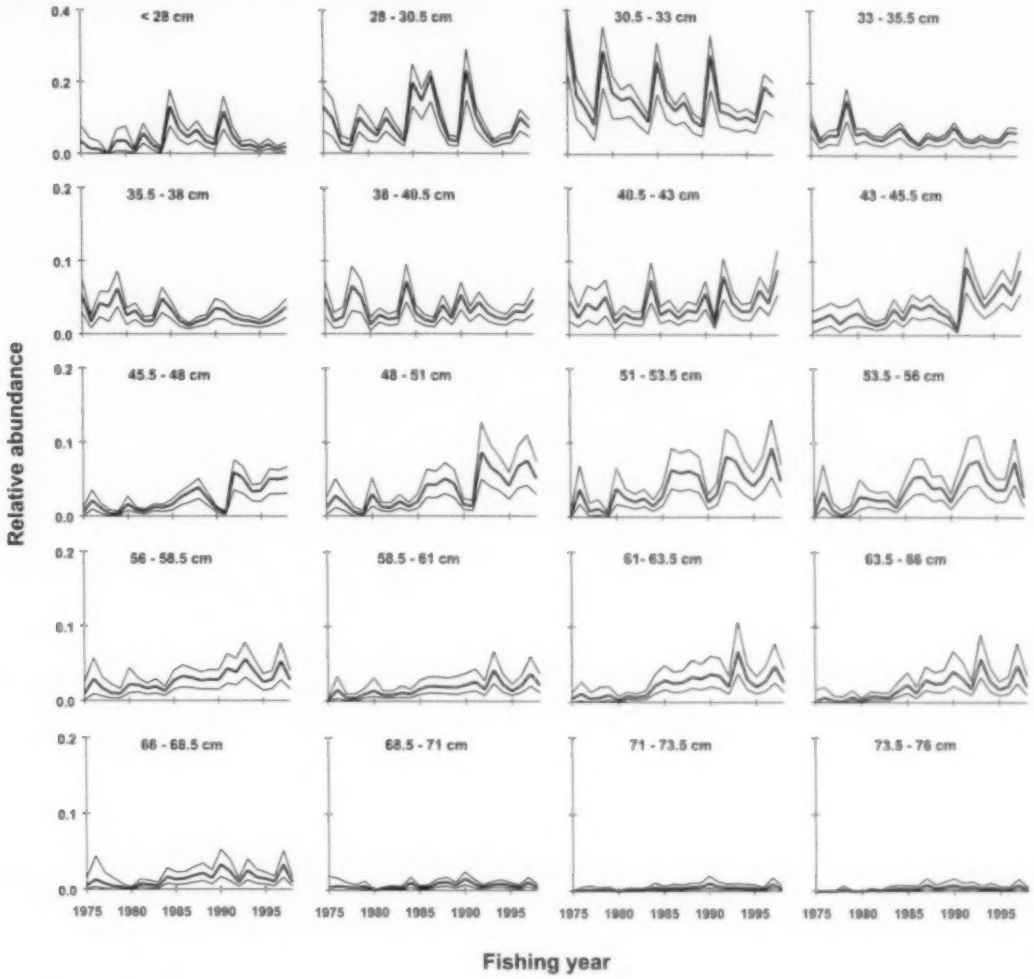

despite having narrow confidence intervals (Figs. 3 and 4), indicating that the recruitment and survival of red drum in Texas bays is highly variable. The estimates for fish under 40.5 cm in length exhibit no discernible long-term trends; however, the estimates for larger fish show a strong increasing trend during the 1980s and 1990s. Age–length data from otoliths collected during the 1990s (Fig. 5) indicate that red drum less than 40.5 cm long in the fall and 46 cm in the spring are nearly all one year old and that red drum less than 53.5 cm long in the fall and 58.5 cm in the spring are nearly all two years old. Most of the remaining catch is composed of fish between three and four years old.

Approximate indices of survival were developed by aggregating the length distributions according to age and dividing the estimated abundance of each year-class by its estimated abundance during the preceding year (Fig. 6). The results suggest the survival of age-1 red drum has increased steadily from very low values in the 1975 to nearly 100% by the late 1990s. The survival of age-2 red drum also seems to have increased since 1975, but leveled off during the mid-1980s and began fluctuating between 50% and 100%. The survival of age-3 and older fish remained very low.

Discussion

The selection models presented in this paper accommodate the possibility that some catch-at-length observations will be known more precisely than others and allow for nonlinear relationships between the optimal length, variance in length, and mesh size. The example showed that gillnet selection for red drum in Texas bays could be explained as a unimodal process approximating a skewed Laplace distribution where the optimal length varies in proportion to mesh size and the variance in proportion to the optimal length (therefore also proportional to mesh size). The proportional relationship between optimal length and mesh size is not surprising and has been demonstrated for many species (see Hamley 1975). The proportional relationship between vari-

© 2002 NRC Canada

Fig. 4. Estimated relative abundance of red drum (*Sciaenops ocellatus*) in Texas bays during the spring (heavy center line) with 90% confidence intervals (thin lines).

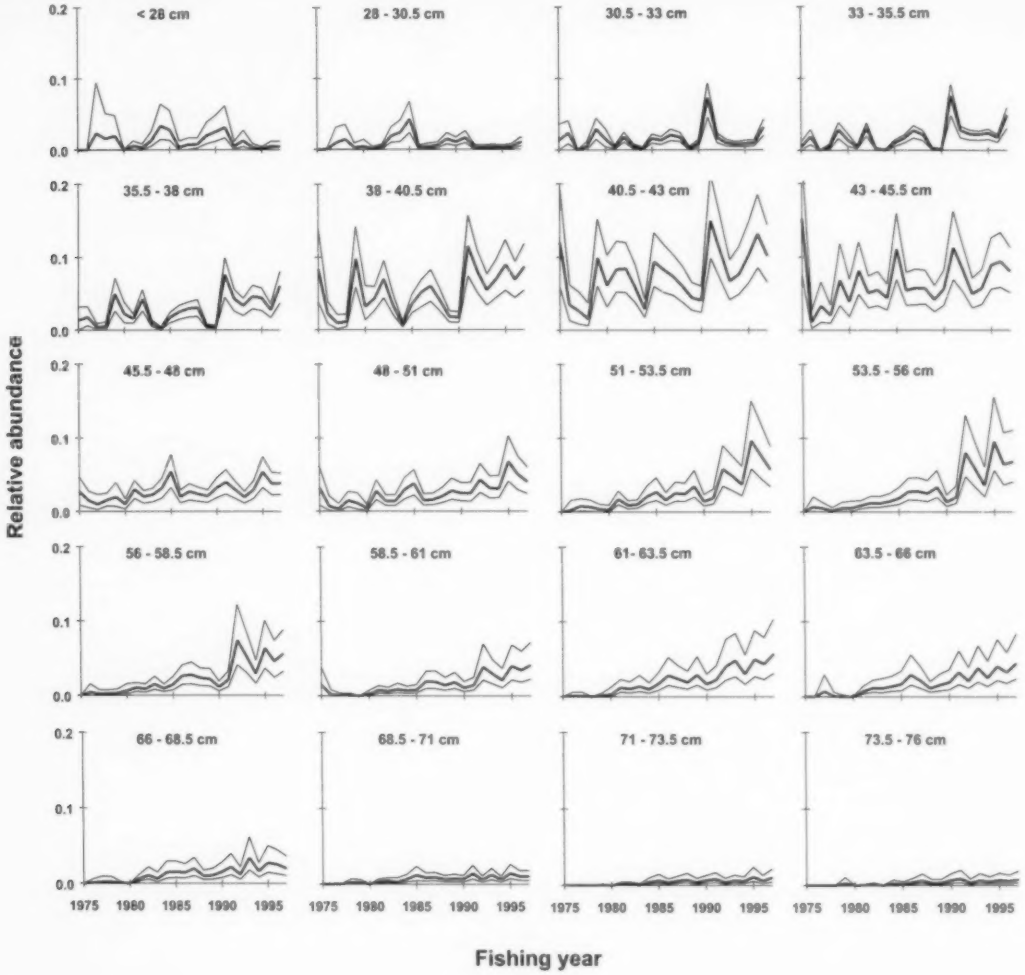

ance and mesh size, on the other hand, is intermediate between the usual assumptions of either constant variance or variance proportional to the square of mesh size. In fact, the "usual" assumptions likely represent the extremes of the relationship and we suggest that allowance always be made for linear forms.

The estimated fishing power for red drum was greater for the spring than for the fall, probably owing to an increase in swimming activity associated with the warmer spring temperatures (see Hensley and Fuls 1998). The estimates also decreased with mesh size, but not as rapidly as the decrease in capture sites per unit of net. This suggests that larger fish may be channeled into the large mesh panels by the adjacent smaller mesh panels or that larger fish cover a greater area of net with each encounter. In any case, the decreasing trend would seem counter to the conventional wisdom that larger meshes are more efficient (Hamley 1975). The conventional wisdom, however, is largely based on fishing power coefficients derived from direct comparisons of gillnet catches with known populations, which implicitly reflect the potential increase in encounter rates with length. When the power estimates from this study were multiplied by the relative encounter rates for the corresponding optimal lengths (with $\tau = 0.8$), the values did indeed increase with mesh size.

The fishing power of gillnets usually decreases as fish and debris accumulate in them (Hamley 1975), causing the catch rates to level off and making the population seem more stable than it actually is (hyperstability). On the other hand, if the target species is attracted by an increase in certain of the entangled items their catch rate may accelerate, causing trends in the population to appear stronger than they actually are (hyperdepletion). If the target species is the predominant item caught, this effect could be estimated by parameterizing fishing power as $p = gE^h$ (and suitably modifying eq. 3), where $h < 1$ would indicate hyperstability and $h > 1$ hyperdepletion (g is a scaling coefficient). Otherwise, it may be

© 2002 NRC Canada

Fig. 5. Distributions of length for ages 1, 2, 3, and 4 during the (*a*) fall and (*b*) spring.

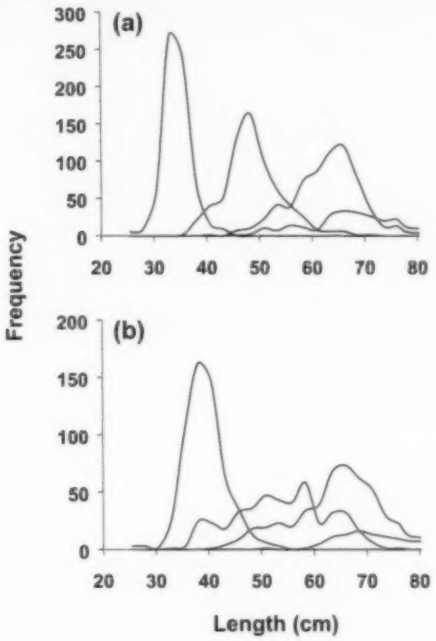

more appropriate to express p as a function of some other covariate like the total number of items entangled. Neither approach appears necessary for the present example as the catch per hour of red drum was not significantly correlated with soak time. Moreover, net saturation was not a frequent problem; less than one percent of the gilling sites were occupied in most sets and less than five percent of the gilling sites were occupied in 99% of the sets. Red drum themselves constituted only a small fraction of the total catch.

The fall abundance of red drum under 40 cm in length (presumably age 1) was estimated to fluctuate without a persistent trend. In part, this appears to be a reflection of recruitment inasmuch as the catch rate of young-of-the-year (age-0) red drum in bag seines also fluctuates with little trending (Hensley and Fuls 1998). However, the age-0 bag seine and lagged age-1 gillnet series are not highly correlated, implying that the survival of age-0 red drum is also highly variable. This contention is supported by observations of increased survival associated with hurricanes (Matlock 1987) and catastrophic kills associated with severe cold fronts (McEachron et al. 1994).

In contrast to fish under 40 cm in length, the abundance and survival of larger red drum appears to have increased a great deal since the early 1980s. This is consistent with increasingly restrictive regulatory changes promulgated by the state of Texas during the 1980s, starting in 1981 when the commercial sale of red drum was prohibited, the minimum length limit was increased from 35.6 to 40.6 cm, and the maximum length limit was lowered to 76.2 cm. In 1988 the minimum length limit was increased to 50.8 cm, the maximum length limit reduced to 71.1 cm, and a creel limit of 3 fish per day was imposed. These regulations effectively eliminated most of the fishing pressure on age-1 and -2 red drum, which is reflected by the very high survival rates indicated in this study.

The fraction of age-3 red drum remaining in the study area was estimated to be very low with little indication of an increasing trend, but the exact magnitude is hard to determine owing to the difficulty in distinguishing age-3 and -4 red drum based on length. To a large extent, the low values may be a reflection of the emigration of maturing 3- and 4-year-old fish out of the bays and into offshore waters, which probably exceeds the loss rate due to fishing and makes any increase in survival difficult to detect. The prohibition on commercial harvest in 1981 and subsequent creel limits may have resulted in a slight increase in spring-to-spring survival of age-3 red drum, but their effect seems to have been mitigated by a shift in recreational effort away from smaller fish (anglers being forced to fill their creel limits with fish within the size limits, most of which are age 3 and 4).

It is noteworthy that the lower confidence limit of the fraction of red drum remaining in the study area occasionally exceeds 1.0, which suggests there may sometimes be a net influx of fish into the study area. This is likely a consequence of episodic movements such as might occur with the passage of cold fronts when red drum are temporarily driven out of the shallow near-shore areas into the deeper waters of the bays. Such variations, however, are effectively random over the time scale considered here and should not affect the long-term trends.

Texas bay systems have experienced a net loss of emergent wetlands and submerged aquatic vegetation since 1975 owing to subsidence, erosion, upland conversion, and dredge-and-fill activities (Galveston Bay National Estuary Program 1995; Texas Parks and Wildlife Department 1999). This raises concerns that the spatial distribution of red drum has changed through time, with a larger fraction concentrating along the remaining healthy shorelines or perhaps using parts of the bay further away from the shore. The former response should not bias the estimated survival and abundance trends because the sampling procedure has not changed, i.e., stations located in the damaged areas are still sampled in the same way. The latter response, however, could lead to a negative bias in the estimated trends because a decreasing fraction of the total population would be available to the nets. However, this too seems unlikely because red drum do not appear to use the open portions of the bay; trawl surveys conducted in these areas by the TPWD have rarely caught red drum and there has not been a discernible increase since the survey began in 1982.

One could argue that the abundance and survival indices may be sensitive to the value of the exponent τ used in the speed-to-length relationship, which was not estimable from the types of data examined in this study and had to be borrowed from a meta-analysis by Blake (1983). However, the rate of increase in abundance was only slightly depressed when the extreme value of 1.0 was used for τ instead of 0.8. Thus, explicit consideration of the uncertainty in τ, if it were possible, would broaden the confidence intervals somewhat, but the general conclusions would remain unchanged.

A reviewer also suggested that a multiplicative error structure might be more appropriate than the weighted least-

© 2002 NRC Canada

Fig. 6. Fraction of red drum in each age-class that remain in the study area after one year (from one fall to the next or one spring to the next) with 90% bootstrap confidence intervals. Panels (*a*) and (*b*) refer to the fraction of age-1 fish remaining at age 2. Panels (*c*) and (*d*) refer to the fraction of age-2 fish remaining at age 3. Panels (*e*) and (*f*) refer to the fraction of age-3 fish remaining at age 4.

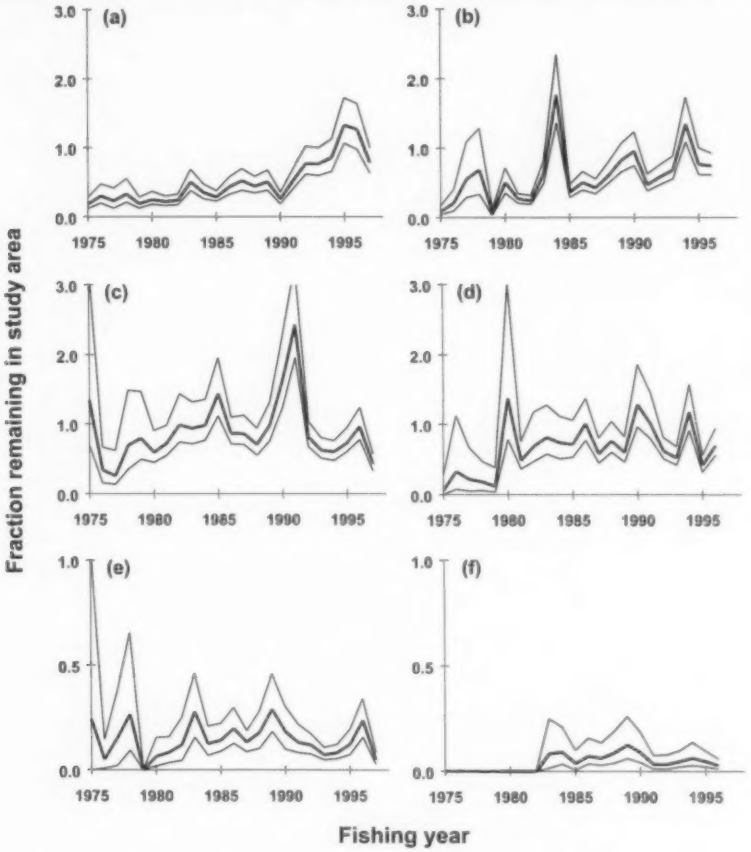

squares approach adopted here, in which case the task would be to minimize

$$\mathcal{L} = \sum_l \sum_k \sum_m (\log_e\{C_{mkl} + z\} - \log_e\{f_{mk} p_{mk} S_{mkl} E_{kl} + z\})^2 \quad (9)$$

The small constant z must be added to each observation if there are catches of zero (as there are in the present example), whereupon the computational burden is greatly increased because there is no closed-form solution for the E terms. Moreover, eq. 9 implies that the variance of C increases in proportion to the squared expectation of C, whereas our data suggest a more linear relationship. For these reasons, a better alternative for the present example might be a Poisson error structure, where one seeks to minimize

$$\mathcal{L} = \sum_l \sum_k \sum_m f_{mk} p_{mk} S_{mkl} E_k - C_{mkl} \log_e\{f_{mk} p_{mk} S_{mkl} E_{kl}\} \quad (10)$$

where

$$E_{kl} = \frac{\sum_m C_{mkl}}{\sum_m f_{mk} p_{mk} S_{mkl}}$$

Note, however, that neither eqs. 9 or 10 allow the variance of C to vary with the number of sets, which are few during the early part of the time series for red drum.

We applied the Poisson error structure to the final selection model in eq. 8 and found that the fishing power estimates for 102- and 126-mm mesh were between 15 and 35% lower than the corresponding weighted least-squares estimates. This translated into proportionally higher abundance estimates for ages 2 and 3 (relative to age 1), which in turn suggested somewhat higher survival rates from age 1 to age 2. Otherwise, the abundance and survival trends were nearly identical to those estimated by the weighted least-squares approach.

Acknowledgments

This paper is dedicated to the memory of Larry McEachron, who succumbed to cancer before the review

© 2002 NRC Canada

process was completed. We thank Carl Walters and two anonymous reviewers for their helpful comments on the manuscript and the Texas Parks and Wildlife Department for releasing the data. Partial funding for the data collection was provided by the U.S. Department of Interior, Fish and Wildlife Service (DJ 15.605, Project F-34-M).

References

Baranov, F.I. 1948. Theory and assessment of fishing gear. Pishchepromizdat, Moscow.

Beamish, F.W.H. 1978. Swimming capacity. *In* Fish physiology. Vol. 7. Locomotion. *Edited by* W.S. Hoar and D.J. Randall. Academic Press, New York. pp. 101–187.

Blake, R.W. 1983. Fish locomotion. Cambridge University Press, New York.

Buckland, S.T., Burnham, K.P., and Augustin, N.H. 1997. Model selection: an integral part of inference. Biometrics, **53**: 603–618

Croxton, F.E., Cowden, D.J., and Klein, S. 1967. Applied general statistics. 3rd ed. Prentice Hall, Englewood Cliffs, N.J.

Efron, B. 1992. Six questions raised by the bootstrap. *In* Exploring the limits of bootstrap. *Edited by* R. LePage and L. Billard. John Wiley and Sons, New York.

Fournier, D.A., Sibert, J.R., Majkowski, J., and Hampton, J. 1990. MULTIFAN a likelihood-based method for estimating growth parameters and age composition from multiple length frequency data sets illustrated using data for southern bluefin tuna (*Thunnus maccoyi*). Can. J. Fish. Aquat. Sci. **47**: 301–317.

Galveston Bay National Estuary Program. 1995. The Galveston Bay Plan. Publication GBNEP-49. Galveston Bay National Estuary Program, Webster, Texas.

Hamley, J.M. 1975. Review of gillnet selectivity. J. Fish. Res. Board Can. **32**: 1943–1969.

Hamley, J.M., and Regier, H.A. 1973. Direct estimates of gillnet selectivity to walleye (*Stizostedion vitreum vitreum*). J. Fish. Res. Board Can. **30**: 817–830.

Helser, T.E., Condrey, R.E., and Geaghan, J.P. 1991. A new method of estimating gillnet selectivity, with an example for spotted seatrout, *Cynoscion nebulosus*. Can. J. Fish. Aquat. Sci. **48**: 487–492.

Hensley, R.A., and Fuls, B.E. 1998. Trends in relative abundance and size of selected finfishes and shellfishes along the Texas coast: November 1975 – December 1996. Texas Parks and Wildlife Department Management Data Series Number 159, 4200 Smith School Road, Austin, TX 78744, U.S.A.

Holt, S.J. 1963. A method of determining gear selectivity and its application. ICNAF–ICES–FAO Joint Sci. Meet. Pap. No. S15 (ICNAF Spec. Publ. No. 5. pp. 106–115).

Hovgard, H. 1996. A two-step approach to estimating selectivity and fishing power of research gill nets used in Greenland waters. Can. J. Fish. Aquat. Sci. **53**: 1007–1013.

Hurvich, C.M., and Tsai, C. 1995. Model selection for extended quasi-likelihood models in small samples. Biometrics, **51**: 1077–1084.

Lagler, K.F. 1968. Capture, sampling and examination of fishes. *In* Methods for assessment of fish production in fresh waters. IBP Handbook 3. *Edited by* W.E. Ricker. Blackwell Scientific Publications, Oxford. pp. 7–45.

Matlock, G.C. 1987. The role of hurricanes in determining year-class strength of red drum. Contrib. Mar. Sci. **30**: 39–47.

McCombie, A.M., and Berst, A.H. 1969. Some effects of shape and structure of fish on selectivity of gill nets. J. Fish. Res. Board Can. **26**: 2681–2689.

McCombie, A.M., and Fry, F.E. 1960. Selectivity of gill nets for lake whitefish, *Coregonus clupeaformis*. Trans. Am. Fish. Soc. **89**: 176–184.

McEachron, L.W., and Green, A.W. 1985. Trends in relative abundance and size of selected finfish in Texas bays: November 1975 – June 1984. Texas Parks and Wildlife Department Management Data Series Number 79. Texas Parks and Wildlife Department, 4200 Smith School Road, Austin , TX 78744, U.S.A.

McEachron, L.W., Matlock, G.C., Bryan, C.E., Unger, P., Cody, T., and Martin, J.H. 1994. Winter mass mortality of animals in Texas Bays. Northeast Gulf Sci. **13**: 121–128.

Okubo, A. 1980. Diffusion and ecological problems: mathematical models. Springer-Verlag, New York.

Porch, C.E. 1998. Some intrinsic limitations of sample variances in stock assessment models. *In* Fishery stock assessment models. *Edited by* F. Funk, T.J. Quinn, II, J. Heifetz, J.N. Ianelli, J.E. Powers, J.F. Schweigert, P.J. Sullivan, and C.-I. Zhang. Alaska Sea Grant College Program Report No. AK-SG-98-01. University of Alaska, Fairbanks. pp. 385–398.

Regier, H.A., and Robson, D.S. 1966. Selectivity of gill nets, especially to lake whitefish. J. Fish. Res. Board Can. **23**: 423–454.

Scheaffer, R.L., Mendenhall, W., and Ott, L. 1979. Elementary survey sampling. 2nd ed. Duxbury Press, North Scituate, Mass.

Seber, G.A.F., and Wild, C.J. 1989. Nonlinear regression. John Wiley and Sons, New York.

Texas Parks and Wildlife Department. 1999. Seagrass conservation plan for Texas. Texas Parks and Wildlife Department, Austin.

Appendix A. Derivation of variance formulae

The catch-at-length observations for each mesh–strata combination, C_{mkl}, were the product of the observed total catch from the mesh (T_{mk}) and the proportion of that catch that belonged to a particular length category (x_{mkl}). We assume the covariance between T and x is small within any given k, in which case the variance of C_{mkl} is

$$V\{C_{mkl}\} \approx T_{mk}^2 V\{p_{mkl}\} + x_{mkl}^2 V\{T_{mk}\}$$

A substantial covariance between T and x might occur if each mesh catches members of several year-classes and year-class strength varies considerably through time—high T values would tend to be associated with high x values for the length categories corresponding to the strong year-class. We do not expect this to be a significant problem in our analysis of Texas red drum because each mesh size catches fish that are predominantly from one age-class (owing to the rapid growth rate of red drum), and year-class strengths do not appear to vary greatly from one year to the next (Hensley and Fuls 1998).

Variance of total catch T

The catches of each individual set i of mesh m in any given k (c_{imk}) can be treated as statistically independent because the sets were separated in time and space and the catches were negligible compared with the local population abundance. If the c_{imk} were also identically distributed, an unbiased estimate of the variance of the total catch T_{mk} by all sets would be

$$V\{T_{mk}\} \approx \frac{n_{mk}}{n_{mk}-1} \sum_i (c_{imk} - \sum_i c_{imk} / n_{mk})^2$$

© 2002 NRC Canada

where n_{mk} is the number of sets with mesh m in strata k. However, in this case, the c_{imk} were not identically distributed because the soak time f_{imk} was not the same for all sets. This being the case, we note that the total catch T_{mk} is simply the product of the total effort and the ratio estimator for the expected catch per unit effort

$$\hat{R}_{mk} = \sum_{i}^{n_{mk}} c_{imk} \Big/ \sum_{i}^{n_{mk}} f_{imk}$$

The soak time of each set was independent of the catch rate; therefore

$$V\{T_{mk}\} = (\sum_{i} f_{imk})^2 V\{\hat{R}_{mk}\} + \hat{R}_{mk}^2 V\left\{\sum_{i} f_{imk}\right\}$$

where $V(\Sigma_i f_{imk})$ is replaced by the equivalent sample statistic and $V(\hat{R}_{mk})$ is given by Scheaffer et al. (1979) as

$$V\{\hat{R}_{mk}\} = \frac{1}{n_{mk}\bar{f}_{mk}^2} \frac{\sum_{i}(c_{imk} - \bar{R}_{mk} f_{imk})^2}{n_{mk} - 1}$$

Variance of the proportion x in each length-class

The observations of length for each mesh and stratum are essentially random samples from the vulnerable fraction of the population. The proportion of the catch falling in each length-class, x_{mkl}, is therefore a random variable with mean μ, sample size ν, and variance $(1 - \mu)\mu/\nu$. As such, Fournier et al. (1990) advocate using the formula

$$V\{p_{mkl}\} = \frac{(1 - \hat{x}_{mkl})\hat{x}_{mkl} + 0.1/L}{\nu_{imk}}$$

where the μ are replaced by the model estimates ($\hat{x}_{mkl}$) and L is the number of length categories. The term $0.1/L$ is included to prevent the expression from tending to zero as x tends to zero.

Replacing the μ with the model estimates presents a problem in the present case because the Es in eq. (3) can no longer be solved for analytically. This leaves us in the unenviable position of having to solve for thousands of parameters numerically. To avoid this we use the perhaps less satisfactory approach of replacing the model estimates with the observed values pooled over all sets within a given stratum. This may cause anomalously low observations of catch-at-length to receive too much weight in the analysis (see Porch 1998), but the effect should not be too serious because a large number of observations are made within each stratum so that the pooled length–frequency distributions should be a fairly good reflection of the true distribution. Moreover, the use of observed values should render the results less sensitive to model mis-specification. Regardless, we believe it to be superior to simply assuming that the variances of all observations are identical.

Appendix B. Bootstrap estimates of variance and bias of parameters

The bias of a statistic $\hat{\theta}(^\circ\mathbf{C})$ as an estimate of a given quantity θ was computed as

$$\text{bias}\{\hat{\theta}(^\circ\mathbf{C})\} = \frac{1}{500}\sum_{B=1}^{500}\hat{\theta}({}^B\mathbf{C}) - \hat{\theta}(\sum{}^B\mathbf{C}/B)$$

where $^\circ\mathbf{C}$ is the matrix of observed catches at length (original data), ${}^B\mathbf{C}$ is a matrix of bootstrapped catches at length, and B is one of 500 bootstrap replications (Efron 1992). Approximate confidence limits were constructed by ordering the results of each bootstrap (the percentile method).

Each bootstrap data set ${}^B\mathbf{C}$ was generated parametrically

$${}^B C_{mkl} = {}^B T_{mk}\, {}^B x_{mkl}$$

$${}^B T_{mk} = \hat{T}_{mk}(^\circ\mathbf{C}) + {}^B\eta$$

Here, $\hat{T}_{mk}(^\circ\mathbf{C})$ is the expected value of total catch obtained when the model was applied to the original data and ${}^B\eta$ represents a random draw from the normal distribution with mean 0 and variance equal to the observed sample variance $V\{T_{mk}\}$. The variable ${}^B x_{mkl}$ represents the bootstrap relative frequency distribution of length generated by drawing with replacement from the corresponding model-estimated relative length–frequency distribution, $\hat{x}_{mkl}(^\circ\mathbf{C})$. The number of draws from $\hat{x}_{mkl}(^\circ\mathbf{C})$ was the lesser of the actual number measured (ν_{mk}) or ${}^B T_{mk}$.

© 2002 NRC Canada

Temporal and spatial variability in elemental composition of otoliths: implications for determining stock identity and connectivity of populations

Bronwyn M. Gillanders

Abstract: Interannual variability in elemental composition of otoliths may confound spatial interpretations. The elemental fingerprints of otoliths of juvenile fish were determined for fish collected from 12 to 15 estuaries in each of three consecutive recruitment years to determine temporal variation in otolith chemistry for each estuary. It was also examined whether there is overlap in elemental fingerprints of fish collected in different years and from different estuaries that may confound subsequent spatial comparisons. Significant differences in otolith chemistry were found among years for individual elements (lithium, manganese, strontium, and barium) and for multi-element fingerprints. Some estuaries showed large variation in multi-element fingerprints among years, whereas others showed little variation among years. There was some overlap of elemental fingerprints of different estuaries, but these were not always for fish collected in the same year. The significant spatial and temporal variation in elemental fingerprints meant that it was possible to confound spatial differences with temporal differences. Therefore, if the natal estuary of the adults is to be determined, a library of elemental fingerprints needs to be built up over time for each estuary rather than a single year-class of juveniles being used as the elemental fingerprint for a number of year-classes of adults.

Résumé : La variation d'une année à l'autre de la composition en éléments chimiques des otolithes peut fausser les interprétations spatiales qu'on peut en tirer. Les empreintes d'éléments chimiques des otolithes ont été déterminées chez de jeunes poissons récoltés dans 12–15 estuaires dans chacune de trois classes de recrutement consécutives dans le but de décrire la variation temporelle de la chimie des otolithes dans chaque estuaire; il s'agissait aussi de vérifier l'existence possible de chevauchement dans les empreintes chimiques des poissons récoltés en différentes années et dans différents estuaires, ce qui pourrait fausser les comparaisons spatiales subséquentes. Il existe des différences significatives dans la chimie des otolithes d'une année à l'autre en ce qui a trait aux empreintes basées sur un (lithium, manganèse, strontium et baryum) ou plusieurs éléments. Dans quelques estuaires, il y a d'importantes variations annuelles dans les empreintes basées sur plusieurs éléments, mais dans d'autres, les variations sont faibles. Il y a du chevauchement entre les empreintes chimiques des différents estuaires, mais ce n'est pas toujours chez des poissons récoltés la même année. Les variations spatiale et temporelle significatives des empreintes chimiques font qu'il est possible de confondre les différences spatiales et les différences temporelles. En conséquence, pour arriver à identifier l'estuaire d'origine d'adultes, il est nécessaire de bâtir au cours des ans une banque d'empreintes chimiques pour chaque estuaire, plutôt que de se fier aux empreintes d'une seule classe de juvéniles pour reconnaître les adultes de plusieurs classes d'âge.

[Traduit par la Rédaction]

Introduction

Estuaries and other sheltered habitats are assumed to be important "nursery" areas for many fishes whose adults are found on reefs. It is generally argued that juvenile fish recruit to estuarine nursery habitats and then move to coastal reefs at greater sizes and ages (Bell and Worthington 1993). However, direct evidence of this process is lacking because of the difficulties of quantifying movement. Thus, the extent to which juveniles occurring in estuarine habitats contribute to adult stocks on coastal reefs is unknown. Recently, natural tags, such as isotopes and elements within otoliths, have shown great promise as a means of determining connectivity among populations (e.g., Gillanders and Kingsford 1996; Campana et al. 2000; Thorrold et al. 2001).

Environmental and physiological information is incorporated into the growing surface of the otolith of fish. The metabolically inert nature of otoliths ensures that deposition of trace elements remains unaltered through time (Campana and Neilson 1985). Deposition occurs in layers over time and differences in microchemistry among the layers can be estimated by reference to the growth zones within the

Received 6 December 2001. Accepted 31 March 2002. Published on the NRC Research Press Web site at http://cjfas.nrc.ca on 18 May 2002.

J16652

B.M. Gillanders. Department of Environmental Biology, The University of Adelaide, SA 5005, Australia (e-mail: Bronwyn.Gillanders@adelaide.edu.au).

 DOI: 10.1139/F02-040 © 2002 NRC Canada

otolith. Such growth zones are routinely used for daily and (or) annual ageing of fish. Trace elements in otoliths can be used as a natural tag to determine past environmental history and to trace movements of fish (e.g., Gillanders and Kingsford 1996).

Differences in elemental fingerprints of juvenile fish have been found among different estuaries, among different streams, and between both estuarine and open coastal as well as offshore and inshore reef habitats (e.g., Gillanders and Kingsford 1996; Thorrold et al. 1998*b*; Gillanders and Kingsford 2000). Such differences in chemical fingerprints among areas provide evidence that the otolith does act as a natural tag (Campana 1999). This means that chemical fingerprints from the juvenile portion of adult otoliths can then be used to classify these fish to their recruitment or "nursery" habitat. However, there is potential for variability in elemental fingerprints of juvenile fish among years, which may subsequently affect classification of adult fish to their recruitment habitats. Recent research suggests that elemental fingerprints of otoliths of juvenile fish in different estuaries may vary among years, largely because there are differences in temperature, salinity, and freshwater inputs between years (Gillanders and Kingsford 2000); therefore, temporal sampling is required.

The general objective of this research was to determine spatial and temporal variation in elemental fingerprints of otoliths of juvenile fish to examine whether the elemental fingerprints of fish from one year are representative of fish from other years. The species chosen for the study was snapper (*Pagrus auratus*; Sparidae) because it has spatially segregated juvenile and adult habitats and is an important fishery species throughout Australia. In New South Wales (NSW), snapper recruit to bare substrata of estuarine habitats where they remain associated for 12–18 months, after which time they leave estuaries for coastal reefs and other habitats over the continental shelf (Bell and Worthington 1993). Within NSW, more than 97% of commercial landings of snapper are from the trap and line fishery, which operates in nearshore and continental shelf waters. Although there are no signs of the large variation in recruitment to the fishery evident in some other snapper populations (e.g., South Australia, McGlennon et al. 2000), year-to-year variation in landings has often been high (Ferrell and Sumpton 1997). Two- and three-year-old fish dominate landings of snapper in all areas of NSW, with fewer than 2% of landings being fish older than 10 years despite a potential longevity in excess of 30 years.

The specific objectives of this study were (*i*) to determine spatial variation in elemental fingerprints of otoliths of juvenile snapper collected in different estuaries and across three years of sampling, (*ii*) to determine temporal variation in elemental fingerprints for each estuary, and (*iii*) to examine if there may be overlap in elemental fingerprints of fish collected in different years and from different estuaries that may confound subsequent spatial comparisons. If there is little temporal variability in elemental fingerprints among estuaries, then fish collected in one year from a number of estuaries could be used to establish an elemental fingerprint for each estuary so that in future years the proportion of adults from each estuary could be determined based on elemental fingerprints of juvenile fish collected in one year. If, however, there is temporal variability in elemental fingerprints among estuaries, then a library of fingerprints may need to be built up encompassing a range of year-classes of juveniles and the birth year of adult fish estimated. The recruitment estuary of adult fish could then be determined with elemental fingerprints of juveniles from the appropriate birth year.

Materials and methods

Sample collection

Juvenile snapper were collected in each of three recruitment seasons (Nov. 1998 – Feb. 1999, Dec. 1999 – Feb. 2000, Dec. 2000 – Jan. 2001, hereafter referred to as 1998–1999, 1999–2000, 2000–2001) to determine variation in elemental fingerprints among estuaries and years. In each year, 10 fish were collected from each of two sites (separated by hundreds of metres to kilometres) in each of 15 estuaries (separated by tens to hundreds of kilometres) spanning 600 km along the coast of NSW (Fig. 1). No juvenile snapper were found in Jervis Bay and Batemans Bay during 1999–2000 and 2000–2001 and in Eden during 1999–2000 recruitment seasons. All fish were collected by hand line and were stored on ice in the field before being dissected upon return to the laboratory. For each fish, the standard length (SL) was measured (range, 43–83 mm SL; average ± standard error, 66.66 ± 0.30 mm SL), and the sagittal otoliths removed, cleaned of adhering tissue in Milli-Q deionized water, air-dried, and placed in Eppendorf microcentrifuge tubes.

Sample preparation and analysis

Otoliths were weighed, cleaned in 1% nitric acid for 5–10 s to remove any possible contamination resulting from weighing, rinsed in Milli-Q water, and placed in acid-washed polycarbonate tubes ready for analysis. The average weight loss between weighing and cleaning of otoliths in 1% acid was 0.2 mg (n = 10 otoliths), which is considered negligible given the average weight of the otoliths (8.03 ± 0.09 mg).

Samples were dissolved overnight in concentrated nitric acid inside a plastic Class 100 (AS 1807) laminar flow cabinet. They were then diluted with Milli-Q water to 1% HNO_3. Blank samples were prepared in a similar manner, but no otolith was present; these were used for blank corrections and to calculate limits of detection. Spiked samples were also analysed at a frequency of every 10 samples to assess instrument drift and recovery. A lab standard, consisting of *Pagrus auratus* otoliths ground to micron-sized particles, was analysed during each session of analysis to assess repeatability of measurements. Elemental concentrations were determined by solution-based inductively coupled plasma-mass spectrometry (ICP-MS; Perkin Elmer SCIEX ELAN model 5000, U.S.A.). All elements were quantified using standards that were matrix-matched (i.e., addition calibration), except Ca and Sr, which were determined using standards made up in 1% HNO_3 (i.e., external calibration).

Preliminary analyses suggested that nine elements [lithium (Li), magnesium (Mg), calcium (Ca), manganese (Mn),

© 2002 NRC Canada

Fig. 1. Map of Australia (inset) and the New South Wales coast showing estuaries in which fish were collected. The meteorological districts are also indicated.

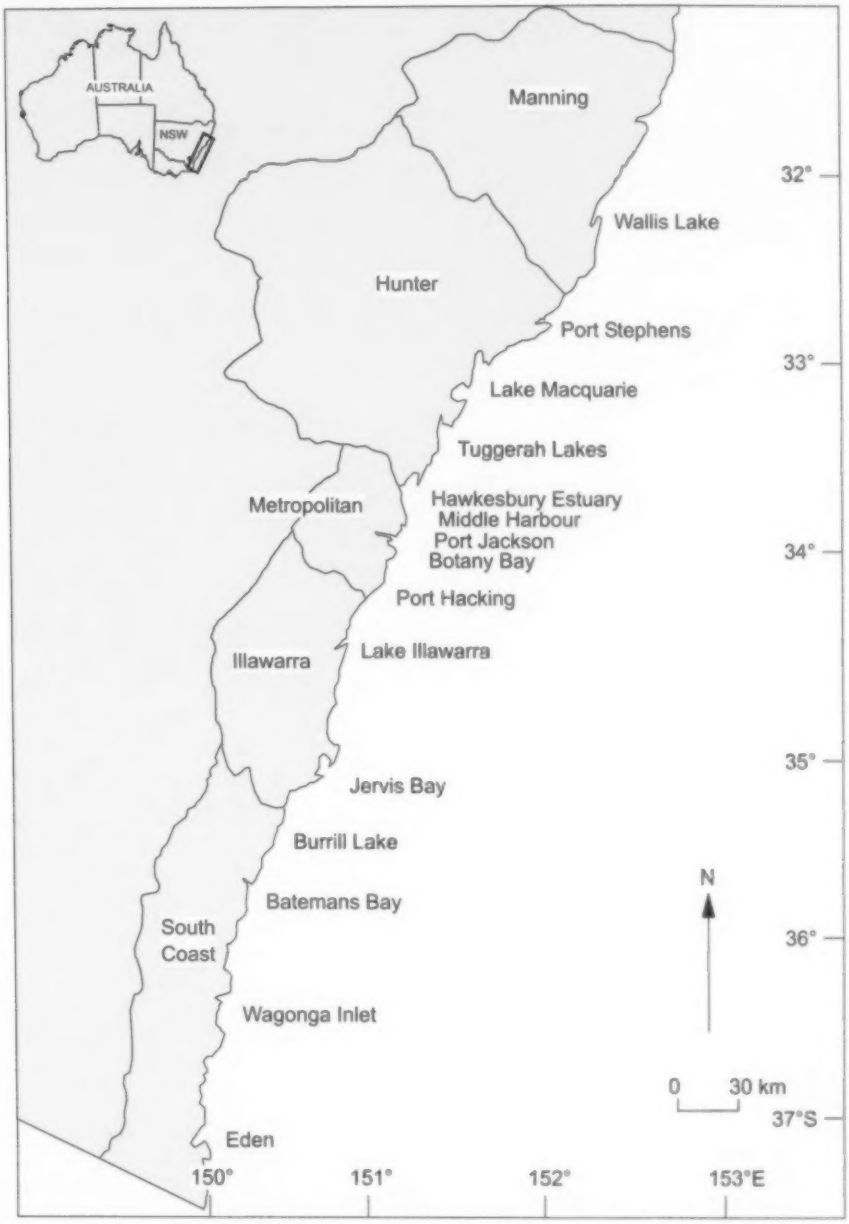

copper (Cu), zinc (Zn), strontium (Sr), barium (Ba), and lead (Pb)] were detectable in otoliths of juvenile snapper using ICP-MS and these elements were chosen for analyses. Cu, Zn, and Pb were frequently below detection limits for otolith samples, Mg showed poor precision, and Ca showed excessive recovery; therefore, these elements were removed from subsequent analyses. Li, Mn, Sr, and Ba were considered quantifiable based on detection limits, precision, and accuracy (see below). Detection limits, which were calculated from the concentration of analyte yielding a signal equivalent to three times the standard deviation of the blank signal, for each of the elements were 0.040 (Li), 0.014 (Mn), 0.082 (Sr), and 0.015 $\mu g \cdot g^{-1}$ (Ba). Mean estimates of precision (%RSD, relative standard deviation) based on replicate measurements (*i*) of our lab standard ($n = 120$) were 12.2% (Li), 16.8% (Mn), 11.5% (Sr), and 12.1% (Ba), and (*ii*) within

© 2002 NRC Canada

otolith samples were 12.2% (Li), 2.8% (Mn), 2.4% (Sr), and 2.7% (Ba). Mean recovery of spiked samples was 95% (Li), 97% (Mn), 98% (Sr), and 84% (Ba).

Statistical analyses

Univariate and multivariate techniques were used to test hypotheses concerning individual elements and multi-element composition of otoliths of snapper. Temporal and spatial variation was analysed by three-factor analyses of variance (ANOVA) for each element. Additional ANOVAs (two factor) were also conducted on each year of data. All factors were treated as random. Site was nested within the interaction of year and estuary for the three-factor design because the same sites could not always be sampled in all years. All analyses were performed on $\ln(x + 1)$-transformed data. The assumption of homogeneity of variance was tested prior to each analysis using Cochran's C test. When data remained heterogeneous after transformation, analyses were still performed, as ANOVA is robust to departures from assumptions where data are balanced and sample sizes are relatively large (Underwood 1997). To ensure balanced data in the three-factor analyses, only estuaries in which fish were collected in all three years were used. Means were compared using Student–Newman–Keuls (SNK) tests, when significant differences were detected.

The Friedman nonparametric test was used to determine whether there was a systematic response or pattern across the estuaries for each year. The Friedman test transforms the data for each year to ranks and then sums the ranks for each estuary. The calculated statistic is approximately distributed as χ^2, and can be compared to χ^2 critical values to determine significance.

Multi-element fingerprints were analysed using nonparametric multivariate ANOVA (NP-MANOVA), using a similar design to the univariate ANOVAs. The NP-MANOVA uses permutations to test multivariate hypotheses (Anderson 2001*a*, 2001*b*). The data were $\ln(x + 1)$ transformed before Euclidean distances between each pair of samples were calculated to obtain a distance matrix. The test statistic was then calculated as the ratio of the sum of squared Euclidean distances among groups divided by the sum of squared distances within groups, and is thus essentially an F ratio (Anderson 2001*b*). For the three-factor design, unrestricted permutation of raw data was used, whereas for the two-factor design, permutation of residuals under the full model was used because the number of levels of the nested factor (site) was 2 and therefore the number of possible permutations could not give P values less than 0.05 (Anderson and Legendre 1999). The units being permuted depend on the term being tested; further details on methods of permutation can be found in Manly (1997) and Anderson and Legendre (1999).

To ensure that differences in fish length and (or) otolith weight among samples did not confound any among estuary differences in elemental composition, the effect of otolith weight on elemental concentrations was examined. Otolith weight was positively correlated with fish length (Pearson's $r = 0.92$, $n = 800$). Three of the four elements (Li, Mn, and Sr) showed small but statistically significant relationships with otolith weight. The effect of otolith weight was removed by subtracting the slope of the regression relationship multiplied by otolith weight from the element data, and the data were re-analysed. This procedure did not modify the significance of any of the results and therefore only the original data are presented.

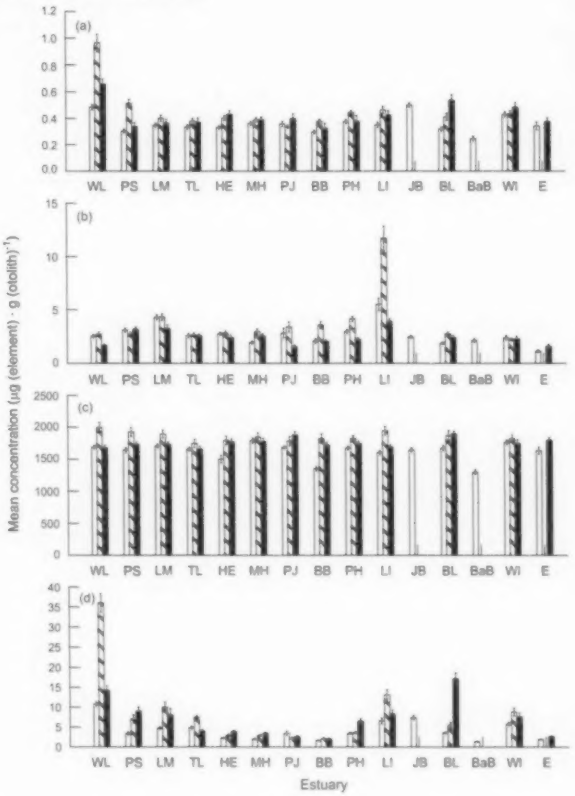

Fig. 2. Mean concentrations (± standard error) of (*a*) Li, (*b*) Mn, (*c*) Sr, and (*d*) Ba in otoliths of juvenile snapper (*Pagrus auratus*) collected over three years in each of two sites within 15 estuaries along the coast of New South Wales, Australia. Data were pooled by estuary (n = 20 fish per estuary per year). Open bars are 1998–1999, hatched bars are 1999–2000, and solid bars are 2000–2001 recruitment seasons. The estuaries from north to south were Wallis Lake (WL), Port Stephens (PS), Lake Macquarie (LM), Tuggerah Lakes (TL), Hawkesbury Estuary (HE), Middle Harbour (MH), Port Jackson (PJ), Botany Bay (BB), Port Hacking (PH), Lake Illawarra (LI), Jervis Bay (JB), Burrill Lake (BL), Batemans Bay (BaB), Wagonga Inlet (WI), and Eden (E). No fish were collected from Jervis Bay and Batemans Bay in 1999–2000 and 2000–2001, and Eden in 1999–2000.

Results

Temporal and spatial variation across three years: individual elements

Variation in otolith chemistry of snapper differed depending on the element. Li and Ba both showed a significant year × estuary interaction (Fig. 2; Table 1). For Li, some estuaries varied among all years (e.g., Wallis Lake) or two of the three years differed (e.g., Port Stephens), whereas other estuaries showed no significant variation among years (e.g.,

© 2002 NRC Canada

Table 1. Results of ANOVA for concentrations of individual elements in otoliths of juvenile snapper collected across three years.

Source	df	MS Li	MS Mn	MS Sr	MS Ba
Time	2	0.2738**	3.8823**	0.4215**	9.5728*
Estuary	11	0.2201***	3.1682***	0.0633	15.7153***
Site (time × estuary)	36	0.0158***	0.2903***	0.0379***	0.8309***
Time × estuary	22	0.0418**	0.5127	0.0537	1.8547*
Residual	648	0.0068	0.0564	0.0107	0.0818
Cochran's *C*		0.0656**	0.0626**	0.0352	0.0510

Note: Cochran's C tests were used to test homogeneity of variances. All data were transformed to $\ln(x + 1)$. $^*P < 0.05$, $^{**}P < 0.01$, $^{***}P < 0.001$. Time and estuary were tested over the time × estuary interaction, the time × estuary interaction was tested over the site (time × estuary) term, and the site (time × estuary) term was tested over the residual. MS, mean square; df, degrees of freedom.

Table 2. Results of ANOVA for concentrations of individual elements in otoliths of juvenile snapper collected during the 1998–1999, 1999–2000, and 2000–2001 recruitment seasons.

Source	df	MS Li	MS Mn	MS Sr	MS Ba
1998–1999					
Estuary	14	0.0484**	1.3024***	0.1659	4.2310***
Site (estuary)	15	0.0097***	0.1691***	0.0766***	0.3268***
Residual	270	0.0032	0.0522	0.0072	0.0627
Cochran's *C*		0.1045*	0.1624**	0.0995*	0.1128**
1999–2000					
Estuary	11	0.1924***	2.4260**	0.0188	10.0851***
Site (estuary)	12	0.0166***	0.5345***	0.0266*	1.0509***
Residual	216	0.0054	0.0557	0.0133	0.0733
Cochran's *C*		0.1723**	0.1157	0.0854	0.1247*
2000–2001					
Estuary	12	0.0768*	0.7723*	0.0170	5.9669**
Site (estuary)	13	0.0213	0.1972***	0.0172	1.0148***
Residual	234	0.0122	0.0570	0.0111	0.0975
Cochran's *C*		0.1018	0.0976	0.0700	0.1184*

Note: Estuary and site were random factors. The degrees of freedom (df) vary across years because in 1999–2000 and 2000–2001 no juvenile snapper were found in Jervis Bay and Batemans Bay and in 1999–2000 no juvenile snapper were found at Eden. MS, mean square. Levels of significance as in Table 1.

Lake Macquarie and Tuggerah Lakes). Although there was variation in Li of otoliths among estuaries in each year, the magnitude of variation differed among the different estuaries. For example, large differences were seen among years for Wallis Lake, but relatively minor differences were found for other estuaries (e.g., Lake Macquarie). For Ba, significant variation among years was largely due to differences found in Wallis Lake and Burrill Lake.

For Mn, significant differences were found among years and estuaries (Fig. 2; Table 1). Concentrations of Mn in otoliths of fish were consistently higher in fish collected during 1999–2000 than in fish collected in the other two years (SNK tests). Fish from Lake Illawarra had consistently higher levels of Mn than fish from the other estuaries. Sr only showed significant variation among years, where concentrations were lower in 1998–1999 than in the other two years.

Spatial variability among estuaries for each of three years: individual elements

Significant differences were found in the otolith chemistry of snapper collected from the different estuaries for all years (Fig. 2; Table 2). Li, Mn, and Ba all showed significant differences among estuaries for each year. In contrast to these results, Sr showed no significant difference among estuaries for any of the years examined.

For Li, otoliths of fish from Wallis Lake had consistently higher levels for all years, although in 1998–1999, fish from Jervis Bay also had high levels. The 12 estuaries in which fish were collected in all three years were ranked for each year according to mean concentration of Li in otoliths of snapper and Friedman's statistic calculated. Although Wallis Lake had the highest levels of Li in each year (rank = 1 for each year), the 12 estuaries differed in their rank across years (Friedman's χ^2 statistic = 19.513, df = 11, non significance (ns) indicating that sums of ranks across years were equal for each estuary and thus the years differed in the way they ranked estuaries).

For Mn, otoliths of fish collected from two estuaries (Lake Illawarra and Lake Macquarie) had higher levels of Mn than fish from all other estuaries in 1998–1999. These same two estuaries were ranked 1 and 2 in terms of concentration of Mn for each of the three years, although in 1999–2000, only Lake Illawarra had higher concentrations of Mn than the other estuaries, and in 2000–2001, Lake Illawarra only differed from three other estuaries (Fig. 2). The 12 estuaries differed in their ranks across years, suggesting that for most estuaries it was difficult to predict where they

© 2002 NRC Canada

Fig. 3. Plots summarizing variation in elemental fingerprints of otoliths of juvenile snapper (*Pagrus auratus*) collected in (*a*) 1998–1999, (*b*) 1999–2000, and (*c*) 2000–2001 from different estuaries along the coast of New South Wales, Australia. The estuaries are designated as in Fig. 1. Shaded areas represent 95% confidence ellipses around the means for each estuary for each canonical variate.

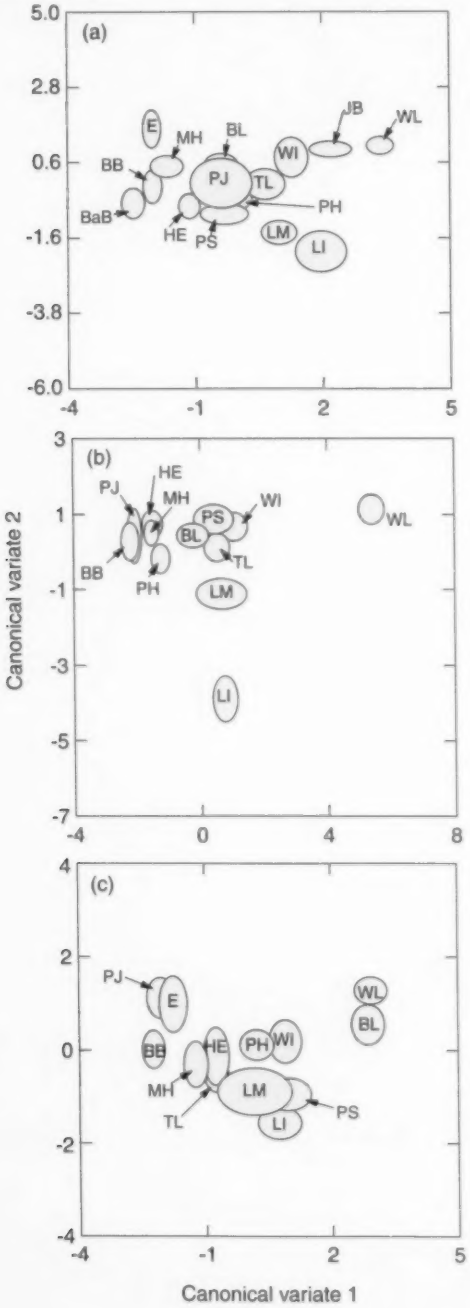

would be ranked and therefore if higher or lower concentrations of Mn may be found.

For Ba, otoliths of fish collected from Wallis Lake had consistently higher concentrations than those of fish collected from the other estuaries, although in 2000–2001 Burrill Lake also had high concentrations. Friedman's χ^2 statistic was significant (27.4615, df = 11, $P < 0.005$) suggesting that ranks of estuaries within each year were similar among years. For example, Wallis Lake was ranked 1 or 2 in all three years (highest concentrations) and Botany Bay had the lowest concentrations in all three years.

Spatial variability among estuaries for each of three years: multi-element fingerprints

Significant differences were found in multi-element fingerprints of otoliths of snapper among estuaries for each of the three years (Fig. 3; Table 3). For all years the 95% confidence ellipses around the mean value for each estuary suggested that a number of estuaries showed significant variation in elemental fingerprints (Fig. 3).

In 1998–1999 there were, however, a group of 5–6 estuaries that showed some overlap in elemental fingerprints, mainly with Port Jackson (Fig. 3*a*). Despite this overlap of some estuaries, there were a number of estuaries that could be distinguished, suggesting that we can track adult fish back to these estuaries. In 1999–2000, two groups of estuaries showed some overlap (Fig. 3*b*). One of these groups included estuaries in the vicinity of Sydney (e.g., Hawkesbury Estuary, Port Jackson, Middle Harbour, Botany Bay). Lake Macquarie, Wallis Lake, and Lake Illawarra clearly differed from the other estuaries (Fig. 3*b*). In 2000–2001, a number of estuaries showed significant variation (e.g., Wallis Lake, Burrill Lake, Botany Bay) and others showed some overlap (e.g., Hawkesbury Estuary and Tuggerah Lakes; Fig. 3*c*).

Consequences of ignoring temporal differences: multi-element fingerprints

Six estuaries were randomly selected from the 12 estuaries in which fish were collected in all three years and used to investigate spatial and temporal variation and the consequences of ignoring temporal variation if it exists. Some estuaries showed large variation among years (e.g., Wallis Lake and Lake Illawarra), others showed variation among years, but less than that seen for Wallis Lake and Lake Illawarra (e.g., Port Stephens and Lake Macquarie), whereas others showed some overlap for two of the three years sampled (e.g., Botany Bay and Wagonga Inlet; Fig. 4*a*, 4*b*, 4*c*).

When the individual years were distinguished, many of the ellipses did not overlap ellipses from other years (Fig. 4*d*). However, some ellipses did overlap those from other years and this overlap did not always involve samples collected in different years from the same estuary. For example, fish collected from Wagonga Inlet in 1998–1999 showed some overlap with those collected from Port Stephens in 1999–2000 (Fig. 4). Likewise, fish collected from Lake Macquarie in 1999–2000 showed some overlap with those collected from Lake Illawarra in 2000–2001. Overlap among years for different estuaries is likely to have consequences for assigning adult fish to recruitment estuaries, especially if juvenile fish are collected from different estuaries in different years and adult fish are not assigned to recruitment estu-

© 2002 NRC Canada

Table 3. Results of NP-MANOVA for multi-element fingerprints in otoliths of juvenile snapper collected during the 1998–1999, 1999–2000, and 2000–2001 recruitment seasons.

	1998–1999		1999–2000		2000–2001	
Source	df	*F*	df	*F*	df	*F*
Estuary	14	9.8727***	11	7.8118***	12	5.4647***
Site(estuary)	15	4.6485***	12	11.0303***	13	7.0327***
Residual	270		216		234	

Note: All data were transformed to $\ln(x + 1)$. df, degrees of freedom. Levels of significance as in Table 1; degrees of freedom as in Table 2.

aries using elemental fingerprints from the year-class of recruits in which they were juveniles (see Discussion).

Discussion

Significant variation in elemental composition of otoliths of juvenile snapper among estuaries was found for all years. There have been few studies that have investigated temporal variability compared to the number examining spatial variability in otolith chemistry. Campana et al. (2000) found that elemental concentrations varied little over 2-year intervals, but more substantive differences were noted for some elements (e.g., Li, Mg, Ba) and some locations over 4- to 13-year intervals. However, a number of other studies have found significant variation in otolith chemistry over 2- to 3-year intervals (Table 4; e.g., Patterson et al. 1999; Gillanders and Kingsford 2000; Rooker et al. 2001). These results suggest that it will not be easy to predict whether there will be interannual variability in elemental fingerprints, but it should not be assumed that there would be no interannual variability.

A number of studies have found significant variation within a year, although the main elements examined in most of these studies were Sr, Na, K, and S (Table 4). In addition, most studies have only examined one site; therefore, it is unknown if some sites may show variation in otolith chemistry over time while others show little or no variation in otolith chemistry. Of the trace elements examined in the present study, Mn has been found to show temporal variability in otolith chemistry over time periods of less than a year (2–6 months), whereas Ba showed significant variability over a 2-month period in one study, but not over a 6-month period in another study (Thorrold et al. 1998*b*; Thorrold and Shuttleworth 2000). No studies have examined variability of Li in otoliths within a year.

The elemental fingerprints allowed some estuaries to be individually distinguished in each year (e.g., Wallis Lake). However, other estuaries could only be distinguished in some years (e.g., Lake Illawarra, Lake Macquarie, Eden), whereas others showed overlap with some estuaries in all years (e.g., estuaries in the vicinity of Sydney). Although there was some overlap in elemental fingerprints among some estuaries, groups of estuaries could usually be distinguished. Other studies have also found variation in elemental fingerprints among different geographic areas (e.g., Campana et al. 1994, 1995), including among estuaries (Thorrold et al. 1998*a*; Gillanders and Kingsford 2000) and between estuaries and coastal reefs (Gillanders and Kingsford 1996). Such differences are frequently used to infer differences in stock structure, but among-estuary and estuary–coastal reef differences have also been used as natural tags of area of origin for juveniles. For each year of sampling, the current data suggest that there were variations in elemental fingerprints in otoliths of snapper that allowed separation of a number of estuaries. Hence, these differences provide a natural tag or area of origin for snapper.

The elemental composition of otoliths of juvenile snapper showed significant spatial and temporal variation, such that it was possible to confound spatial differences with temporal differences. This does not prevent determination of recruitment estuaries of adult fish, but it does suggest that some caution is required when tracking adults back to natal and recruitment regions. Possible confounding of spatial differences with temporal differences may not necessarily be the case for all regions; for example, elemental fingerprints of juvenile fish from Port Phillip Bay (Victoria, Australia) are consistently different from other estuaries, at least over a two-year period (P. Hamer, Marine and Freshwater Resources Institute, Queenscliff, Victoria 3225, Australia, personal communication).

Many past studies have only sampled at one time or sampled different locations at different times and have ignored possible temporal effects. In regions where there is little variation in rainfall and freshwater input to coastal waters, there may be little variation in elemental fingerprints among years, but this needs to be assessed empirically. Sampling different locations in different years may confound spatial differences with temporal differences. For example, if Lake Macquarie had been sampled in 1999–2000 and Lake Illawarra had been sampled in 2000–2001, it would be concluded that there were no significant differences between the two estuaries in terms of elemental fingerprints, whereas if samples were taken from both estuaries in 1999–2000 significant differences would have been found. Thus, it is necessary to sample all locations at similar times.

Despite differences in elemental composition of otoliths among estuaries and over time the mechanisms generating these differences are not well understood. Estuaries show differences in land use varying from intense urban and industrial (e.g., Port Jackson, Botany Bay) to low intensity rural activities (e.g., Port Stephens, Wallis Lake), which may provide a range of potential levels of anthropogenic input that could influence the concentration of elements in the water. There is also likely to be natural variation among estuaries due to different catchments, which may have varying levels of rainfall, rock, soil, and vegetation types. Besides factors influencing trace elements in the water, temperature and salinity are also likely to vary among estuaries. For example, temperatures in December and January 1998–1999 were approximately 4°C lower in Eden than in Botany Bay waters (B.M. Gillanders, unpublished data). Elements in the

© 2002 NRC Canada

Fig. 4. Plots summarizing variation in elemental fingerprints of otoliths of juvenile snapper (*Pagrus auratus*) collected from six of the 15 estuaries in each of three years. (*a*) All six estuaries and years are shown with arrows representing the change from one year to the next for each individual estuary; (*b*) and (*c*) are the same plots as that shown in (*a*) with four and two estuaries shown, respectively, to clarify the changes over time for each individual estuary; and (*d*) is the same plot as that shown in (*a*) but distinguishing among years, rather than among estuaries. The estuaries were Wallis Lake (WL), Port Stephens (PS), Lake Macquarie (LM), Botany Bay (BB), Lake Illawarra (LI), and Wagonga Inlet (WI). Ellipses represent 95% confidence regions around means for each estuary for each canonical variate. In (*d*), solid ellipses represent 1998–1999, shaded ellipses 1999–2000, and open ellipses 2000–2001 recruitment seasons.

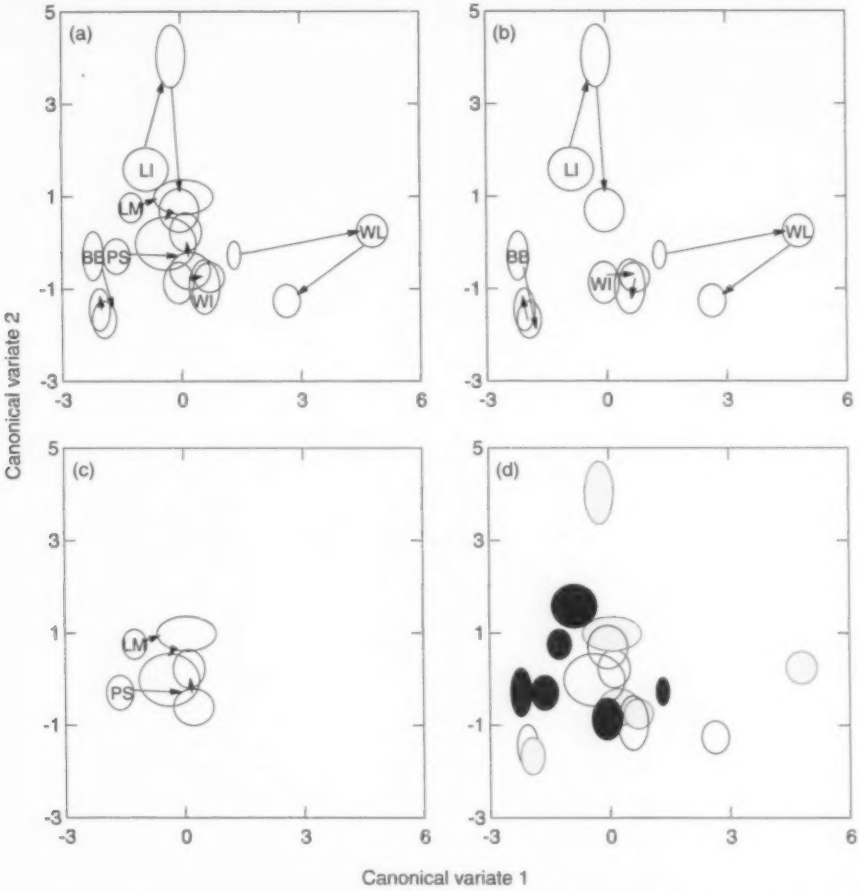

water, temperature, and salinity may also vary not only among estuaries, but also among years. Past studies have shown that these factors can influence microchemistry of otoliths (e.g., Chesney et al. 1998; Bath et al. 2000; Milton and Chenery 2001).

In addition to environmental factors influencing otolith chemistry, a range of other factors (e.g., diet, growth rates, and ontogenetic and physiological effects) may also influence otolith composition in some species (e.g., Sadovy and Severin 1992; Fowler et al. 1995; Limburg 1995). Differences in mean size-at-age of adult snapper have been observed along the coast of NSW (Ferrell and Sumpton 1997) and a positive relationship was found between sea surface temperature and growth of juvenile snapper in New Zealand (Francis 1994). Since sea surface temperature varies among estuaries along the coast of NSW, differences in rates of growth may be found among estuaries. In addition, temperature is likely to have a direct effect on some elements (e.g., Sr, Ba). Although differences in growth rates and diets among estuaries cannot be discounted as possible determinants of otolith composition in snapper, ontogenetic and physiological effects were minimized by analysing otoliths of juvenile fish (0+ years) of similar sizes. In addition, a recent study found that water chemistry had a greater effect on otolith chemistry than did similar levels of trace elements within the diet (Milton and Chenery 2001).

Significant temporal variation in elemental fingerprints among individual estuaries suggests that either the water chemistry (e.g., elements in the water, temperature, and salinity) or ontogenetic and physiological effects may vary among years. I suggest that water chemistry is most likely to vary among years because all fish used in the current study were immature and of a similar size. Juvenile snapper of the size used in the current study would be approximately three to four months old based on previous studies of otolith microstructure (e.g., Bell et al. 1991); therefore, different co-

© 2002 NRC Canada

Table 4. Review of studies examining temporal variation in elemental chemistry of otoliths.

Temporal scale	Elements analysed	Differences	Source
Within years			
2 collections within 6 months at 1 site	Mn, Sr, Ba	Ba and Sr not significant; Mn significant	Thorrold and Shuttleworth (2000)
Aug. and Oct. collections in 1 year	Mg, K, Mn, Sr, Ba	Significant differences among sampling occasions	Thorrold et al. (1998*b*)
4 collections at 3-month intervals over 1 year at 1 site	Mg, Na, P, S, Sr	Seasonal variation observed in canonical variate plot	Edmonds et al. (1995)
8 collections over ~1 year from 1 site	Sr, Na, K, S	Significant seasonal variation for all elements ratioed to Ca	Kalish (1991)
Monthly collections over 1 year at 1 site	Sr, Na, K, S	Significant variation during the year for all elements	Kalish (1989)
Among years			
3 collections over 3 years at 1 site	Li, Mg, Mn, Sr, Ba	Mg, Mn, and Ba showed significant interannual trends	Rooker et al. (2001)
2 collections pooled per year over 2–3 years at 4 sites	Ba, Li, Mg, Mn, Sr	Relatively similar	Campana et al. (2000)
~5 collections over 13 years at 4 areas	Ba, Li, Mg, Sr	Concentrations differed relatively little over 2-year intervals, more substantive differences noted for some elements and some locations after 4- to 13-year intervals	Campana et al. (2000)
Sampled twice ~1 year apart; 2–5 sites in each of 7 estuaries	Ba, Mn, Sr	Significant temporal effects for some or all estuaries	Gillanders and Kingsford (2000)
2 collections in summer of each of 2 years at one site	Zn, Sr, Ba, Pb	Significant differences for Ba	Patterson et al. (1999)
2 collections ~1 year apart; 2 sites sampled at each of 6 locations	Al, Ba, Co, Cu, Hg, Mg, Mn, Pb, Sr, Rb, Ti, Zn	Significant temporal differences for Ba and Mn; results for other elements not reported	Dove and Kingsford (1998)
2 collections ~1 year apart at 5 sites	Li, Na, Mg, Cu, Zn, Sr, Ba	Significant difference between years for all elements except Na	Milton et al. (1997)
2 collections separated by about 2 years at 3 sites	Mg, Na, P, S, Sr, K	S and P showed temporal variation; no statistical analyses for any elements	Edmonds et al. (1995)
3 collections over 3 years	Mg, Na, P, S, Sr	Temporal variation observed in CV plot but elements contributing to differences not mentioned	Edmonds et al. (1995)
2 collections ~2 years apart at 3 sites	B, K, Mg, Mn, Na, Sr	Temporal variation observed in CV plot but elements contributing to differences not mentioned	Edmonds et al. (1992)

Note: Details of the sampling design, elements analysed, and differences over time are given. Within each temporal scale (within years and among years), the table is ordered by year of reference. CV, canonical variate.

horts have been sampled each year. Although fish were collected at similar times (summer) each year, differences in water chemistry may occur among years. Rainfall and subsequent freshwater input to estuaries may vary substantially each year, especially along the coast of NSW. For example, rainfall to the different coastal meteorological regions varied two- to three-fold for the Nov.–Feb. period of the years 1997–1998 to 2000–2001. The northern regions including the Sydney metropolitan region had the highest rainfall in the 1999–2000 period, whereas the southern regions had the highest rainfall in 1998–1999 (South Coast) and in 2000–2001 (Lake Illawarra), suggesting that freshwater effects may vary not only among catchments but also among years. In addition, all catchments did not always have the highest rainfall in the same year.

When determining the recruitment estuaries of adult fish, significant spatial and temporal variation in elemental fingerprints needs to be considered. A library of elemental fingerprints needs to be built up over time for each estuary rather than a single year-class of juveniles being used as the elemental fingerprint for a number of year-classes of adults (as was done in Gillanders and Kingsford 1996). The recruitment estuary of adult fish would then need to be determined based on elemental fingerprints of juveniles from the year-class in which the adults of interest recruited to the estuaries. A region of the otolith similar to that analysed for the juvenile should also be analysed for the adult fish. In addition, it may also be necessary to group some estuaries that show overlap in elemental fingerprints of juveniles before classification or maximum likelihood approaches are used to estimate composition. The grouping of estuaries may not necessarily need to be the same across years, but could be determined from confidence intervals around different estuaries for canonical variate plots.

Numbers of adult fish originating from different estuaries could then be determined for different year-classes of adults.

© 2002 NRC Canada

Thus, spatial models of population replenishment could be developed and patterns of movement of different year-classes established (e.g., Allison et al. 1998). Spatial models of population replenishment would help determine (*i*) whether adults on reefs outside estuaries have come from the estuary closest to them with little transfer from other estuaries or (*ii*) whether the predominant movement is from estuaries close by with few fish remaining on the closest reef to their natal estuary and some moving long distances or (*iii*) whether one estuary essentially sustains coastal reefs of all other estuaries.

Variability in elemental fingerprints over time may also have major implications for determining stock mixing when whole otoliths are used because temporal variability implies that the marker may not remain stable between characterization of stocks and mixing of stocks (see also Campana et al. 2000). Thus, it will be necessary to consider the time interval between when stocks are characterized and when mixed stocks are sampled for estimates of composition.

Although the mechanisms generating spatial and temporal differences in otolith chemistry are not well understood, spatial differences in otolith chemistry suggest that the elemental fingerprints of fish from different estuaries do provide a natural tag of their juvenile habitat. The natural tag for individual estuaries does however vary over time and such temporal differences need to be considered when determining recruitment estuaries of adult fish. Results from models of population replenishment would allow estimates of connectivity between estuaries and coastal regions to be made and could have major implications for fisheries management and conservation of estuarine habitats.

Acknowledgements

I thank Julian Hughes for assisting with collections of fish and preparation of samples and Robert McQuilty (Royal Prince Alfred hospital) for use of the ICP-MS. The study was conducted while the author held Australian Research Council fellowships (APD and QEII) and was funded by the Fisheries Research Development Corporation (No. 98/139).

References

Allison, G.W., Lubchenco, J., and Carr, M.H. 1998. Marine reserves are necessary but not sufficient for marine conservation. Ecol. Appl. **8**: S79–S92.

Anderson, M.J. 2001*a*. A new method for non-parametric multivariate analysis of variance in ecology. Aust. Ecol. **26**: 32–46.

Anderson, M.J. 2001*b*. Permutation tests for univariate or multivariate analysis of variance and regression. Can. J. Fish. Aquat. Sci. **58**: 626–639.

Anderson, M.J., and Legendre, P. 1999. An empirical comparison of permutation methods for tests of partial regression coefficients in a linear model. J. Stat. Comput. Sim. **62**: 271–303.

Bath, G.E., Thorrold, S.R., Jones, C.M., Campana, S.E., McLaren, J.W., and Lam, J.W.H. 2000. Strontium and barium uptake in aragonitic otoliths of marine fish. Geochim. Cosmochim. Acta, **64**: 1705–1714.

Bell, J.D., and Worthington, D.G. 1993. Links between estuaries and coastal rocky reefs in the lives of fishes from south-eastern Australia. *In* Proceedings of the Second International Temperate Reef Symposium. *Edited by* C.B. Battershill, D.R. Schiel, G.P. Jones, R.G. Creese, and A.B. MacDiarmid. NIWA Marine, Wellington, New Zealand. pp. 85–91.

Bell, J.D., Quartararo, N., and Henry, G.W. 1991. Growth of snapper, *Pagrus auratus*, from south-eastern Australia. N.Z. J. Mar. Freshw. Res. **25**: 117–121.

Campana, S.E. 1999. Chemistry and composition of fish otoliths: pathways, mechanisms and applications. Mar. Ecol. Prog. Ser. **188**: 263–297.

Campana, S.E., and Neilson, J.D. 1985. Microstructure of fish otoliths. Can. J. Fish. Aquat. Sci. **42**: 1014–1032.

Campana, S.E., Fowler, A.J., and Jones, C.M. 1994. Otolith elemental fingerprinting for stock discrimination of Atlantic cod (*Gadus morhua*) using laser ablation ICPMS. Can. J. Fish. Aquat. Sci. **51**: 1942–1950.

Campana, S.E., Gagne, J.A., and McLaren, J.W. 1995. Elemental fingerprinting of fish otoliths using ID-ICPMS. Mar. Ecol. Prog. Ser. **122**: 115–120.

Campana, S.E., Chouinard, G.A., Hanson, J.M., Frechet, A., and Brattey, J. 2000. Otolith elemental fingerprints as biological tracers of fish stocks. Fish. Res. **46**: 343–357.

Chesney, E.J., McKee, B.M., Blanchard, T., and Chan, L.-H. 1998. Chemistry of otoliths from juvenile menhaden *Brevoortia patronus*: evaluating strontium, strontium:calcium and strontium isotope ratios as environmental indicators. Mar. Ecol. Prog. Ser. **171**: 261–273.

Dove, S.G., and Kingsford, M.J. 1998. Use of otoliths and eye lenses for measuring trace-metal incorporation in fishes: a biogeographic study. Mar. Biol. (Berlin), **130**: 377–387.

Edmonds, J.S., Lenanton, R.C.J., Caputi, N., and Morita, M. 1992. Trace elements in the otoliths of yellow-eye mullet (*Aldrichetta forsteri*) as an aid to stock identification. Fish. Res. **13**: 39–51.

Edmonds, J.S., Caputi, N., Moran, M.J., Fletcher, W.J., and Morita, M. 1995. Population discrimination by variation in concentrations of minor and trace elements in sagittae of two Western Australian teleosts. *In* Recent developments in fish otolith research. *Edited by* D.H. Secor, J.M. Dean, and S.E. Campana. University of South Carolina Press, Columbia, S.C. pp. 655–670.

Ferrell, D.J., and Sumpton, W. 1997. Assessment of the fishery for snapper (*Pagrus auratus*) in Queensland and New South Wales. Fish. Res. Develop. Corp. Rep. No. 93/074. *Available from* National Library of Australia, Canberra ACT 2600, Australia.

Fowler, A.J., Campana, S.E., Jones, C.M., and Thorrold, S.R. 1995. Experimental assessment of the effect of temperature and salinity on elemental composition of otoliths using solution-based ICPMS. Can. J. Fish. Aquat. Sci. **52**: 1421–1430.

Francis, M.P. 1994. Growth of juvenile snapper, *Pagrus auratus*. N.Z. J. Mar. Freshw. Res. **28**: 201–218.

Gillanders, B.M., and Kingsford, M.J. 1996. Elements in otoliths may elucidate the contribution of estuarine recruitment to sustaining coastal reef populations of a temperate reef fish. Mar. Ecol. Prog. Ser. **141**: 13–20.

Gillanders, B.M., and Kingsford, M.J. 2000. Elemental fingerprints of otoliths of fish may distinguish estuarine 'nursery' habitats. Mar. Ecol. Prog. Ser. **201**: 273–286.

Kalish, J.M. 1989. Otolith microchemistry: validation of the effects of physiology, age and environment on otolith composition. J. Exp. Mar. Biol. Ecol. **132**: 151–178.

Kalish, J.M. 1991. Determinants of otolith chemistry: seasonal variation in the composition of blood plasma, endolymph and otoliths of bearded rock cod *Pseudophycis barbatus*. Mar. Ecol. Prog. Ser. **74**: 137–159.

Limburg, K.E. 1995. Otolith strontium traces environmental his-

© 2002 NRC Canada

tory of subyearling American shad *Alosa sapidissima*. Mar. Ecol. Prog. Ser. **119**: 25–35.

Manly, B.F.J. 1997. Randomization, bootstrap and Monte Carlo methods in biology. Chapman and Hall, London.

McGlennon, D., Jones, G.K., Baker, J., Jackson, W.B., and Kinloch, M.A. 2000. Ageing, catch-at-age and relative year-class strength for snapper (*Pagrus auratus*) in northern Spencer Gulf, South Australia. Mar. Freshw. Res. **51**: 669–677.

Milton, D.A., and Chenery, S.P. 2001. Sources and uptake of trace metals in otoliths of juvenile barramundi (*Lates calcarifer*). J. Exp. Mar. Biol. Ecol. **264**: 47–65.

Milton, D.A., Chenery, S.R., Farmer, M.J., and Blaber, S.J.M. 1997. Identifying the spawning estuaries of the tropical shad, terubok *Tenualosa toli*, using otolith microchemistry. Mar. Ecol. Prog. Ser. **153**: 283–291.

Patterson, H.M., Thorrold, S.R., and Shenker, J.M. 1999. Analysis of otolith chemistry in Nassau grouper (*Epinephelus striatus*) from the Bahamas and Belize using solution-based ICP-MS. Coral Reefs, **18**: 171–178.

Rooker, J.R., Secor, D.H., Zdanowicz, V.S., and Itoh, T. 2001. Discrimination of northern bluefin tuna from nursery areas in the Pacific ocean using otolith chemistry. Mar. Ecol. Prog. Ser. **218**: 275–282.

Sadovy, Y., and Severin, K.P. 1992. Trace elements in biogenic aragonite: correlation of body growth rate and strontium levels in the otoliths of the white grunt, *Haemulon plumieri* (Pisces: Haemulidae). Bull. Mar. Sci. **50**: 237–257.

Thorrold, S.R., and Shuttleworth, S. 2000. In situ analysis of trace elements and isotope ratios in fish otoliths using laser ablation sector field inductively coupled plasma mass spectrometry. Can. J. Fish. Aquat. Sci. **57**: 1–11.

Thorrold, S.R., Jones, C.M., Swart, P.K., and Targett, T.E. 1998*a*. Accurate classification of juvenile weakfish *Cynoscion regalis* to estuarine nursery areas based on chemical signatures in otoliths. Mar. Ecol. Prog. Ser. **173**: 253–265.

Thorrold, S.R., Jones, C.M., Campana, S.E., McLaren, J.W., and Lam, J.W.H. 1998*b*. Trace element signatures in otoliths record natal river of juvenile American shad (*Alosa sapidissima*). Limnol. Oceanogr. **43**: 1826–1835.

Thorrold, S.R., Latkoczy, C., Swart, P.K., and Jones, C.M. 2001. Natal homing in a marine fish metapopulation. Science (Washington, D.C.), **291**: 297–299.

Underwood, A.J. 1997. Experiments in ecology. Their logical design and interpretation using analysis of variance. Cambridge University Press, Cambridge.

© 2002 NRC Canada

Comparative growth and feeding in zebra and quagga mussels (*Dreissena polymorpha* and *Dreissena bugensis*): implications for North American lakes

Brad S. Baldwin, Marilyn S. Mayer, Jeffrey Dayton, Nancy Pau, Johanna Mendilla, Maura Sullivan, Aaron Moore, Aye Ma, and Edward L. Mills

Abstract: In laboratory experiments, quagga mussels (*Dreissena bugensis*) survived as well as zebra mussels (*Dreissena polymorpha*) and equaled or exceeded their growth rate (–3 to 242% change in wet mass) when reared at 6 or 23°C and fed natural seston or *Chlamydomonas* at food levels ranging from 0.05–7.4 $\mu g \cdot L^{-1}$ chlorophyll *a* (chl *a*). Superior growth of quagga mussels was most pronounced at low food levels. We found no significant differences in per capita clearance rates (CR), functional responses, or feeding behavior between zebra and quagga mussels fed *Chlamydomonas*, *Nannochloris*, or mixed suspensions of *Nannochloris* and clay. Per capita CR ranged from 0.018 to 0.402 $L \cdot mussel^{-1} \cdot h^{-1}$ for zebra mussels and from 0.010 to 0.407 $L \cdot mussel^{-1} \cdot h^{-1}$ for quagga mussels. Because quagga mussels had more biomass per unit shell length, we found lower biomass-specific CR for quagga mussels. When fed natural seston, zebra and quagga mussels could selectively reject inorganic material and at the lowest seston level the assimilation efficiency of quagga mussels (81%) was significantly higher than that of zebra mussels (63%). Our experiments suggest that quagga mussels can survive, grow, and feed as well or better than zebra mussels in epilimnetic waters with either low or high productivity.

Résumé : En laboratoire, des moules quagga (*Dreissena bugensis*) gardées à 6 ou 23°C et nourries de seston naturel ou de *Chlamydomonas* en concentrations de 0,05–7,4 $\mu g \cdot L^{-1}$ chlorophylle *a* (chl *a*) survivent aussi bien que les moules zébrées (*Dreissena polymorpha*) et leur taux de croissance est semblable ou supérieur (–3 à 242 % de changement dans la masse humide). La croissance supérieure des moules quagga est surtout évidente aux concentrations faibles de nourriture. Il n'y a pas de différences individuelles significatives dans les taux d'épuration (CR), les réponses fonctionnelles ou les taux d'alimentation entre les moules zébrées et les moules quagga nourries de *Chlamydomonas*, de *Nannochloris* ou de suspensions mixtes de *Nannochloris* et d'argile. Les taux individuels d'épuration (CR) varient de 0,018 à 0,402 $L \cdot moule^{-1} \cdot h^{-1}$ chez les moules zébrées et de 0,010 à 0,407 $L \cdot moule^{-1} \cdot h^{-1}$ chez les moules quagga. Parce que la biomasse par unité de longueur de coquille est plus grande chez les moules quagga, celles-ci ont un CR relatif à la biomasse plus petit. Les moules quagga et les moules zébrées, nourries de seston naturel, savent rejeter de façon sélective les particules inorganiques et, à la concentration la plus faible de seston, l'efficacité de l'assimilation des moules quagga (81 %) est significativement plus élevée que celle des moules zébrés (63 %). Il semble donc que les moules quagga puissent survivre, croître et s'alimenter aussi bien, sinon mieux, que les moules zébrées dans les eaux de l'épilimnion de forte ou de faible productivité.

[Traduit par la Rédaction]

Introduction

The quagga mussel (*Dreissena bugensis*) is the second dreissenid mussel (along with its predecessor, the zebra mussel, *Dreissena polymorpha*) to invade, colonize, and impact North American freshwater ecosystems since 1986. In contrast to zebra mussels, quagga mussels were confined primarily to deepwater habitats of the lower Great Lakes region (i.e., Lake Erie, Lake Ontario, and the St. Lawrence River). However, quagga mussel populations now dominate many of the dreissenid assemblages throughout the profundal and littoral zones of these waters (e.g., Mitchell et al. 1996; Dermott and Kerec 1997; Mills et al. 1999). Such trends in natural populations confirm results from earlier field transplant experiments by MacIsaac (1994), which demonstrated the ability of transplanted quagga mussels to survive well in warm, littoral zone habitats of Lake Erie. Indeed, these North American findings agree in part with observations of Ukrainian dreissenid populations, where littoral habitats once dominated by zebra mussels have been largely replaced

Received 18 July 2001. Accepted 31 March 2002. Published on the NRC Research Press Web site at http://cjfas.nrc.ca on 18 May 2002.
J16454

B.S. Baldwin,[1] M.S. Mayer, M. Sullivan, A. Moore, and A. Ma. Biology Department, St. Lawrence University, Canton, NY 13617, U.S.A.
J. Dayton, N. Pau, J. Mendilla, and E.L. Mills. Department of Natural Resources, Cornell Biological Field Station, 900 Shackelton Point Road, Bridgeport, NY 13030, U.S.A.

[1]Corresponding author (e-mail: bbal@stlawu.edu).

 DOI: 10.1139/F02-043 © 2002 NRC Canada

by quagga mussels (Mills et al. 1996). If similar population shifts occur in Great Lake habitats, and if quagga mussels spread farther into inland lakes and rivers, it raises questions of how quagga mussels might intensify the ecological impacts of dreissenids and whether quagga mussels could become the dominant dreissenid in North America.

Quagga mussels can colonize productive littoral zones of the Great Lakes, but the extent and pace of infestation has been much lower than that of zebra mussels, and to date, there is limited evidence that quagga mussels can, like the zebra mussel, spread to other inland waters (Sea Grant National Aquatic Nuisance Species Clearinghouse 2001). Such inconsistencies may be partly explained by temporal and spatial differences in their introduction and dispersal (see MacIsaac 1994); unresolved biological differences among morphotypes of *Dreissena bugensis* (see Claxton et al. 1998), and (or) improved efforts to restrict human-mediated spread. However, they may also be due to fundamental biological differences of zebra and quagga mussels that can ultimately lead to different ecological impacts.

Profound differences do exist for other sympatric species of mussels like *Mytilus* spp. (e.g., Bayne 1976; Gardner 1994), and similar lines of evidence are suggestive for zebra and quagga mussels. Foremost is the ability of quagga mussels to inhabit and even proliferate in both profundal (e.g., North America, Mills et al. 1999) and littoral zones (e.g., Ukraine, Mills et al. 1996), which indicates a tolerance to different temperature and food regimes than those used by zebra mussels. Indeed, quagga mussels can settle, grow, and spawn over a greater depth and temperature range (Roe and MacIsaac 1997; Claxton and Mackie 1998; Martel et al. 2001) and they may also filter and grow on a wider range of food types and concentrations. Quagga mussels, especially those from profundal zones, may subsist on lower levels of phytoplankton and other food sources (detritus, heterotrophic bacteria and protists, dissolved organic compounds) known to be used by zebra mussels (e.g., Cotner et al. 1995; Lavrentyev et al. 1995; Roditi et al. 2000). If true, not only might quagga mussels feed and grow more efficiently than zebra mussels, they may support large populations on the declining phytoplankton stocks that have been observed in several colonized lakes (e.g., Fahnenstiel et al. 1995; Makarewicz et al. 1999; Idrisi et al. 2001). In fact, this may be one of the reasons why quagga mussels have continued to increase in abundance following initial invasions by zebra mussels (Mills et al. 1996, 1999; Negley et al. 2001). As yet there are no clear distinctions between the feeding rates of zebra and quagga mussels (Zolotareva et al. 1978; Ackerman 1999), but few food types or concentrations have been examined. And while experimental studies have shown great overlap in the growth of zebra and quagga mussels (MacIsaac 1994; Thorp et al. 1998), natural populations of quagga mussels tend to attain longer shell lengths than sympatric zebra mussels (e.g., Mills et al. 1999; Bially and MacIsaac 2000; Negley et al. 2001) indicating greater longevity and (or) growth rates than zebra mussels.

Dreissenid populations continue to grow in the lower Great Lakes (e.g., Dermott and Kerec 1997; Mills et al. 1999; Lozano et al. 2001) and quagga mussels may exert the most widespread impact today in these systems because of their dominance in both profundal and littoral habitats (Mills et al. 1999). However, because of the current paucity of information on the growth, survival, and feeding biology of quagga mussels there remain open questions as to how growing populations of quagga mussels will intensify dreissenid impacts, whether they can spread to and impact inland waters, and whether they represent a substantially different threat to North American ecosystems. We conducted laboratory studies to compare the growth, survival, and feeding biology of quagga and zebra mussels to ascertain if quagga mussels have the potential to increase their populations and intensify dreissenid impacts in productive littoral zone habitats of the Great Lakes or inland lakes. We hypothesized that quagga mussels could survive, grow, and feed at higher rates than zebra mussels under warm or cold temperatures with high or low food conditions.

Materials and methods

Experimental animals

Zebra and quagga mussels were collected from the St. Lawrence River (Cape Vincent, N.Y. and Morristown, N.Y.), Lake Ontario (Oswego, N.Y.), and Lake Erie (Dunkirk, N.Y.) from June and July of 1997–1999. Zebra mussels were also collected from Oneida Lake (Shackelton Point, near Bridgeport, N.Y.) during this period (quagga mussels not present). Mussels were collected using bottom dredges, benthic trawls, or by skin divers. Unless noted otherwise, animals were collected from littoral zone habitats <15 m in depth. Animals were acclimated in the lab to experimental conditions for approximately two weeks before use. Experiments were conducted at St. Lawrence University (SLU) and at the Cornell Biological Field Station (CBFS) located on Oneida Lake. Experiments conducted at SLU used water collected from the St. Lawrence River and those conducted at CBFS used water from Oneida Lake or from Onondaga Lake (Syracuse, N.Y.). In some experiments, mussels were fed natural seston, whereas in other experiments, natural waters were filtered (Gelman A/E; nominal pore size ~1 µm) before use (FLW: filtered lake water) and cultured algae was added for food (*Chlamydomonas reinhardtii* or *Nannochloris* sp.; cultures 90 and LB2291, respectively, from the University of Texas Culture Collection of Algae). Algal stocks were cultured at 18–22°C in aerated 2-L flasks or 15-L carboys (with f/2 medium; Guillard 1975) that were placed near constant fluorescent light and algae were harvested in early stationary phase growth.

Experimental design

We conducted experiments to compare growth, survival, food clearance, and food processing of quagga and zebra mussels. To compare survival and growth of quagga and zebra mussels under conditions simulating profundal and littoral zones of lakes, we conducted three laboratory experiments with animals reared under low or high temperatures (6 and 23°C) and fed low or high levels of food (lake seston or *Chlamydomonas*). We also compared the feeding biology of zebra and quagga mussels in an effort to explain differences in mussel growth and to assess their potential impacts on pelagic systems. Here, a series of experiments were run using natural seston and cultured algae to evaluate their functional response, their reaction to inorganic loads,

© 2002 NRC Canada

their diurnal activity, and their food selection and assimilation. To determine whether quagga mussels tolerate food-limiting conditions better than zebra mussels we compared weight loss and survival of mussels held without food.

Growth experiments

Experimental treatments

We conducted growth experiments using juvenile quagga and zebra mussels 6–9 mm in shell length. Two experiments were conducted in the summer of 1997. In the first, mussels from Lake Ontario were reared at CBFS under conditions simulating the littoral zone of a warm, productive lake. For this, mussels were held at 23°C (±2°C) and were fed seston collected from Onondaga Lake (Syracuse, N.Y.), a site chosen for its high levels of phytoplankton. Individual mussels were reared for 38 days in aerated beakers containing 425 mL of lake seston, which was freshly collected and changed every 2 days. To test the effects of food quantity we fed mussels either undiluted seston (ambient or 100% level) or seston diluted with filtered (pore size 1 μm) Onondaga Lake water to 75, 50, and 25% of ambient levels. For each treatment, 20 individual mussels of each species were tested. The chlorophyll *a* (chl *a*) level of Onondaga Lake seston was measured every 2–3 days on Whatman 934-AH filters (nominal pore size ~1.5 μm) according to Strickland and Parsons (1972). Ambient chl *a* varied from about 1 to 20 $\mu g \cdot L^{-1}$ during the experiment (mean of 4.4 $\mu g \cdot L^{-1}$ ± 1 standard error, SE, of 2.5 $\mu g \cdot L^{-1}$).

In the second 1997 experiment, St. Lawrence River mussels were reared for 43 days at SLU under conditions simulating both the warm littoral zone and the cold profundal zone of a lake during periods of high and low food availability. This experiment used a factorial design with rearing temperatures at 23 or 6°C (±1°C) and food (filtered St. Lawrence River water with *Chlamydomonas*) levels at high (3×10^7 cells$\cdot L^{-1}$) or low (3×10^5 cells$\cdot L^{-1}$) concentrations. Based on chl *a* measurements (as described above for Onondaga Lake samples), these cell concentrations correspond to 5.3 and 0.05 $\mu g \cdot L^{-1}$, respectively. Rearing procedures were conducted as in the first experiment and each treatment tested 20 individual mussels of each species.

A third growth experiment was conducted in the summer of 1998 using seston from Oneida Lake, which has a high but declining phytoplankton biomass owing to filtration by zebra mussels (Idrisi et al. 2001). Beyond testing growth and survival of zebra and quagga mussels in another warm, productive lake we also wanted to evaluate their potential to compete for shared plankton resources. Experiments used three mussel pair combinations (zebra mussels (ZZ), quagga mussels (QQ), and mixed pairs (ZQ)) and two food levels (100 and 25% ambient seston). We used animals collected in early June; specifically, quagga mussels from eastern Lake Erie (zebra mussels were rare or nonexistent from this location) and zebra mussels from Oneida Lake (which has no quagga population). These mussels (two animals, each with a unique permanent ink mark) were reared for 52 days at CBFS (23 ± 1°C) in large containers (4-L pails) and were fed daily with fresh Oneida Lake seston. For each mussel combination, 10 buckets received a high food treatment and 10 received a low food treatment. The high food treatment consisted of seston filtered through an 85-μm screen to remove most zooplankton and large phytoplankton. This treatment was considered the 100% food level. Additional portions of this 85-μm screened water were diluted with filtered (pore size 1 μm) Oneida Lake water to make the 25% food treatment. Rearing procedures were conducted as in the first experiment. Dead animals were replaced with a mussel of the same species and size so as to continue the experimental test for the living mussel. Data for replacement mussels were not included in any analyses.

In this experiment, mean ± 1 SE chl *a* levels were 1.5 ± 0.3 $\mu g \cdot L^{-1}$ for the 25% treatment (range 0.2–7.9 $\mu g \cdot L^{-1}$) compared with 7.4 ± 0.9 $\mu g \cdot L^{-1}$ for the 100% treatment (range 1.2–17.8 $\mu g \cdot L^{-1}$). The dry mass (DM) of Oneida Lake seston was determined by filtering water samples of known volume onto preweighed 25-mm filters (Gelman A/E), drying them at 60°C for a minimum of 24 h, and reweighing. The mean ± 1 SE DM for the 25% treatment was 1.3 ± 0.4 $mg \cdot L^{-1}$ (range 0.7–2.6 $mg \cdot L^{-1}$) compared with that of the 100% treatment, which was 6.8 ± 1.6 $mg \cdot L^{-1}$ (range 2.8–9.2 $mg \cdot L^{-1}$).

Growth measurements

For all three experiments, mussel growth was measured weekly and mortality (dead mussels gaped and did not respond to touch) was assessed at every water change. To accurately measure total mussel growth (3-dimensional changes in shell and tissue) we measured their change in wet mass (WM; live soft tissue + shell mass). Here, initial, final, and weekly measurements were taken for each mussel by drying live animals externally with a tissue and weighing them on an OHAUS balance (model 160D) to the nearest 0.1 mg. We report mussel growth both as percentage change in WM (100 × (final mass – initial mass)/initial mass) and as the instantaneous rate of mass change (which scales for exponential change in mass), calculated according to the following formula:

$$(1) \qquad G = 100(\ln W_2 - \ln W_1)/T$$

where G is the instantaneous rate of mass change (day^{-1}), W_2 is the final mass, W_1 is the initial mass, and T is time in days (MacIsaac 1994). Although our G values do not allow comparisons with published studies reporting rates of mass change as $mass \cdot day^{-1}$, we feel that they are the most appropriate way to compare the growth of our animals among our experimental treatments. For general comparisons with other studies, we also measured the shell length (SL; maximum distance along the anterior–posterior axis) of each mussel to the nearest 0.1 mm at the beginning and end of each experiment using vernier calipers. No data analysis was conducted on SL.

Estimates of organic mass

Based on preliminary observations and measurements, it appeared that quagga mussels had more organic mass (OM; equivalent to "soft tissue dry mass" or "biomass") per unit WM than zebra mussels. To estimate how changes in WM of experimental animals related to likely changes in their OM, we established OM–WM relationships on separate groups of freshly collected mussels from Lake Ontario, the St. Lawrence River, Oneida Lake, and eastern Lake Erie. Here, mus-

© 2002 NRC Canada

sel OM was given as mussel DM (entire animals weighed after being dried at 60°C for 24 h) minus mussel DM after ashing (entire animals reweighed after being ashed at 550°C for 5 h). We also measured OM for a set of quagga mussels used in our clearance rate – body size experiments (see below).

Food clearance

Functional response

To compare how zebra and quagga mussels fed in response to different types and levels of food, we measured their clearance rates over increasing concentrations of cultured algae. (Mussel ingestion rates were not estimated because some of the food they removed from suspension was expelled as pseudofeces in many experiments.) One set of experiments was conducted using mussels held in static feeding chambers containing *Chlamydomonas* (size range of cells 4–8 µm). Additional, more exhaustive experiments were conducted using a flow-through apparatus containing *Nannochloris* (3–5 µm).

The first set of experiments used large zebra and quagga mussels (20–25 mm SL) from the St. Lawrence River that were acclimated for two weeks at SLU at 20 ± 2°C in filtered (pore size 1 µm) river water amended with about 1×10^8 cells·L^{-1} of *Chlamydomonas*. Filtered river water and *Chlamydomonas* were renewed every 24–48 h. For experiments, individual animals (10 per food treatment) were placed in beakers with 250 mL of filtered (pore size 1 µm) river water. After 1 h, *Chlamydomonas* was added to beakers to achieve nominal concentrations of 1×10^7, 5×10^7, or 1×10^8 cells·L^{-1}. Three control beakers (no mussels) were also set up for each food treatment and all beakers in the experiment were gently mixed via aeration. Based on chl *a* measurements of *Chlamydomonas*, these cell concentrations correspond to a range of about 1.8–17.7 µg·L^{-1}. Although some background particles remained in filtered river water, *Chlamydomonas* represented the dominant food source for mussels, given its high cell density and optimal cell size for retention by mussels (Sprung and Rose 1988). However, to count all likely food particles in suspension we expressed food levels as total particles·L^{-1}, as detected on a Coulter Counter (model ZM). Mussels were allowed to feed for about 1 h, whereupon a sample of the remaining algal suspension was removed from each beaker and counted on the Coulter Counter fitted with a 100-µm aperture tube, which counted particles between 2 and 70 µm. A dilute NaCl solution (15%) was added to each sample to provide the conductivity needed for counting (see Sprung and Rose 1988). Mussel clearance rates (the volume of water from which a mussel removed all measurable particles in a given period of time) were determined according to the following formulae (see Baldwin and Newell 1995):

$$k = \ln C_t - \ln C_0/t \quad (2)$$

$$G_0 = [k(C_t - C_0 e^{kt})/1 - e^{kt}]/[1/C_0] \quad (3)$$

$$\mathrm{CR} = VG_0/n \quad (4)$$

where k is the coefficient for growth of particles (h^{-1}), C_t is the particle concentration at time t (particles·L^{-1}), C_0 is the particle concentration at time 0 (particles·L^{-1}), t is time (h), G_0 is the grazing coefficient at initial particle concentration (h^{-1}), CR is clearance rate (L·h^{-1}·mussel^{-1}), V is the volume of the jar (L), and n is the number of mussels.

The second set of experiments used large zebra and quagga mussels (19–22 mm SL) from the St. Lawrence River that were acclimated for two weeks at CBFS in a flow-through feeding system that contained filtered (pore size 1 µm) Oneida Lake water at 20 ± 1°C with *Nannochloris* added at densities ranging from 1×10^7 to 1×10^8 cells·L^{-1}. For experiments, *Nannochloris* was added to the 140-L head tank of the flow-through system to achieve specific food treatments spanning a 0 to 1×10^9 cells·L^{-1} cell density range. Based on chl *a* measurements of *Nannochloris*, these cell concentrations correspond to a range of 0 to about 33 µg·L^{-1}. Mussel clearance rates were measured at the end of a 120-min exposure to each food treatment. Measurements were taken on groups of mussels held in 3-L plastic trays in the flow-through system (flow rates generally ~7 L·min^{-1}). Except where noted, four trays each held 10 zebra mussels (three trays with live mussels, one control tray with empty articulated shells of the appropriate size) and four trays each held 10 quagga mussels (as above). At 120 min, a water sample was collected from the outflow of each tray to calculate a flow rate and to count the number of particles remaining in suspension with the Coulter Counter. Measurements from each tray were considered replicate experimental units. Clearance rates were determined according to the following formula (see Schneider et al. 1998):

$$\mathrm{CR} = [F(P_c - P_e)/P_c]/n \quad (5)$$

where F is flow rate (L·h^{-1}), P_c is the particle concentration of the control chamber (particles·L^{-1}), P_e is the particle concentration of the experimental chamber (particles·L^{-1}), and n is the number of mussels in the tray. To judge the behavioral responses of mussels to each food treatment, the number of actively feeding animals in each tray (shells open and siphons extended) was assessed every 5 min during the 90- to 120-min interval of each feeding trial.

Effect of inorganic particles on clearance rate

To compare how the above zebra and quagga mussels responded to suspended inorganic particles, we measured their clearance rates when fed suspensions of kaolinite clay (hydrated aluminum silicate, Fisher Scientific Co., Pittsburgh, Pa.) in FLW mixed with *Nannochloris* (1×10^7 cells·L^{-1} in all treatments). Experiments were conducted using the flow-through procedure above. Clay concentrations ranged from 0 (control) to 100 mg·L^{-1}. Concentrated stocks of clay suspensions were mixed vigorously in FLW 1–2 days before experiments, were refrigerated, and were diluted for experimental suspensions. Preliminary analyses using the Coulter Counter, different aperture tubes, and size calibration microspheres confirmed that about 70% of clay particles were between 2 and 20 µm.

Day versus night response

To test whether mussels have diurnal feeding activity we measured clearance rates twice daily (12:00 and 23:00) over the course of 48 h using the flow-through procedure above. A different subset of mussels was held under a natural light cycle to which they had been acclimated for four weeks. The

© 2002 NRC Canada

food suspension was refreshed as needed and consisted of *Nannochloris* added at 1×10^7 cells·L^{-1} to FLW. When measuring the filtering activity at night, we used flashlights covered with red cellophane. Prior work showed that zebra mussel feeding activity was not altered by red light (Horgan and Mills 1997) and our preliminary tests confirmed the same for quagga mussels.

Clearance rate and quagga size

To assess the influence of body size on clearance rate, we tested small (SL 5–10 mm), medium (13–15 mm), large (19–22 mm), and extra-large (25–30 mm) quagga mussels using *Nannochloris* added at 1×10^7 cells·L^{-1} to FLW. Extra-large animals were collected from the St. Lawrence River, whereas the other size classes (not available at our St. Lawrence River site) were from Lake Erie. For each size class test, seven trays were filled with live quagga mussels and one control tray held empty, articulated shells of the appropriate size and number. Different numbers of mussels were placed in each tray depending on the size class tested: for small we used 40 individuals, for medium we used 20, and for both large and extra large we used 10. Based on Horgan and Mills (1997), we used larger numbers for smaller size-classes to account for an expected lower individual clearance rate. SL, DM, and OM were measured for each animal following these experiments.

Food processing

Selective feeding

To test the influence of food quality and quantity on the degree to which animals rejected non-nutritious inorganic particles (to selectively ingest organically enriched food mixtures), the quality of material in mussel pseudofeces was compared with each of five food treatments. The quality of pseudofeces and food was expressed as the mass ratio of organic to inorganic (O:I) material and the quantity of food was given as seston DM (see Schneider et al. 1998). We predicted that mussels would reject inorganic components of seston and hence the O:I of pseudofeces would be lower than that of seston.

We established five food treatments of different quality and quantity: (*i*) O:I of 3.98, seston DM (mg·L^{-1}) of 2.24; (*ii*) O:I 3.79, seston 3.46; (*iii*) O:I 1.39, seston 22.33; (*iv*) O:I 0.35, seston 51.39; and (*v*) O:I 0.34, seston 95.67. All treatments included unfiltered Oneida Lake seston (OLS), which was pumped from the lake using a near-bottom intake pipe that drew seston at either low flow rates (mainly suspended seston) or high flow rates (pulling in suspended seston and stirred-up bottom detritus and fine sediments). Food treatments 4 and 5 were amended with fresh lake sediments sieved through a 150-μm screen and treatment 5 was also amended with *Nannochloris* at 1×10^9 cells·L^{-1}.

Prior to the experiments, large mussels (SL 19–22 mm) collected from the St. Lawrence River were acclimated at CBFS for four weeks in unfiltered seston pumped continuously from Oneida Lake. Experiments were conducted under flow-through conditions as described above, with three trays for each species and each tray containing 10 individuals. Animals were allowed to acclimate to each food condition for 90 min prior to the start of each experiment. Afterwards, the bottom of each tray was cleaned of settled food and biodeposits. Following another 30 min of feeding, pseudofeces (collected by pipet) and samples of suspended food were collected from each tray. Samples of food or pseudofeces were filtered onto pre-ashed and pre-weighed 25-mm filters (Gelman A/E). These filters were then dried at 60°C for 24 h, reweighed (total DM), ashed at 550°C for 5 h, and reweighed to determine inorganic and organic DM. The quantity of pseudofeces produced was reported as mg DM·mussel^{-1} and the quality as O:I.

Food assimilation

We compared the assimilation efficiencies (AE) of zebra and quagga mussels and the degree to which they were affected by food quality. After being fed the five food treatments in the experiments described above, animals were rinsed and placed in trays of FLW for 2 h, and newly expelled fecal material from the animals in each tray was collected by pipet and processed as above. Estimates of AE were calculated according to Conover (1966)

$$(6) \qquad AE = 100[(RF - RE)/(1 - RE)RF]$$

where RF and RE are mass ratios of OM to DM in food and feces, respectively. As reported by Schneider et al. (1998), this technique underestimates AE in cases where mussels selectively feed (i.e., reject inorganics in pseudofeces). Species comparisons were made only when neither species selectively fed or when there was no difference in selection among species.

Starvation experiment

To assess which mussel species could better resist loss of body mass, we reared St. Lawrence River quagga and zebra mussels at CBFS in aged, seston-free tap water. For this experiment, animals were collected in July and held and fed at CBFS until they were used in the experiment. Here, 18 adults of each species (mean SL ~19 mm) were held in individual 400-mL jars containing aerated tap water that was changed every 7–10 days over a period of 110 days (September to December). Lab temperatures tracked outside air temperatures during the fall as they declined from 20.5 to 10°C. Other rearing procedures and animal length and WM measurements were conducted as in our growth experiments.

Statistical analyses

Data were compared using analysis of variance (ANOVA) and Bonferroni multiple comparison tests on data that were transformed using a modified square-root procedure or an arcsine transformation (MINITAB release 13, MINITAB Inc., State College, Pa.). Trends in growth or feeding were analyzed using regression and comparisons of slopes and intercepts were made using a proxy variable macro in the regression analysis (R. Lock, St. Lawrence University, Canton, N.Y., personal communication). Other data from mussel feeding experiments were compared using *t* tests. All relationships were considered significant at $P < 0.05$.

Results

Growth experiments

Despite differences in both the sources of mussels and of foods, and over a wide range of food concentrations, we

© 2002 NRC Canada

Table 1. Conditions of growth experiments (see text for details) and mean growth responses (wet mass) of zebra mussels (Z, *Dreissena polymorpha*) and quagga mussels (Q, *Dreissena bugensis*).

Experiment	Temp (°C)	Time (days)	Food treatment	Mean chl *a* ($\mu g \cdot L^{-1}$)	Instantaneous growth (day^{-1})		Percent change	
					Zebra	Quagga	Zebra	Quagga
1. Onondaga seston	23	38	25 (%)	1.1	0.03 (0.01, 0.06)	0.57 (0.47, 0.69)*	1.2 (0.4, 2.5)	24.7 (20.2, 29.9)*
			50 (%)	2.2	0.11 (0.07, 0.16)	0.78 (0.66, 0.92)*	4.3 (2.5, 6.6)	34.9 (29.3, 40.8)*
			75 (%)	3.3	0.09 (0.05, 0.14)	0.63 (0.52, 0.75)*	3.7 (2.0, 5.9)	27.6 (22.7, 32.9)*
			100 (%)	4.4	0.17 (0.15, 0.24)	0.71 (0.59, 0.84)*	7.1 (4.8, 10.0)	31.3 (26.1, 36.9)*
2. *Chlamydomonas*	6	43	Low	0.05	–0.031 (–0.058, –0.013)	0.021 (0.007, 0.044)*	–1.35 (–2.64, –0.49)	1.00 (0.29, 2.14)*
	23	43	Low	0.05	–0.013 (–0.032, –0.002)	0.007 (–0.003, 0.010)*	–0.51 (–1.39, –0.06)	0.19 (–0.02, 1.04)*
	6	43	High	5.3	0.016 (0.004, 0.037)	0.317 (0.251, 0.392)*	0.75 (0.16, 1.77)	15.70 (12.29, 19.52)*
	23	43	High	5.3	0.451 (0.369, 0.542)	1.450 (1.295, 1.613)*	22.38 (18.20, 26.99)	90.99 (82.12, 100.32)*
					Zebra (ZZ)	Quagga (QQ)	Zebra (ZZ)	Quagga (QQ)
3. Oneida seston	23	52	25 (%)	1.56	–0.09 (–0.22, –0.02)	0.12 (0.04, 0.26)	–2.76 (–9.79, –0.04)	7.53 (2.33, 15.70)
	23	52	100 (%)	8.68	2.26 (1.87, 2.69)*	1.24 (0.97, 1.54)	242.05 (207.24, 279.56)*	110.07 (89.75, 132.47)
					Zebra (ZQ)	Quagga (ZQ)	Zebra (ZQ)	Quagga (ZQ)
3. Oneida seston	23	52	25 (%)	1.56	–0.02 (–0.11, 0.06)	–0.02 (–0.13, 0.05)	–3.73 (–10.38, –0.07)	–0.35 (–4.85, 1.04)
	23	52	100 (%)	8.68	2.13 (1.79, 2.32)	1.48 (1.07, 1.95)	228.59 (196.33, 260.16)	124.14 (94.12, 158.30)

Note: All data are back-transformed and because standard errors (SE) are asymmetrical they are given as (mean – SE, mean + SE). Growth data for Oneida Lake experiment are given for species in ZZ, QQ, and ZQ pairs. Asterisks denote significantly higher rates of one species over another in that treatment. N = 4–20 for all experiments.

generally found that juvenile quagga mussels grew as well or better than zebra mussels (Table 1). In the experiment using Onondaga Lake seston, quagga mussels had significantly higher instantaneous growth rates than zebra mussels (2-way ANOVA, $F_{[1,78]} = 97.7$, $P < 0.0001$) and this was true at each food level tested (Bonferroni multiple comparison test; $P < 0.05$). Interestingly, for each mussel species, there was no significant difference in growth among food levels tested (Bonferroni multiple comparison test; $P < 0.05$) and as a result, there was no overall effect of food level on mussel growth (2-way ANOVA, $F_{[3,78]} = 2.0$, $P = 0.121$). (Analysis of percent change in WM produced virtually identical results.) Mean instantaneous growth rates for quagga mussels ranged from 0.57 to 0.78 day^{-1} (back-transformed data) in comparison with 0.03 to 0.17 day^{-1} for zebra mussels (Table 1). As a result, quagga mussel growth was from 4 to 19 times greater than zebra mussels, with the greatest difference at the lowest food level. In terms of percent change in WM over the 38-day period, quagga mussel growth ranged from a 25 to 35% increase compared to a 1–7% increase for zebra mussels (Table 1). Mortality rates were very low for both mussels; no quagga mussels died and only one zebra mussel died (at the 75% food level).

In the experiment using *Chlamydomonas*, quagga mussels had significantly higher instantaneous growth rates than zebra mussels (3-way ANOVA, $F_{[1,145]} = 57.9$, $P < 0.0001$) and this was true at each food–temperature combination (Bonferroni multiple comparison test; $P < 0.05$) except the low food × 23°C treatment. Mussel growth responded more strongly to food level (3-way ANOVA, $F_{[1,145]} = 206.3$, $P < 0.0001$) than to temperature (3-way ANOVA, d.f. = 1, $F = 35.8$, $P < 0.0001$). However, the effects of food on growth were dependent on mussel species (3-way ANOVA, food*species interaction, $F_{[1,145]} = 44.2$, $P = 0.007$) and temperature (3-way ANOVA, food*temperature interaction, $F_{[1,145]} = 54.1$, $P < 0.0001$). (Analysis of percent change in WM produced virtually identical results.)

Mean instantaneous growth rates for quagga mussels ranged from 0.01 to 1.45 day^{-1} (back-transformed data) in comparison to –0.03 to 0.45 day^{-1} for zebra mussels (Table 1). Quagga mussel growth was positive under all experimental conditions, whereas zebra mussels showed negative growth under low food levels, regardless of temperature. Under high food level, quagga mussel growth was about three times greater than zebra mussel growth at high temperature and as high as 19 times greater than zebra mussel growth at low temperature. Also under the high food treatment, temperature had a much greater effect on zebra mussel growth (27 times greater at high temperature than low temperature), than on quagga mussel growth (five times greater at high temperature). In terms of percent change in WM over the 43-day period, quagga mussel growth ranged from a 0.2 to a

© 2002 NRC Canada

Table 2. Comparisons of organic mass (OM) ratios to dry mass (DM) or wet mass (WM) between groups of freshly collected zebra mussels (Z, *Dreissena polymorpha*) and quagga mussels (Q, *Dreissena bugensis*) from different sites.

Source	Date	Species	*N*	Size range (mm)	OM/DM (%)	OM/WM (%)
SLR (Cape Vincent)	May	Q	43	5 to 10	20.2 (0.9) **	9.4 (0.5) **
	1997	Z	79		11.1 (0.4)	5.2 (0.2)
SLR (Cape Vincent)	June	Q	40	5 to 9	3.51 (0.75) **	1.6 (0.5) *
	1998	Z	32		2.82 (0.13)	1.3 (0.1)
Lake Erie (Dunkirk)	June	Q	81	5 to 9	9.74 (1.40) **	4.8 (0.8) **
	1998	Z	109		2.07 (0.09)	1.1 (0.1)
Lake Erie (Dunkirk)	June	Q	81	5 to 9	9.34 (1.40) **	4.5 (0.6) **
Oneida Lake	1998	Z	124		1.77 (0.10)	0.7 (0.1)

Note: Data are mean (± standard error) ratio values (mg· mg^{-1}) expressed as percentages. Species were compared using 2-sample *t* tests. SLR, St. Lawrence River.

* $P < 0.01$.

** $P < 0.001$.

91% increase in WM compared with a –1.35 to 22.4% increase for zebra mussels (Table 1). Mortality rates were low for zebra (5–10%) and quagga mussels (0–10%, with the exception of 35% at the low food × 6°C treatment).

In the experiment using Oneida Lake seston, which had the highest level of food, the instantaneous growth rates of zebra mussels in ZZ pairs and quagga mussels in QQ pairs were similar at the 25% food level but zebra mussels grew faster at the 100% level. We detected no overall effect of species on instantaneous growth rates (2-way ANOVA, $F_{[1,59]} = 0.93$, $P = 0.340$), but growth rates for both species were significantly higher in the 100% versus the 25% food level (2-way ANOVA, $F_{[1,59]} = 83.9$, $P < 0.0001$) and there was a significant interaction effect, meaning that zebra mussel growth rates increased more than quagga mussels between the 25 and 100% food treatments (2-way ANOVA, species*food, $F_{[1,59]} = 11.2$, $P < 0.001$). There were no differences in the growth of zebra and quagga mussels at the 25% food level (Bonferroni multiple comparison test; $P > 0.05$), but zebra mussels grew faster at the 100% level (Bonferroni multiple comparison test; $P < 0.05$). Average zebra mussel (ZZ) growth rates increased dramatically from the low food level (–0.09 day^{-1}) to the high food level (2.26 day^{-1}) as, to a lesser extent, did quagga mussels (QQ) (0.12 day^{-1} versus 1.24 day^{-1}; Table 1). Mortality of zebra mussels (ZZ) was 2.3 times higher than quagga mussels (QQ) (25 versus 11%) in the high food treatment and 1.7 times higher (79 versus 47%) in the low food treatment.

In our test of interspecific competition there was no significant difference in the growth rates of zebra mussels grown in the ZZ treatment as compared with zebra mussels in the ZQ treatment (2-way ANOVA, $F_{[1,42]} = 0.016$, $P = 0.901$). Likewise, there was no significant difference found in growth rates of quagga mussels in the QQ pairing and quagga mussels in the ZQ pairing (2-way ANOVA, $F_{[1,51]} = 1.39$, $P = 0.244$). Furthermore, within the ZQ treatments, neither zebra mussels nor quagga mussels grew better than their potential competitor. Here, the difference in growth between paired competitors was not different from zero at either the 25 (one sample *t* test; $P = 0.887$) or 100% (one sample *t* test; $P = 0.206$) food levels. As before, growth in the ZQ treatment was significantly higher at the 100% food level for both zebra (2-way ANOVA, $F_{[1,42]} = 97.3$, $P < 0.001$) and quagga (2-way ANOVA, $F_{[1,51]} = 39.2$, $P < 0.0001$) mussels. The increases in growth rate from the 25 to the 100% food level were not significantly different between the two species (2-way ANOVA, $F_{[1,42]} = 0.97$, $P = 0.331$). The average growth rates of zebra mussels paired with quagga mussels were –0.02 and 2.13 day^{-1} for the 25 and 100% food levels, respectively, whereas those for quagga mussels were –0.02 and 1.48 day^{-1} (Table 1). Mortality of zebra mussels (ZQ) was ~2.7 times higher than quagga mussels (ZQ) (80 versus 30%) in the low food treatment, but it was lower than quagga mussels (0 versus 10%) in the high food treatment. As with animals in the ZZ and QQ parings, both species showed higher mortality at lower food levels. However, although food affected mortality, the identity of the potential competitor did not.

Estimates of OM

In freshly collected dreissenids, covering different sites and times, we found that quagga mussels had significantly higher ratios than zebra mussels for both OM per unit WM and OM per unit DM (Table 2). Given this, it is probable that the differences in growth reported above for experiments 1–3 (WM) are conservative in that quagga mussels likely added more OM than did zebra mussels. For our most extensive data set (St. Lawrence River, May 1997) we found the following relationships between OM (in mg) and dreissenid SL (in mm) or WM (in mg): (*i*) quagga mussels ($n = 95$) $OM = 0.0209SL^{2.53}$ ($r^2 = 0.90$) and $OM = 0.0637WM + 1.79$ ($r^2 = 0.98$); (*ii*) zebra mussel ($n = 445$) $OM = 0.0296SL^{2.26}$ ($r^2 = 0.76$) and $OM = 0.0337WM + 1.15$ ($r^2 = 0.86$). Regression analysis showed that slope terms for quagga mussel equations were significantly greater ($P < 0.01$ for all tests) than those for zebra mussels, but there were no differences in intercepts ($P > 0.231$ for all tests).

Food clearance

Functional response

We found similar clearance rates for zebra and quagga mussels in experiments using *Chlamydomonas* in small beakers and *Nannochloris* under flow-through conditions. We detected no significant differences in clearance rates (CR) among zebra and quagga mussels over the three test concentrations of *Chlamydomonas* (2-way ANOVA, $F_{[1,59]} = 3.01$, $P = 0.089$), but there was a significant effect of food level on CR (2-way ANOVA, $F_{[2,59]} = 52.22$, $P < 0.0001$). Here, CR were similar over the two lower concentrations of

© 2002 NRC Canada

Fig. 1. Clearance rates (CR) of zebra (*Dreissena polymorpha*; solid columns) and quagga (*Dreissena bugensis*; open columns) mussels fed filtered St. Lawrence River water with different concentrations of *Chlamydomonas* at 20°C. Data are means ± standard error. (*a*) Clearance rates per mussel. (*b*) Clearance rates per milligram of mussel organic mass.

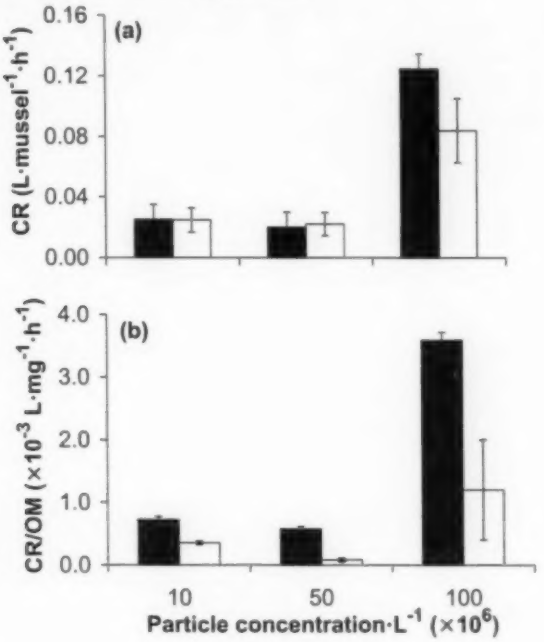

Fig. 2. Functional response of zebra (*Dreissena polymorpha*; solid symbols) and quagga (*Dreissena bugensis*; open symbols) mussels fed filtered Oneida Lake water with different concentrations (log scale) of *Nannochloris* at 20°C. Data are clearance rates (CR) for mussels from each of three replicate feeding trays. Exponential regressions provided the best fit to zebra mussel (black line) and quagga mussel (gray line) data (see text). (*a*) Clearance rates per mussel. (*b*) Clearance rates per milligram of mussel organic weight.

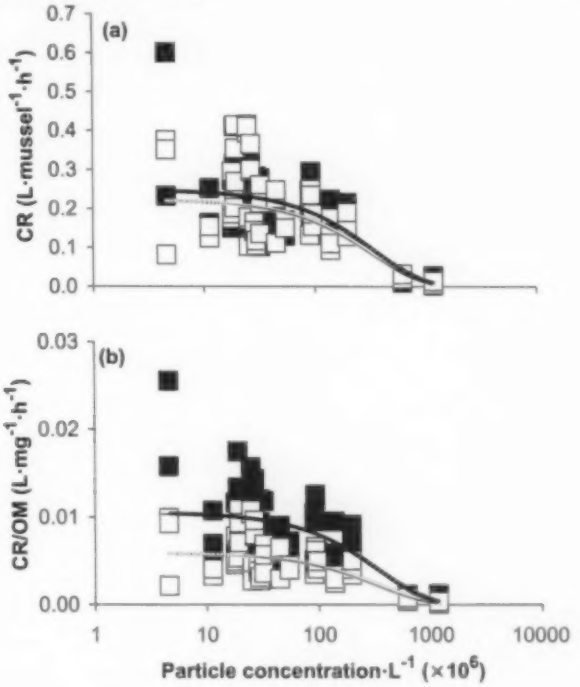

Chlamydomonas (Fig. 1*a*), but both zebra and quagga mussels increased their CR at the highest food level (Bonferroni multiple comparison test; $P < 0.05$). The range of CR seen in this experiment (0.020–0.125 L·mussel^{-1}·h^{-1}) was generally lower than that seen in the *Nannochloris* experiment reported below.

Species differences are apparent when CR are normalized to OM (Fig. 1*b*). Using the OM relationships reported above, we estimated that the quagga mussels we used had about twice the amount of OM as did zebra mussels with similar SL (quagga mussel mean SL = 24.7 mm, OM = 69.8 mg; zebra mussel mean SL = 22.8 mm, OM = 34.7 mg). Tests of CR/OM (L·mg^{-1}·h^{-1}) revealed significant differences among zebra and quagga mussels (2-way ANOVA, $F_{[1,59]} = 30.98$, $P < 0.0001$) at each of the three test concentrations of *Chlamydomonas* (Bonferroni multiple comparison test; $P < 0.05$). In fact, zebra mussels had CR/OM values 2–7 times higher than quagga mussels. Mussel CR/OM values also varied with food level (2-way ANOVA, $F_{[2,59]} = 49.53$, $P < 0.0001$), with the highest values at 100×10^6 particles·L^{-1} and lower, equivalent values over the two lower food concentrations (Bonferroni multiple comparison test; $P < 0.05$). Again, the range of CR/OM values seen in this experiment ($0.08–3.39 \times 10^{-3}$ L·mg^{-1}·h^{-1}) was generally lower than that seen in the *Nannochloris* experiment reported below.

In over 20 different concentrations of *Nannochloris*, the range of CR for zebra mussels (0.018–0.402 L·mussel^{-1}·h^{-1}) greatly overlapped that of quagga mussels (0.010–0.407 L·mussel^{-1}·h^{-1}) (Fig. 2*a*). The trends in CR for both species were similar and they appear to follow a Type I functional response (e.g., Chow-Fraser and Sprules 1992), indicating a high and roughly constant CR over low food concentrations and a dramatic decline in CR as food levels increase (Fig. 2*a*). Based on exponential curve fits, CR for zebra mussels are related to food particle concentrations according to CR (L·mussel^{-1}·h^{-1}) = $0.249e^{-0.00286x}$ ($r^2 = 0.75$) in comparison with quagga mussels, where CR = $0.223e^{-0.00293x}$ ($r^2 = 0.76$). Regression analyses of these data showed a significant decline in CR as food increased for both species ($P < 0.0001$ for all tests) and indicated that the slopes and intercepts of these relationships did not differ between species ($P = 0.273$ for all tests). We found no species difference in the percent of actively feeding mussels (shells open and siphons extended) in this experiment (2-way ANOVA, $F_{[1,141]} = 3.56$, $P = 0.068$), but there was a difference in activity among particle concentrations (2-way ANOVA, $F_{[19,141]} = 6.79$, $P < 0.0001$), where activity at the highest concentration (80–82%) was lower than that at other food levels (86–99%) (Bonferroni multiple comparison test; $P < 0.05$).

By comparison, if the clearance rates of these experimental animals are normalized to their OM (quagga mussel mean SL = 19.2 mm, OM = 36.9 mg; zebra mussel mean

© 2002 NRC Canada

Fig. 3. Clearance rates (CR) of zebra (*Dreissena polymorpha*; filled symbols) and quagga (*Dreissena bugensis*; open symbols) mussels fed filtered Oneida Lake water additions of either (*a*, *b*) *Nannochloris* and suspended clay or (*c*) *Nannochloris* alone. Data are clearance rates (CR) for mussels from each of three replicate feeding trays. Linear regressions provided the best fit to zebra mussel (black line) and quagga mussel (gray line) data (see text). (*a*) Clearance rates per mussel for all clay levels. (*b*) Clearance rates per mussel for select clay levels with particle concentrations spanning 36–91 × 10^6 particles·L^{-1}. (*c*) Clearance rates per mussel from functional response experiment (Fig. 2) over select particle concentrations spanning 32–96 × 10^6 particles·L^{-1}.

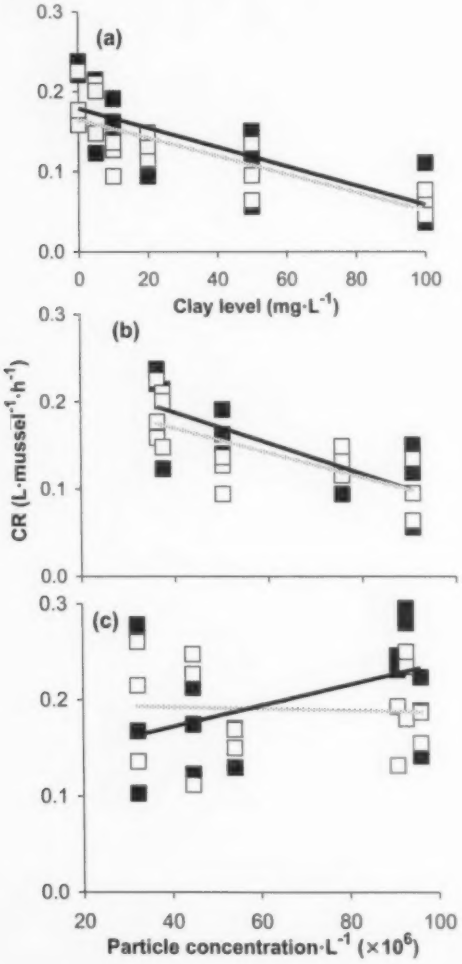

SL = 19.4 mm, OM = 24.6 mg), then it is again evident that zebra mussels had CR/OM values about two times higher than quagga mussels (Fig. 2*b*). For both species, regression analyses showed a significant decline in CR/OM as food increased ($P < 0.0001$), and even though slopes of the regressions were equal ($P = 0.827$), the intercept for zebra mussels was significantly greater than that for quagga mussels ($P < 0.0001$). Based on exponential curve fits, CR/OM for zebra mussels are related to food particle concentrations according to CR/OM (L·mg^{-1}·h^{-1}) = $0.011e^{-0.0029x}$ ($r^2 = 0.75$) in comparison with quagga mussels where CR/OM = $0.006e^{-0.0029x}$ ($r^2 = 0.76$).

Effect of inorganic particles on clearance rate

As clay levels increased from 0 to 100 mg·L^{-1} (with *Nannochloris* at 10^7 cells·L^{-1} in all treatments), CR for both species decreased significantly (regression, $P < 0.0001$ for both species; Fig. 3*a*). Mean CR decreased from 0.210 to 0.072 L·mussel^{-1}·h^{-1} for zebra mussels and from 0.187 to 0.061 L·mussel^{-1}·h^{-1} for quagga mussels. The regression for zebra mussel CR on clay concentration was CR = 0.179 – 0.0012 clay ($r^2 = 0.52$) as compared with quagga mussels CR = 0.166 – 0.0012 clay ($r^2 = 0.61$). There were no differences in slopes or intercepts between species ($P > 0.433$ for all tests), thereby indicating equivalent CR patterns in zebra and quagga mussels. Mussels also showed similar trends in feeding activity. We detected no difference in activity among species (2-way ANOVA, $F_{[1,35]} = 3.26$, $P = 0.082$), but activity did vary with clay levels (2-way ANOVA, $F_{[5,35]} = 22.32$, $P < 0.0001$), where activity at the highest two concentrations (50–70%) was lower than that at lower clay levels (80–100%) (Bonferroni multiple comparison test; $P < 0.05$).

Because food suspensions were also counted on the Coulter Counter, we compared mussel CR responses in this experiment (added clay) to those of the previous experiment (no added clay) over similar particle concentrations (roughly 30–100 × 10^6 particles·L^{-1}) to judge whether the presence of clay itself affected CR. Using regression analyses we found significant declines in CR for both zebra ($P < 0.001$) and quagga mussels ($P = 0.003$) in the clay experiment (Fig. 3*b*), but not in the functional response experiment without clay (zebra mussel $P = 0.091$, quagga mussel $P = 0.836$; Fig. 3*c*). This indicates that both species of mussel reduced their clearance rates in response to increasing levels of clay. In part, mussels may also have reduced their clearance rates in response to a higher actual level of suspended particles since about 30% of clay particles were <2 µm and below the detection level of the standard aperture tube used on the Coulter Counter.

Day versus night response

We compared daytime (12:00) and nighttime clearance rates (23:00) for zebra and quagga mussels over a 48-h period following a four-week acclimation period to diurnal conditions and food (*Nannochloris* added to Oneida Lake water). We found no significant difference in CR between species during the day (1-way ANOVA, $F_{[1,11]} = 0.0$, $P = 0.954$), but a significantly higher CR for zebra mussels at night (1-way ANOVA, $F_{[1,11]} = 13.7$, $P = 0.004$). Mean daytime CR values were 0.091 L·mussel^{-1}·h^{-1} for zebra mussels and 0.092 L·mussel^{-1}·h^{-1} for quagga mussels. However, the mean night-time CR for zebra mussels (0.083 L·mussel^{-1}·h^{-1}) was nearly three times greater than that for quagga mussels (0.028 L·mussel^{-1}·h^{-1}).

To test each species for diurnal variation in CR, we examined the difference in night-time and daytime CR (N – D). Here, N – D values for zebra mussels were not significantly different from zero (2-tailed *t* test, $P = 0.743$), showing no diurnal variation. For quagga mussels, average daytime CR was 3.3 times greater than night-time CR and yet the N – D test was borderline nonsignificant (2-tailed *t* test, $P = 0.055$).

© 2002 NRC Canada

We detected no difference in the level of feeding activity (70–100%) among species (2-way ANOVA, $F_{[1,23]} = 4.43$, $P = 0.052$) or time (2-way ANOVA, $F_{3,23} = 3.00$, $P = 0.061$).

Clearance rate and quagga size

Quagga mussel CR (range 0.0176–0.3260 L·mussel^{-1}·h^{-1}) showed a significant increase with body size, whether expressed as SL, DM, or OM (regression, $P < 0.001$ for all tests). As conventional expressions as power functions, quagga mussel CR (L·mussel^{-1}·h^{-1}) were (*i*) CR = 0.0009SL(mm)$^{1.5853}$ ($r^2 = 0.63$), (*ii*) CR = 0.2221DM(g)$^{0.5419}$ ($r^2 = 0.63$), and (*iii*) CR = 0.7866OM(g)$^{0.6266}$ ($r^2 = 0.63$).

Food processing

Selective feeding

The quality (O:I) of pseudofeces produced by both zebra and quagga mussels was directly related to seston quality but inversely related to seston quantity (Fig. 4*a*). The quality of seston as well as that of pseudofeces changed significantly over different levels of seston quantity (2-way ANOVA, $F_{[3,35]} = 1084.33$, $P < 0.0001$). Seston and pseudofeces quality declined over each of the lowest three amounts of seston but showed no further declines at the highest seston level (Bonferroni multiple comparison test; $P < 0.05$). There was also a significant difference among the quality values of seston and pseudofeces (2-way ANOVA, $F_{[2,35]} = 26.14$, $P < 0.0001$). There were no differences in O:I of pseudofeces among species, but these ratios were lower than those of seston at all but the highest two seston levels (Bonferroni multiple comparison test; $P < 0.05$). This indicates selective feeding by both mussel species when offered food at relatively low seston concentrations (about 3–22 mg·L^{-1}). Negligible pseudofeces were detected at the lowest seston level offered (2.24 mg·L^{-1}). The quantity (mg·mussel^{-1}·h^{-1}) of pseudofeces produced by both zebra and quagga mussels increased with seston quantity (2-way ANOVA, $F_{[4,29]} = 252.13$, $P < 0.0001$), but we detected no difference between species (2-way ANOVA, $F_{[1,29]} = 2.47$, $P = 0.132$) (Fig. 4*b*).

Food assimilation

Both zebra and quagga mussels ingested seston and produced feces at each food treatment. Mean mussel assimilation efficiencies (AE) ranged from about 1 to 82% and were highest over the lowest seston concentrations and highest seston quality (O:I) (Fig. 5). Since both species appeared to selectively remove inorganic constituents of seston at the highest seston O:I levels, the corresponding AE values may be underestimates of actual AE levels. Because there were no species differences detected in mussel pseudofeces composition, we assumed that both species ingested seston of similar quality. We did find differences in AE between zebra and quagga mussels (2-way ANOVA, $F_{[1,29]} = 5.5$, $P = 0.029$) but only at the lowest seston level where quagga AE (81%) exceeded that of zebra mussels (63%) (Bonferroni multiple comparison test; $P < 0.05$).

Starvation experiment

When reared in aged, seston-free tap water, zebra mussels were far more susceptible to mortality than quagga mussels. Over the course of 108 days, 56% of zebra mussels ($n = 10$ out of 18) died, in contrast to only 6% of quagga mussels ($n = 1$ out of 18). The mean ± SE loss of WM for zebra mussels (1.04 ± 0.37 mg·mussel^{-1}·day^{-1}) was about three times greater than that for quagga mussels (0.33 ± 0.08 mg·mussel^{-1}·day^{-1}). However, given the small sample size and the high variation in results the difference in these rates was marginally nonsignificant (Mann–Whitney *U* test, $P = 0.055$).

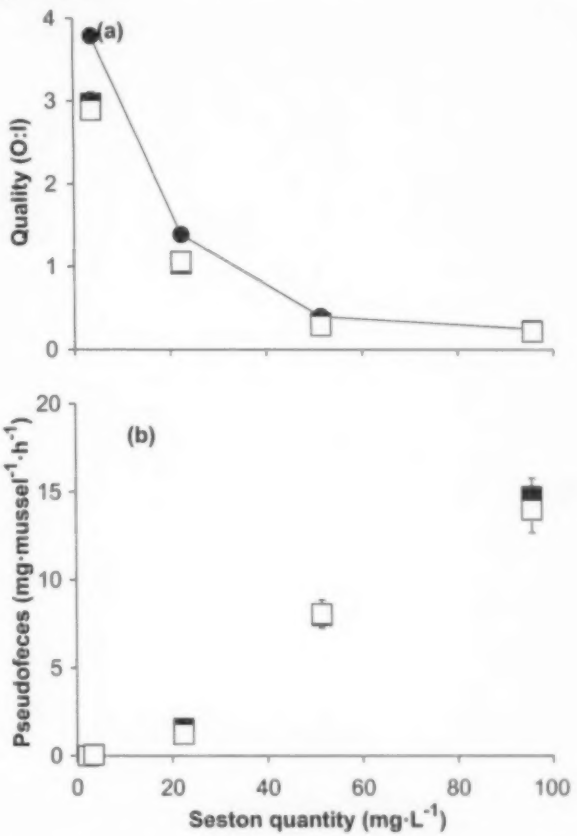

Fig. 4. (*a*) Selective feeding and (*b*) pseudofeces production in zebra (*Dreissena polymorpha*; filled symbols) and quagga (*Dreissena bugensis*; open symbols) mussels fed Oneida Lake seston with different levels of *Nannochloris* and suspended sediments. Data are means ± standard error. (*a*) Organic to inorganic ratios (O:I) of food and pseudofeces from zebra mussels and quagga mussels versus seston quantity. Values below the line (food) indicate enrichment of pseudofeces in inorganic particles (i.e., selective feeding). (*b*) Dry mass of pseudofeces produced by mussels.

Discussion

Comparative growth of zebra and quagga mussels

Our laboratory growth experiments generally showed that survivorship and growth rates of juvenile quagga mussels were equal or superior to those of zebra mussels under environmental conditions (23°C, 1–5 µg·L^{-1} chl *a*) similar to those found in warm, productive surface waters of the lower Great Lakes or inland lakes. In particular, quagga mussels

© 2002 NRC Canada

Fig. 5. Assimilation efficiencies of zebra (*Dreissena polymorpha*; filled symbols) and quagga (*Dreissena bugensis*; open symbols) mussels fed Oneida Lake seston with different levels of *Nannochloris* and suspended sediments. Data are means ± standard error for assimilation efficiencies of zebra mussels and quagga mussels versus either (*a*) seston quality (organic to inorganic ratio, O:I) or (*b*) seston quantity (note log scale).

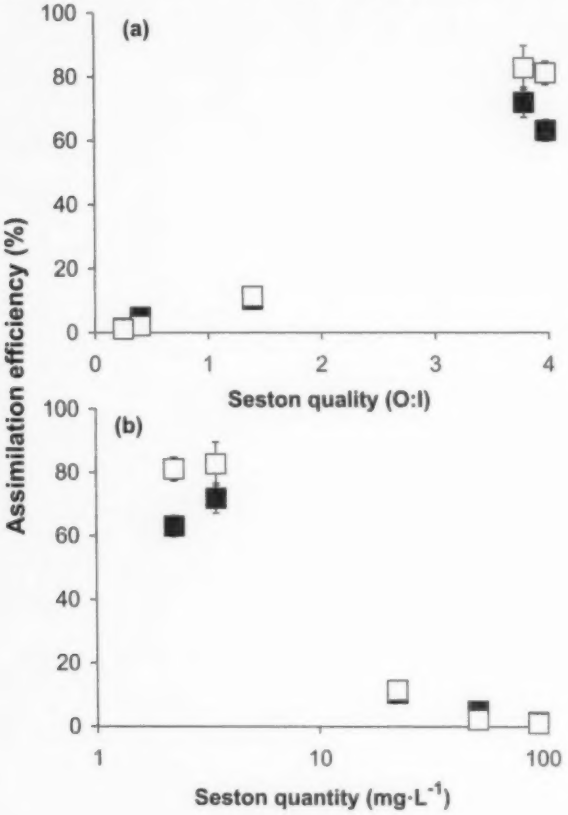

had instantaneous growth rates (WM) from 1 to 19 times faster than those of zebra mussels when fed lake seston or cultured algae (*Chlamydomonas*). These differences in growth may be even larger in terms of biomass since quagga mussels have a greater OM to WM ratio than zebra mussels.

An interesting exception was at the higher, ambient level of Oneida Lake seston (~9 $\mu g \cdot L^{-1}$ chl *a*), where zebra mussels grew 1.4–1.8 times faster than quagga mussels. Even though we observed the fastest growth rates of quagga mussels in this entire study, zebra mussels (originally from Oneida Lake) clearly appeared more adapted to high food levels and more limited by low food levels (growth and mortality). Although data were limited because of high mortality, it is unclear why both species grew at such low rates under the 1.5 $\mu g \cdot L^{-1}$ chl *a* Oneida Lake seston treatment when higher growth was measured for both species in the Onondaga experiment under slightly lower food levels (~1.1 $\mu g \cdot L^{-1}$ chl *a*). Our mean chl *a* level of 1.5 $\mu g \cdot L^{-1}$ was biased upwards by a bloom of phytoplankton (to ~8 $\mu g \cdot L^{-1}$) in the last week of the experiment, so mussels may have experienced a lower food level (~0.9 $\mu g \cdot L^{-1}$) for the majority of the 52-day experiment. In addition, mussels probably received seston that was qualitatively different between Onondaga and Oneida Lakes.

Our results are similar to those reported in an experimental study (MacIsaac 1994) where zebra and quagga mussels were reared for 55 days in cages suspended in the warm and productive western basin of Lake Erie (20–25°C, mean of ~5 $\mu g \cdot L^{-1}$ chl *a*). Here, both small (SL 5 mm) and large (SL 15 mm) quagga mussels grew (change in WM) slightly faster than similar sized zebra mussels, although no significant differences among species were detected. Mortality rates were low for both species and size categories (<10%). Growth rates of small mussels in this field study were much greater than in ours (their maximum of 873% versus our maximum of 242%) owing to a smaller initial mussel size, a longer experimental period, and probably a higher effective level of food due to seston flux through field cages. Our results are similar to those of other studies that report growth as shell length. Here, shell growth of our mussels (–0.007 to 0.024 $mm \cdot day^{-1}$) overlaps with that (0 to ~0.10 $mm \cdot day^{-1}$) of small zebra mussels (SL 5–10 mm) from other laboratory and field studies (e.g., Dorgelo and Smeenk 1988; Smit et al. 1992; Garton and Johnson 2000). Thorp et al. (1998) also compared the growth and survival of large zebra and quagga mussels (SL ~15 mm) that were held for about three months in large tanks containing Ohio River seston (food levels not reported). Under warm conditions (~20–30°C), species growth rates were similar for zebra and quagga mussels collected from southwestern Lake Erie, but quagga mussel survivorship (44%) was somewhat lower than zebra mussels (56%). In another early study that included young-of-the-year (SL 3–10 mm) zebra and quagga mussels sampled on navigation buoys from Lakes Erie and Ontario, Mills et al. (1993) reported greater shell lengths for quagga mussels. Assuming similar settlement times, the difference in mussel sizes could indicate faster growth of quagga mussels under summer epilimnetic conditions.

There is mounting evidence that quagga mussels can colonize littoral zones of the lower Great Lakes (Mitchell et al. 1996; Mills et al. 1999; Bially and MacIsaac 2000) and even thrive under summer temperature and food conditions of epilimnetic habitats in these (MacIsaac 1994) and nearby inland lakes (our study). Certainly this evidence and that from the Ukraine (Mills et al. 1996) should dispel the notion that quagga mussels are restricted to the temperature and food regimes of profundal zones.

Our results also suggest that quagga mussels may grow better than zebra mussels in lakes where food levels are naturally low or declining due to dreissenid filtration. In most of our 23°C experiments, quagga mussels grew more on a given unit of available food than did zebra mussels, particularly at low food levels. For example, the greatest difference in growth rates between quagga and zebra mussels fed Onondaga Lake seston was at the lowest food level offered (~1 $\mu g \cdot L^{-1}$ chl *a*) where quagga mussels grew 19 times faster than zebra mussels. Further, under low concentrations of *Chlamydomonas* (~0.05 $\mu g \cdot L^{-1}$ chl *a*) and of Oneida Lake seston (~1.5 $\mu g \cdot L^{-1}$ chl *a*), quagga mussel growth generally remained positive, whereas zebra mussels actually lost mass. Even under simulated profundal conditions where mussels

© 2002 NRC Canada

were fed low concentrations of *Chlamydomonas* at 6°C, quagga mussels grew marginally and zebra mussels lost mass. In contrast, MacIsaac (1994) reported equivalent declines in mass for juvenile zebra and quagga mussels reared in cages in the eastern basin of Lake Erie (<10°C, mean of ~2 $\mu g \cdot L^{-1}$ chl *a*) and in laboratory experiments found no effect of different food levels on growth as well as higher growth of juvenile zebra mussels at 6°C. However, established field populations of dreissenids in lower Great Lakes habitats with low phytoplankton biomass (eastern basin of Lake Erie, profundal zones) are clearly dominated by quagga mussels (e.g., Mills et al. 1993; Dermott and Kerec 1997; Mills et al. 1999), which normally attain larger sizes than sympatric zebra mussels (e.g., Mills et al. 1993, 1999; Bially and MacIsaac 2000), indicating greater longevity and (or) growth rates. And because lower food levels more dramatically suppressed growth of zebra mussels in our *Chlamydomonas* and Oneida Lake seston experiments, food-limited growth of zebra mussels must be partly responsible for the relative dominance of quagga mussels under low food conditions in nature.

Given that phytoplankton biomass has declined in many lakes colonized by *Dreissena* spp. (e.g., Leach 1993; Fahnenstiel et al. 1995; Idrisi et al. 2001), mussel populations are likely experiencing growth-limiting food conditions. As such, it is reasonable to predict that quagga mussel growth will be less food limited than that of zebra mussels. In fact, this may be one of the reasons why quagga mussels have increased in abundance following initial invasions by zebra mussels (Mills et al. 1996, 1999; Negley et al. 2001). Whether these species compete for food in situ is not known, nor has a clear outcome of resource competition been demonstrated. We did not detect an effect of competitor species on mussel growth in our Oneida Lake seston experiment, even at the lower food level (25% ambient or ~1.3 $mg \cdot L^{-1}$ of dry seston) where growth rates of all mussels were clearly suppressed. Likewise, MacIsaac (1994) found no effect of competition between these species when fed daily with *Chlorella* powder (3.1 and 6.2 $mg \cdot L^{-1}$ treatments) in small-volume (435-mL) jars. Clearly, more investigations are needed on this important question as resource competition may in part explain the displacement of zebra mussels by quagga mussels in the Ukraine (Mills et al. 1996) and it may help forecast potential species shifts in North American dreissenid populations.

Feeding biology of zebra and quagga mussels

We conducted mussel feeding experiments to help explain the species differences we have reported on their growth and field distribution, as well as to assess potential impacts mussels might exert on pelagic systems. Based on the generally faster growth we found for quagga mussels we predicted that they would clear food from suspension at higher rates and (or) for longer time periods than zebra mussels. We also predicted that quagga mussels would selectively ingest and assimilate the organic fraction of seston more effectively than zebra mussels. However, in both the static and flow-through feeding experiments, and using two different species of phytoplankton (*Chlamydomonas*, *Nannochloris*) presented over a wide range of cell densities, we found no significant differences in per capita clearance rates among zebra and quagga mussels. Even the functional responses of both mussels were similar over a wide range of *Nannochloris* (and chl *a*) levels, indicating no species differences in clearance capacity or incipient limiting food concentrations (see Sprung and Rose 1988; Sprung 1995). Further, we did not detect species differences in clearance rates when fed mixed suspensions of *Nannochloris* and different levels of clay, nor did we find significant diurnal variation in their clearance rates or feeding activity (percent of mussels with shells open and siphons extended) in any experiment. At night, quagga mussels may clear food at lower rates than zebra mussels, but more work is needed to establish this conclusively. We conclude that, generally, large (mean SL 22 mm) zebra and quagga mussels clear food from suspension at similar rates and for similar periods of time during a 24-h period at 20°C. We did not estimate species ingestion rates in these experiments since both species often rejected a portion (unquantified) of cleared particles as pseudofeces. However, in our selection and assimilation experiments we did not detect significant differences in the quantity of pseudofeces produced by zebra or quagga mussels (see below). Thus we assume that species ingestion rates in our clearance rate experiments were similar.

Other laboratory studies have also shown similarities in the clearance rates of zebra and quagga mussels. In the only other study to directly compare these mussels, Ackerman (1999) found no differences in the per capita clearance rates of large (SL ~32 mm) or small (SL ~11 mm) zebra and quagga mussels when fed *Chlorella* (~$0.5–3 \times 10^5$ $cells \cdot L^{-1}$) at 20°C. Clearance rates ranged from about 0.1 to 0.4 $L \cdot mussel^{-1} \cdot h^{-1}$ which shows a high degree of overlap with our rates. Zolotareva et al. (1978) reported clearance rates ranging from about 0.002 to 0.011 $L \cdot mussel^{-1} \cdot h^{-1}$ for quagga mussels (SL 5–30 mm) held at 20°C and fed *Chlorella* over a range of cell densities ($0.8–9.8 \times 10^{10}$ $cells \cdot L^{-1}$). We also measured clearance rates for different size quagga mussels (SL 5–30 mm) at 20°C using *Nannochloris* at 1×10^7 $cells \cdot L^{-1}$, but found rates ranging from 0.0176 to 0.0326 $L \cdot mussel^{-1} \cdot h^{-1}$. Most likely, our clearance rates were higher because mussels were given lower food levels than those used by Zolotareva et al. (1978) where, based on the functional response of mussels, one would expect elevated clearance. Together, our three experiments on quagga mussel feeding have found clearance rates similar to those from numerous studies examining zebra mussel feeding under a variety of temperatures using cultured foods and natural seston (e.g., Kryger and Riisgard 1988; Fanslow et al. 1995; Roditi et al. 1996). However, additional studies are needed to resolve possible species differences in particle size retention, selection of different food species, and feeding rates using natural seston presented at relevant field temperatures.

In our study we did find a difference in the biomass-specific clearance rates of zebra and quagga mussels that may partly explain differences in growth rates between these species. In two different feeding experiments we found that large (SL 22 mm) zebra mussels had values of clearance rate per unit OM (CR/OM) that were about 2–7 times higher than those of large quagga mussels. This also appears to be true for a wider size range of mussels (SL 5–30 mm) given that our allometric relation of CR to OM for quagga mussels

© 2002 NRC Canada

($CR = 0.7866OM(g)^{0.6266}$) has smaller power function ($Y = aX^b$) constants (a and b) than those previously developed for zebra mussels fed *Chlorella* ($CR = 6.82OM(g)^{0.88}$; Kryger and Riisgard 1988). Using these equations, calculated CR/OM values for zebra mussels are 2–5 times greater than those for quagga mussels. Assuming that at a given concentration of food these differences in biomass-specific clearance rates reflect a comparable species difference in biomass-specific ingestion rates, quagga mussels may ingest less food to support (or grow) a unit of biomass. So while our juvenile quagga and zebra mussels may show similar per capita clearance and ingestion rates at a given food level, quagga mussels may have used the ingested food more efficiently, as manifested in their greater growth rates. This difference in biomass-specific clearance rates may also help to explain the greater resistance to starvation by quagga mussels and it may help quagga mussels to survive and grow under clear-water conditions or where there is near-bed depletion of food resources (see MacIsaac et al. 1999).

Could the generally faster growth we found for quagga mussels also result from their ability to selectively ingest and assimilate the organic fraction of seston? Whereas zebra and quagga mussels both showed an ability to selectively reject the inorganic fraction of Oneida Lake seston (at least over low to moderate seston levels (~3–22 $mg \cdot L^{-1}$) that are also common in other freshwater habitats; e.g., Fanslow et al. 1995; Roditi et al. 1996; Schneider et al. 1998), we detected no difference in the quality (O:I) or quantity of pseudofeces produced by these species. Our patterns of selection are similar to those reported by Schneider et al. (1998), where zebra mussels fed Illinois River seston produced pseudofeces at concentrations >3 $mg \cdot L^{-1}$ and enriched pseudofeces in inorganics over all but the lowest (<~0.5) quality levels (O:I) of seston. Although our seston experiment did not indicate species differences in selection, it did show that quagga mussels, like zebra mussels, can perceive and reject inorganic material from seston. In addition, our clay experiment also indicated that zebra and quagga mussels perceive and respond to the presence of inorganic particles similarly. Here, both species reduced their clearance rates and feeding activity as the total concentration of particles (particularly clay particles) increased. MacIsaac and Rocha (1995) also found a behavioral reaction by zebra mussels (valve closure) to the presence of clay but they did not increase their avoidance of clay as concentrations were elevated to 250 $mg \cdot L^{-1}$. Our study does not indicate that zebra or quagga mussels ingest different amounts of organic matter via selection, but their ability to enhance ingestion of nutritious organic particles would presumably allow quagga mussels to feed as effectively as zebra mussels in shallow, turbid areas of the littoral zone where resuspension often increases the inorganic fraction of seston.

Faster quagga mussel growth may be linked to higher food assimilation and lower metabolic costs. We did find significantly higher assimilation efficiency by quagga mussels, but only when fed a low concentration of seston (~2 $mg \cdot L^{-1}$). Coincidentally, perhaps, most of our experiments showed higher growth of quagga mussels over low food concentrations. Our estimates of assimilation are similar to those reported by other investigators using zebra mussels and natural seston (Stoeckmann and Garton 1997; Schneider et al. 1998), as are our declines in assimilation over high seston quantity and low seston quality (O:I) (Schneider et al. 1998). However, more work is needed to see whether species differences in assimilation are common in situ where zebra and quagga mussels encounter seston that fluctuates in quantity and quality over daily to seasonal time scales. Complete energy budgets like those constructed for zebra mussels (e.g., Sprung 1995; Stoeckman and Garton 1997; Schneider et al. 1998) are also needed for quagga mussels. Although our starvation experiment is limited in use, the greater mortality of zebra mussels along with their high weight loss suggests that they may have higher metabolic demands than quagga mussels. This may explain, in part, why zebra mussels have higher biomass-specific clearance rates and why they typically grew less than quagga mussels, except where food levels were extremely high (e.g., 100% food treatment using Oneida Lake seston).

Ecological implications

In the lower Great Lakes, quagga mussels likely have widespread, if unmeasured, impacts that may increase in importance if their populations grow and spread. Our results suggest that quagga mussels grow under wider food and temperature conditions than zebra mussels and that they may increase in abundance, particularly where food levels are low. As a result, dreissenid populations in the lower Great Lakes may remain abundant and they may become increasingly dominated by quagga mussels in both profundal zones and littoral zones where phytoplankton biomass has declined (e.g., Mitchell et al. 1996; Mills et al. 1999; E.L. Mills unpublished data). Such trends in the profundal zone may exacerbate declines in native macroinvertebrates like the amphipod *Diporeia*, and in turn alter fish production (e.g., Dermott and Kerec 1997; Nalepa et al. 1998; Lozano et al. 2001). In the littoral zone during summer, quagga mussels may not alter the rates of dreissenid filtration on the pelagic community, but it is unclear whether they are more likely to consume detritus and heterotrophic plankton as they may do in the profundal zone. Because quagga mussels grew as much as 20 times faster than zebra mussels at temperatures as low as 6°C, profundal and littoral zone quagga mussels may also feed more actively under these conditions and thus remove a larger portion of spring phytoplankton blooms (e.g., 3–5°C in Oneida Lake, E.L. Mills, unpublished data; 2–8°C in Lakes Ontario and Erie, Millard et al. 1995; Vega 2000) than zebra mussels, whose optimal feeding rates are between 10 and 20°C (e.g., Walz 1978; Reeders and bij de Vaate 1990; Fanslow et al. 1995). With improved measurements of the biomass of littoral zone quagga populations it should now be possible to estimate their filtration rates at ~20°C over a wide range of chl *a* levels. Further work on quagga mussel clearance of natural seston at colder temperatures will facilitate whole-lake (which include profundal populations) and seasonal filtration estimates.

Will quagga mussels remain confined to the lower Great Lakes? Higher populations in littoral zones should favor their spread to other lakes as may have happened recently in Lake Michigan (Fleisher et al. 2001) and Lake St. Clair (Igor Grigorovich, Department of Biology, University of Windsor, Windsor, Ont., personal communication). Assuming they continue to expand their range, our work indi-

© 2002 NRC Canada

cates high growth and survival of quagga mussels in warm, productive inland lakes such as Onondaga and Oneida and perhaps even in colder water lakes at higher latitudes. And if the population spread of quagga mussels in the Ukraine (Mills et al. 1996) serves as a guide for North America, quagga mussels will spread over decadal time scales and they will become important and possibly dominant members of benthic communities.

Acknowledgements

We thank the captains and crews of the R/V *Seth Green* and the R/V *Argo* for help in collecting mussels from lakes Ontario and Erie, respectively. We are also grateful for the assistance of Mr. Timothy Sinnott and the staff of the New York State Department of Environmental Conservation (NYSDEC). This manuscript benefited greatly from the comments of two anonymous reviewers. Tim Negley, Damon Cone, and Alex Nixon all performed expert lab analyses in support of this study and Robin Lock provided invaluable advice on statistical tests. We thank the U.S. Fish & Wildlife Service (cooperative agreement 50181-J038 with NYSDEC and Cornell University), St. Lawrence University, and Cornell University for financial support. Contribution No. 205 of the Cornell Biological Field Station.

References

Ackerman, J.D. 1999. Effect of velocity on the filter feeding of dreissenid mussels (*Dreissena polymorpha* and *Dreissena bugensis*): implications for trophic dynamics. Can. J. Fish. Aquat. Sci. **56**: 1551–1561.

Baldwin, B.S., and Newell, R.I.E. 1995. Relative importance of different size food particles in the natural diet of oyster larvae (*Crassostrea virginica*). Mar. Ecol. Prog. Ser. **120**: 135–145.

Bayne, B.L. 1976. Marine mussels: their ecology and physiology. Cambridge University Press, Cambridge.

Bially, A., and MacIsaac, H.J. 2000. Fouling mussels (*Dreissena* spp.) colonize soft sediments in Lake Erie and facilitate benthic invertebrates. Freshwater Biol. **43**: 85–97.

Chow-Fraser, P., and Sprules, W.G. 1992. Type-3 functional response in limnetic suspension-feeders, as demonstrated by in situ grazing rates. Hydrobiologia, **232**: 175–191.

Claxton, T.W., and Mackie, G.L. 1998. Seasonal and depth variations in gametogenesis and spawning of *Dreissena polymorpha* and *Dreissena bugensis* in eastern Lake Erie. Can. J. Zool. **76**: 2010–2019.

Claxton, T.W., Wilson, A.B., Mackie, G.L., and Boudling, E.G. 1998. A genetic and morphological comparison of shallow- and deep-water populations of the introduced dreissenid bivalve *Dreissena bugensis*. Can. J. Zool. **76**: 1269–1276.

Conover, R.J. 1966. Assimilation of organic matter by zooplankton. Limnol. Oceanogr. **11**: 338–345.

Cotner, J.B., Gardner, W.S., Johnson, J.R., Sada, R.H., Cavaletto, J.F., and Heath, R.T. 1995. Effects of zebra mussels (*Dreissena polymorpha*) on bacterioplankton: evidence for both size-selective consumption and growth stimulation. J. Gt. Lakes Res. **21**: 517–528.

Dermott, R., and Kerec, D. 1997. Changes to the deepwater benthos of eastern Lake Erie since the invasion of *Dreissena*: 1979–1993. Can. J. Fish. Aquat. Sci. **54**: 922–930.

Dorgelo, J., and Smeenk, J.W. 1988. Contribution to the ecophysiology of *Dreissena polymorpha* (Pallas) (Mollusca: Bivalvia): growth, filtration rate and respiration. Verh. Int. Verein. Limnol. **23**: 2201–2208.

Fahnenstiel, G.L., Lang, G.A., Nalepa, T.F., and Johengen, T.H. 1995. Effects of zebra mussel (*Dreissena polymorpha* Pallas) colonization on water quality parameters in Saginaw Bay, Lake Huron. J. Gt. Lakes Res. **21**: 435–448.

Fanslow, D.L., Nalepa, T.F., and Lang, G.A. 1995. Filtration rates of the zebra mussel (*Dreissena polymorpha*) on natural seston from Saginaw Bay, Lake Huron. J. Gt. Lakes Res. **21:** 489–500.

Fleischer, G.W., DeScorcie, T.J., and Holuszko, J.D. 2001. Lake-wide distribution of *Dreissena* in Lake Michigan, 1999. J. Gt. Lakes Res. **27**: 252–257.

Gardner, J.P.A. 1994. The structure and dynamics of naturally occurring hybrid *Mytilus edulis* Linnaeus, 1758 and *Mytilus galloprovincialis* Lamarck, 1819 (Bivalvia: Mollusca) populations: review and interpretation. Arch. Hydrobiol. (Suppl.), **99**: 37–71.

Garton, D.W., and Johnson, L.E. 2000. Variation in growth rates of the zebra mussel, *Dreissena polymorpha*, within Lake Wawasee. Freshwater Biol. **45**: 443–451.

Guillard, R.R. 1975. Culture of phytoplankton for feeding marine invertebrates. *In* Culture of marine invertebrate animals. *Edited by* W.L. Smith and M.H. Chanley. Plenum Press, New York. pp. 29–60.

Horgan, M.J., and Mills, E.L. 1997. Clearance rates and filtering activity of zebra mussel (*Dreissena polymorpha*): implications for freshwater lakes. Can. J. Fish. Aquat. Sci. **54**: 249–255.

Idrisi, N., Mills, E.L., Rudstam, L.G., and Stewart, D.J. 2001. Impact of zebra mussels (*Dreissena polymorpha*) on the pelagic lower trophic levels of Oneida Lake, New York. Can. J. Fish. Aquat. Sci. **58**: 1–12.

Kryger, J., and Riisgard, H.U. 1988. Filtration rate capacities in 6 species of European freshwater bivalves. Oecologia, **77**: 34–38.

Lavrentyev, P.J., Gardner, W.S, Cavaletto, J.F., and Beaver, J.R. 1995. Effects of the zebra mussel (*Dreissena polymorpha* Pallas) on protozoa and phytoplankton from Saginaw Bay, Lake Huron. J. Gt. Lakes Res. **21**: 545–557.

Leach, J.H. 1993. Impacts of the zebra mussel (*Dreissena polymorpha*) on the water quality and fish spawning reefs in western Lake Erie. *In* Zebra mussels: biology, impacts, and control. *Edited by* T.F. Nalepa and D.W. Schloesser. Lewis Publishers, Inc. (CRC Press), Boca Raton, Fla. pp. 381–397.

Lozano, S.J., Scharold, J.V., and Nalepa, T.F. 2001. Recent declines in benthic macroinvertebrate densities in Lake Ontario. Can. J. Fish. Aquat. Sci. **58**: 518–529.

MacIsaac, H.J. 1994. Comparative growth and survival of *Dreissena polymorpha* and *Dreissena bugensis*, exotic mollusks introduced to the Great Lakes. J. Gt. Lakes Res. **20**: 783–790.

MacIsaac, H.J., and Rocha, R. 1995. Effects of suspended clay on zebra mussel (*Dreissena polymorpha*) faeces and pseudofaeces production. Arch. Hydrobiol. **135**: 53–64.

MacIsaac, H.J., Johannsson, O.E., Ye, J., Spriles, W.G., Leach, J.H., McCorquodale, J.A., and Grigorovich, I.A. 1999. Filtering impacts of an introduced bivalve (*Dreissena polymorpha*) in a shallow lake: application of a hydrodynamic model. Ecosystems, **2**: 338–350.

Makarewicz, J.C., Lewis, T.W., and Bertram, P. 1999. Phytoplankton composition and biomass in the offshore waters of Lake Erie: pre- and post-*Dreissena* introduction (1983–1993). J. Gt. Lakes Res. **25**: 135–148.

Martel, A.L., Baldwin, B.S., Dermott, R.M., and Lutz, R.A. 2001. Species and epilimnion/hypolimnion-related differences in size at larval settlement and metamorphosis in *Dresissena* (Bivalvia). Limnol. Oceanogr. **46**: 707–713.

© 2002 NRC Canada

Millard, E.S., Myles, D.D., Johannsson, O.E., and Ralph, K.M. 1995. Seasonal phosphorous deficiency of Lake Ontario phytoplankton at two index stations: light versus phosphorous limitation of growth. Can. J. Fish. Aquat. Sci. **53**: 1112–1124.

Mills, E.L., Dermott, R.M., Roseman, E.F., Dustin, D., Mellina, E., Conn, D.B., and Spidle, A.P. 1993. Colonization, ecology, and population structure of the "quagga" mussel (Bivalvia: Dreissenidae) in the lower Great Lakes. Can. J. Fish. Aquat. Sci. **50**: 2305–2314.

Mills, E.L., Rosenberg, G., Spidle, A.P., Ludyanskiy, M., Pligin, Y., and May, B. 1996. A review of the biology and ecology of the quagga mussel (*Dreissena bugensis*), a second species of freshwater dreissenid introduced to North America. Am. Zool. **36**: 271–286.

Mills, E.L., Chrisman, J.R., Baldwin, B.S., Howell, T., Owens, R.W., O'Gorman, R., Roseman, E.F., and Raths, M.K. 1999. Changes in the dreissenid community and a shift toward dominance of the quagga mussel (*Dreissena bugensis*) in the lower Great Lakes. J. Gt. Lakes Res. **25**: 187–197.

Mitchell, J.S., Bailey, R.C., and Knapton, R.W. 1996. Abundance of *Dreissena polymorpha* and *Dreissena bugensis* in a warmwater plume: effects of depth and temperature. Can. J. Fish. Aquat. Sci. **53**: 1705–1712.

Nalepa, T.F., Hartson, D.J., Fanslow, D.L., Lang, G.A., and Lozano, S.J. 1998. Decline in benthic macroinvertebrate populations in southern Lake Michigan, 1980–1993. Can. J. Fish. Aquat. Sci. **55**: 2404–2413.

Negley, T.L., Mills, E.L., Baldwin, B.S., O'Gorman, R., and Owens, R.W. 2001. Invasion of Lake Ontario by the zebra mussel (*Dreissena polymorpha*) and quagga mussel (*D. bugensis*): historical development and ecological implications. *In* The state of Lake Ontario. Vol. 1. Ecovision World Monograph Series, Backhuys Publishers, Leiden, The Netherlands.

Reeders, H.H., and bij de Vaate, A. 1990. Zebra mussels (*Dreissena polymorpha*): a new perspective for water quality management. Hydrobiologia, **200/201**: 437–450.

Roditi, H.A., Caraco, N.F., Cole, J.J., and Strayer, D.L. 1996. Filtration of Hudson River water by the zebra mussel (*Dreissena polymorpha*). Estuaries, **19**: 824–832.

Roditi, H.A., Fisher, N.S., and Sanudo-Wilhelmy, S.A. 2000. Uptake of dissolved organic carbon and trace elements by zebra mussels. Nature (London), **407**: 78–80.

Roe, S.L., and MacIsaac, H.J. 1997. Deepwater population structure and reproductive state of quagga mussels (*Dreissena bugensis*) in Lake Erie. Can. J. Fish. Aquat. Sci. **54**: 2428–2433.

Schneider, D.W., Madon, S.P., Stoeckel, J.A., and Sparks, R.E. 1998. Seston quality controls zebra mussel (*Dreissena polymorpha*) energetics in turbid rivers. Oecologia, **117**: 331–341.

Sea Grant National Aquatic Nuisance Species Clearinghouse. 2001. New York Sea Grant, Morgan II SUNY College at Brockport, NY 14420, U.S.A. (http://www.cce.cornell.edu/aquaticinvaders/)

Smit, H., bij de Vaate, A., and Fioole, A. 1992. Shell growth of the zebra mussel (*Dreissena polymorpha* Pallas) in relation to selected physico-chemical parameters in the Lower Rhine and some associated lakes. Arch. Hydrobiol. **124**: 257–280.

Sprung, M. 1995. Physiological energetics of the zebra mussel *Dreissena polymorpha* in lakes. I. Growth and reproductive effort. Hydrobiologia, **304**: 117–132.

Sprung, M., and Rose, U. 1988. Influence of food size and food quantity on the feeding of the mussel *Dreissena polymorpha*. Oecologia, **77**: 526–532.

Stoeckmann, A.M., and Garton, D.W. 1997. A seasonal energy budget for zebra mussel *Dreissena polymorpha* in western Lake Erie. Can. J. Fish. Aquat. Sci. **54**: 2743–2751.

Strickland, J.D.H., and Parsons, T.R. 1972. A practical handbook of seawater analysis. 2nd ed. Bull. Fish. Res. Board Can. No. 167.

Thorp, J.H., Alexander, J.E., Bukaveckas, B.L., Cobbs, G.A., and Bresko, K.L. 1998. Responses of Ohio River and Lake Erie dreissenid molluscs to changes in temperature and turbidity. Can. J. Fish. Aquat. Sci. **55**: 220–229.

Vega, S. 2000. Lower trophic interactions in the eastern basin of Lake Erie after the invasion of dreissenids. M.Sc. thesis, College of Environmental Science and Forestry, The State University of New York, Syracuse.

Walz, N. 1978. The energy balance of the freshwater mussel *Dreissena polymorpha* Pallas in laboratory experiments and in Lake Constance. I. Pattern of activity, feeding and assimilation efficiency. Arch. Hydrobiol. **55**(Suppl.): 83–105.

Zolotareva, V.I, Makhonina, A.V., and Dyga, A.K. 1978. The filtration rate of *Dreissena bugensis* Andrusov. Malacol. Rev. **11**: 96–97.

© 2002 NRC Canada

Estimating riverine fish population size from single- and multiple-pass removal sampling using a hierarchical model

Robin J. Wyatt

Abstract: A hierarchical model is described for estimating population size from single- and multiple-pass removal sampling. The model is appropriate for two-stage sampling schemes, typified by surveys of riverine fish populations, in which multiple sites are surveyed, but a low number of passes are undertaken at each site. The model estimates the average population size within the target area from the raw catch data, and thus allows for differences in the sampling procedure at each site, such as including single-pass sampling. The model also uses the data from all sites to estimate the population size at each individual site. This results in generally improved precision for multiple-pass sites and provides comparable estimates from single-pass sites. A Bayesian approach is described for estimating the parameters of the hierarchical model using sampling importance resampling (SIR). An empirical Bayesian approach, which ignores prior uncertainty but is simpler to implement, is also described. Application of the hierarchical model is illustrated with electrofishing data for 0+ trout (*Salmo trutta*) in the River Inny, U.K.

Résumé : On trouvera ici un modèle hiérarchique qui permet d'estimer la taille d'une population à partir d'un échantillonnage par retraits uniques ou répétés. Le modèle est approprié à un plan d'échantillonnage à deux étapes, comme, par exemple, dans les inventaires de poissons de rivière où de nombreux sites sont inventoriés, mais avec un petit nombre d'échantillonages à chaque site. Le modèle estime la taille moyenne de la population dans la zone ciblée à partir des données brutes de capture et ainsi s'accommode de différences de stratégie d'échantillonnage d'un site à l'autre et peut, en particulier, inclure les données d'un échantillonnage unique. Le modèle utilise aussi les données recueillies à tous les sites pour estimer la taille de la population à chacun des sites. Il en résulte généralement une précision accrue pour les sites échantillonnés à plusieurs reprises et une précision comparable pour les sites échantillonnés une seule fois. Une approche bayésienne, décrite ici, permet d'estimer les paramètres du modèle hiérarchique à l'aide d'un échantillonnage d'importance et d'un rééchantillonnage (modélisation SIR). On trouvera aussi une approche empirique bayésienne qui ignore l'incertitude a priori et qui est plus simple à utiliser. L'étude de données obtenues par pêche électrique sur des truites (*Salmo trutta*) de l'Inny, au Royaume-Uni, illustre le genre d'application qu'on peut faire du modèle hiérarchique.

[Traduit par la Rédaction]

Introduction

Surveys of riverine fish populations typically involve subsampling or two-stage sampling (Cochran 1977; Barnett 1991), in which the fish population is sampled in two distinct stages. In the first stage of sampling, a number of sites are randomly selected from the section or sections of river to which the conclusions of the data analysis are to be applied, termed the target area. In the second stage, a sample of fish is captured at each site from the total number of fish present. The objective of the survey may be either to draw conclusions about the target area as a whole or to draw conclusions about the individual sampling sites.

Received 19 July 2001. Accepted 25 February 2002. Published on the NRC Research Press Web site at http://cjfas.nrc.ca on 18 May 2002.
J16455

R.J. Wyatt. National Salmon and Trout Fisheries Centre, Environment Agency, Rivers House, St. Mellons Business Park, St. Mellons, Cardiff, CF3 0LT, U.K. (e-mail: robin.wyatt@environment-agency.gov.uk).

The statistical methods applied to data collected from two-stage sampling needs to reflect the nested structure of the between-site variation, associated with the first stage of sampling, and the within-site variation, associated with the second stage of sampling. When the interest is in the mean of the target area, standard two-stage sampling equations can be used (Cochran 1977; Barnett 1991), but when the site-specific effects are also of interest, it may be necessary to apply hierarchical or multilevel models (Goldstein 1995; Snijders and Bosker 1999). For simple data such as individual fish lengths and weights, hierarchical models and two-stage sampling equations can be readily applied. However, when the parameter of interest is the abundance of fish, multiple-capture procedures (Seber 1982) are used to collect data from each site, and the analysis of hierarchical data presents a more complex statistical problem.

A common multiple-capture procedure for estimating abundance at a single site is removal sampling, in which fish are repeatedly removed from a closed population without replacement, using constant effort on each pass of a net or electrode. There are numerous statistical methods for estimating the population size at a single site, and many are

 DOI: 10.1139/F02-041 © 2002 NRC Canada

based on a simple binomial model that assumes a constant capture probability between individuals and successive passes (Moran 1951). For example, point estimates of the population size can be obtained from the approximate maximum likelihood method of Zippin (1956) or the exact maximum likelihood method of Carle and Strub (1978). The latter authors also developed a marginal likelihood function weighted by prior knowledge of the capture probability. There is also a range of methods for obtaining interval estimates for the population size (e.g., Schnute 1983; Harding et al. 1984; Hirst 1994). When large numbers of passes are undertaken, it is possible to apply more realistic statistical models that allow for a systematic decline in capture probability between passes (Schnute 1983), random variation in capture probability between passes (Wang and Loneragan 1996; Wang 1999), and random variation in capture probability between individual fish (Lee and Chao 1994; Chao and Chang 1999).

In the context of estimating population size in riverine fish populations, the removal method is applied to multiple sites selected randomly from the target area. When the interest is in the population size of the target area as a whole, a common approach is to apply approximate two-stage sampling equations to the site-specific population estimates. When site areas are constant, the simple random sampling estimator of Bohlin (1981) can be used, or when site areas vary, the ratio estimator of Hankin (1984) may give improved estimates. These estimators give equal weight to the population estimates from each site, which may be inappropriate when the effort or sampling efficiency varies between sites. When the interest is in the site-specific population estimates, the repeated application of removal estimators (e.g., Carle and Strub 1978) inappropriately regards survey sites as independent, fixed treatments. The resulting site-specific population estimates will therefore not correctly reflect that the sites were randomly selected from the target area.

When the objective of a survey is to estimate trends or detect differences in abundance, single-pass removal sampling is commonly used to generate cost-effective indices of relative abundance. Such methods typically involve sampling a measured area of river (Strange et al. 1989; Jones and Stockwell 1995; Mitro and Zale 2000) or sampling for a fixed unit of time (Crozier and Kennedy 1994). Single-pass removal sampling has also been used to estimate population size by calibrating the procedure against estimates from multiple-pass removal sampling. Most calibration studies have used regression models of the population estimates from removal sampling against single-pass catches from the same sites, whereas Mitro and Zale (2000) estimated a mean capture probability from multiple-pass sites and applied it to the single-pass sites.

The objective of this study was to develop a hierarchical model for the raw catch data obtained from single- and multiple-pass sampling. A single hierarchical model would permit the simultaneous estimation of the population size at individual sites and the population size of the target area as a whole. It would therefore replace the use of removal estimators at multiple-pass sites (e.g., Carle and Strub 1978), calibration procedures at single-pass sites (e.g., Mitro and Zale 2000), and approximate two-stage sampling equations for population estimation of the target area (e.g., Hankin 1984).

Hierarchical models can be implemented using frequentist or Bayesian inference, and a Bayesian approach will be developed here. The Bayesian approach to data analysis is well established (O'Hagan 1994; Gelman et al. 1995; Carlin and Louis 2000) and has been contrasted with alternative approaches to statistical inference by Barnett (1999). In Bayesian inference, prior probability distributions are specified for every unknown parameter in the model to reflect the degree of belief regarding possible values of that parameter prior to observing the data. The prior distributions are then modified by the likelihood function of the sample data through the application of Bayes' Theorem to give a posterior probability distribution for the unknown parameters. One advantage of the Bayesian approach is that the posterior distribution allows direct probabilistic statements to be made about the unknown parameters, given the sample data. In contrast, frequentist confidence intervals reflect the long-term performance of the estimation procedure over a large number of data sets. Bayesian methods are becoming increasingly common in fisheries management (Punt and Hilborn 1997; McAllister and Kirkwood 1998), where the probabilistic approach provides a natural basis for decision making. The application of Bayesian inference to hierarchical models is described in detail by Gelman et al. (1995), and has been used to address a wide range of fisheries problems (Liermann and Hilborn 1997; Harley and Myers 2001; Su et al. 2001).

Methods

Alternative models for removal data

Specification of a fixed-effects model for multiple-pass sites

Fixed effects are used to describe treatments imposed by an experiment where it is the effect of those specific choices of treatment that are of interest. A fixed-effects model for a fish population survey therefore regards each of the m sites as independent, fixed treatments. At the ith site ($i = 1, 2, \ldots, m$), k_i passes are undertaken ($k_i \geq 1$) and the number of fish present prior to the jth pass ($j = 1, \ldots, k_i$) is denoted n_{ij}. In common with many simple removal estimators, the capture probability at the ith site (q_i) is assumed constant for all fish and all passes.

The number of fish captured at the ith site on the jth pass (c_{ij}) will follow a binomial distribution

$$c_{ij} \sim \text{binomial}(n_{ij}, q_i)$$

The number of fish remaining after the jth pass is then

$$n_{i,j+1} = n_{ij} - c_{ij}$$

These two equations describe the binomial model on which simple removal estimators are based (Moran 1951). The fixed-effects model can be displayed graphically, where nodes denote the stochastic and deterministic model components and arrows denote the parent–child dependencies between them (Fig. 1*a*). Deterministic nodes are shown to be related to their parents by thick arrows (i.e., $n_{i,j+1}$) and stochastic nodes are either the founder (parentless) nodes (i.e., q_i and n_{i1}) or those shown to be related to their parents by thin arrows (i.e., c_{ij}). Model components that are repeated

© 2002 NRC Canada

Fig. 1. Graphical representation of two statistical models for removal data from several sites. (*a*) A fixed-effects model and (*b*) a hierarchical model. See text for explanation.

(a)

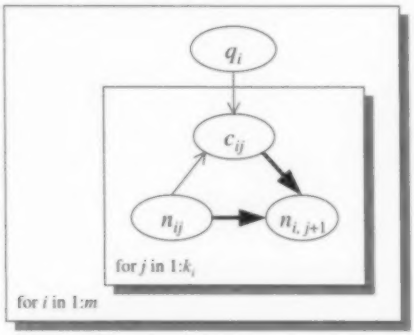

(b)

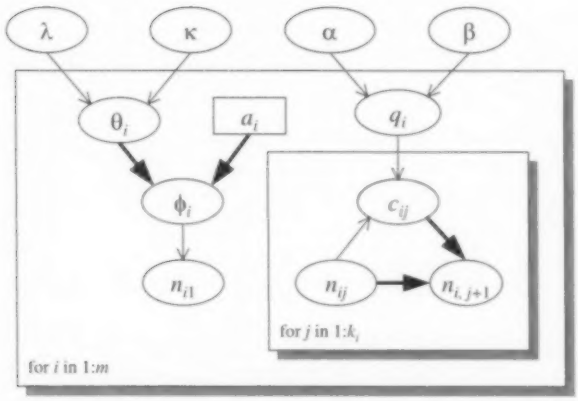

over different sites (i) and passes (j) are enclosed within the rectangular plates. The likelihood function for the fixed-effects model is derived in Appendix A.

Specification of a hierarchical model for single and multiple-pass sites

In contrast to a fixed-effects model, each site in a hierarchical random-effects model is regarded as having been sampled at random from a large population of sites. Only then is it possible to make some inference about this population, and as with a fixed-effects model, inferences about the individual sites can also be made. The between-site variation in fish density as number per area (θ_i) is assumed to follow a gamma distribution, described by the population parameters λ and κ, which are defined in Appendix B.

$$\theta_i \sim \text{gamma}(\lambda, \kappa)$$

The between-site variation in the capture probability (q_i) is assumed to follow a beta distribution, described by the population parameters α and β, also defined in Appendix B.

$$q_i \sim \text{beta}(\alpha, \beta)$$

The gamma distribution is an appropriate choice of probability distribution for a positive, continuous variable like density, and the beta distribution is a common choice for describing proportions. Both the gamma and beta distributions also allow the hierarchical model to be developed algebraically.

The population of fish prior to the first pass at the ith site (n_{i1}, hereafter denoted n_i) will follow a Poisson distribution

$$n_i \sim \text{Poisson}(\phi_i)$$

where $\phi_i = \theta_i a_i$ for a site of area a_i. The hierarchical model can also be displayed graphically, where the site area (a_i) is shown as a rectangle to denote a constant (Fig. 1*b*). With a hierarchical model, the data from all m sites influence the estimate of the population size (n_i) at each site through the shared population parameters. The likelihood function for the hierarchical model is derived in Appendix B.

Comparison of fixed-effects and hierarchical models for multiple-pass sites

Before developing a Bayesian approach in more detail, the relative performance of the fixed-effects and hierarchical models was informally investigated by comparing the likelihood functions for the site-specific population estimates. The likelihood function is central to both Bayesian and frequentist inference, and in the absence of prior information, the frequentist maximum likelihood estimate will be very similar to the mode of the Bayesian posterior distribution. The properties of the two models were compared by calculating the maximum likelihood estimates for the site-specific population sizes from simulated data. Different models will tend to give the same estimates for sites with a large number of passes and a high capture probability, and so the models were compared for data comprising a low number of removals ($k_i = 2$) and a low expected capture probability ($E(q_i) = 0.3$). The expected density of fish ($E(\theta_i)$) was 0.1 m^{-2}, the expected site area ($E(a_i)$) was 200 m^2, and the between-site standard deviation in area was 40 m^2. Three extreme scenarios were considered with different degrees of spatial variability, comprising (*i*) low variability for both capture probability ($V(q_i) = 1.00 \times 10^{-4}$) and density ($V(\theta_i) = 1.00 \times 10^{-6}$), (*ii*) high variability for capture probability ($V(q_i) = 2.25 \times 10^{-2}$), low for density, and (*iii*) low variability for capture probability, high for density ($V(\theta_i) = 1.00 \times 10^{-2}$). Catch data were generated at random from 500 sites, and maximum likelihood estimates of the four population parameters were obtained by finding the values that maximized eq. B.7, using a maximization routine within a spreadsheet. Marginal maximum likelihood estimates for the site-specific population sizes were then obtained from the fixed-effects model (eq. A.2) and the hierarchical model (eq. B.5).

Comparison of mean capture probability method and hierarchical model for single-pass sites

Population estimates from the hierarchical model for single-pass sites were also compared to estimates derived from the mean capture probability method. For each of the fixed-effects estimates ($\hat{n}_i$) for the 500 multiple-pass sites, the capture probability was estimated from the expression (Moran 1951)

$$\hat{q}_i = \frac{t_i}{k_i \hat{n}_i - x_i}$$

© 2002 NRC Canada

where t_i and x_i summarize the data $\underline{c}_i$ at the ith site as follows:

$$t_i = \sum_{j=1}^{k_i} c_{ij} \text{ and } x_i = \sum_{j=1}^{k_i} (k_i - j)c_{ij}$$

Catches from an additional 500 single-pass sites were then simulated. Population estimates for these sites were obtained from the hierarchical model using the population parameter estimates from the multiple-pass sites and from the mean capture probability of the fixed-effects estimates.

Bayesian estimation of the hierarchical model

Marginal posterior distribution for site-specific population size (n_i)

The joint posterior distribution for the population size (n_i) and the capture probability (q_i), conditional on the site-specific catches ($\underline{c}_i$), site area (a_i), and population parameters ($\alpha, \beta, \lambda, \kappa$), is obtained from Bayes' Theorem

$$p(n_i, q_i|\underline{c}_i, a_i, \alpha, \beta, \lambda, \kappa) \propto p(\underline{c}_i|n_i, q_i)\, p(n_i|a_i, \lambda, \kappa)\, p(q_i, \alpha, \beta)$$

where $p(\underline{c}_i|n_i, q_i)$ is the likelihood of the site-specific catch data (eq. A.1), $p(n_i|a_i, \lambda, \kappa)$ is the prior distribution for n_i, conditional on a_i, λ, and κ, and $p(q_i|\alpha, \beta)$ is the prior distribution for q_i, conditional on α and β.

The marginal posterior distribution for the population size, conditional on the population parameters, is therefore given by

$$p(n_i|\underline{c}_i, a_i, \alpha, \beta, \lambda, \kappa) \propto p(\underline{c}_i, n_i|a_i, \alpha, \beta, \lambda, \kappa)$$

Substituting eq. B.4 gives

$$(1) \quad p(n_i|\underline{c}_i, a_i, \alpha, \beta, \lambda, \kappa) \propto \frac{\Gamma(\beta + k_i n_i - x_i - t_i)\Gamma(\kappa + n_i)(\lambda a_i)^{n_i}}{(n_i - t_i)!\Gamma(\alpha + \beta + k_i n_i - x_i)(\lambda a_i + \kappa)^{n_i}}, \quad n_i = t_i, t_i + 1, t_i + 2, \ldots$$

Note that for a single-pass site, $k_i = 1$, and so $t_i = c_{i1}$ and $x_i = 0$.

A simple approximation to the posterior distribution can be obtained by substituting point-estimates of the population parameters into eq. 1.

$$(2) \quad p(n_i|\underline{c}_i, a_i, \hat{\alpha}, \hat{\beta}, \hat{\lambda}, \hat{\kappa}) \propto \frac{\Gamma(\hat{\beta} + k_i n_i - x_i - t_i)\Gamma(\hat{\kappa} + n_i)(\hat{\lambda} a_i)^{n_i}}{(n_i - t_i)!\Gamma(\hat{\alpha} + \hat{\beta} + k_i n_i - x_i)(\hat{\lambda} a_i + \hat{\kappa})^{n_i}}, \quad n_i = t_i, t_i + 1, t_i + 2, \ldots$$

This approximation is sometimes termed an empirical Bayesian approach (Carlin and Louis 2000). However, when the number of sites (m) is small, the uncertainty associated with estimating the population parameters may be important, and a fully Bayesian approach is required. This is achieved by integrating over the joint posterior probability distributions of the population parameters ($p(\alpha, \beta, \lambda, \kappa|\underline{c}, \underline{a})$).

Table 1. Catches (c_{ij}) of 0+ trout from an electrofishing survey of the River Inny, U.K., in 1996.

Site (i)	Area (a_i) (m^2)	Pass (j)		
		1	2	3
1	350.4	30	14	13
2	253.2	16	—	—
3	444.7	41	—	—
4	406.3	28	8	4
5	600.0	11	—	—
6	425.7	11	—	—
7	665.0	18	—	—
8	504.3	11	2	3
9	410.0	8	—	—
10	639.4	3	3	3
11	904.0	0	—	—
12	111.5	14	14	7
13	301.6	11	—	—
14	307.8	17	—	—
15	531.0	19	—	—
16	396.2	44	24	14
17	264.6	44	22	5
18	259.5	35	7	8
19	323.2	42	22	9
20	134.4	10	—	—

$$(3) \quad p(n_i|\underline{c}, \underline{a}) = \int_0^\infty \int_0^\infty \int_0^\infty \int_0^\infty p(n_i|\underline{c}_i, a_i, \alpha, \beta, \lambda, \kappa)\, p(\alpha, \beta, \lambda, \kappa|\underline{c}, \underline{a})\, d\alpha\, d\beta\, d\lambda\, d\kappa$$

To estimate the posterior probability distributions for the site-specific population sizes using a Bayesian or approximate empirical Bayesian approach it is therefore necessary to obtain the joint posterior distribution for the population parameters.

Joint posterior distribution for the population parameters ($\alpha, \beta, \lambda, \kappa$)

The joint posterior distribution for the population parameters $\alpha, \beta, \lambda, \kappa$, conditional on the observed catches ($\underline{c} = \underline{c}_1, \ldots, \underline{c}_m$) and site areas ($\underline{a} = a_1, \ldots, a_m$), is obtained from Bayes' Theorem

$$(4) \quad p(\alpha, \beta, \lambda, \kappa|\underline{c}, \underline{a}) \propto p(\underline{c}|\underline{a}, \alpha, \beta, \lambda, \kappa)\, p(\alpha, \beta)\, p(\lambda, \kappa)$$

where $p(\underline{c}|\underline{a}, \alpha, \beta, \lambda, \kappa)$ is the likelihood of all of the catches from the target area (eq. B.7), $p(\lambda, \kappa)$ is the joint prior distribution for population parameters λ and κ, and $p(\alpha, \beta)$ is the joint prior distribution for population parameters α and β.

The population parameters ($\alpha, \beta, \lambda, \kappa$) are stochastic founder nodes in the model (Fig. 1*b*), and in the absence of any prior information require the specification of locally uninformative prior distributions. The choice of prior distributions in Bayesian inference is a complex subject, and in practical applications, it is important that the sensitivity of the posterior distributions to the choice of prior is evaluated. For demonstration purposes, the joint prior distribution for population parameters λ and κ was chosen to be uniform on the log mean population density ($\log(\lambda)$) and associated variability ($\kappa^{-1/2}$). On the original scale, the joint prior is

© 2002 NRC Canada

Fig. 2. Comparison of site-specific population estimates from simulated multiple-removal data for the fixed-effects and hierarchical models. Three data sets were used with different degrees of spatial variability. (*a*) Low variability for both capture probability and density, (*b*) high variability for capture probability, low for density, and (*c*) low variability for capture probability, high for density.

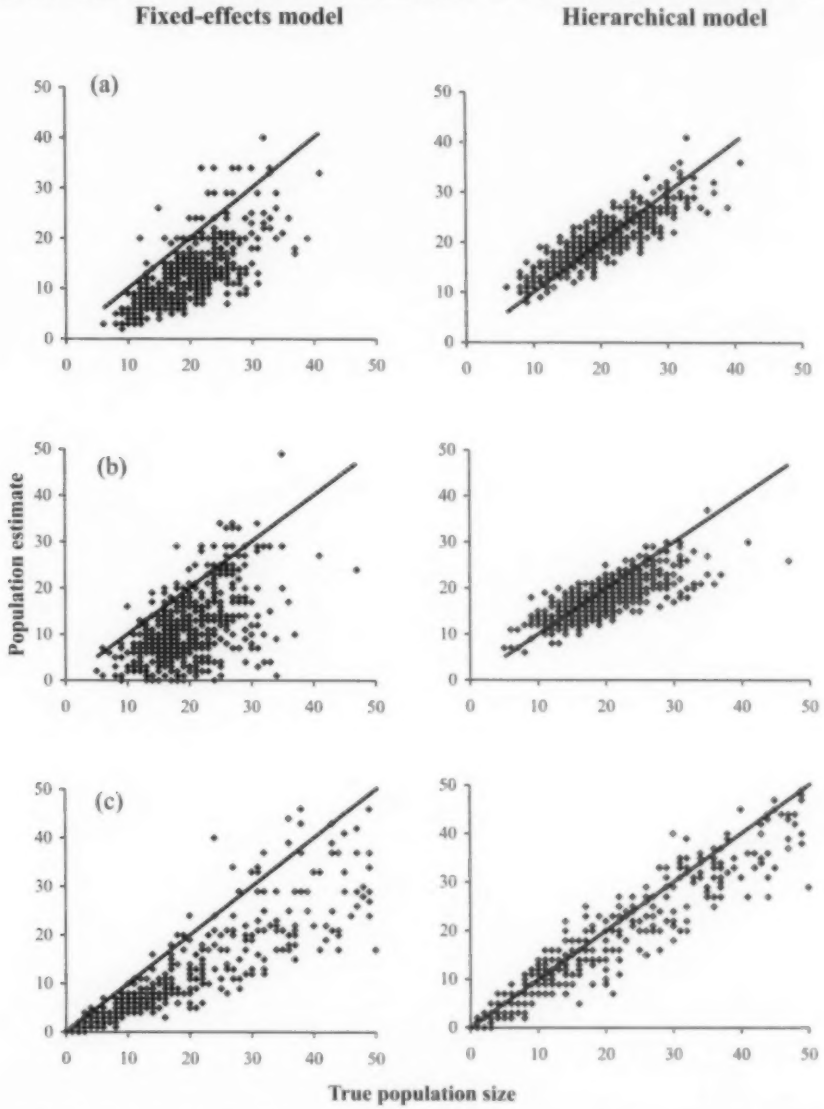

therefore $p(\lambda, \kappa) \propto \lambda^{-1}\kappa^{-3/2}$ ($\lambda > 0$, $\kappa > 0$). The joint prior distribution for population parameters α and β was chosen to be uniform on the mean capture probability ($\alpha/(\alpha + \beta)$) and associated variability ($(\alpha + \beta)^{-1/2}$). On the original scale, the joint prior is obtained by multiplying by the appropriate Jacobian to give $p(\alpha, \beta) \propto (\alpha + \beta)^{-5/2}$ ($\alpha > 0$, $\beta > 0$).

Point estimates of the population parameters, required for the empirical Bayesian approach, can be readily obtained by finding the values that maximize eq. 4, using the maximization routine within a spreadsheet. Posterior distributions for the population parameters, required for the fully Bayesian approach, necessitate the use of a simulation method. Random samples from the joint posterior density of the population parameters (eq. 4) were obtained using the sampling importance resampling (SIR) algorithm (Rubin 1988), programmed in BASIC. Twenty thousand samples were first drawn from importance functions for $\log(\lambda)$, $\kappa^{-1/2}$, $\alpha/(\alpha + \beta)$, and $(\alpha + \beta)^{-1/2}$. The importance functions need to be simple approximations to the desired posterior distributions and from which random samples can be drawn using standard methods (e.g., Ripley 1987). A beta distribution was used for $\alpha/(\alpha + \beta)$, a normal distribution for $\log(\lambda)$, and gamma distributions were used for $\kappa^{-1/2}$ and $(\alpha + \beta)^{-1/2}$. Suitable values for the parameters of the importance functions were selected iteratively before the full simulation was undertaken. For each sample of the four population parameters from the importance functions, the likelihood was calculated (eq. B.7). The 20 000 samples were then resampled 1000

© 2002 NRC Canada

Fig. 3. Comparison of site-specific population estimates from simulated single-removal data for the mean capture probability method and the hierarchical model. Three data sets were used with different degrees of spatial variability (see Fig. 2).

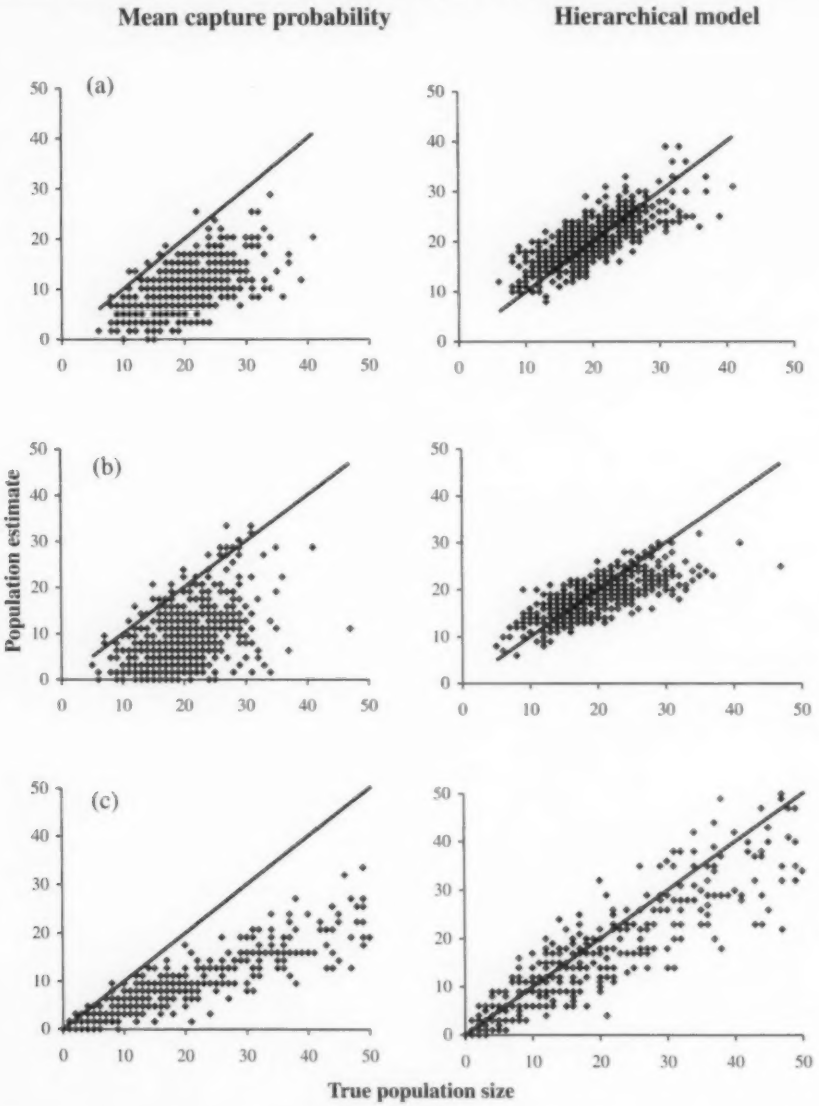

times with probability proportional to the importance ratio (= likelihood/importance) to provide samples from the joint posterior distribution of the population parameters. The marginal posterior distributions for the site-specific population sizes were then obtained by normalizing the conditional posterior distributions (eq. 1) and numerically integrating over the sample of 1000 values from the joint posterior distribution of the population parameters (eq. 3).

Application

Application to the River Inny

The hierarchical model was applied to historical catches obtained from an electrofishing survey of 0+ trout (*Salmo trutta*) populations in the River Inny, a tributary of the River Tamar, England (Table 1). The river had been stratified into sections of relatively uniform habitat, and multiple- and single-pass sites selected at random from each. Data were collected from nine multiple-pass sites and 11 single-pass sites. The joint posterior distribution of the four population parameters (eq. 4) was estimated for all 20 sites and for comparative purposes, was re-estimated after excluding the 11 single-pass sites. Posterior distributions were then obtained for the population size at all sites based on a hierarchical model using a fully Bayesian approach (eq. 3) and the simple, but approximate, empirical Bayesian approach (eq. 2).

Model checking

Model checking for a fixed-effects model for removal sampling will necessarily consider the assumptions associ-

© 2002 NRC Canada

Fig. 4. Sample of 1000 numbers from the posterior distributions of the following population parameters: log mean density ($\log(\lambda)$) and associated variability ($\kappa^{-1/2}$), and mean capture probability ($\alpha/(\alpha + \beta)$) and associated variability ($(\alpha + \beta)^{-1/2}$).

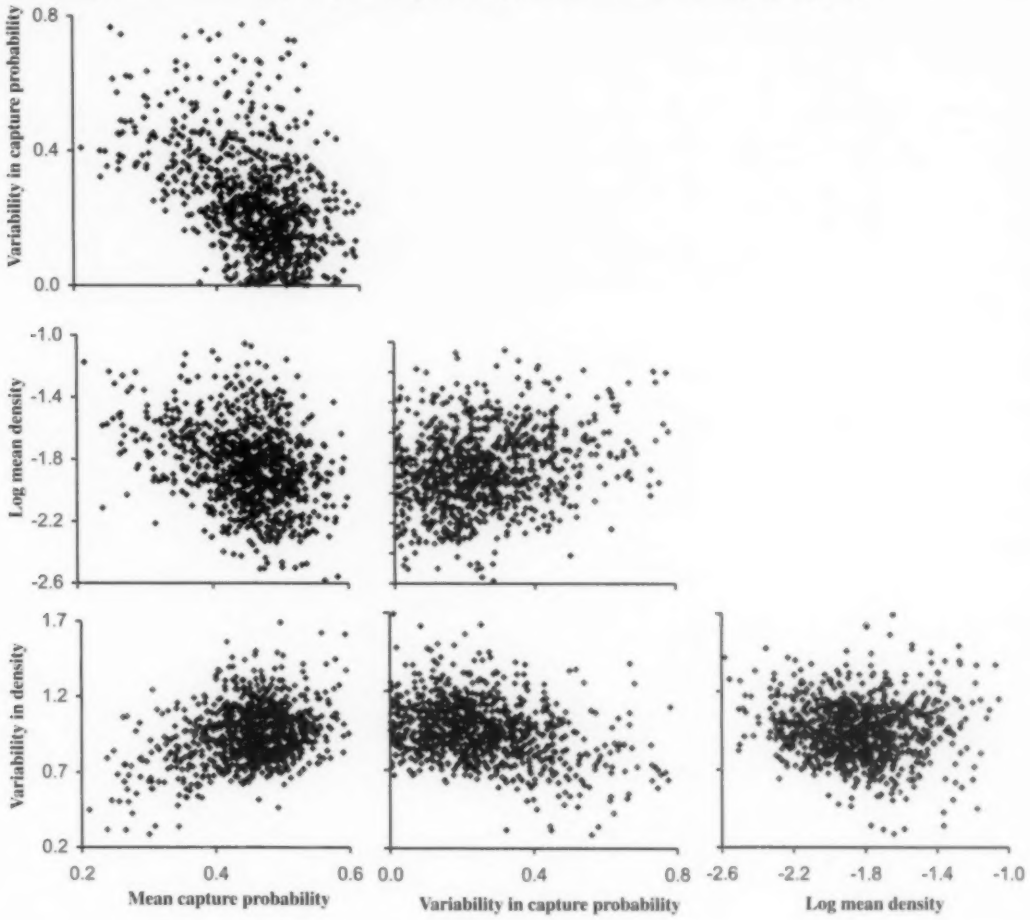

ated with the second stage of sampling, like the constancy of capture probability between passes, and has been considered in detail by other authors. For the hierarchical model, however, the assumptions associated with the first stage of sampling are also important, and will be considered here. There are a number of possible criteria that can be used to assess the fit of a model in Bayesian inference. One approach is to compare each observed data point to a posterior predictive distribution (Gelfand et al. 1992). Ideally, the predictive distribution is based on a separate set of evaluation data, but if this is not available, cross-validation can be undertaken by comparing each data point to the predictive distribution estimated from the remainder of the data. An approximation to cross-validation was undertaken on the catches obtained on the first pass at each site (c_{i1}).

The predictive distribution was obtained by numerically integrating the probability of observing a catch on the first pass, conditional on the site area and population parameters (eq. B.6), over the posterior distribution of the population parameters (eq. 4).

$$p(c_{i1}|\underline{c}, \underline{a}) = \int_0^\infty\int_0^\infty\int_0^\infty\int_0^\infty p(c_{i1}|a_i, \alpha, \beta, \lambda, \kappa) \; p(\alpha, \beta, \lambda, \kappa|\underline{c}, \underline{a})\, d\alpha\, d\beta\, d\lambda\, d\kappa \quad (5)$$

The probability of obtaining a catch less than or equal to the observed catch on the first pass at each site was calculated from eq. 5. These probabilities were plotted against the ranked sites to informally illustrate any departure from the probability model as departure from a straight diagonal line.

The fit of the empirical Bayesian estimates could be investigated more simply by comparing the catches to the posterior predictive distribution obtained by substituting point estimates for the population parameters into eq. B.6.

$$p(c_{i1}|a_i, \hat{\alpha}, \hat{\beta}, \hat{\lambda}, \hat{\kappa}) = \sum_{n_i=t_i}^{\infty} p(c_{i1}, n_i|a_i, \hat{\alpha}, \hat{\beta}, \hat{\lambda}, \hat{\kappa})$$

© 2002 NRC Canada

Table 2. Summary of the marginal posterior distributions for the population parameters.

Parameter	Sites	2.5th percentile	Median	97.5th percentile
Log mean density ($\log(\lambda)$)	All	–2.31	–1.86	–1.30
	Multiple pass only	–2.08	–1.47	–0.52
Mean capture probability ($\alpha/(\alpha + \beta)$)	All	0.287	0.461	0.565
	Multiple pass only	0.354	0.483	0.578
Variability in density ($\kappa^{-1/2}$)	All	0.592	0.943	1.331
	Multiple pass only	0.542	0.927	1.632
Variability in capture probability ($(\alpha + \beta)^{-1/2}$)	All	0.009	0.220	0.626
	Multiple pass only	0.020	0.208	0.573

Fig. 5. Posterior probability distributions for the site-specific population sizes from the Bayesian estimation of the hierarchical model. Multiple-pass sites are denoted by the heavier lines.

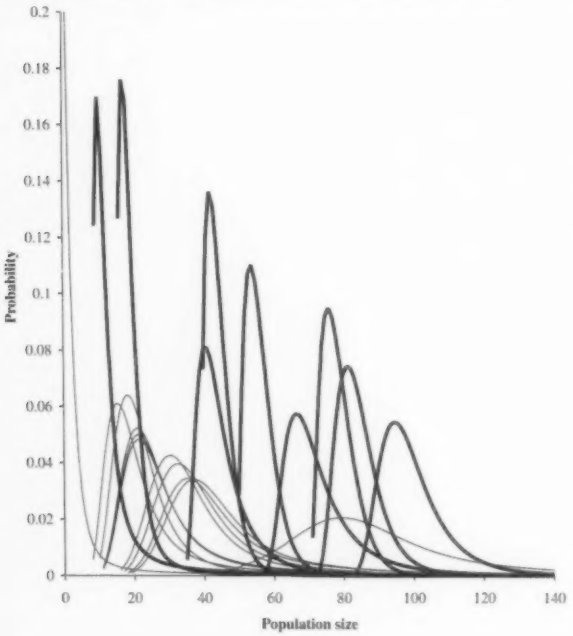

Results and discussion

In a fixed-effects model for removal data at multiple sites, each site is regarded as independent of all other sites, and the population estimate for a site is based on the catches from that site alone. The site-specific population estimates from the fixed-effects model (Fig. 2) are identical to those obtained from the repeated application of the maximum weighted likelihood estimator of Carle and Strub (1978). The estimates exhibit a negative bias, which is particularly pronounced at low capture probabilities (Carle and Strub 1978), and a large sampling variance associated with the low number of removals. In a hierarchical model, site-specific population estimates are obtained from all of the catch data within the target area. The resulting estimates, often termed "shrunk" estimates, are closer to the mean population density ($E(\theta_i)$) and capture probability ($E(q_i)$) than their nonhierarchical counterparts. This shrinkage discounts the likely contribution from the within-site variance and is intuitively satisfactory since very high or low population estimates may be due partly to error in their estimation. The overall degree of shrinkage will be greatest in situations where there is low between-site variance in capture probability (Fig. 2*a* and 2*c*) or population density (Fig. 2*a* and 2*b*). Furthermore, the degree of shrinkage at a particular site will be greater for sites furthest from the mean capture probability or population density and for sites with high within-site variance (low capture probabilities or number of passes). The overall result of shrinkage within the hierarchical model for removal data is to reduce bias and variance of the site-specific estimates (Fig. 2).

The single-pass estimates obtained from the hierarchical model (Fig. 3) perform better than those based on the mean capture probability since they are calculated directly from the raw catch data from all sites, and not indirectly from the biased population estimates at the multiple-pass sites (Fig. 2). Furthermore, in situations where there is a high between-site variation in capture probability, but a relatively low between-site variation in population density (Fig. 3*b*), the hierarchical model can use the density information to improve estimates. A further advantage of the hierarchical approach for single-pass sites is that the estimation procedure is the same as for multiple-pass sites, allowing direct comparison between methods without the confounding influence of different estimation procedures.

The primary objective of a two-stage sampling programme may often be to make inferences about the target area as a whole. The hierarchical model provides a probability distribution for the population parameters relating to population size and capture probability (Fig. 4) from which point estimates and probability intervals can be obtained if required (Table 2). As might be expected, some degree of association is evident between the parameters for the River Inny, such as a negative association between the mean capture probability and mean density (Fig. 4). Unlike the two-stage sampling equations of Bohlin (1981) and Hankin (1984), these population parameters have been estimated directly from the raw catch data, rather than indirectly from the site-specific population estimates. This will correctly allow for the widely different quality of information obtained from each site (Table 1), and in particular allows the direct integration of single- and multiple-pass sites. The advantage of including the single-pass sites can be seen in the substantial reduction in the mean density from 0.229 m^{-2} for multiple-pass

© 2002 NRC Canada

Fig. 6. Population estimates and 95% probability intervals for single (◇) and multiple (◆) pass removal sites on the River Inny, U.K., using a hierarchical model. Estimates obtained from (*a*) fully Bayesian estimation and (*b*) approximate empirical Bayesian estimation.

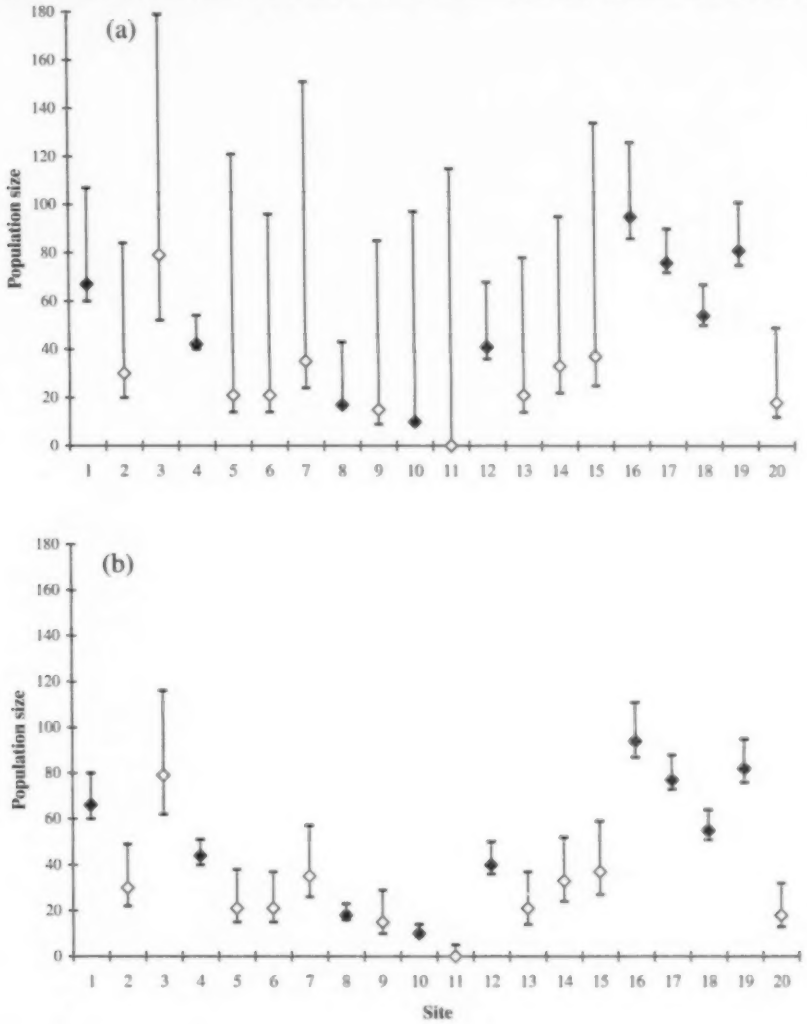

sites only to 0.155 m^{-2} for all sites (Table 2), reflecting the generally lower densities at the single-pass sites (Fig. 5). The increase in the sample size from nine to 20 also results in a narrowing of the 95% probability intervals for the mean density (Table 2).

To undertake a fully Bayesian hierarchical analysis will require the use of computer-intensive techniques like the SIR algorithm. Whereas computer routines for undertaking such techniques are readily programmed and are becoming commonly available, the empirical Bayesian approach (eq. 2) provides a simple way to obtain approximate posterior probability distributions for the site-specific population sizes. On the River Inny, however, there was considerable estimation error for the population parameters (Fig. 4; Table 2) due to the small sample of only nine multiple-pass sites. This results in very wide 95% probability intervals for the site-specific population estimates at the single-pass sites (Figs. 5 and 6*a*). The empirical Bayesian point-estimates for the population size at single-pass sites (Fig. 6*b*) are identical to those from the Bayesian analysis (Fig. 6*a*); however, the empirical Bayesian approach underestimates the width of the probability intervals because the estimation error in the population parameters is ignored. The empirical Bayesian approach is therefore more appropriate for surveys with a higher number of multiple-pass sites, where the site-specific posterior probability distributions from the empirical Bayesian approach will approach the exact distributions provided by the fully Bayesian approach.

The hierarchical model provides a reasonable fit to the catch data (Fig. 7), but there is some evidence that the catches on the first pass at sites 10 and 11 are unexpectedly low. At site 11, a single-pass site, it is not possible to determine whether the catch of zero reflects an unusually low capture probability compared to the beta distribution or an

© 2002 NRC Canada

Fig. 7. Probability of obtaining a catch less than or equal to the observed catch on the first pass based on the posterior predictive distribution for the hierarchical model. Solid diamonds denote multiple-pass sites and open squares denote single-pass sites.

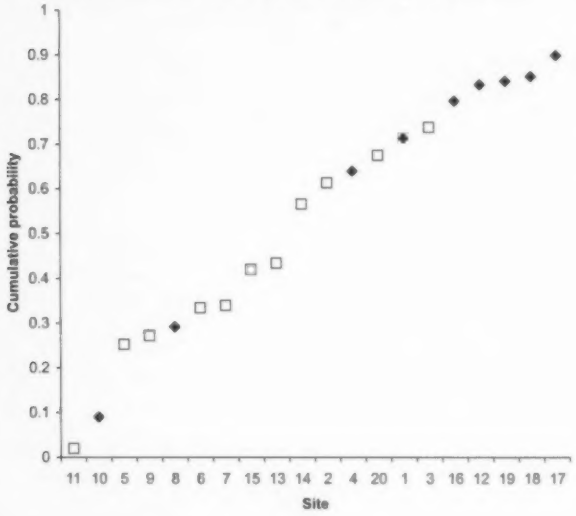

unusually low population density compared to the gamma distribution. At site 10, however, the poor depletion (Table 1) suggests that it is the capture probability that is unusually low. These two sites are adjacent, so further investigation may determine whether any common environmental factors may be causing some departure from the probability model. Any evidence of a poor fit of the basic hierarchical model to a particular data set may suggest areas where the model could be improved. For example, the hierarchical model could be readily extended to include environmental variables that influence the population density or capture probability, either as a basis for stratification or as covariates. Other areas in which the model could be generalized might include an allowance for a variable capture efficiency between fish or passes, a finite population of survey sites when the target area is small, and spatial autocorrelation within the data. Such refinements may require the use of more sophisticated computational strategies than those suggested here.

The hierarchical model provides a natural approach to analyzing removal data from two-stage sampling schemes. A single analysis of the raw catch data from all sites within the target area provides a number of advantages over the more usual approach of analysing the removal data from each site in isolation. These advantages will be most pronounced when a large number of sites are sampled, but when a low number of passes are undertaken at some or all of the sites. Although such data are commonly obtained from surveys of riverine fish populations, the hierarchical model could readily be applied to removal data for any animal population.

Acknowledgements

This work was funded by the Environment Agency Research and Development programme. The electrofishing data for the River Inny were provided by Kelvin Broad. The author would like to thank Julian Ellis for critically reviewing an early version of this manuscript. The improvements suggested by the anonymous referees are gratefully acknowledged. The views expressed by the author are not necessarily those of the Environment Agency.

References

Barnett, V. 1991. Sample survey. Principles and methods. 2nd ed. Edward Arnold, London.

Barnett, V. 1999. Comparative statistical inference. 3rd ed. Wiley, Chichester.

Bohlin, T. 1981. Methods of estimating total stock, smolt output and survival of salmonids using electrofishing. Rep. Inst. Freshwater Res. Drottningholm, **59**: 5–14.

Carle, F.L., and Strub, M.R. 1978. A new method for estimating population size from removal data. Biometrics, **34**: 621–630.

Carlin, B., and Louis, T. 2000. Bayes and empirical Bayes methods for data analysis. 2nd ed. Chapman and Hall, London.

Chao, A., and Chang, S.-H. 1999. An estimating function approach to the inference of catch-effort models. Environ. Ecol. Stat. **6**: 313–334.

Cochran, W.G. 1977. Sampling techniques. 3rd ed. Wiley, New York.

Crozier, W.W., and Kennedy, G.J.A. 1994. Application of semi-quantitative electrofishing to juvenile salmonid stock surveys. J. Fish Biol. **45**: 159–164.

Gelfand, A.E., Dey, D.K., and Chang, H. 1992. Model determination using predictive distributions with implementation via sampling-based methods. *In* Bayesian statistics 4. *Edited by* J.M. Bernardo, J.O. Berger, A.P. Dawid, and A.F.M. Smith. Oxford University Press, Oxford. pp. 147–168.

Gelman, A., Carlin, J., Stern, H., and Rubin, D. 1995. Bayesian data analysis. Chapman and Hall, London.

Goldstein, H. 1995. Multilevel statistical models. Arnold, London.

Hankin, D.G. 1984. Multistage sampling designs in fisheries research: application in small streams. Can. J. Fish. Aquat. Sci. **41**: 1575–1591.

Harding, C.M., Heathwood, A.W., Hunt, R.G., and Read, K.L.Q. 1984. The estimation of animal population size by the removal method. Appl. Stat. **33**: 196–202.

Harley, S.J., and Myers, R.A. 2001. Hierarchical Bayesian models of length-specific catchability of research trawl surveys. Can. J. Fish. Aquat. Sci. **58**: 1569–1584.

Hirst, D. 1994. An improved removal method for estimating animal abundance. Biometrics, **50**: 501–505.

Jones, M.L., and Stockwell, J.D. 1995. A rapid assessment procedure for the enumeration of salmonine populations in streams. N. Am. J. Fish. Manag. **15**: 551–562.

Lee, S.-M., and Chao, A. 1994. Estimating population size via sample coverage for closed capture-recapture models. Biometrics, **50**: 88–97.

Liermann, M., and Hilborn, R. 1997. Depensation in fish stocks: a hierarchic Bayesian meta-analysis. Can. J. Fish. Aquat. Sci. **54**: 1976–1984.

McAllister, M.K., and Kirkwood, G.P. 1998. Bayesian stock assessment: a review and example application using the logistic model. ICES J. Mar. Sci. **55**: 1031–1060.

Mitro, M.G., and Zale, A.V. 2000. Predicting fish abundance using single-pass removal sampling. Can. J. Fish. Aquat. Sci. **57**: 951–961.

Moran, P.A.P. 1951. A mathematical theory of animal trapping. Biometrika, **38**: 307–311.

© 2002 NRC Canada

O'Hagan, A. 1994. Bayesian inference. Kendall's advanced theory of statistics. Vol. 2b. Arnold, London.

Press, W.H., Teukolsky, S.A., Vetterling, W.T., and Flannery, B.P. 1996. Numerical recipes in Fortran 77. The art of scientific computing. 2nd ed. Cambridge University Press, Cambridge.

Punt, A.E., and Hilborn, R. 1997. Fisheries stock assessment and decision analysis: the Bayesian approach. Rev. Fish Biol. Fish. **7**: 35–63.

Ripley, B.D. 1987. Stochastic simulation. John Wiley & Sons, New York.

Rubin, D.B. 1988. Using the SIR algorithm to simulate posterior distributions. *In* Bayesian statistics 3. *Edited by* J.M. Bernardo, M.N. Degroot, D.V. Lindley, and A.M. Smith. Clarendon Press, Oxford. pp. 385–402.

Schnute, J. 1983. A new approach to estimating populations by the removal method. Can. J. Fish. Aquat. Sci. **40**: 2153–2169.

Seber, G.A.F. 1982. The estimation of animal abundance. 2nd ed. Griffin, London.

Snijders, T.A.G., and Bosker R.J. 1999. Multilevel analysis. An introduction to basic and advanced multilevel modelling. Sage, London.

Sprott, J.C. 1991. Numerical recipes. Routines and examples in BASIC. Companion manual to Numerical recipes: the art of scientific computing. Cambridge University Press, Cambridge.

Strange, C.D., Aprahamian, M.W., and Winstone, A.J. 1989. Assessment of a semi-quantitative electric fishing sampling technique for juvenile Atlantic salmon *Salmo salar* L., and trout, *Salmo trutta* L., in small streams. Aquac. Fish. Manag. **20**: 485–492.

Su, Z., Adkison, M.D., and Van Alen, B.W. 2001. A hierarchical Bayesian model for estimating historical salmon escapement and escapement timing. Can. J. Fish. Aquat. Sci. **58**: 1648–1662.

Wang, Y.-G. 1999. Estimating equations for removal data analysis. Biometrics, **55**: 1263–1268.

Wang, Y.-G., and Loneragan, N.R. 1996. An extravariation model for improving confidence intervals of population size estimates from removal data. Can. J. Fish. Aquat. Sci. **53**: 2533–2539.

Zippin, C. 1956. An evaluation of the removal method of estimating animal populations. Biometrics, **12**: 163–189.

Appendix A. Derivation of the likelihood function for the fixed-effects model for multiple-pass sites

The probability of catching c_{ij} fish from a population of n_{ij} at the ith site on the jth pass, given a capture probability q_i, will follow a binomial distribution

$$p(c_{ij}|n_{ij}, q_i) = \frac{n_{ij}!}{(n_{ij} - c_{ij})!\,c_{ij}!} q_i^{c_{ij}} (1 - q_i)^{n_{ij} - c_{ij}},$$

$$0 \le q_i \le 1$$

The number of fish remaining after the jth pass is given by

$$n_{i,j+1} = n_{ij} - c_{ij}$$

The likelihood of a particular catch vector ($\underline{c}_i = c_{i1}, \ldots, c_{ik_i}$) at a site with initial population n_{i1} is therefore given by

$$p(\underline{c}_i|n_{i1}, q_i) = \prod_{j=1}^{k_i} p(c_{ij}|n_{i1}, q_i)$$

Thus, denoting n_{i1} by n_i

$$(A.1) \quad p(\underline{c}_i|n_i, q_i) = \frac{n_i!}{(n_i - t_i)!\,y_i} q_i^{t_i} (1 - q_i)^{k_i n_i - x_i - t_i}$$

where t_i, x_i, and y_i summarize the data $\underline{c}_i$ at the ith site as follows:

$$t_i = \sum_{j=1}^{k_i} c_{ij},\ x_i = \sum_{j=1}^{k_i} (k_i - j)c_{ij},\ \text{and}\ y_i = \prod_{j=1}^{k_i} c_{ij}!$$

A marginal likelihood for n_i can be obtained by integrating over all possible values of q_i.

$$p(\underline{c}_i|n_i) = \int_0^1 p(\underline{c}_i|n_i, q_i)\mathrm{d}q_i$$

$$(A.2) \quad p(\underline{c}_i|n_i) \propto \frac{n_i!(k_i n_i - x_i - t_i)!}{(n_i - t_i)!(k_i n_i - x_i + 1)!}$$

This marginal likelihood function is equivalent to the weighted likelihood function of Carle and Strub (1978), assuming a uniform prior distribution for q.

Appendix B. Derivation of the likelihood function for the hierarchical model for single and multiple-pass sites

The variation in density (θ_i) between sites is assumed to follow a gamma distribution

$$(B.1) \quad p(\theta_i|\lambda, \kappa) = \left(\frac{\kappa}{\lambda}\right)^{\kappa} \frac{\theta_i^{\kappa-1} e^{-\kappa\theta_i/\lambda}}{\Gamma(\kappa)}, \qquad \lambda > 0, \kappa > 0$$

where $\Gamma()$ is the gamma function, which can be evaluated using standard routines (Sprott 1991; Press et al. 1996), and is available as a function in most spreadsheet packages. The expectation and variance of θ_i are

$$E(\theta_i) = \lambda$$

$$V(\theta_i) = \lambda^2/\kappa$$

The variation in catch probability (q_i) between sites is assumed to follow a beta distribution

$$(B.2) \quad p(q_i|\alpha, \beta) = \frac{q_i^{\alpha-1}(1 - q_i)^{\beta-1}}{B(\alpha, \beta)}, \qquad \alpha > 0, \beta > 0$$

where $B()$ is the beta function, which is related to the gamma function by the expression

$$B(u, v) = \Gamma(u)\Gamma(v)/\Gamma(u + v)$$

The expectation and variance of q_i are

$$E(q_i) = \frac{\alpha}{\alpha + \beta}$$

$$V(q_i) = \frac{\alpha\beta}{(\alpha + \beta)^2(\alpha + \beta + 1)}$$

The probability of the population size (n_i), given the density of fish θ_i, will follow a Poisson distribution

© 2002 NRC Canada

(B.3) $$p(n_i|\theta_i, a_i) = \frac{e^{-\phi_i}\phi_i^{n_i}}{n_i!}, \qquad n_i = 0,1,2,\ldots, \quad \theta_i \geq 0$$

where $\phi_i = \theta_i a_i$ for a site of area a_i.

The joint probability of the catch data ($\underline{c}_i$) and a population size n_i at the ith site, conditional on the site area a_i and the population parameters $\alpha, \beta, \lambda, \kappa$, is obtained by integrating out the two nuisance parameters n_i and q_i

$$p(\underline{c}_i, n_i|a_i, \alpha, \beta, \lambda, \kappa) = \int_0^1 p(\underline{c}_i|n_i, q_i)p(q_i|\alpha, \beta)\mathrm{d}q_i$$

$$\int_0^\infty p(n_i|\theta_i, a_i)p(\theta_i|\lambda, \kappa)\mathrm{d}\theta_i$$

Substituting eqs. A.1, B.1, B.2, and B.3 gives

(B.4) $$p(\underline{c}_i, n_i|a_i, \alpha, \beta, \lambda, \kappa)$$

$$= \frac{(\lambda a_i)^{n_i}\kappa^{\kappa}\Gamma(\kappa + n_i)B(\alpha + t_i, \beta + k_i n_i - x_i - t_i)}{(\lambda a_i + \kappa)^{n_i+\kappa}\Gamma(\kappa)(n_i - t_i)!\,B(\alpha, \beta)y_i}$$

Note that for a single-pass site, $k_i = 1$, and so $t_i = c_{i1}$, $y_i = c_{i1}!$, and $x_i = 0$. Equation B.4 can be evaluated efficiently using a sequential equation

(B.5) $$p(\underline{c}_i, n_i|a_i, \alpha, \beta, \lambda, \kappa) =$$

$$p(\underline{c}_i, n_i - 1)\frac{\lambda a_i(\kappa + n_i - 1)}{(\lambda a_i + \kappa)(n_i - t_i)} \prod_{j=1}^{k_i}\frac{\beta + k_i n_i - x_i - t_i - j}{\alpha + \beta + k_i n_i - x_i - j}, \quad n_i > t_i$$

The marginal probability of the catch data at the ith site, conditional on the site area and population parameters is therefore obtained by integrating out the nuisance parameter n_i, that is, by summing from $n_i = t_i$ to ∞. This gives

(B.6) $$p(\underline{c}_i|a_i, \alpha, \beta, \lambda, \kappa) = \sum_{n_i=t_i}^{\infty} p(\underline{c}_i, n_i|a_i, \alpha, \beta, \lambda, \kappa)$$

This summation has to be evaluated numerically to a high value of n_i using the sequential equation (B.5). The likelihood of obtaining a particular set of catch data ($\underline{c} = \underline{c}_1, \ldots, \underline{c}_m$) from sites with area ($\underline{a} = a_1, \ldots, a_m$) is therefore

(B.7) $$p(\underline{c}|\underline{a}, \alpha, \beta, \lambda, \kappa) = \prod_{i=1}^{m} p(\underline{c}_i|a_i, \alpha, \beta, \lambda, \kappa)$$

© 2002 NRC Canada

Functional response of kokanee salmon (*Oncorhynchus nerka*) to *Daphnia* at different light levels

Marci L. Koski and Brett M. Johnson

Abstract: In laboratory experiments, fingerling kokanee salmon (*Oncorhynchus nerka*, 3–8 g) were presented with varying densities of zooplankton prey (*Daphnia* spp.) ranging from 3 to 55 *Daphnia*·L^{-1}, under three light intensities (30, 15, and 0.1 lx). Kokanee exhibited a type I functional response at 0.1 lx (*Daphnia* consumption·min^{-1} = 1.74 prey·L^{-1}), a light level typical of moonlit epilimnetic conditions, but shifted to a type II functional response at higher light levels. Both 15 and 30 lx light levels occur during crepuscular periods when kokanee feeding is maximal in the wild, and consumption rates at these light levels were not significantly different (*Daphnia* consumption·min^{-1} = (163.6 prey·L^{-1})(42.2 prey·L^{-1})$^{-1}$). The shift from the type I to type II functional response may be attributed to a foraging mode switch and the incorporation of search time instead of random encounters with prey. Using these models to simulate feeding rates in a Colorado reservoir, attenuation of light intensity and prey density between the epilimnion and hypolimnion resulted in a 100-fold increase in predicted feeding duration. Functional responses that incorporate environmental characteristics like light are important components of foraging models that seek to understand fish consumption, growth, and behavior.

Résumé : Des expériences de laboratoire ont mis en présence des estivaux du kokani (*Oncorhynchus nerka*) de 3–8 g avec diverses densités de proies zooplanctoniques (*Daphnia* spp.) à raison de 3–55 *Daphnia*·L^{-1} sous trois intensités lumineuses (30, 15 et 0,1 lux). Les kokanis ont une réponse fonctionnelle de type I (consommation de *Daphnia*·min^{-1} = 1,74 proie·L^{-1}) à 0,1 lux, un éclairement qui correspond aux conditions de nuit dans l'épilimnion par clair de lune; la réponse fonctionnelle est de type II aux intensités plus élevées. Des éclairements de 15 et de 30 lx prévalent pendant les heures du crépuscule qui sont les périodes d'alimentation maximale des kokanis en nature et les taux de consommation à ces éclairements ne diffèrent pas significativement (consommation de *Daphnia*·min^{-1} = (163,6 proies·L^{-1})(42,2 proies·L^{-1})$^{-1}$). Le passage d'une réponse fonctionnelle de type I à une de type II peut être dû à un changement de mode de quête de nourriture et à l'incorporation du temps de recherche des proies au modèle (au lieu de la simple rencontre des proies par hasard). Ces modèles utilisés pour simuler les taux d'alimentation dans un réservoir du Colorado montrent que l'atténuation de l'intensité lumineuse et de la densité des proies qui se produit entre l'épilimnion et l'hypolimnion cause une augmentation de l'ordre de 100 fois de la durée prédite de l'alimentation. Les réponses fonctionnelles qui incorporent les caractéristiques de l'environnement, telles que la lumière, sont des composantes importantes des modèles de quête de nourriture qui visent à expliquer la consommation alimentaire, la croissance et le comportement des poissons.

[Traduit par la Rédaction]

Introduction

Planktivorous fishes can have profound influences on the abundance and distribution (Levy 1990; DeVries and Stein 1992), size structure (O'Brien 1979; Vanni 1987), and species composition of zooplankton assemblages (Brooks and Dodson 1965; Christoffersen et al. 1993). The impact of their feeding activities can "cascade" to lower trophic levels and affect primary producers and water quality (Carpenter and Kitchell 1993). Furthermore, because they are often prey for piscivores, planktivorous fishes are a major conduit for channeling energy from plankton to higher trophic levels. Thus, our understanding of trophic dynamics and energy flow in lentic systems could be improved by learning more about the feeding behavior of planktivorous fishes.

A fundamental framework for studying feeding behavior is the functional response. Functional response quantifies consumption rate of a predator as a function of prey density (Holling 1959, 1966). A type I functional response is often observed in filter feeders whose prey is distributed homogeneously in the environment. Consumption rate increases linearly with prey density until saturation occurs. Handling time is an important constraint in the type II functional response. As prey density increases, more time is spent handling or processing prey, and less time is spent searching for it until, at prey saturation, all time is spent handling prey. Planktivorous fishes that particulate-feed or gulp-feed, or that forage in environments where prey are patchy, typically exhibit a type II functional response (Smith 1998). The type III functional response arises when multiple prey types are

Received 11 July 2001. Accepted 18 April 2002. Published on the NRC Research Press Web site at http://cjfas.nrc.ca on 21 May 2002.
J16440

M.L. Koski[1] and B.M. Johnson. Department of Fishery and Wildlife Biology, Colorado State University, Fort Collins, CO 80523-1474, U.S.A.

[1]Corresponding author (e-mail: mkoski@lamar.colostate.edu).

 DOI: 10.1139/F02-045 © 2002 NRC Canada

available and switching behavior occurs (Smith 1998). As the density of one prey type increases, a search image is developed and the predator switches to feeding on that prey. As with the type II functional response, handling time limits feeding rate at high prey density.

Kokanee salmon (*Oncorhynchus nerka*) are well suited to quantitative feeding studies because their diet is simple. They are usually zooplanktivorous, and in many systems they consume large cladocerans exclusively throughout their lives (Finnell and Reed 1969; Eggers 1978; Stockwell et al. 1999). Kokanee are also popular sport fish and are actively managed in coldwater lakes and reservoirs throughout the western United States and Canada. Additionally, this species has been the subject of several bioenergetics models that predict growth or consumption as functions of physiology and characteristics of the environment (Beauchamp et al. 1989; Bevelhimer and Adams 1993; Stockwell and Johnson 1999). However, little is known about how environmental factors such as zooplankton density and light intensity affect kokanee feeding behavior.

The only known work on kokanee functional response was by Hyatt (1980). He conducted feeding experiments to fit a relationship between maximum feeding rate and zooplankton density that suggested a type II functional response. However, the generality of Hyatt's study was limited because of the low temperature (10°C) and low prey densities (0.4–2.3 *Daphnia*·L^{-1}) in the trials. Further, the shape of the response at higher prey densities typical of mesotrophic systems is unknown. More recently, Stockwell and Johnson (1997) used a theoretical approach to estimate feeding rates, including such factors as reaction distance, fish swimming speed, and handling time in the functional response model. However, predicted feeding rates can be highly variable because estimating foraging rate in this manner relies on many parameters that are either unknown or subject to change.

Although functional response by definition relates feeding rate to prey density, other factors may influence feeding rates as well. Light level should affect feeding rate because of its influence on reaction distance and search volume (Ali 1959; Townsend and Risebrow 1982; Link and Edsall 1996). For most salmonids, minimum feeding rates can occur at approximately 0.001–3.4 lx (corresponding to clear starry nights at moonlight levels in the epilimnion), but a threshold light level of roughly 3.4 lx is required for maximum feeding rates (Ali 1959), which typically occurs during crepuscular periods (here defined as times of twilight where the sun is below the horizon during dusk and dawn; some light is reflected back to the earth's surface from the upper atmosphere (U.S. Naval Observatory 2001)). Many populations of *O. nerka* perform diel vertical migrations (DVM; Eggers 1978; Levy 1990; Bevelhimer and Adams 1993), exposing them to both spatial and temporal gradients in light intensity. Therefore, foraging models for kokanee should incorporate a light-dependent functional response. In this study, we conducted laboratory experiments to quantify the effects of prey density and light intensity on kokanee feeding behavior. We were especially interested in kokanee feeding rate at higher prey densities characteristic of mesotrophic reservoirs in Colorado and elsewhere. We then used the models derived from our laboratory experiments to investigate how vertical gradients in light and food would affect kokanee foraging in the wild by calculating feeding rate and feeding duration with data collected from Blue Mesa Reservoir, Colo., in 1994.

Materials and methods

Laboratory procedures

We conducted feeding trials with young-of-the-year kokanee, presenting individual fish with a range of *Daphnia* densities at three different light intensities. One hundred kokanee fingerlings (age 2 months, mean mass 3 g, 4.5 cm total length) were obtained from Roaring Judy state fish hatchery near Gunnison, Colo., three months prior to the start of experiments. Fish were housed in a 655-L tank at 11–13°C, with a water flow-through rate of 60 mL·s^{-1}; the dissolved oxygen level was maintained at 8.2 mg·L^{-1}. Ambient light level in the laboratory was 190 lx (12 h light : 12 h dark); shaded areas in the trough were accessible to fish at all times. Kokanee were fed a low ration of trout chow pellets (<1% body weight per day) and were periodically given live *Daphnia* to acclimate them to eating natural prey (see Vinyard et al. 1982). *Daphnia pulex* and *Daphnia galeata* were collected and reared in filtered river water in 38-L tanks at room temperature. *Daphnia* were fed a 2:1 diet of *Selenastrum* algae and YTC (yeast – trout chow – Cerophyll (cereal leaves)).

Experimental arenas were round plastic containers (bottom diameter 48 cm, top diameter 61 cm, height 38 cm), painted a medium shade of gray inside. Arenas were filled with 35 L well water (0.04 NTU (nephelometric turbidity units)) that was aerated during the acclimation period and feeding trial to aid in distribution of *Daphnia* in the arena. We acknowledge that other studies have shown increased feeding rates with increased turbulence as a result of amplified encounter rates (i.e., Landry et al. 1995; Dower et al. 1998); however, with aeration we were dispersing prey instead of leaving them concentrated near a feeder tube. Light was manipulated by varying the number of screens in front of 91.5 cm fluorescent-bulbs (400- to 700-nm wavelength), which were suspended above the arenas so that light was reflected off the arena house ceiling into the arena (roughly 75 cm below).

The day before trials, single kokanee fingerlings were placed in experimental arenas and acclimated without food for an average of 19.7 h. Whereas kokanee forage in schools in the wild, preliminary trials indicated that dominance hierarchies in small groups (2–3 fish) biased feeding rates, so we used only one fish per trial. During this acclimation period, light level remained constant and at the level at which the trial would occur and water temperature was allowed to naturally increase (without heaters) overnight from the ambient temperature of the holding tank to approximately 19°C (Table 1), a temperature more representative of that found in the epilimnion of regional reservoirs in midsummer. Because kokanee exhibit DVM in the wild, this magnitude of temperature change simulated the range of temperatures kokanee experience when migrating to the epilimnion to forage.

We controlled for learning during trials by ensuring that each fish in a set of trials had the same level of previous experience with the experimental procedure; for all three light levels (except for the second set of trials run at 30 lx), each

© 2002 NRC Canada

Table 1. Experimental conditions by light level.

Light, lx	*n*	Mean fish mass, g	Mean temp., °C	Mean *Daphnia* length, mm	Mean time acclimated, h	Mean trial length, min	Prey density (*Daphnia*·L^{-1})	
							Lowest	Highest
30 (1)	30	3.53	21.0	1.50	20.0	9.61	3.0	26.0
30 (2)	24	8.16	19.5	2.03	17.7	9.44	3.0	55.7
30	54	5.59	20.4	1.73	18.9	9.53	3.0	55.7
15	26	5.05	19.3	1.43	20.1	9.57	3.0	25.9
15 and 30	80	5.41	20.0	1.63	19.3	9.54	3.0	55.7
0.1	30	6.11	18.3	1.47	20.6	9.61	3.0	37.6

Note: 30 (1) was the first set of trials run at 30 lx and 30 (2) was the second set of trials run at 30 lx (to control for learning); these trials were combined in our analyses to compose the 30 lx level. The last two rows (15 and 30, and 0.1 lx) represent two groups of trials, one for each data set (high light and low light, respectively). *n*, number of observations; temp., temperature.

fish had previously been through an experimental procedure exactly once. For the second set of trials run at 30 lx all fish had been through two previous trials. All fish used in feeding trials were randomly selected.

Trials began with the introduction of 3–55 *Daphnia*·L^{-1}. The density of *Daphnia* each fish was exposed to during the trial was chosen arbitrarily in that we did not sequentially run *Daphnia* densities starting low and ending high; densities were largely determined by *Daphnia* availability in our zooplankton cultures. After running numerous trials using several *Daphnia* densities, we filled in the gaps of missing *Daphnia* densities to the best of our abilities to have a somewhat even density distribution. In low-density trials (3–5 *Daphnia*·L^{-1}), the *Daphnia* to be introduced were counted individually so that the number of *Daphnia* eaten during the trial was known exactly. Because of the large number of *Daphnia* required for trials at >5 *Daphnia*·L^{-1}, we estimated the number introduced using a subsampling procedure in which six 5-mL aliquots were enumerated with a dissecting microscope and plankton wheel and then averaged (the average standard deviation for these means was 3.83 *Daphnia*, with an average coefficient of variation of 11.3%). *Daphnia* densities in trials were usually less than 30 L^{-1}, as we had originally set out to examine feeding rates at densities greater than those Hyatt (1980) used. Then we decided to run trials at even higher densities (near 55 *Daphnia*·L^{-1}), but after only two trials we deemed high-density trials impractical because they required too much time to count *Daphnia* before the start of trials. Though influential, we could not eliminate these two 55 *Daphnia*·L^{-1} trials in our analyses because they did not fail for any reason.

At the start of the trial, the initial dose of *Daphnia* was introduced through a feeder tube, which extended from outside of the arena housing to approximately 8 cm below the water surface in the arenas. To keep prey density relatively constant throughout the trial as *Daphnia* were consumed, we replenished the prey supply by adding *Daphnia* throughout the trial. At the beginning of each minute during the trial period (except for the first minute when the initial dose of *Daphnia* was added), a 5-mL volume "shot" of *Daphnia* in water was introduced through the feeder tube. The number of *Daphnia* to be introduced each minute for each density was estimated from pilot trials in which we visually enumerated all prey eaten by the kokanee at various prey densities. The number of *Daphnia* in each 5-mL replenishment shot was estimated in the same manner as for the initial dose. Trials were videotaped to determine when fish started feeding and to make behavioral observations.

At the end of the 10-min trial period, kokanee were removed from the arena and were slowly brought back down to holding tank temperatures. The uneaten *Daphnia* were filtered from the arena and counted under a dissecting microscope. To accurately determine feeding rate, the exact time spent feeding was obtained by reviewing videotapes of feeding trials. Because kokanee did not start feeding immediately upon *Daphnia* being introduced to the arena, actual time spent feeding varied for each trial. Videotapes were reviewed for each light level and actual time spent feeding was averaged and applied to all trials within that light level that were not videotaped (Table 1). Feeding trials at the 15-lx light level were not taped so actual time spent feeding at this light level was determined by averaging all other trial times. Typically, at the onset of the feeding trial, kokanee were positioned near the bottom of the feeding arena and were relatively still. We considered the fish to have begun feeding at the time it made its first strike at a prey item (kokanee were particulate-feeding, not filter-feeding); usually, the kokanee would accelerate rapidly towards the water surface, quickly strike a single *Daphnia*, then rapidly swim back down towards the bottom of the arena at a pronounced angle (anywhere between 15° and 75° from the direction of attack). After this initial attack, kokanee usually repeated this sequence several times and then rapid feeding would commence with several strikes made in a single attack. This sequence of initial attacks was short in length compared with the rest of the trial (lasting for approximately 10–15 s) and did not appreciably change the average consumption rate, so it was included in the total foraging time. After the initial attacks, the kokanee generally remained in the water column and used the entire arena to forage on *Daphnia*; kokanee did not appear to focus on the feeding tube as a food source (aeration kept the *Daphnia* evenly distributed throughout the arena). Consumption rates were determined by subtracting the number of *Daphnia* left over from the estimated number of *Daphnia* originally added to the arena plus the number of *Daphnia* added to the arena during the trial. The difference, the number eaten by the fish, was then divided by the trial time to obtain feeding rate (number of *Daphnia* eaten per minute). Percent change between the beginning and ending *Daphnia* densities in each trial was calculated by dividing the change in *Daphnia* density by the original *Daphnia* density. We slightly overestimated *Daphnia* consumption rates,

© 2002 NRC Canada

as *Daphnia* density among trials increased by an average of 9%, with a standard deviation of 38%; 25% of the trials had a density change of 50% or greater (only two points were identified as outliers using Cook's *D* and standard residuals analysis in SAS statistical software (SAS Institute Inc. 2001) and were removed from data analysis).

Three different light levels were used to determine the effect of light on kokanee consumption rate. The timing of the 30- and 15-lx light level trials overlapped each other because we had access to two arena houses, which provided us with two light level setups. The 0.1-lx trials were conducted after the 30-lx set, so that the timing of these trials also slightly overlapped the 15-lx light level trials. In total, the first set of trials took approximately five months to complete. Six months after the completion of the first set of trials, another set of trials was run at 30 lx to determine the effect of growth and learning on consumption rate; at this point, all fish used in this latter set of trials were 1 year and 3 months old and had experienced trial conditions twice previously.

Statistical analysis

A generalized linear models procedure (PROC GLM in SAS) was used to identify any covariates (fish mass, temperature, acclimation time, and *Daphnia* size) that were potentially important when data were classed by light level. Using this same procedure, we tested for differences between the first and second sets of trials run at 30 lx to determine if there were effects of growth or learning throughout the trial period. We then tested for differences in consumption rates among light levels within the range of *Daphnia* densities that we used in feeding trials. Two data sets (low light and high light) were created by pooling sets of trials for which light level was not a significant factor.

To fit functional response curves, linear and nonlinear analyses were performed for both the low light and high light data sets using PROC GLM and NLIN in SAS. Nonlinear curves were fit to the equation

$$(1) \qquad N = \frac{(\beta_0 P)}{(\beta_1 + P)}$$

where N is consumption rate of the predator (*Daphnia*·min^{-1}), P is prey density (*Daphnia*·L^{-1}), β_0 is maximum consumption rate (*Daphnia*·min^{-1}), and β_1 is the prey density (*Daphnia*·L^{-1}) at which consumption rate reaches half its maximum (Real 1979). Equation 1 can also be solved as a number, where N' is the total number of prey items eaten during the feeding trial (T, min) and β_0' is the maximum possible number of prey eaten during the trial (β_1 will remain the same). Although trials were not conducted below 3 *Daphnia*·L^{-1}, the intercepts for all functional response curves were forced through zero because kokanee do feed at extremely low prey densities (Hyatt 1980) and no suggestion of a negative intercept existed.

R^2 values were calculated for all functional response curves as the ratio of the explained sum of squares (ESS) over the corrected total sum of squares (corr. TSS) when ESS = corr. TSS – residual sum of squares (RSS). Akaike's information criterion (AIC_c, AIC corrected for small sample size) was also used to help determine which functional response model (linear vs. nonlinear) was most appropriate for each data set. AIC is corrected for small sample size by adding $(2k(k+1))(n-k-1)^{-1}$ to AIC to obtain AIC_c. Here, n is the number of trials for each data set and k is the number of estimable parameters in the model including one for σ^2. AIC/ AIC_c is a powerful tool used for model selection and is applied on a relative scale where the most appropriate model is the one with the lowest AIC_c value (Burnham and Anderson 1998). The difference in AIC_c values can also be a measure of how alternative models compare: a difference of <2 units indicates substantial support for a competing model, a difference between 3 and 7 units indicates considerably less support, and a difference of 10 or more units between the best and competing model indicates essentially no support for the competitor (Burnham and Anderson 1998).

Holling's disc equation (1959, 1966; Houck and Strauss 1985) can also be used to fit the type II functional response using PROC NLIN

$$(2) \qquad N' = \frac{(aTP)}{(1 + aT_h P)}$$

Note that in this equation, N' is the total number of prey eaten during the foraging period, T (min). In addition, T_h is handling time (min·prey^{-1}) and a is rate of successful search, which is equal to the volume of foraging habitat a predator can search during a unit of time (volume·time^{-1}, in L·min^{-1}) (Madenjian and Carpenter 1991). Rate of successful search (a) is composed of several components, including reaction distance of the predator, predator and prey velocity, and capture success (Holling 1966). Equation 2 can be solved as a rate by dividing both sides of the equation by T. By treating N' as total number of *Daphnia* eaten for both eqs. 1 and 2, these equations can be linked by defining β_0' as $T \cdot T_h^{-1}$ and β_1 as $(a \cdot T_h)^{-1}$ (Gotelli 1998) and deriving the following relationship:

$$(3) \qquad \beta_0' = \beta_1 Ta = \frac{T}{T_h}$$

The relationship between eqs. 1 and 2 can be seen by multiplying the numerator and denominator of eq. 2 by $(a \cdot T_h)^{-1}$ and substituting β_0' and β_1 with the above terms to arrive at eq. 1 (in terms of N') (Gotelli 1998). Equation 1 was used to obtain values for β_0 and β_1; we then used PROC NLIN to calculate T_h and a for the high light model with eq. 3 (β_0 was multiplied by the average time spent feeding to obtain β_0'). Both a and T_h could be calculated using eq. 2 with similar results.

Predicting foraging behavior

To investigate how realistic summertime gradients in light and food density in the field might affect kokanee foraging, we used the two functional response models to predict feeding rate and feeding duration (time to fill the stomach) in Blue Mesa Reservoir, Colo. Blue Mesa Reservoir is a 3700-ha coldwater impoundment on the Gunnison River, in southwest Colorado. We used an algorithm developed by Janiczcek and DeYoung (1987) to determine incident light intensity at Gunnison, Colo., for time of day and date, and then calculated ambient light intensity by depth with an extinction coefficient (h) derived from Idso and Gilbert (1974)

© 2002 NRC Canada

(4) $$\eta = 1.7 z_{sd}^{-1}$$

where z_{sd} is Secchi depth in metres. Light intensity (I_z) at depths of 1-m intervals (z) was calculated using the following relationship (Horne and Goldman 1994):

(5) $$I_z = I_0 e^{-\eta z}$$

We evaluated feeding rate and duration of kokanee on three separate dates in 1994 (21 May, 10 June, and 16 Sept.) at times of civil twilight (beginning in the morning or ending in the evening when the sun is geometrically six degrees below the horizon), 30 min after sunrise, and at noon, throughout depths of 0–30 m. *Daphnia* densities at depths of 0–5, 5–10, 10–15, and 15–30 m were obtained from Clark-Bumpus field samples taken on the dates of interest from the Sapinero Basin of Blue Mesa Reservoir (B.M. Johnson, unpublished data). By knowing light level and prey density at a given location, we predicted the corresponding consumption rate with β_0 and β_1 from our models. For all locations where light level was above Ali's (1959) minimum light required for maximum feeding rates (3.40 lx), we used the high light model to predict feeding rates; for all locations where light level was between 0.001 and 3.40 lx we used the low light model to predict feeding rates; below 0.001 lx (minimum light level required for minimum feeding rates) we assumed that it was too dark for kokanee to feed. We then estimated maximum stomach capacity in grams as a function of fish mass (Brett 1971, who used fish 2–350 g)

(6) $$\text{capacity} = \frac{\text{mass} \cdot (14.1 - 4.95 \cdot \log(\text{mass}))}{100}$$

The average length of *Daphnia* in kokanee stomach samples collected at Blue Mesa Reservoir during the summer of 1997 was 1.84 mm (Stockwell et al. 1999); we calculated wet mass (mg) for individual *Daphnia* of this size according to Stockwell and Johnson (1999). We then calculated how many *Daphnia* of this mass could be eaten by a 5-g kokanee (which fall within the range of fish used by Brett 1971) and determined time to satiation (stomach fullness) using the feeding rate we calculated for each depth and prey density.

Results

Light level and *Daphnia* density were highly significant predictors of kokanee feeding rate and functional response. When all data were grouped together and classed by light level in a generalized linear model, only light level ($p < 0.0001$) and *Daphnia* density ($p < 0.0001$) were significant factors in predicting feeding rate; the effects of all other factors tested were not significant (fish mass $p = 0.10$, temperature $p = 0.59$, *Daphnia* size $p = 0.52$, experience level $p = 0.32$, and acclimation time $p = 0.67$). The two sets of trials run at 30 lx were not significantly different from each other (PROC GLM in SAS: intercept $p = 0.86$, slope $p = 0.43$). This supported our hypothesis that there was no effect of growth or learning during the entire trial process, so the two 30-lx sets of trials were combined. Highest feeding rates were obtained with the intermediate light level, 15 lx, but were not significantly different from rates at 30 lx (least squares means test in SAS, $p = 0.28$), so these two sets of trials were also pooled to form the high light data set. Feeding rates obtained at the 0.1-lx light level (the low light data set) were significantly lower than in both the 15- and 30-lx light level trials (least squares means test, $p < 0.0001$).

We fit linear and nonlinear functional response curves to both of the data sets to obtain our two final models (Fig. 1). For these two models, we selected a different functional response shape for each. We chose a linear, type I fit with intercept forced through zero for the low light model

(7) $$N = 1.74V$$

When PROC NLIN in SAS was applied to the low light data set the type I functional response shape was still evident; we ultimately selected the linear model for the low light data set because PROC NLIN calculated an unrealistically high maximum consumption rate and AIC_c results supported the linear rather than nonlinear model (R^2 values for each curve were very similar; 0.62 and 0.61, respectively) (Table 2). Whereas a linear model predicts an infinitely high maximum consumption rate (higher than that of the nonlinear model), we have no data that indicates what type of functional response would occur over a larger range of prey densities; therefore, the type I functional response is adequate in describing feeding rates at low light over the range of *Daphnia* densities used in our feeding trials. A nonlinear type II functional response fit best for the high light data

(8) $$N = \frac{(163.3V)}{(42.2 + V)}$$

In support of this decision, the AIC_c value for the nonlinear model was much lower than that of the linear model when intercepts were forced through zero, and the R^2 value for the nonlinear model (0.58) was greater than that of the linear model (0.42) (Table 2).

Using the type II functional response model obtained at the high light level, we estimated a and T_h. a in our high light model was 3.86 $L \cdot min^{-1}$ ($p < 0.0001$). We calculated a prey T_h of 0.36 $s \cdot Daphnia^{-1}$ ($p < 0.0001$).

Light intensity at Blue Mesa Reservoir during the summer of 1994 varied greatly with time of day, depth, and month. Secchi depth was lowest in mid-June (2.9 m) and highest in mid-September (7.4 m, Fig. 2*a*). *Daphnia* densities at Blue Mesa Reservoir were highest near the surface (0–5 m: 9.5, 18.2, and 11.3 L^{-1} on 21 May, 10 June, and 16 Sept., respectively) and lowest at 15–30 m (2.0, 0.2, and 0.2 L^{-1}). Estimated consumption rates were highest in mid-June at the surface (49 min^{-1}), and lowest between 15 and 30 m in mid-June and mid-September (0.3–0.8 min^{-1}). Feeding rates in late May were intermediate, ranging from 30 to 3 min^{-1} through depths of 1–30 m. We estimated a 5-g kokanee to have a maximum stomach capacity of 0.53 g, which is able to hold 3261 *Daphnia* 1.84 mm in length (average wet mass 0.163 mg). Therefore, a 5-g kokanee would need to forage for approximately 1.1 h near the surface in mid-June to reach stomach fullness, as opposed to 14–27 h when located at a depth of 10–15 m, and an impossible 181 h at depths of 15–30 m (Fig. 2*b*). Foraging durations were intermediate and more uniform throughout depth in May (ranging from 1.8 to 18 h). Foraging durations were much more stratified in September (as in June) with relatively low feeding dura-

© 2002 NRC Canada

Fig. 1. (*a*) The low light model was fit using a type I linear regression with intercept forced through zero. (*b*) The high light model was fit using a type II nonlinear function. The broken lines are 95% confidence intervals around the mean.

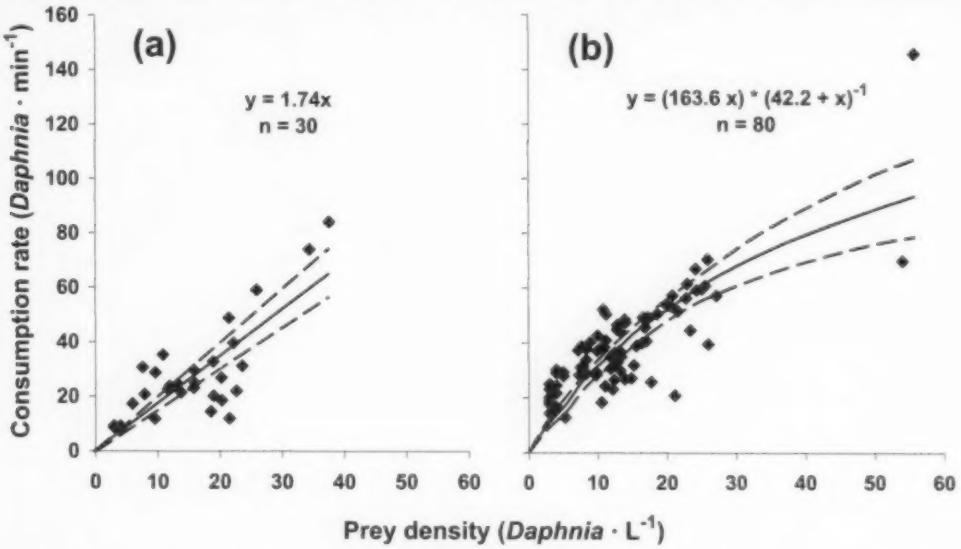

Table 2. Parameter estimates for theoretical linear and nonlinear models for low light and high light data sets.

	Low light		High light	
Data set	Linear model*	Nonlinear model	Linear model	Nonlinear model*
Slope (standard error)	1.74 (0.115)	N/A	2.45 (0.092)	N/A
Slope p value	<0.0001	N/A	<0.0001	N/A
Corrected total df	29	29	79	79
β_0 (standard error)	N/A	$6.41 \cdot 10^{10}$ ($4.25 \cdot 10^{9}$)	N/A	163.6 (30.9)
β_1 (standard error)	N/A	$3.69 \cdot 10^{10}$ (infinity)	N/A	42.2 (11.6)
Model p value	<0.0001	<0.0001	<0.0001	<0.0001
n	30	30	80	80
k	2	3	2	3
RSS	3689.1	3689.1	14 972.4	10 708.2
R^2	0.62	0.61	0.42	0.58
AIC_c	148.8	151.3	422.7	398.1

Note: The intercept for all models is zero. The corrected total degrees of freedom is the sum of the model and error degrees of freedom. n is the number of trials for each data set and k is the number of estimable parameters in the model including one for σ^2. AIC_c calculations are also presented for all models (the lowest AIC_c value within each data set indicates the best model). N/A, not applicable; df, degrees of freedom.

*The final model selected for either the low light or high light data sets.

tions at the surface (1.5–1.9 h) that sharply increased to 68–181 h at depths of 15–30 m.

Discussion

In laboratory trials, kokanee feeding rate increased with zooplankton density. This relationship was modified by light intensity, decreasing consumption rates at very low light levels. When we divided our data into two models (low light and high light), we observed that two different foraging modes occurred at these different light levels that resulted in type I and type II functional response curves, respectively. The rate of increase for the consumption rates at our lowest light level remained constant regardless of prey density, resulting in a type I functional response. Although higher light levels generally resulted in higher consumption rates, the assumption that the feeding rate intercept equals zero resulted in the appearance of a type II functional response with an asymptote of 163.6 *Daphnia*·min^{-1}. Hypothetically, prey density and feeding rate should intercept each other at zero, unless a predator does not begin to forage until a specific prey density is achieved; however, Hyatt's experiments (1980) showed that kokanee feed at very low prey densities (approximately 0.5 *Daphnia*·L^{-1}). Whereas an empirical model may fit a particular data more precisely, using a theoretical model to describe patterns in the data reflects complexities in parameters such as maximum consumption rate, handling time, and rate of successful search.

Changes in light level were associated with a change in foraging mode. In physiological experiments with Pacific

© 2002 NRC Canada

Fig. 2. (*a*) Secchi depth, *Daphnia* density (bars), and temperature (solid line) profiles for Sapinero basin in Blue Mesa Reservoir, Colo., during the summer of 1994. (*b*) Feeding durations (in hours) over depth and time of day, where pre-dawn is civil twilight, and post-dawn is a half hour after dawn (times for Gunnison, Colo., were obtained from the U.S. Naval Observatory). Cross-hatched areas are locations where it was too dark for kokanee (*Oncorhynchus nerka*) to feed. It should be noted that feeding rate and duration patterns at dusk are similar to the dawn patterns shown here.

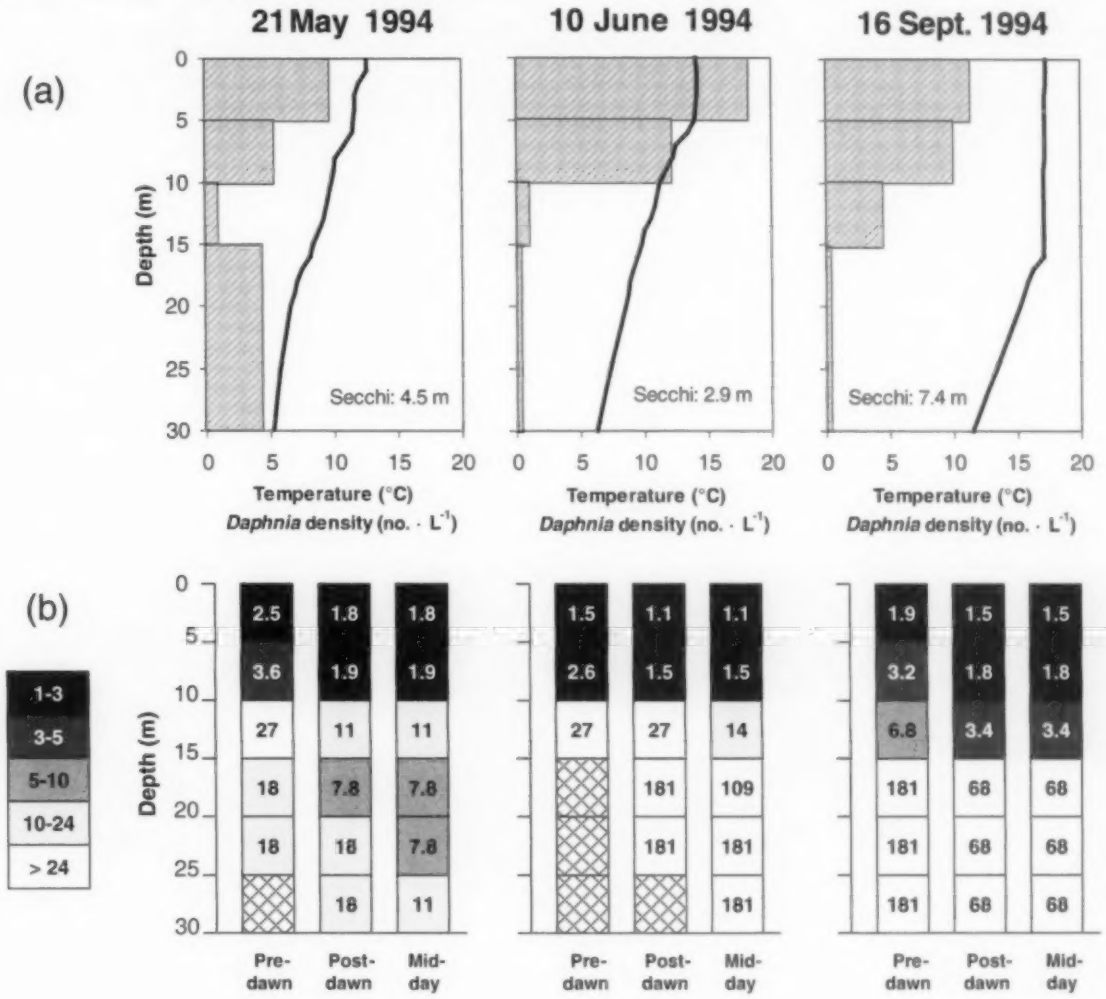

salmon (*Oncorhynchus* spp.), Ali (1959) found that there were minimum light levels required for feeding, as well as light thresholds for minimum and maximum feeding rates. He concluded that most salmon are capable of feeding at light levels corresponding to those on clear nights with a new moon, but maximum feeding rates tend to occur at light levels at or above what is experienced during crepuscular periods. Our 15- and 30-lx light levels (in the high light model), which are very similar to each other relative to the diel range of light intensities in nature, fall just above the lowest light level required to obtain maximum feeding rates. These correspond to light levels in the epilimnion during crepuscular periods, when kokanee are known to feed most heavily in the wild (Eggers 1978; Bevelhimer and Adams 1993). If feeding rate was not limited by the ability to visually detect prey at these light levels, then we would expect kokanee to approach saturation as prey density increased to the point that handling time prevented further increases in feeding rate. In fact, the 163.6 *Daphnia*·min^{-1} asymptote at which maximum feeding rate occurs in our high light model is well within reason (Stockwell and Johnson 1999), but the prey density where this asymptote is reached lies far beyond the 55 *Daphnia*·L^{-1} that we tested in feeding trials.

Alternatively, the 0.1-lx level falls below the threshold for maximum feeding rates, but is still within the range for visual feeding. Owing to the straight-line relationship between density and consumption rate, we believe that consumption rates might be more affected by chance encounters with *Daphnia* which happen to drift in front of the kokanee, a relationship that is very much a function of prey density. In

© 2002 NRC Canada

Fig. 3. The Stockwell and Johnson model (1997) predicts a shift in functional response shape with changes in reaction distance. As reaction distance increases (e.g., light level increases or turbidity decreases), a type II functional response is evident; with lower reaction distances the type II response shifts towards a type I functional response. In this simulation, we used a 5-g fish (*Oncorhynchus nerka*) at 10°C, using a handling time of 0.36 s.

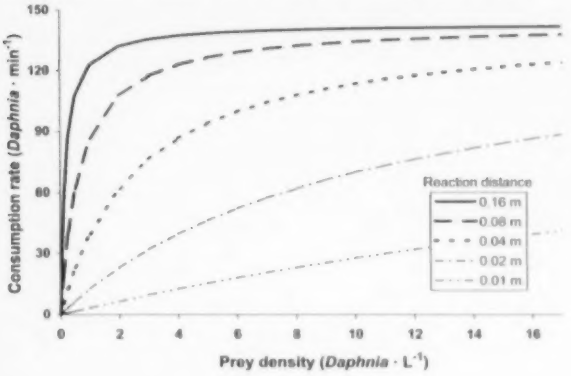

fact, this is what we observed in our feeding trials; at high light intensities (15 and 30 lx), fish actively pursued prey, but at the low light level, fish spent a greater proportion of their time remaining relatively still and striking at *Daphnia* that drifted in front of their snouts. Furthermore, at the high light levels, kokanee selectively fed on larger *Daphnia*; at the low light level, little selectivity occurred reinforcing the notion that prey consumption was largely based on random encounters (M.L. Koski, unpublished data).

The Stockwell and Johnson (1997) model predicted the shift in functional response shape in relationship to light level (Fig. 3). Reaction distance (and search volume) of a fish increases with light level. When reaction distance was manipulated in their model, functional response shape gradually changed from a type II to a type I functional response as reaction distance decreased. Functional responses at low light levels then, close to the minimum feeding threshold, will resemble straight lines; as light level increases, curvature will appear because feeding rate is limited by search time at low prey densities and handling time at high prey densities instead of random encounters with prey.

It is possible that at higher prey densities feeding mode may shift from particulate- to gulp-feeding (Helfman 1990), creating a discontinuity in the functional response curve. In pilot trials with extremely high *Daphnia* densities (hundreds of *Daphnia*·L^{-1}) we observed kokanee gulp-feeding. For every strike, several prey were consumed, but there was no indication of filter feeding. This foraging mode shift could alter the functional response from a type II at low to moderate prey densities, to a type I response when prey density becomes sufficiently high for the fish to consume several prey in a single strike. The end result may be a functional response that is a composite of type II and type I curves. This phenomenon may also explain some of the variation we observed at very high prey densities in feeding trials; some fish may have been gulp-feeding while others were still particulate-feeding.

In addition to obtaining functional response curves at different light levels, we used our functional response models to compare estimated consumption rates and feeding durations of a young-of-the-year kokanee throughout a range of depths in the summer of 1994 at Blue Mesa Reservoir. Stockwell and Johnson (1999) showed that in early summer, choice of foraging depth had little effect on the fish's energy budget because of weak thermal stratification. Thus, prey density and light may be more important environmental variables at this time of year. In fact, there are advantageous locations for a foraging kokanee in the early summer; in May, it is possible for kokanee to feed at intermediate depths (10–25 m) and be able to fill their stomachs during post-dawn and mid-day periods. However, in summer when stratification is more pronounced, there is less of an opportunity for kokanee to choose over a wide range of foraging habitats. In mid-June, a 5-g kokanee could fill its stomach in approximately 1–2 h if it foraged in the upper 10 m of the reservoir after dawn and into the day, but the time required to fill its stomach increases tremendously below 10 m. The stratification observed in June and September foraging rates and durations was caused by different factors. In June, the Secchi depth was fairly low (2.9 m). Although prey abundance was high in the epilimnion, foraging rates dropped off sharply below 10 m because along with a decrease in *Daphnia* density, light level sharply decreased thus lowering visibility and the ability of kokanee to feed at maximum rates. In September, foraging rates and durations were similar to June in the upper 10 m. However, the Secchi depth was 7.4 m; even at a depth of 30 m, light was sufficient for kokanee to feed at maximum rates. In this case, though, foraging was inhibited by *Daphnia* density, limiting foraging rates and dramatically increasing feeding duration below 15 m. Presumably, shorter feeding durations would be advantageous for small fish that must balance energy intake with predation risk. Thus, the vertical structure of the pelagic zone presents planktivorous fishes with important choices about foraging location.

We also found that foraging constraints on the energy budget probably change as kokanee grow. When we applied our high light functional response model to a 5-g kokanee foraging between 0 and 5 m during the post-dawn hours of 10 June 1994, we predicted that the fish would need to forage 1.1 h (at a rate of 49 *Daphnia*·min^{-1}) to fill its stomach once. A 200-g (age-2) kokanee, on the other hand, would have to feed for 11.3 h under the same conditions to fill its stomach. Anecdotal information suggests that this does not occur at Blue Mesa Reservoir; angler catch-per-unit-effort typically falls off greatly by midday in summer because kokanee are not in the epilimnion and feeding much during the day. Thus, the functional response models we developed may not be appropriate for larger kokanee (>age 1), which need to feed at very high rates to satisfy their daily energy requirements. We speculate that larger kokanee may exhibit a foraging mode switch from particulate- to gulp- or filter-feeding to obtain enough food to maintain growth and sustain a larger body size.

Although these experiments better define the shape of the kokanee functional response, additional experiments at extreme (high and low) prey densities and more light levels are necessary to fully understand kokanee feeding behavior in

© 2002 NRC Canada

the wild. We are cautious about concluding we have determined the maximum feeding rate of kokanee; no evidence of an asymptote existed for the low light model, and the asymptote for the high light model is speculative because of the influence of the two high-density points. Regardless of these limitations, our functional response models should be suitable for application in oligotrophic, mesotrophic, or well-mixed systems where kokanee experience zooplankton densities less than 55 *Daphnia*·L^{-1}. Whereas the highest prey densities in the majority of the feeding trials were at or above the maximum average *Daphnia* densities observed in many regional reservoirs (ranging from approximately 5–18 L^{-1}; Schneidervin 1985; Baldwin et al. 2000; Stockwell and Johnson 1999), wild kokanee may seek patches of prey that can have order of magnitude higher densities than the average concentration measured by sampling gear (Pinel-Alloul 1995; Folt and Burns 1999). Feeding trials at prey densities much higher than the 55 L^{-1} we used may be necessary to fully define the asymptotic nature of the functional response and accurately predict kokanee feeding rate at very high prey densities. Further, it would be helpful to obtain kokanee feeding rates at very low *Daphnia* densities (<3 L^{-1}) to evaluate our theoretical assumptions of forcing functional response curves through zero, as well as provide support for our model in very oligotrophic systems.

Clearly, a large suite of factors controls foraging behavior of planktivorous fishes, including those manipulated in our laboratory experiments. For lentic fishes like kokanee, which commonly exhibit DVM, the foraging environment is highly heterogeneous. Strong vertical gradients in food density, temperature, and light are the norm for stratified lakes and reservoirs during the growing season. Predation risk also varies in a complex fashion, depending on the thermal preference of the dominant piscivores. Hence, predicting foraging behavior in the wild requires more than light-dependent functional response curves. However, because of the simple diet of kokanee, and the central importance of energy intake rates, knowledge of the relationship among food density, light, and feeding rate allows one to predict how these fundamental variables may constrain behavior in the wild. We suggest that future studies explore the importance of light even further, examining feeding rates at and around the threshold for maximum feeding rates. Because reaction distance changes significantly at lower light levels, it would be useful to obtain feeding rates at light levels even lower than the threshold, and determine what the threshold actually is (Is it really 3.4 lx as Ali (1959) estimated?). It would also be interesting to examine feeding rates at very high light levels (i.e., midday epilimnetic light levels) to evaluate if light-inhibition cues exist for kokanee that may signal them to stop foraging to avoid predation.

Functions that link predator feeding rates to prey density are powerful tools for exploring the influence of food availability on the foraging behavior of fishes. For visual feeders, including light level explicitly into the functional response is important because light modifies a predator's detection of prey, search time, and feeding rate, and because fish experience tremendous temporal and spatial (especially in lentic systems) variation in the light environment. When incorporated into more elaborate, bioenergetics-based foraging models (e.g., Madenjian and Carpenter 1991; Arrhenius and Hansson 1993; Stockwell and Johnson 1997), functional responses can further allow these models to be used as predictive tools for forecasting how fish growth and behavior respond to environmental perturbations like eutrophication that may alter water clarity or food availability.

Acknowledgements

We are grateful for the help of Tori Stecklein for her assistance in running feeding trials, counting untold thousands of *Daphnia*, and in laboratory maintenance; thanks also to Jeremy Monroe and Todd Stevenson for their help in the lab. Jim zumBrunnen and Ken Burnham provided statistical assistance. We thank the Colorado Division of Wildlife, particularly Terry Robinson, Phil Schlerr, and Pete Walker for providing fish, technical assistance, and supplies. Sture Hansson, Dave Beauchamp, and an anonymous reviewer provided excellent suggestions for improving this manuscript. Funding for this project was provided by the U.S. Bureau of Reclamation, Upper Colorado Region, Salt Lake City, Utah.

References

Ali, M.A. 1959. The ocular structure, retinomotor and photobehavioral responses of juvenile Pacific salmon. Can. J. Zool. **37**: 965–996.

Arrhenius, F., and Hansson, S. 1993. Food consumption of larval, young and adult herring and sprat in the Baltic Sea. Mar. Ecol. Prog. Ser. **96**: 125–137.

Baldwin, C.M., Beauchamp, D.A., and Van Tassell, J.J. 2000. Bioenergetic assessment of temporal food supply and consumption demand by salmonids in the Strawberry Reservoir food web. Trans. Am. Fish. Soc. **129**: 429–450.

Beauchamp, D.A., Stewart, D.J., and Thomas, G.L. 1989. Corroboration of a bioenergetics model for sockeye salmon. Trans. Am. Fish. Soc. **118**: 597–607.

Bevelhimer, M.S., and Adams, S.M. 1993. A bioenergetics analysis of diel vertical migration by kokanee salmon, *Oncorhynchus nerka*. Can. J. Fish. Aquat. Sci. **50**: 2336–2349.

Brett, J.R. 1971. Satiation time, appetite, and maximum food intake of sockeye salmon (*Oncorhynchus nerka*). J. Fish. Res. Board Can. **28**: 409–415.

Brooks, J.L., and Dodson, S.I. 1965. Predation, body size and composition of the plankton. Science (Washington, D.C.), **150**: 28–35.

Burnham, K.P., and Anderson, D.R. 1998. Model selection and inference: a practical information-theoretic approach. Springer-Verlag, New York.

Carpenter, S.R., and Kitchell, J.F. 1993. The trophic cascade in lakes. Cambridge University Press, Cambridge.

Christoffersen, K., Riemann, B., Klysner, A., and Sondergaard, M. 1993. Potential role of fish predation and natural populations of zooplankton in structuring a plankton community in eutrophic lake water. Limnol. Oceanogr. **38**: 561–573.

DeVries, D.R., and Stein, R.A. 1992. Complex interactions between fish and zooplankton: quantifying the role of an open-water planktivore. Can. J. Fish. Aquat. Sci. **49**: 1216–1227.

Dower, J.F., Pepin, P., and Leggett, W.C. 1998. Enhanced gut fullness and an apparent shift in size selectivity by radiated shanny (*Ulvaria subbifurcata*) larvae in response to increased turbidity. Can. J. Fish. Aquat. Sci. **55**: 128–142.

Eggers, D.M. 1978. Limnetic feeding behavior of juvenile sockeye salmon in Lake Washington and predator avoidance. Limnol. Oceanogr. **23**: 1114–1125.

© 2002 NRC Canada

Finnell, L.M., and Reed, E.B. 1969. The diel vertical movements of kokanee salmon, *Oncorhynchus nerka*, in Granby Reservoir, Colorado. Trans. Am. Fish. Soc. **2**: 245–252.

Folt, C.L., and Burns, C.W. 1999. Biological drivers of zooplankton patchiness. Trends Ecol. Evol. **14**: 300–305.

Gotelli, N.J. 1998. A primer of ecology. 2nd ed. Sinauer Associates, Inc., Sunderland, Mass.

Helfman, G.S. 1990. Mode selection and mode switching in foraging animals. Adv. Study Behav. **19**: 249–298.

Holling, C.S. 1959. The components of predation as revealed by a study of small mammal predation of the European pine sawfly. Can. Entomol. **91**: 293–320.

Holling, C.S. 1966. The functional response of predators to prey density and its role in mimicry and population regulation. Mem. Entomol. Soc. Can. **48**: 5–60.

Horne, A.J., and Goldman, C.R. 1994. Limnology. 2nd ed. McGraw-Hill, Inc., New York.

Houck, M.A., and Strauss, R.E. 1985. The comparative study of functional responses: experimental design and statistical interpretation. Can. Entomol. **117**: 617–629.

Hyatt, K.D. 1980. Mechanisms of food resource partitioning and the foraging strategies of rainbow trout (*Salmo gairdneri*) and kokanee (*Oncorhynchus nerka*) in Marion Lake, British Columbia. Ph.D. thesis, The University of British Columbia, Vancouver, B.C., Canada.

Idso, S.B., and Gilbert, R.G. 1974. Universality of Poole and Atkins secchi disk–light extinction equation. J. Appl. Ecol. **11**: 399–401.

Janiczcek, P.M.J., and DeYoung, A.J. 1987. Computer programs for sun and moon illuminance with contingent tables and diagrams. U.S. Naval Observatory Circular, **171**: 1–32.

Landry, F., Miller, T.J., and Leggett, W.C. 1995. The effects of small-scale turbulence on the ingestion rate of fathead minnow (*Pimephales promelas*) larvae. Can. J. Fish. Aquat. Sci. **52**: 1714–1719.

Levy, D.A. 1990. Reciprocal diel vertical migration behavior in planktivores and zooplankton in British Columbia lakes. Can. J. Fish. Aquat. Sci. **47**: 1755–1764.

Link, J., and Edsall, T.A. 1996. The effect of light on lake herring (*Coregonus artedi*) reactive volume. Hydrobiologia, **332**: 131–140.

Madenjian, C.P., and Carpenter, S.R. 1991. Individual-based model for growth of young-of-the-year walleye: a piece of the recruitment puzzle. Ecol. Appl. **1**: 268–279.

O'Brien, W.J. 1979. The predator–prey interaction of planktivorous fish and zooplankton. Am. Sci. **67**: 572–581.

Pinel-Alloul, B. 1995. Spatial heterogeneity as a multiscale characteristic of zooplankton community. Hydrobiologia, **300/301**: 17–42.

Real, L.A. 1979. Ecological determinants of functional response. Ecology, **60**: 481–485.

SAS Institute Inc. 2001. SAS/STAT user's guide, release 8.0 ed. SAS Institute Inc., Cary, N.C.

Schneidervin, R.W. 1985. Zooplankton stocks and the nature of size-selective predation by fishes in Flaming Gorge Reservoir, Wyoming-Utah. M.Sc. thesis, University of Wyoming, Laramie.

Smith, R.L. 1998. Elements of ecology. 4th ed. Menlo Park, Calif.

Stockwell, J.D., and Johnson, B.M. 1997. Refinement and calibration of a bioenergetics-based model for kokanee (*Oncorhynchus nerka*). Can. J. Fish. Aquat. Sci. **54**: 2659–2676.

Stockwell, J.D., and Johnson, B.M. 1999. Field evaluation of a bioenergetics-based foraging model for kokanee (*Oncorhynchus nerka*). Can. J. Fish. Aquat. Sci. **56**(Suppl. 1): 140–151.

Stockwell, J.D., Bonfantine, K.L., and Johnson, B.M. 1999. Kokanee foraging: a *Daphnia* in the stomach is worth two in the lake. Trans. Am. Fish. Soc. **128**: 169–174.

Townsend, C.R., and Risebrow, A.J. 1982. The influence of light level on the functional response of a zooplanktonivorous fish. Oecologia, **53**: 293–295.

U.S. Naval Observatory. 2001. Rise, set, and twilight definitions. Astronomical applications. http://aa.usno.navy.mil/faq/docs/RST_defs.html (accessed 28 Jan. 2002).

Vanni, M.J. 1987. Effects of food availability and fish predation on a zooplankton community. Ecol. Monogr. **57**: 61–88.

Vinyard, G.L., Drenner, R.W., and Hanzel, D.A. 1982. Feeding success of hatchery-reared kokanee salmon when presented with zooplankton prey. Prog. Fish-Cult. **44**: 37–39.

© 2002 NRC Canada

Experimental management for Snake River spring–summer chinook (*Oncorhynchus tshawytscha*): trade-offs between conservation and learning for a threatened species

Charles M. Paulsen and Richard A. Hinrichsen

Abstract: Using Snake River spring–summer chinook (*Oncorhynchus tshawytscha*) as an example, we explore trade-offs between conservation (restoring population abundance to self-sustaining levels) and learning (reliably estimating how management strategies affect productivity). The population has been studied extensively, especially since 1992, when the evolutionarily significant unit (ESU) was listed under the U.S. Endangered Species Act. Understanding both the conservation and learning dimensions is crucial in evaluating management actions. Using a Bayesian simulation model calibrated with 40+ years of spawner–recruit estimates, we performed population viability analyses to examine the biological risks of an array of management strategies. We also performed power analyses to estimate the precision of estimates of the actions' effects. The results suggest that if one can take actions that increase productivity and manage those actions as experiments, one can simultaneously increase fish numbers and reduce the uncertainty about the effects of those actions. However, because more powerful experiments will utilize controls where no action is taken, an experimental approach may increase risks to the ESU when compared to a strategy that tries to maximize productivity as soon as possible.

Résumé : L'exemple de la population de printemps et d'été du saumon quinnat (*Oncorhynchus tshawytscha*) de la rivière Snake nous a permis d'évaluer les compromis entre la conservation (restauration de la densité de la population à un niveau d'autosuffisance) et l'avancement des connaissances (estimation fiable des effets des stratégies de gestion sur la productivité). Cette population a été étudiée en profondeur, particulièrement depuis 1992, lorsqu'elle a été désignée comme unité évolutive importante (ESU, « evolutionarily significant unit ») dans le cadre de la loi américaine sur les espèces menacées (U.S. Endangered Species Act). La compréhension à la fois des aspects de conservation et ceux d'avancement des connaissances est vitale dans l'évaluation des opérations de gestion. À l'aide d'un modèle de simulation bayésien calibré avec des estimations de la relation reproducteurs–recrues sur une période de plus de 40 ans, nous avons pu procéder à des analyses de viabilité dans le but de déterminer les risques biologiques associés à une gamme de stratégies de gestion. Des analyses de puissance ont servi à déterminer la précision des estimations des effets des diverses stratégies. Nos résultats montrent que si on peut procéder à des opérations qui augmentent la productivité et les gérer comme des expériences, on peut accroître la densité des poissons, tout en réduisant l'incertitude associée aux effets de ces opérations. Cependant, parce que des expériences plus rigoureuses nécessitent l'utilisation de témoins qui ne reçoivent aucun traitement, une approche expérimentale pourrait augmenter les risques courus par l'ESU, par comparaison à une stratégie qui cherche à maximiser la productivité le plus rapidement possible.

[Traduit par la Rédaction]

Introduction

Snake River spring–summer chinook (*Oncorhynchus tshawytscha*) were listed by the National Marine Fisheries Service (NMFS) as threatened under the U.S. Endangered Species Act (ESA) in 1992 (NMFS 1995). They have been the subject of intensive study since the early 1970s, and redd (nest) counts in index areas extend back to the late 1950s (Beamesderfer et al. 1997). Trends in spawning abundance have been markedly downward over the past several decades and are especially pronounced since the late 1960s (Fig. 1). Despite the long escapement series, unambiguously identifying the cause(s) of their decline is difficult, because many potential problems for the stocks occurred simultaneously

Received 28 August 2001. Accepted 20 April 2002. Published on the NRC Research Press Web site at http://cjfas.nrc.ca on 24 May 2002.
J16514

C.M. Paulsen.[1] Paulsen Environmental Research Ltd., 16016 SW Boones Ferry Road, Suite 4, Lake Oswego, OR 97035, U.S.A.
R.A. Hinrichsen. Hinrichsen Environmental Services, 3216 NE 45th Place, Suite 303W, Seattle, WA 98105-4028, U.S.A.

[1]Corresponding author (e-mail: cpaulsen@PaulsenEnvironmentalResearch.com).

 DOI: 10.1139/F02-053 © 2002 NRC Canada

Fig. 1. Average spawning escapement over time for seven Snake spring–summer chinook (*Oncorhynchus tshawytscha*) index stocks. Sources: Beamesderfer et al. (1997); Eric Tinus (Oregon Department of Fish and Wildlife, Portland, Oreg., unpublished data).

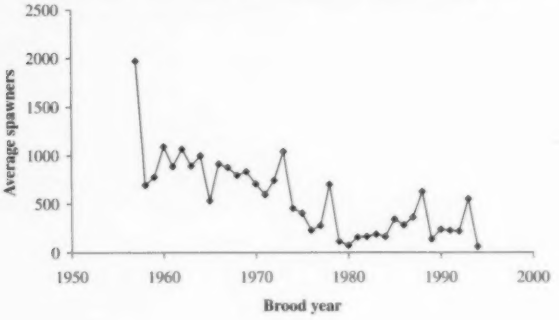

(Karieva et al. 2000; Zabel and Williams 2000; Peters and Marmorek 2001).

One obvious candidate to explain the decline in productivity is the increase in the number of dams that smolts (juvenile downstream migrants) and returning adults must pass to survive and complete their life cycle (e.g., Schaller et al. 1999; Deriso et al. 2001). Declines in productivity may also be caused, in part, by decreases in marine-derived nutrients because of the reduction in salmon carcasses on spawning beds. For some salmonid stocks, especially in coastal streams and lakes, carcasses of spawned-out fish are important nutrient sources, increasing the growth and survival of juveniles (Cederholm et al. 2000; Gresh at al. 2000). Comparable research has not been done for Snake River chinook, but it is plausible that declines in marine-derived nitrogen and phosphorus may play a role, especially for stocks rearing in oligotrophic areas. Other potential confounding effects are numerous. For example, an extensive literature has developed suggesting that decadal changes in ocean conditions are important in explaining large-scale variation in catch for a number of salmon species, including chinook (Hare et al. 1999).

What should managers do in the face of this uncertainty? A common recommendation is to use an adaptive management approach (e.g., Walters 1986; Walters and Sainsbury 1990; Walters et al. 1992). In the fisheries field, situations where harvest rate is the main decision variable have probably received the most attention (e.g., Walters and Sainsbury 1990). However, since harvest rates on Snake spring–summer chinook are presently less than 10% (Beamesderfer et al. 1997), further decreases in harvest will have little effect on stock abundance. Adaptive management models that examine alteration in freshwater habitat are less common and have usually used spawning escapement as the response variable (e.g., Maxell 1999; Williams 1999). If estimates are available for both spawning abundance and age structure of the spawning population, one can make estimates of recruitment (i.e., offspring as adult spawners in future) over time. Recruitment estimates combine both fecundity (eggs per spawner) and survival from egg to adult spawner, so recruits per spawner (*R/S*) may be quite sensitive to changes resulting from management actions.

In this paper we evaluate experimental actions that affect *R/S* based on their power (opportunity for learning) and effect on the population (viability analysis). Our objective is to show where the goals of learning and conservation may collide and where they may coincide for management actions considered for endangered Snake River salmon populations. We examine a status quo action and two illustrative examples: a "do everything" action that effects all stocks simultaneously and a nutrient supplementation action that can be applied to a subset of the index stocks, with the rest used as controls. Each action is evaluated based on power and ability to foster recovery.

Conducting the population viability and power analyses require common elements: retrospective data on spawner abundance and age structure; a model to summarize past and current population dynamics; a prospective model and attendant assumptions to predict future dynamics, with and without management intervention; and illustrative (hypothesized) effect sizes (changes in productivity) associated with management actions. In addition, power analysis requires a model for testing hypotheses about the effect size. The next section outlines the data, models, and derivation of illustrative effects of several hypothetical management actions.

Methods

Data

This section gives an overview of the spawner–recruit run reconstruction. Schaller et al. (1999) review the methods, and Beamesderfer et al. (1997) contain the source data for individual stocks and years. We briefly review ancillary data on parr-to-smolt survival rates used to derive estimates of the potential effects of nutrient supplementation. Finally, we discuss the origin of the recovery standards used as indices of biological risk.

Since the late 1950s, Oregon and Idaho state fisheries biologists have conducted counts of redds in spawning areas for over 20 streams. The seven index stocks used in this analysis are thought to have the most complete and accurate counts and to have minimal spawning by straying hatchery fish (Beamesderfer et al. 1997). Typically, the counts have been done in index areas, a subset of the entire spawning reach used by spring–summer chinook, and the index area counts are expanded to the entire spawning area based on the proportion of each spawning reach sampled. They are expanded further from redds to spawners based on estimates of sex ratios and of prespawning mortality, based on recoveries of female carcasses with substantial numbers of unspawned eggs. This yields estimates of the total spawning population for each index stream and year. Aging of the spawners is based on body size and scale sample analysis on carcasses recovered during the surveys. After assigning each group of recruits to its appropriate group of parents (e.g., age-5 recruits in year t are the progeny of brood year $t - 5$), summing over age classes for each brood yields the total recruits for a brood year.

There are many assumptions involved in the estimation of spawners and recruits. Expansion of redd counts in index areas to total spawners relies on the use of several expansion factors. Comparisons of expanded redd counts with counts of adults at weirs (Marmorek et al. 1996) have not revealed any serious problems, but clearly, errors are possible. Previous work has used estimates of recruitment to the mouth of

© 2002 NRC Canada

the Columbia (e.g., Schaller et al. 1999), which requires additional assumptions and estimates for harvest rates and upstream survival.

We also use ancillary information on survival from parr (fish tagged in rearing areas in their first summer)-to-smolt (downstream migrants at Lower Granite the following spring). These data, Jolly–Seber survival rates for six stocks over a 5-year period, are taken from Paulsen and Fisher (2001) for use in estimating the potential effects of carcass or nutrient supplementation on early life stage survival.

Finally, the recovery standards for each index stock (Table 1) are taken from NMFS planning documents (NMFS 1995). The stocks are presumed to be self-sustaining if they reach their recovery targets and hence would be de-listed under the ESA.

Table 1. Escapement thresholds, 24-year and 48-year recovery (NMFS 1995).

Stock	8-year geometric mean spawning escapement
Imnaha	850
Minam	450
Bear	900
Marsh	450
Sulphur	300
Poverty	850
Johnson	300

Retrospective (historic) population model

The time series of recruits per spawner (*R/S*) exhibits high correlation among the index stocks (e.g., Botsford and Paulsen 2000). In other words, it appears that agents influencing all index stocks account for a large amount of variation in *R/S*. Whether these common factors are anthropogenic, climatological, or some combination of these and other factors is unknown. We exploit the correlations in formulating a model of past stock performance. The retrospective spawner–recruit (*S–R*) model is of the form

$$(1) \qquad \ln(R^r_{i,t}/S^r_{i,t}) = a^r_i - b^r_i S^r_{i,t} + m^r_t + \varepsilon^r_{i,t}$$

where $R^r_{i,t}$ represents recruits (adult offspring returning to spawn) from parent spawners $S^r_{i,t}$ (i denotes stock, t denotes brood year, and r denotes a retrospective or historic estimate for brood years 1957–1994); $S^r_{i,t}$ is spawner numbers returning in year; a^r_i is the Ricker a for stock i; b^r_i is the Ricker b for stock i; m^r_t is the anomaly (from the mean) in productivity in year t common to all index stocks; and $\varepsilon^r_{i,t}$ is a normally distributed process + counting error (white noise).

This is a Ricker (1954) stock–recruit model, modified to include multiple stocks and common variability in productivity, modeled using the m^r_t series. The m^r_t series accounts for changes in productivity common across all stocks. Each m^r_t may be viewed as the coefficient of an explanatory variable that is set to 1 if brood year = t, and 0 otherwise, where the m^r_t are constrained to sum to zero. Note that each m^r_t is assumed to affect fish early in their life history: it affects all recruits from brood year t regardless of age at return. The retrospective model is linear in its parameters and has normally distributed errors; therefore, it can be estimated using any ordinary least squares regression (OLS) package. It is inspired by a more complex model developed by Deriso et al. (2001), which used stocks from both the Snake and lower Columbia rivers and defined recruits as returns to the mouth of the Columbia. Trial applications of these more complex model (C.M. Paulsen and R.A. Hinrichsen, unpublished data) showed power similar to the simpler model used here.

Prospective (predictive) population model

To conduct power and population viability analyses, population numbers (i.e., spawning escapement and subsequent recruits to the spawning grounds) must be projected into the future. To do this, we used a Bayesian simulation model (Gelman et al. 1995) instead of a nonparametric bootstrap approach to obtain better coverage in the tails of the parameter distributions. A parametric bootstrap approach would also have provided better coverage than a nonparametric one; however, both parametric and nonparametric bootstrap and Bayesian approaches yielded similar results (C.M. Paulsen and R.A. Hinrichsen, unpublished data).

The Bayesian model combines the estimates of model parameters (the Ricker a^r_i and Ricker b^r_i for each stock, the m^r_t series, the error terms, and the parameter covariance matrix) with recent estimates of spawning escapement to project index stock spawner and recruit numbers if the future is like the recent past. To simulate the effects of different actions on the population dynamics, the model accommodates hypothetical changes to the productivities (i.e., treatment effects). The prospective model is an age-structured Ricker-type model that produces simulated *S–R* data. In the description of the simulations that follow, an asterisk (*) denotes a simulated quantity

$$(2) \qquad \ln(R^*_{i,t}/S^*_{i,t}) = a^*_i + b^*_i S^*_{i,t} + m^*_t + \Delta m^*_{i,t} + \varepsilon^*_{i,t}$$

$$(3) \qquad R^*_{i,t,a} = \phi^*_{i,t,a} R^*_{i,t}$$

$$(4) \qquad S^*_{i,t} = \sum_{a=4}^{5} R^*_{i,t-a,a}$$

where $R^*_{i,t}$ = total recruits for stock i, year t; $R^*_{i,t,a}$ = age-specific recruits (adult progeny surviving to spawn), stock i, produced by spawners in year t; $\phi^*_{i,t,a}$ = stock-specific maturity schedule; $S^*_{i,t}$ = spawner abundance for stock i, year t; m^*_t = common year effect for all stocks in year t; $\Delta m^*_{i,t}$ = effect of experiment on productivity of stock i in year t (0 for controls); and $\varepsilon^*_{i,t}$ = normal error term with mean 0 and variance σ^{*2}.

The jth simulation proceeded as follows. (*i*) Draw parameter values ($\tilde{m}^j_t$, $\tilde{a}^j_i$, $\tilde{b}^j_i$, $\tilde{\sigma}^j$), $1957 \le t \le 1994$, $1 \le i \le 7$ from the joint posterior distribution assuming a noninformative prior (Gelman et al. 1995), then set $a^{*j}_i = \tilde{a}^j_i$, $b^{*j}_i = \tilde{b}^j_i$, and $\sigma^{*j}_i = \tilde{\sigma}^j_i$, where the tilde (~) denotes a sample from the joint posterior distribution obtained from fitting eq. 1 to retrospective *S–R* data. (*ii*) Initialize simulated spawners using spawner numbers from 1995 to 1999, (i.e., $S^{*j}_{i,t} = S^r_{i,t}$, $1995 \le t \le 1999$). (*iii*) For each future brood year t ($t \ge 2000$), set the maturity schedule, $\phi^{*j}_{i,t,a}$, to a retrospective maturity schedule randomly selected from the 1957–1994 brood years, because no trend in age distributions was apparent in the data. (*iv*) For each year t of the simulation, set m^{*j}_t to a single random sample from ($\tilde{m}^j_{1978}, \ldots, \tilde{m}^j_{1994}$) in step *i*. The 1978–1994 year effects reflect recent conditions, including hydrosystem configuration, hatchery releases, and ocean re-

© 2002 NRC Canada

gime. (*v*) For each future year t, apply the treatment effect, $\Delta m^*_{i,t} = \Delta m_{i,t}$, associated with the management action of interest. This treatment effect is allowed to change with year and index stock. (*vi*) For each future year t, draw the residual $\varepsilon^{*j}_{i,t}$ randomly from the distribution $N(0,(\sigma^{*j})^2)$. (*vii*) Use eqs. 2–4 with draws and estimates described above to create a 100-year simulation of the spawner series for each of the seven index stocks.

The simulation steps *i–vii* were repeated 1000 times for the seven index stocks simultaneously. Simulating population growth in this way allowed us to construct crude posterior probability intervals for the estimated treatment effect sizes and to estimate the probability of exceeding the recovery escapement targets (Table 1).

Population viability analyses

The prospective model is used to calculate a measure of risk known as the recovery probability for each of the index stock and each experimental management action. We estimated the probability of recovery (for each index stock and each management action) as the proportion of trajectories that met the recovery criterion. If the geometric mean of the spawners during years 2016–2023 or 2040–2047 for a given trajectory exceeded a specified escapement threshold (see Data section), then recovery criterion was met; otherwise, it was not. The recovery probabilities are indices of biological risk: the lower the recovery probability, the higher the risk. Each action will have 14 values of risk associated with it: the 24-year and 48-year recovery probabilities for each of the seven index stocks.

Let $S^{*j}_{i,t}$ represent the simulated spawner abundance for stock i, year t, using the jth draw from the posterior distribution of the parameters. Then the probability that stock i met the recovery criterion was estimated by

$$(5) \qquad P^*_i = \sum_{j=1}^{1000} I\left[\sum_{t=y-7}^{y}\{\ln(S^{*j}_{i,t})/8\} - \ln(S^{rec}_i)\right]/1000$$

where y = 2047 and 2023 for the 48-year and 24-year recovery criterion, respectively, S^{rec}_i represents the recovery escapement for stock i, and $I[\ ]$ is the indicator function, which returns the value 1 if its argument is positive, and the value 0 otherwise. That is, $I[\ ]$ returns the value of 1 where the recovery standard is met, and 0 where it is not; thus the P^*_is are the probability of meeting the standards.

Juvenile survival vs. spawner abundance

The model used to estimate the effects of nutrient additions is based on parr–smolt survival estimates (Paulsen and Fisher 2001) and is of the following form:

$$(6) \qquad s_{i,t} = \delta_t + \gamma L_{i,t} + \beta_i S^r_{i,t} + e_{i,t}$$

where i and t represent stock and year, respectively, $s_{i,t}$ is parr-to-smolt survival; δ_t is a regression coefficient representing a year-specific intercept (sum of the δ_t = 0); γ is the estimated coefficient on length; $L_{i,t}$ is length at tagging (mm); β_i is a the stock-specific regression coefficient for spawners; $S^r_{i,t}$ is spawners (a surrogate for nutrient additions); and $e_{i,t}$ is an error term, assumed normally distributed. We estimate this for six index stocks (the Johnson stock has limited tagging data), for approximately seven years each, 1992–1998.

Power analysis

To quantify what can be learned through experimentation, we estimate power: the probability of detecting a significant treatment effect when the true treatment effect is θ. Power calculations require specification of type-I error, a null reference distribution (the sampling distribution of the prospective model for simulated future SR data), and a method to estimate the sampling distribution of the θ estimate, $\hat{\theta}$. The purpose of the power analysis is to imitate how an analyst would estimate θ with data obtained after the experiment has been run in future. In our analysis, we use a two-sided hypothesis test where α = 0.05 using the (Neyman–Pearson) paradigm of fixing the probability of type-I error. Although a one-sided test would increase power, we used a two-sided test to allow for the possibility that putatively beneficial actions might actually decrease productivity (e.g., adding hatchery carcasses might introduce diseases into treated stocks).

The prospective model for generating *S–R* data is given by eqs. 2–4, and the estimation of θ is described below. To quantify the information to be gleaned from different experimental management actions, we use the retrospective and projected *S–R* (derived from the prospective model described above); we then fit a model to these "data" that contains parameters defining a treatment effect. We use two different formulations of the estimating model depending on whether control stocks are used.

In the case where no control stocks are used, the model is

$$(7) \qquad \ln(R^*_{i,t}/S^*_{i,t}) = a_i + b_i S^*_{i,t} + m_t + \varepsilon_{i,t}$$

Note that this is identical to eq. 1, except that the recruit and spawner terms use asterisks (*) to denote the fact that the "data" from 2000 onward are the projected fish numbers from eq. 2, and there is no "r" superscript on the equation's terms. After estimating the parameters of this model using least squares for each of the 1000 simulated outcomes, we calculate

$$(8) \qquad \hat{\theta} = \bar{\hat{m}}_{\text{treatment}} - \bar{\hat{m}}_{\text{control}}$$

where $\bar{\hat{m}}_{\text{treatment}}$ is the sample mean of the estimated common year effects for the treatment years, and $\bar{\hat{m}}_{\text{control}}$ is the sample mean of estimated common year effects for the control years. Having calculated the mean estimate of $\hat{\theta}$ and its standard error, one can then estimate the statistical significance of $\hat{\theta}$.

Estimation of treatment effects proceeds differently when control stocks are used. In this case,

$$(9) \qquad \ln(R^*_{i,t}/S^*_{i,t}) = a_i + b_i S^*_{i,t} + m_t + \Delta m_{i,t} + \varepsilon_{i,t}$$

where $\Delta m_{i,t}$ is zero if i is a control stock or t is a control year and is equal to θ otherwise. This model can be estimated using least squares, and the estimate of the treatment effect is simply the least squares estimate of θ, denoted by $\hat{\theta}$.

For experiments with and without control stocks, to calculate power, we generate 1000 replications of the estimates of $\hat{\theta}$ by fitting eqs. 7 and 9, respectively, to simulated data sets.

© 2002 NRC Canada

Table 2. Estimates of Ricker a_i^r and b_i^r coefficients for the seven index stocks.

	Ricker a_i^r			Ricker b_i^r		
Stock	Value	SE	t value	Value	SE	t value
Imnaha	0.011	0.177	0.063	0.0005	0.0002	3.292*
Minam	0.330	0.143	2.304*	0.0014	0.0002	5.936*
Bear	0.248	0.167	1.486	0.0008	0.0002	4.539*
Marsh	0.101	0.164	0.613	0.0013	0.0003	3.964*
Sulphur	0.359	0.167	2.154*	0.0023	0.0004	5.191*
Poverty	0.365	0.149	2.453*	0.0007	0.0001	4.957*
Johnson	0.422	0.171	2.470*	0.0020	0.0005	4.340*

Note: SE, standard error; *denotes significance at the 0.05 level, df = 213.

Fig. 2. Average recruits per spawner over time for seven Snake spring–summer chinook (*Oncorhynchus tshawytscha*) index stocks. Sources: Beamesderfer at al. (1997); Tinus (Oregon Department of Fish and Wildlife, Portland, Oreg., unpublished data).

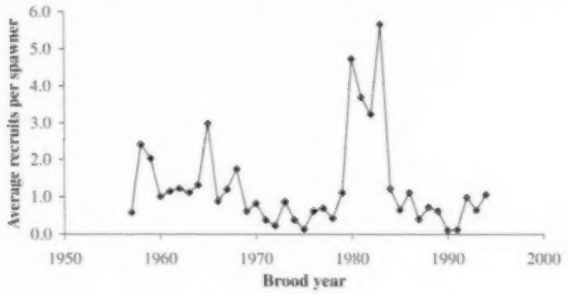

Fig. 3. The m_i^r ordinary least squares series and standard error bars (solid lines). Each vertical bar extends 2 standard errors above and below the point estimate. Least trimmed squares (LTS) estimates (broken line) are shown for comparison.

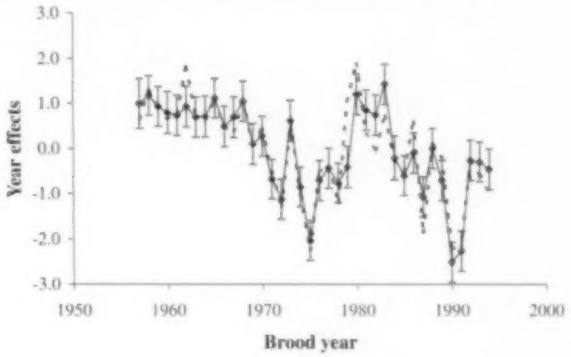

The power estimate is the proportion of the replications for which the null hypothesis of $\theta = 0$ was rejected.

Hypothetical actions and illustrative effect sizes

Power and viability analyses require hypotheses about how actions will affect productivity. We analyze a status quo action, A0, in which 1978–1994 conditions continue indefinitely, and four actions. A1 is a "do everything" action in which productivity is increased as much as possible immediately. In this case, we assume that the increase is left "on" in all years from 2000 forward. A2 is similar to action A1 but with the action turned on and off in alternate years (to reduce confounding) through 2020, after which it is left "on" indefinitely. A3 is an increase in productivity for four of the seven index stocks because of the addition of nutrients or carcasses in rearing areas, with the remaining three stocks serving as controls. Similar to actions A1 and A2, all stocks would receive nutrient additions after 2020. A4 is similar to A3 but with all stocks receiving treatment from the year 2000 onward.

One can view actions A1 and A4 primarily as efforts to increase productivity, whereas actions A2 and A3 sacrifice some increase in productivity in the interest of gaining statistical power. Actions A2 and A3 also reduce possible confounding with other changes unrelated to the management action (e.g., shifts in ocean survival), assuming that the extraneous changes do not have the same schedule as the treatment effects. The last ingredient we need for our power analysis is illustrative effect sizes for the experimental actions. These effect sizes, described in Results, are based on the retrospective results of models represented by eqs. 1 and 6.

Results

Retrospective *R/S* analysis

The Ricker a_i^r estimates are reasonably precise, with standard errors averaging approximately 0.16, but only four are significantly different from zero at a 0.05 level (Table 2). The b_i^r values, on the other hand, are all significantly different from zero, with t values ranging from 3.29 to 5.19. The m_i^r vary widely from year to year, but each individual estimate is reasonably precise, with standard errors ranging from 0.22 to 0.28 (Fig. 2). The variance in the overall series, from 1957 to 1994, is approximately 0.99. The broad pattern of the series over time shows a sustained period of relatively high productivity through about 1967, with lower than average productivity since that time, with the exception of four years of high productivity in the early 1980s. The value of R^2 for the regression is 0.77. Estimates of m_i^r using robust regression technique of least trimmed squares (LTS; Rousseeuw and Leroy 1987) were similar to those using OLS (Fig. 3). Sample variance in the LTS-estimated series over 1978–1994 (1.26) was slightly higher than that of the OLS-estimated series for the same years (1.11). This indicates power to detect changes in productivity would decrease somewhat if LTS were used instead of OLS. The m_i^r estimates ex-

© 2002 NRC Canada

Table 3. Parr-to-smolt survival vs. spawners regression model results.

Stock	Estimated β_i	SE	p value
Bear	0.0003	0.0001	0.0027*
Imnaha	0.0000	0.0000	0.3681
Marsh	0.0007	0.0002	0.0004*
Minam	0.0001	0.0002	0.6501
Poverty	0.0001	0.0001	0.0564
Sulphur	0.0005	0.0007	0.4415

Note: SE, standard error; *denotes significance at the 0.05 level, df = 21.

Table 4. Schedule of treatments, Δm_t, for experimental management actions.

	Management action			
Year	A1	A2	A3	A4
2001	1.4	1.4	0.7 (T), 0 (C)	0.7
2002	1.4	0	0.7 (T), 0 (C)	0.7
2003	1.4	1.4	0.7 (T), 0 (C)	0.7
2004	1.4	0	0.7 (T), 0 (C)	0.7
2005	1.4	1.4	0.7 (T), 0 (C)	0.7
2010	1.4	0	0.7 (T), 0 (C)	0.7
2015	1.4	1.4	0.7 (T), 0 (C)	0.7
2016	1.4	0	0.7 (T), 0 (C)	0.7
2017	1.4	1.4	0.7 (T), 0 (C)	0.7
2018	1.4	0	0.7 (T), 0 (C)	0.7
2019	1.4	1.4	0.7 (T), 0 (C)	0.7
2020	1.4	0	0.7 (T), 0 (C)	0.7
2021+	1.4	1.4	0.7	0.7

Note: A1 is the "do everything" action, applied to all seven index stocks in all years from 2001 onward. A2 is similar but is turned on in odd years only through 2019 and is on for all years thereafter. A3, carcass additions, is applied only to four of the seven index stocks through 2020 and on for all stocks thereafter. Only A3 has both treatment (T) and control (C) stocks. A4 is similar to A3 but is applied to all stocks in all years.

hibit weak autocorrelation, but accounting for this had a negligible effect on the results.

Carcass introductions

Average parr-to-smolt survival (averaging over all six stocks) is about 0.3. Adding the nutrient equivalent of 1000 carcasses would increase average parr-to-smolt survival from a base-case mean of approximately 0.3 to about 0.6. This is calculated using the average for the spawner coefficients (Table 3). That is, future parr-to-smolt survival for treatment stocks = 0.30 + 1000 × 0.0003 = 0.6. This result suggests that adding 1000 carcasses (or their nitrogen–phosphorus equivalents) would roughly double the *R*/*S* ratio. The results, while suggesting that nutrient or carcass additions could improve juvenile survival, are hardly definitive. Although experimental evidence for a link between *R*/*S* and carcass abundance exists in other salmonid ecosystems (Cederholm et al. 2000; Gresh et al. 2000), there is no direct evidence for such effects in Snake River spring–summer chinook.

Table 5. Experimental management model power analysis results.

Last year of experiment	Management action			
	A1	A2	A3	A4
2001	0.23	0.23	0.42	0.11
2002	0.44	0.23	0.67	0.15
2003	0.61	0.45	0.81	0.19
2004	0.72	0.45	0.87	0.24
2005	0.80	0.62	0.92	0.28
2010	0.97	0.79	0.99	0.49
2015	0.99	0.93	1.00	0.64
2020	1.00	0.97	1.00	0.73

Note: A1 is the "do everything" action, applied to all seven index stocks in all years from 2001 onward. A2 is similar but is turned on in odd years only through 2019 and is on for all years thereafter. A3, carcass additions, is applied only to four of the seven index stocks through 2020 and on for all stocks thereafter. Only A3 has both treatment (T) and control (C) stocks. A4 is similar to A3 but is applied to all stocks in all years.

Illustrative effect sizes

As noted above, we simulated a status quo action, A0, with no increase in productivity. Under A0, productivity in the future is assumed to be equal to that of the 1978–1994 brood years, thus, $\theta = 0$. The magnitude of the effect sizes for actions A1 to A4 is based, albeit loosely, on the retrospective results just described. For actions A1 and A2, we make two assumptions. First, we assume that some combination of actions can make the future m_t^* series similar to those from 1957 to 1966, instead of the 1978–1994 series used in the base-case projections (Fig. 3). This yields an increase of approximately 1.2 (the difference between the 1957–1966 m_t^r, mean = 0.85, and that for 1978–1994, mean = –0.32). Second, we assume that although harvest rates might increase somewhat as spawner abundance increases, they will not return to earlier levels, and there will be an additional increase of 0.2 in $\ln(R/S)$ as a result. This results in a θ of 1.4. For actions A3 and A4, we simply use the results from the spawner vs. parr-to-smolt survival regression and assume that for treated stocks, the θ will be 0.7 (i.e., $\ln(2)$), a doubling of recruits per spawner. The schedules for the status quo action and for each experimental management action are summarized in Table 4. We have based the four cases on the empirical estimates as an illustrative example of how one might project effect sizes from available data. One should not take the numerical values used in the power and viability analyses as firm predictions of likely effects of real actions; such predictions are impossible at present. Note that the illustrative effect sizes are substantial: A1 and A2 quadruple *R*/*S*, whereas A3 and A4 double *R*/*S* for treated stocks.

Power analysis

The power analysis results conform to intuition: power increases with the length of the experiments (see Table 5). Several more interesting contrasts are also apparent. First, the carcass experiment with treatment and control stocks (action A3) is clearly the most powerful of the four actions: one can detect treatment effects at $\alpha = 0.05$ with power of 0.81 by 2003. It is more powerful than either A1 or A2, despite having an effect size of half their magnitude. The do-

© 2002 NRC Canada

Table 6. Probabilities that escapement exceeds recovery levels at 48 years for each of the seven index stocks.

		Management action				
Standard	Index stock	Status quo (A0)	A1	A2	A3	A4
24-year recovery	Imnaha	0.00	**0.85**	0.35	0.23	0.22
	Minam	0.00	**0.75**	0.31	0.00	0.23
	Bear	0.00	**0.75**	0.25	0.17	0.17
	Marsh	0.00	**0.57**	0.11	0.00	0.05
	Sulphur	0.00	**0.51**	0.16	0.11	0.10
	Poverty	0.01	**0.85**	0.36	0.01	0.24
	Johnson	0.01	**0.82**	0.47	0.38	0.36
48-year recovery	Imnaha	0.00	**0.91**	**0.90**	0.29	0.29
	Minam	0.00	**0.76**	**0.76**	0.21	0.27
	Bear	0.00	**0.79**	**0.79**	0.24	0.24
	Marsh	0.00	**0.70**	**0.69**	0.08	0.17
	Sulphur	0.00	**0.59**	**0.59**	0.16	0.16
	Poverty	0.00	**0.85**	**0.85**	0.23	0.31
	Johnson	0.01	**0.80**	**0.80**	0.41	0.40

Note: A1 is the "do everything" action, applied to all seven index stocks in all years from 2001 onward. A2 is similar but is turned on in odd years only through 2019 and is on for all years thereafter. A3, carcass additions, is applied only to four of the seven index stocks through 2020 and on for all stocks thereafter. Only A3 has both treatment (T) and control (C) stocks. A4 is similar to A3 but is applied to all stocks in all years. Bolded entries indicate recovery probabilities that exceeded 0.50.

everything action turned on permanently in 2001 (action A1) is a close second, attaining a power of 0.8 by 2005, but the possibility for confounding with unrelated changes in productivity should not be ignored. The do-everything action with alternating treatment and control years (action A2) attains a power of 0.79 by 2010, whereas action A4 (carcass outplants for all stocks) attains power of 0.73 after 20 years.

It may seem surprising that action A1 is a more powerful experiment than action A2. The reason for this is that brood years 1978–1994 are part of the "controls" for both actions A1 and A2. The limiting factor in determining power, for actions with no spatial controls, is the number of treatment years. Therefore, because action A1 is "on" continuously from 2001, it accumulates treatment years twice as fast as action A2, which is turned on and off in alternate years. The result is that action A1 is a more powerful experiment, but one that runs a high risk of confounding with climate change or other phenomena unrelated to the experimental action.

The carcass experiments described by actions A3 and A4 are particularly interesting. Action A3, with treatment and control stocks, gains its statistical power from a combination of two factors: precise estimates of the Ricker a_i^r terms in eq. 1 and the use of untreated control stocks. The power estimates may be viewed as testing whether or not the Ricker a_i^r changes for treatment stocks compared with controls. In contrast, action A4, which has no spatial controls, is not a very powerful experiment even after 20 years.

Population viability analysis

The viability results are also intuitive (Table 6). For A0, the status quo action, the 24-year and 48-year recovery standard (Pr{Recovery} > 0.50) is not met for any of the stocks. Actions A1 and A2 both meet the 48-year standard, but only action A1 meets the 24-year standard. This is one measure of the increased biological risk of experimentation: because action A2 is turned on and off in years 2001–2020, the shorter-term recovery standard is not met for any of the seven index stocks. The carcass actions A3 and A4 do not meet any standards for any of the stocks because the effect size, 0.7, is simply not large enough to meet the recovery standards. However, for the stocks used as controls in A3 (Minam, Poverty, and Marsh), A4 is more likely to meet the 24-year threshold than A3, although neither action attains the 0.5 NMFS standard.

Discussion

Williams (1999) showed, using computer simulations, that even when doubling habitat carrying capacity doubles recruits, there is enough variability in the *S–R* data that the relationship may not be apparent in data records of realistic length. This is a common problem: the noise inherent in most *S–R* series often dominates biologically meaningful signals (Hinrichsen 2001). The methods we have used estimate the average changes in the ln(*R*/*S*) across all index stocks directly, via the m_i^r series. Because the ln(*R*/*S*) anomalies are correlated among stocks, information gleaned from one stock supplies information about the others. Others have used broadly similar approaches to account for common variability (e.g., Bradford 1994; Adkinson et al. 1996; Peterman et al. 1998). To gauge how long an experiment should last, we estimate how soon a given change in the projected *S–R* series (due to an experimental management action) would be detected in the future (i.e., that the precision of the estimated treatment effect is sufficiently high). Experiments that use spatial controls have much higher likelihood of detecting effects quickly when compared with those that effect all stocks simultaneously, despite having smaller effect sizes. Given the high variability of interannual productivity and survival to recruit, this would strongly support the use of spatial controls in an experimental management design for anadromous salmonids.

© 2002 NRC Canada

Other than carcass or nutrient additions, actions with spatial controls might include habitat alteration or supplementation with hatchery-origin juveniles or adults. Similar designs might be possible elsewhere in the Columbia for the John Day Basin, with three spring chinook stocks, or in the Upper Columbia, also having three index stocks (Wenatchee, Entiat, and Methow). It seems likely that these methods could be used in many river systems with multiple stocks of the same species and life history.

Choosing between actions that increase learning opportunities and those that meet conservation objectives is not really a scientific issue. Instead, it is a decision in which societal values take part (Hinrichsen 2000). To reflect those values, some have suggested scaling the statistical criteria for determining significant effect sizes (Mapstone 1995). Lee (1999) suggests, for example, that an appropriate significance level might be $\alpha = 0.5$ (corresponding to a 50% chance that one concludes that the experimental effect was nonzero when the true effect = 0) instead of the traditional $\alpha = 0.05$ used here. Obviously, this is far less precise than many scientists might recommend, but it would increase power. Similar arguments apply to using one-sided tests rather than the two-sided tests employed here. It acknowledges that, in the real world, the trade-offs between statistical power and other considerations may be different than in the groves of academe.

The amount of time available to conduct an experimental management program is also a resource manager's decision. This constraint may severely limit learning potential in some situations. Recent policy statements by Federal regulators, for example, suggest that the time available for experimentation may be quite short (NMFS 2000). If, within 5 to 8 years, the decline in stock numbers is not reversed, NMFS plans to make a final decision on removal of four Lower Snake River dams. If this schedule is adhered to, and managers want to be at least 80% certain of detecting a significant effect, only experiments with spatial controls will give reliable results within 5 years or so. Even this may be problematic: for actions affecting juveniles, one will need to wait until the "subjects" return as adults before final results are available. This of course will add several years to the duration of an experiment.

Monitoring the results of experiments is obviously crucial to assessing their outcomes. The only monitoring required for the experimental management actions we have discussed is accurate enumeration of adult spawners and harvest rates. However, the stocks in question have been the subject of many monitoring efforts to estimate parr–smolt survival (e.g., Paulsen and Fisher 2001), smolt survival as the fish move downstream through the mainstem Snake and Columbia (e.g., Skalski et al. 1998), and survival from smolt to adult. We suspect that use of life stage specific survival estimates will increase the precision of the effects of actions aimed at life stages, like smolt survival, that are extensively monitored, assuming that increases in life-stage survival translate into increases in spawning escapement. Power analyses using life stage survival estimates is ongoing (C.M. Paulsen, unpublished data). However, most of the life stage survival estimates just noted are unavailable before the early 1990s. This precludes estimates of the effects of dams, ocean cycles, declines in spawner abundance, and other long-term phenomena.

We also believe that the models outlined here could be improved. For example, we found modest nonhomogeneity in the residuals: residual variance tends to differ among stocks (range = 0.09 to 0.46, corresponding to Bear and Sulphur, respectively). In the prospective runs, serial correlation in the year effects was ignored, even though weak first-order autocorrelation was evident. Simulating serial correlation in the year effects, however, did not alter power and changed recovery probabilities only slightly. Nonetheless, errors introduced from these shortcomings likely pale in comparison to the inaccuracy of the projected experimental outcomes and the variance in the m_t^r series. This variance drives the estimated necessary duration of the experiments. Furthermore, we have not tried to identify optimal experimental designs, nor have we examined what might result if one were to undertake several experimental management actions simultaneously. Finally, it may be useful to consider alternative functional forms (e.g., Beverton–Holt) for the *S–R* models.

That said, we believe that explicit modeling of covariability among stocks is the best approach for salmonid stocks spawning in the same geographic area, because estimates of base-case population parameters (e.g., Ricker a_i^r and b_i^r) are otherwise very imprecise. Absent this or a similar strategy, we think it will be impossible to design powerful experimental actions that can achieve reliable results within reasonable time frames.

These results suggest that the biological cost of delaying actions (but not postponing them indefinitely) is relatively modest: A1 and A2 both meet the 48-year standard, but only A1 meets the shorter-term 24-year standard. However, they should be taken with several grains of salt, given our poor understanding of the consequences of management actions. Estimates of effect sizes, including the examples used here, are often little more than enlightened conjecture (Lackey 1999). Possible confounding of actions with unrelated environmental change is also a very real possibility. For example, following several years of very poor returns of wild fish, counts of chinook and steelhead (*Oncorhynchus mykiss*) throughout the Columbia are very high. For example, Snake River wild and hatchery spring–summer chinook adults at Lower Granite Dam are about 11 times the 10-year average (DART 2001). If managers had undertaken (plausibly) beneficial actions in the late 1990s, there would be a strong temptation to attribute the recent high returns to those actions. In a similar vein, had managers instituted new actions in the late 1970s, they would have noted that recruits per spawner in 1981–1984 were higher than any previously observed, only to be disappointed by poor productivity a few years later. The potential for surprises, pleasant and otherwise, not anticipated by population models or modelers is obviously high and must be factored into management decisions.

Acknowledgements

This study was funded by the U.S. Department of Energy, Bonneville Power Administration. The opinions expressed are those of the authors. We are grateful for the efforts of the PATH Experimental Management group, especially Rick

© 2002 NRC Canada

Deriso, Calvin Peters, and Dave Marmorek, for comments on the methodology. We also thank Phil Levin, Lyse Godbout, Mike Lapointe, an associate editor, and two anonymous reviewers for their comments on earlier drafts.

References

Adkinson, M.D., Peterman, R.M., Lapointe, M.F., Gillis, D.M., and Korman, J. 1996. Alternative models of the climatic effects on sockeye, *Oncorhynchus nerka*, productivity in Bristol Bay, Alaska, and the Fraser River, British Columbia. Fish. Oceanogr. **5**: 137–152.

Beamesderfer, R.C.P., Petrosky, C.E., Schaller, H.A., and Langness, O. 1997. Spawner–recruit data for spring and summer chinook salmon populations in Idaho, Oregon, and Washington. *In* Plan for analyzing and testing hypotheses (PATH): report of retrospective analysis for fiscal year 1997. *Compiled and Edited by* D.R. Marmorek and C. Peters. ESSA Technologies Ltd., Vancouver, B.C.

Botsford, L.W., and Paulsen, C.M. 2000. Assessing covariability among populations in the presence of intraseries correlation: Columbia River spring–summer chinook salmon (*Oncorhynchus tshawytscha*) stocks. Can. J. Fish. Aquat. Sci. **57**: 616–627.

Bradford, M.J. 1994. Trends in the abundance of chinook salmon (*Oncorhynchus tshawytscha*) of the Nechako River, British Columbia. Can. J. Fish. Aquat. Sci. **51**: 965–973.

Cederholm, C.J., Johnson, D.H., Bilby, R.E., Dominguez, L.G., Garrett, A.M., Graeber, W.H., Greda, E.L., Kunze, M.D., Marcot, B.G., Palmisano, J.F., Plotnikoff, R.W., Pearcy, W.G., Simenstad, C.A., and Trotter, P.C. 2000. Pacific salmon and wildlife—ecological contexts, relationships, and implications for management. Special Edition Technical Report, Washington Department of Fish and Wildlife, Olympia, Wash.

DART (Data Access in Real Time). 2001. http://www.cbr.washington.edu/dart/adult.html

Deriso, R.B., Marmorek, D.R., and Parnell, I.J. 2001. Retrospective patterns of differential mortality and common year-effects experienced by spring and summer chinook salmon (*Oncorhynchus tshawytscha*) of the Columbia River. Can. J. Fish. Aquat. Sci. **58**: 2419–2430.

Gelman, A., Carlin, J.B., Stern, H.S., and Rubin, D.B. 1995. Bayesian data analysis. Chapman & Hall, New York.

Gresh, T., Lichatowich, J., and Schoonmaker, P. 2000. An estimation of historic and current levels of salmon production in the northeast pacific ecosystem: evidence of a nutrient deficit in the freshwater systems of the pacific northwest. Fisheries (Bethesda), **25**: 15–21.

Hare, S.R., Mantua, N.J., and Francis, R.C. 1999. Inverse production regimes: Alaska and west coast Pacific salmon. Fisheries (Bethesda), **24**: 6–14.

Hinrichsen, R.A. 2000. Are there scientific criteria for putting short-term conservation ahead of learning? No. Response to Kai N. Lee 1999: "Appraising Adaptive Management". Conserv. Ecol. **4**(1): r7 (URL: http://www.consecol.org/vol4/iss1/resp7).

Hinrichsen, R.A. 2001. High variability of spawner–recruit data hampers learning. Can. J. Fish. Aquat. Sci. **58**: 769–776.

Karieva, P., Marvier, M., and McClure, M. 2000. Recovery and management options for spring/summer chinook salmon in the Columbia River Basin. Science (Washington, D.C.), **290**: 977–979.

Lackey, R.T. 1999. The savvy salmon technocrat: life's little rules. Environ. Practice, **1**(3): 156–161.

Lee, K.N. 1999. Appraising adaptive management. Conserv. Ecol. **3**: 3 (URL: http://www.consecol.org/vol3/iss2/art3).

Mapstone, B.D. 1995. Scalable decision rules for environmental impact studies: effect sizes, type I, and type II errors. Ecol. Appl. **5**: 401–410.

Maxell, B.A. 1999. A power analysis on the monitoring of bull trout using redd counts. N. Am. J. Fish. Manag. **19**: 860–866.

Marmorek, D.R., and Peters, C. (*Editors*). 1996. Plan for analyzing and testing hypotheses (PATH): final report of retrospective analysis for fiscal year 1996. ESSA Technologies Ltd., Vancouver, B.C.

NMFS (National Marine Fisheries Service). 1995. Biological opinion: reinitiation of consultation on 1994–1998 operations of the Columbia River power system and juvenile transportation program in 1994–1998. Endangered Species Act, section 7 consultation. NMFS, Portland, Oreg.

NMFS 2000. Endangered species act status of West Coast salmon and steelhead (URL: http://www.nwr.noaa.gov/1salmon/salmesa/pubs/1pgr.pdf).

Paulsen, C.M., and Fisher, T.R. 2001. Statistical relationship between Snake River spring/summer chinook salmon parr-to-smolt survival and indices of land use. Trans. Am. Fish. Soc. **130**: 347–358

Peterman, R.M., Pyper, B.J., Lapointe, M.F., and Adkison, M.D. 1998. Patterns of covariation in survival rates of British Columbia and Alaskan sockeye salmon (*Oncorhynchus nerka*) stocks. Can. J. Fish. Aquat. Sci. **55**: 2503–2517.

Peters, C.N., and Marmorek, D.R. 2001. Application of decision analysis to evaluate recovery actions for threatened Snake River spring and summer chinook salmon (*Oncorhynchus tshawytscha*). Can. J. Fish. Aquat. Sci. **58**: 2431–2446.

Ricker, W.E. 1954. Stock and recruitment. J. Fish. Res. Board Can. **11**: 559–623.

Rousseeuw, P.J., and Leroy, A.M. 1987. Robust regression and outlier detection. Wiley, New York.

Schaller, H.A., Petrosky, C.E., and Langness, O.P. 1999. Contrasting patterns of productivity and survival rates for stream-type chinook salmon (*Oncorhynchus tshawytscha*) populations of the Snake and Columbia rivers. Can. J. Fish. Aquat. Sci. **56**: 1031–1045.

Skalski, J.R., Smith, S.G., Iwamoto, R.N., Williams, J.G., and Hoffman, A. 1998. Use of passive integrated transponder tags to estimate survival of migrant juvenile salmonids in the Snake and Columbia rivers. Can. J. Fish. Aquat. Sci. **55**: 1484–1493.

Walters, C.J. 1986. Adaptive management of renewable resources. Macmillan, New York.

Walters, C.J., and Sainsbury, K.J. 1990. Design of a large-scale experiment for measuring the effects of fishing on the Great Barrier Reef. Manuscript Report, Great Barrier Reef Marine Park Authority, Townsville, Queensland, Australia.

Walters, C.J., Gunderson, L., and Holling, C.S. 1992. Experimental policies for water management in the Everglades. Ecol. Appl. **2**: 189–202.

Williams, J.G. 1999. Stock dynamics and adaptive management of habitat: an evaluation based on simulations. N. Am. J. Fish. Manag. **19**: 329–341.

Zabel, R.W., and Williams, J.G. 2000. Comments on "Contrasting patterns of productivity and survival rates for stream-type chinook salmon (*Oncorhynchus tshawytscha*) populations of the Snake and Columbia rivers" by Schaller et al. (1999). Can. J. Fish. Aquat. Sci. **57**: 1739–1741.

© 2002 NRC Canada

Crustacean zooplankton communities in lakes recovering from acidification

W. Keller, N.D. Yan, K.M. Somers, and J.H. Heneberry

Abstract: Large reductions in sulphur emissions at the Sudbury, Ont., Canada, smelters in recent decades have resulted in decreased lake acidity, and biological improvements have followed. Lakes in the Sudbury area offer a very unique opportunity to develop our understanding of the processes regulating biological restructuring in aquatic ecosystems recovering from acidification. Here, we examine changes in crustacean zooplankton communities that have accompanied the chemical recovery of Whitepine and Sans Chambre lakes, near Sudbury, over the last two decades. In both these formerly acidic lakes, pH has increased to ~6.0, and some zooplankton community recovery has occurred. However, zooplankton communities have not completely recovered based on multivariate comparisons with the community composition of reference lakes. Although a number of acid-sensitive species have appeared, many did not persist, or did not achieve abundances typical of the reference lakes. This indicates that zooplankton community recovery will most likely depend on biotic and abiotic interactions within these lakes and not on factors affecting species dispersal. Both chemical and biological factors have large influences on biological recovery processes. Assessing biological recovery is very important since the restoration of healthy aquatic communities is a major objective of large-scale sulphur emission control programs.

Résumé : Les réductions importantes des émissions de soufre dans les fonderies de Sudbury, Ont., Canada, au cours des dernières décennies ont entraîné une diminution de l'acidité des lacs et, par conséquent, une amélioration des conditions biologiques. Les lacs de la région de Sudbury fournissent ainsi une occasion unique de comprendre les processus de restructuration des écosystèmes aquatiques qui se remettent de l'acidification. Nous examinons ici les changements dans les communautés des crustacés du zooplancton qui ont suivi l'amélioration des conditions chimiques au cours des 20 dernières années dans les lacs Whitepine et Sans-Chambre, près de Sudbury. Dans ces deux lacs autrefois acidifiés, le pH a augmenté à ~6,0 et une certaine récupération de la communauté du zooplancton s'est produite. Cependant, des comparaisons multidimensionnelles avec des lacs témoins révèlent que les communautés zooplanctoniques ne sont pas totalement rétablies. Bien qu'un nombre d'espèces sensibles à l'acidité soient apparues, plusieurs n'y sont pas demeurées ou n'ont pas réussi à atteindre les densités habituelles des lacs témoins. Cela indique que le rétablissement de la communauté zooplanctonique dépendra très probablement d'interactions biotiques et abiotiques à l'intérieur de ces lacs, plutôt que de facteurs reliés à la dispersion des espèces. Tant les facteurs chimiques que biologiques agissent fortement sur les processus de récupération biologique. L'évaluation de la récupération biologique est très importante, car la restauration de la santé des communautés aquatiques est l'un des objectifs principaux des programmes de contrôle à grande échelle des émissions de soufre.

[Traduit par la Rédaction]

Introduction

Excessive acid deposition has acidified many thousands of lakes, with resulting damage to their biological communities (Schindler 1988). During the 1980s and 1990s, massive sulphur emission control programs were implemented in many areas including Canada, the United States, and Europe to combat the global problem of acid deposition. With the implementation of emission control programs, it was expected that conditions in affected aquatic ecosystems would improve, and the focus of acid rain assessment programs began to change from documenting damage to investigating ecosystem recovery.

Other than in the Sudbury, Ont., Canada, area, evidence of the chemical recovery of lakes is only beginning to emerge from regions where sulphur emissions and deposition have

Received 21 September 2001. Accepted 31 March 2002. Published on the NRC Research Press Web site at http://cjfas.nrc.ca on 24 May 2002.
J16542

W. Keller[1] **and J.H. Heneberry.** Ontario Ministry of the Environment, Cooperative Freshwater Ecology Unit, Laurentian University, Ramsey Lake Road, Sudbury, ON P3E 2C6, Canada.
N.D. Yan. Biology Department, York University, 4700 Keele Street, Toronto, ON M3J 1P3, Canada.
K.M. Somers. Ontario Ministry of the Environment, Dorset Environmental Science Centre, P.O. Box 39, Dorset, ON P0A 1E0, Canada.

[1]Corresponding author (e-mail: bkeller@vianet.on.ca).

 DOI: 10.1139/F02-042 © 2002 NRC Canada

been reduced (Stoddard et al. 1999). Evidence of biological recovery from lake acidification is even more limited. Lake-scale manipulations (Keller et al. 1990*a*; Degerman et al. 1995; Sampson et al. 1995) indicate that biological improvements should follow the water quality improvements expected to result from sulphur emission reductions. However, evidence of the natural recovery of aquatic communities from acidification is rare.

Some biological recovery, as well as striking chemical recovery, has been documented in lakes around Sudbury (Keller et al. 1992*a*, 1999) where emission reductions from area metal smelters were particularly large and began in the early 1970s. However, since recovery is at an early stage in many Sudbury area lakes, previous studies have not allowed detailed examination of long-term recovery patterns in lakes, which had reached pH levels that would not be expected to still severely limit acid-sensitive aquatic biota. A pH of about 6.0 appears to be necessary for the protection of many acid-sensitive taxa (Schindler 1988; Havens et al. 1993). With continuing chemical recovery in the Sudbury area, some lakes have now reached pH ~ 6.0. This chemical recovery permits evaluation of the natural biological recovery that has followed water quality improvements in lakes that have not had direct chemical manipulations. There can, of course, be different definitions of recovery. Here we accept that various outcomes may reasonably be expected from the biological recovery process (Keller and Yan 1998; Keller et al. 1999) and we consider recovery as the return to a typical, not necessarily a pre-stress, condition. Assessments of biological recovery are very important to the evaluation of acid rain controls, since the protection and restoration of aquatic communities is a major ultimate objective of emission reduction programs. Empirical documentation of the patterns of recovery in damaged lakes also offers important opportunities to increase our more general understanding of the processes regulating aquatic community structure and biodiversity.

This paper examines long-term patterns in crustacean plankton communities in two Sudbury area lakes that have exhibited chemical recovery to pH ~ 6.0, in response to smelter emission reductions. To assess recovery in the crustacean zooplankton communities of these two lakes we have followed the approach of Yan et al. (1996), and compare temporal patterns in univariate and multivariate measures of community structure over a two-decade period to comparable spatial survey data for a set of 47 reference lakes, near Dorset, Ont., that have not shown any general temporal trends in pH during the study period. The range of variability in the zooplankton community data for the reference lakes provides our recovery targets.

Methods

Study lakes

The Sudbury lakes studied (Fig. 1), Whitepine (lat 47°17′N, long 80°50′W) and Sans Chambre (lat 46°43′N, long 81°07′W), are within the large area historically affected by the Sudbury smelter emissions. A summary of general physical and chemical characteristics of the lakes is provided in Table 1. As part of the widespread water quality improvements seen in this region (Keller et al. 1992*b*), these lakes have decreased in acidity following the implementation of large reductions (about 90% since the peak in the 1960s) in sulphur emissions from the Sudbury area metal smelters during the 1970s and 1990s. Both these lakes had average pH < 5.5 when monitoring commenced in 1980, a pH level at which substantial effects on sensitive zooplankton species are expected (Keller et al. 1990*b*; Havens et al. 1993). Both lakes now have average pH > 6.0 (Fig. 2).

The Dorset reference lakes are located about 200 km southeast of Sudbury (Fig. 1) and are zoogeographically similar to the Sudbury lakes with respect to zooplankton (Sprules 1977). The lakes span a range of chemistry and morphometry, which encompasses the conditions in Whitepine and Sans Chambre lakes. General physical and chemical characteristics of the Dorset lakes are summarized in Table 1. Additional descriptions of the Dorset lakes are provided in Yan et al. (1996).

Sampling and analysis

Zooplankton were collected from both of the Sudbury lakes between 1980 and 1999. Whitepine Lake was sampled in all years, whereas some years (1982, 1984, 1986, 1987) were not included in the monitoring of Sans Chambre Lake. Samples were usually collected monthly during the ice-free season; however, sampling frequency was higher in some years in the early 1980s, and slightly reduced in some years in the mid-1990s (Tables 2 and 3). The 47 Dorset reference lakes were sampled monthly during the ice-free season for one year each (1983, 1984, 1987, or 1988).

All zooplankton samples were collected as vertical tows through the water column with 12.5-cm-diameter, 80-μm-mesh nets. Metered nets were used for the Dorset lakes and for the Sudbury lakes after 1981 to allow correction for filtration efficiency. Data for Sudbury lakes from 1980 and 1981 were adjusted for filtration efficiency by applying the mean efficiency for metered net collections in each lake during the 1980s. Single hauls from 1 m above bottom were taken in Sans Chambre Lake. In Whitepine Lake and each of the Dorset lakes, a series of hauls from three to seven fixed depths in the water column, at a single site, was taken and composited. Depths were chosen so that the composite sample was weighted to account for lake stratum volume.

Samples were preserved with buffered sugar formalin to a final formalin concentration of 4%. Subsequently, a minimum of 250 crustacean zooplankton were identified and counted. Cladocera and mature Copepoda were identified to species and immature Copepoda were identified to suborder. To deal with changes in nomenclature over the course of the study we have combined counts of different species of *Diaphanosoma* to genus, have combined *Daphnia dentifera* with *Daphnia mendotae*, and have combined *Daphnia pulicaria* and *Daphnia catawba* with *Daphnia pulex*.

Annual average species richness per collection and abundance were determined by averaging monthly data. Where more than one sample was available for a month, these values were averaged, to provide a monthly value, before generating annual averages. High numbers of animals (up to ~500 and ~700 animals per sample, in Whitepine and Sans Chambre, respectively) were counted in some samples in a few early years. Because richness is related to the number of

© 2002 NRC Canada

Fig. 1. Locations of Whitepine and Sans Chambre lakes, near Sudbury, Ont., Canada, and the Dorset reference lakes.

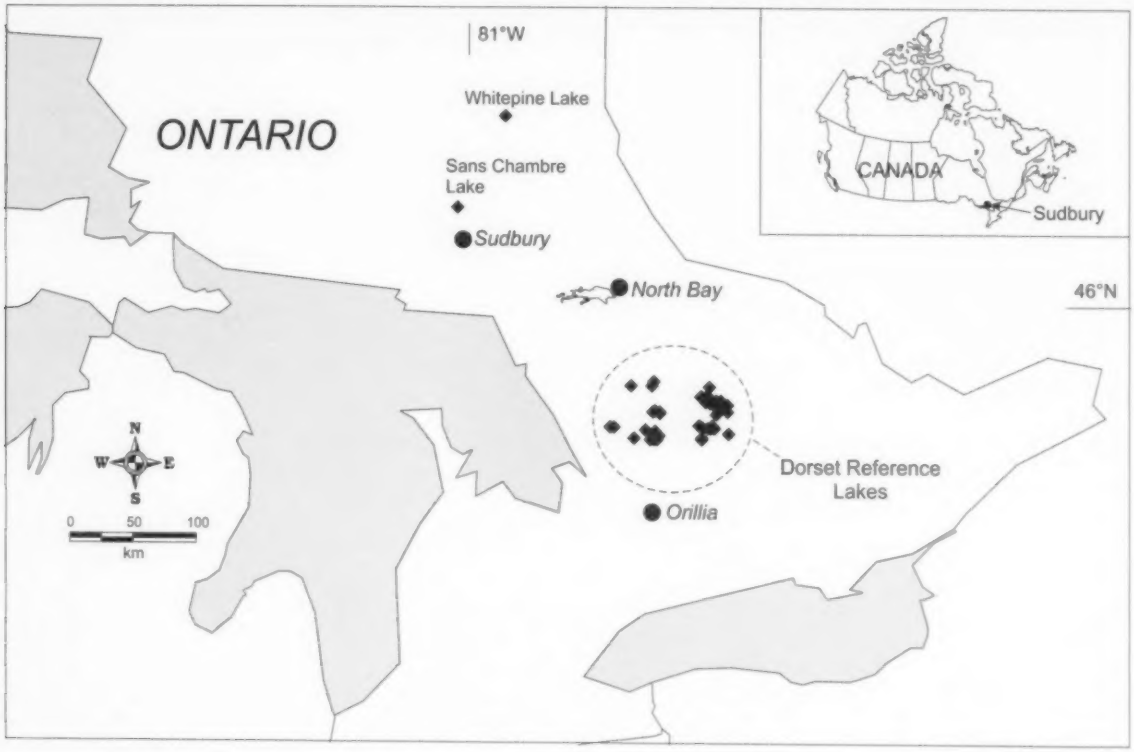

Table 1. General characteristics of the Sudbury and Dorset study lakes.

	Dorset		Sudbury	
	pH > 6.0 (n = 22)	pH < 6.0 (n = 25)	Whitepine	Sans Chambre
Distance from Sudbury (km)	~200	~200	89	30
Area (ha)	13.1–679.0	7.2–195.0	66.9	14.5
Mean depth (m)	5.2–22.0	1.8–12.4	5.9	5.6
Max. depth (m)	13.7–61.0	5.8–36.5	22.0	15.0
Secchi depth (m)	2.9–7.9	1.3–9.3	6.4	4.5
pH	6.0–6.7	5.3–5.9	6.3	6.2
Ca ($mg \cdot L^{-1}$)	2.1–4.0	1.2–2.8	1.8	1.7
Total P ($\mu g \cdot L^{-1}$)	4–18	4–22	5	8
DOC ($mg \cdot L^{-1}$)	1.5–5.5	1.5–8.7	2.5	2.9

Note: Sudbury chemistry data are ice-free period averages of monthly samples from 1999. Dorset chemistry data are ice-free period averages of monthly samples from one of 1983, 1984, 1987, or 1988. Max, maximum; DOC, dissolved organic carbon.

animals counted, richness for these lakes was standardized to a count of 250 animals, using relationships that had been established previously (Keller and Yan 1991). No correction was applied to the Dorset reference lakes because approximately 250 animals were counted in all samples.

Following Yan et al. (1996) we employed correspondence analysis (CA) to generate our multivariate metrics of zooplankton community structure. Our input to the CA was average annual species abundance data transformed to $\log(x + 1) + 0.2$. The factor of 0.2 was applied to further downweight the influence of uncommon species (K. Somers, unpublished data). The rarest species, including *Acantholeberis curvirostris*, *Acroperus harpae*, *Eubosmina coregoni*, *Eucyclops speratus*, and *Aglaodiaptomus leptopus*, were excluded from the analyses. Analyses were run separately for Whitepine Lake with the reference lakes, and for Sans Chambre Lake with the reference lakes.

Results

Species occurrences and abundances

During the 1980s and 1990s, 31 and 24 species of crustacean plankton were recorded in Whitepine and Sans Chambre lakes, respectively (Tables 2 and 3). Between 8 and 16, and 6 and 16 species were found in any one year in Whitepine and Sans Chambre lakes, respectively, but evalua-

© 2002 NRC Canada

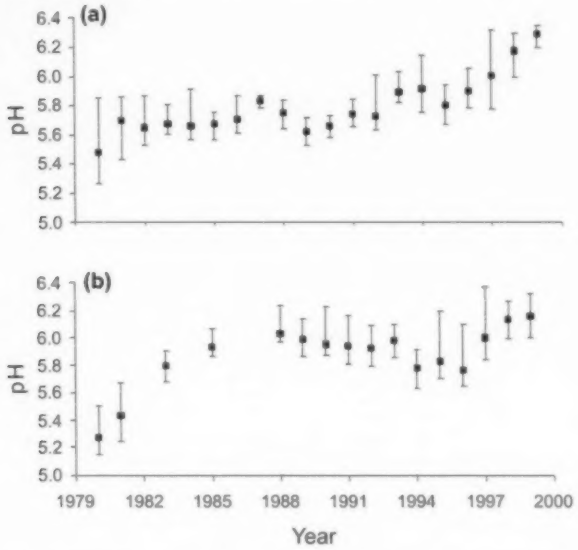

Fig. 2. Average annual pH during the ice-free season (error bars indicate the range in values) for (*a*) Whitepine and (*b*) Sans Chambre lakes.

tion of total annual richness in the Sudbury lakes is complicated by variable sampling frequency (Tables 2 and 3) since sampling effort can greatly influence total richness estimates (Arnott et al. 1998).

A number of species were detected in all, or almost all, study years. These included *Cyclops bicuspidatus thomasi*, *Cyclops scutifer*, *D. pulex*, *Holopedium gibberum*, *Bosmina* spp., and *Leptodiaptomus minutus* in Whitepine Lake (Table 2), and *Bosmina* spp., *C. scutifer*, *H. gibberum*, *L. minutus*, *Orthocyclops modestus*, and *Mesocyclops edax* in Sans Chambre Lake (Table 3). Species that were not detected at the beginning of our studies, but later appeared and persisted in the communities as common species included *Epischura lacustris* and *Eubosmina longispina* in Whitepine Lake (Table 2), and *D. pulex*, *Tropocyclops extensus*, *Daphnia ambigua*, and *E. lacustris* in Sans Chambre Lake (Table 3). Species that occurred throughout our period of record but showed alternating periods of presence or absence, often for several consecutive years, included *Chydorus sphaericus*, *D. ambigua*, *D. mendotae*, *Diaphanosoma* sp., *M. edax*, and *T. extensus* in Whitepine Lake, and *D. mendotae*, *Skistodiaptomus oregonensis*, and *C. b. thomasi* in Sans Chambre Lake (Table 3). Other species collected in these lakes were generally rare, occurring in 25% or less of the study years, and restricted to limited or sporadic occurrences (Tables 2 and 3).

Overall differences ($p < 0.05$) in species abundances between the reference lakes and both Whitepine and Sans Chambre lakes included higher abundances of *D. longiremis*, *S. oregonensis*, *Diaphanosoma* sp., *Neobosmina tubicen*, *D. retrocurva*, *D. dubia*, and *D. mendotae*, and lower abundances of *D. pulex* and *C. scutifer*, in the reference lakes (one-way analysis of variance (ANOVA), Bonferroni multiple comparisons test).

Species richness

There were substantial between-year variations in average zooplankton community richness (Fig. 3); however, in both Sudbury lakes average species richness per collection increased ($p < 0.05$) over the study period based on regressions of richness against year (Whitepine, $r = 0.55$; Sans Chambre, $r = 0.78$). Average richness was also correlated ($p < 0.05$) with average annual pH (Whitepine, $r = 0.42$; Sans Chambre, $r = 0.70$), which was correlated ($p < 0.05$) with year (Whitepine, $r = 0.83$; Sans Chambre, $r = 0.70$).

Comparison of the long-term patterns in the average richness of the Sudbury lakes with the average richness in the Dorset reference lakes with pH > 6.0 (Fig. 3) indicated that in the 1990s, richness values for both Sudbury lakes fell within the range of reference lake variability (mean ± 2 standard deviations = 7.8–12.3) in some years. By this metric, communities have shown recovery.

Multivariate community structure

The first two CA axes explained 39% of the transformed variation in species abundances when Whitepine Lake was included, and 43% of the transformed variation when Sans Chambre Lake was included (species scores for the axes are shown in Fig. 4*a*, 4*b*). In the Whitepine Lake CA, axis I (21% explained variation) was correlated ($p < 0.05$) with dissolved organic carbon (DOC; $r = -0.50$), total phosphorus (TP; $r = -0.34$), and calcium (Ca; $r = -0.26$), and axis II (18% explained variation) was correlated with pH ($r = 0.60$), aluminum (Al; $r = -0.58$), TP ($r = -0.50$), DOC ($r = -0.38$), and Ca ($r = 0.26$). In the ordination with Sans Chambre Lake, axis I (28% explained variation) was correlated ($p < 0.05$) with TP ($r = 0.46$), pH ($r = -0.41$), and Al ($r = 0.36$), and axis II (15% explained variation) was correlated with DOC ($r = -0.63$), Al ($r = -0.43$), pH ($r = 0.42$), TP ($r = -0.36$), and Ca ($r = 0.30$).

Temporally, Whitepine Lake shifted toward higher positive scores on CA axis II during the study period. Axis II scores increased significantly ($r = 0.81$, $p < 0.05$) over the study period based on a regression against sequential year of sampling. This trajectory indicates recovery, since higher positive scores on CA axis II are characteristic of the reference lakes with pH > 6.0 (Fig. 5*a*). However, Whitepine Lake scores never occupied the same region in ordination space on axis I as the reference lakes.

Community structure, as defined by lake scores from CA, changed little in Sans Chambre Lake over the past two decades (Fig. 5*b*). Throughout this study period Sans Chambre Lake did not move in a consistent manner toward the region in the ordination occupied by the reference lakes. There were no significant correlations between axis I or axis II scores and sequential years based on linear regressions ($p > 0.05$).

Discussion

Two decades of monitoring, during conditions of decreasing lake acidity, did reveal evidence of recovery in the crustacean zooplankton communities in Whitepine and Sans Chambre lakes. A number of "new" species became established, and persisted in the zooplankton communities of the lakes. The fact that some of these species, such as *E. lacustris*, are quite acid sensitive (Keller and Yan 1998) indicates that these biological changes are consistent with improved water quality conditions. Average species richness

© 2002 NRC Canada

Table 2. Percent occurrence of crustacean zooplankton in ice-free period samples from Whitepine Lake, 1980–1999.

Species	Species abbreviation	1980 (7)	1981 (13)	1982 (13)	1983 (11)	1984 (5)	1985 (6)	1986 (6)	1987 (6)	1988 (5)
Calanoid copepodid	Cal copep	100	85	92	91	80	83	100	100	100
Cyclopoid copepodid	Cyc copep	100	100	100	100	100	100	100	100	100
Cyclops bicuspidatus thomasi	C b thom	29	31	85	91	60	83	100	83	60
Cyclops scutifer	C scut	71	77	85	82	60	67	50	67	20
Daphnia pulex	D pulex	57	85	85	91	60	83	100	67	80
Holopedium gibberum	H gibb	100	62	69	100	100	100	83	83	60
Leptodiaptomus minutus	L minu	100	100	100	91	80	100	100	100	100
Nauplius	nauplius	100	100	100	100	100	100	100	100	100
Bosmina spp.	Bos spp	86	77	85	100	100	67	33	83	100
Epischura lacustris	E lacus	0	0	15	27	20	50	83	67	60
Bosmina (Eubosmina) longispina	E long	0	0	0	0	0	0	0	17	100
Mesocyclops edax	M edax	57	54	15	64	0	0	0	0	40
Daphnia ambigua	D ambig	71	62	46	0	40	0	0	17	0
Daphnia mendotae	D men	14	8	0	9	0	0	0	0	0
Tropocyclops extensus	T ext	0	8	0	27	0	33	17	17	20
Chydorus sphaericus	C sphaer	29	8	54	82	0	17	0	0	0
Diaphanosoma sp.	Diaph sp	0	0	8	0	0	0	0	0	40
Alona sp.	Alona sp	0	0	0	0	0	0	0	17	20
Bosmina (Neobosmina) tubicen	N tub	0	0	0	0	0	0	0	17	20
Leptodora kindtii	L kind	0	23	15	9	0	0	0	17	0
Alona affinis	A affin	14	15	0	0	0	0	0	0	0
Alona guttata	A gutt	0	0	8	18	0	0	0	0	0
Bosmina (Eubosmina) coregoni	E core	0	0	0	0	0	0	0	0	0
Daphnia longiremis	D long	0	0	0	0	0	0	0	0	0
Eucyclops speratus	E sper	0	0	8	0	0	0	0	0	0
Acantholeberis curvirostris	A curv	0	0	0	0	0	0	17	0	0
Acroperus harpae	A harp	0	0	8	0	0	0	0	0	0
Ceriodaphnia sp.	Cerio sp	0	0	0	0	0	17	0	0	0
Cyclops vernalis	C vern	0	0	0	0	0	0	0	0	20
Daphnia retrocurva	D retro	0	0	8	0	0	0	0	0	0
Eucyclops neomacruroides	E neom	0	0	0	0	0	0	0	0	0
Latona setifera	L seti	0	0	0	0	0	0	0	0	0
Sida crystallina	S crys	0	0	0	9	0	0	0	0	0
Skistodiaptomus oregonensis	S oreg	0	0	0	0	0	0	17	0	0

Note: Taxa are listed in order of decreasing overall occurrence in years. *Daphnia dubia* (species abbreviation D dubia) present in Dorset Reference

per collection in both lakes increased substantially to levels approaching, or in some years falling within, the range of variability observed in the reference lakes with pH > 6.0. Whether species richness will increase further remains to be seen.

Despite the positive responses to reduced acidity that have occurred, zooplankton communities in the two Sudbury lakes have not truly "recovered" when recovery is defined as the lake positions with respect to our two CA axes. The trajectory of community change in Whitepine Lake, determined by CA, clearly indicates recovery; however, in both Whitepine and Sans Chambre lakes, community structure never completely resembled reference lake conditions.

This interpretation of the multivariate patterns in species composition presumes that the range of variability in the reference lake data does provide suitable targets for recovery in our study lakes. The Dorset lakes provide the only comparably collected zooplankton reference data set that is available to help evaluate the responses of our Sudbury lakes. The reference lakes were, however, only sampled during the 1980s, whereas our Sudbury lake data also extend through the 1990s. Therefore, we cannot be completely certain that these reference data are fully representative of the 1990s, a decade with, for example, different weather patterns than the 1980s. Such uncertainty underscores the need for additional efforts to establish current biological reference data sets to aid in assessments of the status of aquatic ecosystems affected by acidification and other anthropogenic stressors.

The reference and study areas are nonetheless zoogeographically similar, and lakes in both areas were sampled by comparable protocols. The reference lakes encompass the range of physico-chemical conditions in the Sudbury lakes, although the Sudbury lakes do tend to lie at the clear, small, low ionic strength end of the distribution of these characteristics in the reference lakes. The major overall difference between the Sudbury lakes and the Dorset lakes is in the comparative scarcity of a number of acid-sensitive zooplankton species in the Sudbury lakes, a difference that is attributable to the greater degree and duration of acidification damage around Sudbury. Collectively, this evidence indicates that the reference lakes are suitable for our comparisons.

© 2002 NRC Canada

1989 (6)	1990 (7)	1991 (6)	1992 (7)	1993 (6)	1994 (6)	1995 (3)	1996 (3)	1997 (5)	1998 (5)	1999 (6)	% of years (20)
100	100	100	100	100	100	100	100	100	100	100	100
100	100	100	100	100	100	100	100	100	100	100	100
67	71	67	71	67	67	67	67	60	80	67	100
83	57	83	57	50	67	67	67	60	40	50	100
83	71	100	100	100	100	100	67	100	100	100	100
83	100	100	100	100	83	67	100	100	60	100	100
100	100	100	100	100	100	100	100	100	100	100	100
100	100	100	100	100	100	100	100	100	100	100	100
83	29	33	0	50	33	67	33	60	60	83	95
17	43	100	86	100	50	33	67	60	80	50	90
83	86	100	100	100	100	100	100	100	100	83	65
67	0	33	14	33	17	0	0	60	40	67	65
0	57	33	0	17	0	0	33	40	0	17	55
0	14	0	14	17	17	33	33	0	0	0	45
0	14	0	0	0	0	0	0	40	0	50	45
0	29	0	0	17	0	33	0	0	0	0	40
17	57	83	14	17	0	0	0	0	0	33	40
0	0	0	0	0	17	0	0	20	40	0	25
33	14	17	0	0	0	0	0	0	0	0	25
0	0	33	0	0	0	0	0	0	0	0	25
0	0	0	0	0	0	0	0	0	0	0	10
0	0	0	0	0	0	0	0	0	0	0	10
0	0	0	0	17	17	0	0	0	0	0	10
0	0	0	0	0	33	33	0	0	0	0	10
0	0	0	0	0	0	0	0	0	20	0	10
0	0	0	0	0	0	0	0	0	0	0	5
0	0	0	0	0	0	0	0	0	0	0	5
0	0	0	0	0	0	0	0	0	0	0	5
0	0	0	0	0	0	0	0	0	0	0	5
0	0	0	0	0	0	0	0	0	0	0	5
0	0	0	0	0	0	33	0	0	0	0	5
0	14	0	0	0	0	0	0	0	0	0	5
0	0	0	0	0	0	0	0	0	0	0	5
0	0	0	0	0	0	0	0	0	0	0	5

Lakes, but not in either of the Sudbury study lakes. Number in parentheses under year represents the total number of samples (*n*).

A number of factors may be involved in regulating biological recovery in these lakes. Both Whitepine and Sans Chambre lakes are headwaters, thus it might be expected that colonization opportunities from external sources could be limited. Invasion rates can be highly variable for different zooplankton species (Jenkins and Buikema 1998) and variability in factors such as invasion sequence and rate (Patrick 1967; Robinson and Edgemon 1988) may account for the variable temporal trajectories observed in lakes recovering from acidification.

Most zooplankton colonization experiments and studies (e.g., Jenkins and Buikema 1998; Shurin 2000) have been comparatively short term (one year or less), and small scale with respect to surface area. They may not completely reflect the ultimate role of dispersal in determining community composition on the scale of decades in larger natural systems. Extended monitoring studies, as reported here, offer an important complement to experimental studies examining factors regulating aquatic communities, because they reveal the actual long-term, lake-scale patterns of community change.

Long-term monitoring studies also have the advantage that species have had a long temporal window for colonization, whether the vector of colonization is transport from sources external to the lake (Maguire 1963; Schlichting and Sides 1969) or from the sediment egg bank (De Stasio 1989; Hairston 1996). It is likely that most species in the species pool will be detected, even if they are rare, when sampling extends through decades. Examination of the two-decade record for Whitepine and Sans Chambre lakes revealed that a number of acid-sensitive (Keller at al. 1990*b*; Havens et al. 1993) species, including *D. mendotae*, *D. retrocurva*, and *S. oregonensis*, which were important in defining our CA axes, were present at times in both lakes, but never became common. This suggests that dispersal was not ultimately a major limitation to their establishment in the lake communities.

The incomplete recovery, as indicated by multivariate analyses of the zooplankton community in Whitepine and Sans Chambre lakes, may reflect the limitations of time and unsuitable water quality. A pH of at least 6.0 appears to be necessary for the survival of many acid-sensitive zooplankton species (Keller at al. 1990*b*; Havens et al. 1993). A number of these species, which were relatively common in the

© 2002 NRC Canada

Table 3. Percent occurrence of crustacean zooplankton in ice-free period samples from Sans Chambre Lake, 1980–1999.

Species	Species abbreviation	1980 (4)	1981 (13)	1983 (6)	1985 (6)	1988 (6)	1989 (6)	1990 (6)	1991 (7)	1992 (9)	1993 (9)	1994 (6)	1995 (7)	1996 (4)	1997 (5)	1998 (5)	1999 (6)	% of Years (16)
Bosmina spp.	Bos spp	100	85	83	100	50	83	67	71	89	89	100	43	25	100	80	83	100
Calanoid copepodid	Cal copep	100	100	100	100	100	100	100	100	100	100	100	100	100	100	100	100	100
Cyclopoid copepodid	Cyc copep	100	100	100	100	100	100	100	100	100	100	100	100	100	100	100	100	100
Cyclops scutifer	C scut	50	62	100	83	50	83	50	43	44	56	67	86	50	40	40	50	100
Holopedium gibberum	H gibb	100	100	83	100	83	83	100	100	100	1 00	83	1 00	100	1 00	100	100	100
Leptodiaptomus minutus	L minu	100	100	100	83	100	100	100	100	100	100	100	100	100	100	100	100	100
Mesocyclops edax	M edax	100	62	100	67	67	50	33	71	44	89	67	86	50	60	60	67	100
Nauplius	nauplius	100	100	100	100	100	100	100	100	100	100	100	100	100	100	100	100	100
Orthocyclops modestus	O mode	100	54	17	0	83	33	83	71	44	56	83	100	25	80	100	83	94
Daphnia pulex	D pulex	0	0	100	100	100	100	100	100	100	100	83	71	100	80	100	100	88
Tropocyclops extensus	T ext	0	0	50	33	17	33	50	86	33	22	50	71	50	80	40	83	88
Daphnia ambigua	D ambig	0	0	0	0	100	67	83	43	11	78	83	43	0	40	40	100	69
Epischura lacustris	E lacus	0	0	0	0	17	17	17	43	44	11	17	29	25	40	20	0	69
Cyclops bicuspidatus thomasi	C b thom	0	8	0	17	17	0	33	29	11	11	17	0	0	0	0	17	56
Daphnia mendotae	D men	0	0	0	0	0	0	0	14	11	0	17	14	0	20	0	33	38
Skistodiaptomus oregonensis	S oreg	0	0	0	0	0	0	17	14	11	0	17	0	0	20	0	0	31
Aglaodiaptomus leptopus	A lept	0	0	0	0	0	0	0	0	0	0	0	0	50	100	60	50	25
Daphnia sp.	Daph sp	0	0	0	0	17	17	17	0	0	22	0	0	0	0	0	0	25
Alona sp.	Alona sp	0	0	0	0	0	17	0	0	0	0	0	0	0	0	20	17	19
Bosmina (Eubosmina) longispina	E long	0	0	0	0	0	0	33	0	0	0	17	0	0	0	0	0	13
Chydorus globosus	C glob	0	0	0	0	0	0	0	0	0	0	33	29	0	0	0	0	13
Chydorus sphaericus	C sphaer	0	0	0	0	0	0	0	0	11	0	17	0	0	0	0	0	13
Daphnia retrocurva	D retro	0	0	0	0	17	0	0	0	11	0	0	0	0	0	0	0	13
Polyphemus pediculus	P pedi	0	0	17	17	0	0	0	0	0	0	0	0	0	0	0	0	13
Bosmina (Neobosmina) tubicen	N tub	0	0	0	0	0	0	0	0	0	0	0	0	0	20	0	0	6
Bosmina (Eubosmina) coregoni	E core	0	0	0	0	0	0	0	0	0	0	0	14	0	0	0	0	6
Sida crystallina	S crys	0	8	0	0	0	0	0	0	0	0	0	0	0	0	0	0	6

Note: Taxa are listed in order of decreasing overall occurrence in years. *Daphnia dubia* (species abbreviation D dubia) present in Dorset Reference Lakes, but not in either of the Sudbury study lakes. Number in parentheses represents the total number of samples (*n*).

© 2002 NRC Canada

Fig. 3. Average annual ice-free period richness per collection, for crustacean zooplankton in Whitepine (○) and Sans Chambre (▲) lakes, 1980–1999, in comparison to the Dorset reference lakes with pH > 6.0.

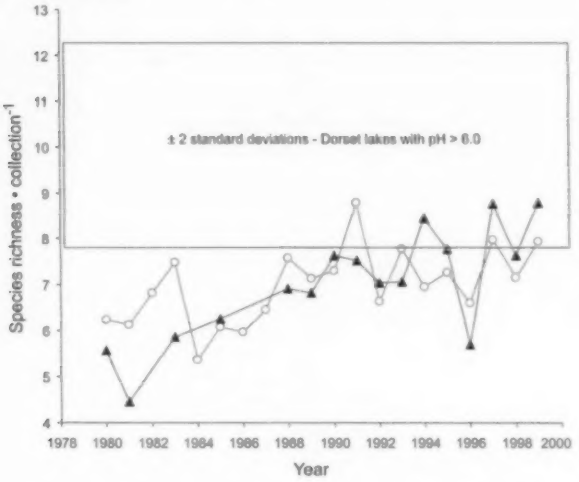

Fig. 4. (*a*) Crustacean zooplankton species scores on correspondence analysis (CA) axes for the ordination with Whitepine Lake and the reference lakes. Species abbreviations are identified in Table 2. (*b*) Crustacean zooplankton species scores on CA axes for the ordination with Sans Chambre Lake and the reference lakes. Species abbreviations are identified in Table 3.

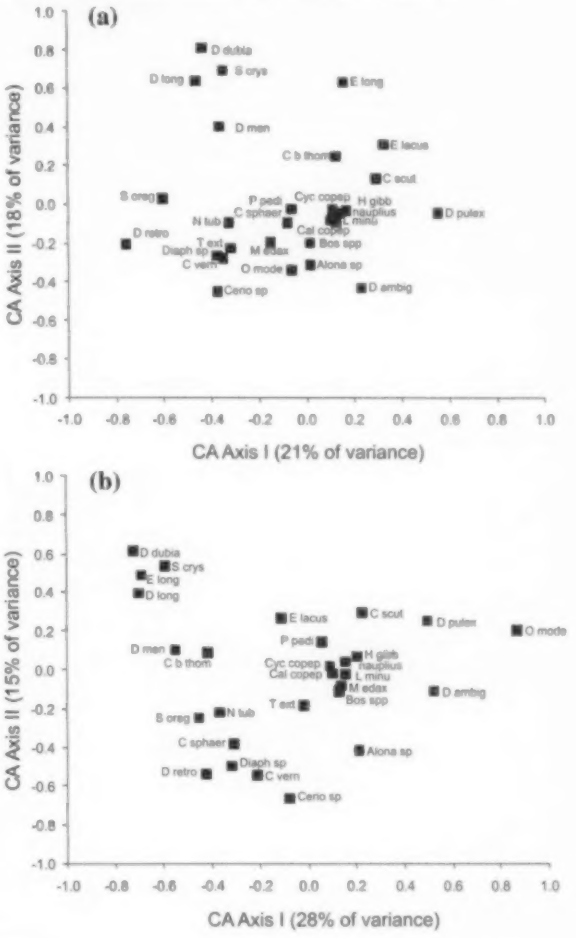

reference lakes and were important in defining community structure in the CA ordinations, are still rare in the Sudbury study lakes. Recovery of the crustacean zooplankton community was observed within a decade after the liming of Nelson Lake, near Sudbury (Yan et al. 1996), and zooplankton communities appear to have recovered in other Sudbury area lakes that have had pH > 6.0 for over a decade (Holt and Yan 2003). However, average pH > 6.0 has only been achieved very recently in Whitepine and Sans Chambre lakes, and pH minima are still slightly under 6.0. Despite two decades of monitoring, it appears that additional time, given conditions of suitable habitat quality, may be required for complete recovery of these communities.

Other factors also appear to be involved in regulating the recovery process in these lakes. The observation that community structure did show some evidence of recovery in Whitepine Lake, but showed very little change in Sans Chambre Lake, even though the extent of pH changes was generally similar, suggests that different mechanisms of control may currently dominate in these lakes. Biological as well as chemical factors may be important influences on the recovery of zooplankton communities (Keller and Yan 1998), and in some very important respects, Whitepine and Sans Chambre lakes differ in their biological characteristics.

Whitepine Lake has always had abundant fish during our study period, although the community composition has changed dramatically, from dominance by yellow perch (*Perca flavescens*) to lake trout (*Salvelinus namaycush*) (Gunn and Mills 1998). This change in the fish community may have favoured the recovery of zooplankton species through the relaxation of fish planktivory (Keller and Yan 1998). Not surprisingly, given the abundant fish and relatively nutrient poor status, abundances of the predatory invertebrate, *Chaoborus*, are very low in Whitepine Lake (late summer abundances of 1–11 animals·m^{-3} based on sampling in 1982–1984 and 1988; W. Keller, unpublished data) and are unlikely to have affected zooplankton species abundances through predation.

In contrast, Sans Chambre Lake was essentially fishless at the beginning of our studies, containing only a few individuals of brown bullhead (*Ictalurus nebulosus*) and central mudminnow (*Umbra limi*). The lake was successfully stocked with smallmouth bass (*Micropterus dolomieu*) in the early 1980s, but predation by smallmouth bass does not appear to exert a strong direct effect on pelagic invertebrates including crustacean zooplankton and *Chaoborus*. *Chaoborus* abundance in Sans Chambre Lake is high, with late summer abundances of 107 animals·m^{-3} and 124 animals·m^{-3} in 2000 and 2001, respectively (W. Keller, unpublished data). *Chaoborus* predation can exert a large effect on crustacean zooplankton at *Chaoborus* abundances of more than 30–50 animals·m^{-3} (Nyberg 1984; Yan et al. 1991). *Chaoborus* predation can decimate and even eliminate some zooplankton species, including comparatively small *Daphnia* species such as *D. mendotae* and *D. retrocurva* (Vanni 1988), which are rare in Sans Chambre

© 2002 NRC Canada

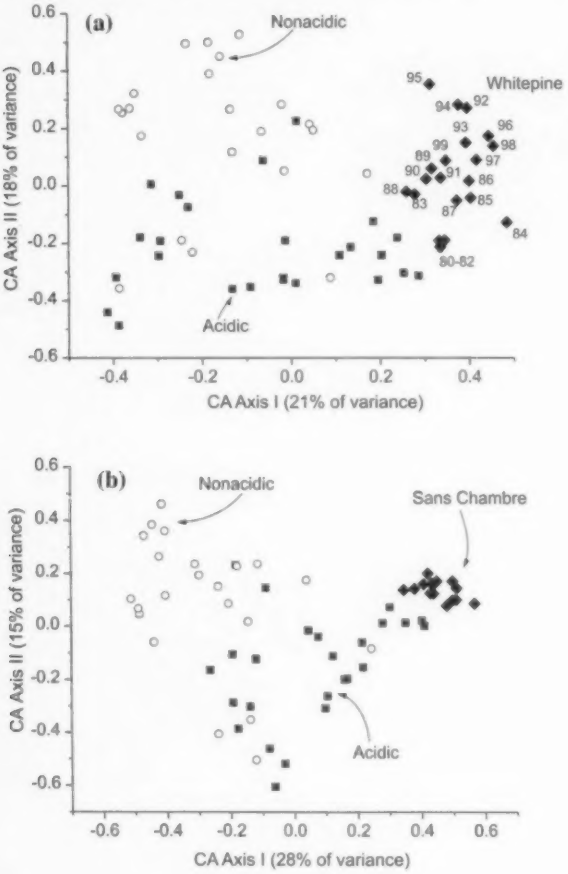

Fig. 5. (*a*) Lake scores on correspondence analysis (CA) axes for the ordination with Whitepine Lake and the reference lakes. (*b*) Lake scores on CA axes for the ordination with Sans Chambre Lake and the reference lakes.

Lake. The current characteristics of the Sans Chambre Lake zooplankton community, including scarcity of small *Daphnia*, absence of *Diaphanosoma birgei*, dominance by *D. pulex*, and the frequent occurrence of *A. leptopus* and *O. modestus*, are consistent with communities in fishless lakes exhibiting high *Chaoborus* predation (Vanni 1988; Arnott and Vanni 1993; Keller and Conlon 1994).

Thus, biological resistance (Nyberg 1984; Keller and Yan 1998) through intensive invertebrate predation is probably limiting the recovery of zooplankton in Sans Chambre Lake. *Chaoborus* abundance varies widely in the reference lakes (Persaud and Yan 2001) but none of the near-neutral reference lakes are fishless. Based on its size of 14.5 ha, Sans Chambre Lake was probably also not fishless prior to acidification (Matuszek et al. 1990), and therefore our recovery targets based on reference data would be valid for that lake. Substantial recovery of zooplankton communities in this lake may require not just suitable water quality, but biological intervention through stocking of planktivorous fish. It is likely that a reduction in invertebrate predation pressure will be needed before the zooplankton community can respond to reduced acidity.

The recovery of damaged aquatic ecosystems after the removal of stress is a very complex, poorly understood process (Cairns 1990; Power 1999). In general, the factors affecting biological recovery fall into two categories: (*i*) chemical, physical, and biological factors related to habitat quality, and (*ii*) factors related to the dispersal of organisms. Understanding the relative roles of processes operating within lakes versus processes related to dispersal is essential to the development of our knowledge of aquatic ecosystem recovery, and is also fundamental to addressing broader ecological questions about the factors regulating biodiversity in aquatic systems. Whether these different processes are termed local versus regional (e.g., Lukaszewski et al. 1999; Shurin et al. 2000) or internal versus external (e.g., Keller and Yan 1998), a key question is if community structure is primarily regulated by factors affecting the dispersal of species, or by factors affecting the survival and persistence of species.

The re-establishment of some zooplankton species including hypolimnetic forms and the "glacial opportunists" is expected to be limited by dispersal abilities (Schindler 1987; Keller and Yan 1998) and the regional species pool will have an overriding effect on local species assemblages. However, increasing experimental evidence is emerging that demonstrates the importance of "local" processes in determining zooplankton community structure (Arnott and Vanni 1993; Lukaszewski et al. 1999; Shurin 2000). Different mechanisms appear to be the primary current controls on zooplankton community recovery in Whitepine (duration of suitable habitat conditions) and Sans Chambre (biological resistance) lakes. However, both these examples provide empirical evidence for the importance of within-lake factors as controls on biological recovery. Our results suggest that the successful establishment of most common zooplankton species in these lakes as they recover from acidification will mainly depend on biotic and abiotic interactions, not on factors affecting species dispersal.

Acknowledgements

This paper is a contribution from the Aquatic Restoration Group of the Cooperative Freshwater Ecology Unit, a partnership between Laurentian University, the Ontario Ministry of the Environment, the Ontario Ministry of Natural Resources, Inco Limited, Falconbridge Limited, and Environment Canada. We thank Shelley Arnott and the Journal referees for helpful comments on the manuscript, and Peggy Gale and Jim Carbone for their many years of help collecting zooplankton samples.

References

Arnott, S.E., and Vanni, M.J. 1993. Zooplankton assemblages in fishless bog lakes: influence of biotic and abiotic factors. Ecology, **74**: 2361–2380.

Arnott, S.E., Magnuson, J.J., and Yan, N.D. 1998. Crustacean zooplankton species richness—single and multiple-year estimates. Can. J. Fish. Aquat. Sci. **55**: 1573–1582.

Cairns, J. 1990. Lack of a theoretical basis for predicting rate and pathways of recovery. Environ. Manag. **14**: 517–526.

© 2002 NRC Canada

Degerman, E., Henrikson, L., Hermann, J., and Nyberg, P. 1995. The effects of liming on aquatic fauna. *In* Liming of acidified surface waters. *Edited by* L. Henrikson and W.Y. Brodin. Springer-Verlag, Heidelberg. pp. 221–282.

De Stasio, B.T., Jr. 1989. The seed bank of a freshwater crustacean: copepodology for the plant ecologist. Ecology, **70**: 1377–1389.

Gunn, J.M., and Mills, K.H. 1998. The potential for restoration of acid-damaged lake trout lakes. Restor. Ecol. **6**: 390–397.

Hairston, N.G., Jr. 1996. Zooplankton egg banks as biotic reservoirs in changing environments. Limnol. Oceanogr. **41**: 1087–1092.

Havens, K.E., Yan, N.D., and Keller, W. 1993. Lake acidification: effects on crustacean zooplankton populations. Environ. Sci. Technol. **27**: 1621–1624.

Holt, C.A., and Yan, N.D. 2003. Recovery of zooplankton communities from acidification in Killarney Park, Ontario, 1971–2000: pH 6 as a recovery goal. Ambio. In press.

Jenkins, D.J., and Buikema, A.L., Jr. 1998. Do similar communities develop in similar sites? A test with zooplankton structure and function. Ecol. Monogr. **68**: 421–443.

Keller, W., and Conlon, M. 1994. Crustacean zooplankton communities and lake morphometry in Precambrian Shield lakes. Can. J. Fish. Aquat. Sci. **51**: 2424–2434.

Keller, W., and Yan, N.D. 1991. Recovery of crustacean zooplankton species richness in Sudbury area lakes following water quality improvements. Can. J. Fish. Aquat. Sci. **48**: 1635–1644.

Keller, W., and Yan, N.D. 1998. Biological recovery from acidification: zooplankton communities as a model of patterns and processes. Restor. Ecol. **6**: 364–375.

Keller, W., Dodge, D.P., and Booth, G.M. 1990*a*. Experimental lake neutralization program: overview of neutralization studies in Ontario. Can. J. Fish. Aquat. Sci. **47**: 410–411.

Keller, W., Yan, N.D., Holtze, K.E., and Pitblado, J.R. 1990*b*. Inferred effects of lake acidification on *Daphnia galeata mendotae*. Environ. Sci. Technol. **24**: 1259–1261.

Keller, W., Gunn, J.M., and Yan, N.D. 1992*a*. Evidence of biological recovery in acid stressed lakes near Sudbury, Canada. Environ. Pollut. **78**: 79–85.

Keller, W., Pitblado, J.R., and Carbone, J. 1992*b*. Chemical responses of acidic lakes in the Sudbury, Ontario, area to reduced smelter emissions, 1981–1989. Can. J. Fish. Aquat. Sci. **49**(Suppl. 1): 25–32.

Keller, W., Gunn, J., and Yan, N. 1999. Acid rain: perspectives on lake recovery. J. Aquat. Ecosyst. Stress Recovery, **6**: 207–216.

Lukaszewski, Y., Arnott, S.E., and Frost, T.M. 1999. Regional versus local processes in determining zooplankton community composition of Little Rock Lake, Wisconsin, U.S.A. J. Plankton Res. **21**: 991–1003.

Maguire, B., Jr. 1963. The passive dispersal of small aquatic organisms and their colonization of isolated bodies of water. Ecol. Monogr. **33**: 61–185.

Matuszek, J.E., Goodier, J., and Wales, D.L. 1990. The occurrence of cyprinidae and other small fish species in relation to pH of Ontario lakes. Trans. Am. Fish. Soc. **119**: 850–861.

Nyberg, P. 1984. Impact of *Chaoborus* predation on planktonic crustacean communities in some acidified and limed forest lakes in Sweden. Rep. Inst. Freshw. Res. Drottningholm, **61**: 154–166.

Patrick, R. 1967. The effect of invasion rate, species pool, and size of area on the structure of the diatom community. Proc. Natl. Acad. Sci. U.S.A., **58**: 1335–1342.

Persaud, A.D., and Yan, N.D. 2001. Accounting for spatial variability in the design of sampling programmes for *Chaoborus* larvae. J. Plankton Res. **23**: 279–285.

Power, M. 1999. Recovery in aquatic ecosytems: an overview of knowledge and needs. J. Aquat. Ecosyst. Stress Recovery, **6**: 253–257.

Robinson, J.V., and Edgemon, M.A. 1988. An experimental evaluation of the effect of invasion history on community structure. Ecology, **69**: 1410–1417.

Sampson, C.J., Brezonik, P.L., Frost, T.M., Webster, K.E., and Simonson, T.D. 1995. Experimental acidification of Little Rock Lake, Wisconsin: the first four years of chemical and biological recovery. Water Air Soil Pollut. **85**: 1713–1719.

Schindler, D.W. 1987. Detecting ecosystem responses to anthropogenic stresses. Can. J. Fish. Aquat. Sci. **44**(Suppl. 1): 6–25.

Schindler, D.W. 1988. Effects of acid rain on freshwater ecosystems. Science (Washington, D.C.), **239**: 149–157.

Schlichting, H.E., Jr., and Sides, S.L. 1969. The passive transport of aquatic microoorganisms by selected Hemiptera. J. Ecol. **57**: 759–764.

Shurin, J.B. 2000. Dispersal limitation, invasion resistance and the structure of pond zooplankton communities. Ecology, **81**: 3062–3073.

Shurin, J.B., Liebold, M.A., Havel, J.E., and Pinel-Alloul, B. 2000. Local and regional species richness: a scale-independent test for saturation. Ecology, **81**: 3074–3086.

Sprules, W.G. 1977. Crustacean zooplankton communities as indicators of limnological conditions: an approach using principal component analysis. J. Fish. Res. Board Can. **34**: 389–395.

Stoddard, J.L., Jeffries, D.S., Lukewille, A., Clair, T.A., Dillon, P.J., Driscoll, C.T., Forsius, M., Johannessen, M., Kahl, J.S., Kellogg, J.H., Kemp, A., Mannio, J., Monteith, D.T., Murdoch, P.S., Patrick, S., Rebsdorf, A., Skjelkvale, B.L., Stainton, M.P., Traen, T., van Dam, H., Webster, K.E., and Wilander, A. 1999. Regional trends in aquatic recovery from acidification in North America and Europe. Nature (London), **401**: 575–578.

Vanni, M.J. 1988. Freshwater zooplankton community structure: introduction of large invertebrate predators and large herbivores to a small species community. Can. J. Fish. Aquat. Sci. **45**: 1758–1770.

Yan, N.D., Keller, W., MacIsaac, H.J., and McEachern, L.J. 1991. Regulation of zooplankton community structure in an acidic lake by *Chaoborus*. Ecol. Appl. **1**: 52–65.

Yan, N.D., Keller, W., Somers, K.M., Pawson, T.W., and Girard, R.G. 1996. Recovery of crustacean zooplankton communities from acid and metal contamination: comparing manipulated and reference lakes. Can. J. Fish. Aquat. Sci. **53**: 1301–1327.

© 2002 NRC Canada

PERSPECTIVE

Dynamics of the Lake Michigan food web, 1970–2000

Charles P. Madenjian, Gary L. Fahnenstiel, Thomas H. Johengen, Thomas F. Nalepa, Henry A. Vanderploeg, Guy W. Fleischer, Philip J. Schneeberger, Darren M. Benjamin, Emily B. Smith, James R. Bence, Edward S. Rutherford, Dennis S. Lavis, Dale M. Robertson, David J. Jude, and Mark P. Ebener

Abstract: Herein, we document changes in the Lake Michigan food web between 1970 and 2000 and identify the factors responsible for these changes. Control of sea lamprey (*Petromyzon marinus*) and alewife (*Alosa pseudoharengus*) populations in Lake Michigan, beginning in the 1950s and 1960s, had profound effects on the food web. Recoveries of lake whitefish (*Coregonus clupeaformis*) and burbot (*Lota lota*) populations, as well as the buildup of salmonine populations, were attributable, at least in part, to sea lamprey control. Based on our analyses, predation by salmonines was primarily responsible for the reduction in alewife abundance during the 1970s and early 1980s. In turn, the decrease in alewife abundance likely contributed to recoveries of deepwater sculpin (*Myoxocephalus thompsoni*), yellow perch (*Perca flavescens*), and burbot populations during the 1970s and 1980s. Decrease in the abundance of all three dominant benthic macroinvertebrate groups, including *Diporeia*, oligochaetes, and sphaeriids, during the 1980s in nearshore waters (≤50 m deep) of Lake Michigan, was attributable to a decrease in primary production linked to a decline in phosphorus loadings. Continued decrease in *Diporeia* abundance during the 1990s was associated with the zebra mussel (*Dreissena polymorpha*) invasion, but specific mechanisms for zebra mussels affecting *Diporeia* abundance remain unidentified.

Résumé : On trouvera ici une étude des changements dans le réseau alimentaire du lac Michigan de 1970 à 2000 et des facteurs qui en sont responsables. Le contrôle des populations de la grande lamproie marine (*Petromyzon marinus*) et du gaspareau (*Alosa pseudoharengus*), qui a débuté dans les années 1950 et 1960, a eu un impact considérable sur le réseau alimentaire. Le rétablissement des populations du grand corégone (*Coregonus clupeaformis*) et de la lotte (*Lota lota*) et l'accroissement des populations de salmonidés sont dus, au moins en partie, au contrôle de la lamproie.

Received 22 March 2001. Accepted 25 January 2002. Published on the NRC Research Press Web site at http://cjfas.nrc.ca on 24 May 2002.
J16279

C.P. Madenjian[1] and G.W. Fleischer. U.S. Geological Survey, Great Lakes Science Center, 1451 Green Road, Ann Arbor, MI 48105, U.S.A.
G.L. Fahnenstiel. National Oceanic and Atmospheric Administration, Great Lakes Environmental, Research Laboratory, Muskegon Field Station, 1431 Beach Street, Muskegon, MI 49441, U.S.A.
T.H. Johengen. Cooperative Institute for Limnology and Ecosystem Research, University of Michigan, 2200 Bonisteel Boulevard, Ann Arbor, MI 48109, U.S.A.
T.F. Nalepa and H.A. Vanderploeg. National Oceanic and Atmospheric Administration, Great Lakes Environmental, Research Laboratory, 2205 Commonwealth Boulevard, Ann Arbor, MI 48105, U.S.A.
P.J. Schneeberger. Michigan Department of Natural Resources, Marquette Fisheries Station, 484 Cherry Creek Road, Marquette, MI 49855, U.S.A.
D.M. Benjamin. Atlantic States Marine Fisheries Commission, 444 Eye Street, Washington, DC 20005, U.S.A.
E.B. Smith and J.R. Bence. Department of Fisheries and Wildlife, Michigan State University, East Lansing, MI 48824, U.S.A.
E.S. Rutherford. Institute for Fisheries Research, University of Michigan, Ann Arbor, MI 48109, U.S.A.
D.S. Lavis. U.S. Fish and Wildlife Service, Ludington Biological Station, 229 South Jebavy Drive, Ludington, MI 49431, U.S.A.
D.M. Robertson. U.S. Geological Survey, Water Resources Division, 8505 Research Way, Middleton, WI 53562, U.S.A.
D.J. Jude. Center for Great Lakes and Aquatic Sciences, University of Michigan, 501 East University, 717 Dennison Building, Ann Arbor, MI 48109, U.S.A.
M.P. Ebener. Inter-Tribal Fisheries and Assessment Program, Chippewa Ottawa Resource Authority, 179 West Three Mile Road, Sault Ste. Marie, MI 49783, U.S.A.

[1]Corresponding author (e-mail: chuck_madenjian@usgs.gov).

 DOI: 10.1139/F02-044 © 2002 NRC Canada

D'après nos analyses, la réduction de la densité des gaspareaux dans les années 1970 et au début des années 1980 est due principalement à la prédation par les salmonidés. À son tour, la réduction des gaspareaux a sans doute contribué au rétablissement des populations du chabot de profondeur (*Myoxocephalus thompsoni*), de la perchaude (*Perca flavescens*) et de la lotte dans les années 1970 et 1980. Durant les années 1980, la décroissance de la densité des trois groupes dominants de macroinvertébrés benthiques, *Diporeia*, les oligochètes et les sphériidés, dans les eaux côtières (≤50 m de profondeur) du lac Michigan est attribuable à une diminution de la production primaire lié à une réduction des apports de phosphore. La poursuite du déclin des densités de *Diporeia* dans les années 1990 est associée à l'invasion de la moule zébrée (*Dreissena polymorpha*), bien que les mécanismes précis de l'effet des moules sur *Diporeia* n'aient pas encore été identifiés.

[Traduit par la Rédaction]

Introduction

The objective of the first symposium on Salmonid Communities in Oligotrophic Lakes (SCOL-1) was to identify the effects of the three major anthropogenic stressors of cultural eutrophication, fishery exploitation, and exotic species introductions on fish communities, especially salmonid communities, in the five Laurentian Great Lakes (Wells and McLain 1972, 1973). As part of the SCOL-1 effort, Wells and McLain (1973) examined the changes in Lake Michigan fish communities from 1880 to 1970. One of the major conclusions from their study was that sea lamprey (*Petromyzon marinus*) and alewife (*Alosa pseudoharengus*) invasions between 1930 and 1950 more profoundly affected fish communities in Lake Michigan than either accelerated eutrophication or fishery exploitation. Nevertheless, Wells and McLain (1973) ascribed the population collapse of larger deepwater ciscoes, including *Coregonus nigripinnis* and *Coregonus johannae*, to overfishing. Wells and McLain (1973) did acknowledge that accelerated eutrophication and other pollution may have caused some changes in fish communities of Lake Michigan during 1880–1970; however, evidence to support this contention was not very strong. In retrospect, SCOL-1 was a milestone in that it marked the first attempt to explain changes in fish communities of the Laurentian Great Lakes during 1880–1970 in the context of anthropogenic stressors to the ecosystem.

The Lake Michigan food web has undergone tremendous changes since 1970. For example, alewife abundance declined substantially during the 1970s and early 1980s (Jude and Tesar 1985; Eck and Wells 1987). Bloater (*Coregonus hoyi*) abundance increased dramatically during the early 1980s, peaked in the late 1980s, and declined during the 1990s (Eck and Wells 1987; TeWinkel et al. 2002). Biomass of the salmonine population increased steadily from 1965 to 1986 (Stewart and Ibarra 1991). Phosphorus loadings to Lake Michigan decreased during the 1980s as a result of federally mandated water quality control measures (Johengen et al. 1994). The three major groups of benthic macroinvertebrates, namely the amphipod *Diporeia*, oligochaete worms (Oligochaeta), and fingernail clams (Sphaeriidae), decreased substantially in abundance in southern Lake Michigan at sites shallower than 50 m between 1980 and 1993 (Nalepa et al. 1998). The midsummer epilimnetic phytoplankton community in offshore waters (>40 m deep) shifted from a blue-green and green algae dominated community in the 1970s to a phytoflagellate dominated community in the 1980s (Fahnenstiel and Scavia 1987*a*). The summer zooplankton community in offshore waters changed abruptly during the early 1980s from a community dominated by calanoid copepods to a community dominated by the large-bodied cladoceran *Daphnia pulicaria* (Evans and Jude 1986). The predatory cladoceran *Bythotrephes cederstroemi*, an invader from Eurasia, became established in Lake Michigan by 1986 (Lehman 1987). By 1993, the zebra mussel (*Dreissena polymorpha*), an invader from the Ponto-Caspian region, had colonized hard substrates within 7 km of shore between Waukegan and Michigan City (Nalepa et al. 1998). Presence of round goby (*Neogobius melanostomus*), a fish invader from the Ponto-Caspian region, was first documented in 1994 (Clapp et al. 2001).

Herein, we document dynamics of the Lake Michigan food web from 1970 through 2000, and then identify factors likely responsible for these ecosystem changes. As in SCOL-1, we address the potential effects of anthropogenic stressors on fish communities in Lake Michigan. Since the time of SCOL-1, the list of anthropogenic stressors to the Great Lakes ecosystems has been expanded to include contaminants and global climate change. We also re-examine conclusions from the SCOL-1 study, in light of the wealth of information on the Lake Michigan food web that has become available since 1970. As has been surmised from studies of other ecosystems (Likens 1989), we would expect that long-term observation and study are needed before we can begin to understand the dynamics of an ecosystem as large and complex as Lake Michigan. Therefore, we analyze the available long-term series of observations on phytoplankton, zooplankton, benthic macroinvertebrate, and fish communities in Lake Michigan to identify factors that may be responsible for changes that have occurred since 1970. Aquatic ecosystem structure can be regulated from the bottom up (McQueen et al. 1989), as well as from the top down (Kitchell and Carpenter 1993). How extensively have top-down and bottom-up effects pervaded the Lake Michigan food web? With this synthesis, we answer that question.

Long-term trends in phosphorus loading and nutrient dynamics

In Lake Michigan, phosphorus is the major nutrient that limits phytoplankton growth and has the greatest potential to adversely affect the lake's ecosystem (Schelske and Stoermer 1971; Schelske et al. 1974). Fortunately, phospho-

© 2002 NRC Canada

Fig. 1. Annual estimates of total phosphorus loading to Lake Michigan, including Green Bay, for 1974–1991 and 1994–1995.

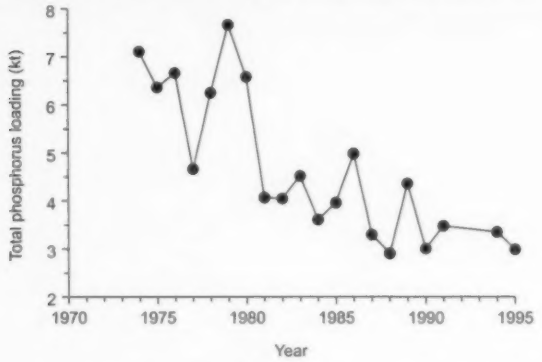

rus is also the easiest nutrient to control, primarily because phosphorus has no gaseous phase. Thus, regulation of phosphorus has been the primary management strategy for controlling eutrophication in the Great Lakes. Billions of dollars have been spent to reduce phosphorus inputs to the Great Lakes, and success has been documented in the lower Great Lakes (Johengen et al. 1994).

Phosphorus control programs substantially reduced phosphorus loadings to Lake Michigan (Fig. 1). Total annual loading decreased from over 6.5 kilotonnes (kt) in 1980 to about 4 kt in 1981, coincident with control of most point sources from major water treatment plants and phosphorus bans on detergents. Loadings further decreased between 1981 and the late 1980s, before appearing to level off during the 1990s (Fig. 1). During 1994 and 1995, annual load estimates ranged from 3 to 3.5 kt.

Based on available data (Johengen et al. 1994; Makarewicz et al. 1998; T. Johengen, unpublished data), nitrate and silica concentrations in epilimnetic waters of Lake Michigan increased between 1976 and 1999. Increases were apparent for both spring maximum and summer minimum concentrations within the epilimnion. Increased nitrate levels have likely resulted from increased tributary loads, in response to human population growth and increases in industrial and agricultural activity (Vollenweider 1970), as well as from increased atmospheric loading, as was clearly demonstrated for Lake Superior (Bennet 1986). Silica concentrations would be expected to increase from an increase in anthropogenic loading, a decrease in the burial rate of silica to the sediment, or a decrease in rates with which dissolved silica is biologically utilized. Rate of use of silica by biota would decrease if species composition of the diatom community shifted toward smaller or less-silicified diatoms, or if there was an overall decrease in production rates of the diatom community.

Dynamics of phytoplankton and primary production

In toto, the evidence indicated that primary production in offshore waters of Lake Michigan trended neither upward nor downward during the last 25 years. Total phytoplankton abundance, measured as chlorophyll *a* concentration, in offshore waters (>50 m deep) of Lake Michigan varied without trend during 1983–1998 (Fig. 2*a*), a finding corroborated by Fahnenstiel et al. (1998), who showed that phytoplankton abundance, measured as carbon, in offshore waters of Lake Michigan did not change between the 1986–1988 and 1993–1995 time periods. Addition of chlorophyll data from Brooks and Torke (1977) to the time series demonstrated no trends in offshore phytoplankton abundance since 1973 (Fig 2*a*). Similarly, total phosphorus concentration (TP) in the water column during spring, an indicator of primary production (Fahnenstiel et al. 1998), fluctuated about a constant level during 1976–1998 (Fig. 2*b*).

Fig. 2. (*a*) Average annual chlorophyll *a* concentration and (*b*) average spring total phosphorus concentration (from March until water temperature reached 4°C) in Lake Michigan at offshore (100–110 m) stations off Grand Haven (●) and Muskegon (▽), Mich., 1976–1998. Also included are chlorophyll *a* data for offshore Lake Michigan waters off Milwaukee, Wis., 1973–1974 (○) (Brooks and Torke 1977).

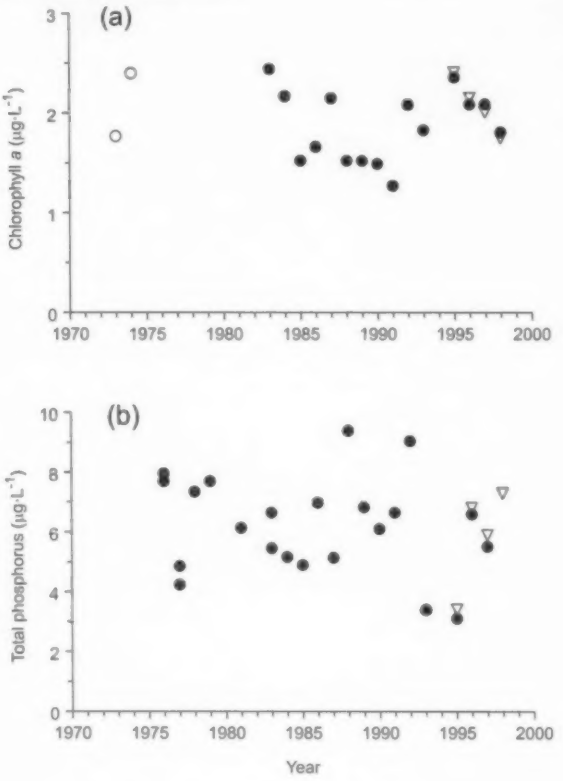

In contrast, species composition of the phytoplankton community in offshore waters of Lake Michigan underwent substantial changes in the past 30 years. Community structure during summer stratification shifted from one dominated by blue-green and green algae during the early 1970s to one dominated by phytoflagellates during the early 1980s (Fahnenstiel and Scavia 1987*a*). Summertime dominance of phytoflagellates has continued into the 1990s (Makarewicz

© 2002 NRC Canada

et al. 1998). Diatoms have composed the bulk of the phytoplankton community during the spring isothermal mixing period since 1970.

In Lake Michigan, a deep chlorophyll layer typically forms in the upper hypolimnion and lower metalimnion during summer stratification, and this layer contributes between 5 and 10% of the annual total chlorophyll and annual primary production within the lake (Fahnenstiel and Scavia 1987*b*). Size of the deep chlorophyll layer increased between the 1970s and 1980s. This increase was attributed to greater light penetration caused by increased grazing due to increased abundance of the very large-bodied zooplankter *D. pulicaria* (Scavia et al. 1986). This change in epilimnetic zooplankton composition did not persist for more than a few years (Evans 1992), and a shift back to smaller-bodied zooplankton apparently led to a reduction in the size and concentration of the deep chlorophyll layer (Fahnenstiel and Scavia 1987*c*; G. Fahnenstiel, unpublished data).

Although a long-term series of observations on phytoplankton abundance was not available for most of the 1970–2000 time period, the available data suggested that phytoplankton abundance and production in nearshore waters of Lake Michigan have decreased during the past 30 years. Schelske et al. (1980) intensively surveyed spring TP and chlorophyll *a* concentrations in nearshore waters of the eastern side of the lake during 1972. Nearshore waters in the vicinity of the Cook Power Plant in the southeastern section of the lake was consistently sampled for chlorophyll *a* concentration during 1973–1981. Similar sampling was conducted during the recent Episodic Events – Great Lakes Experiment (EEGLE) study from 1998–2000 in the same nearshore waters of Lake Michigan (G. Fahnenstiel, unpublished data). Comparison of data between the two time periods indicated that chlorophyll *a* concentration decreased by more than 50% and spring TP decreased by 40% between the 1970s and the 1998–2000 time period. These declines in phytoplankton abundance and production were likely attributable to the reduction in phosphorus loading (Fig. 1).

Owing to lack of regular assessments of the species composition of the phytoplankton community in nearshore waters, changes in phytoplankton community structure were difficult to firmly establish. Diatoms were the predominant group during spring mixing in the 1990s (G. Fahnenstiel, unpublished data), just as they were in the 1970s (Chang and Rossman 1988). The springtime community was dominated by small centric diatoms (such as *Stephanodiscus*) in nearshore waters and by large centric diatoms (such as *Aulacoseira*) in offshore waters (Fahnenstiel and Scavia 1987*a*; G. Fahnenstiel, unpublished data). Relative abundance of blue-green algae during summer increased from the 1970s to the 1980s in nearshore waters (Chang and Rossman 1988). Blue-green algae continued to be important in nearshore waters during summer stratification in the 1990s (G. Fahnenstiel, unpublished data).

During the 1970s, silica may have limited the production of diatoms during the end of the spring diatom bloom in both nearshore and offshore waters of Lake Michigan (Schelske et al. 1986; Scavia and Fahnenstiel 1987).

Dynamics of major benthic macroinvertebrate groups

The three major benthic macroinvertebrate groups found in Lake Michigan have been the amphipod *Diporeia*, oligochaete worms (Oligochaeta), and fingernail clams (Sphaeriidae) (Nalepa et al. 1998). Benthic surveys conducted in the southern basin have been sufficiently consistent and thorough to construct a long-term record of abundances of these groups since 1965. Overall, abundances of *Diporeia*, oligochaetes, and sphaeriids increased between the 1960s and the early 1980s (Fig. 3). The magnitude of the increase varied with group and depth interval. Long-term trends in abundance during 1980–1993 differed between nearshore (≤50 m) and offshore (>50 m) depth zones of southern Lake Michigan (Nalepa et al. 1998, 2000*a*). In the nearshore, abundances of all three groups declined between 1980 and 1993 (Fig. 3*a*, 3*b*). In contrast, abundances of *Diporeia*, oligochaetes, and sphaeriids in the offshore zone exhibited no distinct trends over the same time period (Fig. 3*c*, 3*d*). This difference in temporal trends of benthic macroinvertebrate abundances between nearshore and offshore zones may have been due to differences in temporal trends in phytoplankton abundance between the two zones. In large deep lakes like Lake Michigan, abundance of the dominant groups of benthic macroinvertebrates tends to be directly proportional to the amount of available food (Saether 1980). Increased phytoplankton abundance leads to increased amounts of organic material settling to the bottom region, thereby providing more potential food for macrobenthos. As noted above, phytoplankton abundance and primary production appeared to decrease in nearshore waters of Lake Michigan between the 1970s and 1990s, whereas no change was detected in offshore waters. The decrease in primary production in nearshore waters was probably due to the reduction in phosphorus loadings to the lake. Nutrient inputs from tributaries is better coupled with primary production in nearshore waters than in offshore waters (Schelske 1977). Finally, the zebra mussel invasion, in addition to the reduction in primary production, may have partly contributed to the decrease in *Diporeia* abundance in the nearshore region during the early 1990s (Nalepa et al. 2000*a*).

Continued decline of *Diporeia* in the nearshore region during the 1990s coincided with the invasion of Lake Michigan by the zebra mussel (Nalepa et al. 2000*a*, 2000*b*). By 1993, zebra mussels had colonized hard substrates within 7 km of shore between Waukegan and Michigan City. Zebra mussel density continued to increase at sites <50 m deep in southern Lake Michigan between 1992 and 1999 (Nalepa et al. 2000*a*). Disappearance of *Diporeia* from several southern locations in waters shallower than 50 m was first observed in 1992, and this zone of disappearance spread northward by 1999 (T. Nalepa, unpublished data). The specific mechanism by which zebra mussels could have reduced *Diporeia* abundance remains unclear. If these drastic reductions in *Diporeia* density were to continue to spread throughout the lake, including deeper waters, the effects on the Lake Michigan food web may be substantial. *Diporeia* represents a major link between pelagic production and upper trophic levels

© 2002 NRC Canada

Fig. 3. Average annual abundances of the dominant macroinvertebrate groups in the southern basin of Lake Michigan, in selected years over 1965–1993, within (*a*) the 16- to 30-m depth contour, (*b*) the 31- to 50-m depth contour, (*c*) the 51- to 80-m depth contour, and (*d*) the >80-m depth contour. Error bar represents one standard error for average total annual abundance. Solid bar represents *Diporeia*, open bar represents Sphaeriidae, and hatched bar represents Oligochaeta.

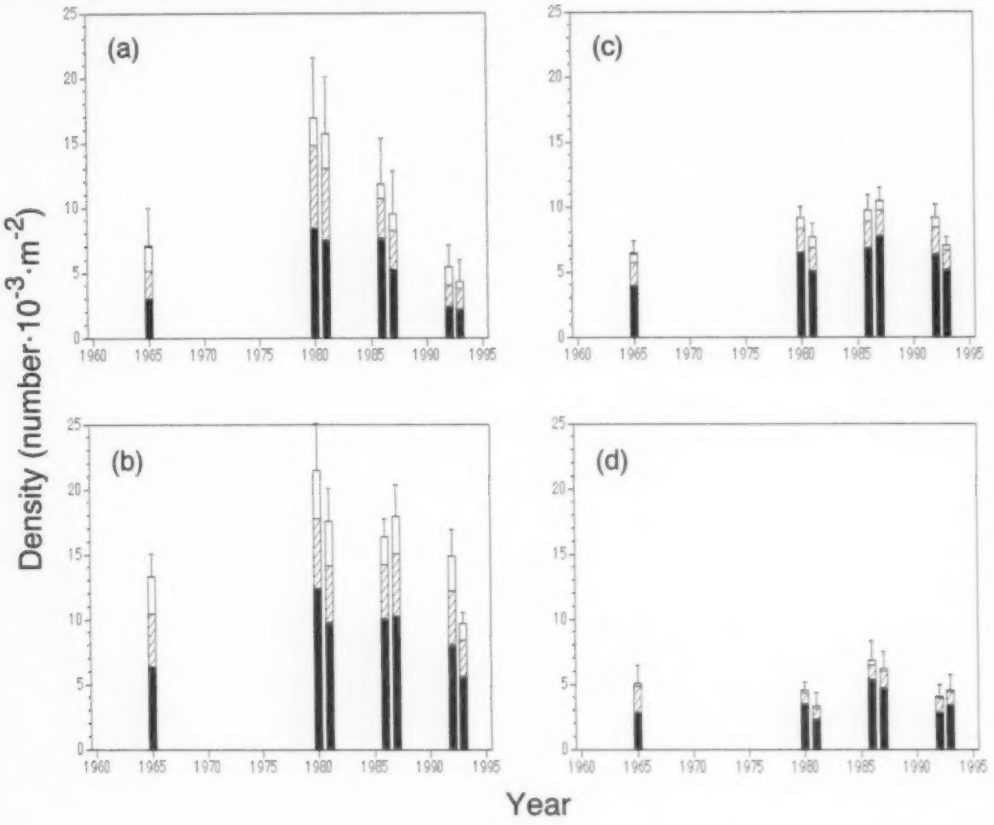

in Lake Michigan, and *Diporeia* exhibits a higher lipid content than other benthic macroinvertebrates (Gardner et al. 1985). If *Diporeia* were sufficiently reduced in abundance on a lake-wide basis, then fish heavily reliant on *Diporeia* as a food source would have to switch to other prey. Consequences of such diet switching on the growth and survival of these fishes remain unknown.

Although surveys by Nalepa (1987) and Nalepa et al. (1998) have documented changes in macroinvertebrate communities in areas deeper than 15 m, community changes have also occurred in shallower regions of Lake Michigan. The zebra mussel invasion has resulted in increased abundance of chironomids and the amphipod *Gammarus* in the shallow, rocky habitats of southern Lake Michigan (Kuhns and Berg 1999).

Dynamics of zooplankton

Long-term trends in zooplankton community structure and abundance have been documented for nearshore waters (≤50 m deep) of southeastern Lake Michigan in the vicinity of the Cook Power Plant between 1972 and 1984 by Evans and Jude (1986) and Evans (1992), and for a large portion of the offshore region (>50 m deep) during 1983–1992 by Makarewicz et al. (1995). In deeper (30- to 40-m) waters sampled by Evans and Jude (1986), summer daphnid assemblage shifted from a 1972–1976 community strongly dominated by the medium-bodied *Daphnia retrocurva* to a 1977–1981 community strongly dominated by the large-bodied *D. galeata mendotae*, to a 1982–1984 community dominated by the very large-bodied *D. pulicaria*. In contrast, *Daphnia retrocurva* dominated the daphnid community in shallower waters in the Cook Plant vicinity from 1972 to 1984. Additionally, abundance of daphnids in shallower waters was substantially higher during 1972–1980 than during 1981–1984. Evans and Jude (1986) attributed this decrease in daphnid abundance to increased predation pressure exerted by the yellow perch (*Perca flavescens*) population, which increased dramatically in size between 1980 and 1984. Evans and Jude (1986) concluded that the appearance of the very large-bodied *D. pulicaria* in the deeper waters during 1982–1984 was possibly related to a decline in alewife abundance during the 1970s and early 1980s. Wells (1970) contended that increased alewife abundance in offshore waters of Lake

© 2002 NRC Canada

Fig. 4. (*a*) Estimated lake-wide biomass of alewife (light shading), rainbow smelt (solid), deepwater sculpin (open), and bloater (dark shading) in Lake Michigan, 1973–1999. Estimates based on annual bottom trawl surveys performed by the USGS–GLSC. (*b*) Estimated lake-wide biomass of lake trout (light shading), brown trout (dark shading), rainbow trout (open), coho salmon (vertical bars), and chinook salmon (solid) in Lake Michigan, 1965–1998. Biomass was estimated using age-specific population models. See text for more details on modeling.

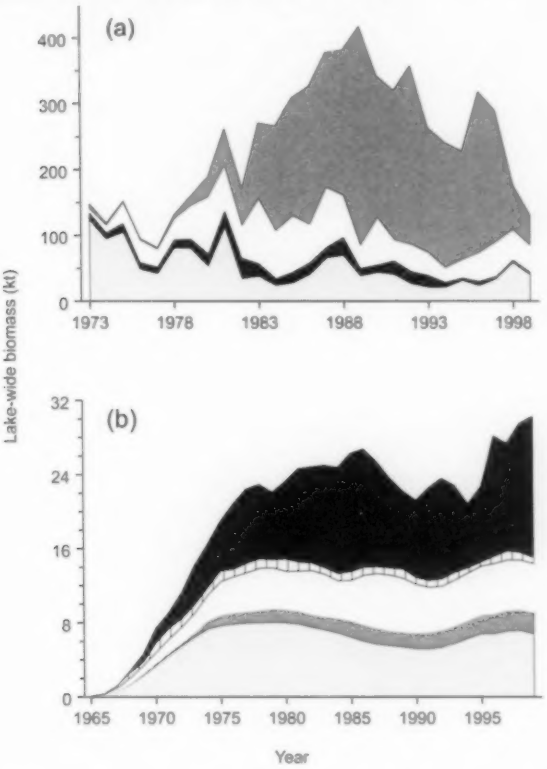

Michigan during the late 1950s and early 1960s led to a shift in the size structure of the summer zooplankton community from large-bodied to small-bodied copepods and cladocerans. Evidence to support the contention that high abundance of alewives in 1966 resulted in a zooplankton community dominated by small-bodied forms was compelling; however, relatively low alewife abundance did not necessarily imply that very large-bodied zooplankters would dominate the zooplankton community (Evans 1992).

Although species composition of the crustacean zooplankton community changed considerably during 1983–1992 in offshore waters of Lake Michigan, crustacean zooplankton biomass varied without trend during that time (Makarewicz et al. 1995). Furthermore, in comparing their data with observations by Scavia et al. (1986), Makarewicz et al. (1995) concluded that crustacean zooplankton biomass during the summer in offshore waters of Lake Michigan showed no trend between 1975 and 1992. *Daphnia pulicaria* was an important constituent of the daphnid community in 1983, but subsequently declined in abundance until nearly disappearing from the lake by 1987 (Makarewicz et al. 1995). Overall, *Diaptomus* dominated the zooplankton community during 1983–1992. Increases in rotifer biomass between 1983 and 1992 were correlated with increases in unicellular algae (Makarewicz et al. 1995). Based on correlation analysis, Makarewicz et al. (1995) suggested that alewives during 1983–1992 were probably not playing a dominant role in affecting zooplankton biomass and size structure except for the size structure of calanoid copepods. However, alewife abundance remained relatively low during this time period (Fig. 4). Preliminary examination of zooplankton samples during 1994–1999 suggested that no major changes in species composition or abundance had occurred since the Makarewicz et al. (1995) study (J. Cavaletto, NOAA Great Lakes Environmental Research Laboratory, Ann Arbor, MI 48105, U.S.A., personal communication).

Invasion of Lake Michigan by the predatory cladoceran *Bythotrephes cederstroemi* in 1986 appeared to have caused some changes in zooplankton community structure (Makarewicz et al. 1995). For example, the decrease in *Daphnia retrocurva* abundance after 1986 was most likely attributable to predation by *Bythotrephes* (Lehman and Cáceres 1993).

Other than the increase in rotifer biomass between 1983 and 1992, evidence for changes in zooplankton community structure and abundance originating from bottom-up effects was not strong (Makarewicz et al. 1995). Furthermore, the issue of whether changes in top-down control from alewives or from *Bythotrephes* led to changes in phytoplankton abundance or composition remains contentious (Evans 1992; Makarewicz et al. 1998).

Abundance of *Mysis relicta*, a common prey of alewife, bloater, rainbow smelt (*Osmerus mordax*), and lake whitefish (*Coregonus clupeaformis*), in southern Lake Michigan has remained relatively stable from the 1970s through 1998 (Pothoven et al. 2000). *Mysis* is an important predator of zooplankton in Lake Michigan. Whereas micrograzers (protozoans and ciliates) are an important component of the Lake Michigan food web (Fahnenstiel et al. 1998), insufficient data are available to characterize temporal trends in their abundance or their community structure.

Dynamics of the prey fish community

Alewife

The alewife invasion during the 1940s greatly altered the fish community of Lake Michigan. Declines in abundances of emerald shiner (*Notropis atherinoides*), deepwater sculpin (*Myoxocephalus thompsoni*), yellow perch, and bloater during the 1960s have been attributed to the alewife invasion (Wells and McLain 1973). Also, alewife predation on lake trout (*Salvelinus namaycush*) fry may represent a serious impediment to lake trout rehabilitation in the lower four Great Lakes (Krueger et al. 1995).

One of the reasons for launching a major stocking program for salmon and trout in Lake Michigan in 1965 was to reduce alewife abundance, which had reached nuisance levels during the 1960s (Hatch et al. 1981; Rutherford 1997). Alewives have dominated the diet of these stocked salmonines (Stewart and Ibarra 1991; Madenjian et al.

© 2002 NRC Canada

1998*a*), and to a lesser extent, have also been eaten by burbot (Fratt et al. 1997).

Stocking of salmonines appeared to be effective in controlling alewife abundance. Alewife abundance decreased during the 1970s and early 1980s, coincident with the buildup of salmonines (Fig. 4). Alewife abundance has neither trended upward nor downward since the early 1980s, concomitant with relatively high levels of salmonine biomass within the lake. Lake-wide alewife biomass in 1973, based on bottom trawl surveys conducted by the U.S. Geological Survey (USGS) Great Lakes Science Center (GLSC), was estimated at 125 kt, whereas lake-wide biomass estimates averaged only 37 kt between 1984 and 1999 (Fig. 4*a*). Furthermore, additional GLSC trawling data indicated that the alewife decline was well underway by 1970 (Krause 1999). Although the lake-wide surveys of prey fish populations did not begin until 1973, GLSC bottom trawling was conducted at selected ports along the eastern and southern portions of the lake since 1962 (Hatch et al. 1981). Krause (1999), accounting for the reduced set of sampling locations during 1962–1972 by using a mixed model approach, estimated that lake-wide abundance of alewives in Lake Michigan was about twice as high in 1969 than it was in 1973. Further, the 1966 abundance was estimated at more than five times higher than the 1969 abundance. However, the decrease between 1966 and 1969 was partially attributable to a die-off occurring in 1967 (Brown 1972). Finally, Madenjian et al. (1986), using trend analysis, demonstrated a significant decline in alewife abundance in southeastern waters of Lake Michigan between 1973 and 1982.

Eck and Brown (1985) proposed that cold temperatures regulated alewife abundance in Lake Michigan, because a portion of the decline in alewife abundance during the 1970s and early 1980s coincided with relatively cold weather. However, 1973–1999 data for alewife abundance and temperature do not support this contention. The alewife population did not rebound even though the cold years of 1977–1982 were followed by relatively warm years of 1983 and 1985–1992 (Fig. 4*a*; T. Karl, NOAA National Climatic Data Center, Asheville, NC 28801, U.S.A., unpublished data). Furthermore, annual alewife abundance during the 1973–1999 time period was poorly correlated ($r = -0.03$, $P = 0.8711$, $n = 27$) with heating degree days at Muskegon (Mich.), an indicator of winter severity (Eck and Brown 1985). In contrast, annual alewife abundance during the 1973–1998 time period showed a significant, negative relationship ($r = -0.54$, $P = 0.0058$, $n = 26$) with estimated annual lake-wide consumption of alewives by salmonines.

The length–frequency distribution of Lake Michigan alewives did not drastically change between 1973 and 1999. Alewife growth rate and condition did not exhibit a trend between 1984 and 1995; however, alewife condition declined by about 15% after 1995 (C. Madenjian, unpublished data). Nearly all of the diet of adult alewives in Lake Michigan from 1970 to 1995 has been composed of zooplankton (chiefly cladocerans and copepods), *Diporeia*, and *Mysis* (Davis et al. 1997). Lipid content in alewives neither increased nor decreased between 1969 and 1995 (Madenjian et al. 2000), and modal length of adult alewives in bottom trawls has shown no trend since 1973 (C. Madenjian, unpublished data). The recent decline in alewife condition may be linked to the recent decline in *Diporeia* abundance.

Fig. 5. Abundance of (*a*) adult (>120 mm total length) and (*b*) age-0 bloaters in Lake Michigan, 1973–1999, based on annual bottom trawl surveys performed by the USGS–GLSC. Catch per unit of effort (CPUE) expressed in number of fish caught per 10-min bottom trawl tow. Horizontal line represents mean catch rate for entire time period.

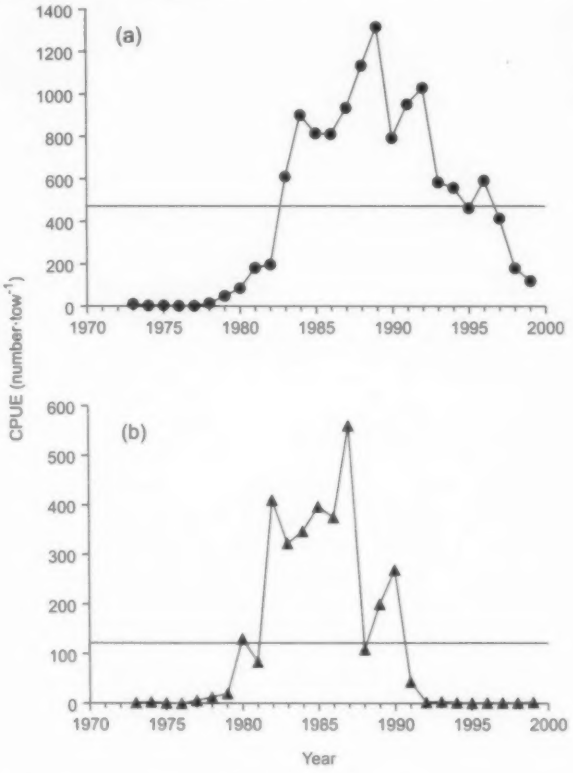

Bloater

Abundance of age-1 and older (hereafter referred to as adult) bloater in Lake Michigan has undergone dramatic changes in the last 30 years (Fig. 5*a*). Bloater recruitment started to increase in 1977, and relatively large year-classes were produced during 1980–1990 (Fig. 5*b*). Since 1992, however, year-class strength has been very weak. Temporal trends in abundance of adult bloater corresponded well with temporal trends in age-0 abundance. Adult abundance increased exponentially during 1977–1983 and then continued to increase, albeit at a slower rate, until 1989 (Fig. 5*a*). Since peaking in 1989, adult abundance has decreased. Examination of bottom trawl data for years 1962–1972, when spatial coverage of the lake during fall surveys was incomplete, suggested that adult bloater abundance had also peaked sometime during the late 1950s or early 1960s (G. Fleischer, unpublished data).

Reasons for rise and fall in bloater abundance between 1970 and 2000 were not clear. Decline in bloater abundance during the 1960s was attributed to alewives interfering with

© 2002 NRC Canada

bloater reproduction (Wells and McLain 1973). However, alewife abundance was relatively low during 1992–1999, when bloater year-class strength was very low. Jude and Tesar (1985) proposed that release from commercial exploitation, more than release from alewife interference, stimulated bloater recovery beginning in the late 1970s. However, exploitation rate on bloaters during the late 1980s and early 1990s was only about 1% per year, yet bloater abundance has been declining since 1989. We propose a new hypothesis to explain the pattern in bloater abundance in Lake Michigan for the past 40 years: bloater abundance in Lake Michigan follows a cycle with a period of about 30 years. Further, the cycle appears to be mainly independent of interactions with other fish populations or humans, and some type of density-dependent feedback may be involved in maintaining these cycles.

Growth and lipid content of bloaters in Lake Michigan have varied with population size, whereas diet composition has been consistent. As abundance increased during the 1980s, both growth rate and lipid content decreased (Madenjian et al. 2000; TeWinkel et al. 2002). *Diporeia* and *Mysis* have remained the mainstay of adult bloater diet in Lake Michigan (Davis et al. 1997). Sex ratio of the bloater population became skewed, with females predominating, during the late 1980s (TeWinkel et al. 2002).

Rainbow smelt

Rainbow smelt became established in Lake Michigan by 1936 (Wells and McLain 1972, 1973). This naturalized population of rainbow smelt continues to be exploited by commercial fisheries, albeit at lesser yields compared with bloater (S. Nelson, USGS Great Lakes Science Center COMCAT database, Ann Arbor, MI 48105, U.S.A.). Adult rainbow smelt have remained an important diet constituent for intermediate-sized (400- to 600-mm total length) lake trout in nearshore waters of Lake Michigan since the 1970s (Madenjian et al. 1998*a*). Also, rainbow smelt represented an important diet component for salmon during 1983–1987 (Stewart and Ibarra 1991).

While relatively low during 1973–1977, lake-wide biomass (as estimated via bottom trawling) of rainbow smelt increased during 1977–1982 (Fig. 4*a*). On average, lake-wide biomass of rainbow smelt was relatively high during 1982–1992, but then declined between 1992 and 1997. Reasons for the decline were not obvious. It seems unlikely that predation on rainbow smelt by salmonines has increased substantially since 1987 (see section on Dynamics of the salmonine community).

Mean total length of adult rainbow smelt in Lake Michigan decreased approximately 10% from 1973 to 1987, with no appreciable decrease since 1987 (G. Fleischer, unpublished data). The decrease in rainbow smelt size was most likely attributable to an increase in predation due to buildup of salmonine biomass. Lipid content of rainbow smelt did not exhibit any definitive trend from the early 1970s to 1995 (Madenjian et al. 2000). Diet of adult rainbow smelt in Lake Michigan has consisted primarily of *Mysis* and small fish, especially young-of-the-year (YOY) alewife, during both the 1970s and 1994–1995 (Davis et al. 1997).

Fig. 6. Abundance of slimy (●) and deepwater (▽) sculpins in Lake Michigan, 1973–1999, based on annual bottom trawl surveys performed by the USGS–GLSC. Catch per unit of effort (CPUE) expressed in (*a*) number and (*b*) kilograms of fish caught per 10-min bottom trawl tow.

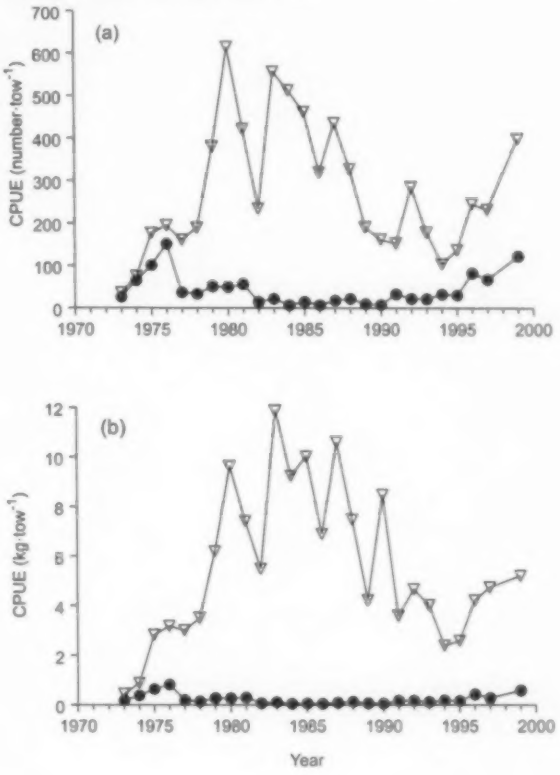

Deepwater sculpin

A substantial portion of the diet of burbot in Lake Michigan is composed of deepwater sculpins (Fratt et al. 1997). To a lesser degree, deepwater sculpins are also eaten by lake trout (Madenjian et al. 1998*a*). Abundance of deepwater sculpin in Lake Michigan increased rapidly between 1973 and 1983 (Fig. 6). After peaking in the early 1980s, deepwater sculpin lake-wide biomass declined until 1991, but showed no further decline after 1991 (Fig. 4*a*). Rapid increase in population size during 1973–1983 was most likely attributable to the decrease in alewife abundance during that time; Wells and McLain (1972, 1973) proposed that the decline in deepwater sculpin abundance during the 1960s was due to interference, by alewives, with deepwater sculpin recruitment. Alewives may consume the pelagic fry of deepwater sculpins. The decrease in deepwater sculpin abundance between the early 1980s and 1991 was probably due to increased predation by the recovering burbot population, which increased in size during the 1980s but appeared to level off in size during the 1990s (Fig. 7). *Diporeia* has dominated deepwater sculpin diet in Lake Michigan during 1970–1995 (Davis et al. 1997).

© 2002 NRC Canada

Fig. 7. Abundance of burbot in Lake Michigan, 1973–1999, based on annual bottom trawl surveys performed by the USGS–GLSC. Catch per unit of effort (CPUE) expressed in number of fish caught per 10-min bottom trawl tow.

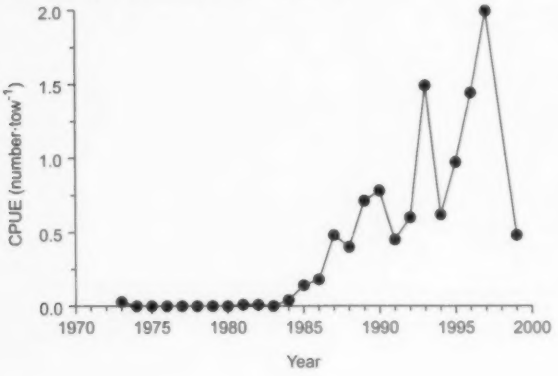

Slimy sculpin

Slimy sculpin (*Cottus cognatus*) has typically been preyed upon by juvenile lake trout in Lake Michigan, at least since the 1970s (Madenjian et al. 1998*a*). To a lesser degree, slimy sculpins are also eaten by burbot (Fratt et al. 1997). Long-term trends in slimy sculpin abundance, as determined by bottom trawl surveys, appeared to be related to changes in the spatial distribution of newly stocked lake trout. Slimy sculpin abundance decreased during the 1970s and early 1980s, remained relatively low during most of the 1980s, and then increased during the 1990s (Fig. 6). Prior to 1986, most of the lake trout stocking in Lake Michigan occurred relatively close to shore, but stocking emphasis was placed on offshore refuge areas beginning in 1986 (Holey et al. 1995). An increase in predation on slimy sculpins with increased lake trout population size during the 1970s probably caused the decrease in slimy sculpin abundance during the 1970s (Eck and Wells 1987). With the shift to predominantly offshore stocking in 1986, predation on slimy sculpins in areas of the lake trawled by USGS–GLSC likely declined, and this decline in predation allowed the increase in slimy sculpin abundance observed during the 1990s. Slimy sculpins in Lake Michigan have fed predominantly on *Diporeia* since the 1960s (Davis et al. 1997).

Dynamics of the salmonine community

Background

Stocking of salmonine fishes into Lake Michigan has had a profound effect on the lake's food web. Large-scale stocking of salmonines began in 1965, and has continued to the present. The rationale for stocking salmonines was (*i*) to control abundance of alewives, which had become a nuisance, (*ii*) to initiate a valuable sport fishery, (*iii*) to possibly initiate naturalized populations of introduced salmonines, and (*iv*) to rehabilitate the lake trout population (Holey et al. 1995; Rutherford 1997). The five species of salmonines currently stocked in Lake Michigan are lake trout, chinook salmon (*Oncorhynchus tshawytscha*), coho salmon (*Oncorhynchus kisutch*), rainbow trout (*Oncorhynchus mykiss*), and brown trout (*Salmo trutta*).

Long-term trends in biomass, production, and consumption

Lake-wide biomass and production of the five salmonine species was estimated using age-specific population models to track abundance at age over time. For all species except chinook salmon, our modeling approach was similar to the one used by Jones et al. (1993) for Lake Ontario salmonines. Using estimates of gross conversion efficiency (GCE) from bioenergetics modeling (Stewart and Ibarra 1991), lake-wide consumption of prey by salmonine populations was calculated using the production–conversion efficiency method of Ney (1990) where gross production is divided by GCE to estimate consumption. For chinook salmon, population modeling techniques outlined in Benjamin and Bence (2002) were used to estimate biomass, production, and consumption. Recruitment was quantified as the number of individuals entering the lake population, and equaled the sum of hatchery and naturally reproduced production. Salmonine stocking records have been summarized by the U.S. Fish and Wildlife Service (C. Bronte, Green Bay Fishery Resources Office, Green Bay, WI 54311, U.S.A., salmonine stocking database) and Benjamin (1998). Natural reproduction by chinook and coho salmon, as well as rainbow trout, was quantified using previously developed methods (Rutherford 1997). We assumed that natural recruitment to lake trout and brown trout populations has been negligible since 1965 (Holey et al. 1995; Rutherford 1997).

Salmonine biomass in Lake Michigan increased from 0.039 kt in 1965 to nearly 27 kt in 1986, then declined during the late 1980s, driven by a decline in abundance of chinook salmon, which has accounted for over 40% of the total salmonine biomass since 1980 (Fig. 4*b*). This decrease in chinook salmon biomass has been attributed to an outbreak of bacterial kidney disease (BKD) within the chinook salmon population (Kabre 1993). Presumably due to a decrease in BKD-induced mortality, chinook salmon biomass increased during 1994–1998, and salmonine biomass was estimated at nearly 30 kt in 1998 (Fig. 4*b*). For the most part, temporal trends in gross production mimicked trends in salmonine biomass. Annual gross production of salmonine biomass increased from 0.235 kt in 1965 to nearly 23 kt in 1998. Ratio of annual gross production to biomass (P/B) generally varied from 0.8 to 1.0.

Consumption of prey by Lake Michigan salmonines increased from only 1 kt in 1965 to 130.5 kt in 1998 (Fig. 8). Since 1977, the chinook salmon population has been responsible for approximately 50% of the consumption by salmonines (Fig. 8*a*). Most predation by salmonines in Lake Michigan has been directed at alewives (Fig. 8*b*). Alewives (both small and large sizes combined) represented, on average, 69.2% of total annual consumption from 1985 to 1998, with a maximum of 79.7% in 1998. Annual consumption of alewives by salmonines exceeded 90 kt in 1996 and 1998. Chinook salmon have been responsible for 62% of the predation on alewives by salmonines since 1980.

An important factor driving salmonine biomass and production, as well as consumption of prey by salmonines, was trends in the recruitment of young fish to the salmonine

© 2002 NRC Canada

Fig. 8. (*a*) Estimated consumption of prey by lake trout (light shading), brown trout (dark shading), rainbow trout (open), coho salmon (vertical bars), and chinook salmon (solid) in Lake Michigan, 1965–1998. (*b*) Estimated consumption of large alewives (solid), small alewives (open), and other fish (shading) by salmonines in Lake Michigan, 1965–1998. Consumption was estimated using age-specific population models coupled with bioenergetics models. See text for more details on modeling.

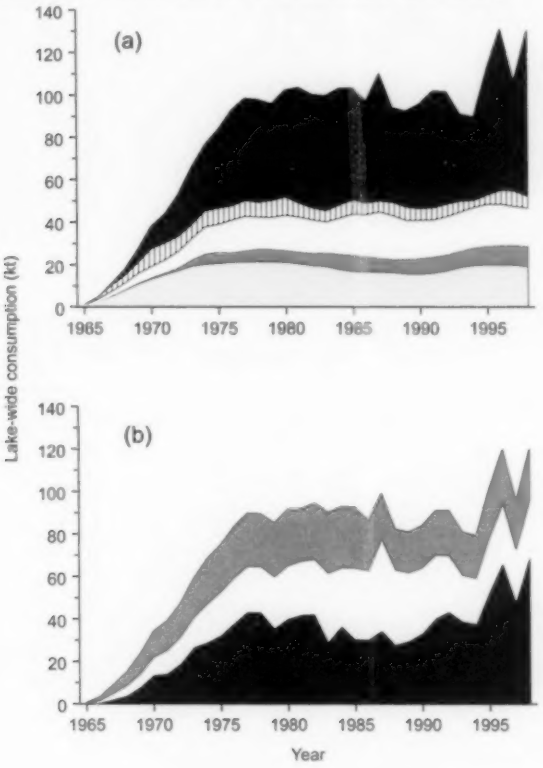

stocks. Natural recruitment of chinook salmon has increased from 1970 to the present. We estimated that annual natural recruitment of chinook salmon approached 2 million smolts during the 1990s. In some years, natural recruitment represented nearly 40% of the total annual recruitment of chinook salmon (Rutherford 1997).

Long-term trends in diet and growth

Growth rate of chinook salmon in Lake Michigan declined during the early 1980s (Stewart and Ibarra 1991), but then increased during the late 1980s and early 1990s (Wesley 1996). The increase could have been a compensatory response to the decline in chinook salmon abundance following the BKD outbreak (Wesley 1996). Growth rate again declined during the late 1990s. Alewife has always been the most prominent component of chinook salmon diet. However, alewife was of greater importance in chinook salmon diet during the 1970s than during 1983–1987, when rainbow smelt was an important diet constituent and when alewives in the diet tended to be smaller than in the 1970s or 1994–1995 (Stewart and Ibarra 1991; R. Elliott, U.S. Fish and Wildlife Service, Green Bay, WI 54311, U.S.A., personal communication).

Growth rate of lake trout remained relatively constant between the 1970s and 2000 (Madenjian et al. 1998*a*; J. Jonas, Michigan Department of Natural Resources, Charlevoix, MI 49720, U.S.A., unpublished data). Overall, alewife has remained the most important component in adult lake trout diet. Nevertheless, bloater was a noteworthy constituent, contributing up to 35% of the diet of adult lake trout in nearshore waters of southeastern Lake Michigan between 1985 and 1995. In contrast, adult lake trout diet in nearshore Wisconsin waters did not appear to change appreciably since the 1970s (Madenjian et al. 1998*a*). Lipid content of lake trout in Lake Michigan did not substantially change between 1970 and 1995 (Madenjian et al. 2000).

Changing fisheries

Sport fisheries for Lake Michigan salmonines greatly expanded from the mid-1960s to 1985, in response to increased salmonine abundance (Bence and Smith 1999). With decline of chinook salmon abundance in the late 1980s, angling effort declined. Harvest of rainbow trout increased during the late 1980s and has remained relatively high during the 1990s (Bence and Smith 1999). Chinook salmon harvest nearly doubled between 1994 and 1998, but the 1998 harvest was still less than 30% of the 1986 harvest. Lake trout have been harvested continually both recreationally and commercially since 1970 (Bence and Smith 1999).

Lake trout rehabilitation

Lake trout were extirpated from Lake Michigan during the 1950s, presumably because of overfishing and sea lamprey predation (Wells and McLain 1973). Since 1965, an average of about 2.4 million lake trout yearlings have been stocked into Lake Michigan each year. As part of the lake trout rehabilitation effort, two offshore refuges were established during 1984–1985 (Holey et al. 1995). The Northern Refuge encompassed a complex of shallow-water (0- to 20-m) spawning reefs, whereas the Southern or Midlake Refuge included four large deep-water (45- to 80-m) spawning reefs. Fishing for lake trout continues to be prohibited in both refuges. Emphasis on stocking the two refuges began in 1986, when stocking rates in nearshore zones sharply declined.

Although the stocking program has yielded a substantial number of spawners, documentation of natural reproduction by lake trout in Lake Michigan since 1965 has been extremely sparse (Holey et al. 1995). This negligible amount of successful natural reproduction appeared to be due to several factors. Contaminants, once thought to strongly interfere with lake trout reproduction in Lake Michigan, have recently been shown not to be a significant hindrance, while thiamine deficiency is now seen as a likely factor (Fitzsimons et al. 1999). By previously established criteria, density of spawning lake trout in the Northern Refuge was sufficiently high to allow for successful natural reproduction (Madenjian and DeSorcie 1999). Perhaps hatchery reared lake trout are so inefficient at reproducing that considerably higher densities of spawners or a higher density of older (age >10 years) spawners are required for successful natural reproduction. Density of lake trout spawners on Sheboygan Reef in the Midlake Refuge exceeded the relatively high density of 175

© 2002 NRC Canada

Fig. 9. Annual commercial harvest of lake whitefish from Lake Michigan, 1970–1998.

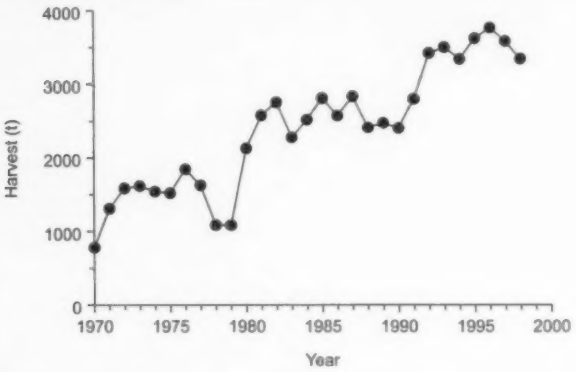

Fig. 10. Mean condition factor, K, for age-4 (●), age-5 (▲), and age-6 (■) lake whitefish in northern Lake Michigan, 1985–1998. $K = 10^5 \cdot W \cdot L^{-3}$, where W is weight (g) and L is total length (mm).

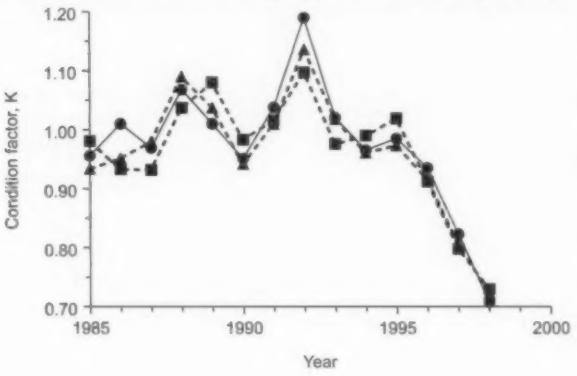

fish per 305 m of gill net during the late 1990s and a substantial proportion of these spawners was composed of fish >10 years old, yet no signs of natural recruitment have been observed (M. Toneys and P. McKee, Wisconsin Department of Natural Resources, Sturgeon Bay, WI 54235, U.S.A., unpublished data). Perhaps alewife predation on lake trout fry has also been playing an important role in suppressing natural reproduction by lake trout (Krueger et al. 1995).

Dynamics of other fish populations

Sea lamprey

Treatment of Lake Michigan tributaries, beginning in the late 1950s, with the lampricide 3-trifluoromethyl-4-nitrophenol (TFM) led to an estimated 80–90% decline in the abundance of adult sea lamprey in Lake Michigan by 1966 (Lavis et al. 2002). Lampricide treatment in streams continues to be the primary strategy for controlling the sea lamprey population in Lake Michigan.

Population sizes of spawning-phase sea lamprey in all Lake Michigan tributaries each year since 1977 have been estimated using a regression model, which incorporated relative abundance data from assessment traps in tributaries and estimates of stream discharge rates (Lavis et al. 2002). This long-term series indicates that numbers of spawning sea lampreys in Lake Michigan tributaries increased during 1977–1984, showed no trend between 1984 and 1995, and then increased again during 1995–1999. The two increases occurred primarily in northern tributaries to the lake. The first increase was attributed to an immigration of adult sea lampreys from northern Lake Huron, whereas the second increase was probably due to a decrease in sea lamprey control measures for Lake Michigan (G. Christie, Great Lakes Fishery Commission, Ann Arbor, MI 48105, U.S.A., personal communication). Lake-wide estimates of spawning sea lamprey population size ranged between 32 000 and 117 000 sea lampreys (Lavis et al. 2002).

Long-term trends for incidence of fresh sea lamprey wounds on lake trout in Lake Michigan mimicked long-term trends for sea lamprey abundance. Wounding rates in southern waters of the lake have remained nearly unchanged for the last 25 years, whereas an increase in wounding rates has been observed in northeastern waters since 1978 (Lavis et al. 2002). Overall, lamprey-induced annual mortality, estimated from wounding rate, for Lake Michigan lake trout was relatively low, averaging less than 7% for most years during 1984–1998.

Lake whitefish

Lake whitefish is the most important commercial fish in Lake Michigan. Tribal and state-licensed commercial fishers from Michigan and Wisconsin continue to exploit lake whitefish. Lake whitefish are taken in trap nets, gill nets, trawls, and pound nets.

Since 1970, annual commercial harvest of lake whitefish has more than tripled (Fig. 9), reflecting a lake-wide increase in abundance. A dramatic decline in lake whitefish abundance during the late 1950s was linked primarily with sea lamprey predation (Wells and McLain 1972). Thus, there can be little doubt that the impressive recovery of the lake whitefish population in Lake Michigan since 1970 was partially driven by sea lamprey control (Eck and Wells 1987). Stocking of lake trout also afforded extra protection from sea lamprey predation because lake trout are favored prey for sea lampreys (Wells and McLain 1972). The decrease in mean size of adult rainbow smelt during the 1970s and 1980s and decreased rainbow smelt abundance during the 1990s may have also contributed to the lake whitefish recovery because large rainbow smelt may prey upon lake whitefish fry (Wells and McLain 1973). During the last 30 years, exploitation has not impaired the ability of the adult lake whitefish population to produce large year-classes. This is true even though contemporary stocks of lake whitefish have been subjected to high exploitation rates, leading to total annual mortality that sometimes exceeded 80% (M. Ebener and J. Bence, unpublished data).

Lake whitefish size-at-age declined in Lake Michigan during the 1990s. Moreover, condition factor dropped rapidly between 1995 and 1998 (Fig. 10). Reduced growth rate during the 1990s may have resulted from density-dependent factors, as sustained high levels of lake whitefish abundance resulted in increased intraspecific competition for food resources. Other factors may also have been involved. For example, zebra mussel density increased substantially in northern Lake Michigan during the same time that lake whitefish condition declined precipitously (T. Nalepa, un-

© 2002 NRC Canada

published data). Hoyle et al. (1999) linked poor body condition of lake whitefish in Lake Ontario with zebra mussel invasion of the lake; perhaps expansion of the zebra mussel population also had a negative effect on lake whitefish condition in Lake Michigan.

Burbot

Diet of adult burbot (*Lota lota*) in Lake Michigan has been diverse and has included both fish and benthic invertebrates, especially crayfish (Fratt et al. 1997; S. Hart and J. Jonas, Michigan Department of Natural Resources, Charlevoix, MI 49720, U.S.A., unpublished data). In deeper waters (>39 m), deepwater sculpin has been an important component of burbot diet since the 1930s.

The burbot population in Lake Michigan was greatly reduced in size because of sea lamprey predation during the 1950s (Wells and McLain 1973). Recovery of the population began, albeit very slowly, during the late 1960s and 1970s (Eck and Wells 1987). However, rapid increase in abundance occurred in the 1980s (Fig. 7). Thus, burbot recovery was delayed for more than 10 years compared with lake whitefish recovery, even though both recoveries are attributed to sea lamprey control. Eshenroder and Burnham-Curtis (1999) contended that this delay was due to alewife interference with burbot reproduction. Burbot larvae are pelagic; therefore, they are susceptible to predation by alewives. Alewife density may have decreased sufficiently during the 1970s to allow for a strong recovery by the burbot population during the 1980s. According to bottom trawl surveys conducted by the USGS–GLSC, lake-wide abundance of burbot increased exponentially during the 1980s and then leveled off during the 1990s (Fig. 7). As mentioned above, patterns in the long-term series for abundances, coupled with diet data for burbot, suggested that predation by burbot has maintained the deepwater sculpin population at a level lower than that observed during the early 1980s (Figs. 6 and 7). Based on GLSC bottom trawl surveys, lake-wide biomass of burbot in Lake Michigan proper averaged about 9.7 kt during 1990–1999.

Yellow perch

The yellow perch population in Lake Michigan has yielded valuable sport and commercial fisheries (Wells and McLain 1973). During the 1980s and 1990s, yellow perch was the most popular sport-caught fish (Bence and Smith 1999).

Decline in yellow perch abundance in Lake Michigan during the 1960s has been attributed to the alewife invasion (Wells 1977), indicating that the levels of alewives characteristic of the 1960s and early 1970s were sufficiently high to interfere with yellow perch reproduction.

With strong year-classes produced in 1980 and 1983–1988, yellow perch abundance in Lake Michigan increased during the 1980s (Jude and Tesar 1985; Eck and Wells 1987; Makauskas and Clapp 2000). This recovery in the yellow perch population has been attributed to the decline in alewife abundance during the 1970s (Jude and Tesar 1985; Eck and Wells 1987). Lake-wide abundance of yellow perch remained relatively high during 1985–1990, but then decreased during 1990–1995 because year-class strength was weak during 1989–1993 (Makauskas and Clapp 2000). Year-class strength remained weak during 1995–1997 and in 1999, but was moderate in 1998. No single factor could explain poor recruitment of yellow perch in Lake Michigan proper between 1989 and 1997. Lake-wide abundance of alewife was as low during 1989–1997 as it was during 1983–1988 (Fig. 4), and therefore it seems unlikely that interference by alewives was primarily responsible for poor recruitment during 1989–1997 throughout the lake. Nonetheless, Shroyer and McComish (2000) reported a negative relationship between yellow perch year-class strength and alewife abundance in Indiana waters of Lake Michigan during 1984–1996. Skewing of the sex ratio (more males than females) during 1992–1996 may have partially contributed to poor recruitment (Makauskas and Clapp 2000). Skewed sex ratio in the yellow perch population may have been due to commercial harvest operations, because females grow faster than males and the commercial fishery targets larger individuals. Perhaps the number of female spawners was so diminished that the probability of producing a moderate or large size year-class was low. During some years, slow rate of warming of nearshore waters in the spring may have partially contributed to production of weak year-classes (Makauskas and Clapp 2000). Finally, data from Illinois waters suggested that bottom-up effects, namely low zooplankton abundance during June and July, may also have been partly responsible for poor recruitment, presumably because survival of yellow perch fry was reduced due to low food availability (Makauskas and Clapp 2000).

Walleye

Walleye (*Stizostedion vitreum*) has been one of the most ecologically and economically important fishes in Michigan waters of Green Bay (Schneeberger 2000). Other centers of relatively high walleye density in Lake Michigan included southern Green Bay and the Muskegon vicinity of eastern Lake Michigan. Walleye abundance in Lake Michigan fluctuated greatly during the 1900s and these fluctuations have been attributed to overexploitation, deterioration of water quality (in southern Green Bay), loss of habitat (in southern Green Bay), and interference by alewives with walleye reproduction.

Walleye abundance in Green Bay declined precipitously during the 1960s, but rebounded during the 1970s because of management actions that included stocking and imposition of restrictions on commercial and recreational fishing (Schneeberger 2000). Today, the walleye population in Little Bay de Noc (northern Green Bay) supports a world-class recreational fishery, and reduction in stocking rates is now being considered by managers because the fishery is nearly self-sustaining. Walleye diet in northern Green Bay has remained consistent between the 1960s and 1990s, with rainbow smelt and alewives representing the bulk of the diet (Schneeberger 2000).

Lake sturgeon

Population size of lake sturgeon (*Acipenser fulvescens*) (for individuals ≥22.7 kg in weight) in Lake Michigan during 1825–1890 has been estimated to have been between 145 000 and 2 406 000 individuals (Hay-Chmielewski and Whelan 1997). The lake sturgeon population in Lake Michigan collapsed during the early 1900s owing to over-

© 2002 NRC Canada

exploitation and habitat degradation (Wells and McLain 1973). During the 1990s, small populations of lake sturgeon have been associated with at least 13 tributaries (Hay-Chmielewski and Whelan 1997). With continued removal of dams on tributaries anticipated in the near future, the size of lake sturgeon population in Lake Michigan should increase as more suitable spawning habitat becomes available.

Emerald shiner

The emerald shiner (*Notropis atherinoides*) population in Lake Michigan crashed during the early 1960s, coincident with buildup of the alewife population (Wells and McLain 1973). Apparently, alewives fed on the pelagic eggs and larvae of the emerald shiner. Emerald shiner abundance has remained at very low levels during 1970–2000 (D. Jude, unpublished data; J. Dettmers, Illinois Natural History Survey, Zion, IL 60099, U.S.A., unpublished data; R. Rost, Wisconsin Department of Natural Resources, Peshtigo, WI 54157, U.S.A., unpublished data), suggesting that the relatively low alewife abundance during 1984–2000 was still sufficiently high to interfere with emerald shiner reproduction.

Round goby

The round goby, an invader from the Ponto-Caspian region, established populations in Calumet Harbor (southern Lake Michigan) and in several harbors on both the east and west sides of Lake Michigan including Milwaukee, Sturgeon Bay, Escanaba, Grand Haven, Muskegon, and Charlevoix during the 1990s (Clapp et al. 2001). Zebra mussels form a substantial portion of the diet of round gobies in the Great Lakes (C. Knight, Ohio Department of Natural Resources, Fairport, OH 44077, U.S.A., personal communication; M. Thomas, Michigan Department of Natural Resources, Mt. Clemens, MI 48045, U.S.A., personal communication). In turn, round gobies are preyed upon by several species of fish. The precipitous decline of mottled sculpin (*Cottus bairdi*) abundance in Calumet Harbor, as well as decreases in abundances of johnny darter (*Etheostoma nigrum*) and logperch (*Percina caprodes*) in Lake St. Clair, has been linked to the round goby invasion (Janssen and Jude 2001; M. Thomas, Michigan Department of Natural Resources, Mt. Clemens, MI 48045, U.S.A., personal communication). It remains to be seen whether these seemingly negative effects of round gobies on sculpins and darters will be confined to shallow and protected waters of Lake Michigan.

Lake herring

Lake herring (*Coregonus artedi*) was once a prominent member of the fish community in Lake Michigan, and the lake herring population once supported a valuable commercial fishery (Wells and McLain 1973). The crash in the lake herring population during the 1950s has been attributed to overexploitation and interference by rainbow smelt with lake herring reproduction (Wells and McLain 1973). Although there have been no signs of a lake-wide recovery, a recent increase in lake herring abundance in Grand Traverse Bay of northern Lake Michigan has been observed. Sport harvest of lake herring in Grand Traverse Bay indicated the presence of lake herring at very low levels in 1985 and 1993, but sport harvest increased three- to seven-fold during 1995–1998 compared with the 1993 harvest (G. Rakoczy, Michigan Department of Natural Resources, Charlevoix, MI 49720, U.S.A., personal communication).

Contaminants and global climate change stressors

Contaminants

The issue of contaminants acting as stressors to Great Lakes biota emerged in the 1970s (Evans 1988). Consequently, the governments of the United States and Canada negotiated the Great Lakes Water Quality Agreement in 1972, and revised this agreement in 1978. This agreement led to many remedial actions to improve the quality of Great Lakes waters. Additionally, production of polychlorinated biphenyls (PCBs) was banned, use of the pesticide DDT (1,1,1-trichloro-2,2-bis[*p*-chlorophenyl]ethane) was discontinued, and uses of the organochlorine pesticides chlordane and dieldrin were restricted in both the United States and Canada during the 1970s.

As a consequence of the abovementioned measures, concentrations of most contaminants in Lake Michigan biota decreased substantially between 1970 and 2000. For example, total PCB concentration in Lake Michigan zooplankton decreased between 1982 and 1995 (A. Trowbridge and D. Swackhamer, University of Minnesota, Minneapolis, MN 55455, U.S.A., personal communication). Total PCB concentration in *Mysis*, *Diporeia*, prey fishes, and salmonines of Lake Michigan decreased by roughly an order of magnitude between 1975 and 1995 (DeVault et al. 1996; Madenjian et al. 1998*b*, 1998*c*). During the 1970s and early 1980s, decreases were observed in total DDT, dieldrin, and oxychlordane concentrations in lake trout (DeVault et al. 1996), and in PCB, oxychlordane, DDT, and dieldrin concentrations in herring gull (*Larus argentatus*) eggs (Pekarik and Weseloh 1998). In contrast, toxaphene concentrations in lake trout did not decrease between 1986 and 1992 (DeVault et al. 1996).

Very few lake-wide temporal changes in Lake Michigan biota between 1970 and 2000 have been shown to be directly linked to stressor effects exerted by contaminants. The dramatic increase in double-crested cormorant (*Phalacrocorax auritus*) population size during the late 1980s and 1990s was due, at least in part, to the substantial reduction of contaminant levels within the lake ecosystem during the 1970s (Weseloh et al. 1995). Number of double-crested cormorant nests on islands within Lake Michigan (including Green Bay) increased exponentially from 75 nests in 1977 to 4743 nests during 1989–1990, and then to 28 158 nests in 1997 (F.J. Cuthbert, University of Minnesota, St. Paul, MN 55108, U.S.A., personal communication). Weseloh et al. (1983) documented shell thinning with high egg breakage and high egg loss (95%) with concomitant reproductive failure in Great Lakes cormorants during the early 1970s, and also reported high DDE (a metabolite of DDT) concentrations in cormorant eggs. Apparently, high concentration of DDE in the cormorants was causing eggshell thinning and reproductive failure. Increased predation by the exploding population of double-crested cormorants in Lake Michigan may have caused a reduction in abundance of smallmouth bass (*Micropterus dolomieui*) in the vicinity of Beaver Island in northern Lake Michigan; however, research results to date

© 2002 NRC Canada

are not conclusive (D. Peterson, Central Michigan University, Mt. Pleasant, MI 48859, U.S.A., personal communication). To the best of our knowledge, no lake-wide temporal changes in phytoplankton communities, benthic invertebrate communities, zooplankton communities, or fish communities in Lake Michigan have been shown to be directly attributable to contaminant effects (Evans 1988). Nevertheless, contaminants may have influenced health of brown bullhead (*Ameiurus nebulosus*) populations in certain tributaries (Baumann et al. 1996).

Global climate change

An increase in atmospheric carbon dioxide enhances heat retention (Regier et al. 1990). Burning fossil fuels and changes in land use are correlated with an increase in carbon dioxide concentration in the earth's atmosphere, and therefore global climate change likely represents an anthropogenic stressor to the global environment. Although not all climatologists agree as to the nature, extent, intensity, and timing of the effects of increased carbon dioxide content in the earth's atmosphere, there is general consensus that climate warming will occur (Regier et al. 1990; Doak and Morris 1999).

Magnuson et al. (1997) predicted the effects of changes in thermal regimes associated with global climate change on primary production, zooplankton biomass, maximum sustainable fishery yield, growth and consumption by fish, fish reproduction and overwinter survival, success of invasions by exotic fish species, and dissolved oxygen concentration in the Great Lakes. For Lake Michigan, McCormick (1990) used computer simulation modeling to explore potential changes in thermal structure and cycle of Lake Michigan under three different scenarios for global climate change. Using predictions from McCormick (1990), Magnuson et al. (1990) forecasted that thermal habitat within Lake Michigan will increase under global warming scenarios for fish species from all thermal guilds. Additionally, Magnuson et al. (1997) reported that global warming has been predicted to eventually cause a 0.99- to 2.48-m decrease in Lake Michigan's water level; however, these researchers did not specifically address effects of this lowering of lake level on Lake Michigan biota.

Based on available data, we are unable to ascribe any of the lake-wide changes in the Lake Michigan food web during 1970–2000 to global climate change, mainly because insufficient data are available to establish long-term, lake-wide trends in water temperature characteristics in Lake Michigan or to clearly show that a long-term trend in water temperature characteristics is linked to global climate change. Long-term trends in water temperatures were not consistent between two sites in Lake Michigan, including one site at St. Joseph, along the southeastern shore of Lake Michigan, and another at the southern end of Green Bay (McCormick and Fahnenstiel 1999). Moreover, even though the duration of summer thermal stratification increased significantly at St. Joseph during 1960–1992, McCormick and Fahnenstiel (1999) cautioned that the series did not extend far enough back in time to resolve whether the trend was part of a natural cycle or was caused by anthropogenic activity. Finally, recent low water levels in Lake Michigan can be explained by quasi-periodicity in water level fluctuations (periods of roughly 30 and 150 years) and by unusually low rainfall during 1998 and 1999, without evoking a global climate change effect (T. Thompson, Indiana Geological Survey, Bloomington, IN 47405, U.S.A., personal communication).

Discussion

Sea lamprey control and top-down effects

Whereas Wells and McLain (1973) concluded that sea lamprey and alewife invasions had a greater effect on the Lake Michigan fish community than any of the other anthropogenic stressors during 1940–1970, control of sea lamprey and alewife populations was paramount in effecting changes within the Lake Michigan ecosystem during 1970–2000. Spectacular recovery of the lake whitefish population in Lake Michigan between 1965 and 2000 was partially attributable to sea lamprey control. Further, control of sea lamprey, beginning in the 1950s, enabled the successful stocking effort launched during the 1960s to increase salmonine biomass. In turn, salmonine populations, especially the chinook salmon population, were primarily responsible for the decline in alewife abundance during the 1970s and early 1980s. Strong recovery of burbot during the 1980s was probably fueled by control of both sea lamprey and alewife. Moreover, recovery of deepwater sculpin during the 1970s was most likely facilitated by reduction in alewife density. Also, relaxation of the interference effect by alewives on yellow perch reproduction is the most plausible explanation for the rapid increase in yellow perch abundance during the 1980s. Finally, the sudden increase in abundance of the very large-bodied cladoceran *D. pulicaria* during the 1980s was probably also due to reduction in alewife abundance.

Evidence that predation by salmonines drove the reduction in alewife abundance is strong. Decline in alewife abundance during the 1970s and early 1980s was well synchronized with buildup of salmonine populations. Moreover, the period of relatively low alewife abundance between 1984 and 2000 coincided with high predation by salmonines on alewives, as estimated by our modeling. Alewives have dominated salmonine diets in Lake Michigan from the 1960s through the 1990s. Additionally, annual alewife abundance since the early 1970s was much better correlated with estimates of annual consumption of alewives by salmonines than with cold temperatures. Based on our estimates of alewife consumption by salmonines, the commercial fishery for alewives was a relatively minor contributor to the observed decrease in alewife abundance. Annual commercial harvest of alewives from Lake Michigan averaged about 15 kt during 1973–1984 (S. Nelson, USGS–GLSC COMCAT database, Ann Arbor, MI 48105, U.S.A.), whereas annual consumption of alewives by salmonines averaged about 60 kt over the same time period. The Lake Michigan commercial fishery for alewives was closed in 1991 and has not been reopened.

Intensive stocking of salmon and trout into Lake Michigan can be viewed as a manipulation of the ecosystem. Lake-wide monitoring of prey fish populations has provided considerable insight into predator–prey dynamics within the Lake Michigan ecosystem. Predator–prey interaction between chinook salmon and alewife has been one of the strongest trophic links within the ecosystem since the 1970s.

© 2002 NRC Canada

Continued monitoring of prey fish populations, as well as surveillance of other components of the ecosystem, should provide further understanding of the Lake Michigan food web. Such long-term studies are especially appropriate for ecosystem manipulations (Pace and Cole 1989).

Bottom-up effects

Several changes within the Lake Michigan ecosystem during 1970–2000 may be attributable to bottom-up effects. Decline in abundance of all three dominant benthic macroinvertebrate groups, including *Diporeia*, oligochaetes, and sphaeriids, between 1980 and 1993 in nearshore (≤50 m deep) waters of Lake Michigan was believed to be chiefly due to a decrease in primary production in nearshore waters. Although long-term data for spring total phosphorus, an indicator of primary production, in nearshore waters of Lake Michigan were not available, comparison of measurements during 1998–2000 with measurements from the early 1970s suggested a decrease in primary production over this time period. In contrast, long-term data were readily available for offshore waters, and these data showed no long-term trend in primary production during 1973–1998. Similarly, abundances of the three major groups of benthic macroinvertebrates in offshore waters did not trend upward or downward during this time period. The apparent decline in primary production in nearshore waters of Lake Michigan between the 1970s and 1998–2000 was likely due to the decrease in phosphorus loadings between 1980 and 1987. The continued decrease in *Diporeia* abundance during the 1990s in nearshore waters of southern and southeastern Lake Michigan coincided with the zebra mussel invasion, although a specific mechanism whereby zebra mussels may have reduced *Diporeia* abundance remains unidentified.

Have bottom-up effects, including the apparent reduction in nearshore primary production and the continued decline of *Diporeia*, already precipitated a decrease in abundances of important fish populations in Lake Michigan? No clear effects are evident yet. The decrease in bloater abundance during the 1990s was attributed to an extended period of very low recruitment, which may be related to intraspecific mechanisms rather than bottom-up effects. Lake-wide abundances of alewife, salmonines, burbot, lake whitefish, and sculpins have not decreased during the 1990s. Even though data from Illinois waters suggested that bottom-up effects may have partly contributed to a prolonged period of low yellow perch recruitment, available data were insufficient to support the contention that a long-term decrease in zooplankton abundance was primarily responsible for the extended period of low recruitment. Rainbow smelt abundance decreased during 1992–1999; however, explanations for trends in rainbow smelt abundance, as determined by GLSC bottom trawl surveys over the past 30 years, are not obvious. Eck and Wells (1987) also experienced difficulty in interpreting long-term trends in rainbow smelt abundance.

Have these bottom-up effects already influenced growth rates or condition of Lake Michigan fishes? The decrease in lake whitefish condition between 1995 and 1998 may have been partially due to some bottom-up effects. An increase in proportion of zebra mussels or a decrease in proportion of *Diporeia* in lake whitefish diet could have led to reduced lake whitefish condition. The recent decline in alewife condition may be due to bottom-up effects. Bloater growth rate declined between 1973 and 1994, during which time the population increased tremendously in size. However, bloater growth rate has actually increased during 1994–1999, as the population has undergone a drastic decrease in size. To detect future impacts of bottom-up effects on fish populations, surveillance of fish abundance, growth rates, lipid content, and condition should be continued. Zebra mussel abundance in Lake Michigan has not yet peaked, and the quagga mussel (*Dreissena bugensis*) invasion of Lake Michigan has just begun (Nalepa et al. 2001).

Overexploitation of fish stocks

Overall, overexploitation of fish populations appeared to play a relatively minor role in shaping the Lake Michigan food web during 1970–2000. Commercial harvest of yellow perch during the 1990s may have contributed to a skewing of the sex ratio (relatively low number of female spawners), which may have contributed to prolonging the period of low recruitment to the yellow perch population. Yellow perch recruitment remained low during 1989–1997. Consequently, the yellow perch commercial fishery in Lake Michigan was closed by 1998.

Bythotrephes and round goby invasions

Although invasions by *Bythotrephes* and round goby have caused some changes to the Lake Michigan food web during the late 1980s and 1990s, the earlier invasions by sea lamprey and alewife had more serious consequences for the Lake Michigan fish community. Through predation, *Bythotrephes* may have reduced the abundance of certain smaller cladocerans. However, the impact of this reduction on the rest of the Lake Michigan ecosystem remains undefined. Total phytoplankton biomass in offshore waters has exhibited no long-term trends since the early 1970s. Although species composition of the zooplankton community has undergone substantial changes, total zooplankton biomass in offshore waters of Lake Michigan has shown no long-term trends since the 1970s. Abundance of *Mysis* in offshore waters has not changed appreciably since the 1970s. Alewife abundance has neither increased nor decreased since the time of the *Bythotrephes* invasion, and salmonine biomass has remained relatively high throughout the occupation of the lake by *Bythotrephes*. Moreover, *Bythotrephes* has been a relatively minor component of the diets of the prey fish and salmonine communities in Lake Michigan since the late 1980s (Davis et al. 1997; R. Elliott, U.S. Fish and Wildlife Service, Green Bay, WI 54311, U.S.A., personal communication). The round goby invasion was linked to the decline of mottled sculpin in Calumet Harbor. To date, however, no lake-wide changes in abundance of any Lake Michigan biota have been ascribed to the round goby invasion.

Contaminants and global climate change stressors

Although bans on use of pesticides and PCBs have led to dramatic declines in contaminant concentrations of Lake Michigan biota between 1970 and 2000, very few lake-wide changes in abundances of Lake Michigan biota have been shown to be directly attributable to stressor effects from contaminants. Rapid increase in the double-crested cormorant

© 2002 NRC Canada

population associated with Lake Michigan during the late 1980s and 1990s was partially due to substantial reduction of contaminant levels within the lake ecosystem during the 1970s (Weseloh et al. 1995). To date, lake-wide consequences of this increase in cormorant abundance on the rest of the lake ecosystem remain unclear.

We were unable to attribute any of the lake-wide changes in the Lake Michigan food web between 1970 and 2000 to global climate change effects. That is not to say that global climate change has not already had some effect on the Lake Michigan ecosystem. Rather, time series for water temperature characteristics are not sufficiently long to resolve whether recent trends were part of a natural cycle or were forced by anthropogenic activity. Furthermore, insufficient data were available to identify a common long-term trend in water temperature characteristics across several locations in the lake. We would expect that ecological changes associated with global climate change would occur much more slowly than changes induced by invasions of exotic species.

Other effects

Finally, we would like to point out that one of the major changes occurring in the Lake Michigan food web between 1970 and 2000 may not have been driven by any of the anthropogenic stressors mentioned above. Rise in bloater abundance during the 1980s and fall in bloater abundance during the 1990s may simply have represented natural oscillations in bloater population size. In other words, bloater abundance may exhibit quasi-regular natural cycles, with a period of approximately 30 years. Through density-dependent mechanisms, bloaters may be regulating their own abundance, largely independent of human interventions or interactions with other fishes. Given that bloater longevity in Lake Michigan is at least 12 years (G. Fleischer, unpublished data), a 30-year cycle in their abundance would be in accord with theory developed by Nisbet (1997) for delayed-feeback population cycles.

Acknowledgments

This paper would not have been possible without the efforts of the Lake Michigan Technical Committee, including chairperson M. Holey, as well as D. Clapp, B. Eggold, R. Hess, J. Kubisiak, S. Marcquenski, E. Olson, M. Toneys, and G. Wright. We thank L. Wells, senior author of the SCOL-1 paper for Lake Michigan, for providing helpful comments. M. Hansen and S. Kerr also reviewed the manuscript. With this paper, we pay tribute to the memory of Heang T. Tin, a pioneer of larval fish ecology in Lake Michigan. This work was supported in part by Michigan Sea Grant College Program grants R/FM-1 and R/GL-46 to J.R.B. This article is Contribution 1172 of the USGS–GLSC, GLERL contribution No. 1224, and CGLAS contribution No. 622. This publication is a result of work sponsored by the Cooperative Institute for Limnology and Ecosystems Research under cooperative agreement NA67RJ0148 from the Office of Oceanic and Atmospheric Research, National Oceanic and Atmospheric Administration, U.S. Department of Commerce.

References

Baumann, P.C., Smith, I.R., and Metcalfe, C.D. 1996. Linkages between chemical contaminants and tumors in benthic Great Lakes fish. J. Gt. Lakes Res. **22**: 131–152.

Bence, J.R., and Smith, K.D. 1999. An overview of recreational fisheries of the Great Lakes. *In* Great Lakes fisheries and policy management: a binational perspective. *Edited by* W.W. Taylor and C.P. Ferreri. Michigan State University Press, East Lansing, Mich. pp. 259–306.

Benjamin, D.M. 1998. Chinook salmon (*Oncorhynchus tshawytscha*) population dynamics in Lake Michigan, 1985–1996. M.Sc. thesis, Michigan State University, East Lansing.

Benjamin, D.M., and Bence, J.R. 2002. Statistical catch-at-age analysis of chinook salmon in Lake Michigan, 1985–1996. Fisheries Research Report, Fisheries Division, Michigan Department of Natural Resources, Ann Arbor.

Bennet, E.B. 1986. The nitrifying of Lake Superior. Ambio, **15**: 272–275.

Brooks, A.S., and Torke, B.G. 1977. Vertical and seasonal distribution of chlorophyll *a* in Lake Michigan. J. Fish. Res. Board Can. **34**: 2280–2287.

Brown, E.H., Jr. 1972. Population biology of alewives, *Alosa pseudoharengus*, in Lake Michigan, 1949–70. J. Fish. Res. Board Can. **29**: 477–500.

Chang, W.Y.B., and Rossman, R. 1988. Changes in the abundance of blue-green algae related to nutrient loadings in the nearshore zone of Lake Michigan. Hydrobiologia, **157**: 271–278.

Clapp, D.F., Schneeberger, P.J., Jude, D.J., Madison, G., and Pistis, C. 2001. Monitoring round goby (*Neogobius melanostomus*) population expansion in eastern and northern Lake Michigan. J. Gt. Lakes Res. **27**: 335–341.

Davis, B.M., Savino, J.F., and Ogilvie, L.M. 1997. Diets of forage fish in Lake Michigan. U.S. Environmental Protection Agency Report EPA/IAG DW14947692-01-0, Chicago, Ill.

DeVault, D.S., Hesselberg, R., Rodgers, P.W., and Feist, T.J. 1996. Contaminant trends in lake trout and walleye from the Laurentian Great Lakes. J. Gt. Lakes Res. **22**: 884–895.

Doak, D.F., and Morris, W. 1999. Detecting population-level consequences of ongoing environmental change without long-term monitoring. Ecology, **80**: 1537–1551.

Eck, G.W., and Brown, E.H., Jr. 1985. Lake Michigan's capacity to support lake trout (*Salvelinus namaycush*) and other salmonines: an estimate based on the status of prey populations in the 1970s. Can. J. Fish. Aquat. Sci. **42**: 449–454.

Eck, G.W., and Wells, L. 1987. Recent changes in Lake Michigan's fish community and their probable causes, with emphasis on the role of the alewife (*Alosa pseudoharengus*). Can. J. Fish. Aquat. Sci. **44**(Suppl. 2): 53–60.

Eshenroder, R.L., and Burnham-Curtis, M.K. 1999. Species succession and sustainability of the Great Lakes fish community. *In* Great Lakes fisheries and policy management: a binational perspective. *Edited by* W.W. Taylor and C.P. Ferreri. Michigan State University Press, East Lansing. pp. 145–184.

Evans, M.S. 1988. Toxic contaminants and ecosystem health: a Great Lakes focus. John Wiley & Sons, New York.

Evans, M.S. 1992. Historic changes in Lake Michigan zooplankton community structure: the 1960s revisited with implications for top-down control. Can. J. Fish. Aquat. Sci. **49**: 1734–1749.

Evans, M.S., and Jude, D.J. 1986. Recent shifts in *Daphnia* community structure in southeastern Lake Michigan: a comparison of the inshore and offshore regions. Limnol. Oceanogr. **31**: 56–67.

Fahnenstiel, G.L., and Scavia, D. 1987*a*. Dynamics of Lake Michigan phytoplankton: recent changes in surface and deep communities. Can. J. Fish. Aquat. Sci. **44**: 509–514.

Fahnenstiel, G.L., and Scavia, D. 1987*b*. Dynamics of Lake Michi-

© 2002 NRC Canada

gan phytoplankton: primary production and growth. Can. J. Fish. Aquat. Sci. **44**: 499–508.

Fahnenstiel, G.L., and Scavia, D. 1987*c*. Dynamics of Lake Michigan phytoplankton: the deep chlorophyll layer. J. Gt. Lakes Res. **13**: 285–295.

Fahnenstiel, G.L., Krause, A.E., McCormick, M.J., Carrick, H.J., and Schelske, C.L. 1998. The structure of the planktonic food-web in the St. Lawrence Great Lakes. J. Gt. Lakes Res. **24**: 531–554.

Fitzsimons, J.D., Brown, S.B., Honeyfield, D.C., and Hnath, J.G. 1999. A review of early mortality syndrome (EMS) in Great Lakes salmonids: relationship with thiamine deficiency. Ambio, **28**: 9–15.

Fratt, T.W., Coble, D.W., Copes, F., and Brusewitz, R.E. 1997. Diet of burbot in Green Bay and western Lake Michigan with comparison to other waters. J. Gt. Lakes Res. **23**: 1–10.

Gardner, W.S., Nalepa, T.F., Frez, W.A., Cichocki, E.A., and Landrum, P.F. 1985. Seasonal patterns in lipid content of Lake Michigan macroinvertebrates. Can. J. Fish. Aquat. Sci. **42**: 1827–1832.

Hatch, R.W., Haack, P.M., and Brown, E.H., Jr. 1981. Estimation of alewife biomass in Lake Michigan, 1967–1978. Trans. Am. Fish. Soc. **110**: 575–584

Hay-Chmielewski, E.M., and Whelan, G.E. 1997. Lake sturgeon rehabilitation strategy.Special Report 18, Fisheries Division, Michigan Department of Natural Resources, Ann Arbor.

Holey, M.E., Rybicki, R.W., Eck, G.W., Brown, E.H., Jr., Marsden, J.E., Lavis, D.S., Toneys, M.L., Trudeau, T.N., and Horrall, R.M. 1995. Progress toward lake trout restoration in Lake Michigan. J. Gt. Lakes Res. **21**(Suppl. 1): 128–151.

Hoyle, J.A., Schaner, T., Casselman, J., and Dermott, R. 1999. Changes in lake whitefish (*Coregonus clupeaformis*) stocks in eastern Lake Ontario following *Dreissena* mussel invasion. Gt. Lakes Res. Rev. **4**(2): 5–10.

Janssen, J., and Jude, D.J. 2001. Recruitment failure of mottled sculpin *Cottus bairdi* in southern Lake Michigan, induced by the newly introduced round goby *Neogobius melanostomus*. J. Gt. Lakes Res. **27**: 319–328.

Johengen, T.H., Johansson, O.E., Pernie, G.L., and Millard, E.S. 1994. Temporal and seasonal trends in nutrient dynamics and biomass measures in Lakes Michigan and Ontario in response to phosphorus control. Can. J. Fish. Aquat. Sci. **51**: 2570–2578.

Jones, M.L., Koonce, J.F., and O'Gorman, R. 1993. Sustainability of hatchery-dependent salmonine fisheries in Lake Ontario: the conflict of predator demand and prey supply. Trans. Am. Fish. Soc. **122**: 1019–1030.

Jude, D.J., and Tesar, F.J. 1985. Recent changes in the inshore forage fish of Lake Michigan. Can. J. Fish. Aquat. Sci. **42**: 1154–1157.

Kabre, J.A. 1993. Impact of *Renibacterium saloninarum* on non-lipid energy, lipid and water contents in liver of infected chinook salmon during fall and spring in Lake Michigan, 1990–1992. Ph.D. thesis, Michigan State University, East Lansing.

Kitchell, J.F., and Carpenter, S.R. 1993. Cascading trophic interactions. *In* The trophic cascade in lakes. *Edited by* S.R. Carpenter and J.F. Kitchell. Cambridge University Press, New York. pp. 1–14.

Krause, A.E. 1999. Sampling variability of ten fish species and population dynamics of alewife (*Alosa pseudoharengus*) and bloater (*Coregonus hoyi*) in Lake Michigan. M.Sc. thesis, Michigan State University, East Lansing.

Krueger, C.C., Perkins, D.L., Mills, E.L., and Marsden, J.E. 1995. Predation by alewives on lake trout fry in Lake Ontario: role of an exotic species in preventing restoration of a native species. J. Gt. Lakes Res. **21**(Suppl. 1): 458–469.

Kuhns, L.A., and Berg, M.B. 1999. Benthic invertebrate community responses to round goby (*Neogobius melanostomus*) and zebra mussel (*Dreissena polymorpha*) invasion in southern Lake Michigan. J. Gt. Lakes Res. **25**: 910–917.

Lavis, D.S., Henson, M.P., Johnson, D.A., Koon, E.M., and Ollila, D.J. 2002. A case history of sea lamprey control in Lake Michigan: 1979–1999. J. Gt. Lakes Res. **28**(Suppl. 1). In press.

Lehman, J.T. 1987. Palearctic predator invades North American Great Lakes. Oecologia, **74**: 478–480.

Lehman, J.T., and Cáceres, C.A. 1993. Food web responses to species invasion by a predatory invertebrate: *Bythotrephes* in Lake Michigan. Limnol. Oceanogr. **38**: 879–891.

Likens, G.E. (*Editor*). 1989. Preface. *In* Long-term studies in ecology—approaches and alternatives. Springer-Verlag, New York. pp. ix–xi.

Madenjian, C.P., and DeSorcie, T.J. 1999. Status of lake trout rehabilitation in the Northern Refuge of Lake Michigan. N. Am. J. Fish. Manag. **19**: 658–669.

Madenjian, C.P., Jude, D.J., and Tesar, F.J. 1986. Intervention analysis of power plant impact on fish populations. Can. J. Fish. Aquat. Sci. **43**: 819–829.

Madenjian, C.P., DeSorcie, T.J., and Stedman, R.M. 1998*a*. Ontogenic and spatial patterns in diet and growth of lake trout in Lake Michigan. Trans. Am. Fish. Soc. **127**: 236–252.

Madenjian, C.P., Hesselberg, R.J., DeSorcie, T.J., Schmidt, L.J., Stedman, R.M., Quintal, R.T., Begnoche, L.J., and Passino-Reader, D.R. 1998*b*. Estimate of net trophic transfer efficiency of PCBs to Lake Michigan lake trout from their prey. Environ. Sci. Technol. **32**: 886–891.

Madenjian, C.P., Elliott, R.F., Schmidt, L.J., DeSorcie, T.J., Hesselberg, R.J., Quintal, R.T., Begnoche, L.J., Bouchard, P.M., and Holey, M.E. 1998*c*. Net trophic transfer efficiency of PCBs to Lake Michigan coho salmon from their prey. Environ. Sci. Technol. **32**: 3063–3067.

Madenjian, C.P., Elliott, R.F., DeSorcie, T.J., Stedman, R.M., O'Connor, D.V., and Rottiers, D.V. 2000. Lipid concentrations in Lake Michigan fishes: seasonal, spatial, ontogenetic, and long-term trends. J. Gt. Lakes Res. **26**: 427–444.

Magnuson, J.J., Meisner, J.D., and Hill, D.K. 1990. Potential changes in the thermal habitat of Great Lakes fish after global climate warming. Trans. Am. Fish. Soc. **119**: 254–264.

Magnuson, J.J., Webster, K.E., Assel, R.A., Bowser, C.J., Dillon, P.J., Eaton, J.G., Evans, H.E., Fee, E.J., Hall, R.J., Mortsch, L.R., Schindler, D.W., and Quinn, F.H. 1997. Potential effects of climate changes on aquatic systems: Laurentian Great Lakes and Precambrian Shield Region. Hydrol. Process. **11**: 825–871.

Makarewicz, J.C., Bertram, P., Lewis, T., and Brown, E.H., Jr. 1995. A decade of predatory control of zooplankton species composition of Lake Michigan. J. Gt. Lakes Res. **21**: 620–640.

Makarewicz, J.C., Bertram, P., and Lewis, T.W. 1998. Changes in phytoplankton size-class abundance and species composition coinciding with changes in water chemistry and zooplankton community structure of Lake Michigan, 1983 to 1992. J. Gt. Lakes Res. **24**: 637–657.

Makauskas, D., and Clapp, D. 2000. Status of yellow perch in Lake Michigan and Yellow Perch Task Group progress report. *In* Minutes of 2000 Annual Meeting of the Lake Michigan Committee. Great Lakes Fishery Commission, Ann Arbor, Mich.

McCormick, M.J. 1990. Potential changes in thermal structure and cycle of Lake Michigan due to global warming. Trans. Am. Fish. Soc. **119**: 254–264.

McCormick, M.J., and Fahnenstiel, G.L. 1999. Recent climatic trends in nearshore water temperatures in the St. Lawrence Great Lakes. Limnol. Oceanogr. **44**: 530–540.

© 2002 NRC Canada

McQueen, D.J., Johannes, M.R.S., Post, J.R., Stewart, T.J., and Lean, D.R.S. 1989. Bottom-up and top-down impacts on freshwater pelagic community structure. Ecol. Monogr. **59**: 289–309.

Nalepa, T.F. 1987. Long term changes in the macrobenthos of southern Lake Michigan. Can. J. Fish. Aquat. Sci. **44**: 515–524.

Nalepa, T.F., Hartson, D.J., Fanslow, D.L., Lang, G.A., and Lozano, S.J. 1998. Declines in benthic macroinvertebrate populations in southern Lake Michigan, 1980–1993. Can. J. Fish. Aquat. Sci. **55**: 2402–2413.

Nalepa, T.F., Fanslow, D.L., and Lang, G.A. 2000*a*. Trends in benthic macroinvertebrate populations in southern Lake Michigan over the past several decades. Internationale Vereinigung für Theoretische und Angewandte Limnologie Verhandlungen, **27**: 2540–2545.

Nalepa, T.F., Hartson, D.J., Buchanan, J., Cavaletto, J.F., Lang, G.A., and Lozano, S.J. 2000*b*. Spatial variation in density, mean size, and physiological condition of the holarctic amphipod *Diporeia* spp. in Lake Michigan. Freshwater Biol. **43**: 107–119.

Nalepa, T.F., Schloesser, D.W., Pothoven, S.A., Horndorp, D.W., Fanslow, D.L., Tuchman, M.L., and Fleischer, G.W. 2001. First finding of the amphipod *Echinogammarus ischnus* and the mussel *Dreissena bugensis* in Lake Michigan. J. Gt. Lakes Res. **27**: 384–391.

Ney, J.J. 1990. Trophic economics in fisheries—assessment of demand–supply relationship between predator and prey. Rev. Aquat. Sci. **2**: 55–81.

Nisbet, R.M. 1997. Delay differential equations for structured populations. *In* Structured population models in marine, terrestrial, and freshwater systems. *Edited by* S. Tuljapurkar and H. Caswell. Chapman and Hall, New York. pp. 89–118.

Pace, M.L., and Cole, J.J. 1989. What questions, systems, or phenomena warrant long-term study? *In* Long-term studies in ecology—approaches and alternatives. *Edited by* G.E. Likens. Springer-Verlag, New York. pp. 183–185.

Pekarik, C., and Weseloh, D.V. 1998. Organochlorine contaminants in herring gull eggs from the Great Lakes, 1974–1995: change point regression analysis and short-term regression. Environ. Monit. Assess. **53**: 77–115.

Pothoven, S.A., Fahnenstiel, G.L., Vanderploeg, H.A., and Luttenton, M. 2000. Population dynamics of *Mysis relicta* in southeastern Lake Michigan, 1995–1998. J. Gt. Lakes Res. **26**: 357–365.

Regier, H.A., Magnuson, J.J., and Coutant, C.C. 1990. Introduction to proceedings: symposium on effects of climate change on fish. Trans. Am. Fish. Soc. **119**: 173–175.

Rutherford, E.S. 1997. Evaluation of natural reproduction, stocking rates, and fishing regulations for steelhead *Oncorhynchus mykiss*, chinook salmon *O. tschawytscha*, and coho salmon *O. kisutch* in Lake Michigan. Federal Aid in Sport Fish Restoration, Project F-35-R-22, Final Report. Michigan Department of Natural Resources, Ann Arbor, Mich.

Saether, O.A. 1980. The influence of eutrophication on deep lake benthic invertebrate communities. Prog. Water Technol. **12**: 161–180.

Scavia, D., and Fahnenstiel, G.L. 1987. Dynamics of Lake Michigan phytoplankton: mechanisms controlling epilimnetic communities. J. Gt. Lakes Res. **13**: 103–120.

Scavia, D., Fahnenstiel, G.L., Evans, M.S., Jude, D.J., and Lehman, J.T. 1986. Influence of salmonid predation and weather on long-term water quality trends in Lake Michigan. Can. J. Fish. Aquat. Sci. **43**: 435–443.

Schelske, C.L. 1977. Trophic status and nutrient loading for Lake Michigan. *In* North American project—a study of U.S. water bodies: a report for the Organization of Economic Cooperation and Development. Ecol. Res. Series, U.S. EPA, Rep. No. EPA-600/3-77-086, Corvallis, Oreg.

Schelske, C.L., and Stoermer, E.F. 1971. Eutrophication, silica, and predicted changes in algal quality in Lake Michigan. Science (Washington, D.C.), **173**: 423–424.

Schelske, C.L., Rothman, E.D., Stoermer, E.F., and Santiago, M.A. 1974. Responses of phosphorus limited Lake Michigan phytoplankton to factorial enrichments with nitrogen and phosphorus. Limnol. Oceanogr. **19**: 409–419.

Schelske, C.L., Feldt, L.E., and Simmons, M.S. 1980. Phytoplankton and physical-chemical conditions in selected rivers and the coastal zone of Lake Michigan, 1972. Gt. Lakes Res. Div. Publ. No. 19. University of Michigan, Ann Arbor, Mich.

Schelske, C.L., Stoermer, E.F., Fahnenstiel, G.L., and Haibach, M. 1986. Phosphorus enrichment, silica limitation, and biogeochemical silica depletion in the Great Lakes. Can. J. Fish. Aquat. Sci. **43**: 407–415.

Schneeberger, P.J. 2000. Population dynamics of contemporary yellow perch and walleye stocks in Michigan waters of Green Bay, Lake Michigan, 1988–96. Fisheries Research Report 2055, Michigan Department of Natural Resources, Ann Arbor, Mich.

Shroyer, S.M., and McComish, T.S. 2000. Relationship between alewife abundance and yellow perch recruitment in southern Lake Michigan. N. Am. J. Fish. Manag. **20**: 220–225.

Stewart, D.J., and Ibarra, M. 1991. Predation and production by salmonine fishes in Lake Michigan, 1978–1988. Can. J. Fish. Aquat. Sci. **48**: 909–922.

TeWinkel, L.M., Kroeff, T., Fleischer, G.W., and Toneys, M. 2002. Population dynamics of bloaters (*Coregonus hoyi*) in Lake Michigan, 1973–1998. *In* Biology and management of coregonid fishes—1999. Arch. Hydrobiol. Special Issues: Advances in Limnology, **57**: 307–320.

Vollenweider, R. 1970. Scientific fundamentals of the eutrophication of lakes and flowing waters, with particular reference to nitrogen and phosphorus as factors responsible in eutrophication. OECD Publications, Paris.

Wells, L. 1970. Effects of alewife predation on zooplankton populations in Lake Michigan. Limnol. Oceanogr. **15**: 556–565.

Wells, L. 1977. Changes in yellow perch (*Perca flavescens*) populations of Lake Michigan, 1954–75. J. Fish. Res. Board Can. **34**: 1821–1829.

Wells, L., and McLain, A.L. 1972. Lake Michigan: effects of exploitation, introductions, and eutrophication on the salmonid community. J. Fish. Res. Board Can. **29**: 889–898.

Wells, L., and McLain, A.L. 1973. Lake Michigan—man's effects on native fish stocks and other biota. Gt. Lakes Fish. Comm. Tech. Rep. No. 20.

Weseloh, D.V., Teeple, S.M., and Gilbertson, M. 1983. Double-crested cormorants of the Great Lakes: egg-laying parameters, reproductive failure, and contaminant residues in eggs, Lake Huron 1972–1973. Can. J. Zool. **61**: 427–436.

Weseloh, D.V., Ewins, P.J., Struger, J., Mineau, P., Bishop, C.A., Postupalsky, S., and Ludwig, J.P. 1995. Double-crested cormorants of the Great Lakes: changes in population size, breeding distribution and reproductive output between 1913 and 1991. Colon. Waterbirds, **18**(Spec. Publ. 1): 48–59.

Wesley, J.K. 1996. Age and growth of chinook salmon in Lake Michigan: verification, current analysis, and past trends. M.Sc. thesis, University of Michigan, Ann Arbor.

© 2002 NRC Canada

Workshop on Rebuilding Abalone Stocks in British Columbia

By/par Alan Campbell

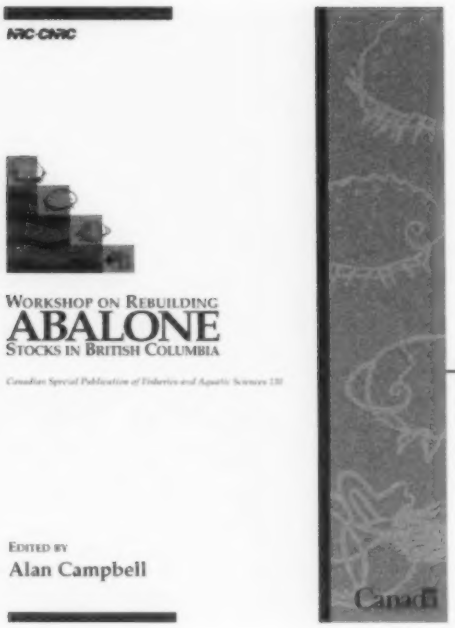

$42.95/42,95 $

Other countries $42.95 US
À l'étranger 42,95 $US

Softcover / Edition brochée
158 pages
ISBN 0-660-18292-0 ISSN 0706-6481
NRC No./N° du CNRC 42841
(Can. Spec. Publ. Fish. Aquat. Sci. No. 130)

Orders may be submitted by mail or fax to: Les commandes peuvent être soumises par courrier ou par télécopieur à :

Order Office/Bureau des commandes
NRC Research Press/Presses scientifique du CNRC
National Research Council/Conseil national de recherches
Ottawa, ON K1A 0R6, Canada
Telephone/Téléphone : (613) 990-2254
Fax/Télécopieur : (613) 952-7656
E-mail: research.press@nrc.ca
Courriel : presses.scientifiques@cnrc.ca
Website: http://researchpress.nrc.ca
Site web : http://pressesscientifiques.cnrc.ca

PLEASE PRINT/LETTRES MOULÉES

☐ Payment enclosed / Paiement inclus
Charge to/ Imputer à ☐ Visa ☐ MasterCard ☐ AMEX
Account no./N° de compte
Expiry date/Date d'expiration

Name/Nom

Signature

Address/Adresse

City/Ville Province

Postal code/Code postal Country/Pays

Telephone/Téléphone Fax/Télécopieur

E-mail/courriel

Prepayment required unless order is accompanied by a purchase order number. Cheques or money orders should be made payable to : "Receiver General for Canada, Credit NRC". For all orders outside Canada, rates are in U.S. Dollars. All sales are final.
Les commandes doivent être payées d'avance à moins qu'elles ne soient accompagnées d'un numéro de bon de commande. Les chèques ou mandats doivent être libellés au « Receveur général du Canada, crédit du CNRC ». Toutes les ventes sont finales.

Salmonine Introductions to the Laurentian Great Lakes: An Historical Review and Evaluation of Ecological Effects

By/par Stephen S. Crawford

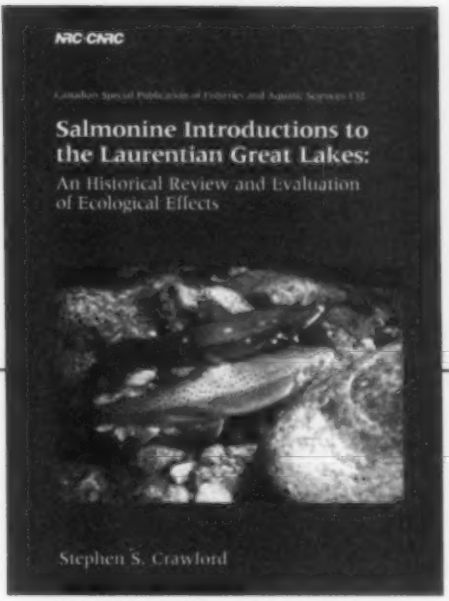
NRC CNRC
Salmonine Introductions to the Laurentian Great Lakes:
An Historical Review and Evaluation of Ecological Effects
Stephen S. Crawford

$42.95/42,95 $

Other countries $42.95 US
À l'étranger 42,95 $US

Softcover / Edition brochée
205 pages
ISBN 0-660-17639-4 ISSN 0706-6481
(Can. Spec. Publ. Fish. Aquat. Sci. 132)
NRC No. / N° du CNRC 42734

Orders may be submitted by mail or fax to: Les commandes peuvent être soumises par courrier ou par télécopieur à :

Order Office/Bureau des commandes
NRC Research Press/Presses scientifique du CNRC
National Research Council/Conseil national de recherches
Ottawa, ON K1A 0R6, Canada
Telephone/Téléphone : (613) 990-2254
Fax/Télécopieur : (613) 952-7656
E-mail: research.press@nrc.ca
Courriel : presses.scientifiques@cnrc.ca
Website: http://researchpress.nrc.ca
Site web : http://pressesscientifiques.cnrc.ca

PLEASE PRINT/LETTRES MOULÉES

☐ Payment enclosed / Paiement inclus ☐ Charge to/ Imputer à ☐ Visa ☐ MasterCard ☐ AMEX

Account no./N° de compte | Expiry date/Date d'expiration

Name/Nom

Signature

Address/Adresse

City/Ville | Province

Postal code/Code postal | Country/Pays

Telephone/Téléphone | Fax/Télécopieur

E-mail/courriel

Prepayment required unless order is accompanied by a purchase order number. Cheques or money orders should be made payable to : "Receiver General for Canada, Credit NRC". For all orders outside Canada, rates are in U.S. Dollars. All sales are final.
Les commandes doivent être payées d'avance à moins qu'elles ne soient accompagnées d'un numéro de bon de commande. Les chèques ou mandats doivent être libellés au « Receveur général du Canada, crédit du CNRC ». Toutes les ventes sont finales.

Marine Protected Areas and Fisheries Closures in British Columbia

By/par Glen S. Jamieson and/et Joanne Lessard

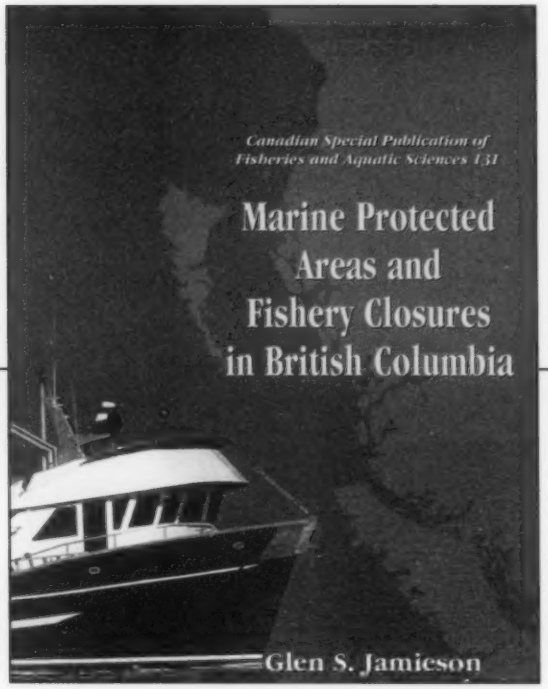
Canadian Special Publication of Fisheries and Aquatic Sciences 131
Marine Protected Areas and Fishery Closures in British Columbia
Glen S. Jamieson

$69.95/69,95 $

Other countries $69.95 US
À l'étranger 69,95 $US

Softcover / Edition brochée
414 pages
ISBN 0-660-17788-9 ISSN 0706-6481
NRC No./N° du CNRC 42846
(Can. Spec. Publ. Fish. Aquat. Sci. No. 131)

Orders may be submitted by mail or fax to: Les commandes peuvent être soumises par courrier ou par télécopieur à :

Order Office/Bureau des commandes

NRC Research Press/Presses scientifique du CNRC
National Research Council/Conseil national de recherches
Ottawa, ON K1A 0R6, Canada
Telephone/Téléphone : (613) 990-2254
Fax/Télécopieur : (613) 952-7656
E-mail: research.press@nrc.ca
Courriel : presses.scientifiques@cnrc.ca
Website: http://researchpress.nrc.ca
Site web : http://pressesscientifiques.cnrc.ca

PLEASE PRINT/LETTRES MOULÉES

☐ Payment enclosed / Paiement inclus ☐ Charge to/ Imputer à ☐ Visa ☐ MasterCard ☐ AMEX

Account no./N° de compte | Expiry date/Date d'expiration

Name/Nom

Signature

Address/Adresse

City/Ville | Province

Postal code/Code postal | Country/Pays

Telephone/Téléphone | Fax/Télécopieur

E-mail/courriel

Prepayment required unless order is accompanied by a purchase order number. Cheques or money orders should be made payable to : "Receiver General for Canada, Credit NRC". For all orders outside Canada, rates are in U.S. Dollars. All sales are final.
Les commandes doivent être payées d'avance à moins qu'elles ne soient accompagnées d'un numéro de bon de commande. Les chèques ou mandats doivent être libellés au « Receveur général du Canada, crédit du CNRC ». Toutes les ventes sont finales.

Robin J. Wyatt	**695–706**	Estimating riverine fish population size from single- and multiple-pass removal sampling using a hierarchical model
Marci L. Koski and Brett M. Johnson	**707–716**	Functional response of kokanee salmon (*Oncorhynchus nerka*) to *Daphnia* at different light levels
Charles M. Paulsen and Richard A. Hinrichsen	**717–725**	Experimental management for Snake River spring–summer chinook (*Oncorhynchus tshawytscha*): trade-offs between conservation and learning for a threatened species
W. Keller, N.D. Yan, K.M. Somers, and J.H. Heneberry	**726–735**	Crustacean zooplankton communities in lakes recovering from acidification
	PERSPECTIVE	PERSPECTIVE
Charles P. Madenjian, Gary L. Fahnenstiel, Thomas H. Johengen, Thomas F. Nalepa, Henry A. Vanderploeg, Guy W. Fleischer, Philip J. Schneeberger, Darren M. Benjamin, Emily B. Smith, James R. Bence, Edward S. Rutherford, Dennis S. Lavis, Dale M. Robertson, David J. Jude, and Mark P. Ebener	**736–753**	Dynamics of the Lake Michigan food web, 1970–2000

National Research Council Canada
Ottawa, Canada K1A 0R6

Conseil national de recherches Canada
Ottawa, Canada K1A 0R6

Postage paid at Ottawa
Publications mail
Registration No. 1240579

Port payé à Ottawa
Poste-publication
Enregistrement n° 1240579

USPS periodical postage paid at Champlain, N.Y.

Canadian Journal of Fisheries and Aquatic Sciences

Volume 59, Number 4, April 2002

Journal canadien des sciences halieutiques et aquatiques

Volume 59, numéro 4, avril 2002

RAPID COMMUNICATIONS		COMMUNICATIONS RAPIDES
Peter K. Weber, Ian D. Hutcheon, Kevin D. McKeegan, and B. Lynn Ingram	**587–591**	Otolith sulfur isotope method to reconstruct salmon (*Oncorhynchus tshawytscha*) life history
C.M. Waluda, P.N. Trathan, C.D. Elvidge, V.R. Hobson, and P.G. Rodhouse	**592–596**	Throwing light on straddling stocks of *Illex argentinus*: assessing fishing intensity with satellite imagery
Ransom A. Myers and Terrance J. Quinn II	**597–601**	Estimating and testing non-additivity in fishing mortality: implications for detecting a fisheries collapse
ARTICLES		ARTICLES
W.A. Montevecchi, D.K. Cairns, and R.A. Myers	**602–612**	Predation on marine-phase Atlantic salmon (*Salmo salar*) by gannets (*Morus bassanus*) in the Northwest Atlantic
George R. Pess, David R. Montgomery, E. Ashley Steel, Robert E. Bilby, Blake E. Feist, and Harvey M. Greenberg	**613–623**	Landscape characteristics, land use, and coho salmon (*Oncorhynchus kisutch*) abundance, Snohomish River, Wash., U.S.A.
M.R. Heupel and C.A. Simpfendorfer	**624–632**	Estimation of mortality of juvenile blacktip sharks, *Carcharhinus limbatus*, within a nursery area using telemetry data
David W. Crowder and Panayiotis Diplas	**633–645**	Vorticity and circulation: spatial metrics for evaluating flow complexity in stream habitats
Marc Ringuette, Martin Castonguay, Jeffrey A. Runge, and François Grégoire	**646–656**	Atlantic mackerel (*Scomber scombrus*) recruitment fluctuations in relation to copepod production and juvenile growth
Clay E. Porch, Mark R. Fisher, and Lawrence W. McEachron	**657–668**	Estimating abundance from gillnet samples with application to red drum (*Sciaenops ocellatus*) in Texas bays
Bronwyn M. Gillanders	**669–679**	Temporal and spatial variability in elemental composition of otoliths: implications for determining stock identity and connectivity of populations
Brad S. Baldwin, Marilyn S. Mayer, Jeffrey Dayton, Nancy Pau, Johanna Mendilla, Maura Sullivan, Aaron Moore, Aye Ma, and Edward L. Mills	**680–694**	Comparative growth and feeding in zebra and quagga mussels (*Dreissena polymorpha* and *Dreissena bugensis*): implications for North American lakes

Continued on inside back cover / Suite au verso

Canada

Printed in Canada by / Imprimé au Canada par
University of Toronto Press Inc.
Typesetting by / Typographie par
NRC Research Press / Presses scientifiques du CNRC

0706-652X(200204)59:4;1-C